

REVIEW OF THE QCD SUM RULES FOR EXOTIC STATES

Zhi-Gang Wang¹

Department of Physics, North China Electric Power University, Baoding 071003, P. R. China

Abstract

We review the exotic states, such as the X , Y , Z , T and P states, and present their possible assignments based on the QCD sum rules. We present many predictions which can be confronted to the experimental data in the future to diagnose the exotic states. Furthermore, we also mention other theoretical methods.

Contents

1	Introduction	2
1.1	$X(3872)$	2
1.2	$X(3915)$, $X(3940)$, $Y(3940)$, $Z(3930)$, $X(4160)$, $X(3860)$, $X(3960)$	3
1.3	$\eta_c(3945)$, $h_c(4000)$, $\chi_{c1}(4010)$, $h_c(4300)$	4
1.4	$X(4140)$, $X(4274)$, $X(4500/4475)$, $X(4700/4710)$, $X(4685/4650)$, $X(4630/4800)$	4
1.5	$X(4350)$	5
1.6	$X_0(2900)$, $X_1(2900)$, $T_{c\bar{s}}(2900)$	5
1.7	$X(5568)$	6
1.8	$X(6600)$, $X(6900)$, $X(7300)$	6
1.9	$Y(4260/4230)$, $Y(4360/4320)$, $Y(4390)$, $Y(4500)$, $Y(4660)$, $Y(4710/4750/4790)$	7
1.10	$Z_c(3900/3885)$, $Z_c(4020/4025)$, $Z_{cs}(3985/4000)$, $Z_{cs}(4123)$, $Z_{cs}(4220)$	8
1.11	$Z_1(4050)$, $Z_1(4250)$, $Z_c(4100)$	9
1.12	$Z_c(4430)$, $Z_c(4600)$	9
1.13	$Z_c(4200)$, $Z_{c\bar{s}}(4600)$, $Z_{c\bar{s}}(4900)$, $Z_{c\bar{s}}(5200)$	10
1.14	$Z_b(10610)$, $Z_b(10650)$, $Y(10750)$	10
1.15	$T_{cc}(3875)$	11
1.16	$P_c(4312)$, $P_c(4380)$, $P_c(4440)$, $P_c(4457)$, $P_c(4337)$, $P_{cs}(4338)$, $P_{cs}(4459)$	11
1.17	$d^*(2380)$	12
2	Theoretical foundations	12
2.1	Typical theoretical methods and possible assignments	12
2.1.1	Threshold cusps, Triangle singularities or genuine Resonances	12
2.1.2	Dynamical Generated Resonances and Molecular States	15
2.1.3	$Q\bar{Q}$ states with coupled channel effects	16
2.1.4	Hybrid and Tetraquark states in Born-Oppenheimer approximation	16
2.1.5	Tetraquarks in diquark models	17
2.1.6	Tetraquark states with Lattice QCD	20
2.2	Multiquark states with the QCD sum rules	21
2.3	Are QCD sum rules reliable to study multiquark states	24
2.4	Energy scale dependence of the QCD sum rules	34
3	$\bar{3}3$ type tetraquark states	41
3.1	Hidden-heavy tetraquark states	41
3.1.1	Tetraquark states with positive parity	42
3.1.2	Tetraquark states with the first radial excitations	60
3.1.3	Tetraquark states with negative parity	64
3.1.4	Tetraquark states with an explicit P-wave	74
3.2	Doubly heavy tetraquark states	76
3.3	Fully heavy tetraquark states	82

¹E-mail: zgwang@aliyun.com.

4	11 type tetraquark states	88
4.1	Hidden heavy tetraquark states	89
4.2	Doubly heavy tetraquark states	98
5	Hidden heavy pentaquark states	104
5.1	$\bar{3}\bar{3}\bar{3}$ type pentaquark states	105
5.2	11 type pentaquark states	121
6	Singly-heavy exotic states	128
6.1	Singly-heavy tetraquark states	128
6.2	Singly-heavy pentaquark states	130
7	Strong decays of exotic states	137
7.1	Strong decays of the $Y(4500)$ as an example	140
7.2	Light-cone QCD sum rules for the $Y(4500)$ as an example	151
8	Conclusion and Perspective	157

1 Introduction

In 1964, Gell-Mann suggested that multiquark states beyond the minimal valence quark constituents $q\bar{q}$ and qqq might exist [1], a quantitative model for the tetraquark states with the quark constituents $qq\bar{q}\bar{q}$ was developed by Jaffe using the MIT bag model in 1977 [2, 3]. Later, the five-quark baryons with the quark constituents $qqqq\bar{q}$ were developed [4], while the name pentaquark was introduced by Lipkin [5]. Also in 1964, Dyson and Xuang studied the dibaryon or six-quark states based on the $SU(6)$ symmetry [6], for more literatures on this subject, one can consult Refs.[7, 8]. The QCD allows the existence of multiquark states and hybrid states which contain not only quarks but also gluonic degrees of freedom [9, 10, 11].

Before observation of the $X(3872)$ by the Belle collaboration in 2003 [12], the most promising and most hot subject is the nature of the light mesons below 1 GeV, are they traditional 3P_0 states, tetraquark states or molecular states? [2, 3, 13, 14, 15, 16]. In fact, the observation of the $X(3872)$ stimulates more motivations and curiosities in exploring the nature of the light scalar mesons [17, 18, 19, 20, 21, 22, 23, 24, 25, 26, 27, 28, 29], for more references, see the reviews [30, 31, 32]. However, it is an un-resolved problem until now. There have been several excellent reviews of the exotic states with emphasis on different aspects [33, 34, 35, 36, 37, 38, 39, 40, 41, 42, 43, 44, 45, 46, 47].

Firstly, let us see the experimental data on the exotic states pedagogically and dogmatically in the order X , Y , Z , T and P sequentially, and sort out of the exotic states according to the masses from low to high roughly. In fact, there are relations among those X , Y and Z states in one way or the other, it is impossible to sort out them distinctly, the most related ones are grouped together into one sub-section. Furthermore, we would like to emphasize the assignment based on the QCD sum rules at the end of every sub-section if there exists a room, as the predicted spectroscopy based on the QCD sum rules cannot accommodate all the exotic states. Other possible assignments would be presented in Sects.3, 4, 5 and 6.1.

1.1 $X(3872)$

In 2003, the Belle collaboration observed a narrow charmonium-like state $X(3872)$ with the mass $3872.0 \pm 0.6 \pm 0.5$ MeV near the $D\bar{D}^*$ threshold in the $\pi^+\pi^-J/\psi$ mass spectrum in the exclusive processes $B^\pm \rightarrow K^\pm\pi^+\pi^-J/\psi$ [12]. The evidences for the decay modes $X(3872) \rightarrow \gamma J/\psi, \gamma\psi'$ observed by the Belle and BaBar collaborations imply the positive charge conjugation $C = +$ [48, 49, 50]. Angular correlations between final state particles $\pi^+\pi^-J/\psi$ analyzed by the CDF,

Belle and LHCb collaborations favor the $J^{PC} = 1^{++}$ assignment [51, 52, 53, 54]. It is a possible candidate for the tetraquark state [55, 56, 57, 58, 59, 60, 61, 62], (not) molecular state ([63]) [64, 65, 66, 67, 68, 69, 70, 71, 72, 73, 74, 75, 76, 77, 78, 79, 80, 81, 82, 83, 84], (not) traditional charmonium $\chi_{c1}(2P)$ ([85]) [86, 87, 88], threshold cusp [89], etc. However, none of those available assignment has won an overall consensus, its nature is still under heated debates, the very narrow width and exotic branching fractions make it a hot potato, the door remains open for another binding mechanism. The QCD sum rules allow both the color $\bar{\mathbf{3}}\mathbf{3}$ -type and $\mathbf{11}$ -type tetraquark assignments, see Table 9 in Sect.3.1.1 and Table 44 in Sect.4.1.

1.2 $X(3915)$, $X(3940)$, $Y(3940)$, $Z(3930)$, $X(4160)$, $X(3860)$, $X(3960)$

In 2005, the Belle collaboration observed the $Y(3940)$ in the B -decays $B \rightarrow KY(3940) \rightarrow K\omega J/\psi$ [90], later, the BaBar collaboration confirmed the $Y(3940)$ in the $\omega J/\psi$ mass spectrum with a mass about 3.915 GeV in the decays $B \rightarrow K\omega J/\psi$ [91, 92].

In 2007, the Belle collaboration observed the $X(3940)$ in the process $e^+e^- \rightarrow J/\psi X(3940)$ with the subprocess $X(3940) \rightarrow D^*\bar{D}$ [93]. In 2008, the Belle collaboration confirmed the $X(3940)$ in the same process, and observed the $X(4160)$ in the subprocess $X(4160) \rightarrow D^*\bar{D}^*$ [94].

In 2010, the $X(3915)$ was observed in the process $\gamma\gamma \rightarrow J/\psi\omega$ by the Belle collaboration [95], then the BaBar collaboration determined its quantum numbers $J^P = 0^+$ [96], it is a good candidate for the conventional charmonium $\chi_{c0}(2P)$. The $Y(3940)$ and $X(3915)$ could be the same particle, and is denoted as the $\chi_{c0}(3915)$ with the assignment $J^{PC} = 0^{++}$ in *The Review of Particle Physics* [97].

In 2006, the $Z(3930)$ was observed in the process $\gamma\gamma \rightarrow J/\psi\omega$ by the Belle collaboration [98], then confirmed by the BaBar collaboration in the same process [99], the two collaborations both determined its quantum numbers to be $J^{PC} = 2^{++}$, and it is widely assigned as the $\chi_{c2}(3930)$ [97].

In 2017, the Belle collaboration performed a full amplitude analysis of the process $e^+e^- \rightarrow J/\psi D\bar{D}$, and observed a new charmonium-like state $X^*(3860)$ which decays to the $D\bar{D}$ pair, the measured mass and width are 3862^{+26+40}_{-32-13} MeV and $201^{+154+88}_{-67-82}$ MeV, respectively [100]. The $J^{PC} = 0^{++}$ hypothesis is favored over the 2^{++} hypothesis at the level of 2.5σ , and the Belle collaboration assigned the $X^*(3860)$ as an alternative $\chi_{c0}(2P)$ state [100].

In 2020, the LHCb collaboration performed an amplitude analysis of the $B^+ \rightarrow D^+D^-K^+$ decays and observed that it is necessary to include the $\chi_{c0}(3930)$ and $\chi_{c2}(3930)$ with the $J^{PC} = 0^{++}$ and 2^{++} respectively in the D^+D^- channel, and to include the $X_0(2900)$ and $X_1(2900)$ with the $J^P = 0^+$ and 1^- respectively in the D^-K^+ channel [101, 102]. The measured Breit-Wigner masses and widths are

$$\begin{aligned}\chi_{c0}(3930) &: M = 3923.8 \pm 1.5 \pm 0.4 \text{ MeV}, \quad \Gamma = 17.4 \pm 5.1 \pm 0.8 \text{ MeV}, \\ \chi_{c2}(3930) &: M = 3926.8 \pm 2.4 \pm 0.8 \text{ MeV}, \quad \Gamma = 34.2 \pm 6.6 \pm 1.1 \text{ MeV},\end{aligned}\tag{1}$$

and the $\chi_{c0}(3915)$ and $\chi_{c0}(3930)$ can be identified as the $\chi_{c0}(2P)$.

In 2023, the LHCb collaboration announced the observation of the $X(3960)$ in the $D_s^+D_s^-$ mass spectrum in the $B^+ \rightarrow D_s^+D_s^-K^+$ decays, and the assignment $J^{PC} = 0^{++}$ is favored [103], the measured Breit-Wigner mass and width are $3956 \pm 5 \pm 10$ MeV and $43 \pm 13 \pm 8$ MeV, respectively.

The thresholds of the $D_s^+D_s^-$ and D^+D^- are 3938 MeV and 3739 MeV, respectively, which favors assigning the $X(3960)$ and $\chi_{c0}(3930)$ as the same particle. However, the ratio of the branching fractions [103],

$$\frac{\Gamma(X \rightarrow D^+D^-)}{\Gamma(X \rightarrow D_s^+D_s^-)} = 0.29 \pm 0.09 \pm 0.10 \pm 0.08,\tag{2}$$

implies the exotic nature of this state, as it is harder to excite an $s\bar{s}$ pair from the vacuum compared with the $u\bar{u}$ or $d\bar{d}$ pair, and the traditional charmonium states predominantly decay into the $D\bar{D}$ and $D^*\bar{D}^*$ states rather than into the $D_s\bar{D}_s$ and $D_s^*\bar{D}_s^*$ states. In addition, there is no room for

the $X(3860)$, so, at least one of the $X(3860)$, $X(3915)$, $\chi_{c0}(3930)$ and $X(3960)$ should be exotic state [104, 105, 106, 107].

For example, the updated nonrelativistic potential model (NR) and Godfrey-Isgur relativized potential model (GI) indicate that the 2P charmonium states have the masses (NR; GI)[108],

$$\begin{aligned}\chi_{c2}(2P) &: 3972 \text{ MeV}, 3979 \text{ MeV}, \\ \chi_{c1}(2P) &: 3925 \text{ MeV}, 3953 \text{ MeV}, \\ \chi_{c0}(2P) &: 3852 \text{ MeV}, 3916 \text{ MeV},\end{aligned}\tag{3}$$

even the assignments of the $\chi_{c0}(2P)$ and $\chi_{c2}(2P)$ are not comfortable enough.

We can identify the $X(3915)$, $Y(3940)$ and $\chi_{c0}(3930)$ as the same particle tentatively, and assign it as the color **33**-type scalar tetraquark state based on the QCD sum rules, see Table 9 in Sect.3.1.1, furthermore, there exists a room for the $X(3860)$. On the other hand, we can assign the $X(3960)$ as the color **33**-type or **11**-type tetraquark state, see Table 10 in Sect.3.1.1 and Table 44 in Sect.4.1.

1.3 $\eta_c(3945)$, $h_c(4000)$, $\chi_{c1}(4010)$, $h_c(4300)$

In 2024, the LHCb collaboration explored the decays $B^+ \rightarrow D^{*+}D^-K^+$ and $D^{*-}D^+K^+$, and observed four charmonium(-like) states $\eta_c(3945)$, $h_c(4000)$, $\chi_{c1}(4010)$ and $h_c(4300)$ with the quantum numbers $J^{PC} = 0^{-+}$, 1^{+-} , 1^{++} and 1^{+-} respectively in the $D^{*\pm}D^\mp$ mass spectrum [109]. The measured Breit-Wigner masses and widths are

$$\begin{aligned}\eta_c(3945) &: M = 3945^{+28}_{-17}{}^{+37}_{-28} \text{ MeV}, \Gamma = 130^{+92}_{-49}{}^{+101}_{-70} \text{ MeV}, \\ h_c(4000) &: M = 4000^{+17}_{-14}{}^{+29}_{-22} \text{ MeV}, \Gamma = 184^{+71}_{-45}{}^{+97}_{-61} \text{ MeV}, \\ \chi_{c1}(4010) &: M = 4012.5^{+3.6}_{-3.9}{}^{+4.1}_{-3.7} \text{ MeV}, \Gamma = 62.7^{+7.0}_{-6.4}{}^{+6.4}_{-6.6} \text{ MeV}, \\ h_c(4300) &: M = 4307.3^{+6.4}_{-6.6}{}^{+3.3}_{-4.1} \text{ MeV}, \Gamma = 58^{+28}_{-16}{}^{+28}_{-25} \text{ MeV}.\end{aligned}\tag{4}$$

The updated nonrelativistic potential model (NR) and Godfrey-Isgur relativized potential model (GI) indicate that the 3S/2P/3P charmonium states have the masses (NR; GI) [108],

$$\begin{aligned}\eta_c(3S) &: 4043 \text{ MeV}, 4064 \text{ MeV}, \\ \chi_{c1}(2P) &: 3925 \text{ MeV}, 3953 \text{ MeV}, \\ \chi_{c1}(3P) &: 4271 \text{ MeV}, 4317 \text{ MeV}, \\ h_c(2P) &: 3934 \text{ MeV}, 3956 \text{ MeV}, \\ h_c(3P) &: 4279 \text{ MeV}, 4318 \text{ MeV},\end{aligned}\tag{5}$$

the assignments $\eta_c(3945)$, $h_c(4000)$ and $\chi_{c1}(4010)$ in Ref.[109] are rather marginal.

Based on the predictions of the QCD sum rules, we can assign the $h_c(4000)$ and $\chi_{c1}(4010)$ as the color **33**-type tetraquark states tentatively based on the QCD sum rules, see Table 9 in Sect.3.1.1.

1.4 $X(4140)$, $X(4274)$, $X(4500/4475)$, $X(4700/4710)$, $X(4685/4650)$, $X(4630/4800)$

In 2009, the CDF collaboration observed the $X(4140)$ in the $J/\psi\phi$ mass spectrum in the $B^+ \rightarrow J/\psi\phi K^+$ decays with a significance larger than 3.8σ [110]. In 2011, the CDF collaboration confirmed the $Y(4140)$ in the $B^\pm \rightarrow J/\psi\phi K^\pm$ decays with a significance greater than 5σ , and observed an evidence for the $X(4274)$ with an approximate significance of 3.1σ [111]. In 2013, the CMS collaboration also confirmed the $X(4140)$ in the $B^\pm \rightarrow J/\psi\phi K^\pm$ decays [112].

In 2016, the LHCb collaboration performed the first full amplitude analysis of the $B^+ \rightarrow J/\psi\phi K^+$ decays, confirmed the $X(4140)$ and $X(4274)$ in the $J/\psi\phi$ mass spectrum, and determined

the spin-parity to be $J^P = 1^+$ [113, 114]. Moreover, the LHCb collaboration observed two new particles $X(4500)$ and $X(4700)$ in the $J/\psi\phi$ mass spectrum, and determined the spin-parity to be $J^P = 0^+$ [113, 114]. The measured masses and widths are

$$\begin{aligned} X(4140) : M &= 4146.5 \pm 4.5_{-2.8}^{+4.6} \text{ MeV}, \Gamma = 83 \pm 21_{-14}^{+21} \text{ MeV}, \\ X(4274) : M &= 4273.3 \pm 8.3_{-3.6}^{+17.2} \text{ MeV}, \Gamma = 56 \pm 11_{-11}^{+8} \text{ MeV}, \\ X(4500) : M &= 4506 \pm 11_{-15}^{+12} \text{ MeV}, \Gamma = 92 \pm 21_{-20}^{+21} \text{ MeV}, \\ X(4700) : M &= 4704 \pm 10_{-24}^{+14} \text{ MeV}, \Gamma = 120 \pm 31_{-33}^{+42} \text{ MeV}. \end{aligned} \quad (6)$$

If they are tetraquark states, their quark constituents must be $cs\bar{c}\bar{s}$. The S-wave $J/\psi\phi$ systems have the $J^{PC} = 0^{++}, 1^{++}, 2^{++}$, while the P-wave $J/\psi\phi$ systems have the $J^{PC} = 0^{-+}, 1^{-+}, 2^{-+}, 3^{-+}$. The LHCb's data rule out the 0^{++} or 2^{++} $D_s^{*+}D_s^{*-}$ molecule assignments.

In 2021, the LHCb collaboration performed an improved full amplitude analysis of the exclusive process $B^+ \rightarrow J/\psi\phi K^+$, observed the $X(4685)$ ($X(4630)$) in the $J/\psi\phi$ mass spectrum with the $J^P = 1^+$ (1^-) and Breit-Wigner masses and widths,

$$\begin{aligned} X(4685) : M &= 4684 \pm 7_{-16}^{+13} \text{ MeV}, \Gamma = 126 \pm 15_{-41}^{+37} \text{ MeV}, \\ X(4630) : M &= 4626 \pm 16_{-110}^{+18} \text{ MeV}, \Gamma = 174 \pm 27_{-73}^{+134} \text{ MeV}, \end{aligned} \quad (7)$$

furthermore, they observed the $Z_{cs}(4000)$ and $Z_{cs}(4220)$ with the $J^P = 1^+$ in the $J/\psi K^+$ mass spectrum and confirmed the four old particles [115].

In 2024, the LHCb collaboration performed the first full amplitude analysis of the decays $B^+ \rightarrow \psi(2S)K^+\pi^+\pi^-$, and they developed an amplitude model with 53 components comprising 11 hidden-charm exotic states, for example, the $X(4475)$, $X(4650)$, $X(4710)$ and $X(4800)$ in the $\psi(2S)\rho^0(770)$ mass spectrum with the $J^P = 0^+, 1^+, 0^+$ and 1^- , respectively, while the $X(4800)$ is just an effective description of generic partial wave-function [116].

The $X(4475)$, $X(4650)$, $X(4710)$ and $X(4800)$ have the isospin $(I, I_3) = (1, 0)$, while the $X(4500)$, $X(4685)$, $X(4700)$ and $X(4630)$ have the isospin $(I, I_3) = (0, 0)$ according to the final states $\psi(2S)\rho^0(770)$ and $J/\psi\phi$. A possible explanation is that those states are genuinely different states, if the $X(4475)$ state is the $c\bar{c}(u\bar{u} - d\bar{d})$ isospin partner of the $X(4500)$ interpreted as the $c\bar{c}s\bar{s}$ state, we would generally expect a larger mass difference of $M_{X(4500)} - M_{X(4475)} \approx 200 \text{ MeV}$ rather than several MeV. The un-normal light-flavor $SU(3)$ breaking effects make them difficult to assign in the scenario of tetraquark states.

Based on the predictions of the QCD sum rules, we can assign the $X(4140)$, $X(4274)$, $X(4500)$, $X(4685)$ and $X(4700)$ as the color $\mathbf{\bar{3}3}$ -type tetraquark states with the positive parity tentatively, see Table 10 in Sect.3.1.1, and assign the $X(4630)$ as the color $\mathbf{\bar{3}3}$ -type tetraquark state with the negative parity tentatively, see Table 23 in Sect.3.1.3.

1.5 $X(4350)$

In 2010, the Belle collaboration measured the process $\gamma\gamma \rightarrow \phi J/\psi$ for the $\phi J/\psi$ mass distributions and observed a narrow peak of $8.8_{-3.2}^{+4.2}$ events with a significance of 3.2σ [117]. The mass and width are $(4350.6_{-5.1}^{+4.6} \pm 0.7) \text{ MeV}$ and $(13.3_{-9.1}^{+17.9} \pm 4.1) \text{ MeV}$ respectively. However, the $X(4350)$ is not confirmed by other experiments.

1.6 $X_0(2900)$, $X_1(2900)$, $T_{c\bar{s}}(2900)$

In 2020, the LHCb collaboration reported a narrow peak in the D^-K^+ invariant mass spectrum in the decays $B^\pm \rightarrow D^+D^-K^\pm$ [101, 102]. The peak could be reasonably parameterized in terms of two Breit-Wigner resonances:

$$\begin{aligned} X_0(2900) : J^P &= 0^+, M = 2866 \pm 7 \pm 2 \text{ MeV}, \Gamma = 57 \pm 12 \pm 4 \text{ MeV}, \\ X_1(2900) : J^P &= 1^-, M = 2904 \pm 5 \pm 1 \text{ MeV}, \Gamma = 110 \pm 11 \pm 4 \text{ MeV}. \end{aligned} \quad (8)$$

They are the first exotic hadrons with fully open flavor, the valence quarks are $u\bar{d}\bar{c}\bar{s}$ [101, 102]. The narrow peak can be assigned as the color **33**-type tetraquark state with the $J^P = 0^+$ [118, 119, 120, 121], its radial/orbital excitation [122], non-tetraquark state [123], $D^*\bar{K}^*$ molecular state [121, 124, 125, 126, 127, 128], triangle singularity [129], etc.

In 2023, the LHCb collaboration observed the tetraquark candidates $T_{c\bar{s}}^{0/++}(2900)$ with the spin-parity $J^P = 0^+$ in the processes $B^+ \rightarrow D^- D_s^+ \pi^+$ and $B^0 \rightarrow \bar{D}^0 D_s^+ \pi^-$ with the significance larger than 9σ [130, 131]. The measured Breit-Wigner masses and widths are

$$\begin{aligned} T_{c\bar{s}}^0(2900) &: M = 2.892 \pm 0.014 \pm 0.015 \text{ GeV}, \Gamma = 0.119 \pm 0.026 \pm 0.013 \text{ GeV}, \\ T_{c\bar{s}}^{++}(2900) &: M = 2.921 \pm 0.017 \pm 0.020 \text{ GeV}, \Gamma = 0.137 \pm 0.032 \pm 0.017 \text{ GeV}, \end{aligned} \quad (9)$$

respectively, and they belong to a new type of open-charm tetraquark states with the c and \bar{s} quarks. The $X_0(2900)$, $T_{c\bar{s}}^0(2900)$ and $T_{c\bar{s}}^{++}(2900)$ can be accommodated in the light flavor $SU(3)_F$ symmetry sextet.

We can assign the $X_0(2900)$, $T_{c\bar{s}}^0(2900)$ and $T_{c\bar{s}}^{++}(2900)$ as the color **33**-type tetraquark states with the $J^P = 0^+$ tentatively based on the QCD sum rules, see Sect.6.1.

1.7 $X(5568)$

In 2016, the D0 collaboration observed a narrow structure $X(5568)$ in the decays $X(5568) \rightarrow B_s^0 \pi^\pm$ with significance of 5.1σ [132]. The mass and natural width are $5567.8 \pm 2.9^{+0.9}_{-1.9}$ MeV and $21.9 \pm 6.4^{+5.0}_{-2.5}$ MeV, respectively. The $B_s^0 \pi^\pm$ systems consist of two quarks and two antiquarks of four different flavors, just like the $T_{c\bar{s}}(2900)$ with the $J^P = 0^+$ observed 7 years later in the $D_s^+ \pi^+ / D_s^+ \pi^-$ mass spectrum by the LHCb collaboration [130, 131]. The D0 collaboration fitted the $B_s^0 \pi^\pm$ systems with the S-wave Breit-Wigner parameters, the favored assignments are $J^P = 0^+$, but the assignments $J^P = 1^+$ cannot be excluded according to decays $X(5568) \rightarrow B_s^* \pi^+ \rightarrow B_s^0 \pi^+ \gamma$, where the low-energy photon is not detected. It can be assigned as a $us\bar{b}\bar{d}$ tetraquark state with the $J^{PC} = 0^{++}$ [133, 134, 135, 136, 137], however, the $X(5568)$ is not confirmed by the LHCb, CMS, ATLAS and CDF collaborations [138, 139, 140, 141].

1.8 $X(6600)$, $X(6900)$, $X(7300)$

In 2020, the LHCb collaboration reported evidences of two fully-charm tetraquark candidates in the $J/\psi J/\psi$ mass spectrum [142]. They observed a broad structure above the $J/\psi J/\psi$ threshold ranging from 6.2 to 6.8 GeV and a narrow structure at about 6.9 GeV with the significance of larger than 5σ . In addition, they also observed some vague structures around 7.2 GeV.

In 2023, the ATLAS collaboration observed statistically significant excesses in the $J/\psi J/\psi$ channel, which are consistent with a narrow resonance at about 6.9 GeV and a broader structure at much lower mass. And they also observed a statistically significant excess at about 7.0 GeV in the $J/\psi \psi'$ channel [143].

In 2024, the CMS collaboration observed three resonant structures in the $J/\psi J/\psi$ mass spectrum with the masses 6638^{+43+16}_{-38-31} MeV, 6847^{+44+48}_{-28-20} MeV and 7134^{+48+41}_{-25-15} MeV, respectively [144]. While in the no-interference model, the measured Breit-Wigner masses and widths are [144],

$$\begin{aligned} X(6600) &: M = 6552 \pm 10 \pm 12 \text{ MeV}, \Gamma = 124^{+32}_{-26} \pm 33 \text{ MeV}, \\ X(6900) &: M = 6927 \pm 9 \pm 4 \text{ MeV}, \Gamma = 122^{+24}_{-21} \pm 18 \text{ MeV}, \\ X(7300) &: M = 7287^{+20}_{-18} \pm 5 \text{ MeV}, \Gamma = 95^{+59}_{-40} \pm 19 \text{ MeV}. \end{aligned} \quad (10)$$

The two-meson pairs $J/\psi J/\psi$, $J/\psi \psi'$, $\psi' \psi'$, $h_c h_c$, $\chi_{c0} \chi_{c0}$, $\chi_{c1} \chi_{c1}$ and $\chi_{c2} \chi_{c2}$ lie at 6194 MeV, 6783 MeV, 7372 MeV, 7051 MeV, 6829 MeV, 7021 MeV and 7112 MeV, respectively [97], it is difficult to assign the $X(6600)$, $X(6900)$ and $X(7300)$ as the charmonium-charmonium molecular states without introducing coupled channel effects.

We can assign the $X(6600)$, $X(6900)$ and $X(7300)$ as the color $\bar{\mathbf{33}}$ -type tetraquark states tentatively based on the QCD sum rules, see Table 41 in Sect.3.3.

1.9 $Y(4260/4230)$, $Y(4360/4320)$, $Y(4390)$, $Y(4500)$, $Y(4660)$, $Y(4710/4750/4790)$

In 2005, the BaBar collaboration studied the initial-state radiation process $e^+e^- \rightarrow \gamma_{ISR}\pi^+\pi^-J/\psi$ and observed the $Y(4260)$ in the $\pi^+\pi^-J/\psi$ mass spectrum, the measured mass and width are $(4259 \pm 8_{-6}^{+2})$ MeV and $(88 \pm 23_{-4}^{+6})$ MeV, respectively [145]. Subsequently the $Y(4260)$ was confirmed by the Belle and CLEO collaborations [146, 147], the Belle collaboration also observed an evidence for a very broad structure $Y(4008)$ in the $\pi^+\pi^-J/\psi$ mass spectrum.

In 2007, the Belle collaboration studied the initial-state radiation process $e^+e^- \rightarrow \gamma_{ISR}\pi^+\pi^-\psi'$, and observed the $Y(4360)$ and $Y(4660)$ in the $\pi^+\pi^-\psi'$ mass spectrum at $(4361 \pm 9 \pm 9)$ MeV with a width of $(74 \pm 15 \pm 10)$ MeV and $(4664 \pm 11 \pm 5)$ MeV with a width of $(48 \pm 15 \pm 3)$ MeV, respectively [148, 149], then the $Y(4660)$ was confirmed by the BaBar collaboration [150].

In 2008, the Belle collaboration studied the initial-state radiation process $e^+e^- \rightarrow \gamma_{ISR}\Lambda_c^+\Lambda_c^-$, observed a clear peak $Y(4630)$ in the $\Lambda_c^+\Lambda_c^-$ mass spectrum just above the $\Lambda_c^+\Lambda_c^-$ threshold, and determined the mass and width to be (4634_{-7-8}^{+8+5}) MeV and (92_{-24-21}^{+40+10}) MeV, respectively [151]. Thereafter, the $Y(4660)$ and $Y(4630)$ are taken as the same particle according to the uncertainties of the masses and widths, for example, in *The Review of Particle Physics* [97].

In 2014, the BESIII collaboration searched for the production of $e^+e^- \rightarrow \omega\chi_{cJ}$ with $J = 0, 1, 2$, and observed a resonance in the $\omega\chi_{c0}$ cross section, the measured mass and width are $4230 \pm 8 \pm 6$ MeV and $38 \pm 12 \pm 2$ MeV, respectively [152].

In 2016, the BESIII collaboration measured the cross sections of the process $e^+e^- \rightarrow \pi^+\pi^-h_c$, and observed two structures, the $Y(4220)$ has a mass of $4218.4 \pm 4.0 \pm 0.9$ MeV and a width of $66.0 \pm 9.0 \pm 0.4$ MeV respectively, and the $Y(4390)$ has a mass of $4391.6 \pm 6.3 \pm 1.0$ MeV and a width of $139.5 \pm 16.1 \pm 0.6$ MeV respectively [153].

Also in 2016, the BESIII collaboration precisely measured the cross section of the process $e^+e^- \rightarrow \pi^+\pi^-J/\psi$ and observed two resonant structures, which agree with the $Y(4260)$ and $Y(4360)$, respectively. The first resonance has a mass of $4222.0 \pm 3.1 \pm 1.4$ MeV and a width of $44.1 \pm 4.3 \pm 2.0$ MeV, while the second one has a mass of $4320.0 \pm 10.4 \pm 7.0$ MeV and a width of $101.4_{-19.7}^{+25.3} \pm 10.2$ MeV [154].

In 2022, the BESIII collaboration observed two resonant structures in the K^+K^-J/ψ mass spectrum, one is the $Y(4230)$ and the other is the $Y(4500)$, which was observed for the first time with the Breit-Wigner mass and width $4484.7 \pm 13.3 \pm 24.1$ MeV and $111.1 \pm 30.1 \pm 15.2$ MeV, respectively [155].

In 2023, the BESIII collaboration observed three enhancements in the $D^{*-}D^{*0}\pi^+$ mass spectrum in the Born cross sections of the process $e^+e^- \rightarrow D^{*0}D^{*-}\pi^+$, the first and third resonances are the $Y(4230)$ and $Y(4660)$, respectively, while the second resonance has the Breit-Wigner mass and width $4469.1 \pm 26.2 \pm 3.6$ MeV and $246.3 \pm 36.7 \pm 9.4$ MeV, respectively, and is roughly compatible with the $Y(4500)$ [156].

Also in 2023, the BESIII collaboration observed three resonance structures in the $D_s^{*+}D_s^{*-}$ mass spectrum, the two significant structures are consistent with the $\psi(4160)$ and $\psi(4415)$, respectively, while the third structure is new, and has the Breit-Wigner mass and width 4793.3 ± 7.5 MeV and 27.1 ± 7.0 MeV, respectively, therefore is named as $Y(4790)$ [157].

Also in 2023, the BESIII collaboration observed a new resonance $Y(4710)$ in the K^+K^-J/ψ mass spectrum with a significance over 5σ , the measured Breit-Wigner mass and width are $4708_{-15}^{+17} \pm 21$ MeV and $126_{-23}^{+27} \pm 30$ MeV, respectively [158].

In 2024, the BESIII collaboration measured the Born cross sections for the processes $e^+e^- \rightarrow \omega\chi_{c1}$ and $\omega\chi_{c2}$, and observed the well established $\psi(4415)$ in the $\omega\chi_{c2}$ mass spectrum [159]. In addition, they observed a new resonance in the $\omega\chi_{c1}$ mass spectrum, and measured the mass and width as $4544.2 \pm 18.7 \pm 1.7$ MeV and $116.1 \pm 33.5 \pm 1.7$ MeV, respectively, which are also roughly compatible with the $Y(4500)$.

Also in 2024, the BESIII collaboration studied the processes $e^+e^- \rightarrow \omega X(3872)$ and $\gamma X(3872)$, and observed that the relatively large cross section for the $e^+e^- \rightarrow \omega X(3872)$ process is mainly due to the enhancement about 4.75 GeV, which maybe indicate a potential structure in the $e^+e^- \rightarrow \omega X(3872)$ cross section [160]. If the enhancement is confirmed in the future by enough experimental data, there maybe exist another Y state, the $Y(4750)$.

We should bear in mind, in 2023, the BESIII collaboration studied the process $e^+e^- \rightarrow \Lambda_c^+ \Lambda_c^-$ at twelve center-of-mass energies from 4.6119 to 4.9509 GeV, determined the Born cross sections and effective form-factors with unprecedented precision, and obtained flat cross sections about 4.63 GeV, which does not indicate the resonant structure $Y(4630)$ [161].

The charmonium-like candidates $Y(4260/4230)$, $Y(4360/4320)$, $Y(4390)$, $Y(4500)$, $Y(4660)$ and $Y(4710/4750/4790)$ with the $J^{PC} = 1^{--}$ overwhelm the accommodating capacity of the traditional $c\bar{c}$ model, some of them should be multiquark states.

Based on the predictions of the QCD sum rules, we can assign the $Y(4260/4230)$, $Y(4360/4320)$, $Y(4390)$ and $Y(4750)$ as the color **33**-type tetraquark states with an explicit P-wave between the diquark and antidiquark tentatively, see Table 33 in Sect. **3.1.4**, and assign the $Y(4360)$, $Y(4390)$, $Y(4500)$, $Y(4660)$, $Y(4710)$ and $Y(4790)$ as the color **$\bar{3}3$** -type tetraquark states with an implicit P-wave in the diquark or antidiquark tentatively, see Tables 22-23 in Sect. **3.1.3**.

1.10 $Z_c(3900/3885)$, $Z_c(4020/4025)$, $Z_{cs}(3985/4000)$, $Z_{cs}(4123)$, $Z_{cs}(4220)$

In 2013, the BESIII collaboration studied the process $e^+e^- \rightarrow \pi^+\pi^- J/\psi$ at a center-of-mass energy of 4.260 GeV, and observed a structure $Z_c^\pm(3900)$ in the $\pi^\pm J/\psi$ mass spectrum with a mass of $(3899.0 \pm 3.6 \pm 4.9)$ MeV and a width of $(46 \pm 10 \pm 20)$ MeV [162], at the same time, the Belle collaboration studied the process $e^+e^- \rightarrow \gamma_{ISR} \pi^+\pi^- J/\psi$ using initial-state radiation, and observed a structure $Z_c^\pm(3900)$ in the $\pi^\pm J/\psi$ mass spectrum with a mass of $(3894.5 \pm 6.6 \pm 4.5)$ MeV and a width of $(63 \pm 24 \pm 26)$ MeV [163]. Then this structure was confirmed by the CLEO collaboration [164].

Also in 2013, the BESIII collaboration studied the process $e^+e^- \rightarrow (D^* \bar{D}^*)^\pm \pi^\mp$ at $\sqrt{s} = 4.26$ GeV, and observed a structure $Z_c^\pm(4025)$ near the $(D^* \bar{D}^*)^\pm$ threshold in the π^\mp recoil mass spectrum [165]. The measured mass and width are $(4026.3 \pm 2.6 \pm 3.7)$ MeV and $(24.8 \pm 5.6 \pm 7.7)$ MeV, respectively [165]. Slightly later, the BESIII collaboration studied the process $e^+e^- \rightarrow \pi^+\pi^- h_c$ at \sqrt{s} from 3.90 GeV to 4.42 GeV, and observed a distinct structure $Z_c(4020)$ in the $\pi^\pm h_c$ mass spectrum, the measured mass and width are $(4022.9 \pm 0.8 \pm 2.7)$ MeV and $(7.9 \pm 2.7 \pm 2.6)$ MeV, respectively [166].

In 2014, the BESIII collaboration studied the process $e^+e^- \rightarrow \pi D \bar{D}^*$ at $\sqrt{s} = 4.26$ GeV, and observed a distinct charged structure $Z_c(3885)$ in the $(D \bar{D}^*)^\pm$ mass spectrum [167]. The measured mass and width are $(3883.9 \pm 1.5 \pm 4.2)$ MeV and $(24.8 \pm 3.3 \pm 11.0)$ MeV, respectively, and the angular distribution of the $\pi Z_c(3885)$ system favors the assignment $J^P = 1^+$ [167].

We tentatively identify the $Z_c(3900)$ and $Z_c(3885)$ as the same particle according to the uncertainties of the masses and widths [60]. In 2017, the BESIII collaboration established the spin-parity of the $Z_c(3900)$ to be $J^P = 1^+$ [168].

In 2021, the BESIII collaboration observed an excess near the $D_s^- D^{*0}$ and $D_s^{*-} D^0$ thresholds in the K^+ recoil-mass spectrum with the significance of 5.3σ in the processes $e^+e^- \rightarrow K^+(D_s^- D^{*0} + D_s^{*-} D^0)$ [169]. The Breit-Wigner mass and width of the new structure $Z_{cs}(3985)$ were measured as $3985.2_{-2.0}^{+2.1} \pm 1.7$ MeV and $13.8_{-5.2}^{+8.1} \pm 4.9$ MeV, respectively.

The $Z_c(3885)$ and $Z_{cs}(3985)$ have similar production modes,

$$\begin{aligned} e^+e^- &\rightarrow Z_c^-(3885) \pi^+ \rightarrow (D \bar{D}^*)^- \pi^+, \\ e^+e^- &\rightarrow Z_{cs}^-(3985) K^+ \rightarrow (D_s^- D^{*0} + D_s^{*-} D^0) K^+, \end{aligned} \quad (11)$$

and they should be cousins and have similar properties.

Also in 2021, the LHCb collaboration reported two new exotic states with the valence quarks $c\bar{c}u\bar{s}$ in the $J/\psi K^+$ mass spectrum in the decays $B^+ \rightarrow J/\psi \phi K^+$ [115]. The most significant

state $Z_{cs}^+(4000)$ has a mass of $4003 \pm 6_{-14}^{+4}$ MeV, a width of $131 \pm 15 \pm 26$ MeV, and the spin-parity $J^P = 1^+$, while the broader state $Z_{cs}^+(4220)$ has a mass of $4216 \pm 24_{-30}^{+43}$ MeV, a width of $233 \pm 52_{-73}^{+97}$ MeV, and the spin-parity $J^P = 1^+$ or 1^- (with a 2σ difference in favor of the first hypothesis) [115]. Considering the large difference between the widths, the $Z_{cs}(3985)$ and $Z_{cs}(4000)$ are unlikely to be the same particle.

In 2023, the BESIII collaboration reported an excess of the $Z_{cs}^-(4123) \rightarrow D_s^{*-} D^{*0}$ candidate at a mass of $(4123.5 \pm 0.7 \pm 4.7)$ MeV with a significance of 2.1σ in the process $e^+e^- \rightarrow K^+ D_s^{*-} D^{*0} + c.c.$ [170]. The $Z_{cs}^-(4123)$ is consistent with the tetraquark state with the valence quarks $c\bar{c}s\bar{u}$, spin-parity-charge-conjugation $J^{PC} = 1^{+-}$, a mass 4.11 ± 0.08 GeV and a width 22.71 ± 1.65 MeV predicted in previous work based on the QCD sum rules [171].

The charmonium-like states $Z_c(3900/3885)$, $Z_c(4020/4025)$, $Z_{cs}(3985/4000)$, $Z_{cs}(4123)$ and $Z_{cs}(4220)$ have non-zero electric charge, and are excellent candidates for the tetraquark (molecular) states [171, 172].

Based on the predictions of the QCD sum rules, we can assign the $Z_c(3900/3885)$, $Z_c(4020)$, $Z_{cs}(3985/4000)$ and $Z_{cs}(4123)$ as the color $\mathbf{\bar{3}3}$ -type tetraquark states, see Table 9 and Table 11 in Sect. 3.1.1, or $\mathbf{11}$ -type tetraquark states, see Table 44 in Sect. 4.1.

1.11 $Z_1(4050)$, $Z_1(4250)$, $Z_c(4100)$

In 2008, the Belle collaboration reported the first observation of two resonance-like structures $Z_1^+(4050)$ and $Z_2^+(4250)$ exceeding 5σ in the $\pi^+\chi_{c1}$ mass spectrum near 4.1 GeV in the exclusive decays $\bar{B}^0 \rightarrow K^-\pi^+\chi_{c1}$ [173]. The Breit-Wigner masses and widths are $M_1 = 4051 \pm 14_{-41}^{+20}$ MeV, $\Gamma_1 = 82_{-17-22}^{+21+47}$ MeV, $M_2 = 4248_{-29-35}^{+44+180}$ MeV and $\Gamma_2 = 177_{-39-61}^{+54+316}$ MeV, respectively. However, the BaBar collaboration observed no evidence for the $Z_1^+(4050)$ and $Z_2^+(4250)$ states in the $\pi^+\chi_{c1}$ mass spectrum in the exclusive decays $\bar{B}^0 \rightarrow \pi^+\chi_{c1}K^-$ and $B^+ \rightarrow \pi^+\chi_{c1}K_S^0$ [174].

In 2018, the LHCb collaboration observed an evidence for the $\eta_c\pi^-$ resonant structure $Z_c(4100)$ with the significance larger than 3σ in a Dalitz plot analysis of the $B^0 \rightarrow \eta_c K^+\pi^-$ decays, the measured mass and width are $4096 \pm 20_{-22}^{+18}$ MeV and $152 \pm 58_{-35}^{+60}$ MeV respectively [175]. The assignments $J^P = 0^+$ and 1^- are both consistent with the experimental data. However, the $Z_c(4100)$ is not confirmed by other experiments until now.

1.12 $Z_c(4430)$, $Z_c(4600)$

In 2007, the Belle collaboration observed a distinct peak in the $\pi^\pm\psi'$ mass spectrum in the decays $B \rightarrow K\pi^\pm\psi'$, the mass and width are $(4433 \pm 4 \pm 2)$ MeV and (45_{-13-13}^{+18+30}) MeV, respectively [176]. In 2009, the Belle collaboration observed a signal for the decay $Z(4430)^+ \rightarrow \pi^+\psi'$ from a Dalitz plot analysis of the decays $B \rightarrow K\pi^+\psi'$ [177]. In 2013, the Belle collaboration performed a full amplitude analysis of the decays $B^0 \rightarrow \psi' K^+\pi^-$ to reach the favored assignments $J^P = 1^+$ [178].

In 2014, the LHCb collaboration analyzed the $B^0 \rightarrow \psi'\pi^-K^+$ decays by performing a four-dimensional fit of the amplitude, and provided the first independent confirmation of the $Z^-(4430)$ resonance and established its spin-parity $J^P = 1^+$. The measured Breit-Wigner mass and width are $(4475 \pm 7_{-25}^{+15})$ MeV and $(172 \pm 13_{-34}^{+37})$ MeV, respectively [179], which excludes the possibility of assigning the $Z_c(4430)$ as the D^*D_1 molecular state with the spin-parity $J^P = 0^-$ [180], although it lies near the D^*D_1 threshold.

The Okubo-Zweig-Iizuka-suppressed decays

$$\begin{aligned} Z_c(3900) &\rightarrow J/\psi\pi, \\ Z_c'(4430) &\rightarrow \psi'\pi \end{aligned} \quad (12)$$

are expected to take place easily, and the energy gaps have the relation $M_{Z_c'} - M_{Z_c} = m_{\psi'} - m_{J/\psi}$, the $Z_c(4430)$ can be assigned as the first radial excitation of the $Z_c(3900)$ [56, 181, 182], which was proposed before the J^P of the $Z_c(3900)$ were determined by the BESIII collaboration [168].

In 2019, the LHCb collaboration performed an angular analysis of the weak decays $B^0 \rightarrow J/\psi K^+ \pi^-$, examined the $m(J/\psi \pi^-)$ versus the $m(K^+ \pi^-)$ plane, and observed two possible resonant structures in the vicinity of the energies $m(J/\psi \pi^-) = 4200$ MeV and 4600 MeV, respectively [183], the structure $Z_c(4600)$ has not been confirmed by other experiments yet. According to the mass gaps $M_{Z_c(4600)} - M_{Z_c(4020)} \approx M_{Z_c(4430)} - M_{Z_c(3900)}$, we can tentatively assign the $Z_c(4600)$ as the first radial excitation of the $Z_c(4020)$ [184, 185].

Based on the predictions of the QCD sum rules, we can assign the $Z_c(4430)$ and $Z_c(4600)$ as the first radial excitations of the color $\mathbf{\bar{3}3}$ -type tetraquark states, see Table 9 in Sect.3.1.1 and Table 17 in Sect.3.1.2.

1.13 $Z_c(4200)$, $Z_{\bar{c}s}(4600)$, $Z_{\bar{c}s}(4900)$, $Z_{\bar{c}s}(5200)$

In 2014, the Belle collaboration analyzed the decays $\bar{B}^0 \rightarrow K^- \pi^+ J/\psi$ and observed a resonance $Z_c(4200)$ in the $J/\psi \pi^+$ mass spectrum with a statistical significance more than 6.2σ , the measured mass and width are 4196^{+31+17}_{-29-13} MeV and $370^{+70+70}_{-70-132}$ MeV, respectively, the preferred assignment is $J^P = 1^+$ [186].

In 2019, the LHCb collaboration performed an angular analysis of the decays $B^0 \rightarrow J/\psi K^+ \pi^-$, examined the $m(J/\psi \pi^-)$ versus the $m(K^+ \pi^-)$ plane, and observed two structures in the vicinity of the energies $m(J/\psi \pi^-) = 4200$ MeV and 4600 MeV, respectively [183].

In 2024, the LHCb collaboration performed the first full amplitude analysis of the decays $B^+ \rightarrow \psi(2S) K^+ \pi^+ \pi^-$, and they developed an amplitude model with 53 components comprising 11 hidden-charm exotic states, for example, the $Z_c(4200)$ and $Z_c(4430)$ in the $\psi(2S) \pi^+$ mass spectrum with the $J^P = 1^+$; the $Z_{\bar{c}s}(4600)$ and $Z_{\bar{c}s}(4900)$ in the $\psi(2S) K^*(892)$ mass spectrum with the $J^P = 1^+$, which might be the radial excitations of the $Z_{\bar{c}s}(4000)$ in the scenario of tetraquark states with the valence quarks $c\bar{c}d\bar{s}$; the $Z_{\bar{c}s}(4000)$, $Z_c(4055)$ and $Z_{\bar{c}s}(5200)$ are effective descriptions of generic partial wave-functions with the $J^P = 1^+$, 1^- and 1^- , respectively [116]. The spin-parity of the $Z_c(4200)$ is determined to be 1^+ for the first time with a significance exceeding 5σ .

We group the $Z_c(4200)$ with the $Z_{\bar{c}s}(4600)$, $Z_{\bar{c}s}(4900)$ and $Z_{\bar{c}s}(5200)$ together into one-subsection as its assignment is still an open problem, and we would like to revisit this subject to discuss the possible assignment based on the QCD sum rules in Sect.3.1.

1.14 $Z_b(10610)$, $Z_b(10650)$, $Y(10750)$

In 2011, the Belle collaboration reported the first observation of the $Z_b(10610)$ and $Z_b(10650)$ in the $\pi^\pm \Upsilon(1, 2, 3S)$ and $\pi^\pm h_b(1, 2P)$ mass spectra associated with a single charged pion in the $\Upsilon(5S)$ decays, the quantum numbers $I^G(J^P) = 1^+(1^+)$ are favored [187]. Subsequently, the Belle collaboration updated the measured parameters $M_{Z_b(10610)} = (10607.2 \pm 2.0)$ MeV, $M_{Z_b(10650)} = (10652.2 \pm 1.5)$ MeV, $\Gamma_{Z_b(10610)} = (18.4 \pm 2.4)$ MeV and $\Gamma_{Z_b(10650)} = (11.5 \pm 2.2)$ MeV, respectively [188]. In 2013, the Belle collaboration observed the $\Upsilon(5S) \rightarrow \Upsilon(1, 2, 3S) \pi^0 \pi^0$ decays for the first time, and obtained the neutral $Z_b^0(10610)$ in a Dalitz analysis of the decays to the final states $\Upsilon(2, 3S) \pi^0$ [189].

In 2019, the Belle collaboration observed a resonance structure $Y(10750)$ in the $e^+ e^- \rightarrow \Upsilon(nS) \pi^+ \pi^-$ ($n = 1, 2, 3$) cross sections [190]. The Breit-Wigner mass and width are $10752.7 \pm 5.9^{+0.7}_{-1.1}$ MeV and $35.5^{+17.6+3.9}_{-11.3-3.3}$ MeV, respectively. The $Y(10750)$ is observed in the $\Upsilon(nS) \pi^+ \pi^-$ mass spectrum with $n = 1, 2, 3$, its quantum numbers are $J^{PC} = 1^{--}$.

The Belle II collaboration confirmed the $Y(10750)$ in the processes $e^+ e^- \rightarrow \omega \chi_{b1}(1P)$, $\omega \chi_{b2}(1P)$ [191], $\pi^+ \pi^- \Upsilon(1S)$, $\pi^+ \pi^- \Upsilon(2S)$ [192], and observed no evidence in the processes $e^+ e^- \rightarrow \omega \eta_b(1S)$, $\omega \chi_{b0}(1P)$ [193], $\pi^+ \pi^- \Upsilon(3S)$ [192].

Based on the predictions of the QCD sum rules, we can assign the $Z_b(10610)$ and $Z_b(10650)$ as the color $\mathbf{\bar{3}3}$ -type or $\mathbf{11}$ -type tetraquark states tentatively, see Sect.3.1.1 and Sect.4.1, and assign

the $Y(10750)$ as the color $\bar{\mathbf{33}}$ -type tetraquark state with an explicit P-wave between the diquark and antiquark tentatively, see Sect. **3.1.4**.

1.15 $T_{cc}(3875)$

In 2021, the LHCb collaboration formally announced observation of the exotic state $T_{cc}^+(3875)$ just below the $D^0 D^{*+}$ threshold [194, 195]. The Breit-Wigner mass and width are $\delta M_{BW} = -273 \pm 61 \pm 5_{-14}^{+11}$ KeV below the $D^0 D^{*+}$ threshold and $\Gamma_{BW} = 410 \pm 165 \pm 43_{-38}^{+18}$ KeV [194, 195]. The exotic state $T_{cc}^+(3875)$ is consistent with the ground isoscalar tetraquark state with the valence quarks $cc\bar{u}\bar{d}$ and spin-parity $J^P = 1^+$, and exploring the DD mass spectrum disfavors interpreting the $T_{cc}^+(3875)$ as an isovector state. The observation of the $T_{cc}^+(3875)$ is a great breakthrough beyond the Ξ_{cc}^{++} for hadron physics, and it is the first doubly-charmed tetraquark candidate with the typical quark configuration $cc\bar{u}\bar{d}$.

Based on the predictions of the QCD sum rules, we can assign the $T_{cc}(3875)$ as the color $\bar{\mathbf{33}}$ -type or $\mathbf{11}$ -type tetraquark state tentatively based on the QCD sum rules, see Sect. **3.2** and Sect. **4.2**.

1.16 $P_c(4312)$, $P_c(4380)$, $P_c(4440)$, $P_c(4457)$, $P_c(4337)$, $P_{cs}(4338)$, $P_{cs}(4459)$

In 2015, the LHCb collaboration observed two exotic structures $P_c(4380)$ and $P_c(4450)$ in the $J/\psi p$ mass spectrum in the $\Lambda_b^0 \rightarrow J/\psi K^- p$ decays [196]. The $P_c(4380)$ has a mass of $4380 \pm 8 \pm 29$ MeV and a width of $205 \pm 18 \pm 86$ MeV, while the $P_c(4450)$ has a mass of $4449.8 \pm 1.7 \pm 2.5$ MeV and a width of $39 \pm 5 \pm 19$ MeV. The preferred spin-parity assignments of the $P_c(4380)$ and $P_c(4450)$ are $J^P = \frac{3}{2}^-$ and $\frac{5}{2}^+$, respectively [196].

In 2019, the LHCb collaboration studied the $\Lambda_b^0 \rightarrow J/\psi K^- p$ decays with a data sample, which is an order of magnitude larger than that previously analyzed, and observed a narrow pentaquark candidate $P_c(4312)$ in the $J/\psi p$ mass spectrum. Furthermore, the LHCb collaboration confirmed the pentaquark structure $P_c(4450)$, and observed that it consists of two narrow overlapping peaks $P_c(4440)$ and $P_c(4457)$ [197]. The measured masses and widths are

$$\begin{aligned} P_c(4312) : M &= 4311.9 \pm 0.7_{-0.6}^{+6.8} \text{ MeV}, \Gamma = 9.8 \pm 2.7_{-4.5}^{+3.7} \text{ MeV}, \\ P_c(4440) : M &= 4440.3 \pm 1.3_{-4.7}^{+4.1} \text{ MeV}, \Gamma = 20.6 \pm 4.9_{-10.1}^{+8.7} \text{ MeV}, \\ P_c(4457) : M &= 4457.3 \pm 0.6_{-1.7}^{+4.1} \text{ MeV}, \Gamma = 6.4 \pm 2.0_{-1.9}^{+5.7} \text{ MeV}. \end{aligned} \quad (13)$$

In 2021, the LHCb collaboration reported an evidence of a hidden-charm pentaquark candidate $P_{cs}(4459)$ with the strangeness $S = -1$ in the $J/\psi \Lambda$ mass spectrum with a significance of 3.1σ in the $\Xi_b^- \rightarrow J/\psi K^- \Lambda$ decays [198], the Breit-Wigner mass and width are

$$P_{cs}(4459) : M = 4458.8 \pm 2.9_{-1.1}^{+4.7} \text{ MeV}, \Gamma = 17.3 \pm 6.5_{-5.7}^{+8.0} \text{ MeV}, \quad (14)$$

and the spin-parity have not been determined yet up to now.

In 2022, the LHCb collaboration observed an evidence for a structure $P_c(4337)$ in the $J/\psi p$ and $J/\psi \bar{p}$ systems in the $B_s^0 \rightarrow J/\psi p \bar{p}$ decays with a significance about $3.1 - 3.7\sigma$ depending on the J^P hypothesis [199], the Breit-Wigner mass and width are

$$P_c(4337) : M = 4337_{-4-2}^{+7+2} \text{ MeV}, \Gamma = 29_{-12-14}^{+26+14} \text{ MeV}. \quad (15)$$

Its existence is still need confirmation and its spin-parity are not measured yet.

In 2023, the LHCb collaboration observed an evidence for a new structure $P_{cs}(4338)$ in the $J/\psi \Lambda$ mass distribution in the $B^- \rightarrow J/\psi \Lambda \bar{p}$ decays [200], the measured Breit-Wigner mass and width are

$$P_{cs}(4338) : M = 4338.2 \pm 0.7 \pm 0.4 \text{ MeV}, \Gamma = 7.0 \pm 1.2 \pm 1.3 \text{ MeV}, \quad (16)$$

and the favored spin-parity is $J^P = \frac{1}{2}^-$.

The $P_{cs}(4338)$ and $P_{cs}(4459)$ are observed in the $J/\psi\Lambda$ mass spectrum, they have the isospin $I = 0$, as the strong decays conserve isospin. The $P_c(4312)$, $P_c(4380)$, $P_c(4440)$, $P_c(4457)$, $P_{cs}(4459)$ and $P_{cs}(4338)$ lie slightly below or above the thresholds of the charmed meson-baryon pairs $\bar{D}\Sigma_c$, $\bar{D}\Sigma_c^*$, $\bar{D}^*\Sigma_c$, $\bar{D}^*\Sigma_c'$, $\bar{D}\Xi_c'$ ($\bar{D}\Xi_c^*$, $\bar{D}^*\Xi_c$, $\bar{D}^*\Xi_c'$) and $\bar{D}\Xi_c$, respectively. It is difficult to identify the $P_c(4337)$ as the molecular state without resorting to the help of large coupled-channel effects due to lacking nearby meson-baryon thresholds. Or the $P_c(4312)$ and $P_c(4337)$ are the same particle, such a possibility cannot be excluded at the present time.

Based on the predictions of the QCD sum rules, we can assign the $P_c(4312)$, $P_c(4337)$, $P_c(4380)$, $P_c(4440)$, $P_c(4457)$ and $P_{cs}(4459)$ as the color **333**-type pentaquark states tentatively, see Table 50 and Table 52 in Sect.5.1, and assign the $P_c(4312)$, $P_c(4380)$, $P_c(4440)$, $P_c(4457)$, $P_{cs}(4338)$ and $P_{cs}(4459)$ as the color **11**-type pentaquark states, see Table 54 in Sect.5.2.

1.17 $d^*(2380)$

In 2014, the scientists in the WASA-at-COSY collaboration and SAID data analysis center performed exclusive and kinematically complete high-statistics measurements of the polarized $\vec{n}p$ scattering through the quasifree process $\vec{d}p \rightarrow np + p_{\text{spectator}}$ in the energy region of the narrow resonance-like structure d^* with the $I(J^P) = 0(3^+)$, and confirmed their (WASA-at-COSY collaboration) early observation of the $d^*(2380)$ in the double-pionic fusion channels, they produced a resonance pole in the ${}^3D_3 - {}^3G_3$ coupled partial waves at $2380 \pm 10 - i40 \pm 5$ MeV [201, 202], — in accordance with the $\Delta\Delta$ dibaryon resonance [203, 204, 205, 206, 207]. And we will revisit this subject at the end of Sect.4.2.

2 Theoretical foundations

In this section, we would like to review the typical theoretical methods and related possible assignments concisely, then focus on the QCD sum rules in the subsequent sub-sections, see Sects.2.2, 2.3 and 2.4.

2.1 Typical theoretical methods and possible assignments

There have been tremendous progresses on the hadron spectrum containing two heavy quarks experimentally since the observation of the $X(3872)$. It is surprising that many resonant structures lie around thresholds of a pair of heavy hadrons. A natural conjecture is that they are possible deuteron-like two-particle bound states bound via attractive interactions induced by one-pion exchange or one-boson exchange [63, 65, 67, 72, 76, 208, 209, 210, 211, 212, 213, 214, 215], it is only a possibility. In the heavy quark limit, the $Q_3\bar{q}_3$ mesons and $Q_3[qq]_3$ baryons have the antiquark-diquark symmetry, $\bar{q}_3 \leftrightarrow [qq]_3$, therefore the $Q\bar{q}q'\bar{Q}$ and $Q[qq]q'\bar{Q}$ systems could be analyzed in the same theoretical scheme, in this sub-section, we would like to focus on the tetraquark systems. Someone maybe wonder: are they threshold cusps, triangle singularities or genuine resonances? As there always exist threshold cusps at the S-wave thresholds or triangle singularities near the thresholds. Firstly, let us see the outcomes based on the (non)relativistic effective field theory.

2.1.1 Threshold cusps, Triangle singularities or genuine Resonances

Not all peaks in the invariant mass distributions are genuine resonances, they often arise due to the nearby kinematical singularities of the transition amplitudes in the complex energy plane. Those singularities (or Landau singularities) occur when the intermediate particles are on the mass-shell. The simplest case is the cusp at the normal two-body threshold, there always exists a cusp at the S-wave threshold of two particles coupling to the final states, while a more complicated case is the so-called triangle singularity. They maybe produce observable effects if the involved interactions are

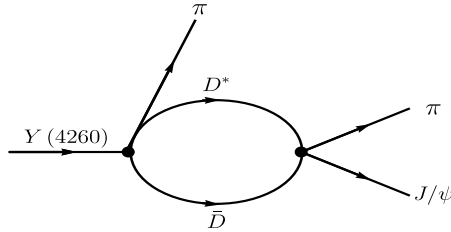


Figure 1: A Feynman diagram for the decay $Y(4260) \rightarrow J/\psi \pi^+ \pi^-$ maybe lead to threshold cusp.

strong enough, sometimes, even mimic the behavior of a resonance. It is important to distinguish kinematic singularities from genuine resonances. We would like to give an example concerning the exotic states $Y(4260)$ and $Z_c(3900)$ to illustrate their possible assignments in the scenarios of threshold cusps, triangle singularities and genuine resonances.

The threshold cusp is determined by masses of the involved particles, how strong the cusp depends on detailed dynamics and the cusp could be rather dramatic if there is a nearby pole, thus it plays an important role in studying the exotic states [216]. For example, the $X(3872)$, $Z_c(3900)$, $Z_c(4020)$, $Z_b(10610)$ and $Z_b(10650)$ lie near the $D^0 \bar{D}^{*0}$, $D \bar{D}^*$, $D^* \bar{D}^*$, $B \bar{B}^*$ and $B^* \bar{B}^*$ thresholds, respectively, their quantum numbers are the same as the corresponding S-wave meson pairs although the J^{PC} of the $Z_c(4020)$ have not been fully determined yet [97].

The $X(3872)$ was assigned to be a threshold cusp by Bugg [89], subsequently, he realized that the very narrow line shapes in the $J/\psi \rho$ and $D^0 \bar{D}^{*0}$ channels could not be fitted with only a threshold cusp, and a resonance or virtual state pole was necessary [217].

In a modified threshold cusp model [218, 219], see the Feynman diagram shown in Fig.1 as an example, both the inelastic ($J/\psi \pi$, $h_c \pi$) and elastic ($D \bar{D}^*$, $D^* \bar{D}^*$) decay modes were considered for the $Z_c(3900)$ and $Z_c(4020)$, analogous discussions are applied to the $Z_b(10610)$ and $Z_b(10650)$. A Gaussian form-factor was chosen for all the vertices including the tree-level ones. Then the experimental data for the $J/\psi \pi$ and $D \bar{D}^*$ mass spectra for the $Z_c(3900)$ and the $D^* \bar{D}^*$ and $h_c \pi$ mass spectra for the $Z_c(4020)$ could be fitted very good, exotic resonances are not required to account for the experimental data. However, the fitting quality depends crucially on the cutoff parameter in the Gaussian form-factor.

The triangle singularity is determined by the masses of the intermediate particles plus the invariant masses of the external ones, therefore the triangle singularities are sensitive to the kinematic variables, the peak position and peak shape change according to the variations of the external energies. More precisely, the triangle singularities are determined by the scalar triangle loop integral, which does not depend on the orbital angular momentum for each vertex, however, sharp triangle singularity peaks are constrained to the S-wave internal particles, as momentum power factor weakens the singular behavior in other cases [216].

In the initial single-pion emission (ISPE) mechanism, the triangle diagrams contribute to threshold cusps, see Fig.2 for a typical Feynman diagram. This mechanism was suggested firstly to study the exotic structures $Z_b(10610)$ and $Z_b(10650)$, Chen and Liu introduced a dipole form-factor to accompany the exchanged B -meson propagator and took account of the $B \bar{B}$, $B \bar{B}^*$, $B^* \bar{B}$ and $B^* \bar{B}^*$ triangle loop diagrams, and produced sharp cusps right around the $Z_b(10610)$ and $Z_b(10650)$ structures in the $\Upsilon(1S, 2S, 3S) \pi$ and $h_b(1P, 2P) \pi$ mass spectra, but observed no cusp at the $B \bar{B}$ threshold [220]. Similarly, Chen, Liu and Matsuki took account of the $D \bar{D}$, $D \bar{D}^*$, $D^* \bar{D}$ and $D^* \bar{D}^*$ triangle loop diagrams and the intermediate $f_0(600)$ and $f_0(980)$ to study the decays $Y(4260) \rightarrow J/\psi \pi \pi$, and observed two peaks, the $Z_c(3900)$ and its reflection [221]. And they studied other processes with possible triangle singularities [222].

In Ref.[223], Dong, Guo and Zou show that the threshold cusp appears as a peak only for

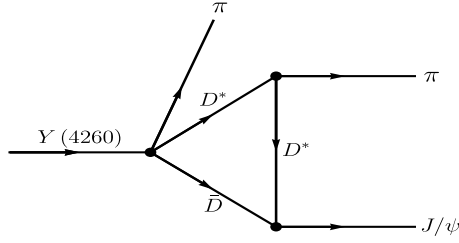


Figure 2: A Feynman diagram for the decay $Y(4260) \rightarrow J/\psi \pi^+ \pi^-$ in the ISPE mechanism.

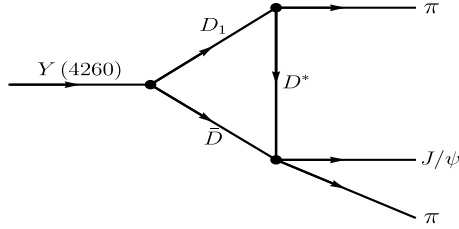


Figure 3: The Feynman diagram for the decays $Y(4260) \rightarrow J/\psi \pi^+ \pi^-$ in the molecule scenario with re-scattering mechanism.

channels with attractive interaction, and the cusp's width is inversely proportional to the reduced mass for the relevant threshold. There should be threshold structures at any threshold of a $q\bar{Q}$ and $Q\bar{q}$ (Qqq) pair, which have attractive interaction at threshold, in the invariant mass distribution of a $Q\bar{Q}$ state and a $q\bar{q}$ (qqq) state coupling to the $q\bar{Q}$ and $Q\bar{q}$ (Qqq) pair, and the structure becomes more pronounced if there is a near-threshold pole.

In Ref.[224], Liu and Li suppose the $Y(4260)$ as a $D_1\bar{D}$ molecular state to study its decays, see Fig.3 as an example, and observe that under special kinematic configurations, the triangle singularity maybe occur in the re-scattering amplitude, which can change the threshold behavior significantly. Obvious threshold enhancements or narrow cusp structures appear quite naturally without introducing a genuine resonance, but cannot exclude existence of a genuine resonance, such a mechanism also works for the pentaquark structures [225, 226].

If the $Y(4260)$ have a large $D_1\bar{D}$ molecular component, the decays $Y(4260) \rightarrow J/\psi \pi^+ \pi^-$ can occur through the re-scattering process [227, 228, 229], see Fig.3. The singularity regions provide an ideal environment for forming bound states or resonances. Although the $Y(4260)$ lies slightly below the $D_1(2420)\bar{D}$ threshold, the triangle singularity in the $J/\psi \pi^\pm$ invariant mass distribution of the re-scattering amplitude is still near the physical boundary and can influence the $J/\psi \pi^\pm$ invariant mass distribution around the $D^*\bar{D}$ threshold significantly [227]. Despite the importance of the triangle diagram contribution, it is insisted that a $Z_c(3900)$ resonance was still needed in order to fit to the narrow peak observed in experiments [224, 227, 230, 231]. The diagrams similar to Fig.3 also play an important role in the hidden-bottom sector [232, 233].

The resonance pole can be incorporated by constructing a unitarized coupled-channel scattering T -matrix by fitting to the experimental data, the best fit still demands the T -matrix to have a resonant or virtual pole near the $D\bar{D}^*$ threshold, which can be interpreted as the $Z_c(3900)$ [234]. The molecule assignment provides a natural explanation for the resonance-like structure $Z_c(3900)$ in the $Y(4260)$ decays [229, 234], the kinematical threshold cusp cannot produce a narrow peak

in the invariant mass distribution in the elastic channel in contrast with a genuine S-matrix pole [235].

In a similar scenario, Szczepaniak suggests that the $Z_c(3900)$ peak could be attributed to the $D_0^*(2300)\bar{D}^*D$ loop instead of the $D_1(2420)\bar{D}D^*$ loop, which is in the physical region by neglecting the width of the $D_0^*(2300)$ [236]. The triangle singularities can produce enhancement potentially in the amplitude consistent with the experimental data qualitatively.

In Ref.[237], Chen, Du and Guo perform a unified description of the $\pi^+\pi^-$ and $J/\psi\pi^\pm$ mass distributions for the $e^+e^- \rightarrow J/\psi\pi^+\pi^-$ and the D^0D^{*-} mass distribution for the $e^+e^- \rightarrow D^0D^{*-}\pi^+$ at $\sqrt{s} = 4.23$ and 4.26 GeV. They take account of the open-charm meson loops containing triangle singularities, the $J/\psi\pi-D\bar{D}^*$ coupled-channel interaction respecting unitarity, and the strong $\pi\pi-K\bar{K}$ final-state interaction using dispersion relations, which lead to a precise determination of the pole mass and width ($3880.7 \pm 1.7 \pm 22.4$) MeV and ($35.9 \pm 1.4 \pm 15.3$) MeV, respectively, and indicate the molecular and non-molecular components are of similar importance for the structure $Z_c(3900)$.

Precisely measuring the near threshold structures plays an important role in diagnosing the heavy-hadron interactions, therefore understanding the puzzling hidden-charm and hidden-bottom structures. Furthermore, it is important to search for the resonant structures in processes free of triangle singularities, such as the photo-production and pion-induced production processes in the e^+e^- and pp collisions [238, 239, 240]. For a recent review on the production of the exotic hadrons in the pp and nuclear collisions, see Ref.[241].

2.1.2 Dynamical Generated Resonances and Molecular States

If we take the traditional heavy mesons as the elementary degrees of freedom, then we construct the heavy meson effective Lagrangian according to the chiral symmetry, hidden-local symmetry and heavy quark symmetry [242, 243, 244]. It is easy to obtain the two-meson scattering amplitudes V . Then we have three choices:

Firstly, we unitarize the amplitudes by taking account of the intermediate two-meson loops with the coupled channel effects through the Bethe-Salpeter or Lippmann-Schwinger equation with on-shell factorization [245, 246],

$$\begin{aligned} T &= V + VGV + VGVGV + \cdots, \\ &= [1 - VG]^{-1} V, \end{aligned} \quad (17)$$

where the G is the loop function, see Fig.4 for a diagrammatical representation. Then we explore the analytical properties of the full amplitudes T , and try to find the poles in the complex Riemann sheets, such as the bound states, virtual states and resonances. Such discussions are applied to the baryon-meson systems directly.

Bound states appear as poles on the physical sheet, and only appear on the real s -axis below the lowest threshold by causality. Virtual states also appear on the real s -axis, however, on the unphysical Riemann sheet. Resonances appear as poles on an unphysical Riemann sheet close to the physical one with non-zero imaginary part, and they appear in conjugate pairs. For example, the loosely bound states $X(3872)$, $Y(3940)$, $Z_c(3900)$, $Z_b(10610)$, $Z_b(10650)$ [70, 75, 247, 248, 249, 250, 251, 252, 253, 254], the hidden-charm pentaquark resonances [255, 256, 257, 258, 259]. We usually apply Weinberg's compositeness condition to estimate the hadronic molecule components [260, 261, 262, 263, 264, 265, 266].

Secondly, we take the scattering amplitudes V as interaction kernels, solve the quasi-potential Bethe-Salpeter or Lippmann-Schwinger equation with the coupled channel effects directly, then explore the analytical properties of the full amplitudes [267, 268, 269, 270, 271, 272, 273], or obtain the bound energies directly to estimate the bound states [76, 274, 275, 276, 277, 278].

Thirdly, we reduce the scattering amplitudes to interaction potentials in the momentum space in terms of the Breit approximation and introduce monopole form-factors associated with the exchanged particles. Generally, we should introduce form-factors in each interaction vertex, which

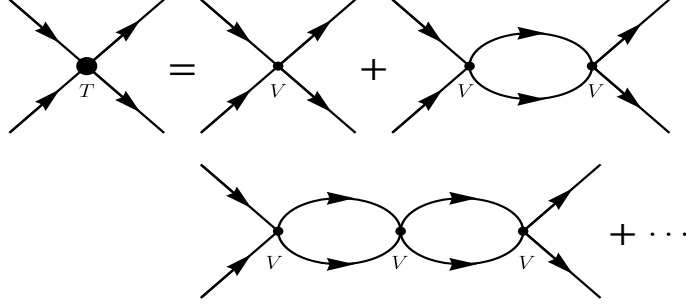


Figure 4: Summing the two-meson loops through the Bethe-Salpeter equation.

reflects the off-shell effect of the exchanged meson and the structure effect, because the components of the molecular states and exchanged mesons are not point particles. Then we perform the Fourier transformation to obtain the potential in the coordinate space, finally we solve the Schrodinger equation directly to obtain the binding energy [63, 279, 280, 281, 282, 283, 284, 285, 286, 287, 288, 289].

2.1.3 $Q\bar{Q}$ states with coupled channel effects

In the famous GI model, the charmonium $\chi_{c1}(2^3P_1)$ has the mass about 3953 MeV [86], which is about 100 MeV above the $X(3872)$ lying near the $D^0\bar{D}^{*0}$ threshold, the strong coupling to the nearby threshold maybe lead to some DD^* molecular configuration. Furthermore, pure charmonium assignment cannot interpret the high $\gamma\psi'$ decay rate [290].

We can extend the constituent quark models to include the meson-meson Fock components, and write the physical charmonium (bottomonium) states in terms of $|\Psi\rangle$,

$$|\Psi\rangle = \sum_{\alpha} c_{\alpha} |\psi_{\alpha}\rangle + \sum_{\beta} \chi_{\beta}(P) |\phi_1 \phi_2 \beta\rangle \quad (18)$$

where the $|\psi_{\alpha}\rangle$ are the $Q\bar{Q}$ eigenstates, the ϕ_i are $Q\bar{q}$ or $q\bar{Q}$ eigenstates, $|\phi_1 \phi_2 \beta\rangle$ are the two-meson state with β quantum numbers, and the $\chi_{\beta}(P)$ is the relative wave function between the two mesons. Then we solve the Schrodinger equation directly [291, 292, 293, 294, 295, 296, 297, 298, 299, 300].

2.1.4 Hybrid and Tetraquark states in Born-Oppenheimer approximation

Due to the large ratio of the mass of a nucleus to that of the electron, the electrons respond almost instantaneously to the motion of the nuclei. The energy of the electrons combined with the repulsive Coulomb energy of the nuclei defines a Born-Oppenheimer potential. Accordingly, due to the large ratio of the heavy-quark mass m_Q to the energy scale Λ_{QCD} associated with the gluon field, the gluons respond almost instantaneously to the motion of the heavy quarks Q and \bar{Q} [301, 302, 303, 304, 305, 306].

In the static limit, the Q and \bar{Q} serve as two color-sources separated by a distance r , the ground-state flavor-singlet Born-Oppenheimer potential $V_{\Sigma_g^+}(r)$ is defined by the minimal energy of the gluonic configurations, whose small and large r limiting behaviors are qualitatively compatible with the simple phenomenological Cornell potential, thus the $V_{\Sigma_g^+}(r)$ describes the traditional heavy quarkonium states. The excited Born-Oppenheimer potentials $V_{\Gamma}(r)$ are defined as the minimal energies of the excited configurations for the gluon and light-quark fields with the quantum numbers Γ [301, 302, 303].

The hybrid states $\bar{Q}GQ$ are energy levels of a heavy quark pair $Q\bar{Q}$ in the excited flavor-singlet Born-Oppenheimer potentials, the hybrid potentials. Juge, Kuti and Morningstar calculated many

flavor-singlet potentials using the quenched lattice QCD [307]. There have been some works on the lowest lying hybrid potentials using lattice QCD with two flavors of dynamical Wilson fermions [308, 309]. At large r , the hybrid potential $V_{\Gamma}(r)$ is a flux-tube extending between the Q and \bar{Q} . At small r , the hybrid potential approaches the repulsive color-Coulomb potential between a Q and \bar{Q} in a color-octet state. In the limit $r \rightarrow 0$, the Q and \bar{Q} sources reduce to a single local color-octet $Q\bar{Q}$ source. The energy levels of the flavor-singlet gluon and light-quark field configurations bound to a static color-octet source are called static hybrid mesons. The most effective pictorial representation of the hybrid states is the flux-tube model. Lattice QCD simulations show that two static quarks Q and \bar{Q} at large distances are confined by approximately cylindrical regions of the color fields [307, 308, 309].

The $\bar{Q}Q\bar{q}q$ tetraquark states are energy levels in the Born-Oppenheimer potentials with nonsinglet (excited singlet) flavor quantum numbers, the tetraquark potentials, which are distinguished by the quantum numbers, $u\bar{u} \pm d\bar{d}$, $u\bar{d}$, $d\bar{u}$, $s\bar{q}$, $s\bar{s}$, etc. At large r , the minimal-energy configuration consists of two static mesons localized near the Q and \bar{Q} sources. At small r , the minimal-energy configuration is the flavor-singlet Σ_g^+ potential accompanied by one or two pions (two or three pions), depending on the quantum numbers Γ . There have been works on the energies of static adjoint mesons using the quenched lattice QCD [310]. The static adjoint mesons are energy levels of the light-quark and gluon fields with nonsinglet flavor quantum numbers bound to a static color-octet source.

The heavy quark motion is restored by solving the Schrodinger equation in each of those potentials, and many X , Y and Z mesons could be assigned as the bound states with the Born-Oppenheimer potentials [301, 302, 303, 304, 305, 306].

2.1.5 Tetraquarks in diquark models

If we take the quarks in color triplet $\mathbf{3}$ as the basic constituents, then we could construct the hadrons according to the $SU(3)$ symmetry. For the traditional mesons,

$$q\mathbf{3} \otimes \bar{q}\bar{\mathbf{3}} \rightarrow [\bar{q}q]\mathbf{1}.$$

For the traditional baryons,

$$q\mathbf{3} \otimes q\mathbf{3} \otimes q\mathbf{3} \rightarrow [qqq]\mathbf{1}.$$

For the tetraquark molecular states,

$$q\mathbf{3} \otimes \bar{q}\bar{\mathbf{3}} \otimes q\mathbf{3} \otimes \bar{q}\bar{\mathbf{3}} \rightarrow [\bar{q}q]\mathbf{1}[\bar{q}q]\mathbf{1} \oplus [\bar{q}q]\mathbf{8}[\bar{q}q]\mathbf{8} \rightarrow [\bar{q}q\bar{q}q]\mathbf{1} \oplus [\bar{q}q\bar{q}q]\mathbf{1},$$

and we usually call the color $\mathbf{11}$ type structures as the molecular states. For the tetraquark states,

$$q\mathbf{3} \otimes q\mathbf{3} \otimes \bar{q}\bar{\mathbf{3}} \otimes \bar{q}\bar{\mathbf{3}} \rightarrow [qq]\bar{\mathbf{3}}[\bar{q}\bar{q}]\mathbf{3} \oplus [qq]\mathbf{6}[\bar{q}\bar{q}]\bar{\mathbf{6}} \rightarrow [qq\bar{q}\bar{q}]\mathbf{1} \oplus [qq\bar{q}\bar{q}]\mathbf{1},$$

and we usually call the color $\bar{\mathbf{33}}$ type structures as the tetraquark states. For the pentaquark molecular states,

$$q\mathbf{3} \otimes q\mathbf{3} \otimes q\mathbf{3} \otimes q\mathbf{3} \otimes \bar{q}\bar{\mathbf{3}} \rightarrow [qqq]\mathbf{1}[\bar{q}q]\mathbf{1} \rightarrow [qqqq\bar{q}]\mathbf{1}.$$

For the pentaquark states,

$$q\mathbf{3} \otimes q\mathbf{3} \otimes q\mathbf{3} \otimes q\mathbf{3} \otimes \bar{q}\bar{\mathbf{3}} \rightarrow [qq]\bar{\mathbf{3}}[qq]\bar{\mathbf{3}}[\bar{q}]\bar{\mathbf{3}} \rightarrow [qqqq\bar{q}]\mathbf{1}.$$

If we take the viewpoint of the quantum field theory, the scattering amplitude for one-gluon exchange is proportional to,

$$\left(\frac{\lambda^a}{2}\right)_{ij} \left(\frac{\lambda^a}{2}\right)_{kl} = -\frac{N_c + 1}{4N_c} (\delta_{ij}\delta_{kl} - \delta_{il}\delta_{kj}) + \frac{N_c - 1}{4N_c} (\delta_{ij}\delta_{kl} + \delta_{il}\delta_{kj}), \quad (19)$$

where the λ^a is the Gell-Mann matrix, the i, j, k, m and l are color indexes, the N_c is the color number, and $N_c = 3$ in the real world. The negative sign in front of the antisymmetric antitriplet **3** indicates the interaction is attractive, which favors formation of the diquarks in color antitriplet, while the positive sign in front of the symmetric sextet **6** indicates the interaction is repulsive, which disfavors formation of the diquarks in color sextet.

In this sub-sub-section, we would like to focus on the tetraquark states, as the extension to the pentaquark states is straightforward. Now we define the color factor,

$$\hat{C}_i \cdot \hat{C}_j = \frac{\lambda_i^a}{2} \cdot \frac{\lambda_j^a}{2}, \quad (20)$$

where the subscripts i and j denote the quarks, $\langle \hat{C}_i \cdot \hat{C}_j \rangle = -\frac{2}{3}$ and $\frac{1}{3}$ for the **3** and **6** diquark $[qq]$, respectively, and $\langle \hat{C}_i \cdot \hat{C}_j \rangle = -\frac{4}{3}$ and $\frac{1}{6}$ for the **1** and **8** quark-antiquark $\bar{q}q$, respectively. If we define $\hat{C}_{12} \cdot \hat{C}_{34} = (\hat{C}_1 + \hat{C}_2) \cdot (\hat{C}_3 + \hat{C}_4)$, then $\langle \hat{C}_{12} \cdot \hat{C}_{34} \rangle = -\frac{4}{3}$ and $-\frac{10}{3}$ for the **33** and **66** type tetraquark states. It is feasible to take both the **33** and **66** diquark configurations to explore the tetraquark states, while the preferred or usually chosen configuration is of the **33** type.

The color-spin Hamiltonian can be written as [311],

$$H = - \sum_{i \neq j} \kappa_{ij} S_i \cdot S_j \frac{\lambda_i^a}{2} \cdot \frac{\lambda_j^a}{2}, \quad (21)$$

the color factor $\frac{\lambda_i^a}{2} \cdot \frac{\lambda_j^a}{2}$ can be absorbed into the chromomagnetic couplings κ_{ij} after taking matrix elements between the **33** type tetraquark states.

In 2004, Maiani et al introduced the simple spin-spin Hamiltonian,

$$H = 2m_{[cq]} + 2(\kappa_{cq})_{\bar{\mathbf{3}}} (S_c \cdot S_q + S_{\bar{c}} \cdot S_{\bar{q}}) + 2\kappa_{q\bar{q}} (S_q \cdot S_{\bar{q}}) + 2\kappa_{c\bar{q}} (S_c \cdot S_{\bar{q}} + S_{\bar{c}} \cdot S_q) + 2\kappa_{c\bar{c}} (S_c \cdot S_{\bar{c}}), \quad (22)$$

to study the hidden-charm tetraquark states in the diquark model, where the m_{cq} is the charmed diquark mass [55]. They took the $X(3872)$ with the $J^{PC} = 1^{++}$ as the basic input and predicted a mass spectrum for the **33** type hidden-charm tetraquark states with the $J^{PC} = 0^{++}, 1^{+-}$ and 2^{++} . Maiani et al assigned the $J^{PC} = 1^{+-}$ charged resonance in the $Y(4260) \rightarrow \pi^+ \pi^- J/\psi$ decays as the $X(3882)$ or $Z(3882)$ according to the BESIII and Belle data, however, there is no evidence for the lower resonance $X(3754)$ or $Z(3754)$ [312]. In fact, in the Type-I diquark model, see the Hamiltonian in Eq.(22) [55], the predicted masses 3754 MeV and 3882 MeV for the $J^{PC} = 1^{+-}$ states are smaller than that of the tetraquark candidates $Z_c(3900)$ and $Z_c(4020)$ observed later, respectively [162, 163, 165, 166, 167].

In 2005, Maiani et al assigned the $Y(4260)$ to be the first orbital excitation of the $[cs][\bar{c}\bar{s}]$ state by including the spin-orbit interaction, and obtained a crucial prediction that the $Y(4260)$ should decay predominantly in the $D_s \bar{D}_s$ channel [313]. The decay model $Y(4260) \rightarrow D_s \bar{D}_s$ has not been observed yet up to now. In 2009, Drenska, Faccini and Polosa studied the $[cs][\bar{c}\bar{s}]$ tetraquark states with the $J^{PC} = 0^{++}, 0^{-+}, 0^{--}, 1^{++}, 1^{+-}, 1^{-+}$ and 1^{--} by computing the mass spectrum and decay modes [314].

In 2014, Maiani et al restricted the dominant spin-spin interactions to the ones within each diquark, and simplify the effective Hamiltonian,

$$H = 2m_{[cq]} + 2\kappa_{cq} (S_c \cdot S_q + S_{\bar{c}} \cdot S_{\bar{q}}), \quad (23)$$

which could describe the hierarchy of the masses of the $X(3872)$, $Z_c(3900)$, $Z_c(4020)$ very well in the scenario of tetraquark states [56], furthermore, they introduced a spin-orbit interaction to interpret the Y states,

$$H = M_{00} + B_c \frac{L^2}{2} - 2aL \cdot S + 2\kappa_{cq} (S_c \cdot S_q + S_{\bar{c}} \cdot S_{\bar{q}}), \quad (24)$$

where the M_{00} , B_c and a are parameters to be fitted experimentally. Then they sorted the tetraquark states in terms of $|S_{qc}, S_{\bar{q}\bar{c}}; S, L; J\rangle$, where the L is the angular momentum between the diquark and antidiquark, $\vec{S}_{qc} = \vec{S}_q + \vec{S}_c$, $\vec{S}_{\bar{q}\bar{c}} = \vec{S}_{\bar{q}} + \vec{S}_{\bar{c}}$, $\vec{S} = \vec{S}_{qc} + \vec{S}_{\bar{q}\bar{c}}$, $\vec{J} = \vec{S} + \vec{L}$, and assigned the $Y(4008)$, $Y(4260)$, $Y(4290/4220)$ and $Y(4630)$ to be the tetraquark states $|0, 0; 0, 1; 1\rangle$, $\frac{1}{\sqrt{2}}(|1, 0; 1, 1; 1\rangle + |0, 1; 1, 1; 1\rangle)$, $|1, 1; 0, 1; 1\rangle$ and $|1, 1; 2, 1; 1\rangle$, respectively. The effective Hamiltonian, see Eq.(23), is referred to as the Type-II diquark model. Then the mass spectrum of the $[cs][\bar{c}\bar{s}]$ tetraquark states was explored [315], and applied to study the LHCb's $J/\psi\phi$ resonances [316].

In 2017, Maiani, Polosa and Riquer introduced a hypothesis that the diquarks and antidiquarks in tetraquarks are separated by a potential barrier to answer the long standing questions challenging the diquark-antidiquark model of exotic resonances [317].

In 2018, Ali et al analyzed the P-wave hidden-charm tetraquark states in the diquark model using an effective Hamiltonian incorporating the dominant spin-spin, spin-orbit and tensor interactions,

$$H = 2m_{\mathcal{D}} + \frac{B_{\mathcal{D}}}{2}L^2 + 2a_Y L \cdot S + b_Y (3S_1 \cdot \vec{n} S_2 \cdot \vec{n} - S_1 \cdot S_2) + 2\kappa_{cq} (S_q \cdot S_c + S_{\bar{q}} \cdot S_{\bar{c}}), \quad (25)$$

where $\vec{n} = \frac{\vec{r}}{r}$, the S_1 and S_2 are the spins of the $\bar{\mathbf{3}}$ diquark $\mathcal{D} ([qc])$ and $\mathbf{3}$ antidiquark $\bar{\mathcal{D}} ([\bar{q}\bar{c}])$, respectively, the $m_{\mathcal{D}}$, B_Y , a_Y and b_Y are parameters to be fitted experimentally [318]. And their updated analysis indicate that it is favorable to assign the $Y(4220)$, $Y(4330)$, $Y(4390)$, $Y(4660)$ as the tetraquark states $|0, 0; 0, 1; 1\rangle$, $\frac{1}{\sqrt{2}}(|1, 0; 1, 1; 1\rangle + |0, 1; 1, 1; 1\rangle)$, $|1, 1; 0, 1; 1\rangle$ and $|1, 1; 2, 1; 1\rangle$, respectively.

In 2021, Maiani, Polosa and Riquer suggested that the $Z_{cs}(3985)$ and $Z_{cs}(4003)$ are two different particles, and there exist two $SU(3)_f$ nonets with the $J^{PC} = 1^{++}$ and 1^{+-} , respectively, thus they could assign the $X(3872)$, $Z_c(3900)$, $Z_{cs}(3985)$, $Z_{cs}(4003)$ and $X(4140)$ consistently [319].

Again, let us turn to the chromomagnetic interaction model, see Eq.(21), and choose the $\bar{\mathbf{3}}\mathbf{3}$ plus $\bar{\mathbf{6}}\bar{\mathbf{6}}$ configurations and $\mathbf{11}$ plus $\mathbf{88}$ configurations as two independent representations (or basis) respectively to explore the mass spectrum of the exotic states and their decay channels, and have obtained many successful descriptions [320, 321, 322, 323, 324].

In the dynamical diquark picture, Brodsky, Hwang and Lebed assume that the $\mathcal{D}\bar{\mathcal{D}}$ pair forms promptly at the production point, and rapidly separates due to the kinematics of the production process, as the diquark and antidiquark are colored objects, they cannot separate asymptotically far apart; they create a color flux tube or string between them. If sufficient energy is available, the string would break to create an additional $q\bar{q}$ pair, and rearrange into a baryon-antibaryon pair, for example, the $\Lambda_c \bar{\Lambda}_c$ pair. The overlap of the wave-functions between the quark and antiquark is suppressed greatly, due to the large spatial separation between the diquark and antidiquark pair, therefore, the transition rate is suppressed and leads to small exotic widths [57]. The exotic mass spectrum is calculated in this picture [325, 326, 327, 328, 329, 330, 331].

In the relativized quark model, the Hamiltonian can be written as,

$$H = \sum_{i=1}^4 (p_i^2 + m_i^2)^{1/2} + \sum_{i<j} V_{ij}^{\text{conf}} + \sum_{i<j} V_{ij}^{\text{oge}} \quad (26)$$

where the V_{ij}^{conf} is the linear confining potential, the V_{ij}^{oge} is the one-gluon exchange potential including a Coulomb and a hyperfine term. Then the $\bar{\mathbf{3}}\mathbf{3}$ type configurations or both the $\bar{\mathbf{3}}\mathbf{3}$ and $\bar{\mathbf{6}}\bar{\mathbf{6}}$ type configurations are taken into account to solve the Schrodinger equations to obtain the mass spectrum [332, 333, 334, 335, 336, 337, 338, 339, 340, 341].

In the quasipotential approach, Ebert et al take the $\bar{\mathbf{3}}\mathbf{3}$ -type configurations to study the hidden-charm (hidden-bottom, charm-bottom or fully-heavy) tetraquark mass spectrum by solving the Schrodinger type equations, where an effective one-gluon exchange potential plus a linear confining potential are adopted [59, 342, 343, 344].

In the constituent quark model, all possible quark configurations satisfying the Pauli principle are explored by solving the Schrodinger equation with the potential kernel containing the confinement plus one-gluon-exchange plus (or not plus) one-meson-exchange interactions [345, 346, 347, 348, 349, 350, 351, 352], while in the color flux-tube model, a multi-body interacting confinement potential instead of a two-body interacting confinement potential is chosen [353, 354].

2.1.6 Tetraquark states with Lattice QCD

Lattice QCD provides rather accurate and reliable calculations for the hadrons which lie well below strong-decay threshold and do not decay strongly, the physical information is commonly extracted from the discrete energy spectrum. The physical system with specified quantum numbers is created from the vacuum $|0\rangle$ using an operator \mathcal{O}_j^\dagger at time $t=0$, then this system propagates for a time t before being annihilated by an operator \mathcal{O}_i . The spectral decomposition is performed to express the correlators $C_{ij}(t)$ in terms of the energies E_n and overlaps Z_j^n of the eigenstates $|n\rangle$,

$$C_{ij}(t) = \langle 0 | \mathcal{O}_i(t) \mathcal{O}_j^\dagger(0) | 0 \rangle = \sum_n Z_i^n Z_j^{n*} e^{-E_n t}, \quad (27)$$

$Z_i^n \equiv \langle 0 | \mathcal{O}_i | n \rangle$. The correlators $C_{ij}(t)$ are calculated on the lattice and their time-dependence is used to extract the E_n and Z_n^i [355, 356]. The lattice QCD has been applied extensively to study the exotic states [357, 358, 359, 360, 361, 362, 363, 364].

In the energy region near or above the strong decay thresholds, the masses of the bound states and resonances are inferred from the finite-volume scattering matrix of one-channel elastic or multiple-channel inelastic scattering. Various approaches with varying degrees of mathematical rigour have been used in the simulations [365]. The simplest example is a one-channel elastic scattering with the partial wave l , where the scattering matrix $S(p)$ satisfying unitarity $SS^\dagger = 1$ is parameterized in terms of the phase shift $\delta_l(p)$,

$$\begin{aligned} S(p) &= e^{2i\delta_l(p)} = 1 + 2iT(p), \\ T(p) &= \frac{1}{\cot(\delta_l(p)) - i}, \end{aligned} \quad (28)$$

the phase shift $\delta_l(p)$ for the S-wave scattering is extracted using the well-established and rigorous Luscher's relation [366, 367, 368], which applies for the elastic scattering below and above threshold. The phase shifts $\delta(p)$ provide copious information about the masses of resonances and bound states. In the vicinity of a hadronic resonance with a mass m_R and a width Γ , the cross section has a Breit-Wigner-type shape with the value $\delta(s = m_R^2) = \frac{\pi}{2}$,

$$T(p) = \frac{-\sqrt{s} \Gamma(p)}{s - m_R^2 + i\sqrt{s} \Gamma(p)} = \frac{1}{\cot \delta(p) - i}. \quad (29)$$

Below and above threshold, the $p \cot \delta(p)$ can be expanded by the effective range approximation,

$$p \cot \delta(p) = \frac{1}{a} + \frac{1}{2} r p^2, \quad (30)$$

where the a is the scattering length and the r is the effective range. On the other hand, the bound state (B) is realized when the scattering amplitude $T(p)$ has a pole at the value $p_B = i|p_B|$,

$$T = \frac{1}{\cot(\delta(p_B)) - i} = \infty, \quad (31)$$

the location of this shallow bound state can be obtained by parameterizing $\delta(p)$ near the threshold and finding the p_B which satisfies $\cot(\delta(p_B)) = i$. Most of the exotic candidates are above several two-hadron thresholds, and have more than one decay channels, which requires determining the

scattering matrix for the coupled-channel nonelastic scattering matrix elements [369, 370, 371, 372, 373].

The HALQCD collaboration use the HALQCD approach to extract the coupled-channel scattering matrix [374, 375], the HALQCD approach is based on the lattice determination of the potential $V(r)$ between different channels, then employs the Nambu-Bethe-Salpeter equation to extract the masses of the bound states.

2.2 Multiquark states with the QCD sum rules

The QCD sum rules were introduced by Shifman, Vainshtein and Zakharov in 1979 to study the conventional mesons [376, 377], then they were extended to study the conventional baryons by Ioffe [378]. The QCD sum rules are analytic and fully relativistic, and approach the bound state problem in QCD from short distances and move to longer distances step by step by including the non-perturbative effects so as to extract information on the hadronic properties.

In the past years, the QCD sum rules have been applied widely to study the hadronic properties, such as the masses of the quarks; masses and decay constants of the light and heavy mesons and baryons; form-factors of the mesons and baryons; valence quark distributions and spin structure functions of the nucleons; structure functions of the photon, pseudoscalar, vector and axialvector mesons; hadronic matrix elements for the $K^0 - \bar{K}^0$, $B_d - \bar{B}_d$, $B_s - \bar{B}_s$ mixing; strong coupling constants and magnetic moments of the mesons and baryons; parameters of the effective field theories; spectroscopy and properties of the exotic states; hadrons in the nuclear matter; properties of hadronic matter at high temperature and density, etc [46, 47, 379, 380, 381, 382, 383, 384, 385, 386, 387, 388]. Especially since 2007, the QCD sum rules have been applied extensively to study the X , Y , Z , T and P states, which are the typical multiquark candidates [46, 47, 58, 60, 81]. For the early works on the exotic states, we can consult Refs.[389, 390, 391, 392, 393, 394, 395, 396, 397, 398, 399, 400].

In this sub-section, we would like to illustrate the general procedure of the QCD sum rules for the masses of the conventional hadrons and multiquark states concisely.

At the beginning point, let us write down the general two-point vacuum correlation functions,

$$\Pi(p) = i \int d^4x e^{ip \cdot x} \langle 0 | T \{ J(x) J^\dagger(0) \} | 0 \rangle, \quad (32)$$

where the $J(x)$ are the local currents consist of quark-gluon fields with specified quantum numbers, and the T denotes the time-ordering operation. For the conventional mesons and baryons, the currents $J(x)$ have been explored extensively [381], for the multiquark states, the currents $J(x)$ can be constructed straightforwardly.

At the large squared momentum region $P^2 = -p^2 \gg \Lambda_{QCD}^2$, the integral in Eq.(32) is dominated by small spatial distances and time intervals,

$$t \sim |\vec{x}| \sim \frac{1}{\sqrt{P^2}} \ll r, \quad (33)$$

to avoid fast exponential oscillating, where the hadron size $r \sim \frac{1}{\Lambda_{QCD}}$. If we set $\Lambda_{QCD} = (200 - 300) \text{ MeV}$, then the hadron size $r \sim 0.7 - 1.0 \text{ fm}$. Therefore, at the condition of large hadron size, say $r \gg 1 \text{ fm}$, the local currents $J(x)$ are questionable to interpolate the corresponding hadrons.

Now let us take it for granted that the exotic states have the size $r \leq 1 \text{ fm}$, just like the conventional mesons and baryons, could be interpolated by the local currents $J(x)$ tacitly. For example, the charge radii of the π^\pm , K^\pm and p are $\sqrt{\langle r^2 \rangle} = 0.659 \pm 0.004 \text{ fm}$, $0.560 \pm 0.031 \text{ fm}$ and $0.8409 \pm 0.0004 \text{ fm}$ respectively from the Particle Data Group [97]. We extend the QCD sum rules on the conventional mesons and baryons to study the multiquark states directly with a simple replacement of the interpolating currents, and would like to come back to this subject again in Sect.2.3.

A Lorentz invariant vacuum average can be expressed as

$$\langle 0|T \{J(x)J^\dagger(0)\} |0\rangle = \int d\tau \exp(i\tau x^2) f(\tau), \quad (34)$$

where the $f(\tau)$ is a function. Then

$$\Pi(p^2) = i \int d\tau \int d^4x \exp(i\tau x^2) \exp(iP^2/4\tau) f(\tau). \quad (35)$$

The dominant contributions to the $\Pi(p^2)$ come from the region,

$$x^2 \sim \frac{1}{\tau} \sim \frac{1}{P^2}. \quad (36)$$

In the limit $P^2 \rightarrow \infty$, we reach the light-cone $x^2 \sim 0$, which is a necessary but not yet sufficient condition for the short-distance dominance, we have to constrain $|\vec{x}| \sim \frac{1}{\sqrt{P^2}}$.

Now we focus on the quark-gluon degrees of freedom and calculate the correlation functions using Wilson's operator product expansion to separate the physics of short and long distances,

$$\Pi(p^2) = \sum_n C_n(p^2, \mu) \langle \mathcal{O}_n(\mu) \rangle, \quad (37)$$

where the $C_n(p^2, \mu)$ are the Wilson's coefficients encoding short-distance contributions, the $\langle \mathcal{O}_n(\mu) \rangle$ are vacuum expectations of the local operators with dimension n . The short-distance contributions at $p^2 > \mu^2$ are encoded in the coefficients $C_n(p^2, \mu)$, the long-distance contributions at $p^2 < \mu^2$ are absorbed into the vacuum condensates $\langle \mathcal{O}_n(\mu) \rangle$ [385]. If $\mu \gg \Lambda_{QCD}$, the Wilson coefficients $C_n(p^2, \mu)$ depend only on short-distance dynamics, the vacuum condensates $\langle \mathcal{O}_n(\mu) \rangle$ embody the long-distance effects. The lowest condensate is vacuum expectation of the unit operator $\langle \mathcal{O}_0(\mu) \rangle$ associated with the perturbative contributions. The vacuum condensates with dimensions $n = 3, 4, 5, 6, \dots$ are quark condensate $\langle \bar{q}q \rangle$, gluon condensate $\langle \frac{\alpha_s G G}{\pi} \rangle$, mixed condensate $\langle \bar{q}g_s \sigma G q \rangle$, four-quark condensate $\langle \bar{q}q \rangle^2$, \dots , which parameterize the non-perturbative effects or soft gluons and quarks. We can consult Refs.[381, 385] for the basic techniques in performing the operator product expansion.

If there exist m heavy quark lines and n light-quark lines in the correlation functions $\Pi(p^2)$, each heavy quark line emits a gluon and each light quark line contributes a quark-antiquark pair, we obtain a quark-gluon operator,

$$\underbrace{G_{\mu\nu} \cdots G_{\alpha\beta}} \underbrace{\bar{q}q \bar{q}q \cdots \bar{q}q \bar{q}q}, \quad (38)$$

which is of dimension $2m + 3n$, we should perform the operator product expansion up to the vacuum condensates of dimension $2m + 3n$ at least [60, 61, 81, 82, 83]. For example, $m = 3$ and $n = 4$, we should calculate the vacuum condensates of dimension 18, see Fig.5. When $m = n = 1$, we obtain the conventional $Q\bar{q}$ mesons, it is obvious that we should calculate the mixed condensate $\langle \bar{q}g_s \sigma G q \rangle$.

Then we obtain the Källen-Lehmann representation through dispersion relation at the quark-gluon degrees of freedom,

$$\Pi_{QCD}(p^2) = \frac{1}{\pi} \int_{\Delta^2}^{\infty} ds \frac{\text{Im}\Pi_{QCD}(s)}{s - p^2}, \quad (39)$$

where the Δ^2 denotes the thresholds.

At the hadron degrees of freedom, we insert a complete set of intermediate hadronic states $|n\rangle$ with the same quantum numbers as the currents $J(x)$ into the correlation functions $\Pi(p^2)$, and

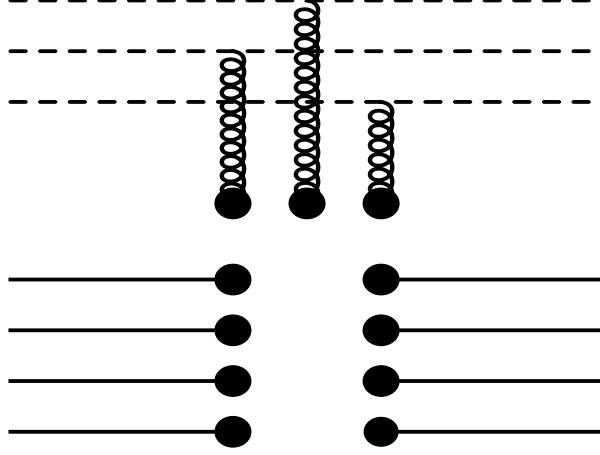


Figure 5: The counting role for the truncation of the operator product expansion, where the solid lines and dashed lines represent the light quarks and heavy quarks, respectively.

take account of the current-hadron couplings to obtain the analytical expressions, again we obtain the Källen-Lehmann representation through dispersion relation,

$$\Pi_H(p^2) = \frac{1}{\pi} \int_{\Delta^2}^{\infty} ds \frac{\text{Im}\Pi_H(s)}{s - p^2}, \quad (40)$$

where

$$\rho_H(s) = \frac{\text{Im}\Pi_H(s)}{\pi} = \sum_n |\langle 0 | J(0) | n \rangle|^2 \delta(s - M_n^2), \quad (41)$$

the subscript H denotes the hadron side.

According to the Quark-Hadron duality, we introduce the continuum threshold parameters s_0 , and match the QCD side with hadron side of the correlation functions $\Pi(p^2)$,

$$\frac{1}{\pi} \int_{\Delta^2}^{s_0} ds \frac{\text{Im}\Pi_H(s)}{s - p^2} = \frac{1}{\pi} \int_{\Delta^2}^{s_0} ds \frac{\text{Im}\Pi_{QCD}(s)}{s - p^2}. \quad (42)$$

An important point is the choice of the continuum threshold s_0 , which is a physical parameter that should be determined from the hadronic spectrum. Then we perform the Borel transformation,

$$\Pi(T^2) = \mathcal{B}[\Pi(P^2)] \equiv \lim_{\substack{P^2, n \rightarrow \infty \\ P^2/n = T^2}} \frac{(P^2)^{n+1}}{(n)!} \left(-\frac{d}{dP^2} \right)^n \Pi(P^2), \quad (43)$$

with $P^2 = -p^2$ to obtain the QCD sum rules,

$$\frac{1}{\pi} \int_{\Delta^2}^{s_0} ds \text{Im}\Pi_H(s) \exp\left(-\frac{s}{T^2}\right) = \frac{1}{\pi} \int_{\Delta^2}^{s_0} ds \text{Im}\Pi_{QCD}(s) \exp\left(-\frac{s}{T^2}\right), \quad (44)$$

where the T^2 is the Borel parameter. Some typical and useful examples of the Borel transformation are given in the Appendix. If only the ground state is taken, then

$$\frac{\text{Im}\Pi_H(s)}{\pi} = \lambda_H^2 (s - M_H^2), \quad (45)$$

we obtain the QCD sum rules,

$$\lambda_H^2 \exp\left(-\frac{M_H^2}{T^2}\right) = \frac{1}{\pi} \int_{\Delta^2}^{s_0} ds \text{Im}\Pi_{QCD}(s) \exp\left(-\frac{s}{T^2}\right), \quad (46)$$

where the M_H is the mass of the ground state of the conventional hadron or multi-quark state, the λ_H is the pole residue.

It is obvious that the Borel transformation wipes out any eventual subtraction terms in the correlation functions and suppresses the continuum contributions exponentially, therefore, it improves the convergent behavior of the dispersion integral. Furthermore, it suppresses the higher-dimensional operators in the operator product expansion factorially, which contain inverse powers of the P^2 , see Eq.(481), thus justifies truncation of the operator product expansion and favors a good convergent behavior.

Finally, we eliminate the pole residue λ_H to obtain the QCD sum rules for the ground state mass,

$$M_H^2 = \frac{-\frac{d}{d\tau} \int_{\Delta^2}^{s_0} ds \text{Im}\Pi_{QCD}(s) \exp(-\tau s)}{\int_{\Delta^2}^{s_0} ds \text{Im}\Pi_{QCD}(s) \exp(-\tau s)} \Big|_{\tau=\frac{1}{T^2}}. \quad (47)$$

In the QCD sum rules, we choose some phenomenological inputs which limit the accuracy of this method to be around 10% – 20% [388].

2.3 Are QCD sum rules reliable to study multi-quark states

Any color singlet four-quark and five-quark currents $J(x)$ can be written as $J(x) = J_A^i(x)J_B^i(x)$, where the $J_A^i(x)$ and $J_B^i(x)$ are color singlet clusters with $i = 1, 2, 3, \dots$, for example,

$$\begin{aligned} J_\mu(x) &= \frac{\varepsilon^{ijk}\varepsilon^{lmn}}{\sqrt{2}} \left\{ u_j^T(x) C \gamma_5 c_k(x) \bar{d}_m(x) \gamma_\mu C \bar{c}_n^T(x) - u_j^T(x) C \gamma_\mu c_k(x) \bar{d}_m(x) \gamma_5 C \bar{c}_n^T(x) \right\}, \\ &= \frac{1}{2\sqrt{2}} \left\{ i\bar{c}i\gamma_5 c \bar{d}\gamma_\mu u - i\bar{c}\gamma_\mu c \bar{d}i\gamma_5 u + \bar{c}u \bar{d}\gamma_\mu \gamma_5 c - \bar{c}\gamma_\mu \gamma_5 u \bar{d}c \right. \\ &\quad \left. - i\bar{c}\gamma^\nu \gamma_5 c \bar{d}\sigma_{\mu\nu} u + i\bar{c}\sigma_{\mu\nu} c \bar{d}\gamma^\nu \gamma_5 u - i\bar{c}\sigma_{\mu\nu} \gamma_5 u \bar{d}\gamma^\nu c + i\bar{c}\gamma^\nu u \bar{d}\sigma_{\mu\nu} \gamma_5 c \right\}, \end{aligned} \quad (48)$$

for the four-quark current [60, 401], and

$$\begin{aligned} J(x) &= \varepsilon^{ila}\varepsilon^{ijk}\varepsilon^{lmn} u_j^T(x) C \gamma_5 d_k(x) u_m^T(x) C \gamma_5 c_n(x) C \bar{c}_a^T(x), \\ &= -\frac{1}{4} \mathcal{S}_{ud} \gamma_5 c \bar{c} u + \frac{1}{4} \mathcal{S}_{ud} \gamma^\lambda \gamma_5 c \bar{c} \gamma_\lambda u + \frac{1}{8} \mathcal{S}_{ud} \sigma^{\lambda\tau} \gamma_5 c \bar{c} \sigma_{\lambda\tau} u + \frac{1}{4} \mathcal{S}_{ud} \gamma^\lambda c \bar{c} \gamma_\lambda \gamma_5 u + \frac{i}{4} \mathcal{S}_{ud} c \bar{c} i\gamma_5 u \\ &\quad + \frac{1}{4} \mathcal{S}_{ud} \gamma_5 u \bar{c} c - \frac{1}{4} \mathcal{S}_{ud} \gamma^\lambda \gamma_5 u \bar{c} \gamma_\lambda c - \frac{1}{8} \mathcal{S}_{ud} \sigma^{\lambda\tau} \gamma_5 u \bar{c} \sigma_{\lambda\tau} c - \frac{1}{4} \mathcal{S}_{ud} \gamma^\lambda u \bar{c} \gamma_\lambda \gamma_5 c - \frac{i}{4} \mathcal{S}_{ud} u \bar{c} i\gamma_5 c, \end{aligned} \quad (49)$$

for the five-quark current [402], where the components $\mathcal{S}_{ud}\Gamma c = \varepsilon^{ijk} u_i^T C \gamma_5 d_j \Gamma c_k$.

According to the pioneer works [403, 404, 405], in the coordinate space, we write the two-hadron-reducible contributions as

$$\Pi_{RE}(x) = \langle 0|T \left\{ J_A^i(x) J_A^{j\dagger}(0) \right\} |0\rangle \langle 0|T \left\{ J_B^i(x) J_B^{j\dagger}(0) \right\} |0\rangle, \quad (50)$$

and the two-hadron-irreducible contributions as

$$\Pi_{IR}(x) = \langle 0|T \left\{ J(x) J^\dagger(0) \right\} |0\rangle - \langle 0|T \left\{ J_A^i(x) J_A^{j\dagger}(0) \right\} |0\rangle \langle 0|T \left\{ J_B^i(x) J_B^{j\dagger}(0) \right\} |0\rangle. \quad (51)$$

At the phenomenological side of the correlation functions, we can write the two-hadron-reducible contributions as

$$\Pi_{RE}(p^2) = |\lambda_{AB}|^2 \frac{i}{(2\pi)^4} \int d^4 q \frac{i}{q^2 - M_A^2} \frac{i}{(p-q)^2 - M_B^2}, \quad (52)$$

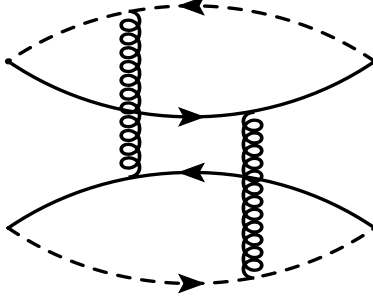


Figure 6: The nonfactorizable Feynman diagrams of the order $\mathcal{O}(\alpha_s^2)$ for the color singlet-singlet type currents, other diagrams obtained by interchanging of the heavy quark lines (dashed lines) and light quark lines (solid lines) are implied.

where the couplings

$$\langle 0 | J_A^i(0) | A(q) \rangle \langle 0 | J_B^i(0) | B(p-q) \rangle = \lambda_{AB}, \quad (53)$$

and the λ_{AB} could be estimated phenomenologically [403, 404, 405, 406].

In the correlation functions for the color singlet-singlet type currents [407, 408], Lucha, Melikhov and Sazdjian assert that the Feynman diagrams can be divided into factorizable and nonfactorizable diagrams in the color space, the contributions at the order $\mathcal{O}(\alpha_s^k)$ with $k \leq 1$, which are factorizable in the color space, are exactly canceled out by the meson-meson scattering states at the hadron side, the nonfactorizable diagrams, if have a Landau singularity, begin to make contributions to the tetraquark (molecular) states, the tetraquark (molecular) states begin to receive contributions at the order $\mathcal{O}(\alpha_s^2)$, see Fig.6.

In Ref.[409], we examine the assertion of Lucha, Melikhov and Sazdjian in details and use two examples for the currents $J_\mu(x)$ and $J_{\mu\nu}(x)$ to illustrate that the Landau equation is of no use in the QCD sum rule for the tetraquark molecular states, where

$$\begin{aligned} J_\mu(x) &= \frac{1}{\sqrt{2}} \left[\bar{u}(x) i\gamma_5 c(x) \bar{c}(x) \gamma_\mu d(x) + \bar{u}(x) \gamma_\mu c(x) \bar{c}(x) i\gamma_5 d(x) \right], \\ J_{\mu\nu}(x) &= \frac{1}{\sqrt{2}} \left[\bar{s}(x) \gamma_\mu c(x) \bar{c}(x) \gamma_\nu \gamma_5 s(x) - \bar{s}(x) \gamma_\nu \gamma_5 c(x) \bar{c}(x) \gamma_\mu s(x) \right]. \end{aligned} \quad (54)$$

Firstly, we cannot assert that the factorizable Feynman diagrams in color space are exactly canceled out by the meson-meson scattering states, because the meson-meson scattering state and tetraquark molecular state both have four valence quarks, which can be divided into two color-neutral clusters. We cannot distinguish which Feynman diagrams contribute to the meson-meson scattering state or tetraquark molecular state based on the two color-neutral clusters [409].

Secondly, the quarks and gluons are confined objects, they cannot be put on the mass-shell, it is questionable to assert that the Landau equation is applicable for the quark-gluon bound states [410].

If we insist on applying the Landau equation to study the Feynman diagrams, we should choose the pole masses rather than the \overline{MS} masses to warrant mass poles. As the tetraquark (molecular) states begin to receive contributions at the order $\mathcal{O}(\alpha_s^2)$ [407, 408], it is reasonable to take the pole masses \hat{m}_Q as,

$$\hat{m}_Q = m_Q(m_Q) \left[1 + \frac{4}{3} \frac{\alpha_s(m_Q)}{\pi} + f \left(\frac{\alpha_s(m_Q)}{\pi} \right)^2 + g \left(\frac{\alpha_s(m_Q)}{\pi} \right)^3 \right], \quad (55)$$

see Refs.[411, 412] for the explicit expressions of the f and g . If the Landau equation is applicable for the tetraquark (molecular) states, it is certainly applicable for the traditional charmonium and

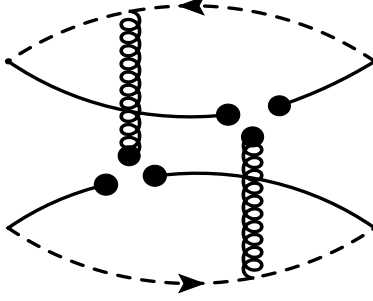


Figure 7: The nonfactorizable Feynman diagrams contribute to the vacuum condensates $\langle \bar{q}g_s\sigma Gq \rangle^2$ for the color singlet-singlet type currents, where the solid lines and dashed lines denote the light quarks and heavy quarks, respectively.

bottomonium states. In the case of the c -quark (b -quark), the pole mass $\hat{m}_c = 1.67 \pm 0.07$ GeV ($\hat{m}_b = 4.78 \pm 0.06$ GeV) from the Particle Data Group [411], the Landau singularity appears at the s -channel $\sqrt{s} = \sqrt{p^2} = 2\hat{m}_c = 3.34 \pm 0.14$ GeV $> M_{\eta_c}/M_{J/\psi}$ ($2\hat{m}_b = 9.56 \pm 0.12$ GeV $> M_{\eta_b}/M_{\Upsilon}$). It is unreliable that the masses of the charmonium (bottomonium) states lie below the threshold $2\hat{m}_c$ ($2\hat{m}_b$) for the η_c and J/ψ (η_b and Υ) [409].

Thirdly, the nonfactorizable Feynman diagrams which have the Landau singularities begin to appear at the order $\mathcal{O}(\alpha_s^0/\alpha_s^1)$ rather than at the order $\mathcal{O}(\alpha_s^2)$, and make contributions to the tetraquark molecular states, if the assertion (only nonfactorizable Feynman diagrams which have Landau singularities make contributions to the tetraquark molecular states) of Lucha, Melikhov and Sazdjian is right.

The nonfactorizable contributions appear at the order $\mathcal{O}(\alpha_s)$ due to the operators $\bar{q}g_sGq\bar{q}g_sGq$, which come from the Feynman diagrams shown in Fig.7. If we insist on choosing the pole mass and applying the Landau equation to study the diagrams, we obtain a sub-leading Landau singularity at the s -channel $s = p^2 = 4\hat{m}_c^2$. From the operators $\bar{q}g_sGq\bar{q}g_sGq$, we obtain the vacuum condensate $\langle \bar{q}g_s\sigma Gq \rangle^2$, where the g_s^2 is absorbed into the vacuum condensate. The nonfactorizable Feynman diagrams appear at the order $\mathcal{O}(\alpha_s^0)$ or $\mathcal{O}(\alpha_s^1)$, not at the order $\mathcal{O}(\alpha_s^2)$ asserted in Refs.[407, 408].

In fact, for the triply-heavy dibaryon-type currents $\eta(x)$ and $\eta_\mu(x)$,

$$\begin{aligned}\eta(x) &= J_c^T(x)C\gamma_5J_{cc}(x), \\ \eta_\mu(x) &= J_c^T(x)C\gamma_\mu J_{cc}(x), \\ J_c(x) &= \varepsilon^{ijk}q_i^T(x)C\gamma_\alpha q_j(x)\gamma^\alpha\gamma_5c_k(x), \\ J_{cc}(x) &= \varepsilon^{ijk}c_i^T(x)C\gamma_\alpha c_j(x)\gamma^\alpha\gamma_5q_k(x),\end{aligned}\tag{56}$$

even in the lowest order Feynman diagrams, there are both connected and disconnected contributions in the color space [413], see Fig.8. From the first diagram in Fig.8, we can obtain both connected and disconnected Feynman diagrams, the connected contributions appear due to the quark-gluon operators $\bar{q}g_sGq\bar{q}g_sGq$ [413], which are of the order $\mathcal{O}(\alpha_s^1)$ and come from the Feynman diagrams shown in Fig.9.

Fourthly, the Landau equation serves as a kinematical equation in the momentum space, and does not depend on the factorizable and nonfactorizable properties of the Feynman diagrams in the color space.

In the leading order, the factorizable Feynman diagrams shown in Fig.10 can be divided into two color-neutral clusters, however, in the momentum space, they are nonfactorizable diagrams, the basic integrals are of the form,

$$\int d^4q d^4k d^4l \frac{1}{(p+q-k+l)^2 - m_c^2} \frac{1}{q^2 - m_q^2} \frac{1}{k^2 - m_q^2} \frac{1}{l^2 - m_c^2}.\tag{57}$$

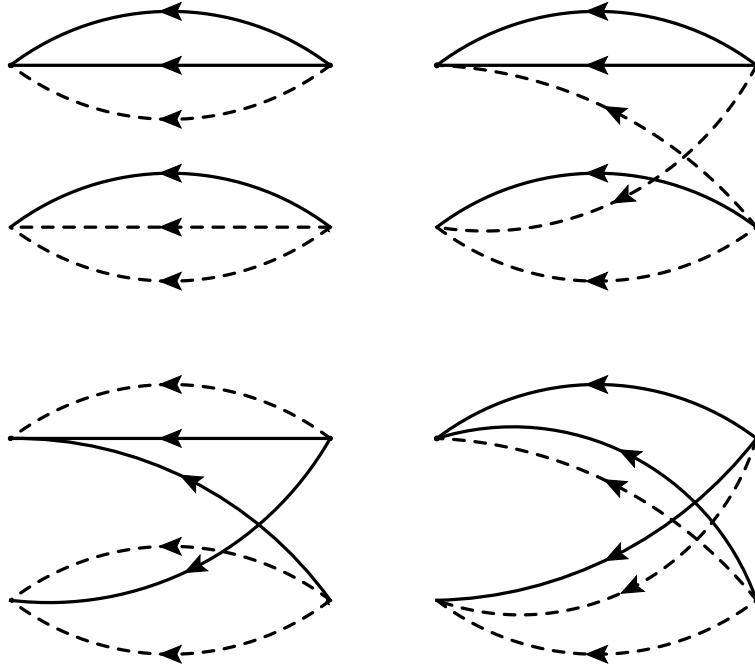


Figure 8: The lowest order Feynman diagrams for the triply-heavy dibaryon states, where the solid lines and dashed lines represent the light quarks and heavy quarks, respectively.

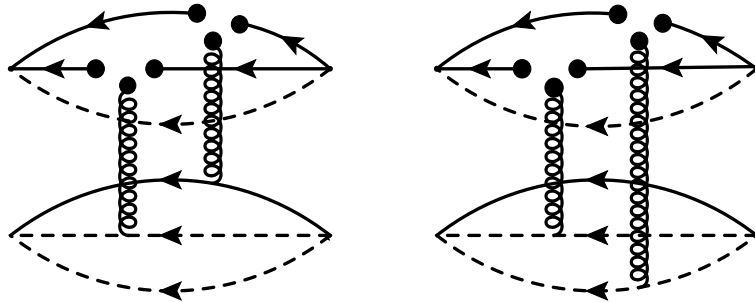


Figure 9: The connected Feynman diagrams originate from the first diagram in Fig.8, other diagrams obtained by interchanging of the heavy quark lines (dashed lines) or light quark lines (solid lines) are implied.

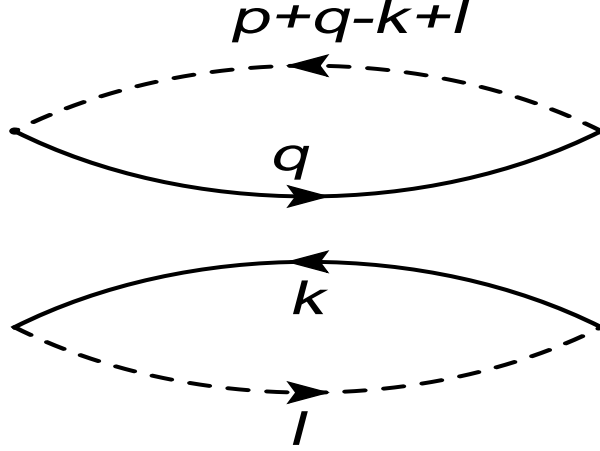


Figure 10: The Feynman diagrams for the lowest order contributions, where the solid lines and dashed lines represent the light quarks and heavy quarks, respectively.

If we choose the pole masses, there exists a Landau singularity at $s = p^2 = (\hat{m}_u + \hat{m}_d + \hat{m}_c + \hat{m}_{\bar{c}})^2$, which is just a signal of a four-quark intermediate state. We cannot assert that it is a signal of a two-meson scattering state or a tetraquark molecular state, because the meson-meson scattering state and tetraquark molecular state both have four valence quarks, q, \bar{q}, c and \bar{c} , which form two color-neutral clusters.

Fifthly, only formal QCD sum rules for the tetraquark (molecular) states are obtained based on the assertion of Lucha, Melikhov and Sazdjian in Refs.[407, 408], no feasible QCD sum rules are obtained up to now.

Sixthly, we carry out the operator product expansion in the deep Euclidean space, $-p^2 \rightarrow \infty$, then obtain the physical spectral densities at the quark-gluon level through dispersion relation [376, 377],

$$\rho_{QCD}(s) = \frac{1}{\pi} \text{Im} \Pi(s + i\epsilon) |_{\epsilon \rightarrow 0}, \quad (58)$$

where the $\Pi(s)$ denotes the correlation functions. The Landau singularities require that the squared momentum $p^2 = (\hat{m}_u + \hat{m}_d + \hat{m}_c + \hat{m}_{\bar{c}})^2$ in the Feynman diagrams, see Fig.10 and Eq.(57), it is questionable to perform the operator product expansion.

Seventhly, we choose the local four-quark or five-quark currents, while the traditional mesons and baryons are spatial extended objects and have mean spatial sizes $\sqrt{\langle r^2 \rangle} \neq 0$, for example, $\sqrt{\langle r^2 \rangle_{E, \Sigma_c^{++}}} = 0.48 \text{ fm}$, $\sqrt{\langle r^2 \rangle_{M, \Sigma_c^{++}}} = 0.83 \text{ fm}$, $\sqrt{\langle r^2 \rangle_{M, \Sigma_c^0}} = 0.81 \text{ fm}$ from the lattice QCD, where the subscripts E and M stand for the electric and magnetic radii, respectively [414], $\sqrt{\langle r^2 \rangle_{M, \Sigma_c^{++}}} = 0.77 \text{ fm}$, $\sqrt{\langle r^2 \rangle_{M, \Sigma_c^0}} = 0.52 \text{ fm}$, $\sqrt{\langle r^2 \rangle_{M, \Sigma_c^+}} = 0.81 \text{ fm}$, $\sqrt{\langle r^2 \rangle_{M, \Xi_c^{'+}}} = 0.55 \text{ fm}$, $\sqrt{\langle r^2 \rangle_{M, \Xi_c'^0}} = 0.79 \text{ fm}$ from the self-consistent $SU(3)$ chiral quark-soliton model [415], $\sqrt{\langle r^2 \rangle_{D^+}} = 0.43 \text{ fm}$, $\sqrt{\langle r^2 \rangle_{D^0}} = 0.55 \text{ fm}$ from the light-front quark model [416], $\sqrt{\langle r^2 \rangle_{J/\psi}} = 0.41 \text{ fm}$, $\sqrt{\langle r^2 \rangle_{\chi_{c2}}} = 0.71 \text{ fm}$ from the screened potential model [88]. Local currents couple potentially to the compact objects having the average spatial sizes as that of the typical heavy mesons and baryons, not to the two-particle scattering states with average spatial size $\sqrt{\langle r^2 \rangle} \geq 1.0 \text{ fm}$, which is too large to be interpolated by the local currents [417, 418].

Now we take a short digression to give a **short notice**. In the QCD sum rules, as we choose the local currents, the four-quark and five-quark states are all compact objects, they are **33**-type, **66**-type, **11**-type or **88**-type tetraquark states, and **333**-type or **11**-type pentaquark states, although we usually call the **11**-type states as the molecular states.

Now, let us write down the correlation functions $\Pi_{\mu\nu}(p)$ and $\Pi_{\mu\nu\alpha\beta}(p)$ for the two currents shown in Eq.(54),

$$\Pi_{\mu\nu}(p) = i \int d^4x e^{ip \cdot x} \langle 0 | T \{ J_\mu(x) J_\nu^\dagger(0) \} | 0 \rangle, \quad (59)$$

$$\Pi_{\mu\nu\alpha\beta}(p) = i \int d^4x e^{ip \cdot x} \langle 0 | T \{ J_{\mu\nu}(x) J_{\alpha\beta}^\dagger(0) \} | 0 \rangle. \quad (60)$$

If we assume the four-quark currents couple potentially both to the two-meson scattering states and molecular states, then we can express the $J_\mu(x)$ and $J_{\mu\nu}(x)$ in terms of the heavy meson fields,

$$J_\mu(x) = \frac{1}{\sqrt{2}} \frac{f_D m_D^2}{m_c} f_{D^*} m_{D^*} [D^0(x) D_\mu^{*-}(x) + D_\mu^{*0}(x) D^-(x)] \\ + \frac{1}{\sqrt{2}} \frac{f_D m_D^2}{m_c} f_{D_0} [D^0(x) i \partial_\mu D_0^-(x) + i \partial_\mu D_0^0(x) D^-(x)] + \lambda_Z Z_{c,\mu}(x) + \dots, \quad (61)$$

$$J_{\mu\nu}(x) = \frac{1}{\sqrt{2}} f_{D_s^*} m_{D_s^*} f_{D_{s1}} m_{D_{s1}} [D_{s,\mu}^{*+}(x) D_{s1,\nu}^-(x) - D_{s1,\nu}^+(x) D_{s,\mu}^{*-}(x)] \\ - \frac{1}{\sqrt{2}} f_{D_s^*} m_{D_s^*} f_{D_s} [D_{s,\mu}^{*+}(x) \partial_\nu D_s^-(x) - \partial_\nu D_s^+(x) D_{s,\mu}^{*-}(x)] \\ + \frac{1}{\sqrt{2}} f_{D_{s0}} f_{D_{s1}} m_{D_{s1}} [i \partial_\mu D_{s0}^+(x) D_{s1,\nu}^-(x) - D_{s1,\nu}^+(x) i \partial_\mu D_{s0}^-(x)] \\ - \frac{1}{\sqrt{2}} f_{D_{s0}} f_{D_s} [i \partial_\mu D_{s0}^+(x) \partial_\nu D_s^-(x) - \partial_\nu D_s^+(x) i \partial_\mu D_{s0}^-(x)] \\ - \tilde{\lambda}_{X^-} \varepsilon_{\mu\nu\alpha\beta} i \partial^\alpha X_c^{-\beta}(x) - \tilde{\lambda}_{X^+} [i \partial_\mu X_{c,\nu}^+(x) - i \partial_\nu X_{c,\mu}^+(x)] + \dots, \quad (62)$$

where we have taken the standard definitions for the decay constants of the traditional mesons and pole residues of the tetraquark molecular states,

$$\langle 0 | J_\mu(0) | Z_c(p) \rangle = \lambda_Z \varepsilon_\mu(p), \quad (63)$$

$$\langle 0 | J_{\mu\nu}(0) | X_c^-(p) \rangle = \tilde{\lambda}_{X^-} \varepsilon_{\mu\nu\alpha\beta} \varepsilon^\alpha(p) p^\beta, \\ \langle 0 | J_{\mu\nu}(0) | X_c^+(p) \rangle = \tilde{\lambda}_{X^+} [\varepsilon_\mu(p) p_\nu - \varepsilon_\nu(p) p_\mu], \quad (64)$$

$\lambda_{X^\pm} = \tilde{\lambda}_{X^\pm} M_{X^\pm}$, the Z_c , X^- and X^+ have the $J^{PC} = 1^{+-}$, 1^{-+} and 1^{++} , respectively, the $\varepsilon_\mu(p)$ are the polarization vectors, we introduce the superscripts \mp to denote the parity.

It is straightforward to obtain the hadronic representation,

$$\Pi_{\mu\nu}(p) = \Pi(p^2) \left(-g_{\mu\nu} + \frac{p_\mu p_\nu}{p^2} \right) + \dots, \quad (65)$$

$$\Pi_{\mu\nu\alpha\beta}(p) = \Pi_-(p^2) \left(g_{\mu\alpha} g_{\nu\beta} - g_{\mu\beta} g_{\nu\alpha} - g_{\mu\alpha} \frac{p_\nu p_\beta}{p^2} - g_{\nu\beta} \frac{p_\mu p_\alpha}{p^2} + g_{\mu\beta} \frac{p_\nu p_\alpha}{p^2} + g_{\nu\alpha} \frac{p_\mu p_\beta}{p^2} \right) \\ + \Pi_+(p^2) \left(-g_{\mu\alpha} \frac{p_\nu p_\beta}{p^2} - g_{\nu\beta} \frac{p_\mu p_\alpha}{p^2} + g_{\mu\beta} \frac{p_\nu p_\alpha}{p^2} + g_{\nu\alpha} \frac{p_\mu p_\beta}{p^2} \right), \quad (66)$$

where

$$\Pi(p^2) = \frac{\lambda_Z^2}{M_Z^2 - p^2} + \Pi_{TW}(p^2) + \dots, \\ \Pi_-(p^2) = P_-^{\mu\nu\alpha\beta} \Pi_{\mu\nu\alpha\beta}(p) = \frac{\lambda_{X^-}^2}{M_{X^-}^2 - p^2} + \Pi_{TW}^-(p^2) + \dots, \\ \Pi_+(p^2) = P_+^{\mu\nu\alpha\beta} \Pi_{\mu\nu\alpha\beta}(p) = \frac{\lambda_{X^+}^2}{M_{X^+}^2 - p^2} + \dots, \quad (67)$$

we project out the components $\Pi_-(p^2)$ and $\Pi_+(p^2)$ by introducing the operators $P_-^{\mu\nu\alpha\beta}$ and $P_+^{\mu\nu\alpha\beta}$ respectively,

$$\begin{aligned} P_-^{\mu\nu\alpha\beta} &= \frac{1}{6} \left(g^{\mu\alpha} - \frac{p^\mu p^\alpha}{p^2} \right) \left(g^{\nu\beta} - \frac{p^\nu p^\beta}{p^2} \right), \\ P_+^{\mu\nu\alpha\beta} &= \frac{1}{6} \left(g^{\mu\alpha} - \frac{p^\mu p^\alpha}{p^2} \right) \left(g^{\nu\beta} - \frac{p^\nu p^\beta}{p^2} \right) - \frac{1}{6} g^{\mu\alpha} g^{\nu\beta}, \end{aligned} \quad (68)$$

$$\begin{aligned} \Pi_{TW}(p^2) &= \frac{\lambda_{DD^*}^2}{16\pi^2} \int_{\Delta_1^2}^{s_0} ds \frac{1}{s-p^2} \frac{\sqrt{\lambda(s, m_D^2, m_{D^*}^2)}}{s} \left[1 + \frac{\lambda(s, m_D^2, m_{D^*}^2)}{12sm_{D^*}^2} \right] \\ &\quad + \frac{\lambda_{DD_0}^2}{16\pi^2} \int_{\Delta_2^2}^{s_0} ds \frac{1}{s-p^2} \frac{\sqrt{\lambda(s, m_D^2, m_{D_0}^2)}}{s} \frac{\lambda(s, m_D^2, m_{D_0}^2)}{12s} + \dots, \end{aligned} \quad (69)$$

$$\begin{aligned} \Pi_{TW}^-(p^2) &= \frac{\lambda_{D_s^* D_{s1}}^2}{16\pi^2} \int_{\Delta_3^2}^{s_0} ds \frac{1}{s-p^2} \frac{\sqrt{\lambda(s, m_{D_s^*}^2, m_{D_{s1}}^2)}}{s} \left[1 + \frac{\lambda(s, m_{D_s^*}^2, m_{D_{s1}}^2)}{12sm_{D_s^*}^2} \frac{\lambda(s, m_{D_s^*}^2, m_{D_{s1}}^2)}{12sm_{D_{s1}}^2} \right] \\ &\quad + \frac{\lambda_{D_s^* D_s}^2}{16\pi^2} \int_{\Delta_4^2}^{s_0} ds \frac{1}{s-p^2} \frac{\sqrt{\lambda(s, m_{D_s^*}^2, m_{D_s}^2)}}{s} \frac{\lambda(s, m_{D_s^*}^2, m_{D_s}^2)}{12s} \\ &\quad + \frac{\lambda_{D_{s0} D_{s1}}^2}{16\pi^2} \int_{\Delta_5^2}^{s_0} ds \frac{1}{s-p^2} \frac{\sqrt{\lambda(s, m_{D_{s0}}^2, m_{D_{s1}}^2)}}{s} \frac{\lambda(s, m_{D_{s0}}^2, m_{D_{s1}}^2)}{12s} + \dots, \end{aligned} \quad (70)$$

where $\lambda_{DD^*}^2 = \frac{f_D^2 m_D^4 f_{D^*}^2 m_{D^*}^2}{m_c^2}$, $\Delta_1^2 = (m_D + m_{D^*})^2$, $\lambda_{DD_0}^2 = \frac{f_D^2 m_D^4 f_{D_0}^2}{m_c^2}$, $\Delta_2^2 = (m_D + m_{D_0})^2$, $\lambda_{D_s^* D_{s1}}^2 = f_{D_s^*}^2 m_{D_s^*}^2 f_{D_{s1}}^2 m_{D_{s1}}^2$, $\Delta_3^2 = (m_{D_s^*} + m_{D_{s1}})^2$, $\lambda_{D_s^* D_s}^2 = f_{D_s^*}^2 m_{D_s^*}^2 f_{D_s}^2 m_{D_s}^2$, $\Delta_4^2 = (m_{D_s^*} + m_{D_s})^2$, $\lambda_{D_{s0} D_{s1}}^2 = f_{D_{s0}}^2 f_{D_{s1}}^2 m_{D_{s1}}^2$, $\Delta_5^2 = (m_{D_{s0}} + m_{D_{s1}})^2$ and $\lambda(a, b, c) = a^2 + b^2 + c^2 - 2ab - 2bc - 2ca$.

The traditional hidden-flavor mesons have the normal quantum numbers, $J^{PC} = 0^{-+}, 0^{++}, 1^{--}, 1^{+-}, 1^{++}, 2^{--}, 2^{-+}, 2^{++}, \dots$. The component $\Pi_-(p^2)$ receives contributions with the exotic quantum numbers $J^{PC} = 1^{-+}$, the component $\Pi_+(p^2)$ receives contributions with the normal quantum numbers $J^{PC} = 1^{++}$. We choose the component $\Pi_-(p^2)$ with the exotic quantum numbers $J^{PC} = 1^{-+}$ and discard the component $\Pi_+(p^2)$ with the normal quantum numbers $J^{PC} = 1^{++}$. Thereafter, we will neglect the superscript $-$ in the X_c^- for simplicity.

According to the assertion of Lucha, Melikhov and Sazdjian [407, 408], all contributions of the order $\mathcal{O}(\alpha_s^k)$ with $k \leq 1$ are exactly canceled out by the two-meson scattering states, we set

$$\begin{aligned} \Pi(p^2) &= \Pi_{TW}(p^2) + \dots, \\ \Pi_-(p^2) &= \Pi_{TW}^-(p^2) + \dots, \end{aligned} \quad (71)$$

at the hadron side [409]. Then let us take the quark-hadron duality below the continuum threshold s_0 and perform Borel transformation with respect to the variable $P^2 = -p^2$ to obtain the QCD sum rules:

$$\begin{aligned} \Pi_{TW}(T^2) &= \frac{\lambda_{DD^*}^2}{16\pi^2} \int_{\Delta_1^2}^{s_0} ds \frac{\sqrt{\lambda(s, m_D^2, m_{D^*}^2)}}{s} \left[1 + \frac{\lambda(s, m_D^2, m_{D^*}^2)}{12sm_{D^*}^2} \right] \exp\left(-\frac{s}{T^2}\right) \\ &\quad + \frac{\lambda_{DD_0}^2}{16\pi^2} \int_{\Delta_2^2}^{s_0} ds \frac{\sqrt{\lambda(s, m_D^2, m_{D_0}^2)}}{s} \frac{\lambda(s, m_D^2, m_{D_0}^2)}{12s} \exp\left(-\frac{s}{T^2}\right) \\ &= \kappa \int_{4m_c^2}^{s_0} ds \rho_{Z, QCD}(s) \exp\left(-\frac{s}{T^2}\right), \end{aligned} \quad (72)$$

$$\begin{aligned}
\Pi_{TW}^-(T^2) &= \frac{\lambda_{D_s^* D_{s1}}^2}{16\pi^2} \int_{\Delta_3^2}^{s_0} ds \frac{\sqrt{\lambda(s, m_{D_s^*}^2, m_{D_{s1}}^2)}}{s} \left[1 + \frac{\lambda(s, m_{D_s^*}^2, m_{D_{s1}}^2)}{12sm_{D_s^*}^2} \frac{\lambda(s, m_{D_s^*}^2, m_{D_{s1}}^2)}{12sm_{D_{s1}}^2} \right] \exp\left(-\frac{s}{T^2}\right) \\
&+ \frac{\lambda_{D_s^* D_s}^2}{16\pi^2} \int_{\Delta_4^2}^{s_0} ds \frac{\sqrt{\lambda(s, m_{D_s^*}^2, m_{D_s}^2)}}{s} \frac{\lambda(s, m_{D_s^*}^2, m_{D_s}^2)}{12s} \exp\left(-\frac{s}{T^2}\right) \\
&+ \frac{\lambda_{D_{s0} D_{s1}}^2}{16\pi^2} \int_{\Delta_5^2}^{s_0} ds \frac{\sqrt{\lambda(s, m_{D_{s0}}^2, m_{D_{s1}}^2)}}{s} \frac{\lambda(s, m_{D_{s0}}^2, m_{D_{s1}}^2)}{12s} \exp\left(-\frac{s}{T^2}\right) \\
&= \kappa \int_{4m_c^2}^{s_0} ds \rho_{X, QCD}(s) \exp\left(-\frac{s}{T^2}\right), \tag{73}
\end{aligned}$$

the explicit expressions of the QCD spectral densities $\rho_{Z, QCD}(s)$ and $\rho_{X, QCD}(s)$ are given in Ref.[409]. We introduce the parameter κ to measure the deviations from 1, if $\kappa \approx 1$, we could get the conclusion tentatively that the two-meson scattering states can saturate the QCD sum rules. Then we differentiate Eqs.(72)-(73) with respect to $\frac{1}{T^2}$, and obtain two additional QCD sum rules,

$$-\frac{d\Pi_{TW}(T^2)}{d(1/T^2)} = -\kappa \frac{d}{d(1/T^2)} \int_{4m_c^2}^{s_0} ds \rho_{Z, QCD}(s) \exp\left(-\frac{s}{T^2}\right), \tag{74}$$

$$-\frac{d\Pi_{TW}^-(T^2)}{d(1/T^2)} = -\kappa \frac{d}{d(1/T^2)} \int_{4m_c^2}^{s_0} ds \rho_{X, QCD}(s) \exp\left(-\frac{s}{T^2}\right). \tag{75}$$

Thereafter, we will denote the QCD sum rules in Eqs.(74)-(75) as the QCDSR I, and the QCD sum rules in Eqs.(72)-(73) as the QCDSR II.

On the other hand, if the two-meson scattering states cannot saturate the QCD sum rules, we have to introduce the tetraquark molecular states to saturate the QCD sum rules,

$$\lambda_{Z/X}^2 \exp\left(-\frac{M_{Z/X}^2}{T^2}\right) = \int_{4m_c^2}^{s_0} ds \rho_{Z/Z, QCD}(s) \exp\left(-\frac{s}{T^2}\right), \tag{76}$$

then we differentiate Eq.(76) with respect to $\frac{1}{T^2}$, and obtain two QCD sum rules for the masses of the tetraquark molecular states,

$$M_{Z/X}^2 = \frac{-\frac{d}{d(1/T^2)} \int_{4m_c^2}^{s_0} ds \rho_{Z/X, QCD}(s) \exp\left(-\frac{s}{T^2}\right)}{\int_{4m_c^2}^{s_0} ds \rho_{Z/X, QCD}(s) \exp\left(-\frac{s}{T^2}\right)}. \tag{77}$$

In Fig.11, we plot the values of the κ with variations of the Borel parameters T^2 with the continuum threshold parameters $\sqrt{s_0} = 4.40 \text{ GeV}$ and 5.15 GeV for the $\bar{u}c\bar{c}d$ and $\bar{s}c\bar{c}s$ two-meson scattering states, respectively. From Fig.11, we can see explicitly that the values of the κ increase monotonically and quickly with the increase of the Borel parameters T^2 , no platform appears, which indicates that the QCD sum rules in Eqs.(72)-(73) obtained according to the assertion of Lucha, Melikhov and Sazdjian are unreasonable. Reasonable QCD sum rules lead to platforms flat enough or not flat enough, rather than no evidence of platforms, the two-meson scattering states cannot saturate the QCD sum rules.

We saturate the hadron side of the QCD sum rules with the tetraquark molecular states alone, and study the QCD sum rules shown in Eqs.(76)-(77). In Fig.12, we plot tetraquark molecule masses with variations of the Borel parameters T^2 . From the Fig.12, we observe that there appear Borel platforms in the Borel windows indeed, the relevant results are shown explicitly in Table 1, we adopt the energy scale formula $\mu = \sqrt{M_{X/Z}^2 - 4 \times (1.84 \text{ GeV})^2}$ to choose the best energy scales

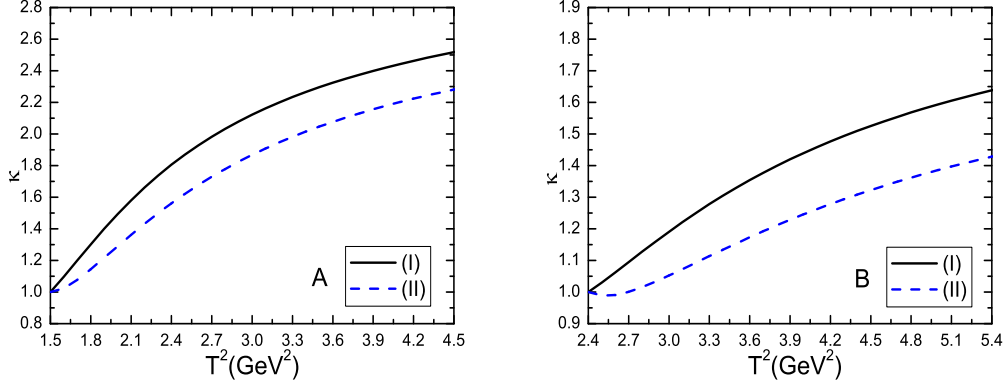


Figure 11: The κ with variations of the Borel parameters T^2 , where the A and B correspond to the $\bar{u}c\bar{c}d$ and $\bar{s}c\bar{c}s$ meson-meson scattering states, respectively, the (I) and (II) correspond to QCDSR I and II, respectively, the κ values are normalized to be 1 for the Borel parameters $T^2 = 1.5 \text{ GeV}^2$ and 2.4 GeV^2 , respectively.

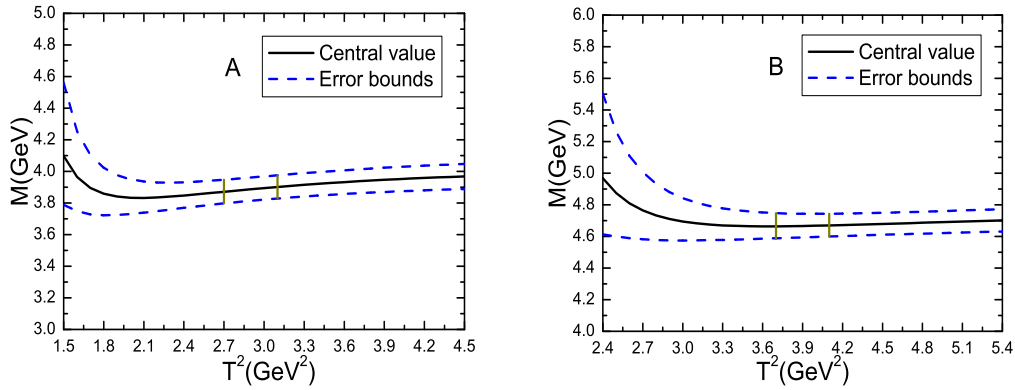


Figure 12: The masses with variations of the Borel parameters T^2 , where the A and B correspond to the $\bar{u}c\bar{c}d$ and $\bar{s}c\bar{c}s$ tetraquark molecular states, respectively, the regions between the two vertical lines are the Borel windows.

of the QCD spectral densities. The tetraquark molecular states alone can satisfy the QCD sum rules [409]. We obtain the prediction $M_Z = 3.89 \pm 0.09 \text{ GeV}$ and $M_X = 4.67 \pm 0.08 \text{ GeV}$, which are consistent with the $Z_c(3900)$ observed by the BESIII and Belle collaborations [162, 163] and the $X(4630)$ **observed one-year latter** by the LHCb collaboration [115]. If we have taken account of the light-flavor $SU(3)$ breaking effects of the energy scale formula, the fit between the theoretical calculation and experimental measurement would be better for the $X(4630)$.

The local currents do suppress but do not forbid the couplings between the four-quark currents and two-meson scattering states, as the overlaps of the wave-functions are very small [417], furthermore, the quantum field theory does not forbid the couplings between the four-quark currents and two-meson scattering states if they have the same quantum numbers. We study the contributions of the intermediate meson-meson scattering states $D\bar{D}^*$, $J/\psi\pi$, $J/\psi\rho$, etc besides the tetraquark molecular state Z_c to the correlation function $\Pi_{\mu\nu}(p)$ as an example,

$$\Pi_{\mu\nu}(p) = -\frac{\hat{\lambda}_Z^2}{p^2 - \hat{M}_Z^2 - \Sigma_{D\bar{D}^*}(p^2) - \Sigma_{J/\psi\pi}(p^2) - \Sigma_{J/\psi\rho}(p^2) + \dots} \tilde{g}_{\mu\nu}(p) + \dots, \quad (78)$$

where $\tilde{g}_{\mu\nu}(p) = -g_{\mu\nu} + \frac{p_\mu p_\nu}{p^2}$. We choose the bare quantities $\hat{\lambda}_Z$ and \hat{M}_Z to absorb the divergences in the self-energies $\Sigma_{D\bar{D}^*}(p^2)$, $\Sigma_{J/\psi\pi}(p^2)$, $\Sigma_{J/\psi\rho}(p^2)$, etc. The renormalized energies satisfy the relation $p^2 - M_Z^2 - \overline{\Sigma}_{D\bar{D}^*}(p^2) - \overline{\Sigma}_{J/\psi\pi}(p^2) - \overline{\Sigma}_{J/\psi\rho}(p^2) + \dots = 0$, where the overlines above the self-energies denote that the divergent terms have been subtracted. As the tetraquark molecular state Z_c is unstable, the relation should be modified, $p^2 - M_Z^2 - \text{Re}\overline{\Sigma}_{D\bar{D}^*}(p^2) - \text{Re}\overline{\Sigma}_{J/\psi\pi}(p^2) - \text{Re}\overline{\Sigma}_{J/\psi\rho}(p^2) + \dots = 0$, and $-\text{Im}\overline{\Sigma}_{D\bar{D}^*}(p^2) - \text{Im}\overline{\Sigma}_{J/\psi\pi}(p^2) - \text{Im}\overline{\Sigma}_{J/\psi\rho}(p^2) + \dots = \sqrt{p^2}\Gamma(p^2)$. The renormalized self-energies contribute a finite imaginary part to modify the dispersion relation,

$$\Pi_{\mu\nu}(p) = -\frac{\lambda_Z^2}{p^2 - M_Z^2 + i\sqrt{p^2}\Gamma(p^2)} \tilde{g}_{\mu\nu}(p) + \dots. \quad (79)$$

If we assign the $Z_c(3900)$ to be the $D\bar{D}^* + D^*\bar{D}$ tetraquark molecular state with the $J^{PC} = 1^{+-}$ [81, 82, 83], the physical width $\Gamma_{Z_c(3900)}(M_Z^2) = (28.2 \pm 2.6) \text{ MeV}$ from the Particle Data Group [411].

We take account of the finite width effect by the simple replacement of the hadronic spectral density,

$$\lambda_Z^2 \delta(s - M_Z^2) \rightarrow \lambda_Z^2 \frac{1}{\pi} \frac{M_Z \Gamma_Z(s)}{(s - M_Z^2)^2 + M_Z^2 \Gamma_Z^2(s)}, \quad (80)$$

where

$$\Gamma_Z(s) = \Gamma_Z \frac{M_Z}{\sqrt{s}} \sqrt{\frac{s - (M_D + M_{D^*})^2}{M_Z^2 - (M_D + M_{D^*})^2}}. \quad (81)$$

Then the hadron sides of the QCD sum rules in Eq.(76) and Eq.(77) undergo the following changes,

$$\begin{aligned} \lambda_Z^2 \exp\left(-\frac{M_Z^2}{T^2}\right) &\rightarrow \lambda_Z^2 \int_{(m_D+m_{D^*})^2}^{s_0} ds \frac{1}{\pi} \frac{M_Z \Gamma_Z(s)}{(s - M_Z^2)^2 + M_Z^2 \Gamma_Z^2(s)} \exp\left(-\frac{s}{T^2}\right), \\ &= (0.78 \sim 0.79) \lambda_Z^2 \exp\left(-\frac{M_Z^2}{T^2}\right), \end{aligned} \quad (82)$$

$$\begin{aligned} \lambda_Z^2 M_Z^2 \exp\left(-\frac{M_Z^2}{T^2}\right) &\rightarrow \lambda_Z^2 \int_{(m_D+m_{D^*})^2}^{s_0} ds s \frac{1}{\pi} \frac{M_Z \Gamma_Z(s)}{(s - M_Z^2)^2 + M_Z^2 \Gamma_Z^2(s)} \exp\left(-\frac{s}{T^2}\right), \\ &= (0.80 \sim 0.81) \lambda_Z^2 M_Z^2 \exp\left(-\frac{M_Z^2}{T^2}\right), \end{aligned} \quad (83)$$

J^{PC}	$T^2(\text{GeV}^2)$	$\sqrt{s_0}(\text{GeV})$	$\mu(\text{GeV})$	pole	$M(\text{GeV})$	$\lambda(10^{-2}\text{GeV}^5)$
$1^{+-}(\bar{u}c\bar{c}d)$	$2.7 - 3.1$	4.40 ± 0.10	1.3	$(40 - 63)\%$	3.89 ± 0.09	1.72 ± 0.30
$1^{-+}(\bar{s}c\bar{c}s)$	$3.7 - 4.1$	5.15 ± 0.10	2.9	$(42 - 60)\%$	4.67 ± 0.08	6.87 ± 0.84

Table 1: The Borel windows, continuum threshold parameters, energy scales of the QCD spectral densities, pole contributions, masses and pole residues of the $\bar{u}c\bar{c}d$ and $\bar{s}c\bar{c}s$ tetraquark molecular states [409].

for the value $\sqrt{s_0} = 4.40 \text{ GeV}$. We can absorb the numerical factors $0.78 \sim 0.79$ and $0.80 \sim 0.81$ into the pole residue with the simple replacement $\lambda_Z \rightarrow 0.89\lambda_Z$ safely, the intermediate meson-loops cannot affect the mass M_Z significantly, but affect the pole residue remarkably, which are consistent with the fact that we obtain the masses of the tetraquark molecular states from a fraction, see Eq.(77).

We obtain the conclusion confidently that it is reliable to study the multiquark states with the QCD sum rules, the contaminations from the two-particle scattering states play a tiny role [409].

2.4 Energy scale dependence of the QCD sum rules

In calculating the Feynman diagrams, we usually adopt the dimensional regularization to regularize the divergences, and resort to wave-function, quark-mass and current renormalizations to absorb the ultraviolet divergences, and resort to the vacuum condensate redefinitions to absorb the infrared divergences. Thus, the correlation functions $\Pi(p^2)$ are free of divergences. And we expect to calculate the $\Pi(p^2)$ at any energy scale μ at which perturbative calculations are feasible, and the physical quantities are independent on the specified energy scale μ . Roughly speaking, the correlation functions $\Pi(p^2)$ are independent on the energy scale approximately,

$$\frac{d}{d\mu}\Pi(p^2) = 0, \quad (84)$$

at least the bare $\Pi(p^2)$ are independent on the energy scale.

We write down the correlation functions $\Pi(p^2)$ for the hidden-charm (or hidden-bottom) four-quark currents, the most commonly chosen currents in studying the X , Y and Z states, in the Källén-Lehmann representation,

$$\Pi(p^2) = \int_{4m_Q^2(\mu)}^{s_0} ds \frac{\rho_{QCD}(s, \mu)}{s - p^2} + \int_{s_0}^{\infty} ds \frac{\rho_{QCD}(s, \mu)}{s - p^2}. \quad (85)$$

In fact, there are subtraction terms neglected at the right side of Eq.(85), which could be deleted after performing the Borel transformation. The $\Pi(p^2)$ should be independent on the energy scale we adopt to perform the operator product expansion, but which does not mean

$$\frac{d}{d\mu} \int_{4m_Q^2(\mu)}^{s_0} ds \frac{\rho_{QCD}(s, \mu)}{s - p^2} \rightarrow 0, \quad (86)$$

due to the two features inherited from the QCD sum rules:

- Perturbative corrections are neglected, even in the QCD sum rules for the traditional mesons, we cannot take account of the radiative corrections up to arbitrary orders, for example, we only have calculated the radiative corrections up to the order $\mathcal{O}(\alpha_s^2)$ for the pseudoscalar D/B mesons up to now [419, 420, 421]. The higher dimensional vacuum condensates are factorized into lower dimensional ones based on the vacuum saturation, for example,

$$\langle \bar{\psi}\Gamma\psi\bar{\psi}\Gamma\psi \rangle = \frac{1}{144} \langle \bar{\psi}\psi \rangle^2 [\text{Tr}(\Gamma)\text{Tr}(\Gamma) - \text{Tr}(\Gamma\Gamma)], \quad (87)$$

where $\psi = u, d$ or s , $\text{Tr} = \text{Tr}_D \text{Tr}_C$, the subscripts denote the Dirac spinor and color spaces, respectively, therefore the energy scale dependence of the higher dimensional vacuum condensates is modified.

- Truncations s_0 which are physical quantities determined by the experimental data set in, the correlations between the thresholds $4m_Q^2(\mu)$ and continuum thresholds s_0 are unknown. Quark-hadron duality is just an assumption.

After performing the Borel transformation, we obtain the integrals

$$\int_{4m_Q^2(\mu)}^{s_0} ds \rho_{QCD}(s, \mu) \exp\left(-\frac{s}{T^2}\right), \quad (88)$$

which are sensitive to the Q -quark mass $m_Q(\mu)$, in other words, the energy scale μ . Variations of the energy scale μ can lead to changes of integral ranges $4m_Q^2(\mu) - s_0$ of the variable ds besides the QCD spectral densities $\rho_{QCD}(s, \mu)$, therefore changes of the Borel windows and predicted hadron masses and pole residues. The strong fine-structure $\alpha_s = \frac{g_s^2}{4\pi}$ appears even in the tree-level,

$$\langle \bar{q} \gamma_\mu t^a q D_\eta g_s G_{\lambda\tau}^a \rangle = \frac{g_\eta \lambda g_{\mu\tau} - g_{\eta\tau} g_{\mu\lambda}}{27} 4\pi \alpha_s \langle \bar{q} q \rangle^2, \quad (89)$$

where $t^a = \frac{\lambda^a}{2}$. Thus we have to deal with the energy scale dependence of the QCD sum rules.

Let us take a short digression and perform some phenomenological analysis. We can describe the heavy four-quark systems $Q\bar{Q}q\bar{q}$ by a double-well potential with two light quarks $q\bar{q}$ lying in the two wells, respectively. In the heavy quark limit, the Q -quark serves as a static well potential and attracts with the light quark q to form a heavy diquark \mathcal{D}_{qQ}^i in color antitriplet,

$$q + Q \rightarrow \mathcal{D}_{qQ}^i, \quad (90)$$

or attracts with the light antiquark \bar{q} to form a meson-like color-singlet cluster (meson-like color-octet cluster),

$$\bar{q} + Q \rightarrow \bar{q}Q (\bar{q}\lambda^a Q), \quad (91)$$

the \bar{Q} -quark serves as another static well potential and attracts with the light antiquark \bar{q} to form a heavy antidiquark $\mathcal{D}_{\bar{q}\bar{Q}}^i$ in color triplet,

$$\bar{q} + \bar{Q} \rightarrow \mathcal{D}_{\bar{q}\bar{Q}}^i, \quad (92)$$

or attracts with the light quark q to form a heavy meson-like color-singlet cluster (meson-like color-octet-cluster),

$$q + \bar{Q} \rightarrow \bar{Q}q (\bar{Q}\lambda^a q). \quad (93)$$

Then

$$\begin{aligned} \mathcal{D}_{qQ}^i + \mathcal{D}_{\bar{q}\bar{Q}}^i &\rightarrow \mathbf{\bar{3}3} - \text{type tetraquark states}, \\ \bar{q}Q + \bar{Q}q &\rightarrow \mathbf{11} - \text{type tetraquark states}, \\ \bar{q}\lambda^a Q + \bar{Q}\lambda^a q &\rightarrow \mathbf{88} - \text{type tetraquark states}, \end{aligned} \quad (94)$$

the two heavy quarks Q and \bar{Q} stabilize the four-quark systems $q\bar{q}Q\bar{Q}$, just as in the case of the $(\mu^- e^+)(\mu^+ e^-)$ molecule in QED [57].

We can also describe the hidden-charm (or hidden-bottom) five-quark systems $qq_1q_2Q\bar{Q}$ by a double-well potential. In the heavy quark limit, the Q -quark (\bar{Q} -quark) serves as a static well potential, the diquark $\mathcal{D}_{q_1q_2}^j$ and quark q lie in the two wells, respectively,

$$\begin{aligned} q_1 + q_2 + \bar{Q} &\rightarrow \mathcal{D}_{q_1q_2}^j + \bar{Q}^k \rightarrow \mathcal{T}_{q_1q_2\bar{Q}}^i, \\ q + Q &\rightarrow \mathcal{D}_{qQ}^i, \end{aligned} \quad (95)$$

or

$$\begin{aligned} q_1 + q_2 + Q &\rightarrow \mathcal{D}_{q_1 q_2}^j + Q^j \rightarrow q_1 q_2 Q, \\ q + \bar{Q} &\rightarrow q \bar{Q}, \end{aligned} \quad (96)$$

where the $\mathcal{T}_{q_1 q_2 \bar{Q}}^i$ denotes the heavy triquark in the color triplet. Then

$$\begin{aligned} \mathcal{D}_{qQ}^i + \mathcal{T}_{q_1 q_2 \bar{Q}}^i &\rightarrow \bar{\mathbf{3}}\bar{\mathbf{3}}\bar{\mathbf{3}} - \text{type pentaquark states}, \\ q_1 q_2 Q + \bar{Q} q &\rightarrow \mathbf{11} - \text{type pentaquark states}. \end{aligned} \quad (97)$$

Now we can obtain the conclusion tentatively that the heavy tetraquark states are characterized by the effective heavy quark masses \mathbb{M}_Q (or constituent quark masses) and the virtuality $V = \sqrt{M_{X/Y/Z}^2 - (2\mathbb{M}_Q)^2}$ (or bound energy not as robust) [81, 422, 423, 424].

In summary, the QCD sum rules have three typical energy scales μ^2 , T^2 , V^2 . It is natural to set the energy scales as,

$$\mu^2 = V^2 = \mathcal{O}(T^2), \quad (98)$$

and we obtain the energy scale formula [424],

$$\mu = \sqrt{M_{X/Y/Z/P}^2 - (2\mathbb{M}_Q)^2}, \quad (99)$$

which works very well for the tetraquark states and pentaquark states. It can improve the convergence of the operator product expansion remarkably and enhance the pole contributions remarkably.

We usually set the small u and d quark masses to be zero, and take account of the light-flavor $SU(3)$ breaking effects by introducing an effective s -quark mass \mathbb{M}_s , thus we reach the modified energy scale formula,

$$\mu = \sqrt{M_{X/Y/Z/P}^2 - (2\mathbb{M}_Q)^2 - \kappa \mathbb{M}_s}, \quad (100)$$

to choose the suitable energy scales of the QCD spectral densities [61, 82, 83, 172, 425], where the $\kappa = 0, 1$ and 2 denote the numbers of the s -quarks, the \mathbb{M}_Q and \mathbb{M}_s have universal values to be commonly used elsewhere.

We can rewrite the energy scale formula in Eq.(99) in the following form,

$$M_{X/Y/Z/P}^2 = \mu^2 + \text{Constants}, \quad (101)$$

where the Constants have the values $4\mathbb{M}_Q^2$ [426]. As we cannot obtain energy scale independent QCD sum rules, we conjecture that the predicted multi-quark masses and the pertinent energy scales of the QCD spectral densities have a Regge-trajectory-like relation, see Eq.(101), where the Constants are free parameters and fitted by the QCD sum rules. Direct calculations have proven that the Constants have universal values and work well. We take account of the light-flavor $SU(3)$ breaking effects, and write down the modified energy scale formula [418],

$$M_{X/Y/Z/P}^2 = (\mu + \kappa \mathbb{M}_s)^2 + \text{Constants}. \quad (102)$$

In Ref.[60], we take the $X(3872)$ and $Z_c(3900)$ as the hidden-charm tetraquark with the $J^{PC} = 1^{++}$ and 1^{+-} , respectively, and explore the energy scale dependence of the QCD sum rules for the exotic states for the first time. In Fig.13, we plot the mass of the $Z_c(3900)$ with variations of the Borel parameter T^2 and energy scale μ for the continuum threshold parameter $\sqrt{s_0} = 4.4 \text{ GeV}$. From the figure, we can see clearly that the mass decreases monotonously with increase of the energy

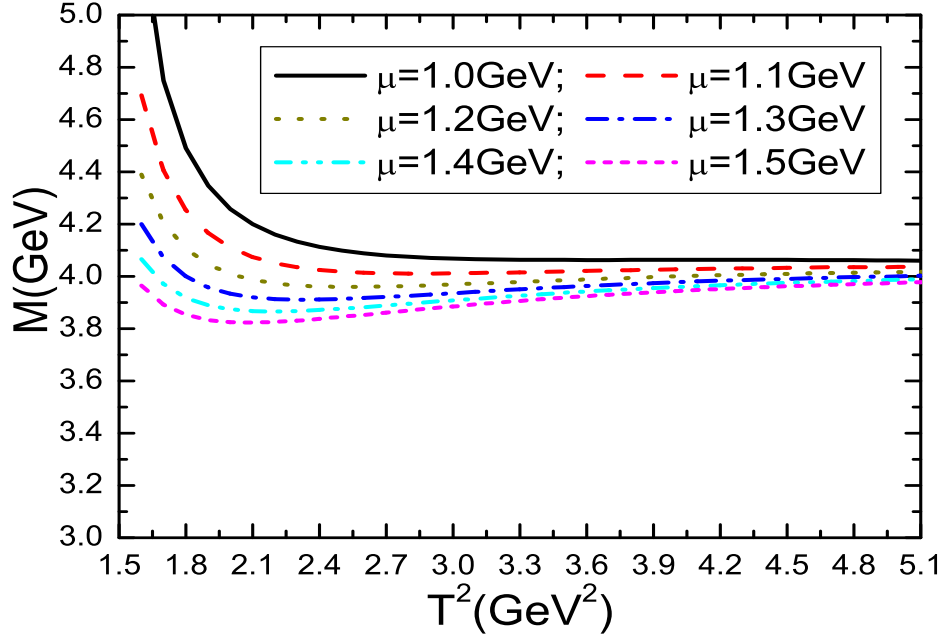


Figure 13: The mass with variation of the Borel parameter T^2 and energy scale μ for the $Z_c(3900)$.

scale. The energy scale $\mu = 1.4$ GeV is the lowest energy scale to reproduce the experimental data [162, 163].

There are three schemes to choose the input parameters at the QCD side of the QCD sum rules:

Scheme I. We take the energy scale formula and its modifications, see Eqs.(99)-(100), to choose the energy scales of the QCD spectral densities in a consistent way.

Scheme II. We take the \overline{MS} (modified-minimal-subtraction) masses for the heavy quarks $m_Q(m_Q)$, and take the light quark masses and vacuum condensates at the energy scale $\mu = 1$ GeV.

Scheme III. We take all the input parameters at the energy scale $\mu = 1$ GeV.

The **Scheme II** is adopted in most QCD sum rules [46, 47, 58, 180, 427, 428, 429, 430, 431, 432, 433, 434, 435, 436, 437, 438, 439, 440, 441, 442, 443, 444, 445, 446, 447, 448, 449, 450, 451, 452, 453, 454, 455, 456, 457, 458, 459, 460, 461] ([462, 463, 464, 465, 466, 467, 468, 469, 470, 471, 472, 473, 474]), where the \overline{MS} masses $m_Q(m_Q)$ are usually smaller than (or equal to) the values from the Particle Data Group (with much smaller pole contributions) [97].

The **Scheme III** was adopted in early works of Wang and his collaborators in 2009-2011 [475, 476, 477, 478, 479, 480, 481, 482, 483, 484, 485, 486], where many elegant four-quark currents were constructed originally.

In Ref.[487], we study the pentaquark molecular states in the three schemes in details and examine their advantages and shortcomings, in **Scheme I** and **III**, we truncate the operator product expansion up to the vacuum condensates of $D = 13$, while in **Scheme II**, we truncate the operator product expansion up to the vacuum condensates of $D = 10$, which is commonly adopted in this case.

We write down the correlation functions $\Pi(p)$, $\Pi_{\mu\nu}(p)$ and $\Pi_{\mu\nu\alpha\beta}(p)$ firstly,

$$\begin{aligned}\Pi(p) &= i \int d^4x e^{ip \cdot x} \langle 0 | T \{ J(x) \bar{J}(0) \} | 0 \rangle, \\ \Pi_{\mu\nu}(p) &= i \int d^4x e^{ip \cdot x} \langle 0 | T \{ J_\mu(x) \bar{J}_\nu(0) \} | 0 \rangle, \\ \Pi_{\mu\nu\alpha\beta}(p) &= i \int d^4x e^{ip \cdot x} \langle 0 | T \{ J_{\mu\nu}(x) \bar{J}_{\alpha\beta}(0) \} | 0 \rangle,\end{aligned}\quad (103)$$

where the currents $J(x) = J^{\bar{D}\Sigma_c}(x)$, $J_\mu(x) = J_\mu^{\bar{D}\Sigma_c^*}(x)$, $J_{\mu\nu}^{\bar{D}^*\Sigma_c}(x)$, $J_{\mu\nu}(x) = J_{\mu\nu}^{\bar{D}^*\Sigma_c^*}(x)$,

$$\begin{aligned}J^{\bar{D}\Sigma_c}(x) &= \bar{c}(x) i \gamma_5 u(x) \varepsilon^{ijk} u_i^T(x) C \gamma_\alpha d_j(x) \gamma^\alpha \gamma_5 c_k(x), \\ J_\mu^{\bar{D}\Sigma_c^*}(x) &= \bar{c}(x) i \gamma_5 u(x) \varepsilon^{ijk} u_i^T(x) C \gamma_\mu d_j(x) c_k(x), \\ J_\mu^{\bar{D}^*\Sigma_c}(x) &= \bar{c}(x) \gamma_\mu u(x) \varepsilon^{ijk} u_i^T(x) C \gamma_\alpha d_j(x) \gamma^\alpha \gamma_5 c_k(x), \\ J_{\mu\nu}^{\bar{D}^*\Sigma_c^*}(x) &= \bar{c}(x) \gamma_\mu u(x) \varepsilon^{ijk} u_i^T(x) C \gamma_\nu d_j(x) c_k(x) + (\mu \leftrightarrow \nu).\end{aligned}\quad (104)$$

We separate the contributions of the molecular states with the $J^P = \frac{1}{2}^\pm, \frac{3}{2}^\pm$ and $\frac{5}{2}^\pm$ unambiguously, then we introduce the weight functions $\sqrt{s} \exp(-\frac{s}{T^2})$ and $\exp(-\frac{s}{T^2})$ to obtain the QCD sum rules at the hadron side,

$$\int_{4m_c^2}^{s_0} ds [\sqrt{s} \rho_{j,H}^1(s) \pm \rho_{j,H}^0(s)] \exp\left(-\frac{s}{T^2}\right) = 2M_\mp \lambda_j^{\mp 2} \exp\left(-\frac{M_\mp^2}{T^2}\right), \quad (105)$$

where the s_0 are the continuum threshold parameters and the T^2 are the Borel parameters, the $\rho_{j,H}^1(s)$ and $\rho_{j,H}^0(s)$ with the $j = \frac{1}{2}, \frac{3}{2}$ and $\frac{5}{2}$ are hadronic spectral densities, the λ_j^\pm are the pole residues.

We perform the operator product expansion to obtain the analytical QCD spectral densities $\rho_{j,QCD}^1(s)$ and $\rho_{j,QCD}^0(s)$ through dispersion relation, then we take the quark-hadron duality below the continuum thresholds s_0 and introduce the weight functions $\sqrt{s} \exp(-\frac{s}{T^2})$ and $\exp(-\frac{s}{T^2})$ to obtain the QCD sum rules:

$$2M_- \lambda_j^{-2} \exp\left(-\frac{M_-^2}{T^2}\right) = \int_{4m_c^2}^{s_0} ds [\sqrt{s} \rho_{j,QCD}^1(s) + \rho_{j,QCD}^0(s)] \exp\left(-\frac{s}{T^2}\right). \quad (106)$$

For the technical details, one can consult Ref.[487] or Sect.5.1.

We differentiate Eq.(106) with respect to $\tau = \frac{1}{T^2}$, then eliminate the pole residues to obtain the molecule masses,

$$M_-^2 = \frac{-\frac{d}{d\tau} \int_{4m_c^2}^{s_0} ds [\sqrt{s} \rho_{QCD}^1(s) + \rho_{QCD}^0(s)] \exp(-\tau s)}{\int_{4m_c^2}^{s_0} ds [\sqrt{s} \rho_{QCD}^1(s) + \rho_{QCD}^0(s)] \exp(-\tau s)}, \quad (107)$$

where $\rho_{QCD}^1(s) = \rho_{j,QCD}^1(s)$ and $\rho_{QCD}^0(s) = \rho_{j,QCD}^0(s)$.

We show the Borel windows T^2 , continuum threshold parameters s_0 , energy scales of the QCD spectral densities and pole contributions of the ground states explicitly in Table 2. In the **Scheme III**, the pole contributions are less than 25%, which are too small, and the **Scheme III** could be abandoned. On the other hand, the convergent behaviors of the operator product expansion have relation **Scheme I** > **Scheme II** > **Scheme III**.

At last, we take account of all uncertainties of the input parameters, and obtain the masses and pole residues of the molecular states, which are shown explicitly in Table 3 and Figs.14-15.

In Figs.14-15, we plot the masses at much larger ranges of the Borel parameters than the Borel windows. The predicted masses in the **Scheme I** decrease monotonously and quickly with increase

	J^P	D	$\mu(\text{GeV})$	$T^2(\text{GeV}^2)$	$s_0(\text{GeV}^2)$	pole
$\bar{D}^0 \Sigma_c^+(2455)$	$\frac{1}{2}^-$	13	2.2	3.1 – 3.5	25.0 ± 1.0	(41 – 62)%
		10	1.0	2.7 – 3.1	24.5 ± 1.0	(38 – 63)%
		13	1.0	3.4 – 4.2	21.5 ± 1.0	(7 – 24)%
$\bar{D}^0 \Sigma_c^{*+}(2520)$	$\frac{3}{2}^-$	13	2.4	3.3 – 3.7	25.5 ± 1.0	(39 – 59)%
		10	1.0	2.8 – 3.2	25.5 ± 1.0	(40 – 64)%
		13	1.0	3.5 – 4.3	22.0 ± 1.0	(7 – 23)%
$\bar{D}^{*0} \Sigma_c^+(2455)$	$\frac{3}{2}^-$	13	2.5	3.3 – 3.7	26.5 ± 1.0	(40 – 60)%
		10	1.0	2.8 – 3.2	26.5 ± 1.0	(40 – 65)%
		13	1.0	3.7 – 4.6	23.0 ± 1.0	(5 – 19)%
$\bar{D}^{*0} \Sigma_c^{*+}(2520)$	$\frac{5}{2}^-$	13	2.6	3.4 – 3.8	27.0 ± 1.0	(39 – 59)%
		10	1.0	3.0 – 3.4	27.5 ± 1.0	(39 – 62)%
		13	1.0	3.5 – 4.4	23.5 ± 1.0	(7 – 25)%

Table 2: The truncations of the operator product expansion D , energy scales μ , Borel parameters T^2 , continuum threshold parameters s_0 and pole contributions for the hidden-charm pentaquark molecular states, where the $\mu = 1 \text{ GeV}$ denote the energy scale of the vacuum condensates, and the data are listed in **Scheme I**, **II**, **III** sequentially [487].

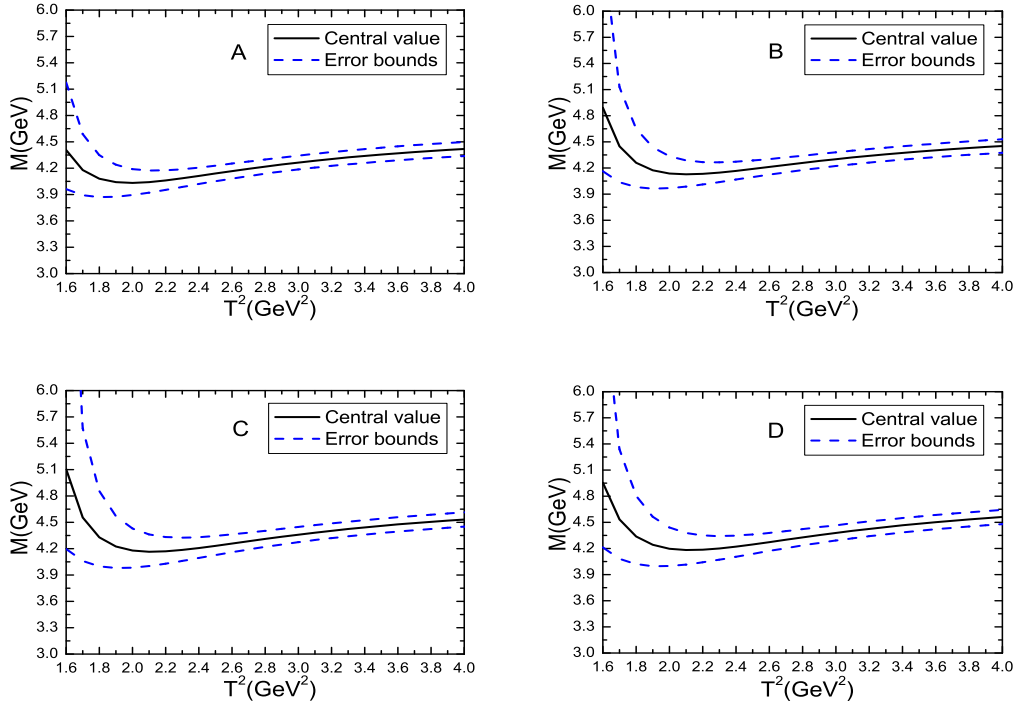


Figure 14: The masses of the molecular states with variations of the Borel parameter T^2 in the **Scheme I**, where the A, B, C and D denote the molecular states $\bar{D}\Sigma_c$, $\bar{D}\Sigma_c^*$, $\bar{D}^*\Sigma_c$ and $\bar{D}^*\Sigma_c^*$, respectively.

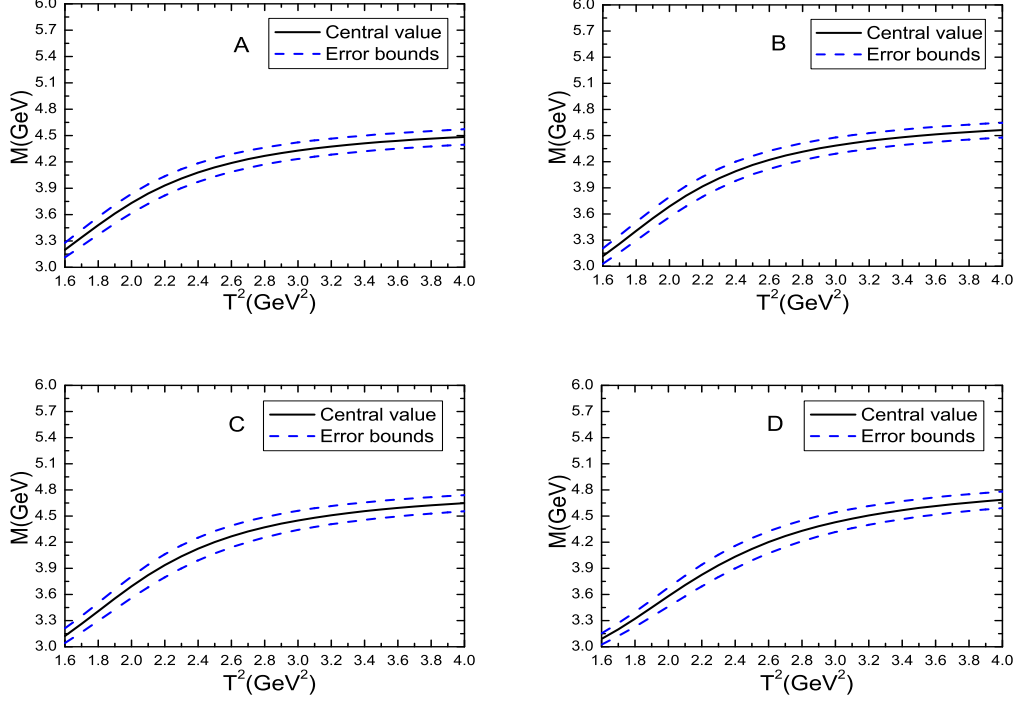


Figure 15: The masses of the molecular states with variations of the Borel parameter T^2 in the **Scheme II**, where the A, B, C and D denote the molecular states $\bar{D}\Sigma_c$, $\bar{D}\Sigma_c^*$, $\bar{D}^*\Sigma_c$ and $\bar{D}^*\Sigma_c^*$, respectively.

	J^P	D	$\mu(\text{GeV})$	$M(\text{GeV})$	$\lambda(10^{-3}\text{GeV}^6)$	Thresholds (MeV)
$\bar{D}^0 \Sigma_c^+(2455)$	$\frac{1}{2}^-$	13	2.2	$4.32^{+0.11}_{-0.11}$	$1.95^{+0.37}_{-0.33}$	4318
		10	1.0	$4.30^{+0.14}_{-0.17}$	$1.00^{+0.27}_{-0.24}$	
		13	1.0	$4.30^{+0.09}_{-0.10}$	$0.77^{+0.19}_{-0.15}$	
$\bar{D}^0 \Sigma_c^+(2520)$	$\frac{3}{2}^-$	13	2.4	$4.39^{+0.10}_{-0.11}$	$1.23^{+0.21}_{-0.20}$	4382
		10	1.0	$4.39^{+0.14}_{-0.17}$	$0.64^{+0.16}_{-0.15}$	
		13	1.0	$4.38^{+0.10}_{-0.09}$	$0.47^{+0.11}_{-0.09}$	
$\bar{D}^{*0} \Sigma_c^+(2455)$	$\frac{3}{2}^-$	13	2.5	$4.46^{+0.11}_{-0.12}$	$2.31^{+0.41}_{-0.38}$	4460
		10	1.0	$4.45^{+0.16}_{-0.20}$	$1.15^{+0.31}_{-0.29}$	
		13	1.0	$4.48^{+0.11}_{-0.10}$	$0.88^{+0.19}_{-0.18}$	
$\bar{D}^{*0} \Sigma_c^+(2520)$	$\frac{5}{2}^-$	13	2.6	$4.50^{+0.12}_{-0.12}$	$1.74^{+0.31}_{-0.28}$	4524
		10	1.0	$4.51^{+0.16}_{-0.19}$	$0.93^{+0.25}_{-0.22}$	
		13	1.0	$4.51^{+0.11}_{-0.10}$	$0.66^{+0.15}_{-0.12}$	

Table 3: The masses and pole residues of the hidden-charm pentaquark molecular states, where the data are listed in **Scheme I, II, III** sequentially [487].

of the Borel parameters at the region $T^2 \leq 2.0 \text{ GeV}^2$, then reach small platforms and increase slowly with increase of the Borel parameters. The predicted masses in the **Scheme II** increase monotonously and quickly with increase of the Borel parameters at the region $T^2 < 2.6 \text{ GeV}^2$, then increase slowly and steadily with increase of the Borel parameters. It is obvious that the flatness of the platforms have relation **Scheme I** > **Scheme II**.

Both the predictions in the **Scheme I** and **II** support assigning the $P_c(4312)$ as the $\bar{D}\Sigma_c$ molecular state with the $J^P = \frac{1}{2}^-$, assigning the $P_c(4380)$ as the $\bar{D}\Sigma_c^*$ molecular state with the $J^P = \frac{3}{2}^-$, assigning the $P_c(4440/4457)$ as the $\bar{D}^*\Sigma_c$ molecular state with the $J^P = \frac{3}{2}^-$ or the $\bar{D}^*\Sigma_c^*$ molecular state with the $J^P = \frac{5}{2}^-$. However, if we take account of the vacuum condensates of the dimensions of $D = 11$ and 13 in the **Scheme II**, we would obtain a mass about 200 MeV larger than the corresponding one given in Table 3, so we prefer the **Scheme I** [487].

3 $\bar{3}3$ type tetraquark states

3.1 Hidden-heavy tetraquark states

The scattering amplitude for one-gluon exchange is proportional to,

$$\left(\frac{\lambda^a}{2}\right)_{ij} \left(\frac{\lambda^a}{2}\right)_{kl} = -\frac{1}{3}(\delta_{ij}\delta_{kl} - \delta_{il}\delta_{kj}) + \frac{1}{6}(\delta_{ij}\delta_{kl} + \delta_{il}\delta_{kj}), \quad (108)$$

the negative (positive) sign in front of the antisymmetric antitriplet $\bar{\mathbf{3}}$ (symmetric sextet $\mathbf{6}$) indicates the interaction is attractive (repulsive), which favors (disfavors) formation of the diquarks in color $\bar{\mathbf{3}}$ ($\mathbf{6}$). We usually construct the $\bar{\mathbf{3}}\mathbf{3}$ type color-singlet four-quark currents $J_{\bar{\mathbf{3}}\mathbf{3}}$ to interpolate the tetraquark states,

$$J_{\bar{\mathbf{3}}\mathbf{3}} = \varepsilon^{kij} \varepsilon^{kmn} q_i^T C \Gamma q'_j \bar{q}_m \Gamma' C \bar{q}_n'^T, \quad (109)$$

where the q and q' are the quarks, the Γ and Γ' are the Dirac γ -matrixes. The color factor has the relation,

$$\varepsilon^{kij} \varepsilon^{kmn} = \delta_{im} \delta_{jn} - \delta_{in} \delta_{jm}. \quad (110)$$

With the simple replacement,

$$\delta_{im} \delta_{jn} - \delta_{in} \delta_{jm} \rightarrow \delta_{im} \delta_{jn} + \delta_{in} \delta_{jm}, \quad (111)$$

we obtain the corresponding $\mathbf{6}\bar{\mathbf{6}}$ type currents $J_{\mathbf{6}\bar{\mathbf{6}}}$,

$$J_{\mathbf{6}\bar{\mathbf{6}}} = q_i^T C \Gamma q'_j \bar{q}_i \Gamma' C \bar{q}_j'^T + q_i^T C \Gamma q'_j \bar{q}_j \Gamma' C \bar{q}_i'^T. \quad (112)$$

If the $J_{\mathbf{6}\bar{\mathbf{6}}}$ type currents satisfy the Fermi-Dirac statistics, the quantum field theory does not forbid their existence. In fact, in the potential quark models, we usually take both the $\bar{\mathbf{3}}\mathbf{3}$ and $\mathbf{6}\bar{\mathbf{6}}$ diquark configurations, see Sect.2.1.5. The $\mathbf{6}\bar{\mathbf{6}}$ type currents are also widely used in literatures [34, 42, 121, 134, 185, 437, 488, 489, 490, 491, 492, 493].

Or we construct the $\mathbf{8}\mathbf{8}$ type currents directly to interpolate the exotic states [455, 459, 494, 495, 496, 497], although the one-gluon exchange induced interaction is repulsive in this channel, see Sect.2.1.5. In Ref.[496], we take the $Z_c(4200)$ as the $\mathbf{8}\mathbf{8}$ type axial-vector molecule-like state, and construct the $\mathbf{8}\mathbf{8}$ type axial-vector current to study its mass and width with the QCD sum rules, the numerical results support assigning the $Z_c(4200)$ as the $\mathbf{8}\mathbf{8}$ type molecule-like state with the $J^{PC} = 1^{+-}$. Furthermore, we discuss the possible assignments of the $Z_c(3900)$, $Z_c(4200)$ and $Z(4430)$ as the $\bar{\mathbf{3}}\mathbf{3}$ type tetraquark states with the $J^{PC} = 1^{+-}$.

3.1.1 Tetraquark states with positive parity

The one-gluon-exchange induced attractive interactions favor formation of the diquarks in the color antitriplet, flavor antitriplet and spin singlet [311], while the most favored configurations are the scalar and axialvector diquark states [498, 499, 500, 501, 502, 503, 504]. The QCD sum rules indicate that the heavy-light scalar and axialvector diquark states have almost degenerate masses [498, 499, 500], while the masses of the light axialvector diquark states lie about (150 – 200) MeV above that of the light scalar diquark states [501, 502, 503, 504], if they have the same valence quarks.

The diquarks $\varepsilon^{ijk} q_j^T C \Gamma q'_k$ in the $\bar{\mathbf{3}}$ have five structures in the Dirac spinor space, where $C\Gamma = C\gamma_5, C, C\gamma_\mu\gamma_5, C\gamma_\mu$ and $C\sigma_{\mu\nu}$ for the scalar, pseudoscalar, vector, axialvector and tensor diquarks, respectively. In the non-relativistic quark model, a P-wave changes the parity by contributing a factor $(-)^L = -$ with the angular momentum $L = 1$. The $C\gamma_5$ and $C\gamma_\mu$ diquark states have the spin-parity $J^P = 0^+$ and 1^+ , respectively, the corresponding C and $C\gamma_\mu\gamma_5$ diquark states have the spin-parity $J^P = 0^-$ and 1^- , respectively, the effects of the P-waves are embodied in the underlined γ_5 in the $C\gamma_5\gamma_5$ and $C\gamma_\mu\gamma_5$. The tensor diquark states have both the $J^P = 1^+$ and 1^- components, we project out the 1^+ and 1^- components explicitly, and introduce the symbols \tilde{A} and \tilde{V} to represent them respectively. We would like to give an example on the heavy-light tensor diquarks to illustrate how to perform the projection.

Under parity transformation \hat{P} , the tensor diquarks have the properties,

$$\begin{aligned}\hat{P}\varepsilon^{ijk} q_j^T(x) C\sigma_{\mu\nu}\gamma_5 Q_k(x) \hat{P}^{-1} &= \varepsilon^{ijk} q_j^T(\tilde{x}) C\sigma^{\mu\nu}\gamma_5 Q_k(\tilde{x}), \\ \hat{P}\varepsilon^{ijk} q_j^T(x) C\sigma_{\mu\nu} Q_k(x) \hat{P}^{-1} &= -\varepsilon^{ijk} q_j^T(\tilde{x}) C\sigma^{\mu\nu} Q_k(\tilde{x}),\end{aligned}\quad (113)$$

where the four vectors $x^\mu = (t, \vec{x})$ and $\tilde{x}^\mu = (t, -\vec{x})$. We introduce the four vector $t^\mu = (1, \vec{0})$ and project out the 1^+ and 1^- components explicitly [505],

$$\begin{aligned}\hat{P}\varepsilon^{ijk} q_j^T(x) C\sigma_{\mu\nu}^t \gamma_5 Q_k(x) \hat{P}^{-1} &= +\varepsilon^{ijk} q_j^T(\tilde{x}) C\sigma_{\mu\nu}^t \gamma_5 Q_k(\tilde{x}), \\ \hat{P}\varepsilon^{ijk} q_j^T(x) C\sigma_{\mu\nu}^v \gamma_5 Q_k(x) \hat{P}^{-1} &= -\varepsilon^{ijk} q_j^T(\tilde{x}) C\sigma_{\mu\nu}^v \gamma_5 Q_k(\tilde{x}), \\ \hat{P}\varepsilon^{ijk} q_j^T(x) C\sigma_{\mu\nu}^v Q_k(x) \hat{P}^{-1} &= +\varepsilon^{ijk} q_j^T(\tilde{x}) C\sigma_{\mu\nu}^v Q_k(\tilde{x}), \\ \hat{P}\varepsilon^{ijk} q_j^T(x) C\sigma_{\mu\nu}^t Q_k(x) \hat{P}^{-1} &= -\varepsilon^{ijk} q_j^T(\tilde{x}) C\sigma_{\mu\nu}^t Q_k(\tilde{x}),\end{aligned}\quad (114)$$

where $\sigma_{\mu\nu}^t = \frac{i}{2}[\gamma_\mu^t, \gamma_\nu^t]$, $\sigma_{\mu\nu}^v = \frac{i}{2}[\gamma_\mu^v, \gamma_\nu^t]$, $\gamma_\mu^v = \gamma \cdot t t_\mu$, $\gamma_\mu^t = \gamma_\mu - \gamma \cdot t t_\mu$. We can also introduce the P-wave explicitly in the $C\gamma_5$ and $C\gamma_\mu$ diquarks and obtain the vector diquarks $\varepsilon^{ijk} q_j^T C\gamma_5 \overleftrightarrow{\partial}_\mu q'_k$ and tensor diquarks $\varepsilon^{ijk} q_j^T C\gamma_\mu \overleftrightarrow{\partial}_\nu q'_k$, where the derivative $\overleftrightarrow{\partial}_\mu = \overrightarrow{\partial}_\mu - \overleftarrow{\partial}_\mu$ embodies the P-wave effects.

We can also adopt the covariant derivative with the simple replacement $\partial_\mu \rightarrow D_\mu = \partial_\mu - ig_s G_\mu$, then the four-quark currents are gauge covariant, however, gluonic components are introduced, we have to deal with both valence quarks and gluons.

Now let us construct the $\bar{\mathbf{33}}$ -type four-quark currents to interpolate the hidden-charm tetraquark states with the $J^{PC} = 0^{++}, 1^{+-}, 1^{++}$ and 2^{++} ,

$$\begin{aligned}J_{SS}(x) &= \varepsilon^{ijk} \varepsilon^{imn} u_j^T(x) C\gamma_5 c_k(x) \bar{d}_m(x) \gamma_5 C\bar{c}_n^T(x), \\ J_{AA}(x) &= \varepsilon^{ijk} \varepsilon^{imn} u_j^T(x) C\gamma_\mu c_k(x) \bar{d}_m(x) \gamma^\mu C\bar{c}_n^T(x), \\ J_{\tilde{A}\tilde{A}}(x) &= \varepsilon^{ijk} \varepsilon^{imn} u_j^T(x) C\sigma_{\mu\nu}^v c_k(x) \bar{d}_m(x) \sigma_v^{\mu\nu} C\bar{c}_n^T(x), \\ J_{VV}(x) &= \varepsilon^{ijk} \varepsilon^{imn} u_j^T(x) C\gamma_\mu \gamma_5 c_k(x) \bar{d}_m(x) \gamma_5 \gamma^\mu C\bar{c}_n^T(x), \\ J_{\tilde{V}\tilde{V}}(x) &= \varepsilon^{ijk} \varepsilon^{imn} u_j^T(x) C\sigma_{\mu\nu}^t c_k(x) \bar{d}_m(x) \sigma_t^{\mu\nu} C\bar{c}_n^T(x), \\ J_{PP}(x) &= \varepsilon^{ijk} \varepsilon^{imn} u_j^T(x) Cc_k(x) \bar{d}_m(x) C\bar{c}_n^T(x),\end{aligned}\quad (115)$$

$$\begin{aligned}
J_{-,\mu}^{SA}(x) &= \frac{\varepsilon^{ijk}\varepsilon^{imn}}{\sqrt{2}} \left[u_j^T(x) C \gamma_5 c_k(x) \bar{d}_m(x) \gamma_\mu C \bar{c}_n^T(x) - u_j^T(x) C \gamma_\mu c_k(x) \bar{d}_m(x) \gamma_5 C \bar{c}_n^T(x) \right], \\
J_{-,\mu\nu}^{AA}(x) &= \frac{\varepsilon^{ijk}\varepsilon^{imn}}{\sqrt{2}} \left[u_j^T(x) C \gamma_\mu c_k(x) \bar{d}_m(x) \gamma_\nu C \bar{c}_n^T(x) - u_j^T(x) C \gamma_\nu c_k(x) \bar{d}_m(x) \gamma_\mu C \bar{c}_n^T(x) \right], \\
J_{-,\mu\nu}^{S\tilde{A}}(x) &= \frac{\varepsilon^{ijk}\varepsilon^{imn}}{\sqrt{2}} \left[u_j^T(x) C \gamma_5 c_k(x) \bar{d}_m(x) \sigma_{\mu\nu} C \bar{c}_n^T(x) - u_j^T(x) C \sigma_{\mu\nu} c_k(x) \bar{d}_m(x) \gamma_5 C \bar{c}_n^T(x) \right], \\
J_{-,\mu}^{\tilde{A}A}(x) &= \frac{\varepsilon^{ijk}\varepsilon^{imn}}{\sqrt{2}} \left[u_j^T(x) C \sigma_{\mu\nu} \gamma_5 c_k(x) \bar{d}_m(x) \gamma^\nu C \bar{c}_n^T(x) - u_j^T(x) C \gamma^\nu c_k(x) \bar{d}_m(x) \gamma_5 \sigma_{\mu\nu} C \bar{c}_n^T(x) \right], \\
J_{-,\mu}^{\tilde{V}V}(x) &= \frac{\varepsilon^{ijk}\varepsilon^{imn}}{\sqrt{2}} \left[u_j^T(x) C \sigma_{\mu\nu} c^k(x) \bar{d}_m(x) \gamma_5 \gamma^\nu C \bar{c}_n^T(x) + u_j^T(x) C \gamma^\nu \gamma_5 c_k(x) \bar{d}_m(x) \sigma_{\mu\nu} C \bar{c}_n^T(x) \right], \\
J_{-,\mu\nu}^{VV}(x) &= \frac{\varepsilon^{ijk}\varepsilon^{imn}}{\sqrt{2}} \left[u_j^T(x) C \gamma_\mu \gamma_5 c_k(x) \bar{d}_m(x) \gamma_5 \gamma_\nu C \bar{c}_n^T(x) - u_j^T(x) C \gamma_\nu \gamma_5 c_k(x) \bar{d}_m(x) \gamma_5 \gamma_\mu C \bar{c}_n^T(x) \right], \\
J_{-,\mu}^{PV}(x) &= \frac{\varepsilon^{ijk}\varepsilon^{imn}}{\sqrt{2}} \left[u_j^T(x) C c_k(x) \bar{d}_m(x) \gamma_5 \gamma_\mu C \bar{c}_n^T(x) + u_j^T(x) C \gamma_\mu \gamma_5 c_k(x) \bar{d}_m(x) C \bar{c}_n^T(x) \right], \quad (116)
\end{aligned}$$

$$\begin{aligned}
J_{+,\mu}^{SA}(x) &= \frac{\varepsilon^{ijk}\varepsilon^{imn}}{\sqrt{2}} \left[u_j^T(x) C \gamma_5 c_k(x) \bar{d}_m(x) \gamma_\mu C \bar{c}_n^T(x) + u_j^T(x) C \gamma_\mu c_k(x) \bar{d}_m(x) \gamma_5 C \bar{c}_n^T(x) \right], \\
J_{+,\mu\nu}^{S\tilde{A}}(x) &= \frac{\varepsilon^{ijk}\varepsilon^{imn}}{\sqrt{2}} \left[u_j^T(x) C \gamma_5 c_k(x) \bar{d}_m(x) \sigma_{\mu\nu} C \bar{c}_n^T(x) + u_j^T(x) C \sigma_{\mu\nu} c_k(x) \bar{d}_m(x) \gamma_5 C \bar{c}_n^T(x) \right], \\
J_{+,\mu}^{\tilde{V}V}(x) &= \frac{\varepsilon^{ijk}\varepsilon^{imn}}{\sqrt{2}} \left[u_j^T(x) C \sigma_{\mu\nu} c_k(x) \bar{d}_m(x) \gamma_5 \gamma^\nu C \bar{c}_n^T(x) - u_j^T(x) C \gamma^\nu \gamma_5 c_k(x) \bar{d}_m(x) \sigma_{\mu\nu} C \bar{c}_n^T(x) \right], \\
J_{+,\mu}^{\tilde{A}A}(x) &= \frac{\varepsilon^{ijk}\varepsilon^{imn}}{\sqrt{2}} \left[u_j^T(x) C \sigma_{\mu\nu} \gamma_5 c_k(x) \bar{d}_m(x) \gamma^\nu C \bar{c}_n^T(x) + u_j^T(x) C \gamma^\nu c_k(x) \bar{d}_m(x) \gamma_5 \sigma_{\mu\nu} C \bar{c}_n^T(x) \right], \\
J_{+,\mu}^{PV}(x) &= \frac{\varepsilon^{ijk}\varepsilon^{imn}}{\sqrt{2}} \left[u_j^T(x) C c_k(x) \bar{d}_m(x) \gamma_5 \gamma_\mu C \bar{c}_n^T(x) - u_j^T(x) C \gamma_\mu \gamma_5 c_k(x) \bar{d}_m(x) C \bar{c}_n^T(x) \right], \\
J_{+,\mu\nu}^{AA}(x) &= \frac{\varepsilon^{ijk}\varepsilon^{imn}}{\sqrt{2}} \left[u_j^T(x) C \gamma_\mu c_k(x) \bar{d}_m(x) \gamma_\nu C \bar{c}_n^T(x) + u_j^T(x) C \gamma_\nu c_k(x) \bar{d}_m(x) \gamma_\mu C \bar{c}_n^T(x) \right], \\
J_{+,\mu\nu}^{VV}(x) &= \frac{\varepsilon^{ijk}\varepsilon^{imn}}{\sqrt{2}} \left[u_j^T(x) C \gamma_\mu \gamma_5 c_k(x) \bar{d}_m(x) \gamma_5 \gamma_\nu C \bar{c}_n^T(x) + u_j^T(x) C \gamma_\nu \gamma_5 c_k(x) \bar{d}_m(x) \gamma_5 \gamma_\mu C \bar{c}_n^T(x) \right], \quad (117)
\end{aligned}$$

where the subscripts \pm denote the positive and negative charge conjugation, respectively, the superscripts or subscripts P , S , $A(\tilde{A})$ and $V(\tilde{V})$ denote the pseudoscalar, scalar, axialvector and vector diquark and antidiquark operators, respectively [61]. With the simple replacements,

$$\begin{aligned}
u &\rightarrow q, \\
\bar{d} &\rightarrow \bar{s}, \quad (118)
\end{aligned}$$

where $q = u, d$, we obtain the corresponding currents for the $c\bar{c}q\bar{s}$ states [172]. Again, with the simple replacements,

$$\begin{aligned}
u &\rightarrow s, \\
\bar{d} &\rightarrow \bar{s}, \quad (119)
\end{aligned}$$

we obtain the corresponding currents for the $c\bar{c}s\bar{s}$ states [425, 506, 507].

We introduce the symbols,

$$\begin{aligned}
J(x) &= J_{SS}(x), J_{AA}(x), J_{\tilde{A}\tilde{A}}(x), J_{VV}(x), J_{\tilde{V}\tilde{V}}(x), J_{PP}(x), \\
J_\mu(x) &= J_{-,\mu}^{SA}(x), J_{-,\mu}^{\tilde{A}A}(x), J_{-,\mu}^{\tilde{V}V}(x), J_{-,\mu}^{PV}(x), J_{+,\mu}^{SA}(x), J_{+,\mu}^{\tilde{V}V}(x), J_{+,\mu}^{\tilde{A}A}(x), J_{+,\mu}^{PV}(x), \\
J_{\mu\nu}(x) &= J_{-,\mu\nu}^{AA}(x), J_{-,\mu\nu}^{\tilde{A}\tilde{A}}(x), J_{-,\mu\nu}^{VV}(x), J_{+,\mu\nu}^{SA}(x), J_{+,\mu\nu}^{AA}(x), J_{+,\mu\nu}^{VV}(x),
\end{aligned} \tag{120}$$

for simplicity.

Under parity transformation \hat{P} , the currents have the properties,

$$\begin{aligned}
\hat{P}J(x)\hat{P}^{-1} &= +J(\tilde{x}), \\
\hat{P}J_\mu(x)\hat{P}^{-1} &= -J^\mu(\tilde{x}), \\
\hat{P}J_{\mu\nu}^{SA}(x)\hat{P}^{-1} &= -J_{SA}^{\mu\nu}(\tilde{x}), \\
\hat{P}J_{\mu\nu}^{AA/VV}(x)\hat{P}^{-1} &= +J_{AA/VV}^{\mu\nu}(\tilde{x}),
\end{aligned} \tag{121}$$

where $x^\mu = (t, \vec{x})$ and $\tilde{x}^\mu = (t, -\vec{x})$, and we have neglected other superscripts and subscripts.

The currents $J(x)$, $J_\mu(x)$ and $J_{\mu\nu}(x)$ have the symbolic quark constituent $\bar{c}\bar{c}\bar{d}u$ with the isospin $I = 1$ and $I_3 = 1$, other currents in the isospin multiplets can be constructed analogously, for example, we write down the isospin singlet current for the $J_{SS}(x)$ directly,

$$J_{SS}^{I=0}(x) = \frac{\varepsilon^{ijk}\varepsilon^{imn}}{\sqrt{2}} \left[u_j^T(x)C\gamma_5 c_k(x)\bar{u}_m(x)\gamma_5 C\bar{c}_n^T(x) + d_j^T(x)C\gamma_5 c_k(x)\bar{d}_m(x)\gamma_5 C\bar{c}_n^T(x) \right]. \tag{122}$$

In the isospin limit, the currents with the symbolic quark constituents $\bar{c}\bar{c}\bar{d}u$, $\bar{c}\bar{c}\bar{u}d$, $\bar{c}\bar{c}\frac{\bar{u}u-\bar{d}d}{\sqrt{2}}$, $\bar{c}\bar{c}\frac{\bar{u}u+\bar{d}d}{\sqrt{2}}$ couple potentially to the hidden-charm tetraquark states with degenerated masses, the currents with the isospins $I = 1$ and 0 lead to the same QCD sum rules. Thereafter, we will denote the Z_c states as the isospin triplet, and the X states as the isospin singlet,

$$\begin{aligned}
Z_c &: \bar{c}\bar{c}\bar{d}u, \bar{c}\bar{c}\bar{u}d, \bar{c}\bar{c}\frac{\bar{u}u-\bar{d}d}{\sqrt{2}}, \\
X &: \bar{c}\bar{c}\frac{\bar{u}u+\bar{d}d}{\sqrt{2}}.
\end{aligned} \tag{123}$$

Accordingly, the Z_{cs} states with the symbolic quark constituents $\bar{c}\bar{c}\bar{s}q$ and isospin $I = \frac{1}{2}$ have degenerated masses.

The currents with the symbolic quark constituents $\bar{c}\bar{c}\frac{\bar{u}u-\bar{d}d}{\sqrt{2}}$ and $\bar{c}\bar{c}\frac{\bar{u}u+\bar{d}d}{\sqrt{2}}$ have definite charge conjugation. We would like to assume that the $\bar{c}\bar{c}\bar{d}u$ type tetraquark states have the same charge conjugation as their charge-neutral cousins.

Under charge conjugation transformation \hat{C} , the currents $J(x)$, $J_\mu(x)$ and $J_{\mu\nu}(x)$ have the properties,

$$\begin{aligned}
\hat{C}J(x)\hat{C}^{-1} &= +J(x) |_{u \leftrightarrow d}, \\
\hat{C}J_{\pm,\mu}(x)\hat{C}^{-1} &= \pm J_{\pm,\mu}(x) |_{u \leftrightarrow d}, \\
\hat{C}J_{\pm,\mu\nu}(x)\hat{C}^{-1} &= \pm J_{\pm,\mu\nu}(x) |_{u \leftrightarrow d},
\end{aligned} \tag{124}$$

where we have neglected other superscripts and subscripts.

Now we write down the correlation functions $\Pi(p)$, $\Pi_{\mu\nu}(p)$ and $\Pi_{\mu\nu\alpha\beta}(p)$,

$$\begin{aligned}
\Pi(p) &= i \int d^4x e^{ip \cdot x} \langle 0 | T \{ J(x) J^\dagger(0) \} | 0 \rangle, \\
\Pi_{\mu\nu}(p) &= i \int d^4x e^{ip \cdot x} \langle 0 | T \{ J_\mu(x) J_\nu^\dagger(0) \} | 0 \rangle, \\
\Pi_{\mu\nu\alpha\beta}(p) &= i \int d^4x e^{ip \cdot x} \langle 0 | T \{ J_{\mu\nu}(x) J_{\alpha\beta}^\dagger(0) \} | 0 \rangle.
\end{aligned} \tag{125}$$

At the hadron side, we insert a complete set of intermediate hadronic states with the same quantum numbers as the currents $J(x)$, $J_\mu(x)$ and $J_{\mu\nu}(x)$ into the correlation functions $\Pi(p)$, $\Pi_{\mu\nu}(p)$ and $\Pi_{\mu\nu\alpha\beta}(p)$ to obtain the hadronic representation [376, 377], and isolate the ground state hidden-charm tetraquark contributions,

$$\begin{aligned}
\Pi(p) &= \frac{\lambda_{Z^+}^2}{M_{Z^+}^2 - p^2} + \dots = \Pi_+(p^2), \\
\Pi_{\mu\nu}(p) &= \frac{\lambda_{Z^+}^2}{M_{Z^+}^2 - p^2} \left(-g_{\mu\nu} + \frac{p_\mu p_\nu}{p^2} \right) + \dots \\
&= \Pi_+(p^2) \left(-g_{\mu\nu} + \frac{p_\mu p_\nu}{p^2} \right) + \dots, \\
\Pi_{\mu\nu\alpha\beta}^{AA,-}(p) &= \frac{\tilde{\lambda}_{Z^+}^2}{M_{Z^+}^2 - p^2} (p^2 g_{\mu\alpha} g_{\nu\beta} - p^2 g_{\mu\beta} g_{\nu\alpha} - g_{\mu\alpha} p_\nu p_\beta - g_{\nu\beta} p_\mu p_\alpha + g_{\mu\beta} p_\nu p_\alpha + g_{\nu\alpha} p_\mu p_\beta) \\
&\quad + \frac{\tilde{\lambda}_{Z^-}^2}{M_{Z^-}^2 - p^2} (-g_{\mu\alpha} p_\nu p_\beta - g_{\nu\beta} p_\mu p_\alpha + g_{\mu\beta} p_\nu p_\alpha + g_{\nu\alpha} p_\mu p_\beta) + \dots \\
&= \tilde{\Pi}_+(p^2) (p^2 g_{\mu\alpha} g_{\nu\beta} - p^2 g_{\mu\beta} g_{\nu\alpha} - g_{\mu\alpha} p_\nu p_\beta - g_{\nu\beta} p_\mu p_\alpha + g_{\mu\beta} p_\nu p_\alpha + g_{\nu\alpha} p_\mu p_\beta) \\
&\quad + \tilde{\Pi}_-(p^2) (-g_{\mu\alpha} p_\nu p_\beta - g_{\nu\beta} p_\mu p_\alpha + g_{\mu\beta} p_\nu p_\alpha + g_{\nu\alpha} p_\mu p_\beta), \\
\Pi_{\mu\nu\alpha\beta}^{S\tilde{A},\pm}(p) &= \frac{\tilde{\lambda}_{Z^-}^2}{M_{Z^-}^2 - p^2} (p^2 g_{\mu\alpha} g_{\nu\beta} - p^2 g_{\mu\beta} g_{\nu\alpha} - g_{\mu\alpha} p_\nu p_\beta - g_{\nu\beta} p_\mu p_\alpha + g_{\mu\beta} p_\nu p_\alpha + g_{\nu\alpha} p_\mu p_\beta) \\
&\quad + \frac{\tilde{\lambda}_{Z^+}^2}{M_{Z^+}^2 - p^2} (-g_{\mu\alpha} p_\nu p_\beta - g_{\nu\beta} p_\mu p_\alpha + g_{\mu\beta} p_\nu p_\alpha + g_{\nu\alpha} p_\mu p_\beta) + \dots \\
&= \tilde{\Pi}_-(p^2) (p^2 g_{\mu\alpha} g_{\nu\beta} - p^2 g_{\mu\beta} g_{\nu\alpha} - g_{\mu\alpha} p_\nu p_\beta - g_{\nu\beta} p_\mu p_\alpha + g_{\mu\beta} p_\nu p_\alpha + g_{\nu\alpha} p_\mu p_\beta) \\
&\quad + \tilde{\Pi}_+(p^2) (-g_{\mu\alpha} p_\nu p_\beta - g_{\nu\beta} p_\mu p_\alpha + g_{\mu\beta} p_\nu p_\alpha + g_{\nu\alpha} p_\mu p_\beta), \\
\Pi_{\mu\nu\alpha\beta}^{AA,+}(p) &= \frac{\lambda_{Z^+}^2}{M_{Z^+}^2 - p^2} \left(\frac{\tilde{g}_{\mu\alpha} \tilde{g}_{\nu\beta} + \tilde{g}_{\mu\beta} \tilde{g}_{\nu\alpha}}{2} - \frac{\tilde{g}_{\mu\nu} \tilde{g}_{\alpha\beta}}{3} \right) + \dots, \\
&= \Pi_+(p^2) \left(\frac{\tilde{g}_{\mu\alpha} \tilde{g}_{\nu\beta} + \tilde{g}_{\mu\beta} \tilde{g}_{\nu\alpha}}{2} - \frac{\tilde{g}_{\mu\nu} \tilde{g}_{\alpha\beta}}{3} \right) + \dots, \tag{126}
\end{aligned}$$

where $\tilde{g}_{\mu\nu} = g_{\mu\nu} - \frac{p_\mu p_\nu}{p^2}$. We add the superscripts \pm in the $\Pi_{\mu\nu\alpha\beta}^{AA,-}(p)$, $\Pi_{\mu\nu\alpha\beta}^{S\tilde{A},\pm}(p)$ and $\Pi_{\mu\nu\alpha\beta}^{AA,+}(p)$ to denote the positive and negative charge conjugation, respectively, and add the superscripts (subscripts) \pm in the Z_c^\pm (the $\Pi_\pm(p^2)$ and $\tilde{\Pi}_\pm(p^2)$ components) to denote the positive and negative parity, respectively. And the $\Pi_{\mu\nu\alpha\beta}^{VV,\pm}(p)$ and $\Pi_{\mu\nu\alpha\beta}^{AA,\pm}(p)$ have the same tensor structures. The pole residues λ_{Z^\pm} are defined by

$$\begin{aligned}
\langle 0 | J(0) | Z_c^+(p) \rangle &= \lambda_{Z^+}, \\
\langle 0 | J_\mu(0) | Z_c^+(p) \rangle &= \lambda_{Z^+} \varepsilon_\mu, \\
\langle 0 | J_{\pm,\mu\nu}^{S\tilde{A}}(0) | Z_c^-(p) \rangle &= \tilde{\lambda}_{Z^-} \varepsilon_{\mu\nu\alpha\beta} \varepsilon^\alpha p^\beta, \\
\langle 0 | J_{\pm,\mu\nu}^{S\tilde{A}}(0) | Z_c^+(p) \rangle &= \tilde{\lambda}_{Z^+} (\varepsilon_\mu p_\nu - \varepsilon_\nu p_\mu), \\
\langle 0 | J_{-,\mu\nu}^{AA/VV}(0) | Z_c^+(p) \rangle &= \tilde{\lambda}_{Z^+} \varepsilon_{\mu\nu\alpha\beta} \varepsilon^\alpha p^\beta, \\
\langle 0 | J_{-,\mu\nu}^{AA/VV}(0) | Z_c^-(p) \rangle &= \tilde{\lambda}_{Z^-} (\varepsilon_\mu p_\nu - \varepsilon_\nu p_\mu), \\
\langle 0 | J_{+,\mu\nu}^{AA/VV}(0) | Z_c^+(p) \rangle &= \lambda_{Z^+} \varepsilon_{\mu\nu}, \tag{127}
\end{aligned}$$

where $\lambda_{Z^\pm} = \tilde{\lambda}_{Z^\pm} M_{Z^\pm}$, the $\varepsilon_{\mu/\alpha}$ and $\varepsilon_{\mu\nu}$ are the polarization vectors. We choose the components $\Pi_+(p^2)$ and $p^2 \tilde{\Pi}_+(p^2)$ to study the hidden-charm tetraquark states.

Z_c	J^{PC}	Currents
$[uc]_S[\bar{dc}]_S$	0^{++}	$J_{SS}(x)$
$[uc]_A[\bar{dc}]_A$	0^{++}	$J_{AA}(x)$
$[uc]_{\tilde{A}}[\bar{dc}]_{\tilde{A}}$	0^{++}	$J_{\tilde{A}\tilde{A}}(x)$
$[uc]_V[\bar{dc}]_V$	0^{++}	$J_{VV}(x)$
$[uc]_{\tilde{V}}[\bar{dc}]_{\tilde{V}}$	0^{++}	$J_{\tilde{V}\tilde{V}}(x)$
$[uc]_P[\bar{dc}]_P$	0^{++}	$J_{PP}(x)$
$[uc]_S[\bar{dc}]_A - [uc]_A[\bar{dc}]_S$	1^{+-}	$J_{-}^{SA}(x)$
$[uc]_A[\bar{dc}]_A$	1^{+-}	$J_{-, \mu\nu}^{AA}(x)$
$[uc]_S[\bar{dc}]_{\tilde{A}} - [uc]_{\tilde{A}}[\bar{dc}]_S$	1^{+-}	$J_{-, \mu\nu}^{SA}(x)$
$[uc]_{\tilde{A}}[\bar{dc}]_A - [uc]_A[\bar{dc}]_{\tilde{A}}$	1^{+-}	$J_{-, \mu\nu}^{AA}(x)$
$[uc]_{\tilde{V}}[\bar{dc}]_V + [uc]_V[\bar{dc}]_{\tilde{V}}$	1^{+-}	$J_{-, \mu\nu}^{\tilde{V}V}(x)$
$[uc]_V[\bar{dc}]_V$	1^{+-}	$J_{-, \mu\nu}^{\tilde{V}V}(x)$
$[uc]_P[\bar{dc}]_V + [uc]_V[\bar{dc}]_P$	1^{+-}	$J_{-, \mu\nu}^{PV}(x)$
$[uc]_S[\bar{dc}]_A + [uc]_A[\bar{dc}]_S$	1^{++}	$J_{+, \mu\nu}^{SA}(x)$
$[uc]_S[\bar{dc}]_{\tilde{A}} + [uc]_{\tilde{A}}[\bar{dc}]_S$	1^{++}	$J_{+, \mu\nu}^{SA}(x)$
$[uc]_{\tilde{V}}[\bar{dc}]_V - [uc]_V[\bar{dc}]_{\tilde{V}}$	1^{++}	$J_{+, \mu\nu}^{\tilde{V}V}(x)$
$[uc]_{\tilde{A}}[\bar{dc}]_A + [uc]_A[\bar{dc}]_{\tilde{A}}$	1^{++}	$J_{+, \mu\nu}^{AA}(x)$
$[uc]_P[\bar{dc}]_V - [uc]_V[\bar{dc}]_P$	1^{++}	$J_{+, \mu\nu}^{PV}(x)$
$[uc]_A[\bar{dc}]_A$	2^{++}	$J_{+, \mu\nu}^{AA}(x)$
$[uc]_V[\bar{dc}]_V$	2^{++}	$J_{+, \mu\nu}^{\tilde{V}V}(x)$

Table 4: The quark constituents and corresponding currents for the hidden-charm tetraquark states [61].

In Table 4, we present the quark constituents and corresponding currents explicitly.

At the QCD side, we carry out the operator product expansion for the correlation functions $\Pi(p)$, $\Pi_{\mu\nu}(p)$ and $\Pi_{\mu\nu\alpha\beta}(p)$. For example, we contract the quark fields in the $\Pi_{\mu\nu}(p)$ with the Wick's theorem, and obtain the results,

$$\begin{aligned}
\Pi_{\mu\nu}(p) = & -\frac{i\varepsilon^{ijk}\varepsilon^{lmn}\varepsilon^{i'j'k'}\varepsilon^{l'm'n'}}{2} \int d^4x e^{ip \cdot x} \\
& \left\{ \text{Tr} \left[\gamma_5 S_c^{kk'}(x) \gamma_5 C U_{jj'}^T(x) C \right] \text{Tr} \left[\gamma_\nu S_c^{n'n}(-x) \gamma_\mu C D_{m'm}^T(-x) C \right] \right. \\
& + \text{Tr} \left[\gamma_\mu S_c^{kk'}(x) \gamma_\nu C U_{jj'}^T(x) C \right] \text{Tr} \left[\gamma_5 S_c^{n'n}(-x) \gamma_5 C D_{m'm}^T(-x) C \right] \\
& \mp \text{Tr} \left[\gamma_\mu S_c^{kk'}(x) \gamma_5 C U_{jj'}^T(x) C \right] \text{Tr} \left[\gamma_\nu S_c^{n'n}(-x) \gamma_5 C D_{m'm}^T(-x) C \right] \\
& \left. \mp \text{Tr} \left[\gamma_5 S_c^{kk'}(x) \gamma_\nu C U_{jj'}^T(x) C \right] \text{Tr} \left[\gamma_5 S_c^{n'n}(-x) \gamma_\mu C D_{m'm}^T(-x) C \right] \right\}, \quad (128)
\end{aligned}$$

where the full quark propagators, $S^{ij}(x) = U^{ij}(x) = D^{ij}(x)$,

$$\begin{aligned}
S^{ij}(x) = & \frac{i\delta_{ij}\not{x}}{2\pi^2 x^4} - \frac{\delta_{ij}m_q}{4\pi^2 x^2} - \frac{\delta_{ij}\langle\bar{q}q\rangle}{12} + \frac{i\delta_{ij}\not{x}m_q\langle\bar{q}q\rangle}{48} - \frac{\delta_{ij}x^2\langle\bar{q}g_s\sigma Gq\rangle}{192} + \frac{i\delta_{ij}x^2\not{x}m_q\langle\bar{q}g_s\sigma Gq\rangle}{1152} \\
& - \frac{ig_s G_{\alpha\beta}^a t_{ij}^a (\not{x}\sigma^{\alpha\beta} + \sigma^{\alpha\beta}\not{x})}{32\pi^2 x^2} - \frac{i\delta_{ij}x^2\not{x}g_s^2\langle\bar{q}q\rangle^2}{7776} - \frac{\delta_{ij}x^4\langle\bar{q}q\rangle\langle g_s^2 GG\rangle}{27648} - \frac{1}{8}\langle\bar{q}_j\sigma^{\mu\nu}q_i\rangle\sigma_{\mu\nu} \\
& - \frac{1}{4}\langle\bar{q}_j\gamma^\mu q_i\rangle\gamma_\mu + \dots, \quad (129)
\end{aligned}$$

and $S_c^{ij}(x) = S_Q^{ij}(x)$,

$$\begin{aligned}
S_Q^{ij}(x) &= \frac{i}{(2\pi)^4} \int d^4k e^{-ik \cdot x} \left\{ \frac{\delta_{ij}}{k - m_Q} - \frac{g_s G_{\alpha\beta}^n t_{ij}^n}{4} \frac{\sigma^{\alpha\beta}(k + m_Q) + (k + m_Q)\sigma^{\alpha\beta}}{(k^2 - m_Q^2)^2} \right. \\
&\quad \left. + \frac{g_s D_\alpha G_{\beta\lambda}^n t_{ij}^n (f^{\lambda\beta\alpha} + f^{\lambda\alpha\beta})}{3(k^2 - m_Q^2)^4} - \frac{g_s^2 (t^a t^b)_{ij} G_{\alpha\beta}^a G_{\mu\nu}^b (f^{\alpha\beta\mu\nu} + f^{\alpha\mu\beta\nu} + f^{\alpha\mu\nu\beta})}{4(k^2 - m_Q^2)^5} + \dots \right\}, \\
f^{\lambda\alpha\beta} &= (k + m_Q)\gamma^\lambda (k + m_Q)\gamma^\alpha (k + m_Q)\gamma^\beta (k + m_Q), \\
f^{\alpha\beta\mu\nu} &= (k + m_Q)\gamma^\alpha (k + m_Q)\gamma^\beta (k + m_Q)\gamma^\mu (k + m_Q)\gamma^\nu (k + m_Q), \tag{130}
\end{aligned}$$

with $Q = c$, $D_\alpha = \partial_\alpha - ig_s G_\alpha^n t^n$ [60, 381, 508], and the \mp correspond to the currents $J_{+,\mu}^{SA}(x)$ and $J_{-,\mu}^{SA}(x)$, respectively. In Eq.(129), we retain the terms $\langle \bar{q}_j \sigma_{\mu\nu} q_i \rangle$ and $\langle \bar{q}_j \gamma_\mu q_i \rangle$ come from the Fierz transformation of the $\langle q_i \bar{q}_j \rangle$ to absorb the gluons emitted from the other quark lines to form $\langle \bar{q}_j g_s G_{\alpha\beta}^a t_{mn}^a \sigma_{\mu\nu} q_i \rangle$ and $\langle \bar{q}_j \gamma_\mu q_i D_\nu g_s G_{\alpha\beta}^a t_{mn}^a \rangle$ to extract the mixed condensate $\langle \bar{q} g_s \sigma G q \rangle$ and four-quark condensate $g_s^2 \langle \bar{q} q \rangle^2$, respectively [60], where $q = u, d$ or s . The condensate $g_s^2 \langle \bar{q} q \rangle^2$ comes from the $\langle \bar{q} \gamma_\mu t^a q g_s D_\eta G_{\lambda\tau}^a \rangle$, $\langle \bar{q}_j D_\mu^\dagger D_\nu^\dagger D_\alpha^\dagger q_i \rangle$ and $\langle \bar{q}_j D_\mu D_\nu D_\alpha q_i \rangle$ rather than comes from the radiative $\mathcal{O}(\alpha_s)$ corrections to the $\langle \bar{q} q \rangle^2$.

In fact, the method of adopting the full propagators in Eq.(128) implies vacuum saturation implicitly, the factorization of the higher dimensional vacuum condensates, for example, see Eq.(87), is already performed. We calculate the higher dimensional vacuum condensates using the formula $t_{ij}^a t_{mn}^a = -\frac{1}{6} \delta_{ij} \delta_{mn} + \frac{1}{2} \delta_{jm} \delta_{in}$ rigorously.

Let us see Eq.(128) again, there are two Q -quark propagators and two q -quark propagators, if each Q -quark line emits a gluon and each q -quark line contributes a quark-antiquark pair, we obtain an operator $G_{\mu\nu} G_{\alpha\beta} \bar{u} u \bar{d} d$ (or $G_{\mu\nu} G_{\alpha\beta} \bar{q} q \bar{s} s$ or $G_{\mu\nu} G_{\alpha\beta} \bar{s} s \bar{s} s$), which is of dimension 10, see the Feynman diagram in Fig.7 for example. We should take account of the vacuum condensates at least up to dimension 10. The higher dimensional vacuum condensates are associated with the $\frac{1}{T^2}$, $\frac{1}{T^4}$ or $\frac{1}{T^6}$, which manifest themselves at small Borel parameter T^2 and play an important role in determining the Borel windows, where they play a minor important role. Therefore, we take account of the vacuum condensates $\langle \bar{q} q \rangle$, $\langle \frac{\alpha_s G G}{\pi} \rangle$, $\langle \bar{q} g_s \sigma G q \rangle$, $\langle \bar{q} q \rangle^2$, $g_s^2 \langle \bar{q} q \rangle^2$, $\langle \bar{q} q \rangle \langle \frac{\alpha_s G G}{\pi} \rangle$, $\langle \bar{q} q \rangle \langle \bar{q} g_s \sigma G q \rangle$, $\langle \bar{q} g_s \sigma G q \rangle^2$ and $\langle \bar{q} q \rangle^2 \langle \frac{\alpha_s G G}{\pi} \rangle$, which are vacuum expectations of the quark-gluon operators of the order $\mathcal{O}(\alpha_s^k)$ with $k \leq 1$. We truncate the operator product expansion in such a way consistently and rigorously. The condensates $\langle g_s^3 G G G \rangle$, $\langle \frac{\alpha_s G G}{\pi} \rangle^2$, $\langle \frac{\alpha_s G G}{\pi} \rangle \langle \bar{q} g_s \sigma G q \rangle$ have the dimensions 6, 8, 9 respectively, but they are vacuum expectations of the quark-gluon operators of the order $\mathcal{O}(\alpha_s^{3/2})$, $\mathcal{O}(\alpha_s^2)$, $\mathcal{O}(\alpha_s^{3/2})$ respectively, and discarded. Furthermore, direct calculations indicate such contributions are tiny indeed [509].

We accomplish the integrals in Eqs.(128)-(130) sequentially by simply setting $d^4 x d^4 k d^4 q \rightarrow d^D x d^D k d^D q$ with $D = 4 - 2\epsilon$ to regularize the divergences, such a simple scheme misses many subtraction terms, which make no contribution in obtaining the imaginary parts through $p^2 \rightarrow p^2 + i\epsilon$. Finally, we obtain the QCD spectral densities $\rho_{QCD}(s)$ through dispersion relation. Now we take a short digression to give an example,

$$\begin{aligned}
\text{Int}(p^2) &= \int_{-\infty}^{+\infty} d^D x d^D k d^D q \frac{\exp[i(p + q + k) \cdot x]}{(q^2 - m_Q^2)^\lambda (k^2 - m_Q^2)^\tau x^{2n}} \\
&= -i \frac{2^{4-2n} \pi^2}{\Gamma(n)} \int_{-\infty}^{+\infty} d^D k d^D q \frac{\Gamma(\alpha)}{(q^2 - m_Q^2)^\lambda (k^2 - m_Q^2)^\tau (p + q + k)^{2\alpha}} \\
&= -i \frac{2^{4-2n} \pi^2}{\Gamma(n)} \frac{i \pi^2}{\Gamma(\tau)} \int_0^1 dx \int_{-\infty}^{+\infty} d^D q \frac{x^{\alpha-1} (1-x)^{\tau-1} \Gamma(\alpha + \tau - \frac{D}{2})}{(q^2 - m_Q^2)^\lambda (x(1-x)(p+q)^2 - (1-x)m_Q^2)^{\alpha+\tau-\frac{D}{2}}} \\
&= \frac{i 2^{4-2n} \pi^6}{\Gamma(\lambda) \Gamma(\tau) \Gamma(n)} \int_0^1 dx \frac{x^{\alpha-1} (1-x)^{\tau-1}}{[x(1-x)]^{\alpha+\tau-\frac{D}{2}}} \int_0^1 dy \frac{y^{\alpha+\tau-\frac{D}{2}-1} (1-y)^{\lambda-1}}{[y(1-y)]^{\alpha+\lambda+\tau-D}} \frac{\Gamma(\alpha + \lambda + \tau - D)}{(p^2 - \tilde{m}_Q^2)^{\alpha+\lambda+\tau-D}}, \tag{131}
\end{aligned}$$

with $\alpha = \frac{D}{2} - n$. We set $D = 4 - 2\epsilon$ and $z = x(1 - y)$, then we obtain,

$$\text{Int}(p^2) = \frac{i 2^{4-2n} \pi^6}{\Gamma(\lambda)\Gamma(\tau)\Gamma(n)} \int_{y_i}^{y_f} dy y^{1-\lambda} \int_{z_i}^{1-y} dz z^{1-\tau} (1-y-z)^{n-1} \frac{\Gamma(\lambda+\tau-n-2+\epsilon)}{(p^2 - \tilde{m}_Q^2)^{\lambda+\tau-n-2+\epsilon}}. \quad (132)$$

In the case $\lambda = \tau = 1$ and $n = 2$, we obtain,

$$\text{Int}(p^2) = i \pi^6 \int_{y_i}^{y_f} dy \int_{z_i}^{1-y} dz (1-y-z) \frac{\Gamma(\epsilon-2)}{(p^2 - \tilde{m}_Q^2)^{\epsilon-2}}, \quad (133)$$

and

$$\frac{1}{\pi} \text{Im Int}(s + i\epsilon) = i \frac{\pi^6}{2} \int_{y_i}^{y_f} dy \int_{z_i}^{1-y} dz (1-y-z) (s - \tilde{m}_Q^2)^2, \quad (134)$$

where $y_f = \frac{1+\sqrt{1-4m_Q^2/s}}{2}$, $y_i = \frac{1-\sqrt{1-4m_Q^2/s}}{2}$, $z_i = \frac{ym_Q^2}{ys-m_Q^2}$ and $\tilde{m}_Q^2 = \frac{m_Q^2}{y} + \frac{m_Q^2}{z}$.

Then we match the hadron side with the QCD side of the components $\Pi_+(p^2)$ and $p^2 \tilde{\Pi}_+(p^2)$ of the correlation functions $\Pi(p)$, $\Pi_{\mu\nu}(p)$ and $\Pi_{\mu\nu\alpha\beta}(p)$ below the continuum thresholds s_0 and perform Borel transformation with respect to $P^2 = -p^2$ to obtain the QCD sum rules:

$$\lambda_{Z^+}^2 \exp\left(-\frac{M_{Z^+}^2}{T^2}\right) = \int_{4m_c^2}^{s_0} ds \rho_{QCD}(s) \exp\left(-\frac{s}{T^2}\right). \quad (135)$$

We derive Eq.(135) with respect to $\tau = \frac{1}{T^2}$, and obtain the QCD sum rules for the masses of the hidden-charm tetraquark states Z_c or X ,

$$M_{Z^+}^2 = -\frac{\int_{4m_c^2}^{s_0} ds \frac{d}{d\tau} \rho_{QCD}(s) \exp(-\tau s)}{\int_{4m_c^2}^{s_0} ds \rho_{QCD}(s) \exp(-\tau s)}. \quad (136)$$

Now let us begin to perform numerical analysis, and write down the energy-scale dependence of the input parameters,

$$\begin{aligned} \langle \bar{q}q \rangle(\mu) &= \langle \bar{q}q \rangle(1\text{GeV}) \left[\frac{\alpha_s(1\text{GeV})}{\alpha_s(\mu)} \right]^{\frac{12}{33-2n_f}}, \\ \langle \bar{s}s \rangle(\mu) &= \langle \bar{s}s \rangle(1\text{GeV}) \left[\frac{\alpha_s(1\text{GeV})}{\alpha_s(\mu)} \right]^{\frac{12}{33-2n_f}}, \\ \langle \bar{q}g_s \sigma G q \rangle(\mu) &= \langle \bar{q}g_s \sigma G q \rangle(1\text{GeV}) \left[\frac{\alpha_s(1\text{GeV})}{\alpha_s(\mu)} \right]^{\frac{2}{33-2n_f}}, \\ \langle \bar{s}g_s \sigma G s \rangle(\mu) &= \langle \bar{s}g_s \sigma G s \rangle(1\text{GeV}) \left[\frac{\alpha_s(1\text{GeV})}{\alpha_s(\mu)} \right]^{\frac{2}{33-2n_f}}, \\ m_c(\mu) &= m_c(m_c) \left[\frac{\alpha_s(\mu)}{\alpha_s(m_c)} \right]^{\frac{12}{33-2n_f}}, \\ m_s(\mu) &= m_s(2\text{GeV}) \left[\frac{\alpha_s(\mu)}{\alpha_s(2\text{GeV})} \right]^{\frac{12}{33-2n_f}}, \\ \alpha_s(\mu) &= \frac{1}{b_0 t} \left[1 - \frac{b_1}{b_0^2} \frac{\log t}{t} + \frac{b_1^2 (\log^2 t - \log t - 1) + b_0 b_2}{b_0^4 t^2} \right], \end{aligned} \quad (137)$$

where $t = \log \frac{\mu^2}{\Lambda_{QCD}^2}$, $b_0 = \frac{33-2n_f}{12\pi}$, $b_1 = \frac{153-19n_f}{24\pi^2}$, $b_2 = \frac{2857-\frac{5033}{9}n_f+\frac{325}{27}n_f^2}{128\pi^3}$, $\Lambda_{QCD} = 210$ MeV, 292 MeV and 332 MeV for the flavors $n_f = 5, 4$ and 3, respectively [510, 511]. Because the c -quark is concerned, we choose the flavor number to be $n_f = 4$.

At the beginning points, we adopt the commonly-used values $\langle \bar{q}q \rangle = -(0.24 \pm 0.01 \text{ GeV})^3$, $\langle \bar{s}s \rangle = (0.8 \pm 0.1) \langle \bar{q}q \rangle$, $\langle \bar{q}g_s \sigma G q \rangle = m_0^2 \langle \bar{q}q \rangle$, $\langle \bar{s}g_s \sigma G s \rangle = m_0^2 \langle \bar{s}s \rangle$, $m_0^2 = (0.8 \pm 0.1) \text{ GeV}^2$, $\langle \frac{\alpha_s GG}{\pi} \rangle = (0.012 \pm 0.004) \text{ GeV}^4$ at the typical energy scale $\mu = 1 \text{ GeV}$ [376, 377, 381, 385], and adopt the \overline{MS} (modified-minimal-subtraction) masses $m_c(m_c) = (1.275 \pm 0.025) \text{ GeV}$ and $m_s(2\text{GeV}) = (0.095 \pm 0.005) \text{ GeV}$ from the Particle Data Group [510].

We apply the modified energy scale formula $\mu = \sqrt{M_{X/Y/Z}^2 - (2\mathbb{M}_c)^2} - \kappa \mathbb{M}_s$ to choose the suitable energy scales of the QCD spectral densities [61, 172, 425], where the \mathbb{M}_c and \mathbb{M}_s are the effective c and s -quark masses respectively, and have universal values to be commonly used elsewhere. We adopt the updated value $\mathbb{M}_c = 1.82 \text{ GeV}$ [512], and take the collective light-flavor $SU(3)$ -breaking effects into account by introducing an effective s -quark mass $\mathbb{M}_s = 0.20 \text{ GeV}$ (0.12 GeV) for the S-wave (P-wave) tetraquark states [82, 83, 171, 172, 418, 425, 513, 514, 515].

The continuum threshold parameters are not completely free parameters, and cannot be determined by the QCD sum rules themselves completely. We often consult the experimental data in choosing the continuum threshold parameters. The $Z_c(4430)$ can be assigned to be the first radial excitation of the $Z_c(3900)$ according to the analogous decays,

$$\begin{aligned} Z_c^\pm(3900) &\rightarrow J/\psi \pi^\pm, \\ Z_c^\pm(4430) &\rightarrow \psi' \pi^\pm, \end{aligned} \quad (138)$$

and the analogous mass gaps $M_{Z_c(4430)} - M_{Z_c(3900)} = 591 \text{ MeV}$ and $M_{\psi'} - M_{J/\psi} = 589 \text{ MeV}$ from the Particle Data Group [56, 181, 182, 411].

We tentatively choose the continuum threshold parameters as $\sqrt{s_0} = M_{X/Z} + 0.60 \text{ GeV}$ and vary the continuum threshold parameters s_0 and Borel parameters T^2 to satisfy the following four criteria:

- Pole dominance at the hadron side;
 - Convergence of the operator product expansion;
 - Appearance of the Borel platforms;
 - Fulfillment of the modified energy scale formula,
- via trial and error.

Thereafter, such criteria are adopted for all the hidden-charm (hidden-bottom) tetraquark (molecular) states, hidden-charm (hidden-bottom) pentaquark (molecular) states, doubly-charm (doubly-bottom) tetraquark (molecular) states, doubly-charm (doubly-bottom) pentaquark (molecular) states, etc.

The pole dominance at the hadron side and convergence of the operator product expansion at the QCD side are two basic criteria, we should satisfy them to obtain reliable QCD sum rules. In the QCD sum rules for the hidden-charm tetraquark and pentaquark states, the largest power of the energy variable s in the QCD spectral densities $\rho_{QCD}(s) \sim s^4$ and s^5 , respectively, which make the integrals,

$$\int_{4m_c^2}^{s_0} ds s^4 \exp\left(-\frac{s}{T^2}\right), \quad \int_{4m_c^2}^{s_0} ds s^5 \exp\left(-\frac{s}{T^2}\right), \quad (139)$$

converge more slowly compared to the traditional hadrons, **it is very difficult to satisfy the two basic criteria at the same time**. We define the pole contributions (PC) by,

$$\text{PC} = \frac{\int_{4m_c^2}^{s_0} ds \rho_{QCD}(s) \exp\left(-\frac{s}{T^2}\right)}{\int_{4m_c^2}^{\infty} ds \rho_{QCD}(s) \exp\left(-\frac{s}{T^2}\right)}, \quad (140)$$

$Z_c(X_c)$	J^{PC}	$T^2(\text{GeV}^2)$	$\sqrt{s_0}(\text{GeV})$	$\mu(\text{GeV})$	pole	$ D(10) $
$[uc]_S[\bar{d}\bar{c}]_S$	0^{++}	$2.7 - 3.1$	4.40 ± 0.10	1.3	$(40 - 63)\%$	$< 1\%$
$[uc]_A[\bar{d}\bar{c}]_A$	0^{++}	$2.8 - 3.2$	4.52 ± 0.10	1.5	$(40 - 63)\%$	$\leq 1\%$
$[uc]_{\tilde{A}}[\bar{d}\bar{c}]_{\tilde{A}}$	0^{++}	$3.1 - 3.5$	4.55 ± 0.10	1.6	$(42 - 62)\%$	$< 1\%$
$[uc]_V[\bar{d}\bar{c}]_V$	0^{++}	$3.7 - 4.1$	5.22 ± 0.10	2.9	$(41 - 60)\%$	$\ll 1\%$
$[uc]_{\tilde{V}}[\bar{d}\bar{c}]_{\tilde{V}}$	0^{++}	$4.9 - 5.7$	5.90 ± 0.10	3.9	$(41 - 61)\%$	$\ll 1\%$
$[uc]_P[\bar{d}\bar{c}]_P$	0^{++}	$5.2 - 6.0$	6.03 ± 0.10	4.1	$(40 - 60)\%$	$\ll 1\%$
$[uc]_S[\bar{d}\bar{c}]_A - [uc]_A[\bar{d}\bar{c}]_S$	1^{+-}	$2.7 - 3.1$	4.40 ± 0.10	1.4	$(40 - 63)\%$	$< 1\%$
$[uc]_A[\bar{d}\bar{c}]_A$	1^{+-}	$3.3 - 3.7$	4.60 ± 0.10	1.7	$(40 - 59)\%$	$\ll 1\%$
$[uc]_S[\bar{d}\bar{c}]_{\tilde{A}} - [uc]_{\tilde{A}}[\bar{d}\bar{c}]_S$	1^{+-}	$3.3 - 3.7$	4.60 ± 0.10	1.7	$(40 - 59)\%$	$\ll 1\%$
$[uc]_{\tilde{A}}[\bar{d}\bar{c}]_A - [uc]_A[\bar{d}\bar{c}]_{\tilde{A}}$	1^{+-}	$3.2 - 3.6$	4.60 ± 0.10	1.7	$(41 - 61)\%$	$\ll 1\%$
$[uc]_{\tilde{V}}[\bar{d}\bar{c}]_V + [uc]_V[\bar{d}\bar{c}]_{\tilde{V}}$	1^{+-}	$3.7 - 4.1$	5.25 ± 0.10	2.9	$(41 - 60)\%$	$\ll 1\%$
$[uc]_V[\bar{d}\bar{c}]_V$	1^{+-}	$5.1 - 5.9$	6.00 ± 0.10	4.1	$(41 - 60)\%$	$\ll 1\%$
$[uc]_P[\bar{d}\bar{c}]_V + [uc]_V[\bar{d}\bar{c}]_P$	1^{+-}	$5.1 - 5.9$	6.00 ± 0.10	4.1	$(41 - 60)\%$	$\ll 1\%$
$[uc]_S[\bar{d}\bar{c}]_A + [uc]_A[\bar{d}\bar{c}]_S$	1^{++}	$2.7 - 3.1$	4.40 ± 0.10	1.4	$(40 - 62)\%$	$\ll 1\%$
$[uc]_S[\bar{d}\bar{c}]_{\tilde{A}} + [uc]_{\tilde{A}}[\bar{d}\bar{c}]_S$	1^{++}	$3.3 - 3.7$	4.60 ± 0.10	1.7	$(40 - 59)\%$	$\ll 1\%$
$[uc]_{\tilde{V}}[\bar{d}\bar{c}]_V - [uc]_V[\bar{d}\bar{c}]_{\tilde{V}}$	1^{++}	$2.8 - 3.2$	4.62 ± 0.10	1.8	$(40 - 63)\%$	$< 2\%$
$[uc]_{\tilde{A}}[\bar{d}\bar{c}]_A + [uc]_A[\bar{d}\bar{c}]_{\tilde{A}}$	1^{++}	$4.6 - 5.3$	5.73 ± 0.10	3.7	$(40 - 60)\%$	$\ll 1\%$
$[uc]_P[\bar{d}\bar{c}]_V - [uc]_V[\bar{d}\bar{c}]_P$	1^{++}	$5.1 - 5.9$	6.00 ± 0.10	4.1	$(40 - 60)\%$	$\ll 1\%$
$[uc]_A[\bar{d}\bar{c}]_A$	2^{++}	$3.3 - 3.7$	4.65 ± 0.10	1.8	$(40 - 60)\%$	$< 1\%$
$[uc]_V[\bar{d}\bar{c}]_V$	2^{++}	$5.0 - 5.8$	5.95 ± 0.10	4.0	$(40 - 60)\%$	$\ll 1\%$

Table 5: The Borel windows, continuum threshold parameters, energy scales of the QCD spectral densities, pole contributions, and contributions of the vacuum condensates of dimension 10 for the ground state $c\bar{c}u\bar{d}$ tetraquark states [61].

while we define the contributions of the vacuum condensates $D(n)$ of dimension n by,

$$D(n) = \frac{\int_{4m_c^2}^{s_0} ds \rho_{QCD,n}(s) \exp\left(-\frac{s}{T^2}\right)}{\int_{4m_c^2}^{s_0} ds \rho_{QCD}(s) \exp\left(-\frac{s}{T^2}\right)}, \quad (141)$$

or

$$D(n) = \frac{\int_{4m_c^2}^{\infty} ds \rho_{QCD,n}(s) \exp\left(-\frac{s}{T^2}\right)}{\int_{4m_c^2}^{\infty} ds \rho_{QCD}(s) \exp\left(-\frac{s}{T^2}\right)}, \quad (142)$$

sometimes we would like to use the notation D_n in stead of $D(n)$. Compared to the criterion in Eq.(142), the criterion in Eq.(141) is strong and leads to larger Borel parameter T^2 . If we only study the ground state contributions, the Eq.(141) is preferred.

After trial and error, we obtain the Borel windows, continuum threshold parameters, energy scales of the QCD spectral densities, pole contributions, and contributions of the vacuum condensates of dimension 10, which are shown explicitly in Tables 5-6.

At the hadron side, the pole contributions are about $(40 - 60)\%$, the pole dominance is well satisfied. It is more easy to obtain the pole contributions $(40 - 60)\%$ with the help of the modified energy scale formula. In Table 6, we provide two sets of data for the scalar tetraquark states, one set data is based on the continuum threshold parameters about $\sqrt{s_0} = M_X + 0.60 \pm 0.10$ GeV with the central values $\sqrt{s_0} < M_Y + 0.60$ GeV (this criterion is also adopted for the tetraquark states with the $J^{PC} = 1^{+-}, 1^{++}$ and 2^{++}), the other set data is based on the continuum threshold parameters about $\sqrt{s_0} = M_X + 0.55 \pm 0.10$ GeV with the central values $\sqrt{s_0} < M_Y + 0.55$ GeV, which will be characterized by the additional symbol * in Tables 6, 8 and 10.

X_c	J^{PC}	$T^2(\text{GeV}^2)$	$\sqrt{s_0}(\text{GeV})$	$\mu(\text{GeV})$	pole	$ D(10) $
$[sc]_S[\bar{s}\bar{c}]_S$	0^{++}	$3.1 - 3.5$	4.65 ± 0.10	1.4	$(40 - 61)\%$	$\ll 1\%$
$[sc]_A[\bar{s}\bar{c}]_A$	0^{++}	$3.1 - 3.5$	4.70 ± 0.10	1.5	$(39 - 60)\%$	$\ll 1\%$
$[sc]_{\tilde{A}}[\bar{s}\bar{c}]_{\tilde{A}}$	0^{++}	$3.4 - 3.9$	4.75 ± 0.10	1.6	$(39 - 61)\%$	$\ll 1\%$
$[sc]_V[\bar{s}\bar{c}]_V$	0^{++}	$4.0 - 4.5$	5.40 ± 0.10	2.8	$(41 - 60)\%$	$\ll 1\%$
$[sc]_{\tilde{V}}[\bar{s}\bar{c}]_{\tilde{V}}$	0^{++}	$5.2 - 6.1$	6.05 ± 0.10	3.7	$(40 - 61)\%$	$\ll 1\%$
$[sc]_P[\bar{s}\bar{c}]_P$	0^{++}	$5.2 - 6.1$	6.10 ± 0.10	3.8	$(40 - 61)\%$	$\ll 1\%$
$[sc]_S[\bar{s}\bar{c}]_S^*$	0^{++}	$2.8 - 3.2$	4.50 ± 0.10	1.3	$(39 - 61)\%$	$\ll 1\%$
$[sc]_A[\bar{s}\bar{c}]_A^*$	0^{++}	$2.7 - 3.1$	4.55 ± 0.10	1.3	$(39 - 62)\%$	$\leq 1\%$
$[sc]_{\tilde{A}}[\bar{s}\bar{c}]_{\tilde{A}}^*$	0^{++}	$3.0 - 3.5$	4.60 ± 0.10	1.4	$(39 - 62)\%$	$\ll 1\%$
$[sc]_V[\bar{s}\bar{c}]_V^*$	0^{++}	$3.6 - 4.1$	5.25 ± 0.10	2.6	$(40 - 62)\%$	$\ll 1\%$
$[sc]_{\tilde{V}}[\bar{s}\bar{c}]_{\tilde{V}}^*$	0^{++}	$4.7 - 5.4$	5.86 ± 0.10	3.5	$(41 - 60)\%$	$\ll 1\%$
$[sc]_P[\bar{s}\bar{c}]_P^*$	0^{++}	$4.8 - 5.6$	5.95 ± 0.10	3.7	$(40 - 61)\%$	$\ll 1\%$
$[sc]_S[\bar{s}\bar{c}]_A - [sc]_A[\bar{s}\bar{c}]_S$	1^{+-}	$3.2 - 3.7$	4.70 ± 0.10	1.5	$(39 - 61)\%$	$\ll 1\%$
$[sc]_A[\bar{s}\bar{c}]_A$	1^{+-}	$3.4 - 3.8$	4.76 ± 0.10	1.6	$(41 - 60)\%$	$\ll 1\%$
$[sc]_S[\bar{s}\bar{c}]_{\tilde{A}} - [sc]_{\tilde{A}}[\bar{s}\bar{c}]_S$	1^{+-}	$3.4 - 3.9$	4.76 ± 0.10	1.6	$(39 - 61)\%$	$\ll 1\%$
$[sc]_{\tilde{A}}[\bar{s}\bar{c}]_A - [sc]_A[\bar{s}\bar{c}]_{\tilde{A}}$	1^{+-}	$3.4 - 3.8$	4.76 ± 0.10	1.6	$(40 - 60)\%$	$\ll 1\%$
$[sc]_{\tilde{V}}[\bar{s}\bar{c}]_V + [sc]_V[\bar{s}\bar{c}]_{\tilde{V}}$	1^{+-}	$4.0 - 4.5$	5.40 ± 0.10	2.8	$(40 - 60)\%$	$\ll 1\%$
$[sc]_V[\bar{s}\bar{c}]_V$	1^{+-}	$5.4 - 6.3$	6.16 ± 0.10	3.8	$(41 - 61)\%$	$\ll 1\%$
$[sc]_P[\bar{s}\bar{c}]_V + [sc]_V[\bar{s}\bar{c}]_P$	1^{+-}	$4.6 - 5.3$	5.70 ± 0.10	3.2	$(41 - 61)\%$	$\ll 1\%$
$[sc]_S[\bar{s}\bar{c}]_A + [sc]_A[\bar{s}\bar{c}]_S$	1^{++}	$3.2 - 3.6$	4.70 ± 0.10	1.5	$(41 - 61)\%$	$\ll 1\%$
$[sc]_S[\bar{s}\bar{c}]_{\tilde{A}} + [sc]_{\tilde{A}}[\bar{s}\bar{c}]_S$	1^{++}	$3.4 - 3.9$	4.76 ± 0.10	1.6	$(39 - 60)\%$	$\ll 1\%$
$[sc]_{\tilde{V}}[\bar{s}\bar{c}]_V - [sc]_V[\bar{s}\bar{c}]_{\tilde{V}}$	1^{++}	$3.2 - 3.6$	4.86 ± 0.10	1.9	$(40 - 61)\%$	$\ll 1\%$
$[sc]_{\tilde{A}}[\bar{s}\bar{c}]_A + [sc]_A[\bar{s}\bar{c}]_{\tilde{A}}$	1^{++}	$4.9 - 5.8$	5.93 ± 0.10	3.5	$(39 - 61)\%$	$\ll 1\%$
$[sc]_P[\bar{s}\bar{c}]_V - [sc]_V[\bar{s}\bar{c}]_P$	1^{++}	$4.6 - 5.4$	5.70 ± 0.10	3.2	$(39 - 61)\%$	$\ll 1\%$
$[sc]_A[\bar{s}\bar{c}]_A$	2^{++}	$3.5 - 4.0$	4.82 ± 0.10	1.8	$(40 - 60)\%$	$\ll 1\%$
$[sc]_V[\bar{s}\bar{c}]_V$	2^{++}	$5.1 - 6.0$	6.05 ± 0.10	3.7	$(40 - 61)\%$	$\ll 1\%$

Table 6: The Borel windows, continuum threshold parameters, energy scales of the QCD spectral densities, pole contributions, and contributions of the vacuum condensates of dimension 10 for the ground state $cs\bar{c}\bar{s}$ tetraquark states [425].

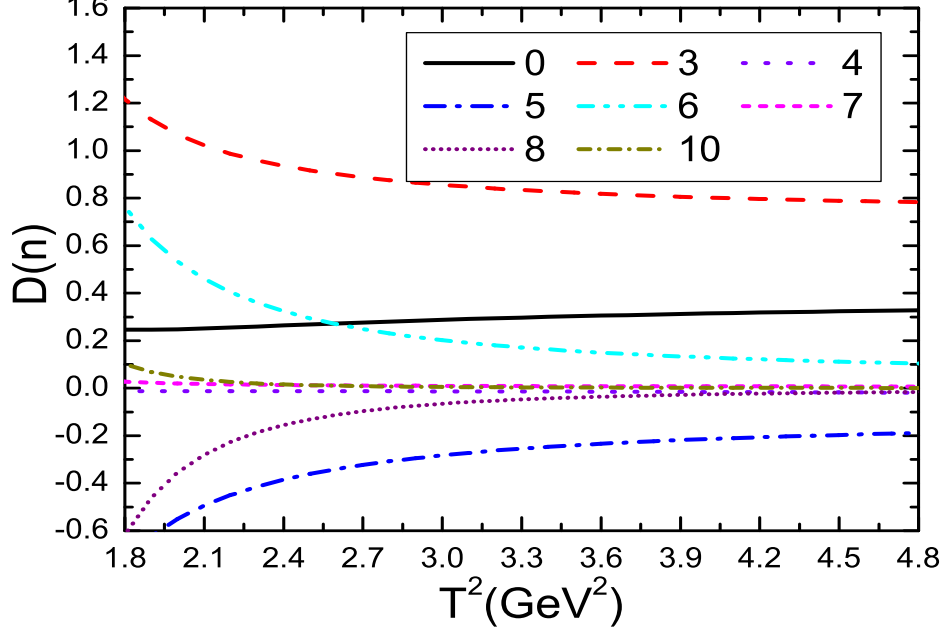


Figure 16: The $D(n)$ with variation of the Borel parameter T^2 for the current $J_{-,μ}^{SA}(x)$.

At the QCD side, the contributions of the vacuum condensates of dimension 10 are $|D(10)| \leq 1\%$ or $\ll 1\%$ except for $|D(10)| < 2\%$ for the $[uc]_{\tilde{V}}[\bar{d}\bar{c}]_V - [uc]_V[\bar{d}\bar{c}]_{\tilde{V}}$ tetraquark state with the $J^{PC} = 1^{++}$, the convergent behavior of the operator product expansion is very good.

In Fig.16, we plot the contributions of the vacuum condensates $D(n)$ with variation of the Borel parameter T^2 for the current $J_{-,μ}^{SA}(x)$. From the figure, we can see clearly that the main contributions come from the $D(0)$, $D(3)$, $D(5)$, $D(6)$ and $D(8)$, while the largest contribution comes from the $D(3)$. Therefore, if we would like to calculate the radiative $\mathcal{O}(\alpha_s)$ corrections, we should calculate the radiative $\mathcal{O}(\alpha_s)$ corrections to the $D(3)$, not just to the $D(0)$. At the present time, only the radiative $\mathcal{O}(\alpha_s)$ corrections to the $D(0)$ are partially calculated [128, 452, 456, 461, 516, 517, 518, 519].

We take account of all the uncertainties of the input parameters and obtain the masses and pole residues of the scalar, axialvector and tensor hidden-charm tetraquark states, which are shown explicitly in Tables 7-8. From Tables 5-8, we could see clearly that the modified energy scale formula $\mu = \sqrt{M_{X/Y/Z}^2 - (2\mathbb{M}_c)^2} - \kappa \mathbb{M}_s$ is well satisfied. In Fig.17, we plot the masses of the $[uc]_S[\bar{d}\bar{c}]_A - [uc]_A[\bar{d}\bar{c}]_S$ and $[uc]_S[\bar{d}\bar{c}]_A + [uc]_A[\bar{d}\bar{c}]_S$ tetraquark states having the spin-parity $J^P = 1^+$ with variations of the Borel parameters at much larger ranges than the Borel widows as an example, there appear platforms in the Borel windows indeed.

In Tables 9-10, we present the possible assignments of the ground state hidden-charm tetraquark states, and revisit the assignments based on the tetraquark scenario, there are rooms for the $X(3860)$, $X(3872)$, $X(3915)$, $X(3960)$, $X(4140)$, $X(4274)$, $X(4500)$, $X(4685)$, $X(4700)$, $Z_c(3900)$, $Z_c(4020)$, $Z_c(4050)$, $Z_c(4055)$, $Z_c(4430)$ and $Z_c(4600)$.

It is not difficult to reproduce the mass of the $X(3872)$ in the scenario of tetraquark state [58, 60, 61], it is a great challenge to reproduce the tiny width 1.19 ± 0.21 MeV from the Particle Data Group consistently [97]. In Ref.[62], we study the strong decays $X(3872) \rightarrow J/\psi \pi^+ \pi^-$, $J/\psi \omega$,

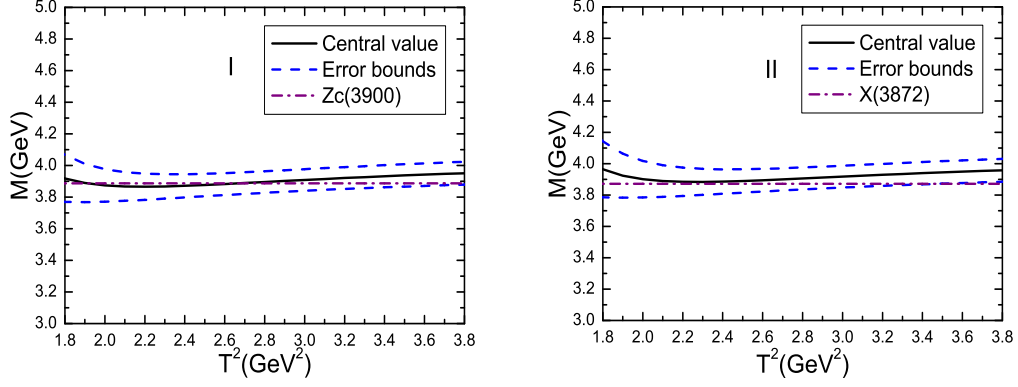


Figure 17: The masses of the $[uc]_S[\bar{d}\bar{c}]_A - [uc]_A[\bar{d}\bar{c}]_S$ (I) and $[uc]_S[\bar{d}\bar{c}]_A + [uc]_A[\bar{d}\bar{c}]_S$ (II) axialvector tetraquark states with variations of the Borel parameters T^2 .

$Z_c(X_c)$	J^{PC}	$M_Z(\text{GeV})$	$\lambda_Z(\text{GeV}^5)$
$[uc]_S[\bar{d}\bar{c}]_S$	0^{++}	3.88 ± 0.09	$(2.07 \pm 0.35) \times 10^{-2}$
$[uc]_A[\bar{d}\bar{c}]_A$	0^{++}	3.95 ± 0.09	$(4.49 \pm 0.77) \times 10^{-2}$
$[uc]_{\tilde{A}}[\bar{d}\bar{c}]_{\tilde{A}}$	0^{++}	3.98 ± 0.08	$(4.30 \pm 0.63) \times 10^{-2}$
$[uc]_V[\bar{d}\bar{c}]_V$	0^{++}	4.65 ± 0.09	$(1.35 \pm 0.22) \times 10^{-1}$
$[uc]_{\tilde{V}}[\bar{d}\bar{c}]_{\tilde{V}}$	0^{++}	5.35 ± 0.09	$(4.87 \pm 0.51) \times 10^{-1}$
$[uc]_P[\bar{d}\bar{c}]_P$	0^{++}	5.49 ± 0.09	$(2.11 \pm 0.21) \times 10^{-1}$
$[uc]_S[\bar{d}\bar{c}]_A - [uc]_A[\bar{d}\bar{c}]_S$	1^{+-}	3.90 ± 0.08	$(2.09 \pm 0.33) \times 10^{-2}$
$[uc]_A[\bar{d}\bar{c}]_A$	1^{+-}	4.02 ± 0.09	$(3.00 \pm 0.45) \times 10^{-2}$
$[uc]_S[\bar{d}\bar{c}]_{\tilde{A}} - [uc]_{\tilde{A}}[\bar{d}\bar{c}]_S$	1^{+-}	4.01 ± 0.09	$(3.02 \pm 0.45) \times 10^{-2}$
$[uc]_{\tilde{A}}[\bar{d}\bar{c}]_A - [uc]_A[\bar{d}\bar{c}]_{\tilde{A}}$	1^{+-}	4.02 ± 0.09	$(6.09 \pm 0.90) \times 10^{-2}$
$[uc]_{\tilde{V}}[\bar{d}\bar{c}]_V + [uc]_V[\bar{d}\bar{c}]_{\tilde{V}}$	1^{+-}	4.66 ± 0.10	$(1.18 \pm 0.21) \times 10^{-1}$
$[uc]_V[\bar{d}\bar{c}]_V$	1^{+-}	5.46 ± 0.09	$(1.72 \pm 0.17) \times 10^{-1}$
$[uc]_P[\bar{d}\bar{c}]_V + [uc]_V[\bar{d}\bar{c}]_P$	1^{+-}	5.45 ± 0.09	$(1.87 \pm 0.19) \times 10^{-1}$
$[uc]_S[\bar{d}\bar{c}]_A + [uc]_A[\bar{d}\bar{c}]_S$	1^{++}	3.91 ± 0.08	$(2.10 \pm 0.34) \times 10^{-2}$
$[uc]_S[\bar{d}\bar{c}]_{\tilde{A}} + [uc]_{\tilde{A}}[\bar{d}\bar{c}]_S$	1^{++}	4.02 ± 0.09	$(3.01 \pm 0.45) \times 10^{-2}$
$[uc]_{\tilde{V}}[\bar{d}\bar{c}]_V - [uc]_V[\bar{d}\bar{c}]_{\tilde{V}}$	1^{++}	4.08 ± 0.09	$(3.67 \pm 0.67) \times 10^{-2}$
$[uc]_{\tilde{A}}[\bar{d}\bar{c}]_A + [uc]_A[\bar{d}\bar{c}]_{\tilde{A}}$	1^{++}	5.19 ± 0.09	$(2.12 \pm 0.24) \times 10^{-1}$
$[uc]_P[\bar{d}\bar{c}]_V - [uc]_V[\bar{d}\bar{c}]_P$	1^{++}	5.46 ± 0.09	$(1.89 \pm 0.19) \times 10^{-1}$
$[uc]_A[\bar{d}\bar{c}]_A$	2^{++}	4.08 ± 0.09	$(4.67 \pm 0.68) \times 10^{-2}$
$[uc]_V[\bar{d}\bar{c}]_V$	2^{++}	5.40 ± 0.09	$(2.32 \pm 0.25) \times 10^{-1}$

Table 7: The masses and pole residues of the ground state hidden-charm tetraquark states [61].

X_c	J^{PC}	$M_X(\text{GeV})$	$\lambda_X(\text{GeV}^5)$
$[sc]_S[\bar{s}\bar{c}]_S$	0^{++}	4.08 ± 0.09	$(3.18 \pm 0.52) \times 10^{-2}$
$[sc]_A[\bar{s}\bar{c}]_A$	0^{++}	4.13 ± 0.09	$(6.02 \pm 1.02) \times 10^{-2}$
$[sc]_{\tilde{A}}[\bar{s}\bar{c}]_{\tilde{A}}$	0^{++}	4.16 ± 0.09	$(5.83 \pm 0.87) \times 10^{-2}$
$[sc]_V[\bar{s}\bar{c}]_V$	0^{++}	4.82 ± 0.09	$(1.70 \pm 0.25) \times 10^{-1}$
$[sc]_{\tilde{V}}[\bar{s}\bar{c}]_{\tilde{V}}$	0^{++}	5.46 ± 0.10	$(5.37 \pm 0.58) \times 10^{-1}$
$[sc]_P[\bar{s}\bar{c}]_P$	0^{++}	5.54 ± 0.10	$(2.13 \pm 0.22) \times 10^{-1}$
$[sc]_S[\bar{s}\bar{c}]_S^*$	0^{++}	3.99 ± 0.09	$(2.41 \pm 0.42) \times 10^{-2}$
$[sc]_A[\bar{s}\bar{c}]_A^*$	0^{++}	4.04 ± 0.09	$(4.24 \pm 0.76) \times 10^{-2}$
$[sc]_{\tilde{A}}[\bar{s}\bar{c}]_{\tilde{A}}^*$	0^{++}	4.08 ± 0.08	$(4.39 \pm 0.69) \times 10^{-2}$
$[sc]_V[\bar{s}\bar{c}]_V^*$	0^{++}	4.70 ± 0.09	$(1.31 \pm 0.23) \times 10^{-1}$
$[sc]_{\tilde{V}}[\bar{s}\bar{c}]_{\tilde{V}}^*$	0^{++}	5.37 ± 0.11	$(4.41 \pm 0.47) \times 10^{-1}$
$[sc]_P[\bar{s}\bar{c}]_P^*$	0^{++}	5.47 ± 0.11	$(1.86 \pm 0.19) \times 10^{-1}$
$[sc]_S[\bar{s}\bar{c}]_A - [sc]_A[\bar{s}\bar{c}]_S$	1^{+-}	4.11 ± 0.10	$(2.91 \pm 0.48) \times 10^{-2}$
$[sc]_A[\bar{s}\bar{c}]_A$	1^{+-}	4.17 ± 0.08	$(3.65 \pm 0.55) \times 10^{-2}$
$[sc]_S[\bar{s}\bar{c}]_{\tilde{A}} - [sc]_{\tilde{A}}[\bar{s}\bar{c}]_S$	1^{+-}	4.17 ± 0.09	$(3.71 \pm 0.57) \times 10^{-2}$
$[sc]_{\tilde{A}}[\bar{s}\bar{c}]_A - [sc]_A[\bar{s}\bar{c}]_{\tilde{A}}$	1^{+-}	4.18 ± 0.09	$(7.50 \pm 1.12) \times 10^{-2}$
$[sc]_{\tilde{V}}[\bar{s}\bar{c}]_V + [sc]_V[\bar{s}\bar{c}]_{\tilde{V}}$	1^{+-}	4.82 ± 0.09	$(1.45 \pm 0.23) \times 10^{-1}$
$[sc]_V[\bar{s}\bar{c}]_V$	1^{+-}	5.57 ± 0.11	$(1.89 \pm 0.19) \times 10^{-1}$
$[sc]_P[\bar{s}\bar{c}]_V + [sc]_V[\bar{s}\bar{c}]_P$	1^{+-}	5.13 ± 0.10	$(1.33 \pm 0.16) \times 10^{-1}$
$[sc]_S[\bar{s}\bar{c}]_A + [sc]_A[\bar{s}\bar{c}]_S$	1^{++}	4.11 ± 0.09	$(2.88 \pm 0.46) \times 10^{-2}$
$[sc]_S[\bar{s}\bar{c}]_{\tilde{A}} + [sc]_{\tilde{A}}[\bar{s}\bar{c}]_S$	1^{++}	4.17 ± 0.09	$(3.67 \pm 0.57) \times 10^{-2}$
$[sc]_{\tilde{V}}[\bar{s}\bar{c}]_V - [sc]_V[\bar{s}\bar{c}]_{\tilde{V}}$	1^{++}	4.29 ± 0.09	$(5.49 \pm 0.92) \times 10^{-2}$
$[sc]_{\tilde{A}}[\bar{s}\bar{c}]_A + [sc]_A[\bar{s}\bar{c}]_{\tilde{A}}$	1^{++}	5.34 ± 0.10	$(2.52 \pm 0.30) \times 10^{-1}$
$[sc]_P[\bar{s}\bar{c}]_V - [sc]_V[\bar{s}\bar{c}]_P$	1^{++}	5.12 ± 0.10	$(1.33 \pm 0.17) \times 10^{-1}$
$[sc]_A[\bar{s}\bar{c}]_A$	2^{++}	4.24 ± 0.09	$(6.03 \pm 0.88) \times 10^{-2}$
$[sc]_V[\bar{s}\bar{c}]_V$	2^{++}	5.49 ± 0.11	$(2.43 \pm 0.26) \times 10^{-1}$

Table 8: The masses and pole residues of the ground state hidden-charm-hidden-strange tetraquark states [425].

$Z_c(X_c)$	J^{PC}	$M_{X/Z}(\text{GeV})$	Assignments	$Z'_c(X'_c)$
$[uc]_S[\bar{d}\bar{c}]_S$	0^{++}	3.88 ± 0.09	? $X(3860)$	
$[uc]_A[\bar{d}\bar{c}]_A$	0^{++}	3.95 ± 0.09	? $X(3915)$	
$[uc]_{\bar{A}}[\bar{d}\bar{c}]_{\bar{A}}$	0^{++}	3.98 ± 0.08		
$[uc]_V[\bar{d}\bar{c}]_V$	0^{++}	4.65 ± 0.09		
$[uc]_{\bar{V}}[\bar{d}\bar{c}]_{\bar{V}}$	0^{++}	5.35 ± 0.09		
$[uc]_P[\bar{d}\bar{c}]_P$	0^{++}	5.49 ± 0.09		
$[uc]_S[\bar{d}\bar{c}]_A - [uc]_A[\bar{d}\bar{c}]_S$	1^{+-}	3.90 ± 0.08	? $Z_c(3900)$? $Z_c(4430)$
$[uc]_A[\bar{d}\bar{c}]_A$	1^{+-}	4.02 ± 0.09	? $Z_c(4020/4055)$? $Z_c(4600)$
$[uc]_S[\bar{d}\bar{c}]_{\bar{A}} - [uc]_{\bar{A}}[\bar{d}\bar{c}]_S$	1^{+-}	4.01 ± 0.09	? $Z_c(4020/4055)$? $Z_c(4600)$
$[uc]_{\bar{A}}[\bar{d}\bar{c}]_A - [uc]_A[\bar{d}\bar{c}]_{\bar{A}}$	1^{+-}	4.02 ± 0.09	? $Z_c(4020/4055)$? $Z_c(4600)$
$[uc]_{\bar{V}}[\bar{d}\bar{c}]_V + [uc]_V[\bar{d}\bar{c}]_{\bar{V}}$	1^{+-}	4.66 ± 0.10	? $Z_c(4600)$	
$[uc]_V[\bar{d}\bar{c}]_V$	1^{+-}	5.46 ± 0.09		
$[uc]_P[\bar{d}\bar{c}]_V + [uc]_V[\bar{d}\bar{c}]_P$	1^{+-}	5.45 ± 0.09		
$[uc]_S[\bar{d}\bar{c}]_A + [uc]_A[\bar{d}\bar{c}]_S$	1^{++}	3.91 ± 0.08	? $X(3872)$	
$[uc]_S[\bar{d}\bar{c}]_{\bar{A}} + [uc]_{\bar{A}}[\bar{d}\bar{c}]_S$	1^{++}	4.02 ± 0.09	? $Z_c(4050)$	
$[uc]_{\bar{V}}[\bar{d}\bar{c}]_V - [uc]_V[\bar{d}\bar{c}]_{\bar{V}}$	1^{++}	4.08 ± 0.09	? $Z_c(4050)$	
$[uc]_{\bar{A}}[\bar{d}\bar{c}]_A + [uc]_A[\bar{d}\bar{c}]_{\bar{A}}$	1^{++}	5.19 ± 0.09		
$[uc]_P[\bar{d}\bar{c}]_V - [uc]_V[\bar{d}\bar{c}]_P$	1^{++}	5.46 ± 0.09		
$[uc]_A[\bar{d}\bar{c}]_A$	2^{++}	4.08 ± 0.09	? $Z_c(4050)$	
$[uc]_V[\bar{d}\bar{c}]_V$	2^{++}	5.40 ± 0.09		
$[uc]_A[\bar{d}\bar{c}]_A$	1^{+-}	4.02 ± 0.09	? $h_c(4000)$	
$[uc]_S[\bar{d}\bar{c}]_{\bar{A}} - [uc]_{\bar{A}}[\bar{d}\bar{c}]_S$	1^{+-}	4.01 ± 0.09	? $h_c(4000)$	
$[uc]_{\bar{A}}[\bar{d}\bar{c}]_A - [uc]_A[\bar{d}\bar{c}]_{\bar{A}}$	1^{+-}	4.02 ± 0.09	? $h_c(4000)$	
$[uc]_S[\bar{d}\bar{c}]_{\bar{A}} + [uc]_{\bar{A}}[\bar{d}\bar{c}]_S$	1^{++}	4.02 ± 0.09	? $\chi_{c1}(4010)$	

Table 9: The possible assignments of the hidden-charm tetraquark states, the isospin limit is implied [61, 184, 425].

X_c	J^{PC}	$M_X(\text{GeV})$	Assignments	X'_c
$[sc]_S[\bar{s}\bar{c}]_S$	0^{++}	4.08 ± 0.09		
$[sc]_A[\bar{s}\bar{c}]_A$	0^{++}	4.13 ± 0.09		? $X(4700)$
$[sc]_{\bar{A}}[\bar{s}\bar{c}]_{\bar{A}}$	0^{++}	4.16 ± 0.09		? $X(4700)$
$[sc]_V[\bar{s}\bar{c}]_V$	0^{++}	4.82 ± 0.09		
$[sc]_{\bar{V}}[\bar{s}\bar{c}]_{\bar{V}}$	0^{++}	5.46 ± 0.10		
$[sc]_P[\bar{s}\bar{c}]_P$	0^{++}	5.54 ± 0.10		
$[sc]_S[\bar{s}\bar{c}]_S^*$	0^{++}	3.99 ± 0.09	? $X(3960)$? $X(4500)$
$[sc]_A[\bar{s}\bar{c}]_A^*$	0^{++}	4.04 ± 0.09		
$[sc]_{\bar{A}}[\bar{s}\bar{c}]_{\bar{A}}^*$	0^{++}	4.08 ± 0.08	? $X(4700)$	
$[sc]_V[\bar{s}\bar{c}]_V^*$	0^{++}	4.70 ± 0.09		
$[sc]_{\bar{V}}[\bar{s}\bar{c}]_{\bar{V}}^*$	0^{++}	5.37 ± 0.11		
$[sc]_P[\bar{s}\bar{c}]_P^*$	0^{++}	5.47 ± 0.11		
$[sc]_S[\bar{s}\bar{c}]_A - [sc]_A[\bar{s}\bar{c}]_S$	1^{+-}	4.11 ± 0.10		
$[sc]_A[\bar{s}\bar{c}]_A$	1^{+-}	4.17 ± 0.08		
$[sc]_S[\bar{s}\bar{c}]_{\bar{A}} - [sc]_{\bar{A}}[\bar{s}\bar{c}]_S$	1^{+-}	4.17 ± 0.09		
$[sc]_{\bar{A}}[\bar{s}\bar{c}]_A - [sc]_A[\bar{s}\bar{c}]_{\bar{A}}$	1^{+-}	4.18 ± 0.09		
$[sc]_{\bar{V}}[\bar{s}\bar{c}]_V + [sc]_V[\bar{s}\bar{c}]_{\bar{V}}$	1^{+-}	4.82 ± 0.09		
$[sc]_V[\bar{s}\bar{c}]_V$	1^{+-}	5.57 ± 0.11		
$[sc]_P[\bar{s}\bar{c}]_V + [sc]_V[\bar{s}\bar{c}]_P$	1^{+-}	5.13 ± 0.10		
$[sc]_S[\bar{s}\bar{c}]_A + [sc]_A[\bar{s}\bar{c}]_S$	1^{++}	4.11 ± 0.09	? $X(4140)$? $X(4685)$
$[sc]_S[\bar{s}\bar{c}]_{\bar{A}} + [sc]_{\bar{A}}[\bar{s}\bar{c}]_S$	1^{++}	4.17 ± 0.09	? $X(4140)$? $X(4685)$
$[sc]_{\bar{V}}[\bar{s}\bar{c}]_V - [sc]_V[\bar{s}\bar{c}]_{\bar{V}}$	1^{++}	4.29 ± 0.09	? $X(4274)$	
$[sc]_{\bar{A}}[\bar{s}\bar{c}]_A + [sc]_A[\bar{s}\bar{c}]_{\bar{A}}$	1^{++}	5.34 ± 0.10		
$[sc]_P[\bar{s}\bar{c}]_V - [sc]_V[\bar{s}\bar{c}]_P$	1^{++}	5.12 ± 0.10		
$[sc]_A[\bar{s}\bar{c}]_A$	2^{++}	4.24 ± 0.09		
$[sc]_V[\bar{s}\bar{c}]_V$	2^{++}	5.49 ± 0.11		

Table 10: The possible assignments of the hidden-charm-hidden-strange tetraquark states [425].

$\chi_{c1}\pi^0$, $D^{*0}\bar{D}^0$ and $D^0\bar{D}^0\pi^0$ via the QCD sum rules according to rigorous quark-hadron duality, and obtain the total decay width about 1 MeV, it is the first time to reproduce the tiny width of the $X(3872)$ via the QCD sum rules. The thresholds of the $J/\psi\rho$ and $J/\psi\omega$ are 3872.16 MeV and 3879.56 MeV respectively, which are larger than the value 3871.64 MeV of the mass of the $X(3872)$ from the Particle Data Group [97] and also lead to the possibility that it may be a $J/\psi\rho$ or $J/\psi\omega$ molecular state [84], the decays $X(3872) \rightarrow J/\psi\pi^+\pi^-$ and $J/\psi\pi^+\pi^-\pi^-$ take place through the virtual ρ and ω mesons, respectively, we introduce form-factors to parameterize the off-shell-ness, however, the arbitrariness in choosing the form-factors would impair the predictive ability.

As far as the $Z_c(3900)$ is concerned, it is not difficult to reproduce its mass and width via the QCD sum rules [60, 61, 520]. It is the benchmark for the **33** type hidden-charm tetraquark states in the simple diquark models [56, 301, 312, 313, 521].

In Table 9, there are enough rooms to accommodate the $h_c(4000)$ and $\chi_{c1}(4010)$ in the scenario of tetraquark states, as the central values of the predicted tetraquark masses happen to coincide with the experimental data from the LHCb collaboration [109]. We should bear in mind that the predictions were made **before** the experimental observation, therefore the calculations are robust enough [61]. While in the traditional charmonium scenario, the h'_c and χ'_{c1} have the masses 3956 MeV and 3953 MeV, respectively [108], there exist discrepancies about 50 – 60 MeV.

The predictions $M_X = 4.11 \pm 0.09$ GeV and 4.17 ± 0.09 GeV for the 1S $[sc]_S[\bar{s}\bar{c}]_A + [sc]_A[\bar{s}\bar{c}]_S$ and $[sc]_S[\bar{s}\bar{c}]_{\bar{A}} + [sc]_{\bar{A}}[\bar{s}\bar{c}]_S$ tetraquark states with the $J^{PC} = 1^{++}$ respectively support assigning the $X(4140)$ and $X(4685)$ as the 1S and 2S $[sc]_S[\bar{s}\bar{c}]_A + [sc]_A[\bar{s}\bar{c}]_S$ or $[sc]_S[\bar{s}\bar{c}]_{\bar{A}} + [sc]_{\bar{A}}[\bar{s}\bar{c}]_S$ tetraquark states respectively. In Refs.[507, 522], we obtain the prediction $M_X = 4.14 \pm 0.10$ GeV for the 1S $[sc]_{\bar{V}}[\bar{s}\bar{c}]_V - [sc]_V[\bar{s}\bar{c}]_{\bar{V}}$ tetraquark state with the $J^{PC} = 1^{++}$ in the old scheme, which supports assigning the $X(4140)$ as the $[sc]_{\bar{V}}[\bar{s}\bar{c}]_V - [sc]_V[\bar{s}\bar{c}]_{\bar{V}}$ tetraquark state.

The prediction $M_X = 4.29 \pm 0.09$ GeV for the 1S $[sc]_{\bar{V}}[\bar{s}\bar{c}]_V - [sc]_V[\bar{s}\bar{c}]_{\bar{V}}$ tetraquark state supports assigning the $X(4274)$ as the $[sc]_{\bar{V}}[\bar{s}\bar{c}]_V - [sc]_V[\bar{s}\bar{c}]_{\bar{V}}$ tetraquark state with the $J^{PC} = 1^{++}$. The calculations in Refs.[507, 522] are updated, as where the light-flavor $SU(3)$ mass-breaking effects in the energy scale formula are not taken into account.

In Ref.[523], the predictions support assigning the $X(4274)$ as the $[sc]_A[\bar{s}\bar{c}]_V - [sc]_V[\bar{s}\bar{c}]_A$ tetraquark state with a relative P-wave between the diquark and antidiquark pairs, such an assignment does not suffer from shortcomings in sense of treating scheme. The $X(4274)$ maybe have two important Fock components.

The $X(4140)$ and $X(4274)$ are also play an important role in establishing the hidden-charm tetraquark states, especially the $X(4140)$. There have been several possible assignments of the $X(4140)$, such as the tetraquark state [315, 316, 332, 333, 425, 507, 522, 524, 525, 526, 527], hybrid state [477, 478, 528] or rescattering effect [529], etc.

In Table 10, we assign the $X(3960)$ and $X(4500)$ as the 1S and 2S $[cs]_S[\bar{c}\bar{s}]_S$ tetraquark states with the $J^{PC} = 0^{++}$, the $X(4700)$ as the 1S $[cs]_V[\bar{c}\bar{s}]_V$ tetraquark state with the $J^{PC} = 0^{++}$; or assign the $X(4700)$ as the 2S $[cs]_A[\bar{c}\bar{s}]_A$ or $[cs]_{\bar{A}}[\bar{c}\bar{s}]_{\bar{A}}$ tetraquark state with the $J^{PC} = 0^{++}$. In Ref.[530], we assign the $X(4500)$ as the $[sc]_{\bar{V}}[\bar{s}\bar{c}]_{\bar{V}}$ tetraquark state with the $J^{PC} = 0^{++}$, where the \bar{V} denotes the diquark with an explicit P-wave. In Ref.[527], Chen et al assign the $X(4500)$ and $X(4700)$ as the D -wave tetraquark states with the quark content $cs\bar{c}\bar{s}$ and $J^P = 0^+$: the $X(4500)$ consists of one D -wave diquark and one S -wave antidiquark, with the antisymmetric color structure **33**; the $X(4700)$ consists of similar diquarks but with the symmetric color structure **66**.

However, there is no room for the $X(4350)$, we should introduce mixing effect to interpret its nature [484].

In fact, the predictions of the QCD sum rules have arbitrariness, and depend on the interpolating currents, truncations of the operator product expansion, convergent behavior, pole contributions, input parameters, etc. Therefore, the predictions maybe quite different, we have to perform systematic investigations with uniform criterion to outcome the shortcomings.

We suggest to study the two-body strong decays to diagnose those hidden-charm tetraquark

states [61, 425], for example,

$$\begin{aligned}
Z_c^\pm(1^{+-}) &\rightarrow \pi^\pm J/\psi, \pi^\pm \psi', \pi^\pm h_c, \rho^\pm \eta_c, (D\bar{D}^*)^\pm, (D^*\bar{D})^\pm, (D^*\bar{D}^*)^\pm, \\
Z_c^\pm(0^{++}) &\rightarrow \pi^\pm \eta_c, \pi^\pm \chi_{c1}, \rho^\pm J/\psi, \rho^\pm \psi', (D\bar{D})^\pm, (D^*\bar{D}^*)^\pm, \\
Z_c^\pm(1^{++}) &\rightarrow \pi^\pm \chi_{c1}, \rho^\pm J/\psi, \rho^\pm \psi', (D\bar{D}^*)^\pm, (D^*\bar{D})^\pm, (D^*\bar{D}^*)^\pm, \\
Z_c^\pm(2^{++}) &\rightarrow \pi^\pm \eta_c, \pi^\pm \chi_{c1}, \rho^\pm J/\psi, \rho^\pm \psi', (D\bar{D})^\pm, (D^*\bar{D}^*)^\pm,
\end{aligned} \tag{143}$$

$$\begin{aligned}
Z_c^0(1^{+-}) &\rightarrow \pi^0 J/\psi, \pi^0 \psi', \pi^0 h_c, \rho^0 \eta_c, (D\bar{D}^*)^0, (D^*\bar{D})^0, (D^*\bar{D}^*)^0, \\
Z_c^0(0^{++}) &\rightarrow \pi^0 \eta_c, \pi^0 \chi_{c1}, \rho^0 J/\psi, \rho^0 \psi', (D\bar{D})^0, (D^*\bar{D}^*)^0, \\
Z_c^0(1^{++}) &\rightarrow \pi^0 \chi_{c1}, \rho^0 J/\psi, \rho^0 \psi', (D\bar{D}^*)^0, (D^*\bar{D})^0, (D^*\bar{D}^*)^0, \\
Z_c^0(2^{++}) &\rightarrow \pi^0 \eta_c, \pi^0 \chi_{c1}, \rho^0 J/\psi, \rho^0 \psi', (D\bar{D})^0, (D^*\bar{D}^*)^0,
\end{aligned} \tag{144}$$

$$\begin{aligned}
X(1^{+-}) &\rightarrow \eta J/\psi, \eta \psi', \eta h_c, \omega \eta_c, (D\bar{D}^*)^0, (D^*\bar{D})^0, (D^*\bar{D}^*)^0, \\
X(0^{++}) &\rightarrow \eta \eta_c, \eta \chi_{c1}, \omega J/\psi, \omega \psi', (D\bar{D})^0, (D^*\bar{D}^*)^0, \\
X(1^{++}) &\rightarrow \eta \chi_{c1}, \omega J/\psi, \omega \psi', (D\bar{D}^*)^0, (D^*\bar{D})^0, (D^*\bar{D}^*)^0, \\
X(2^{++}) &\rightarrow \eta \eta_c, \eta \chi_{c1}, \omega J/\psi, \omega \psi', (D\bar{D})^0, (D^*\bar{D}^*)^0,
\end{aligned} \tag{145}$$

$$\begin{aligned}
X(1^{+-}) &\rightarrow \eta J/\psi, \eta \psi', \eta h_c, \phi \eta_c, D_s \bar{D}_s^*, D_s^* \bar{D}_s, D_s^* \bar{D}_s^*, \\
X(0^{++}) &\rightarrow \eta \eta_c, \eta \chi_{c1}, \phi J/\psi, \phi \psi', D_s \bar{D}_s, D_s^* \bar{D}_s^*, \\
X(1^{++}) &\rightarrow \eta \chi_{c1}, \phi J/\psi, \phi \psi', D_s \bar{D}_s^*, D_s^* \bar{D}_s, D_s^* \bar{D}_s^*, \\
X(2^{++}) &\rightarrow \eta \eta_c, \eta \chi_{c1}, \phi J/\psi, \phi \psi', D_s \bar{D}_s, D_s^* \bar{D}_s^*.
\end{aligned} \tag{146}$$

The LHCb collaboration observed the $h_c(4000)$ and $\chi_{c1}(4010)$ in the $D^{*\pm}D^\mp$ mass spectrum [109], see the two-body strong decays of the Z_c^0 shown in Eq.(144).

As the $c\bar{c}q\bar{s}$ tetraquark states are concerned, we present the predictions based on the direct calculations plus light-flavor $SU(3)$ -breaking effects in Table 11 [171, 172]. In Ref.[171], we tentatively assign the $Z_c(4020/4025)$ as the $A\bar{A}$ -type hidden-charm tetraquark state with the $J^{PC} = 1^{+-}$ according to the analogous properties of the $Z_c(3900/3885)$ and $Z_{cs}(3985/4000)$, and study the $A\bar{A}$ -type tetraquark states without strange, with strange and with hidden-strange via the QCD sum rules in a consistent way. Then we study the hadronic coupling constants of the tetraquark states without strange and with strange via the QCD sum rules based on rigorous quark-hadron duality, and obtain the total decay widths,

$$\begin{aligned}
\Gamma_{Z_{cs}} &= 22.71 \pm 1.65 \text{ (or } \pm 6.60) \text{ MeV}, \\
\Gamma_{Z_c} &= 29.57 \pm 2.30 \text{ (or } \pm 9.20) \text{ MeV},
\end{aligned} \tag{147}$$

and suggest to search for the Z_{cs} state in the mass spectrum of the $h_c K$, $J/\psi K$, $\eta_c K^*$, $D^* \bar{D}_s^*$, $D_s^* \bar{D}^*$. Slightly later, the BESIII collaboration observed an evidence for the $Z_{cs}(4123)$ [170].

With the simple replacement,

$$c \rightarrow b, \tag{148}$$

we obtain the corresponding QCD sum rules for the hidden-bottom tetraquark states. And we would like to present the results from the QCD sum rules in Ref.[531] directly, see Tables 12-13.

In calculations, we use the energy scale formula $\mu = \sqrt{M_{X/Y/Z}^2 - (2\mathbb{M}_b)^2}$ with the effective b -quark mass $\mathbb{M}_b = 5.17 \text{ GeV}$ to determine the ideal energy scales of the QCD spectral densities [532], and choose the continuum threshold parameters $\sqrt{s_0} = Z_b + 0.55 \pm 0.10 \text{ GeV}$ as a constraint to extract the masses and pole residues from the QCD sum rules. The predicted masses $10.61 \pm$

$Z_c(X_c)$	J^{PC}	$M_Z(\text{GeV})$	Assignments
$[uc]_S[\bar{s}\bar{c}]_S$	0^{++}	3.97 ± 0.09	
$[uc]_A[\bar{s}\bar{c}]_A$	0^{++}	4.04 ± 0.09	
$[uc]_{\tilde{A}}[\bar{s}\bar{c}]_{\tilde{A}}$	0^{++}	4.07 ± 0.08	
$[uc]_V[\bar{s}\bar{c}]_V$	0^{++}	4.74 ± 0.09	
$[uc]_{\tilde{V}}[\bar{s}\bar{c}]_{\tilde{V}}$	0^{++}	5.44 ± 0.09	
$[uc]_P[\bar{s}\bar{c}]_P$	0^{++}	5.58 ± 0.09	
$[uc]_S[\bar{s}\bar{c}]_A - [uc]_A[\bar{s}\bar{c}]_S$	1^{+-}	3.99 ± 0.09	? $Z_{cs}(3985)$
$[uc]_A[\bar{s}\bar{c}]_A$	1^{+-}	4.11 ± 0.09	? $Z_{cs}(4123)$
$[uc]_S[\bar{s}\bar{c}]_{\tilde{A}} - [uc]_{\tilde{A}}[\bar{s}\bar{c}]_S$	1^{+-}	4.10 ± 0.09	? $Z_{cs}(4123)$
$[uc]_{\tilde{A}}[\bar{s}\bar{c}]_A - [uc]_A[\bar{s}\bar{c}]_{\tilde{A}}$	1^{+-}	4.11 ± 0.09	? $Z_{cs}(4123)$
$[uc]_{\tilde{V}}[\bar{s}\bar{c}]_V + [uc]_V[\bar{s}\bar{c}]_{\tilde{V}}$	1^{+-}	4.75 ± 0.10	
$[uc]_V[\bar{s}\bar{c}]_V$	1^{+-}	5.55 ± 0.09	
$[uc]_P[\bar{s}\bar{c}]_V + [uc]_V[\bar{s}\bar{c}]_P$	1^{+-}	5.54 ± 0.09	
$[uc]_S[\bar{s}\bar{c}]_A + [uc]_A[\bar{s}\bar{c}]_S$	1^{++}	3.99 ± 0.09	? $Z_{cs}(3985)$
$[uc]_S[\bar{s}\bar{c}]_{\tilde{A}} + [uc]_{\tilde{A}}[\bar{s}\bar{c}]_S$	1^{++}	4.11 ± 0.09	? $Z_{cs}(4123)$
$[uc]_{\tilde{V}}[\bar{s}\bar{c}]_V - [uc]_V[\bar{s}\bar{c}]_{\tilde{V}}$	1^{++}	4.17 ± 0.09	
$[uc]_{\tilde{A}}[\bar{s}\bar{c}]_A + [uc]_A[\bar{s}\bar{c}]_{\tilde{A}}$	1^{++}	5.28 ± 0.09	
$[uc]_P[\bar{s}\bar{c}]_V - [uc]_V[\bar{s}\bar{c}]_P$	1^{++}	5.55 ± 0.09	
$[uc]_A[\bar{s}\bar{c}]_A$	2^{++}	4.17 ± 0.09	
$[uc]_V[\bar{s}\bar{c}]_V$	2^{++}	5.49 ± 0.09	

Table 11: The possible assignments of the ground state hidden-charm tetraquark states with strangeness [171, 172].

Z_b	J^{PC}	$T^2(\text{GeV}^2)$	$\sqrt{s_0}(\text{GeV})$	$\mu(\text{GeV})$	pole	$ D(10) $
$[ub]_S[\bar{d}\bar{b}]_S$	0^{++}	$7.0 - 8.0$	11.16 ± 0.10	2.40	$(44 - 66)\%$	$\leq 3\%$
$[ub]_A[\bar{d}\bar{b}]_A$	0^{++}	$6.4 - 7.4$	11.14 ± 0.10	2.30	$(44 - 68)\%$	$\leq 11\%$
$[ub]_{\tilde{A}}[\bar{d}\bar{b}]_{\tilde{A}}$	0^{++}	$7.2 - 8.2$	11.17 ± 0.10	2.40	$(45 - 66)\%$	$\leq 4\%$
$[ub]_{\tilde{V}}[\bar{d}\bar{b}]_{\tilde{V}}$	0^{++}	$11.4 - 12.8$	12.22 ± 0.10	5.40	$(44 - 61)\%$	$\ll 1\%$
$[ub]_S[\bar{d}\bar{b}]_A - [ub]_A[\bar{d}\bar{b}]_S$	1^{+-}	$7.0 - 8.0$	11.16 ± 0.10	2.40	$(44 - 66)\%$	$< 4\%$
$[ub]_A[\bar{d}\bar{b}]_A$	1^{+-}	$7.1 - 8.1$	11.17 ± 0.10	2.40	$(44 - 65)\%$	$\leq 4\%$
$[ub]_{\tilde{A}}[\bar{d}\bar{b}]_A - [ub]_A[\bar{d}\bar{b}]_{\tilde{A}}$	1^{+-}	$6.9 - 7.9$	11.17 ± 0.10	2.40	$(44 - 66)\%$	$\leq 7\%$
$[ub]_S[\bar{d}\bar{b}]_{\tilde{A}} - [ub]_{\tilde{A}}[\bar{d}\bar{b}]_S$	1^{+-}	$7.1 - 8.1$	11.17 ± 0.10	2.40	$(44 - 66)\%$	$\leq 4\%$
$[ub]_S[\bar{d}\bar{b}]_A + [ub]_A[\bar{d}\bar{b}]_S$	1^{++}	$7.1 - 8.1$	11.18 ± 0.10	2.45	$(44 - 65)\%$	$\leq 3\%$
$[ub]_{\tilde{V}}[\bar{d}\bar{b}]_V - [ub]_V[\bar{d}\bar{b}]_{\tilde{V}}$	1^{++}	$6.8 - 7.8$	11.19 ± 0.10	2.50	$(44 - 66)\%$	$\leq 4\%$
$[ub]_{\tilde{A}}[\bar{d}\bar{b}]_A + [ub]_A[\bar{d}\bar{b}]_{\tilde{A}}$	1^{++}	$9.7 - 11.1$	11.99 ± 0.10	4.90	$(44 - 63)\%$	$\ll 1\%$
$[ub]_A[\bar{d}\bar{b}]_A$	2^{++}	$7.2 - 8.2$	11.19 ± 0.10	2.50	$(44 - 65)\%$	$< 4\%$

Table 12: The Borel parameters, continuum threshold parameters, energy scales of the QCD spectral densities, pole contributions, and contributions of the vacuum condensates of dimension 10 for the ground state hidden-bottom tetraquark states [531].

Z_b	J^{PC}	$M_Z(\text{GeV})$	$\lambda_Z(\text{GeV}^5)$
$[ub]_S[\bar{d}\bar{b}]_S$	0^{++}	10.61 ± 0.09	$(1.10 \pm 0.17) \times 10^{-1}$
$[ub]_A[\bar{d}\bar{b}]_A$	0^{++}	10.60 ± 0.09	$(1.61 \pm 0.25) \times 10^{-1}$
$[ub]_{\bar{A}}[\bar{d}\bar{b}]_{\bar{A}}$	0^{++}	10.61 ± 0.09	$(1.81 \pm 0.27) \times 10^{-1}$
$[ub]_{\bar{V}}[\bar{d}\bar{b}]_{\bar{V}}$	0^{++}	11.66 ± 0.12	3.03 ± 0.31
$[ub]_S[\bar{d}\bar{b}]_A - [ub]_A[\bar{d}\bar{b}]_S$	1^{+-}	10.61 ± 0.09	$(1.08 \pm 0.16) \times 10^{-1}$
$[ub]_A[\bar{d}\bar{b}]_A$	1^{+-}	10.62 ± 0.09	$(1.07 \pm 0.16) \times 10^{-1}$
$[ub]_{\bar{A}}[\bar{d}\bar{b}]_A - [ub]_A[\bar{d}\bar{b}]_{\bar{A}}$	1^{+-}	10.62 ± 0.09	$(2.12 \pm 0.31) \times 10^{-1}$
$[ub]_S[\bar{d}\bar{b}]_{\bar{A}} - [ub]_{\bar{A}}[\bar{d}\bar{b}]_S$	1^{+-}	10.62 ± 0.09	$(1.08 \pm 0.16) \times 10^{-1}$
$[ub]_S[\bar{d}\bar{b}]_A + [ub]_A[\bar{d}\bar{b}]_S$	1^{++}	10.63 ± 0.09	$(1.17 \pm 0.17) \times 10^{-1}$
$[ub]_{\bar{V}}[\bar{d}\bar{b}]_V - [ub]_V[\bar{d}\bar{b}]_{\bar{V}}$	1^{++}	10.63 ± 0.09	$(1.22 \pm 0.20) \times 10^{-1}$
$[ub]_{\bar{A}}[\bar{d}\bar{b}]_A + [ub]_A[\bar{d}\bar{b}]_{\bar{A}}$	1^{++}	11.45 ± 0.14	$(8.52 \pm 1.02) \times 10^{-1}$
$[ub]_A[\bar{d}\bar{b}]_A$	2^{++}	10.65 ± 0.09	$(1.72 \pm 0.24) \times 10^{-1}$

Table 13: The masses and pole residues of the ground state hidden-bottom tetraquark states [531].

0.09 GeV and 10.62 ± 0.09 GeV for the 1^{+-} tetraquark states support assigning the $Z_b(10610)$ and $Z_b(10650)$ to be the hidden-bottom tetraquark states with the $J^{PC} = 1^{+-}$, more theoretical and experimental works are still needed to assign the $Z_b(10610)$ and $Z_b(10650)$ unambiguously according to the partial decay widths.

In the diquark-model, the $Z_b^\pm(10610)$ and $Z_b^\pm(10650)$ are also assigned as the $S\bar{A} - A\bar{S}$ -type and $A\bar{A}$ -type hidden-bottom tetraquark states, respectively [533, 534]. And we could extend this subsection to study the B_c -like tetraquark states [458, 535, 536, 537].

3.1.2 Tetraquark states with the first radial excitations

In this sub-section, we would like to study the first radial excitations of the hidden-charm tetraquark states and make possible assignments of the exotic states. In Ref.[538], M. S. Maier de Sousa and R. Rodrigues da Silva suggest a theoretical scheme to study the double-pole QCD sum rules, and study the quarkonia $\rho(1S, 2S)$, $\psi(1S, 2S)$, $\Upsilon(1S, 2S)$ and $\psi_t(1S, 2S)$, the predicted hadron masses are not good enough, they adopt the experimental masses except for the $\psi_t(1S, 2S)$ to study the decay constants. In Ref.[182], we extend this scheme to study the $Z_c(3900)$ and $Z_c(4430)$ as the ground state and its first radial excitation, respectively, and observed that it is impossible to reproduce the experimental masses at the same energy scale, just as in the case of the $\rho(1S, 2S)$, $\psi(1S, 2S)$ and $\Upsilon(1S, 2S)$ [538], we should resort to the energy scale formula, see Eq.(99), to choose the optimal energy scales independently.

We adopt the correlation functions $\Pi_{\mu\nu}(p)$ and $\Pi_{\mu\nu\alpha\beta}(p)$ [184], see Eq.(125), and set $J_\mu(x) = J_\mu^1(x)$, $J_\mu^2(x)$, $J_\mu^3(x)$, and $J_\mu^1(x) = J_{-, \mu}^{SA}(x)$, $J_\mu^2(x) = J_{-, \mu}^{\bar{A}A}(x)$, $J_\mu^3(x) = J_{-, \mu}^{\bar{V}V}(x)$ and $J_{\mu\nu}(x) = J_{-, \mu\nu}^{AA}(x)$, see Eq.(116).

At the hadron side, if we only take account of the ground state hidden-charm tetraquark states, we obtain the QCD sum rules:

$$\lambda_Z^2 \exp\left(-\frac{M_Z^2}{T^2}\right) = \int_{4m_c^2}^{s_0} ds \rho_{QCD}(s) \exp\left(-\frac{s}{T^2}\right), \quad (149)$$

$$M_Z^2 = -\frac{\int_{4m_c^2}^{s_0} ds \frac{d}{dT} \rho_{QCD}(s) e^{-\tau s}}{\int_{4m_c^2}^{s_0} ds \rho_{QCD}(s) e^{-\tau s}} \Big|_{\tau=\frac{1}{T^2}}. \quad (150)$$

Thereafter, we will refer the QCD sum rules in Eq.(149) and Eq.(150) as QCDSR I.

If we take into account the contributions of the first radially excited tetraquark states Z'_c in the hadronic representation, we can obtain the QCD sum rules,

$$\lambda_Z^2 \exp\left(-\frac{M_Z^2}{T^2}\right) + \lambda_{Z'}^2 \exp\left(-\frac{M_{Z'}^2}{T^2}\right) = \int_{4m_c^2}^{s'_0} ds \rho_{QCD}(s) \exp\left(-\frac{s}{T^2}\right), \quad (151)$$

where the s'_0 is continuum threshold parameter, then we introduce the notations $\tau = \frac{1}{T^2}$, $D^n = \left(-\frac{d}{d\tau}\right)^n$, and resort to the subscripts 1 and 2 to represent the ground state Z_c and first radially excited state Z'_c respectively for simplicity. We rewrite the QCD sum rules as

$$\lambda_1^2 \exp(-\tau M_1^2) + \lambda_2^2 \exp(-\tau M_2^2) = \Pi_{QCD}(\tau), \quad (152)$$

here we introduce the subscript QCD to represent the QCD representation. We derive the QCD sum rules in Eq.(152) in regard to τ to obtain

$$\lambda_1^2 M_1^2 \exp(-\tau M_1^2) + \lambda_2^2 M_2^2 \exp(-\tau M_2^2) = D\Pi_{QCD}(\tau). \quad (153)$$

From Eqs.(152)-(153), we obtain the QCD sum rules,

$$\lambda_i^2 \exp(-\tau M_i^2) = \frac{(D - M_j^2) \Pi_{QCD}(\tau)}{M_i^2 - M_j^2}, \quad (154)$$

where the indexes $i \neq j$. Let us derive the QCD sum rules in Eq.(154) in regard to τ to obtain

$$\begin{aligned} M_i^2 &= \frac{(D^2 - M_j^2 D) \Pi_{QCD}(\tau)}{(D - M_j^2) \Pi_{QCD}(\tau)}, \\ M_i^4 &= \frac{(D^3 - M_j^2 D^2) \Pi_{QCD}(\tau)}{(D - M_j^2) \Pi_{QCD}(\tau)}. \end{aligned} \quad (155)$$

The squared masses M_i^2 satisfy the equation,

$$M_i^4 - bM_i^2 + c = 0, \quad (156)$$

where

$$\begin{aligned} b &= \frac{D^3 \otimes D^0 - D^2 \otimes D}{D^2 \otimes D^0 - D \otimes D}, \\ c &= \frac{D^3 \otimes D - D^2 \otimes D^2}{D^2 \otimes D^0 - D \otimes D}, \\ D^j \otimes D^k &= D^j \Pi_{QCD}(\tau) D^k \Pi_{QCD}(\tau), \end{aligned} \quad (157)$$

the indexes $i = 1, 2$ and $j, k = 0, 1, 2, 3$. Finally we solve above equation analytically to obtain two solutions [182, 538],

$$M_1^2 = \frac{b - \sqrt{b^2 - 4c}}{2}, \quad (158)$$

$$M_2^2 = \frac{b + \sqrt{b^2 - 4c}}{2}. \quad (159)$$

Thereafter, we will denote the QCD sum rules in Eq.(151) and Eqs.(158)-(159) as QCDSR II. In calculations, we observe that if we specify the energy scales of the spectral densities in the QCD representation, only one solution satisfies the energy scale formula $\mu = \sqrt{M_{X/Y/Z}^2 - (2\mathbb{M}_c)^2}$ in the

QCDSR II, we have to abandon the other solution, i.e. the mass M_1 (M_Z). It is the unique feature of our works [182, 184], which is in contrast to Ref.[538].

The Okubo-Zweig-Iizuka supper-allowed decays,

$$\begin{aligned} Z_c &\rightarrow J/\psi\pi, \\ Z'_c &\rightarrow \psi'\pi \\ Z''_c &\rightarrow \psi''\pi, \end{aligned} \tag{160}$$

are expected to take place easily. The energy gaps maybe have the relations $M_{Z'} - M_Z = m_{\psi'} - m_{J/\psi}$ and $M_{Z''} - M_{Z'} = m_{\psi''} - m_{\psi'}$. The charmonium masses are $m_{J/\psi} = 3.0969$ GeV, $m_{\psi'} = 3.686097$ GeV and $m_{\psi''} = 4.039$ GeV from the Particle Data Group [411], $m_{\psi'} - m_{J/\psi} = 0.59$ GeV, $m_{\psi''} - m_{J/\psi} = 0.94$ GeV, we can choose the continuum threshold parameters to be $\sqrt{s_0} = M_Z + 0.59$ GeV and $\sqrt{s'_0} = M_Z + 0.95$ GeV tentatively and vary the continuum threshold parameters and Borel parameters to satisfy the four criteria in Sect 3.1.1.

After trial and error, we obtain the continuum threshold parameters, Borel windows, best energy scales, and contributions of the ground states for the QCDSR I, see Table 14. In Table 14, we write the continuum threshold parameters as $s_0 = 21.0 \pm 1.0$ GeV² rather than as $s_0 = (4.58 \pm 0.11 \text{ GeV})^2$ for the $[uc]_{\bar{A}}[\bar{d}\bar{c}]_A - [uc]_A[\bar{d}\bar{c}]_{\bar{A}}$ and $[uc]_A[\bar{d}\bar{c}]_A$ tetraquark states to remain the same form as in Ref.[512]. Again we obtain the parameters for the QCDSR II using trial and error, see Table 15.

We take the energy scale formula $\mu = \sqrt{M_{X/Y/Z}^2 - (2\mathbb{M}_c)^2}$ to obtain the ideal energy scales of the spectral densities [182, 184].

From Tables 14-15, we can see clearly that the contributions of the single-pole terms are about (40 – 60)% for the QCDSR I, the contributions of the two-pole terms are about (70 – 80)% for the QCDSR II, which satisfy the pole dominance very well. In the QCDSR II, the contributions of the ground states are about (30 – 45)%, which are much less than the ground state contributions in the QCDSR I, we prefer the QCDSR I for the ground states.

We take account of all the uncertainties of the parameters, and obtain the masses and pole residues, which are shown in Tables 16-17. From those Tables, we can see that the ground state tetraquark masses from the QCDSR I and the radially excited tetraquark masses from the QCDSR II satisfy the energy scale formula $\mu = \sqrt{M_{X/Y/Z}^2 - (2\mathbb{M}_c)^2}$, where the updated value of the effective c -quark mass $\mathbb{M}_c = 1.82$ GeV is adopted [512]. In Table 17, we also present the central values of the ground state masses and pole residues extracted from the QCDSR II at the same energy scales. If we examine Table 17, we would observe the ground state masses cannot satisfy the energy scale formula, and should be discarded.

For example, in Fig.18, we plot the ground state masses from the QCDSR I and the first radially excited tetraquark masses from the QCDSR II with variations of the Borel parameters for the $[uc]_S[\bar{d}\bar{c}]_A - [uc]_A[\bar{d}\bar{c}]_S$ and $[uc]_{\bar{A}}[\bar{d}\bar{c}]_A - [uc]_A[\bar{d}\bar{c}]_{\bar{A}}$ states. From the figure, we observe that there indeed appear very flat platforms in the Borel windows.

We present the possible assignments explicitly in Table 9. The predicted mass $M_Z = 4.47 \pm 0.09$ GeV for the 2S $[uc]_S[\bar{d}\bar{c}]_A - [uc]_A[\bar{d}\bar{c}]_S$ tetraquark state exhibits very good agreement with the experimental data $4475 \pm 7_{-25}^{+15}$ MeV from the LHCb collaboration [179], which is in favor of assigning the $Z_c(4430)$ as the first radial excitation of the $[uc]_S[\bar{d}\bar{c}]_A - [uc]_A[\bar{d}\bar{c}]_S$ tetraquark state with the $J^{PC} = 1^{+-}$ [182, 184].

The predicted mass $M_Z = 4.60 \pm 0.09$ GeV for the 2S $[uc]_{\bar{A}}[\bar{d}\bar{c}]_A - [uc]_A[\bar{d}\bar{c}]_{\bar{A}}$ tetraquark state and $M_Z = 4.58 \pm 0.09$ GeV for the 2S $[uc]_A[\bar{d}\bar{c}]_A$ tetraquark state both exhibit very good agreement with the experimental data 4600 MeV from the LHCb collaboration [183], and the predicted mass $M_Z = 4.66 \pm 0.10$ GeV for the 1S $[uc]_{\bar{V}}[\bar{d}\bar{c}]_V + [uc]_V[\bar{d}\bar{c}]_{\bar{V}}$ tetraquark state is also compatible with the experimental data. In summary, there are three tetraquark state candidates with the $J^{PC} = 1^{+-}$ for the $Z_c(4600)$.

The scheme of the QCDSR II and its modification have been applied extensively to study the 2S tetraquark states, such as the $Z_c(4430)$ [182, 184, 185, 464, 539], $Z_c(4600)$ [184, 185], $X(4500)$

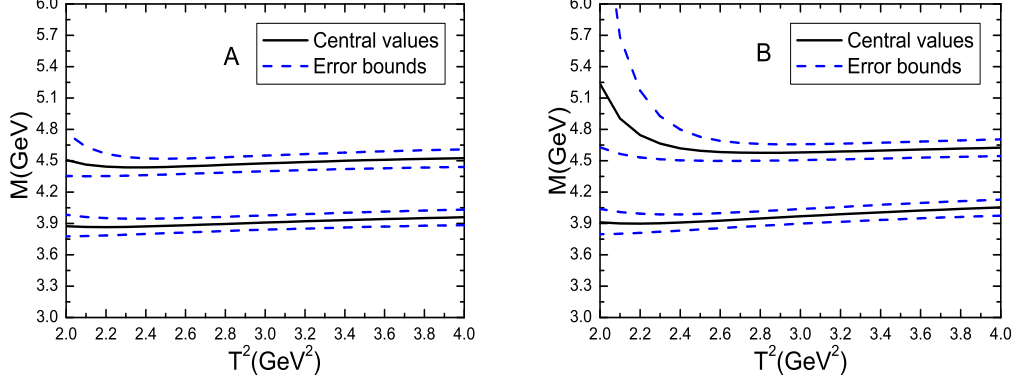


Figure 18: The masses with variations of the Borel parameters T^2 for the axialvector hidden-charm tetraquark states, the A and B represent the $[uc]_S[d\bar{c}]_A - [uc]_A[d\bar{c}]_S$ and $[uc]_{\bar{A}}[d\bar{c}]_A - [uc]_A[d\bar{c}]_{\bar{A}}$ tetraquark states, respectively.

Z_c	$T^2(\text{GeV}^2)$	s_0	$\mu(\text{GeV})$	pole
$[uc]_S[d\bar{c}]_A - [uc]_A[d\bar{c}]_S$	2.7 – 3.1	$(4.4 \pm 0.1 \text{ GeV})^2$	1.4	(40 – 63)%
$[uc]_{\bar{A}}[d\bar{c}]_A - [uc]_A[d\bar{c}]_{\bar{A}}$	3.2 – 3.6	$21.0 \pm 1.0 \text{ GeV}^2$	1.7	(40 – 60)%
$[uc]_{\bar{V}}[d\bar{c}]_V + [uc]_V[d\bar{c}]_{\bar{V}}$	3.7 – 4.1	$(5.25 \pm 0.10 \text{ GeV})^2$	2.9	(41 – 60)%
$[uc]_A[d\bar{c}]_A$	3.2 – 3.6	$21.0 \pm 1.0 \text{ GeV}^2$	1.7	(41 – 61)%

Table 14: The Borel parameters, continuum threshold parameters, energy scales of the QCD spectral densities and pole contributions for the QCDSR I [184].

$Z_c + Z'_c$	$T^2(\text{GeV}^2)$	s_0	$\mu(\text{GeV})$	pole (Z_c)
$[uc]_S[d\bar{c}]_A - [uc]_A[d\bar{c}]_S$	2.7 – 3.1	$(4.85 \pm 0.10 \text{ GeV})^2$	2.6	(72 – 88)% ((35 – 52)%)
$[uc]_{\bar{A}}[d\bar{c}]_A - [uc]_A[d\bar{c}]_{\bar{A}}$	3.2 – 3.6	$(4.95 \pm 0.10 \text{ GeV})^2$	2.8	(64 – 80)% ((30 – 44)%)
$[uc]_A[d\bar{c}]_A$	3.2 – 3.6	$(4.95 \pm 0.10 \text{ GeV})^2$	2.8	(64 – 81)% ((29 – 43)%)

Table 15: The Borel parameters, continuum threshold parameters, energy scales of the QCD spectral densities and pole contributions for the QCDSR II [184].

Z_c	$M_Z(\text{GeV})$	$\lambda_Z(\text{GeV}^5)$
$[uc]_S[d\bar{c}]_A - [uc]_A[d\bar{c}]_S$	3.90 ± 0.08	$(2.09 \pm 0.33) \times 10^{-2}$
$[uc]_{\bar{A}}[d\bar{c}]_A - [uc]_A[d\bar{c}]_{\bar{A}}$	4.01 ± 0.09	$(5.96 \pm 0.94) \times 10^{-2}$
$[uc]_{\bar{V}}[d\bar{c}]_V + [uc]_V[d\bar{c}]_{\bar{V}}$	4.66 ± 0.10	$(1.18 \pm 0.22) \times 10^{-1}$
$[uc]_A[d\bar{c}]_A$	$(2.91 \pm 0.46) \times 10^{-2}$	

Table 16: The masses and pole residues of the 1S states Z_c from the QCDSR I [184].

$Z_c + Z'_c$	$M_Z(\text{GeV})$	$\lambda_Z(\text{GeV}^5)$	$M_{Z'}(\text{GeV})$	$\lambda_{Z'}(\text{GeV}^5)$
$[uc]_S[d\bar{c}]_A - [uc]_A[d\bar{c}]_S$	3.81	1.77×10^{-2}	4.47 ± 0.09	$(6.02 \pm 0.80) \times 10^{-2}$
$[uc]_{\bar{A}}[d\bar{c}]_A - [uc]_A[d\bar{c}]_{\bar{A}}$	3.78	3.94×10^{-2}	4.60 ± 0.09	$(1.35 \pm 0.18) \times 10^{-1}$
$[uc]_A[d\bar{c}]_A$	3.73	1.76×10^{-2}	4.58 ± 0.09	$(6.55 \pm 0.85) \times 10^{-2}$

Table 17: The masses and pole residues of the 1S states Z_c and 2S states Z'_c from the QCDSR II [184].

(as the 2S state of the $X(3915)$) [540, 541], $X(4685)$ (as the 2S state of the $X(4140)$) [522], and $\Lambda_c(2S)$ and $\Xi_c(2S)$ [542], etc.

3.1.3 Tetraquark states with negative parity

In Sect.3.1.1, we study the hidden-heavy tetraquark states with the positive parity, in this subsection, we would like to study the hidden-heavy tetraquark states with the negative parity. Again we choose the diquark operators without explicit P-waves as the elementary building blocks, for detailed discussions about the diquark operators, see the beginning of Sect.3.1.1. Compared to the vector tetraquark states, it is easy to analyze the pseudoscalar tetraquark states, and we would like to present the results directly.

Again, let us adopt the correlation functions $\Pi_{\mu\nu}(p)$ and $\Pi_{\mu\nu\alpha\beta}(p)$ defined in Eq.(125), and write down the currents

$$\begin{aligned} J_\mu(x) &= J_{-,\mu}^{PA}(x), J_{+,\mu}^{PA}(x), J_{-,\mu}^{SV}(x), J_{+,\mu}^{SV}(x), J_{-,\mu}^{\tilde{V}A}(x), J_{+,\mu}^{\tilde{V}A}(x), J_{-,\mu}^{\tilde{A}V}(x), J_{+,\mu}^{\tilde{A}V}(x), \\ J_{\mu\nu}(x) &= J_{-,\mu\nu}^{S\tilde{V}}(x), J_{+,\mu\nu}^{S\tilde{V}}(x), J_{-,\mu\nu}^{P\tilde{A}}(x), J_{+,\mu\nu}^{P\tilde{A}}(x), J_{-,\mu\nu}^{AA}(x), \end{aligned} \quad (161)$$

$$\begin{aligned} J_{-,\mu}^{PA}(x) &= \frac{\varepsilon^{ijk}\varepsilon^{imn}}{\sqrt{2}} \left[u_j^T(x) C c_k(x) \bar{d}_m(x) \gamma_\mu C \bar{c}_n^T(x) - u_j^T(x) C \gamma_\mu c_k(x) \bar{d}_m(x) C \bar{c}_n^T(x) \right], \\ J_{+,\mu}^{PA}(x) &= \frac{\varepsilon^{ijk}\varepsilon^{imn}}{\sqrt{2}} \left[u_j^T(x) C c_k(x) \bar{d}_m(x) \gamma_\mu C \bar{c}_n^T(x) + u_j^T(x) C \gamma_\mu c_k(x) \bar{d}_m(x) C \bar{c}_n^T(x) \right], \\ J_{-,\mu}^{SV}(x) &= \frac{\varepsilon^{ijk}\varepsilon^{imn}}{\sqrt{2}} \left[u_j^T(x) C \gamma_5 c_k(x) \bar{d}_m(x) \gamma_5 \gamma_\mu C \bar{c}_n^T(x) + u_j^T(x) C \gamma_\mu \gamma_5 c_k(x) \bar{d}_m(x) \gamma_5 C \bar{c}_n^T(x) \right], \\ J_{+,\mu}^{SV}(x) &= \frac{\varepsilon^{ijk}\varepsilon^{imn}}{\sqrt{2}} \left[u_j^T(x) C \gamma_5 c_k(x) \bar{d}_m(x) \gamma_5 \gamma_\mu C \bar{c}_n^T(x) - u_j^T(x) C \gamma_\mu \gamma_5 c_k(x) \bar{d}_m(x) \gamma_5 C \bar{c}_n^T(x) \right], \end{aligned} \quad (162)$$

$$\begin{aligned} J_{-,\mu}^{\tilde{V}A}(x) &= \frac{\varepsilon^{ijk}\varepsilon^{imn}}{\sqrt{2}} \left[u_j^T(x) C \sigma_{\mu\nu} c_k(x) \bar{d}_m(x) \gamma^\nu C \bar{c}_n^T(x) - u_j^T(x) C \gamma^\nu c_k(x) \bar{d}_m(x) \sigma_{\mu\nu} C \bar{c}_n^T(x) \right], \\ J_{+,\mu}^{\tilde{V}A}(x) &= \frac{\varepsilon^{ijk}\varepsilon^{imn}}{\sqrt{2}} \left[u_j^T(x) C \sigma_{\mu\nu} c_k(x) \bar{d}_m(x) \gamma^\nu C \bar{c}_n^T(x) + u_j^T(x) C \gamma^\nu c_k(x) \bar{d}_m(x) \sigma_{\mu\nu} C \bar{c}_n^T(x) \right], \\ J_{-,\mu}^{\tilde{A}V}(x) &= \frac{\varepsilon^{ijk}\varepsilon^{imn}}{\sqrt{2}} \left[u_j^T(x) C \sigma_{\mu\nu} \gamma_5 c_k(x) \bar{d}_m(x) \gamma_5 \gamma^\nu C \bar{c}_n^T(x) + u_j^T(x) C \gamma^\nu \gamma_5 c_k(x) \bar{d}_m(x) \gamma_5 \sigma_{\mu\nu} C \bar{c}_n^T(x) \right], \\ J_{+,\mu}^{\tilde{A}V}(x) &= \frac{\varepsilon^{ijk}\varepsilon^{imn}}{\sqrt{2}} \left[u_j^T(x) C \sigma_{\mu\nu} \gamma_5 c_k(x) \bar{d}_m(x) \gamma_5 \gamma^\nu C \bar{c}_n^T(x) - u_j^T(x) C \gamma^\nu \gamma_5 c_k(x) \bar{d}_m(x) \gamma_5 \sigma_{\mu\nu} C \bar{c}_n^T(x) \right], \end{aligned} \quad (163)$$

$$\begin{aligned}
J_{-,\mu\nu}^{S\tilde{V}}(x) &= \frac{\varepsilon^{ijk}\varepsilon^{imn}}{\sqrt{2}} \left[u_j^T(x) C \gamma_5 c_k(x) \bar{d}_m(x) \sigma_{\mu\nu} C \bar{c}_n^T(x) - u_j^T(x) C \sigma_{\mu\nu} c_k(x) \bar{d}_m(x) \gamma_5 C \bar{c}_n^T(x) \right], \\
J_{+,\mu\nu}^{S\tilde{V}}(x) &= \frac{\varepsilon^{ijk}\varepsilon^{imn}}{\sqrt{2}} \left[u_j^T(x) C \gamma_5 c_k(x) \bar{d}_m(x) \sigma_{\mu\nu} C \bar{c}_n^T(x) + u_j^T(x) C \sigma_{\mu\nu} c_k(x) \bar{d}_m(x) \gamma_5 C \bar{c}_n^T(x) \right], \\
J_{-,\mu\nu}^{P\tilde{A}}(x) &= \frac{\varepsilon^{ijk}\varepsilon^{imn}}{\sqrt{2}} \left[u_j^T(x) C c_k(x) \bar{d}_m(x) \gamma_5 \sigma_{\mu\nu} C \bar{c}_n^T(x) - u_j^T(x) C \sigma_{\mu\nu} \gamma_5 c_k(x) \bar{d}_m(x) C \bar{c}_n^T(x) \right], \\
J_{+,\mu\nu}^{P\tilde{A}}(x) &= \frac{\varepsilon^{ijk}\varepsilon^{imn}}{\sqrt{2}} \left[u_j^T(x) C c_k(x) \bar{d}_m(x) \gamma_5 \sigma_{\mu\nu} C \bar{c}_n^T(x) + u_j^T(x) C \sigma_{\mu\nu} \gamma_5 c_k(x) \bar{d}_m(x) C \bar{c}_n^T(x) \right],
\end{aligned} \tag{164}$$

$$J_{-,\mu\nu}^{AA}(x) = \frac{\varepsilon^{ijk}\varepsilon^{imn}}{\sqrt{2}} \left[u_j^T(x) C \gamma_\mu c_k(x) \bar{d}_m(x) \gamma_\nu C \bar{c}_n^T(x) - u_j^T(x) C \gamma_\nu c_k(x) \bar{d}_m(x) \gamma_\mu C \bar{c}_n^T(x) \right], \tag{165}$$

the subscripts \pm denote the positive and negative charge conjugation, respectively, the super-scripts $P, S, A(\tilde{A})$ and $V(\tilde{V})$ denote the pseudoscalar, scalar, axialvector and vector diquark and antidiquark operators, respectively [424, 505, 512, 543, 544]. With the simple replacement,

$$\begin{aligned}
u &\rightarrow s, \\
\bar{d} &\rightarrow \bar{s},
\end{aligned} \tag{166}$$

we reach the corresponding currents for the $c\bar{c}s\bar{s}$ states [424, 544, 545].

Under parity transformation \hat{P} , the current operators $J_\mu(x)$ and $J_{\mu\nu}(x)$ have the properties,

$$\begin{aligned}
\hat{P} J_\mu(x) \hat{P}^{-1} &= +J^\mu(\tilde{x}), \\
\hat{P} \tilde{J}_{\mu\nu}(x) \hat{P}^{-1} &= -\tilde{J}^{\mu\nu}(\tilde{x}), \\
\hat{P} J_{-,\mu\nu}^{AA}(x) \hat{P}^{-1} &= +J_{AA}^{+,\mu\nu}(\tilde{x}),
\end{aligned} \tag{167}$$

according to the properties of the diquark operators,

$$\begin{aligned}
\hat{P} \varepsilon^{ijk} q_j^T(x) C \Gamma c_k(x) \hat{P}^{-1} &= -\varepsilon^{ijk} q_j^T(\tilde{x}) C \gamma^0 \Gamma \gamma^0 c_k(\tilde{x}), \\
\hat{P} \varepsilon^{ijk} \bar{q}_j(x) \Gamma C \bar{c}_k^T(x) \hat{P}^{-1} &= -\varepsilon^{ijk} \bar{q}_j(\tilde{x}) \gamma^0 \Gamma \gamma^0 C \bar{c}_k^T(\tilde{x}),
\end{aligned} \tag{168}$$

where $\tilde{J}_{\mu\nu}(x) = J_{-,\mu\nu}^{S\tilde{V}}(x), J_{+,\mu\nu}^{S\tilde{V}}(x), J_{-,\mu\nu}^{P\tilde{A}}(x), J_{+,\mu\nu}^{P\tilde{A}}(x)$, $x^\mu = (t, \vec{x})$ and $\tilde{x}^\mu = (t, -\vec{x})$. For $\Gamma = 1, \gamma_5, \gamma_\mu, \gamma_\mu \gamma_5, \sigma_{\mu\nu}, \sigma_{\mu\nu} \gamma_5$, we obtain $\gamma^0 \Gamma \gamma^0 = 1, -\gamma_5, \gamma^\mu, -\gamma^\mu \gamma_5, \sigma^{\mu\nu}, -\sigma^{\mu\nu} \gamma_5$. And we rewrite Eq.(167) in more explicit form,

$$\begin{aligned}
\hat{P} J_i(x) \hat{P}^{-1} &= -J_i(\tilde{x}), \\
\hat{P} \tilde{J}_{ij}(x) \hat{P}^{-1} &= -\tilde{J}_{ij}(\tilde{x}), \\
\hat{P} J_{- , 0i}^{AA}(x) \hat{P}^{-1} &= -J_{AA, 0i}^-(\tilde{x}),
\end{aligned} \tag{169}$$

$$\begin{aligned}
\hat{P} J_0(x) \hat{P}^{-1} &= +J_0(\tilde{x}), \\
\hat{P} \tilde{J}_{0i}(x) \hat{P}^{-1} &= +\tilde{J}_{0i}(\tilde{x}), \\
\hat{P} J_{- , ij}^{AA}(x) \hat{P}^{-1} &= +J_{AA, ij}^-(\tilde{x}),
\end{aligned} \tag{170}$$

where $i, j = 1, 2, 3$.

Under charge conjugation transformation \hat{C} , the currents $J_\mu(x)$ and $J_{\mu\nu}(x)$ have the properties,

$$\begin{aligned}\hat{C}J_{\pm,\mu}(x)\hat{C}^{-1} &= \pm J_{\pm,\mu}(x) |_{u \leftrightarrow d}, \\ \hat{C}J_{\pm,\mu\nu}(x)\hat{C}^{-1} &= \pm J_{\pm,\mu\nu}(x) |_{u \leftrightarrow d}.\end{aligned}\quad (171)$$

The currents $J_\mu(x)$ and $J_{\mu\nu}(x)$ have the symbolic quark structure $\bar{c}c\bar{d}u$ with the isospin $I = 1$ and $I_3 = 1$. In the isospin limit, the currents with the symbolic quark structures

$$\bar{c}c\bar{d}u, \bar{c}c\bar{u}d, \bar{c}c\frac{\bar{u}u - \bar{d}d}{\sqrt{2}}, \bar{c}c\frac{\bar{u}u + \bar{d}d}{\sqrt{2}} \quad (172)$$

couple potentially to the hidden-charm tetraquark states with degenerated masses, and the currents with the isospin $I = 1$ and 0 lead to the same QCD sum rules. Only the currents with the symbolic quark structures $\bar{c}c\frac{\bar{u}u - \bar{d}d}{\sqrt{2}}$ and $\bar{c}c\frac{\bar{u}u + \bar{d}d}{\sqrt{2}}$ have definite charge conjugation, again we assume that the tetraquark states $\bar{c}c\bar{d}u$ have the same charge conjugation as their neutral partners.

According to the current-hadron duality, we obtain the hadronic representation,

$$\begin{aligned}\Pi_{\mu\nu}(p) &= \frac{\lambda_{Y_-}^2}{M_{Y_-}^2 - p^2} \left(-g_{\mu\nu} + \frac{p_\mu p_\nu}{p^2} \right) + \dots \\ &= \Pi_-(p^2) \left(-g_{\mu\nu} + \frac{p_\mu p_\nu}{p^2} \right) + \dots, \\ \tilde{\Pi}_{\mu\nu\alpha\beta}(p) &= \frac{\tilde{\lambda}_{Y_-}^2}{M_{Y_-}^2 - p^2} (p^2 g_{\mu\alpha} g_{\nu\beta} - p^2 g_{\mu\beta} g_{\nu\alpha} - g_{\mu\alpha} p_\nu p_\beta - g_{\nu\beta} p_\mu p_\alpha + g_{\mu\beta} p_\nu p_\alpha + g_{\nu\alpha} p_\mu p_\beta) \\ &\quad + \frac{\tilde{\lambda}_{Z_+}^2}{M_{Z_+}^2 - p^2} (-g_{\mu\alpha} p_\nu p_\beta - g_{\nu\beta} p_\mu p_\alpha + g_{\mu\beta} p_\nu p_\alpha + g_{\nu\alpha} p_\mu p_\beta) + \dots \\ &= \tilde{\Pi}_-(p^2) (p^2 g_{\mu\alpha} g_{\nu\beta} - p^2 g_{\mu\beta} g_{\nu\alpha} - g_{\mu\alpha} p_\nu p_\beta - g_{\nu\beta} p_\mu p_\alpha + g_{\mu\beta} p_\nu p_\alpha + g_{\nu\alpha} p_\mu p_\beta) \\ &\quad + \tilde{\Pi}_+(p^2) (-g_{\mu\alpha} p_\nu p_\beta - g_{\nu\beta} p_\mu p_\alpha + g_{\mu\beta} p_\nu p_\alpha + g_{\nu\alpha} p_\mu p_\beta), \\ \Pi_{\mu\nu\alpha\beta}^{AA}(p) &= \frac{\tilde{\lambda}_{Z_+}^2}{M_{Z_+}^2 - p^2} (p^2 g_{\mu\alpha} g_{\nu\beta} - p^2 g_{\mu\beta} g_{\nu\alpha} - g_{\mu\alpha} p_\nu p_\beta - g_{\nu\beta} p_\mu p_\alpha + g_{\mu\beta} p_\nu p_\alpha + g_{\nu\alpha} p_\mu p_\beta) \\ &\quad + \frac{\tilde{\lambda}_{Y_-}^2}{M_{Y_-}^2 - p^2} (-g_{\mu\alpha} p_\nu p_\beta - g_{\nu\beta} p_\mu p_\alpha + g_{\mu\beta} p_\nu p_\alpha + g_{\nu\alpha} p_\mu p_\beta) + \dots \\ &= \tilde{\Pi}_+(p^2) (p^2 g_{\mu\alpha} g_{\nu\beta} - p^2 g_{\mu\beta} g_{\nu\alpha} - g_{\mu\alpha} p_\nu p_\beta - g_{\nu\beta} p_\mu p_\alpha + g_{\mu\beta} p_\nu p_\alpha + g_{\nu\alpha} p_\mu p_\beta) \\ &\quad + \tilde{\Pi}_-(p^2) (-g_{\mu\alpha} p_\nu p_\beta - g_{\nu\beta} p_\mu p_\alpha + g_{\mu\beta} p_\nu p_\alpha + g_{\nu\alpha} p_\mu p_\beta),\end{aligned}\quad (173)$$

where the pole residues are defined by

$$\begin{aligned}\langle 0 | J_\mu(0) | Y_c^-(p) \rangle &= \lambda_{Y_-} \varepsilon_\mu, \\ \langle 0 | \tilde{J}_{\mu\nu}(0) | Y_c^-(p) \rangle &= \tilde{\lambda}_{Y_-} \varepsilon_{\mu\nu\alpha\beta} \varepsilon^\alpha p^\beta, \\ \langle 0 | \tilde{J}_{\mu\nu}(0) | Z_c^+(p) \rangle &= \tilde{\lambda}_{Z_+} (\varepsilon_\mu p_\nu - \varepsilon_\nu p_\mu), \\ \langle 0 | J_{-,\mu\nu}^{AA}(0) | Z_c^+(p) \rangle &= \tilde{\lambda}_{Z_+} \varepsilon_{\mu\nu\alpha\beta} \varepsilon^\alpha p^\beta, \\ \langle 0 | J_{-,\mu\nu}^{AA}(0) | Y_c^-(p) \rangle &= \tilde{\lambda}_{Y_-} (\varepsilon_\mu p_\nu - \varepsilon_\nu p_\mu),\end{aligned}\quad (174)$$

$\lambda_{Z_+} = \tilde{\lambda}_{Z_+} M_{Z_+}$, $\lambda_{Y_-} = \tilde{\lambda}_{Y_-} M_{Y_-}$, the $\varepsilon_{\mu/\alpha}$ are the polarization vectors, we add the superscripts/subscripts \pm to denote the positive and negative parity, respectively, and add the wide-tilde and superscript in the $\Pi_{\mu\nu\alpha\beta}(p)$ to denote the currents $J_{\mu\nu}(x)$ and $J_{-,\mu\nu}^{AA}(x)$, respectively. We choose the components $\Pi_-(p^2)$ and $p^2 \tilde{\Pi}_-(p^2)$ to explore the negative parity hidden-charm tetraquark states [543, 545].

Y_c	J^{PC}	$T^2(\text{GeV}^2)$	$\sqrt{s_0}(\text{GeV})$	$\mu(\text{GeV})$	pole
$[uc]_P[\bar{d}\bar{c}]_A - [uc]_A[\bar{d}\bar{c}]_P$	1^{--}	$3.7 - 4.1$	5.15 ± 0.10	2.9	(43 - 61)%
$[uc]_P[\bar{d}\bar{c}]_A + [uc]_A[\bar{d}\bar{c}]_P$	1^{-+}	$3.7 - 4.1$	5.10 ± 0.10	2.8	(42 - 60)%
$[uc]_S[\bar{d}\bar{c}]_V + [uc]_V[\bar{d}\bar{c}]_S$	1^{--}	$3.2 - 3.6$	4.85 ± 0.10	2.4	(42 - 62)%
$[uc]_S[\bar{d}\bar{c}]_V - [uc]_V[\bar{d}\bar{c}]_S$	1^{-+}	$3.7 - 4.1$	5.15 ± 0.10	2.9	(41 - 60)%
$[uc]_{\tilde{V}}[\bar{d}\bar{c}]_A - [uc]_A[\bar{d}\bar{c}]_{\tilde{V}}$	1^{--}	$3.6 - 4.0$	5.05 ± 0.10	2.7	(42 - 60)%
$[uc]_{\tilde{V}}[\bar{d}\bar{c}]_A + [uc]_A[\bar{d}\bar{c}]_{\tilde{V}}$	1^{-+}	$3.7 - 4.1$	5.15 ± 0.10	2.9	(41 - 60)%
$[uc]_{\tilde{A}}[\bar{d}\bar{c}]_V + [uc]_V[\bar{d}\bar{c}]_{\tilde{A}}$	1^{--}	$3.5 - 3.9$	5.00 ± 0.10	2.6	(42 - 61)%
$[uc]_{\tilde{A}}[\bar{d}\bar{c}]_V - [uc]_V[\bar{d}\bar{c}]_{\tilde{A}}$	1^{-+}	$3.6 - 4.0$	5.05 ± 0.10	2.7	(42 - 61)%
$[uc]_S[\bar{d}\bar{c}]_{\tilde{V}} - [uc]_{\tilde{V}}[\bar{d}\bar{c}]_S$	1^{--}	$3.4 - 3.8$	5.00 ± 0.10	2.6	(42 - 61)%
$[uc]_S[\bar{d}\bar{c}]_{\tilde{V}} + [uc]_{\tilde{V}}[\bar{d}\bar{c}]_S$	1^{-+}	$3.4 - 3.8$	5.00 ± 0.10	2.6	(42 - 61)%
$[uc]_P[\bar{d}\bar{c}]_{\tilde{A}} - [uc]_{\tilde{A}}[\bar{d}\bar{c}]_P$	1^{--}	$3.7 - 4.1$	5.10 ± 0.10	2.8	(43 - 61)%
$[uc]_P[\bar{d}\bar{c}]_{\tilde{A}} + [uc]_{\tilde{A}}[\bar{d}\bar{c}]_P$	1^{-+}	$3.7 - 4.1$	5.10 ± 0.10	2.8	(43 - 61)%
$[uc]_A[\bar{d}\bar{c}]_A$	1^{--}	$3.8 - 4.2$	5.20 ± 0.10	3.0	(42 - 60)%

Table 18: The Borel parameters, continuum threshold parameters, energy scales of the QCD spectral densities and pole contributions for the ground state vector hidden-charm tetraquark states [543].

At the QCD side, we calculate the vacuum condensates up to dimension 10 and take into account the vacuum condensates $\langle \bar{q}q \rangle$, $\langle \frac{\alpha_s GG}{\pi} \rangle$, $\langle \bar{q}g_s \sigma G q \rangle$, $\langle \bar{q}q \rangle^2$, $g_s^2 \langle \bar{q}q \rangle^2$, $\langle \bar{q}q \rangle \langle \frac{\alpha_s GG}{\pi} \rangle$, $\langle \bar{q}q \rangle \langle \bar{q}g_s \sigma G q \rangle$, $\langle \bar{q}g_s \sigma G q \rangle^2$ and $\langle \bar{q}q \rangle^2 \langle \frac{\alpha_s GG}{\pi} \rangle$, which are vacuum expectations of the quark-gluon operators of the order $\mathcal{O}(\alpha_s^k)$ with $k \leq 1$ [543, 545].

We match the hadron side with the QCD side of the components $\Pi_-(p^2)$ and $p^2 \tilde{\Pi}_-(p^2)$ below the continuum thresholds s_0 with the help of the spectral representation, and perform Borel transformation with respect to $P^2 = -p^2$ to obtain the QCD sum rules:

$$\lambda_Y^2 \exp\left(-\frac{M_Y^2}{T^2}\right) = \int_{4m_c^2}^{s_0} ds \rho_{QCD}(s) \exp\left(-\frac{s}{T^2}\right), \quad (175)$$

the explicit expressions of the QCD spectral densities $\rho_{QCD}(s)$ are neglected for simplicity.

We derive Eq.(175) with respect to $\tau = \frac{1}{T^2}$, and obtain the QCD sum rules for the masses of the vector hidden-charm tetraquark states Y_c ,

$$M_Y^2 = -\frac{\int_{4m_c^2}^{s_0} ds \frac{d}{d\tau} \rho_{QCD}(s) \exp(-\tau s)}{\int_{4m_c^2}^{s_0} ds \rho_{QCD}(s) \exp(-\tau s)}. \quad (176)$$

With a simple replacement $c \rightarrow b$, we obtain the corresponding QCD sum rules for the hidden-bottom tetraquark states directly.

We perform the same procedure as in the previous subsections, and obtain the Borel windows, continuum threshold parameters, suitable energy scales of the QCD spectral densities and pole contributions, which are shown explicitly in Tables 18-19. From the Tables, we can see clearly that the pole contributions are about (40 - 60)%, the central values are larger than 50%, the pole dominance is well satisfied. In calculations, we observe that the main contributions come from the perturbative terms, the higher dimensional condensates play a minor important role and the contributions $|D(10)| \ll 1\%$, the operator product expansion converges very good.

We take account of all the uncertainties of the relevant parameters and obtain the masses and pole residues of the hidden-charm (and hidden-strange) tetraquark states with the $J^{PC} = 1^{--}$ and 1^{-+} , which are shown explicitly in Tables 20-21.

In Tables 22-23, we present the possible assignments of the hidden-charm tetraquark states with the $J^{PC} = 1^{--}$ and 1^{-+} obtained in Refs.[543, 545]. Considering the large uncertainties, it

Y_c	J^{PC}	$T^2(\text{GeV}^2)$	$\sqrt{s_0}(\text{GeV})$	$\mu(\text{GeV})$	pole
$[sc]_P[\bar{s}\bar{c}]_A - [sc]_A[\bar{s}\bar{c}]_P$	1^{--}	$4.1 - 4.7$	5.35 ± 0.10	2.9	$(40 - 61)\%$
$[sc]_P[\bar{s}\bar{c}]_A + [sc]_A[\bar{s}\bar{c}]_P$	1^{++}	$4.0 - 4.6$	5.30 ± 0.10	2.8	$(41 - 61)\%$
$[sc]_S[\bar{s}\bar{c}]_V + [sc]_V[\bar{s}\bar{c}]_S$	1^{--}	$3.5 - 4.0$	5.05 ± 0.10	2.5	$(41 - 62)\%$
$[sc]_S[\bar{s}\bar{c}]_V - [sc]_V[\bar{s}\bar{c}]_S$	1^{++}	$4.0 - 4.6$	5.35 ± 0.10	2.9	$(40 - 60)\%$
$[sc]_{\tilde{V}}[\bar{s}\bar{c}]_A - [sc]_A[\bar{s}\bar{c}]_{\tilde{V}}$	1^{--}	$3.9 - 4.5$	5.25 ± 0.10	2.7	$(40 - 61)\%$
$[sc]_{\tilde{V}}[\bar{s}\bar{c}]_A + [sc]_A[\bar{s}\bar{c}]_{\tilde{V}}$	1^{++}	$4.0 - 4.6$	5.35 ± 0.10	2.9	$(40 - 61)\%$
$[sc]_{\tilde{A}}[\bar{s}\bar{c}]_V + [sc]_V[\bar{s}\bar{c}]_{\tilde{A}}$	1^{--}	$3.8 - 4.4$	5.20 ± 0.10	2.7	$(40 - 61)\%$
$[sc]_{\tilde{A}}[\bar{s}\bar{c}]_V - [sc]_V[\bar{s}\bar{c}]_{\tilde{A}}$	1^{++}	$3.9 - 4.5$	5.25 ± 0.10	2.7	$(40 - 61)\%$
$[sc]_S[\bar{s}\bar{c}]_{\tilde{V}} - [sc]_{\tilde{V}}[\bar{s}\bar{c}]_S$	1^{--}	$3.7 - 4.2$	5.20 ± 0.10	2.7	$(41 - 62)\%$
$[sc]_S[\bar{s}\bar{c}]_{\tilde{V}} + [sc]_{\tilde{V}}[\bar{s}\bar{c}]_S$	1^{++}	$3.7 - 4.3$	5.20 ± 0.10	2.7	$(40 - 62)\%$
$[sc]_P[\bar{s}\bar{c}]_{\tilde{A}} - [sc]_{\tilde{A}}[\bar{s}\bar{c}]_P$	1^{--}	$4.1 - 4.7$	5.30 ± 0.10	2.8	$(40 - 60)\%$
$[sc]_P[\bar{s}\bar{c}]_{\tilde{A}} + [sc]_{\tilde{A}}[\bar{s}\bar{c}]_P$	1^{++}	$4.1 - 4.7$	5.30 ± 0.10	2.8	$(40 - 60)\%$
$[sc]_A[\bar{s}\bar{c}]_A$	1^{--}	$4.2 - 4.9$	5.40 ± 0.10	3.0	$(40 - 60)\%$

Table 19: The Borel parameters, continuum threshold parameters, energy scales of the QCD spectral densities and pole contributions for the ground state hidden-charm-hidden-strange tetraquark states [545].

Y_c	J^{PC}	$M_Y(\text{GeV})$	$\lambda_Y(\text{GeV}^5)$
$[uc]_P[\bar{d}\bar{c}]_A - [uc]_A[\bar{d}\bar{c}]_P$	1^{--}	4.66 ± 0.07	$(7.19 \pm 0.84) \times 10^{-2}$
$[uc]_P[\bar{d}\bar{c}]_A + [uc]_A[\bar{d}\bar{c}]_P$	1^{++}	4.61 ± 0.07	$(6.69 \pm 0.80) \times 10^{-2}$
$[uc]_S[\bar{d}\bar{c}]_V + [uc]_V[\bar{d}\bar{c}]_S$	1^{--}	4.35 ± 0.08	$(4.32 \pm 0.61) \times 10^{-2}$
$[uc]_S[\bar{d}\bar{c}]_V - [uc]_V[\bar{d}\bar{c}]_S$	1^{++}	4.66 ± 0.09	$(6.67 \pm 0.82) \times 10^{-2}$
$[uc]_{\tilde{V}}[\bar{d}\bar{c}]_A - [uc]_A[\bar{d}\bar{c}]_{\tilde{V}}$	1^{--}	4.53 ± 0.07	$(1.03 \pm 0.14) \times 10^{-1}$
$[uc]_{\tilde{V}}[\bar{d}\bar{c}]_A + [uc]_A[\bar{d}\bar{c}]_{\tilde{V}}$	1^{++}	4.65 ± 0.08	$(1.13 \pm 0.15) \times 10^{-1}$
$[uc]_{\tilde{A}}[\bar{d}\bar{c}]_V + [uc]_V[\bar{d}\bar{c}]_{\tilde{A}}$	1^{--}	4.48 ± 0.08	$(9.47 \pm 1.27) \times 10^{-2}$
$[uc]_{\tilde{A}}[\bar{d}\bar{c}]_V - [uc]_V[\bar{d}\bar{c}]_{\tilde{A}}$	1^{++}	4.55 ± 0.07	$(1.06 \pm 0.14) \times 10^{-1}$
$[uc]_S[\bar{d}\bar{c}]_{\tilde{V}} - [uc]_{\tilde{V}}[\bar{d}\bar{c}]_S$	1^{--}	4.50 ± 0.09	$(4.78 \pm 0.66) \times 10^{-2}$
$[uc]_S[\bar{d}\bar{c}]_{\tilde{V}} + [uc]_{\tilde{V}}[\bar{d}\bar{c}]_S$	1^{++}	4.50 ± 0.09	$(4.79 \pm 0.66) \times 10^{-2}$
$[uc]_P[\bar{d}\bar{c}]_{\tilde{A}} - [uc]_{\tilde{A}}[\bar{d}\bar{c}]_P$	1^{--}	4.60 ± 0.07	$(6.32 \pm 0.74) \times 10^{-2}$
$[uc]_P[\bar{d}\bar{c}]_{\tilde{A}} + [uc]_{\tilde{A}}[\bar{d}\bar{c}]_P$	1^{++}	4.61 ± 0.08	$(6.36 \pm 0.74) \times 10^{-2}$
$[uc]_A[\bar{d}\bar{c}]_A$	1^{--}	4.69 ± 0.08	$(6.65 \pm 0.81) \times 10^{-2}$

Table 20: The masses and pole residues of the ground state vector hidden-charm tetraquark states [543].

Y_c	J^{PC}	$M_Y(\text{GeV})$	$\lambda_Y(\text{GeV}^5)$
$[sc]_P[\overline{sc}]_A - [sc]_A[\overline{sc}]_P$	1^{--}	4.80 ± 0.08	$(8.97 \pm 1.09) \times 10^{-2}$
$[sc]_P[\overline{sc}]_A + [sc]_A[\overline{sc}]_P$	1^{-+}	4.75 ± 0.08	$(8.34 \pm 1.04) \times 10^{-2}$
$[sc]_S[\overline{sc}]_V + [sc]_V[\overline{sc}]_S$	1^{--}	4.53 ± 0.08	$(5.70 \pm 0.79) \times 10^{-2}$
$[sc]_S[\overline{sc}]_V - [sc]_V[\overline{sc}]_S$	1^{-+}	4.83 ± 0.09	$(8.39 \pm 1.05) \times 10^{-2}$
$[sc]_{\tilde{V}}[\overline{sc}]_A - [sc]_A[\overline{sc}]_{\tilde{V}}$	1^{--}	4.70 ± 0.08	$(1.32 \pm 0.18) \times 10^{-1}$
$[sc]_{\tilde{V}}[\overline{sc}]_A + [sc]_A[\overline{sc}]_{\tilde{V}}$	1^{-+}	4.81 ± 0.09	$(1.43 \pm 0.19) \times 10^{-1}$
$[sc]_{\tilde{A}}[\overline{sc}]_V + [sc]_V[\overline{sc}]_{\tilde{A}}$	1^{--}	4.65 ± 0.08	$(1.23 \pm 0.17) \times 10^{-1}$
$[sc]_{\tilde{A}}[\overline{sc}]_V - [sc]_V[\overline{sc}]_{\tilde{A}}$	1^{-+}	4.71 ± 0.08	$(1.34 \pm 0.17) \times 10^{-1}$
$[sc]_S[\overline{sc}]_{\tilde{V}} - [sc]_{\tilde{V}}[\overline{sc}]_S$	1^{--}	4.68 ± 0.09	$(6.22 \pm 0.82) \times 10^{-2}$
$[sc]_S[\overline{sc}]_{\tilde{V}} + [sc]_{\tilde{V}}[\overline{sc}]_S$	1^{-+}	4.68 ± 0.09	$(6.23 \pm 0.84) \times 10^{-2}$
$[sc]_P[\overline{sc}]_{\tilde{A}} - [sc]_{\tilde{A}}[\overline{sc}]_P$	1^{--}	4.75 ± 0.08	$(7.93 \pm 0.98) \times 10^{-2}$
$[sc]_P[\overline{sc}]_{\tilde{A}} + [sc]_{\tilde{A}}[\overline{sc}]_P$	1^{-+}	4.75 ± 0.08	$(7.94 \pm 0.97) \times 10^{-2}$
$[sc]_A[\overline{sc}]_A$	1^{--}	4.85 ± 0.09	$(8.38 \pm 1.05) \times 10^{-2}$

Table 21: The masses and pole residues of the ground state hidden-charm-hidden-strange tetraquark states [545].

is possible to assign the $X(4630)$ as the $[sc]_S[\overline{sc}]_{\tilde{V}} + [sc]_{\tilde{V}}[\overline{sc}]_S$ state with the $J^{PC} = 1^{-+}$, which has a mass $4.68 \pm 0.09 \text{ GeV}$, see Table 23. In Ref.[409], we prove that it is feasible and reliable to study the multiquark states in the framework of the QCD sum rules, and obtain the prediction for the mass of the $D_s^* \bar{D}_{s1} - D_{s1} \bar{D}_s^*$ molecular state with the exotic quantum numbers $J^{PC} = 1^{-+}$, $M_X = 4.67 \pm 0.08 \text{ GeV}$, which was obtained before the LHCb data and is compatible with the LHCb data. The $X(4630)$ maybe have two important Fock components.

After Ref.[543] was published, the $Y(4500)$ was observed by the BESIII collaboration [155, 156, 159]. At the energy about 4.5 GeV , we obtain three hidden-charm tetraquark states with the $J^{PC} = 1^{--}$, the $[uc]_{\tilde{V}}[\overline{uc}]_A + [dc]_{\tilde{V}}[\overline{dc}]_A - [uc]_A[\overline{uc}]_{\tilde{V}} - [dc]_A[\overline{dc}]_{\tilde{V}}$, $[uc]_{\tilde{A}}[\overline{uc}]_V + [dc]_{\tilde{A}}[\overline{dc}]_V + [uc]_V[\overline{uc}]_{\tilde{A}} + [dc]_V[\overline{dc}]_{\tilde{A}}$ and $[uc]_S[\overline{uc}]_{\tilde{V}} + [dc]_S[\overline{dc}]_{\tilde{V}} - [uc]_{\tilde{V}}[\overline{uc}]_S - [dc]_{\tilde{V}}[\overline{dc}]_S$ tetraquark states have the masses $4.53 \pm 0.07 \text{ GeV}$, $4.48 \pm 0.08 \text{ GeV}$ and $4.50 \pm 0.09 \text{ GeV}$, respectively [543]. In Ref.[546], we study the two-body strong decays systematically, i.e. we obtain thirty QCD sum rules for the hadronic coupling constants based on rigorous quark-hadron duality, then obtain the partial decay widths, therefore the total widths approximately, which are compatible with the experimental data of the $Y(4500)$ from the BESIII collaboration, see Sect.7.1 for details. In Ref.[547], we take the $Y(4500)$ as the $[uc]_{\tilde{A}}[\overline{uc}]_V + [dc]_{\tilde{A}}[\overline{dc}]_V + [uc]_V[\overline{uc}]_{\tilde{A}} + [dc]_V[\overline{dc}]_{\tilde{A}}$ tetraquark state, and study the three-body strong decay $Y(4500) \rightarrow D^{*-} D^{*0} \pi^+$ with the light-cone QCD sum rules, see Sect.7.2 for details.

If only the mass is concerned, the $Y(4660)$ can be assigned as the $[sc]_{\tilde{A}}[\overline{sc}]_V + [sc]_V[\overline{sc}]_{\tilde{A}}$, $[sc]_S[\overline{sc}]_{\tilde{V}} - [sc]_{\tilde{V}}[\overline{sc}]_S$, $[uc]_P[\overline{uc}]_A + [dc]_P[\overline{dc}]_A - [uc]_A[\overline{uc}]_P - [dc]_A[\overline{dc}]_P$ or $[uc]_A[\overline{uc}]_A + [dc]_A[\overline{dc}]_A$ tetraquark state, see Tables 22-23. In other words, the $Y(4660)$ maybe have several important Fock components, we have to study the strong decays in details to diagnose its nature. For example, if we assign the $Y(4660)$ as the $[sc]_{\tilde{A}}[\overline{sc}]_V + [sc]_V[\overline{sc}]_{\tilde{A}}$ or $[sc]_S[\overline{sc}]_{\tilde{V}} - [sc]_{\tilde{V}}[\overline{sc}]_S$ state, then the strong decays $Y(4660) \rightarrow J/\psi f_0(980)$, $\eta_c \phi$, $\chi_{c0} \phi$, $D_s \bar{D}_s$, $D_s^* \bar{D}_s^*$, $D_s \bar{D}_s^*$, $D_s^* \bar{D}_s$, $J/\psi \pi^+ \pi^-$ and $\psi' \pi^+ \pi^-$ are Okubo-Zweig-Iizuka super-allowed, considering the intermediate process $f_0(980) \rightarrow \pi^+ \pi^-$. Up to now, only the decays $Y(4660) \rightarrow J/\psi \pi^+ \pi^-$, $\psi_2(3823) \pi^+ \pi^-$, $\Lambda_c^+ \Lambda_c^-$ and $D_s^+ D_{s1}^-$ have been observed [97], which cannot exclude the assignments $Y(4660) = [uc]_P[\overline{uc}]_A + [dc]_P[\overline{dc}]_A - [uc]_A[\overline{uc}]_P - [dc]_A[\overline{dc}]_P$ or $[uc]_A[\overline{uc}]_A + [dc]_A[\overline{dc}]_A$, as the decay $Y(4660) \rightarrow D_s^+ D_{s1}^-$ can take place through the re-scattering mechanism. We can investigate or search for the neutral Y_c tetraquark states with

Y_c	J^{PC}	$M_Y(\text{GeV})$	Assignments
$[uc]_P[\overline{dc}]_A - [uc]_A[\overline{dc}]_P$	1^{--}	4.66 ± 0.07	? $Y(4660)$
$[uc]_P[\overline{dc}]_A + [uc]_A[\overline{dc}]_P$	1^{-+}	4.61 ± 0.07	
$[uc]_S[\overline{dc}]_V + [uc]_V[\overline{dc}]_S$	1^{--}	4.35 ± 0.08	? $Y(4360/4390)$
$[uc]_S[\overline{dc}]_V - [uc]_V[\overline{dc}]_S$	1^{-+}	4.66 ± 0.09	
$[uc]_{\tilde{V}}[\overline{dc}]_A - [uc]_A[\overline{dc}]_{\tilde{V}}$	1^{--}	4.53 ± 0.07	? $Y(4500)$
$[uc]_{\tilde{V}}[\overline{dc}]_A + [uc]_A[\overline{dc}]_{\tilde{V}}$	1^{-+}	4.65 ± 0.08	
$[uc]_{\tilde{A}}[\overline{dc}]_V + [uc]_V[\overline{dc}]_{\tilde{A}}$	1^{--}	4.48 ± 0.08	? $Y(4500)$
$[uc]_{\tilde{A}}[\overline{dc}]_V - [uc]_V[\overline{dc}]_{\tilde{A}}$	1^{-+}	4.55 ± 0.07	
$[uc]_S[\overline{dc}]_{\tilde{V}} - [uc]_{\tilde{V}}[\overline{dc}]_S$	1^{--}	4.50 ± 0.09	? $Y(4500)$
$[uc]_S[\overline{dc}]_{\tilde{V}} + [uc]_{\tilde{V}}[\overline{dc}]_S$	1^{-+}	4.50 ± 0.09	
$[uc]_P[\overline{dc}]_{\tilde{A}} - [uc]_{\tilde{A}}[\overline{dc}]_P$	1^{--}	4.60 ± 0.07	
$[uc]_P[\overline{dc}]_{\tilde{A}} + [uc]_{\tilde{A}}[\overline{dc}]_P$	1^{-+}	4.61 ± 0.08	
$[uc]_A[\overline{dc}]_A$	1^{--}	4.69 ± 0.08	? $Y(4660)$

Table 22: The possible assignments of the hidden-charm tetraquark states, the isospin limit is implied [543].

Y_c	J^{PC}	$M_Y(\text{GeV})$	Assignments
$[sc]_P[\overline{sc}]_A - [sc]_A[\overline{sc}]_P$	1^{--}	4.80 ± 0.08	? $Y(4790)$
$[sc]_P[\overline{sc}]_A + [sc]_A[\overline{sc}]_P$	1^{-+}	4.75 ± 0.08	
$[sc]_S[\overline{sc}]_V + [sc]_V[\overline{sc}]_S$	1^{--}	4.53 ± 0.08	
$[sc]_S[\overline{sc}]_V - [sc]_V[\overline{sc}]_S$	1^{-+}	4.83 ± 0.09	
$[sc]_{\tilde{V}}[\overline{sc}]_A - [sc]_A[\overline{sc}]_{\tilde{V}}$	1^{--}	4.70 ± 0.08	? $Y(4710)$
$[sc]_{\tilde{V}}[\overline{sc}]_A + [sc]_A[\overline{sc}]_{\tilde{V}}$	1^{-+}	4.81 ± 0.09	
$[sc]_{\tilde{A}}[\overline{sc}]_V + [sc]_V[\overline{sc}]_{\tilde{A}}$	1^{--}	4.65 ± 0.08	? $Y(4660)$
$[sc]_{\tilde{A}}[\overline{sc}]_V - [sc]_V[\overline{sc}]_{\tilde{A}}$	1^{-+}	4.71 ± 0.08	
$[sc]_S[\overline{sc}]_{\tilde{V}} - [sc]_{\tilde{V}}[\overline{sc}]_S$	1^{--}	4.68 ± 0.09	? $Y(4660)$
$[sc]_S[\overline{sc}]_{\tilde{V}} + [sc]_{\tilde{V}}[\overline{sc}]_S$	1^{-+}	4.68 ± 0.09	?? $X(4630)$
$[sc]_P[\overline{sc}]_{\tilde{A}} - [sc]_{\tilde{A}}[\overline{sc}]_P$	1^{--}	4.75 ± 0.08	
$[sc]_P[\overline{sc}]_{\tilde{A}} + [sc]_{\tilde{A}}[\overline{sc}]_P$	1^{-+}	4.75 ± 0.08	
$[sc]_A[\overline{sc}]_A$	1^{--}	4.85 ± 0.09	

Table 23: The possible assignments of the hidden-charm-hidden-strange tetraquark states [545].

	$J_\mu^1(x), \mu = 2.9 \text{ GeV}$	$J_\mu^1(x), \mu = 2.4 \text{ GeV}$	$J_\mu^4(x), \mu = 2.4 \text{ GeV}$	$J_\mu^4(x), \mu = 2.9 \text{ GeV}$
$\lambda_{Y(4220)}$	0.38729	0.29100	0.02632	1.56680
$\lambda_{Y(4320)}$	0.69720	0.20867	3.90360	3.94290
$\lambda_{Y(4390)}$	0.41733	0.41695	0.00000	0.00190
$\lambda_{Y(4660)}$	6.47460	5.93670	0.00000	0.00000

Table 24: The central values of the fitted pole residues, where the unit is 10^{-2} GeV^5 [544].

the $J^{PC} = 1^{--}$ and 1^{-+} through the two-body or three-body strong decays,

$$\begin{aligned} Y_c(1^{--}) &\rightarrow \chi_{c0}\rho/\omega, J/\psi\pi^+\pi^-, J/\psi K\bar{K}, \eta_c\rho/\omega, \chi_{c1}\rho/\omega, \\ Y_c(1^{-+}) &\rightarrow J/\psi\rho/\omega, h_c\rho/\omega. \end{aligned} \quad (177)$$

From Tables 22-23, we observe that there is no room for the $Y(4260/4220)$. In Ref.[544], we choose the currents,

$$\begin{aligned} J_\mu^1(x) &= J_{-, \mu}^{PA}(x) |_{u\bar{d} \rightarrow s\bar{s}}, \\ J_\mu^4(x) &= J_{-, \mu}^{SV}(x) |_{u\bar{d} \rightarrow \frac{u\bar{u}+d\bar{d}}{\sqrt{2}}}, \end{aligned} \quad (178)$$

to interpolate the Y states, and fit the correlation functions,

$$\begin{aligned} \Sigma_{Y=Y(4220), Y(4360), Y(4390), Y(4660)} \lambda_Y^2 \exp\left(-\frac{M_Y^2}{T^2}\right) &= \int_{4m_c^2}^{s_0} ds \rho_{QCD}^1(s) \exp\left(-\frac{s}{T^2}\right), \\ \Sigma_{Y=Y(4220), Y(4360), Y(4390), Y(4660)} \lambda_Y^2 \exp\left(-\frac{M_Y^2}{T^2}\right) &= \int_{4m_c^2}^{s_0} ds \rho_{QCD}^4(s) \exp\left(-\frac{s}{T^2}\right), \end{aligned} \quad (179)$$

by taking the λ_Y as free parameters. We obtain the best values, which are shown in Table 24, at the pertinent energy scales $\mu = 2.4 \text{ GeV}$ for the current $J_\mu^4(x)$ and $\mu = 2.9 \text{ GeV}$ for the current $J_\mu^1(x)$, the values of the pole residue $\lambda_{Y(4220)}$ are very small. Without introducing explicit P-waves, we cannot produce the experimental mass of the $Y(4260/4220)$ in the scenario of tetraquark state.

The $Y(4660)$ has been studied extensively via the QCD sum rules [424, 431, 440, 444, 485, 512, 543, 544, 545, 548], however, no definite conclusion can be obtained, more works are still needed to decipher its structure.

Now let us turn to the pseudoscalar tetraquark states and write down the local currents,

$$J(x) = J_{AV}^+(x), J_{AV}^-(x), J_{PS}^+(x), J_{PS}^-(x), J_{TT}^+(x), J_{TT}^-(x), \quad (180)$$

$$\begin{aligned} J_{AV}^+(x) &= \frac{\varepsilon^{ijk}\varepsilon^{imn}}{\sqrt{2}} \left[q_j^T(x) C \gamma_\mu c_k(x) \bar{q}_m'(x) \gamma_5 \gamma^\mu C \bar{c}_n^T(x) - q_j^T(x) C \gamma_\mu \gamma_5 c_k(x) \bar{q}_m'(x) \gamma^\mu C \bar{c}_n^T(x) \right], \\ J_{AV}^-(x) &= \frac{\varepsilon^{ijk}\varepsilon^{imn}}{\sqrt{2}} \left[q_j^T(x) C \gamma_\mu c_k(x) \bar{q}_m'(x) \gamma_5 \gamma^\mu C \bar{c}_n^T(x) + q_j^T(x) C \gamma_\mu \gamma_5 c_k(x) \bar{q}_m'(x) \gamma^\mu C \bar{c}_n^T(x) \right], \\ J_{PS}^+(x) &= \frac{\varepsilon^{ijk}\varepsilon^{imn}}{\sqrt{2}} \left[q_j^T(x) C c_k(x) \bar{q}_m'(x) \gamma_5 C \bar{c}_n^T(x) + q_j^T(x) C \gamma_5 c_k(x) \bar{q}_m'(x) C \bar{c}_n^T(x) \right], \\ J_{PS}^-(x) &= \frac{\varepsilon^{ijk}\varepsilon^{imn}}{\sqrt{2}} \left[q_j^T(x) C c_k(x) \bar{q}_m'(x) \gamma_5 C \bar{c}_n^T(x) - q_j^T(x) C \gamma_5 c_k(x) \bar{q}_m'(x) C \bar{c}_n^T(x) \right], \\ J_{TT}^+(x) &= \frac{\varepsilon^{ijk}\varepsilon^{imn}}{\sqrt{2}} \left[q_j^T(x) C \sigma_{\mu\nu} c_k(x) \bar{q}_m'(x) \gamma_5 \sigma^{\mu\nu} C \bar{c}_n^T(x) + q_j^T(x) C \sigma_{\mu\nu} \gamma_5 c_k(x) \bar{q}_m'(x) \sigma^{\mu\nu} C \bar{c}_n^T(x) \right], \\ J_{TT}^-(x) &= \frac{\varepsilon^{ijk}\varepsilon^{imn}}{\sqrt{2}} \left[q_j^T(x) C \sigma_{\mu\nu} c_k(x) \bar{q}_m'(x) \gamma_5 \sigma^{\mu\nu} C \bar{c}_n^T(x) - q_j^T(x) C \sigma_{\mu\nu} \gamma_5 c_k(x) \bar{q}_m'(x) \sigma^{\mu\nu} C \bar{c}_n^T(x) \right], \end{aligned} \quad (181)$$

Z_c	J^{PC}	$T^2(\text{GeV}^2)$	$\sqrt{s_0}(\text{GeV})$	$\mu(\text{GeV})$	pole
$[uc]_A[d\bar{c}]_V - [uc]_V[d\bar{c}]_A$	0^{-+}	$3.7 - 4.1$	5.10 ± 0.10	2.7	$(42 - 60)\%$
$[uc]_A[d\bar{c}]_V + [uc]_V[d\bar{c}]_A$	0^{--}	$3.7 - 4.1$	5.10 ± 0.10	2.8	$(42 - 60)\%$
$[uc]_A[\bar{s}\bar{c}]_V - [uc]_V[\bar{s}\bar{c}]_A$	0^{-+}	$3.7 - 4.1$	5.15 ± 0.10	2.7	$(43 - 61)\%$
$[uc]_A[\bar{s}\bar{c}]_V + [uc]_V[\bar{s}\bar{c}]_A$	0^{--}	$3.7 - 4.1$	5.15 ± 0.10	2.8	$(43 - 61)\%$
$[sc]_A[\bar{s}\bar{c}]_V - [sc]_V[\bar{s}\bar{c}]_A$	0^{-+}	$3.8 - 4.2$	5.20 ± 0.10	2.7	$(42 - 60)\%$
$[sc]_A[\bar{s}\bar{c}]_V + [sc]_V[\bar{s}\bar{c}]_A$	0^{--}	$3.8 - 4.2$	5.20 ± 0.10	2.8	$(43 - 60)\%$
$[uc]_P[d\bar{c}]_S + [uc]_S[d\bar{c}]_P$	0^{-+}	$3.7 - 4.1$	5.10 ± 0.10	2.8	$(42 - 60)\%$
$[uc]_P[d\bar{c}]_S - [uc]_S[d\bar{c}]_P$	0^{--}	$3.7 - 4.1$	5.10 ± 0.10	2.8	$(42 - 60)\%$
$[uc]_P[\bar{s}\bar{c}]_S + [uc]_S[\bar{s}\bar{c}]_P$	0^{-+}	$3.7 - 4.1$	5.15 ± 0.10	2.8	$(43 - 61)\%$
$[uc]_P[\bar{s}\bar{c}]_S - [uc]_S[\bar{s}\bar{c}]_P$	0^{--}	$3.7 - 4.1$	5.15 ± 0.10	2.8	$(43 - 61)\%$
$[sc]_P[\bar{s}\bar{c}]_S + [sc]_S[\bar{s}\bar{c}]_P$	0^{-+}	$3.8 - 4.2$	5.20 ± 0.10	2.8	$(43 - 61)\%$
$[sc]_P[\bar{s}\bar{c}]_S - [sc]_S[\bar{s}\bar{c}]_P$	0^{--}	$3.8 - 4.2$	5.20 ± 0.10	2.8	$(43 - 61)\%$
$[uc]_T[d\bar{c}]_T + [uc]_T[d\bar{c}]_T$	0^{-+}	$3.7 - 4.1$	5.10 ± 0.10	2.7	$(41 - 60)\%$
$[uc]_T[\bar{s}\bar{c}]_T + [uc]_T[\bar{s}\bar{c}]_T$	0^{-+}	$3.7 - 4.1$	5.15 ± 0.10	2.7	$(43 - 61)\%$
$[sc]_T[\bar{s}\bar{c}]_T + [sc]_T[\bar{s}\bar{c}]_T$	0^{-+}	$3.8 - 4.2$	5.20 ± 0.10	2.7	$(42 - 60)\%$

Table 25: The Borel parameters, continuum threshold parameters, energy scales of the QCD spectral densities and pole contributions for the pseudoscalar hidden-charm tetraquark states [515].

with $q, q' = u, d, s$, the superscripts \pm symbolize the positive and negative charge-conjugation, respectively, the subscripts P, S, V, A and T stand for the pseudoscalar, scalar, vector, axialvector and tensor diquark operators, respectively [515].

Under parity transformation \hat{P} , the $J(x)$ have the property,

$$\hat{P}J(x)\hat{P}^{-1} = -J(\tilde{x}). \quad (182)$$

Under charge-conjugation transformation \hat{C} , the $J(x)$ have the property,

$$\hat{C}J^\pm(x)\hat{C}^{-1} = \pm J^\pm(x) |_{q \leftrightarrow q'}, \quad (183)$$

and we can prove that the current $J_{TT}^-(x) = 0$ through performing the Fierz-transformation. Again, we take the isospin limit $m_u = m_d$, the four-quark currents with the symbolic quark structures,

$$\bar{c}c\bar{d}u, \bar{c}c\bar{u}d, \bar{c}c\frac{\bar{u}u - \bar{d}d}{\sqrt{2}}, \bar{c}c\frac{\bar{u}u + \bar{d}d}{\sqrt{2}}, \quad (184)$$

couple potentially to the pseudoscalar tetraquark states with degenerated masses. And the four-quark currents with the symbolic quark structures,

$$\bar{c}c\bar{u}s, \bar{c}c\bar{d}s, \bar{c}c\bar{s}u, \bar{c}c\bar{s}d, \quad (185)$$

also couple potentially to the pseudoscalar tetraquark states with degenerated masses according to the isospin symmetry. And we obtain the QCD sum rules routinely.

In Table 25, we present the Borel windows, continuum threshold parameters, energy scales of the QCD spectral densities and pole contributions. From the Table, we can see distinctly that the pole contributions are about $(40 - 60)\%$ at the hadron side, while the central values are larger than 50%, the pole dominance criterion is satisfied very good. On the other hand, the higher vacuum condensates play a minor important role, the operator product expansion converges very well.

We take all the uncertainties of the parameters into account and acquire the masses and pole residues, see Table 26. From Tables 25-26, we can see distinctly that the modified energy scale

Z_c	J^{PC}	$M_Z(\text{GeV})$	$\lambda_Z(\text{GeV}^5)$
$[uc]_A[d\bar{c}]_V - [uc]_V[d\bar{c}]_A$	0^{-+}	4.56 ± 0.08	$(1.33 \pm 0.18) \times 10^{-1}$
$[uc]_A[d\bar{c}]_V + [uc]_V[d\bar{c}]_A$	0^{--}	4.58 ± 0.07	$(1.37 \pm 0.17) \times 10^{-1}$
$[uc]_A[\bar{s}c]_V - [uc]_V[\bar{s}c]_A$	0^{-+}	4.61 ± 0.08	$(1.41 \pm 0.19) \times 10^{-1}$
$[uc]_A[\bar{s}c]_V + [uc]_V[\bar{s}c]_A$	0^{--}	4.63 ± 0.08	$(1.45 \pm 0.19) \times 10^{-1}$
$[sc]_A[\bar{s}c]_V - [sc]_V[\bar{s}c]_A$	0^{-+}	4.66 ± 0.08	$(1.50 \pm 0.20) \times 10^{-1}$
$[sc]_A[\bar{s}c]_V + [sc]_V[\bar{s}c]_A$	0^{--}	4.67 ± 0.08	$(1.53 \pm 0.20) \times 10^{-1}$
$[uc]_P[d\bar{c}]_S + [uc]_S[d\bar{c}]_P$	0^{-+}	4.58 ± 0.07	$(6.92 \pm 0.86) \times 10^{-2}$
$[uc]_P[d\bar{c}]_S - [uc]_S[d\bar{c}]_P$	0^{--}	4.58 ± 0.07	$(6.91 \pm 0.86) \times 10^{-2}$
$[uc]_P[\bar{s}c]_S + [uc]_S[\bar{s}c]_P$	0^{-+}	4.63 ± 0.07	$(7.30 \pm 0.90) \times 10^{-2}$
$[uc]_P[\bar{s}c]_S - [uc]_S[\bar{s}c]_P$	0^{--}	4.63 ± 0.07	$(7.30 \pm 0.90) \times 10^{-2}$
$[sc]_P[\bar{s}c]_S + [sc]_S[\bar{s}c]_P$	0^{-+}	4.67 ± 0.08	$(7.73 \pm 0.97) \times 10^{-2}$
$[sc]_P[\bar{s}c]_S - [sc]_S[\bar{s}c]_P$	0^{--}	4.67 ± 0.08	$(7.73 \pm 0.96) \times 10^{-2}$
$[uc]_T[d\bar{c}]_T + [uc]_T[d\bar{c}]_T$	0^{-+}	4.57 ± 0.08	$(4.62 \pm 0.61) \times 10^{-1}$
$[uc]_T[\bar{s}c]_T + [uc]_T[\bar{s}c]_T$	0^{-+}	4.62 ± 0.08	$(4.89 \pm 0.63) \times 10^{-1}$
$[sc]_T[\bar{s}c]_T + [sc]_T[\bar{s}c]_T$	0^{-+}	4.67 ± 0.08	$(5.19 \pm 0.67) \times 10^{-1}$

Table 26: The masses and pole residues for the ground state pseudoscalar hidden-charm tetraquark states [515].

formula $\mu = \sqrt{M_{X/Y/Z}^2 - (2\mathbb{M}_c)^2} - k m_s(\mu)$ with $k = 0, 1$ or 2 is satisfied, where we subtract the small s -quark mass approximately to account for the small light-flavor $SU(3)$ mass-breaking effects, which is slightly different from Eq.(100).

As can be seen distinctly from Table 26 that the lowest mass of the pseudoscalar hidden-charm tetraquark state with the symbolic quark constituents $c\bar{c}u\bar{d}$ is about 4.56 ± 0.08 GeV, which is much larger than the value $4239 \pm 18_{-10}^{+45}$ MeV from the LHCb collaboration [179]. In 2014, the LHCb collaboration provided the first independent confirmation of the existence of the $Z_c(4430)$ in the $\psi'\pi^-$ mass spectrum and established its spin-parity to be $J^P = 1^+$ [179]. Furthermore, the LHCb collaboration observed a weak evidence for an additional resonance, the $Z_c(4240)$, in the $\psi'\pi^-$ mass spectrum with the preferred spin-parity $J^P = 0^-$ and the Breit-Wigner mass $4239 \pm 18_{-10}^{+45}$ MeV and width $220 \pm 47_{-74}^{+108}$ MeV, respectively with large uncertainties [179]. If the $Z_c(4240)$ is confirmed by further experiments in the future, it is an excellent candidate for the hidden-charm tetraquark state with the $J^{PC} = 0^{--}$, and we should revisit the QCD sum rules for the discrepancy.

In Ref.[437], Chen and Zhu study the hidden-charm tetraquark states with the symbolic quark constituents $c\bar{c}u\bar{d}$ with the QCD sum rules, and obtain the ground state masses 4.55 ± 0.11 GeV for the tetraquark states with the $J^{PC} = 0^{--}$, the masses 4.55 ± 0.11 GeV, 4.67 ± 0.10 GeV, 4.72 ± 0.10 GeV for the tetraquark states with the $J^{PC} = 0^{-+}$. The present predictions are consistent with their calculations, again, we should bear in mind that their interpolating currents and schemes in treating the operator product expansion and input parameters at the QCD side differ from the present work remarkably. Any current with the same quantum numbers and same quark structure as a Fock state in a hadron couples potentially to this hadron, so we can construct several currents to interpolate a hadron, or construct a current to interpolate several hadrons.

From Table 26, we can see explicitly that the central values of the masses of the $J^{PC} = 0^{-+}$ tetraquark states with the symbolic quark constituents $uc\bar{d}\bar{c}$, $uc\bar{s}\bar{c}$, $sc\bar{s}\bar{c}$ are about $4.56 \sim 4.58$ GeV, $4.61 \sim 4.62$ GeV and $4.66 \sim 4.67$ GeV, respectively, the central values of the masses of the $J^{PC} = 0^{--}$ tetraquark states with the symbolic quark constituents $uc\bar{d}\bar{c}$, $uc\bar{s}\bar{c}$ and $sc\bar{s}\bar{c}$ are about 4.58 GeV, 4.63 GeV and 4.67 GeV, respectively. We obtain the conclusion tentatively that the currents $J_{AV}^+(x)$, $J_{PS}^+(x)$ and $J_{TT}^+(x)$ ($J_{AV}^-(x)$ and $J_{PS}^-(x)$) couple potentially to three (two) different pseudoscalar tetraquark states with almost degenerated masses, or to one pseudoscalar

tetraquark state with three (two) different Fock components. As the currents with the same quantum numbers couple potentially to the pseudoscalar tetraquark states with almost degenerated masses, the mixing effects cannot improve the predictions remarkably if only the tetraquark masses are concerned. All in all, we obtain reasonable predictions for the masses of the pseudoscalar tetraquark states without strange, with strange and with hidden-strange, the central values are about $4.56 \sim 4.58$ GeV, $4.61 \sim 4.63$ GeV and $4.66 \sim 4.67$ GeV, respectively.

The following two-body strong decays of the pseudoscalar hidden-charm tetraquark states,

$$\begin{aligned}
Z_c(0^{--}) &\rightarrow \chi_{c1}\rho, \eta_c\rho, J/\psi a_1(1260), J/\psi\pi, D\bar{D}_0 + h.c., D^*\bar{D}_1 + h.c., D^*\bar{D} + h.c., \\
Z_c(0^{-+}) &\rightarrow \chi_{c0}\pi, \eta_c f_0(500), J/\psi\rho, D\bar{D}_0 + h.c., D^*\bar{D}_1 + h.c., D^*\bar{D} + h.c., \\
Z_{cs}(0^{--}) &\rightarrow \chi_{c1}K^*, \eta_c K^*, J/\psi K_1, J/\psi K, D_s\bar{D}_0 + h.c., D\bar{D}_{s0} + h.c., D_s^*\bar{D}_1 + h.c., \\
&\quad D^*\bar{D}_{s1} + h.c., D_s^*\bar{D} + h.c., D^*\bar{D}_s + h.c., \\
Z_{cs}(0^{-+}) &\rightarrow \chi_{c0}K, \eta_c K_0^*(700), J/\psi K^*, D_s\bar{D}_0 + h.c., D\bar{D}_{s0} + h.c., D_s^*\bar{D}_1 + h.c., \\
&\quad D^*\bar{D}_{s1} + h.c., D_s^*\bar{D} + h.c., D^*\bar{D}_s + h.c., \\
Z_{css}(0^{--}) &\rightarrow \chi_{c1}\phi, \eta_c\phi, J/\psi f_1, J/\psi\eta, D_s\bar{D}_{s0} + h.c., D_s^*\bar{D}_{s1} + h.c., D_s^*\bar{D}_s + h.c., \\
Z_{css}(0^{-+}) &\rightarrow \chi_{c0}\eta, \eta_c f_0(980), J/\psi\phi, D_s\bar{D}_{s0} + h.c., D_s^*\bar{D}_{s1} + h.c., D_s^*\bar{D}_s + h.c., \quad (186)
\end{aligned}$$

can take place through the Okubo-Zweig-Iizuka super-allowed fall-apart mechanism, we suggest to search for the pseudoscalar hidden-charm tetraquark states in those channels.

The QCD sum rules obtained in this sub-section can be extended directly to study the tetraquark states in the bottom sector with the simple replacements $c \rightarrow b$ and $\bar{c} \rightarrow \bar{b}$.

3.1.4 Tetraquark states with an explicit P-wave

In the type-II diquark model [56], Maiani et al assign the $Y(4008)$, $Y(4260)$, $Y(4290/4220)$ and $Y(4630)$ as four tetraquark states with the $L = 1$ based on the effective spin-spin and spin-orbit interactions, see Eq.(24). In Ref.[318], A. Ali et al incorporate the dominant spin-spin, spin-orbit and tensor interactions, see Eq.(25), and observe that the preferred assignments of the tetraquark states with the $L = 1$ are the $Y(4220)$, $Y(4330)$, $Y(4390)$, $Y(4660)$. In the diquark model, the quantum numbers of the Y states are shown explicitly in Table 27, where the L is the angular momentum between the diquark and antidiquark, $\vec{S} = \vec{S}_{qc} + \vec{S}_{\bar{q}\bar{c}}$, $\vec{J} = \vec{S} + \vec{L}$, and $L = 1$ denotes the explicit P-wave.

We take the isospin limit, and construct the interpolating currents according to the quantum numbers shown in Table 27,

$$\begin{aligned}
J_\mu^1(x) &= \frac{\varepsilon^{ijk}\varepsilon^{imn}}{\sqrt{2}} u_j^T(x) C \gamma_5 c_k(x) \overset{\leftrightarrow}{\partial}_\mu \bar{d}_m(x) \gamma_5 C \bar{c}_n^T(x), \\
J_\mu^2(x) &= \frac{\varepsilon^{ijk}\varepsilon^{imn}}{\sqrt{2}} u_j^T(x) C \gamma_\alpha c_k(x) \overset{\leftrightarrow}{\partial}_\mu \bar{d}_m(x) \gamma^\alpha C \bar{c}_n^T(x), \\
J_\mu^3(x) &= \frac{\varepsilon^{ijk}\varepsilon^{imn}}{2} \left[u_j^T(x) C \gamma_\mu c_k(x) \overset{\leftrightarrow}{\partial}_\alpha \bar{d}_m(x) \gamma^\alpha C \bar{c}_n^T(x) \right. \\
&\quad \left. + u_j^T(x) C \gamma^\alpha c_k(x) \overset{\leftrightarrow}{\partial}_\alpha \bar{d}_m(x) \gamma_\mu C \bar{c}_n^T(x) \right], \\
J_{\mu\nu}(x) &= \frac{\varepsilon^{ijk}\varepsilon^{imn}}{2\sqrt{2}} \left[u_j^T(x) C \gamma_5 c_k(x) \overset{\leftrightarrow}{\partial}_\mu \bar{d}_m(x) \gamma_\nu C \bar{c}_n^T(x) \right. \\
&\quad + u_j^T(x) C \gamma_\nu c_k(x) \overset{\leftrightarrow}{\partial}_\mu \bar{d}_m(x) \gamma_5 C \bar{c}_n^T(x) \\
&\quad - u_j^T(x) C \gamma_5 c_k(x) \overset{\leftrightarrow}{\partial}_\nu \bar{d}_m(x) \gamma_\mu C \bar{c}_n^T(x) \\
&\quad \left. - u_j^T(x) C \gamma_\mu c_k(x) \overset{\leftrightarrow}{\partial}_\nu \bar{d}_m(x) \gamma_5 C \bar{c}_n^T(x) \right], \quad (187)
\end{aligned}$$

$ S_{qc}, S_{\bar{q}\bar{c}}; S, L; J\rangle$	[56]	[318]	Currents
$ 0, 0; 0, 1; 1\rangle$	$Y(4008)$	$Y(4220)$	$J_\mu^1(x)$
$\frac{1}{\sqrt{2}}(1, 0; 1, 1; 1\rangle + 0, 1; 1, 1; 1\rangle)$	$Y(4260)$	$Y(4330)$	$J_{\mu\nu}(x)$
$ 1, 1; 0, 1; 1\rangle$	$Y(4290/4220)$	$Y(4390)$	$J_\mu^2(x)$
$ 1, 1; 2, 1; 1\rangle$	$Y(4630)$	$Y(4660)$	$J_\mu^3(x)$
$ 1, 1; 2, 3; 1\rangle$			

Table 27: The vector tetraquark states, possible assignments and corresponding vector tetraquark currents, where the mixing effects are neglected [550].

$ S_{qc}, S_{\bar{q}\bar{c}}; S, L; J\rangle$	$\mu(\text{GeV})$	$T^2(\text{GeV}^2)$	$\sqrt{s_0}(\text{GeV})$	pole	$D(10)$
$ 0, 0; 0, 1; 1\rangle$	1.1	$2.2 - 2.8$	4.80 ± 0.10	$(49 - 81)\%$	$\leq 1\%$
$ 1, 1; 0, 1; 1\rangle$	1.2	$2.2 - 2.8$	4.85 ± 0.10	$(45 - 79)\%$	$(1 - 5)\%$
$\frac{1}{\sqrt{2}}(1, 0; 1, 1; 1\rangle + 0, 1; 1, 1; 1\rangle)$	1.3	$2.6 - 3.2$	4.90 ± 0.10	$(46 - 75)\%$	$\ll 1\%$
$ 1, 1; 2, 1; 1\rangle$	1.4	$2.6 - 3.2$	4.90 ± 0.10	$(40 - 71)\%$	$\leq 1\%$

Table 28: The Borel windows T^2 , continuum threshold parameters s_0 , ideal energy scales, pole contributions of the ground states and contributions of the vacuum condensates of dimension 10 [550].

where $\overleftrightarrow{\partial}_\mu = \overrightarrow{\partial}_\mu - \overleftarrow{\partial}_\mu$ embodies the explicit P-wave.

Under charge conjugation transformation \hat{C} , the currents $J_\mu(x)$ and $J_{\mu\nu}(x)$ have the property,

$$\begin{aligned}\hat{C}J_\mu(x)\hat{C}^{-1} &= -J_\mu(x), \\ \hat{C}J_{\mu\nu}(x)\hat{C}^{-1} &= -J_{\mu\nu}(x),\end{aligned}\tag{188}$$

the currents have definite charge conjugation.

We choose the currents $J_\mu(x) = J_\mu^1(x)$, $J_\mu^2(x)$, $J_\mu^3(x)$ and $J_{\mu\nu}(x)$ and resort to the correlation functions in Eq.(125) to study the vector tetraquark states using the modified energy scale formula,

$$\begin{aligned}\mu &= \sqrt{M_{X/Y/Z}^2 - (2M_c + 0.5 \text{ GeV})^2}, \\ &= \sqrt{M_{X/Y/Z}^2 - (4.1 \text{ GeV})^2},\end{aligned}\tag{189}$$

to determine the ideal energy scales of the QCD spectral densities, and reexamine the possible assignments of the Y states [549, 550]. The numerical results are shown explicitly in Tables 28-29.

The predicted mass $M_Y = 4.24 \pm 0.10 \text{ GeV}$ of the $|0, 0; 0, 1; 1\rangle$ tetraquark state is in excellent agreement with the experimental data $M_{Y(4220)} = 4222.0 \pm 3.1 \pm 1.4 \text{ MeV}$ from the BESIII collaboration [154], or $M_{Y(4260)} = 4230.0 \pm 8.0 \text{ MeV}$ from the Particle Data Group [411], which supports assigning the $Y(4260/4220)$ as the $C\gamma_5 \otimes \overleftrightarrow{\partial}_\mu \otimes \gamma_5 C$ type vector tetraquark state. We obtain the **vector hidden-charm tetraquark state with the lowest mass** up to now.

There have been other possible assignments for the $Y(4260)$ states, such as the hybrid states [303, 551, 552, 553, 554], molecular state [227, 229, 280, 555, 556], baryonium states [557, 558], hadro-charmonium state [559], interference effect [560, 561], etc.

From Tables 22 and 29, we can see explicitly that there are no rooms for the $Y(4008)$ and $Y(4750)$ in the hidden-charm tetraquark scenario. If we assign the $Y(4220/4230/4260)$ as the ground state, then we could assign the $Y(4750)$ as its first radial excitation according to the mass gap $M_{Y(4750)} - M_{Y(4260)} = 0.51 \text{ GeV}$ [562].

$ S_{qc}, S_{\bar{q}\bar{c}}; S, L; J\rangle$	$M_Y(\text{GeV})$	$\lambda_Y(10^{-2}\text{GeV}^6)$	Assignments
$ 0, 0; 0, 1; 1\rangle$	4.24 ± 0.10	2.31 ± 0.45	$Y(4220)$
$ 1, 1; 0, 1; 1\rangle$	4.28 ± 0.10	4.93 ± 1.00	$Y(4220/4320)$
$\frac{1}{\sqrt{2}}(1, 0; 1, 1; 1\rangle + 0, 1; 1, 1; 1\rangle)$	4.31 ± 0.10	2.99 ± 0.54	$Y(4320/4390)$
$ 1, 1; 2, 1; 1\rangle$	4.33 ± 0.10	7.35 ± 1.39	$Y(4320/4390)$

Table 29: The masses, pole residues and possible assignments of the vector tetraquark states [550].

We carry out the calculations routinely to obtain two QCD sum rules,

$$\lambda_Y^2 \exp\left(-\frac{M_Y^2}{T^2}\right) = \int_{4m_c^2}^{s_0} ds \rho_{QCD}(s) \exp\left(-\frac{s}{T^2}\right), \quad (190)$$

$$\lambda_Y^2 \exp\left(-\frac{M_Y^2}{T^2}\right) + \lambda_{Y'}^2 \exp\left(-\frac{M_{Y'}^2}{T^2}\right) = \int_{4m_c^2}^{s'_0} ds \rho_{QCD}(s) \exp\left(-\frac{s}{T^2}\right), \quad (191)$$

where the s_0 and s'_0 correspond to the ground states Y and first radial excitations Y' , respectively [562].

We adopt the QCDSR II, see Eq.(151) and Eqs.(158)-(159), to study the radially excited states, and obtain the Borel windows, continuum threshold parameters, suitable energy scales and pole contributions, which are shown explicitly in Tables 30-31. From the tables, we can see explicitly that the pole contributions of the 1P states (the 1P plus 2P states) are about (40–60)% ((67–85)%), the pole dominance is satisfied very well. On the other hand, the contributions from the highest dimensional condensates play a minor important role, $|D(10)| < 3\%$ or $\ll 1\%$ ($< 1\%$ or $\ll 1\%$) for the 1P states (the 1P plus 2P states), the operator product expansion converges very good and better than that in our previous work [550], see Table 28.

The predicted masses and pole residues are presented in Table 32. From Tables 31-32, we can see explicitly that the modified energy scale formula, see Eq.(189), can be well satisfied, and the relations $\sqrt{s_0} = M_Y + 0.50 \sim 0.55 \pm 0.10 \text{ GeV}$ and $\sqrt{s'_0} = M_{Y'} + 0.40 \pm 0.10 \text{ GeV}$ are hold, see Eq.(160).

In Fig.19, we plot the masses of the 1P and 2P hidden-charm tetraquark states with the $J^{PC} = 1^{--}$. From the figure, we can see explicitly that there appear flat platforms in the Borel windows, the uncertainties come from the Borel parameters are rather small.

In Table 33, we present the possible assignments of the vector tetraquark states [562]. From the table, we can see explicitly that there is a room to accommodate the $Y(4750)$, i.e. the $Y(4220/4260)$ and $Y(4750)$ can be assigned as the ground state and first radial excited state of the $C\gamma_5 \overset{\leftrightarrow}{\partial}_\mu \gamma_5 C$ type tetraquark states with the $J^{PC} = 1^{--}$, respectively [562].

We can study the corresponding hidden-bottom tetraquark states with the simple replacement $c \rightarrow b$ in Eq.(187). In Ref.[563], we observe that the $Y(10750)$ observed by the Belle collaboration [190] can be assigned as the $C\gamma_5 \otimes \overset{\leftrightarrow}{\partial}_\mu \gamma_5 C$ type hidden-bottom tetraquark state with the $J^{PC} = 1^{--}$.

3.2 Doubly heavy tetraquark states

In 2016, the LHCb collaboration observed the doubly-charmed baryon state Ξ_{cc}^{++} in the $\Lambda_c^+ K^- \pi^+ \pi^+$ mass spectrum and measured the mass, but did not determine the spin [564]. The Ξ_{cc}^{++} maybe have the spin $\frac{1}{2}$ or $\frac{3}{2}$, we can take the diquark $\varepsilon^{ijk} c_i^T C \gamma_\mu c_j$ as basic constituent to construct the current

$$J(x) = \varepsilon^{ijk} c_i^T(x) C \gamma_\mu c_j(x) \gamma_5 \gamma^\mu u_k(x), \quad (192)$$

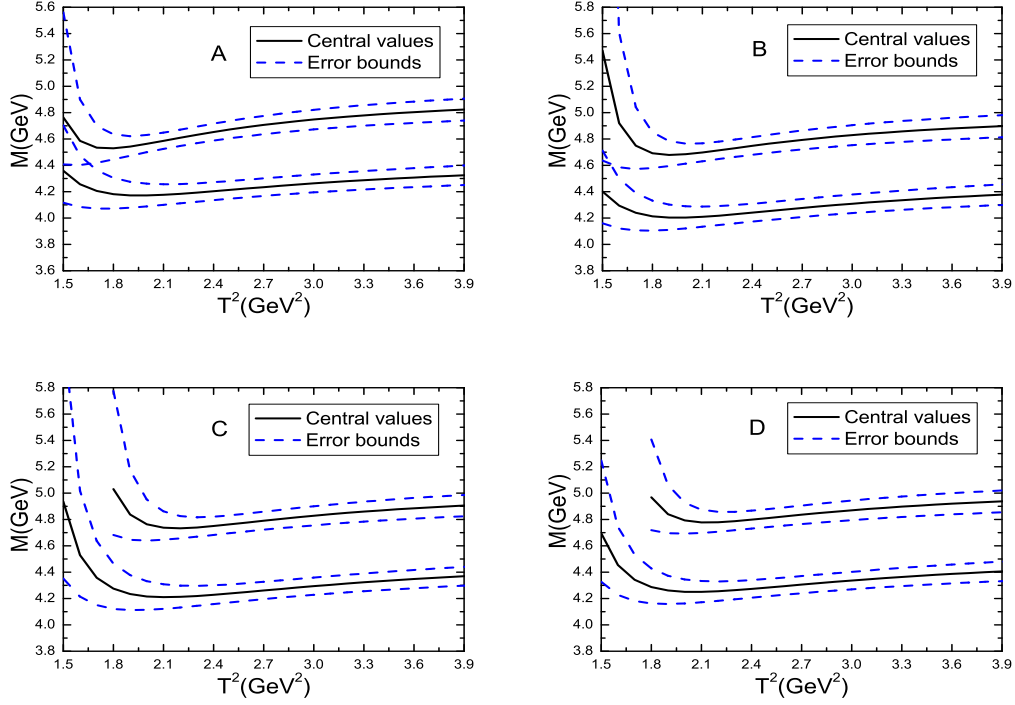


Figure 19: The masses of the vector tetraquark states with variations of the Borel parameters T^2 , where the A , B , C and D stand for the $|0, 0; 0, 1; 1\rangle$, $|1, 1; 0, 0; 1; 1\rangle$, $\frac{1}{\sqrt{2}}(|1, 0; 1, 1; 1\rangle + |0, 1; 1, 1; 1\rangle)$ and $|1, 1; 2, 1; 1\rangle$ states, respectively; the lower lines and upper lines stand for the ground states and first radial excitations, respectively.

$ S_{qc}, S_{\bar{q}\bar{c}}; S, L; J\rangle$	$\mu(\text{GeV})$	$T^2(\text{GeV}^2)$	$\sqrt{s_0}(\text{GeV})$	pole	$D(10)$
$ 0, 0; 0, 1; 1\rangle$	1.1	$2.6 - 3.0$	4.75 ± 0.10	$(40 - 65)\%$	$< 1\%$
$ 1, 1; 0, 1; 1\rangle$	1.2	$2.5 - 2.9$	4.80 ± 0.10	$(39 - 64)\%$	$< 3\%$
$\frac{1}{\sqrt{2}}(1, 0; 1, 1; 1\rangle + 0, 1; 1, 1; 1\rangle)$	1.3	$3.0 - 3.4$	4.85 ± 0.10	$(38 - 60)\%$	$\ll 1\%$
$ 1, 1; 2, 1; 1\rangle$	1.3	$2.7 - 3.1$	4.85 ± 0.10	$(39 - 63)\%$	$< 1\%$

Table 30: The Borel windows T^2 , continuum threshold parameters s_0 , energy scales of the QCD spectral densities, contributions of the ground states, and values of the $D(10)$ [562].

$ S_{qc}, S_{\bar{q}\bar{c}}; S, L; J\rangle$	$\mu(\text{GeV})$	$T^2(\text{GeV}^2)$	$\sqrt{s'_0}(\text{GeV})$	pole	$D(10)$
$ 0, 0; 0, 1; 1\rangle$	2.4	$2.8 - 3.2$	5.15 ± 0.10	$(67 - 85)\%$	$\ll 1\%$
$ 1, 1; 0, 1; 1\rangle$	2.5	$2.6 - 3.0$	5.20 ± 0.10	$(67 - 86)\%$	$< 1\%$
$\frac{1}{\sqrt{2}}(1, 0; 1, 1; 1\rangle + 0, 1; 1, 1; 1\rangle)$	2.6	$3.0 - 3.4$	5.25 ± 0.10	$(67 - 84)\%$	$\ll 1\%$
$ 1, 1; 2, 1; 1\rangle$	2.6	$2.7 - 3.1$	5.25 ± 0.10	$(68 - 87)\%$	$\ll 1\%$

Table 31: The Borel windows T^2 , continuum threshold parameters s'_0 , energy scales of the QCD spectral densities, contributions of the ground states plus first radial excitations, and values of the $D(10)$ [562].

$ S_{qc}, S_{\bar{q}\bar{c}}; S, L; J\rangle$	$M_Y(\text{GeV})$	$\lambda_Y(10^{-2}\text{GeV}^6)$	$M_Y(\text{GeV})$	$\lambda_Y(10^{-2}\text{GeV}^6)$
$ 0, 0; 0, 1; 1\rangle$	4.24 ± 0.09	2.28 ± 0.42	4.75 ± 0.10	8.19 ± 1.23
$ 1, 1; 0, 1; 1\rangle$	4.28 ± 0.09	4.80 ± 0.95	4.81 ± 0.10	18.3 ± 3.0
$\frac{1}{\sqrt{2}}(1, 0; 1, 1; 1\rangle + 0, 1; 1, 1; 1\rangle)$	4.31 ± 0.09	2.94 ± 0.50	4.85 ± 0.09	8.63 ± 1.22
$ 1, 1; 2, 1; 1\rangle$	4.33 ± 0.09	6.55 ± 1.19	4.86 ± 0.10	21.7 ± 3.4

Table 32: The masses and pole residues of the ground states and first radial excitations [562].

$ S_{qc}, S_{\bar{q}\bar{c}}; S, L; J\rangle$	$M_Y(\text{GeV})$	Assignments
$ 0, 0; 0, 1; 1\rangle$ (1P)	4.24 ± 0.09	$Y(4220/4260)$
$ 0, 0; 0, 1; 1\rangle$ (2P)	4.75 ± 0.10	$Y(4750)$
$ 1, 1; 0, 1; 1\rangle$ (1P)	4.28 ± 0.09	$Y(4220/4320)$
$ 1, 1; 0, 1; 1\rangle$ (2P)	4.81 ± 0.10	
$\frac{1}{\sqrt{2}}(1, 0; 1, 1; 1\rangle + 0, 1; 1, 1; 1\rangle)$ (1P)	4.31 ± 0.09	$Y(4320/4390)$
$\frac{1}{\sqrt{2}}(1, 0; 1, 1; 1\rangle + 0, 1; 1, 1; 1\rangle)$ (2P)	4.85 ± 0.09	
$ 1, 1; 2, 1; 1\rangle$ (1P)	4.33 ± 0.09	$Y(4320/4390)$
$ 1, 1; 2, 1; 1\rangle$ (2P)	4.86 ± 0.10	

Table 33: The masses of the vector tetraquark states and possible assignments, where the 1P and 2P denote the ground states and first radial excitations, respectively [562].

or

$$J_\mu(x) = \varepsilon^{ijk} c_i^T(x) C \gamma_\mu c_j(x) u_k(x), \quad (193)$$

to study it with the QCD sum rules [565]. The observation of the doubly-charmed baryon state Ξ_{cc}^{++} has led to a renaissance on the doubly-heavy tetraquark spectroscopy [566, 567, 568]. For a $QQ\bar{q}\bar{q}'$ system, if the two Q -quarks are in long separation, the gluon exchange induced force between them would be screened by the two \bar{q} -quarks, then a loosely $Q\bar{q} - Q\bar{q}'$ type bound state is formed. If the two Q -quarks are in short separation, the QQ pair forms a compact point-like color source in heavy quark limit, and attracts a $\bar{q}\bar{q}'$ pair, which serves as another compact point-like color source, then an exotic $QQ - \bar{q}\bar{q}'$ type tetraquark state is formed. The existence and stability of the $QQ\bar{q}\bar{q}'$ tetraquark states have been extensively discussed in early literatures based on the potential models [569, 570, 571, 572, 573, 574] and heavy quark symmetry [575].

In Ref.[576], we choose the currents $J_\mu(x)$ and $\eta_\mu(x)$ to study the doubly heavy tetraquark states with the $J^P = 1^+$, where

$$\begin{aligned} J_\mu(x) &= \varepsilon^{ijk} \varepsilon^{imn} Q_j^T(x) C \gamma_\mu Q_k(x) \bar{u}_m(x) \gamma_5 C \bar{s}_n^T(x), \\ \eta_\mu(x) &= \varepsilon^{ijk} \varepsilon^{imn} Q_j^T(x) C \gamma_\mu Q_k(x) \bar{u}_m(x) \gamma_5 C \bar{d}_n^T(x), \end{aligned} \quad (194)$$

$Q = c, b$, again, we adopt the correlation functions $\Pi_{\mu\nu}(p)$ in Eq.(125). The tetraquark states are spatial extended objects, not point-like objects, however, we choose the local currents to interpolate them and take all the quarks and antiquarks as the color sources, and neglect the finite size effects.

We rewrite the current $J_\mu(x)$ as

$$\begin{aligned} J_\mu(x) &= Q_j^T(x) C \gamma_\mu Q_k(x) [\bar{u}_j(x) \gamma_5 C \bar{s}_k^T(x) - \bar{u}_k(x) \gamma_5 C \bar{s}_j^T(x)] \\ &= \frac{1}{2} [Q_j^T(x) C \gamma_\mu Q_k(x) - Q_k^T(x) C \gamma_\mu Q_j(x)] [\bar{u}_j(x) \gamma_5 C \bar{s}_k^T(x) - \bar{u}_k(x) \gamma_5 C \bar{s}_j^T(x)] \end{aligned} \quad (195)$$

according to the identity $\varepsilon_{ijk} \varepsilon_{imn} = \delta_{jm} \delta_{kn} - \delta_{jn} \delta_{km}$ in the color space. The current $J_\mu(x)$ is of $\mathbf{\bar{3}} \otimes \mathbf{3}$ type in the color space, we can also construct the current $\tilde{J}_\mu(x)$ satisfying the Fermi-Dirac

	$T^2(\text{GeV}^2)$	$\sqrt{s_0}(\text{GeV})$	$\mu(\text{GeV})$	pole	$M(\text{GeV})$	$\lambda(\text{GeV}^5)$
$cc\bar{u}d$	$2.6 - 3.0$	4.45 ± 0.10	1.3	$(39 - 63)\%$	3.90 ± 0.09	$(2.64 \pm 0.42) \times 10^{-2}$
$cc\bar{u}\bar{s}$	$2.6 - 3.0$	4.50 ± 0.10	1.3	$(41 - 64)\%$	3.95 ± 0.08	$(2.88 \pm 0.46) \times 10^{-2}$
$bb\bar{u}d$	$6.9 - 7.7$	11.14 ± 0.10	2.4	$(41 - 60)\%$	10.52 ± 0.08	$(1.30 \pm 0.20) \times 10^{-1}$
$bb\bar{u}\bar{s}$	$6.8 - 7.6$	11.15 ± 0.10	2.4	$(41 - 61)\%$	10.55 ± 0.08	$(1.33 \pm 0.20) \times 10^{-1}$
$cc\bar{u}d$	$2.6 - 3.0$	4.40 ± 0.10	1.4	$(39 - 62)\%$	3.85 ± 0.09	$(2.60 \pm 0.42) \times 10^{-2}$

Table 34: The Borel windows, continuum threshold parameters, ideal energy scales, pole contributions, masses and pole residues for the doubly heavy tetraquark states [576].

statistics,

$$\tilde{J}_\mu(x) = \frac{1}{2} [Q_j^T(x)C\gamma_5 Q_k(x) + Q_k^T(x)C\gamma_5 Q_j(x)] [\bar{u}_j(x)\gamma_\mu C\bar{s}_k^T(x) + \bar{u}_k(x)\gamma_\mu C\bar{s}_j^T(x)] \quad (196)$$

which is of $\mathbf{6} \otimes \bar{\mathbf{6}}$ type in the color space, and differs from the corresponding current constructed in Ref.[577] slightly.

The color factor defined in Eq.(20) has the values, $\langle \hat{C}_i \cdot \hat{C}_j \rangle = -\frac{2}{3}$ and $\frac{1}{3}$ for the $\bar{\mathbf{3}}$ and $\mathbf{6}$ diquark $[qq]$, respectively. If we define $\hat{C}_{12} \cdot \hat{C}_{34} = (\hat{C}_1 + \hat{C}_2) \cdot (\hat{C}_3 + \hat{C}_4)$, then $\langle \hat{C}_{12} \cdot \hat{C}_{34} \rangle = -\frac{4}{3}$ and $-\frac{10}{3}$ for the $\bar{\mathbf{33}}$ and $\mathbf{66}$ type tetraquark states. The one-gluon exchange induced attractive (repulsive) interaction favors (disfavors) formation of the $\bar{\mathbf{3}}$ ($\mathbf{6}$) diquark state $Q_j^T C\gamma_\mu Q_k - Q_k^T C\gamma_\mu Q_j$ ($Q_j^T C\gamma_5 Q_k + Q_k^T C\gamma_5 Q_j$), while the $\mathbf{66}$ -type tetraquark states are expected to have much smaller masses than that of the $\bar{\mathbf{33}}$ -type tetraquark states according to the $\hat{C}_{12} \cdot \hat{C}_{34}$. Furthermore, the color magnetic interaction, see Eq.(21), leads to mixing between the $\mathbf{66}$ and $\bar{\mathbf{33}}$ -type tetraquark states. In Ref.[577], M. L. Du et al obtain degenerate masses for the $\mathbf{66}$ and $\bar{\mathbf{33}}$ -type tetraquark states based on the QCD sum rules. We should study this subject further.

After tedious but straightforward calculations, we obtain the QCD sum rules for the doubly-heavy tetraquark states [576], which are named as the T states in *The Review of Particle Physics* [97]. According to the energy scale formula in Eq.(99), we suggest an energy scale formula,

$$\mu = \sqrt{M_T^2 - (2\mathbb{M}_Q)^2} - \kappa m_s(\mu), \quad (197)$$

to determine the optimal energy scales of the QCD spectral densities.

There was no experimental candidate for the doubly heavy tetraquark state when performing the calculations [576]. After careful examinations, we choose the effective heavy quark masses $\mathbb{M}_c = 1.84 \text{ GeV}$ and $\mathbb{M}_b = 5.12 \text{ GeV}$, and take account of the $SU(3)$ breaking effect by subtracting the $\kappa m_s(\mu)$. In Table 34, we present the Borel windows T^2 , continuum threshold parameters s_0 , optimal energy scales μ , pole contributions of the ground states, where the same parameters as the ones in the QCD sum rules for the $Z_c(3900)$ are chosen, see the last line.

We take into account all the uncertainties of the relevant parameters, and obtain the values of the masses and pole residues of the Z_{QQ} , which are shown explicitly in Table 34 and Fig.20. From Fig.20, we can see explicitly that there appear platforms in the Borel windows shown in Table 34 indeed. And we suggested to search for the Z_{QQ} states in the Okubo-Zweig-Iizuka super-allowed two-body strong decays

$$\begin{aligned} Z_{cc\bar{u}d} &\rightarrow D^0 D^{*+}, D^+ D^{*0}, \\ Z_{cc\bar{u}\bar{s}} &\rightarrow D^0 D_s^{*+}, D_s^+ D^{*0}, \end{aligned} \quad (198)$$

and weak decays through $b \rightarrow c\bar{c}s$ at the quark level,

$$\begin{aligned} Z_{bb\bar{u}d} &\rightarrow \bar{B}^0 B^{*-}, B^- \bar{B}^{*0} \rightarrow \gamma J/\psi K^- J/\psi \bar{K}^0, \\ Z_{bb\bar{u}\bar{s}} &\rightarrow \bar{B}_s^0 B^{*-}, B^- \bar{B}_s^{*0} \rightarrow \gamma J/\psi \phi J/\psi K^-. \end{aligned} \quad (199)$$

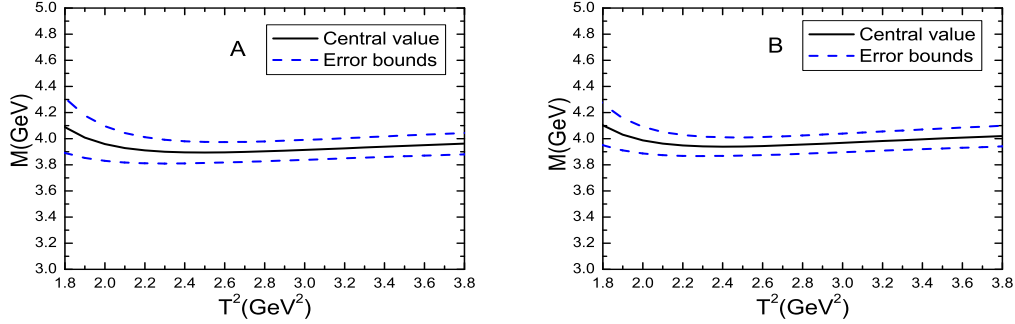


Figure 20: The masses with variations of the Borel parameter T^2 , where the A and B denote the $cc\bar{u}\bar{d}$ and $cc\bar{u}\bar{s}$ tetraquark states, respectively.

In 2021, the LHCb collaboration observed the exotic state $T_{cc}^+(3875)$ just below the $D^0 D^{*+}$ threshold [194, 195]. The Breit-Wigner mass and width are $\delta M_{BW} = -273 \pm 61 \pm 5_{-14}^{+11}$ KeV below the $D^0 D^{*+}$ threshold and $\Gamma_{BW} = 410 \pm 165 \pm 43_{-38}^{+18}$ KeV [194, 195]. While the Particle Data Group fit the Breit-Wigner mass and width to be 3874.83 ± 0.11 MeV and $0.410 \pm 0.165_{-0.057}^{+0.047}$ MeV, respectively [97]. The prediction $M_{Z_{cc\bar{u}\bar{d}}} = 3.90 \pm 0.09$ GeV is in excellent agreement with the LHCb data.

Before the LHCb data, several theoretical groups had made predictions for the T_{cc} masses [276, 285, 336, 342, 345, 351, 354, 360, 361, 566, 567, 576, 577, 578, 579, 580, 581, 582, 583, 584, 585, 586, 587, 588, 589, 590, 591, 592, 593, 594, 595, 596], the predicted masses differ from each other in one way or the other.

In Ref.[578], we resort to the correlation functions $\Pi(p)$ and $\Pi_{\mu\nu\alpha\beta}(p)$ in Eq.(125) and currents

$$\begin{aligned} J(x) &= J_{\bar{u}\bar{d};0}(x), J_{\bar{u}\bar{s};0}(x), J_{\bar{s}\bar{s};0}(x), \\ J_{\mu\nu}(x) &= J_{\mu\nu;1}(x), J_{\mu\nu;2}(x), \\ J_{\mu\nu;1/2}(x) &= J_{\mu\nu;\bar{u}\bar{d};1/2}(x), J_{\mu\nu;\bar{u}\bar{s};1/2}(x), J_{\mu\nu;\bar{s}\bar{s};1/2}(x), \end{aligned} \quad (200)$$

where

$$\begin{aligned} J_{\bar{u}\bar{d};0}(x) &= \varepsilon^{ijk} \varepsilon^{imn} c_j^T(x) C \gamma_\mu c_k(x) \bar{u}_m(x) \gamma^\mu C \bar{d}_n^T(x), \\ J_{\bar{u}\bar{s};0}(x) &= \varepsilon^{ijk} \varepsilon^{imn} c_j^T(x) C \gamma_\mu c_k(x) \bar{u}_m(x) \gamma^\mu C \bar{s}_n^T(x), \\ J_{\bar{s}\bar{s};0}(x) &= \varepsilon^{ijk} \varepsilon^{imn} c_j^T(x) C \gamma_\mu c_k(x) \bar{s}_m(x) \gamma^\mu C \bar{s}_n^T(x), \\ J_{\mu\nu;\bar{u}\bar{d};1/2}(x) &= \varepsilon^{ijk} \varepsilon^{imn} [c_j^T(x) C \gamma_\mu c_k(x) \bar{u}_m(x) \gamma_\nu C \bar{d}_n^T(x) \mp c_j^T(x) C \gamma_\nu c_k(x) \bar{u}_m(x) \gamma_\mu C \bar{d}_n^T(x)], \\ J_{\mu\nu;\bar{u}\bar{s};1/2}(x) &= \varepsilon^{ijk} \varepsilon^{imn} [c_j^T(x) C \gamma_\mu c_k(x) \bar{u}_m(x) \gamma_\nu C \bar{s}_n^T(x) \mp c_j^T(x) C \gamma_\nu c_k(x) \bar{u}_m(x) \gamma_\mu C \bar{s}_n^T(x)], \\ J_{\mu\nu;\bar{s}\bar{s};1/2}(x) &= \varepsilon^{ijk} \varepsilon^{imn} [c_j^T(x) C \gamma_\mu c_k(x) \bar{s}_m(x) \gamma_\nu C \bar{s}_n^T(x) \mp c_j^T(x) C \gamma_\nu c_k(x) \bar{s}_m(x) \gamma_\mu C \bar{s}_n^T(x)], \end{aligned} \quad (201)$$

to study the mass spectrum of the $J^P = 0^+, 1^\pm$ and 2^+ doubly charmed tetraquark states systematically, where the subscripts 0, 1 and 2 denote the spins.

At the phenomenological side, we obtain the hadronic representation and isolate the ground state contributions,

$$\Pi(p) = \frac{\lambda_Z^2}{M_Z^2 - p^2} + \dots = \Pi_0(p^2), \quad (202)$$

$$\begin{aligned}
\Pi_{\mu\nu\alpha\beta;1}(p) &= \frac{\tilde{\lambda}_Z^2}{M_Z^2 - p^2} (p^2 g_{\mu\alpha} g_{\nu\beta} - p^2 g_{\mu\beta} g_{\nu\alpha} - g_{\mu\alpha} p_\nu p_\beta - g_{\nu\beta} p_\mu p_\alpha + g_{\mu\beta} p_\nu p_\alpha + g_{\nu\alpha} p_\mu p_\beta) \\
&\quad + \frac{\tilde{\lambda}_Y^2}{M_Y^2 - p^2} (-g_{\mu\alpha} p_\nu p_\beta - g_{\nu\beta} p_\mu p_\alpha + g_{\mu\beta} p_\nu p_\alpha + g_{\nu\alpha} p_\mu p_\beta) + \dots, \\
&= \Pi_Z(p^2) (p^2 g_{\mu\alpha} g_{\nu\beta} - p^2 g_{\mu\beta} g_{\nu\alpha} - g_{\mu\alpha} p_\nu p_\beta - g_{\nu\beta} p_\mu p_\alpha + g_{\mu\beta} p_\nu p_\alpha + g_{\nu\alpha} p_\mu p_\beta) \\
&\quad + \Pi_Y(p^2) (-g_{\mu\alpha} p_\nu p_\beta - g_{\nu\beta} p_\mu p_\alpha + g_{\mu\beta} p_\nu p_\alpha + g_{\nu\alpha} p_\mu p_\beta), \tag{203}
\end{aligned}$$

$$\begin{aligned}
\Pi_{\mu\nu\alpha\beta;2}(p) &= \frac{\lambda_Z^2}{M_Z^2 - p^2} \left(\frac{\tilde{g}_{\mu\alpha} \tilde{g}_{\nu\beta} + \tilde{g}_{\mu\beta} \tilde{g}_{\nu\alpha}}{2} - \frac{\tilde{g}_{\mu\nu} \tilde{g}_{\alpha\beta}}{3} \right) + \dots, \\
&= \Pi_2(p^2) \left(\frac{\tilde{g}_{\mu\alpha} \tilde{g}_{\nu\beta} + \tilde{g}_{\mu\beta} \tilde{g}_{\nu\alpha}}{2} - \frac{\tilde{g}_{\mu\nu} \tilde{g}_{\alpha\beta}}{3} \right), \tag{204}
\end{aligned}$$

where $\tilde{g}_{\mu\nu} = g_{\mu\nu} - \frac{p_\mu p_\nu}{p^2}$, the pole residues λ_Z and λ_Y are defined analogous to Eq.(127) with the simple replacements $Z^- \rightarrow Y$ and $Z^+ \rightarrow Z$, and $\lambda_Y = \tilde{\lambda}_Y M_Y$, $\lambda_Z = \tilde{\lambda}_Z M_Z$.

We perform the calculations routinely, and obtain the QCD sum rules for the masses and pole residues from the components $\Pi_0(p^2)$, $\Pi_{1;A}(p^2)$, $\Pi_{1;V}(p^2)$ and $\Pi_2(p^2)$, respectively, where $\Pi_{1;A}(p^2) = p^2 \Pi_Z(p^2)$ and $\Pi_{1;V}(p^2) = p^2 \Pi_Y(p^2)$. Again, we adopt the modified energy scale formula in Eq.(197) to determine the best energy scales of the QCD spectral densities.

After trial and error, we obtain the Borel windows T^2 , continuum threshold parameters s_0 , optimal energy scales μ , pole contributions, see Table 35. From the Table, we can see clearly that the pole dominance can be well satisfied. In calculations, we observe that for the $J^P = 1^-$ tetraquark states, the operator product expansion is well convergent, while in the case of the $J^P = 0^+$, 1^+ and 2^+ tetraquark states, the contributions of the vacuum condensates of dimensions 6, 8, 10 have the hierarchy $|D(6)| \gg |D(8)| \gg |D(10)|$, the operator product expansion is also convergent. At last, we take account of all uncertainties of the relevant parameters, and obtain the values of the masses and pole residues, which are shown explicitly in Table 35.

The centroids of the masses of the $C\gamma_\mu \otimes \gamma_\nu C$ type tetraquark states are

$$\begin{aligned}
M_{C\gamma_\mu \otimes \gamma_\nu C}(cc\bar{u}\bar{d}) &= \frac{M_{cc\bar{u}\bar{d};0^+} + 3M_{cc\bar{u}\bar{d};1^+} + 5M_{cc\bar{u}\bar{d};2^+}}{9} = 3.92 \text{ GeV}, \\
M_{C\gamma_\mu \otimes \gamma_\nu C}(cc\bar{u}\bar{s}) &= \frac{M_{cc\bar{u}\bar{s};0^+} + 3M_{cc\bar{u}\bar{s};1^+} + 5M_{cc\bar{u}\bar{s};2^+}}{9} = 3.99 \text{ GeV}, \\
M_{C\gamma_\mu \otimes \gamma_\nu C}(cc\bar{s}\bar{s}) &= \frac{M_{cc\bar{s}\bar{s};0^+} + 3M_{cc\bar{s}\bar{s};1^+} + 5M_{cc\bar{s}\bar{s};2^+}}{9} = 4.04 \text{ GeV}, \tag{205}
\end{aligned}$$

which are slightly larger than the centroids of the masses of the corresponding $C\gamma_\mu \otimes \gamma_5 C$ type tetraquark states,

$$\begin{aligned}
M_{C\gamma_\mu \otimes \gamma_5 C}(cc\bar{u}\bar{d}) &= 3.90 \text{ GeV}, \\
M_{C\gamma_\mu \otimes \gamma_5 C}(cc\bar{u}\bar{s}) &= 3.95 \text{ GeV}, \tag{206}
\end{aligned}$$

the lowest states are the $C\gamma_\mu \otimes \gamma_5 C$ type tetraquark states, which is consistent with our naive expectation that the axialvector (anti)diquarks have larger masses than the corresponding scalar (anti)diquarks. The lowest centroids $M_{cc\bar{u}\bar{d};0^+} = 3.87 \text{ GeV}$ and $M_{cc\bar{u}\bar{s};0^+} = 3.94 \text{ GeV}$ originate from the spin splitting, in other words, the spin-spin interaction between the doubly heavy diquark and light antidiquark. In fact, the predicted masses have uncertainties, the centroids of the masses are not the super values, all values within uncertainties make sense.

The QCD sum rules indicate that the masses of the light axialvector diquark states lie about $(150 - 200) \text{ MeV}$ above that of the light scalar diquark states [501, 502, 503, 504], if they have the same valence quarks. Therefore, the centroids of the masses of the $C\gamma_\mu \otimes \gamma_\nu C$ type tetraquark

states should be larger than 4.0 GeV, the present calculations maybe under-estimate the doubly-heavy tetraquark masses. If we take the simple replacement $m_s(\mu) \rightarrow \mathbb{M}_s$ in the modified energy scale formula in Eq.(197), the predictions should be improved, about +100 MeV.

After observation of the $T_{cc}(3875)$, several new works on the $T_{cc}(3875)$ in the $\bar{\mathbf{3}}\mathbf{3}$ type tetraquark scenario appear [324, 472, 597, 598, 599, 600, 601]. Roughly speaking, the centroid of the $C\gamma_\alpha \otimes \gamma_\beta C$ type tetraquark states maybe lie about 100 MeV above the corresponding $C\gamma_\alpha \otimes \gamma_5 C$ type tetraquark states, and more works are still needed.

The doubly-charmed tetraquark states with the $J^P = 0^+, 1^+$ and 2^+ lie near the corresponding charmed meson pair thresholds, the decays are Okubo-Zweig-Iizuka super-allowed,

$$\begin{aligned}
Z_{cc\bar{u}\bar{d};0^+} &\rightarrow D^0 D^+, \\
Z_{cc\bar{u}\bar{s};0^+} &\rightarrow D^0 D_s^+, \\
Z_{cc\bar{s}\bar{s};0^+} &\rightarrow D_s^+ D_s^+, \\
Z_{cc\bar{u}\bar{d};1^+} &\rightarrow D^0 D^{*+}, D^+ D^{*0}, \\
Z_{cc\bar{u}\bar{s};1^+} &\rightarrow D^0 D_s^{*+}, D_s^+ D^{*0}, \\
Z_{cc\bar{s}\bar{s};1^+} &\rightarrow D_s^+ D_s^{*+}, \\
Z_{cc\bar{u}\bar{d};2^+} &\rightarrow D^0 D^+, D^{*0} D^{*+}, \\
Z_{cc\bar{u}\bar{s};2^+} &\rightarrow D^0 D_s^+, \\
Z_{cc\bar{s}\bar{s};2^+} &\rightarrow D_s^+ D_s^+,
\end{aligned} \tag{207}$$

but the available phase spaces are very small, thus the decays are kinematically depressed, the doubly charmed tetraquark states with the $J^P = 0^+, 1^+$ and 2^+ maybe have small widths. On the other hand, the doubly charmed tetraquark states with the $J^P = 1^-$ lie above the corresponding charmed meson pair thresholds, the decays are Okubo-Zweig-Iizuka super-allowed,

$$\begin{aligned}
Y_{cc\bar{u}\bar{d};1^-} &\rightarrow D^0 D^+, D^0 D^{*+}, D^+ D^{*0}, \\
Y_{cc\bar{u}\bar{s};1^-} &\rightarrow D^0 D_s^+, D^0 D_s^{*+}, D_s^+ D^{*0}, \\
Y_{cc\bar{s}\bar{s};1^-} &\rightarrow D_s^+ D_s^+, D_s^+ D_s^{*+},
\end{aligned} \tag{208}$$

and the available phase spaces are large, thus the decays are kinematically facilitated, the doubly charmed tetraquark states with the $J^P = 1^-$ should have large widths.

3.3 Fully heavy tetraquark states

The exotic states $Z_c(3900)$, $Z_c(4020)$, $Z_c(4430)$, $T_{cc}(3875)$, $P_c(4312)$, $P_c(4380)$, $P_c(4440)$, $P_c(4457)$, $Z_b(10610)$, $Z_b(10650)$, \dots are excellent candidates for the multiquark states, which consist two heavy quarks and two or three light quarks, we have to deal with both the heavy and light degrees of freedom of the dynamics. If there exist multiquark configurations consist of fully heavy quarks, the dynamics is much simple at first glance, and the $QQ\bar{Q}\bar{Q}$ tetraquark states have been studied extensively before the LHCb data [323, 333, 346, 349, 493, 569, 602, 603, 604, 605, 606, 607, 608, 609, 610, 611, 612, 613].

The quarks have color $SU(3)$ symmetry, we can construct the tetraquark states according to the routine quark \rightarrow diquark \rightarrow tetraquark,

$$(\mathbf{3} \otimes \mathbf{3}) \otimes (\bar{\mathbf{3}} \otimes \bar{\mathbf{3}}) \rightarrow (\bar{\mathbf{3}} \oplus \mathbf{6}) \otimes (\mathbf{3} \oplus \bar{\mathbf{6}}) \rightarrow (\bar{\mathbf{3}} \otimes \mathbf{3}) \oplus (\mathbf{6} \otimes \bar{\mathbf{6}}) \rightarrow (\mathbf{1} \oplus \mathbf{8}) \oplus \dots \tag{209}$$

For the $\bar{\mathbf{3}}$ diquarks, only the operators $\varepsilon^{ijk} Q_j^T C \gamma_\mu Q_k$ and $\varepsilon^{ijk} Q_j^T C \sigma_{\mu\nu} Q_k$ could exist due to Fermi-Dirac statistics, and we usually take the operators $\varepsilon^{ijk} Q_j^T C \gamma_\mu Q_k$ to construct the four-quark

	$T^2(\text{GeV}^2)$	$\sqrt{s_0}(\text{GeV})$	$\mu(\text{GeV})$	pole	$M(\text{GeV})$	$\lambda(\text{GeV}^5)$
$cc\bar{u}d(0^+)$	2.4 – 2.8	4.40 ± 0.10	1.2	(38 – 63)%	3.87 ± 0.09	$(3.90 \pm 0.63) \times 10^{-2}$
$cc\bar{u}\bar{s}(0^+)$	2.6 – 3.0	4.50 ± 0.10	1.3	(38 – 62)%	3.94 ± 0.10	$(4.92 \pm 0.89) \times 10^{-2}$
$cc\bar{s}\bar{s}(0^+)$	2.6 – 3.0	4.55 ± 0.10	1.3	(39 – 63)%	3.99 ± 0.10	$(5.31 \pm 0.99) \times 10^{-2}$
$cc\bar{u}d(1^+)$	2.6 – 3.0	4.45 ± 0.10	1.3	(39 – 62)%	3.90 ± 0.09	$(3.44 \pm 0.54) \times 10^{-2}$
$cc\bar{u}\bar{s}(1^+)$	2.6 – 3.0	4.50 ± 0.10	1.3	(40 – 64)%	3.96 ± 0.08	$(3.78 \pm 0.59) \times 10^{-2}$
$cc\bar{s}\bar{s}(1^+)$	2.7 – 3.1	4.55 ± 0.10	1.3	(39 – 62)%	4.02 ± 0.09	$(4.11 \pm 0.68) \times 10^{-2}$
$cc\bar{u}d(2^+)$	2.7 – 3.1	4.50 ± 0.10	1.4	(39 – 62)%	3.95 ± 0.09	$(5.67 \pm 0.90) \times 10^{-2}$
$cc\bar{u}\bar{s}(2^+)$	2.8 – 3.2	4.55 ± 0.10	1.4	(38 – 60)%	4.01 ± 0.09	$(6.27 \pm 1.02) \times 10^{-2}$
$cc\bar{s}\bar{s}(2^+)$	2.8 – 3.2	4.60 ± 0.10	1.4	(39 – 61)%	4.06 ± 0.09	$(6.78 \pm 1.12) \times 10^{-2}$
$cc\bar{u}d(1^-)$	3.3 – 3.9	5.20 ± 0.10	2.9	(50 – 73)%	4.66 ± 0.10	$(1.31 \pm 0.17) \times 10^{-1}$
$cc\bar{u}\bar{s}(1^-)$	3.4 – 4.0	5.25 ± 0.10	2.9	(49 – 71)%	4.73 ± 0.11	$(1.40 \pm 0.19) \times 10^{-1}$
$cc\bar{s}\bar{s}(1^-)$	3.7 – 4.3	5.30 ± 0.10	2.9	(49 – 72)%	4.78 ± 0.11	$(1.48 \pm 0.19) \times 10^{-1}$

Table 35: The Borel windows, continuum threshold parameters, optimal energy scales, pole contributions, masses and pole residues for the doubly charmed tetraquark states [578].

currents $J(x)$ and $J_{\mu\nu}(x)$ [610, 611], where $J_{\mu\nu}(x) = J_{\mu\nu}^1(x)$, $J_{\mu\nu}^2(x)$, and

$$\begin{aligned}
J(x) &= \varepsilon^{ijk} \varepsilon^{imn} Q_j^T(x) C \gamma_\mu Q_k(x) \bar{Q}_m(x) \gamma^\mu C \bar{Q}_n^T(x), \\
J_{\mu\nu}^1(x) &= \varepsilon^{ijk} \varepsilon^{imn} \{ Q_j^T(x) C \gamma_\mu Q_k(x) \bar{Q}_m(x) \gamma_\nu C \bar{Q}_n^T(x) - Q_j^T(x) C \gamma_\nu Q_k(x) \bar{Q}_m(x) \gamma_\mu C \bar{Q}_n^T(x) \}, \\
J_{\mu\nu}^2(x) &= \frac{\varepsilon^{ijk} \varepsilon^{imn}}{\sqrt{2}} \{ Q_j^T(x) C \gamma_\mu Q_k(x) \bar{Q}_m(x) \gamma_\nu C \bar{Q}_n^T(x) + Q_j^T(x) C \gamma_\nu Q_k(x) \bar{Q}_m(x) \gamma_\mu C \bar{Q}_n^T(x) \},
\end{aligned} \tag{210}$$

then resort to the correlation functions $\Pi(p)$ and $\Pi_{\mu\nu\alpha\beta}(p)$ shown in Eq.(125) to obtain the QCD sum rules.

In Ref.[493], Chen et al construct the currents $\eta^i(x)$, $\eta_\mu^k(x)$ and $\eta_{\mu\nu}^j(x)$ with $i = 1, 2, 3, 4, 5$, $k = 1, 2$ and $j = 1, 2$, to interpolate the $QQ\bar{Q}\bar{Q}$ tetraquark states with the $J^{PC} = 0^{++}$, 1^{+-} and 2^{++} , respectively,

$$\begin{aligned}
\eta^i(x) &= Q_a^T(x) C \Gamma^i Q_b(x) \bar{Q}_a(x) \Gamma^i C \bar{Q}_b^T(x), \\
\eta_\mu^1(x) &= Q_a^T(x) C \gamma_\mu \gamma_5 Q_b(x) \bar{Q}_a(x) C \bar{Q}_b^T(x) - Q_a^T(x) C Q_b(x) \bar{Q}_a(x) \gamma_\mu \gamma_5 C \bar{Q}_b^T(x), \\
\eta_\mu^2(x) &= Q_a^T(x) C \sigma_{\mu\nu} \gamma_5 Q_b(x) \bar{Q}_a(x) \gamma^\nu C \bar{Q}_b^T(x) - Q_a^T(x) C \gamma^\nu Q_b(x) \bar{Q}_a(x) \sigma_{\mu\nu} \gamma_5 C \bar{Q}_b^T(x), \\
\eta_{\mu\nu}^j(x) &= Q_a^T(x) C \Gamma_\mu^j Q_b(x) \bar{Q}_a(x) \Gamma_\nu^j C \bar{Q}_b^T(x) + Q_a^T(x) C \Gamma_\nu^j Q_b(x) \bar{Q}_a(x) \Gamma_\mu^j C \bar{Q}_b^T(x),
\end{aligned} \tag{211}$$

where $\Gamma^1 = \gamma_5$, $\Gamma^2 = \gamma_\mu \gamma_5$, $\Gamma^3 = \sigma_{\mu\nu}$, $\Gamma^4 = \gamma_\mu$, $\Gamma^5 = 1$, $\Gamma_\mu^1 = \gamma_\mu$, $\Gamma_\mu^2 = \gamma_\mu \gamma_5$, the a and b are color indexes. The $C\gamma_5$, C , $C\gamma_\mu \gamma_5$ are antisymmetric, while the $C\gamma_\mu$, $C\sigma_{\mu\nu}$, $C\sigma_{\mu\nu} \gamma_5$ are symmetric. The currents $\eta^{1/2/5}(x)$, $\eta_\mu^1(x)$ and $\eta_{\mu\nu}^2(x)$ are in the color $\bar{\mathbf{66}}$ representation, while the currents $\eta^{3/4}(x)$, $\eta_\mu^2(x)$ and $\eta_{\mu\nu}^1(x)$ are in the color $\bar{\mathbf{33}}$ representation. For more currents and predictions in **Scheme II**, we can consult Ref.[493].

At the hadron side, we isolate the ground state contributions and obtain the results [610, 611],

$$\Pi(p) = \frac{\lambda_X^2}{M_X^2 - p^2} + \cdots = \Pi_S(p^2), \tag{212}$$

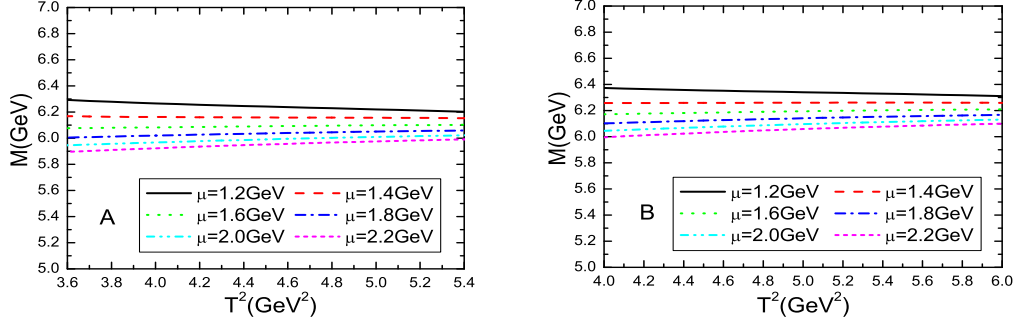


Figure 21: The masses of the $cc\bar{c}\bar{c}$ tetraquark states with variations of the energy scales and Borel parameters, where the A and B denote the $cc\bar{c}\bar{c}(0^{++})$ and $cc\bar{c}\bar{c}(2^{++})$, respectively [610].

$$\begin{aligned}
\Pi_{\mu\nu\alpha\beta}^1(p) &= \frac{\tilde{\lambda}_{Y^+}^2}{M_{Y^+}^2 - p^2} (p^2 g_{\mu\alpha} g_{\nu\beta} - p^2 g_{\mu\beta} g_{\nu\alpha} - g_{\mu\alpha} p_\nu p_\beta - g_{\nu\beta} p_\mu p_\alpha + g_{\mu\beta} p_\nu p_\alpha + g_{\nu\alpha} p_\mu p_\beta) \\
&\quad + \frac{\tilde{\lambda}_{Y^-}^2}{M_{Y^-}^2 - p^2} (-g_{\mu\alpha} p_\nu p_\beta - g_{\nu\beta} p_\mu p_\alpha + g_{\mu\beta} p_\nu p_\alpha + g_{\nu\alpha} p_\mu p_\beta) + \dots, \\
&= \Pi_A(p^2) (p^2 g_{\mu\alpha} g_{\nu\beta} - p^2 g_{\mu\beta} g_{\nu\alpha} - g_{\mu\alpha} p_\nu p_\beta - g_{\nu\beta} p_\mu p_\alpha + g_{\mu\beta} p_\nu p_\alpha + g_{\nu\alpha} p_\mu p_\beta) \\
&\quad + \Pi_V(p^2) (-g_{\mu\alpha} p_\nu p_\beta - g_{\nu\beta} p_\mu p_\alpha + g_{\mu\beta} p_\nu p_\alpha + g_{\nu\alpha} p_\mu p_\beta). \quad (213)
\end{aligned}$$

$$\begin{aligned}
\Pi_{\mu\nu\alpha\beta}^2(p) &= \frac{\lambda_X^2}{M_X^2 - p^2} \left(\frac{\tilde{g}_{\mu\alpha} \tilde{g}_{\nu\beta} + \tilde{g}_{\mu\beta} \tilde{g}_{\nu\alpha}}{2} - \frac{\tilde{g}_{\mu\nu} \tilde{g}_{\alpha\beta}}{3} \right) + \dots, \\
&= \Pi_T(p^2) \left(\frac{\tilde{g}_{\mu\alpha} \tilde{g}_{\nu\beta} + \tilde{g}_{\mu\beta} \tilde{g}_{\nu\alpha}}{2} - \frac{\tilde{g}_{\mu\nu} \tilde{g}_{\alpha\beta}}{3} \right) + \dots, \quad (214)
\end{aligned}$$

where $\tilde{g}_{\mu\nu} = g_{\mu\nu} - \frac{p_\mu p_\nu}{p^2}$, we add the superscripts 1 and 2 to denote the spins, and define the pole residues λ_X and λ_Y with $\lambda_{Y^\pm} = \tilde{\lambda}_{Y^\pm} M_{Y^\pm}$ analogous to Eq.(127) with the simple replacements $Z^+ \rightarrow X$, Y^+ and $Z^- \rightarrow Y^-$.

If we take into account the first radial excited states, we obtain

$$\begin{aligned}
\Pi_{S/T}(p^2) &= \frac{\lambda_X^2}{M_X^2 - p^2} + \frac{\lambda_{X'}^2}{M_{X'}^2 - p^2} + \dots, \\
\Pi_{A/V}(p^2) &= \frac{\tilde{\lambda}_{Y^\pm}^2}{M_{Y^\pm}^2 - p^2} + \frac{\tilde{\lambda}_{Y'^\pm}^2}{M_{Y'^\pm}^2 - p^2} + \dots. \quad (215)
\end{aligned}$$

Again we take the quark-hadron duality below the continuum thresholds s_0 and s'_0 , respectively, and perform the Borel transformation with respect to the variable $P^2 = -p^2$ to obtain the QCD sum rules:

$$\lambda_{X/Y}^2 \exp\left(-\frac{M_{X/Y}^2}{T^2}\right) = \int_{16m_c^2}^{s_0} ds \int_{z_i}^{z_f} dz \int_{t_i}^{t_f} dt \int_{r_i}^{r_f} dr \rho(s, z, t, r) \exp\left(-\frac{s}{T^2}\right), \quad (216)$$

$$\begin{aligned}
\lambda_{X/Y}^2 \exp\left(-\frac{M_{X/Y}^2}{T^2}\right) + \lambda_{X'/Y'}^2 \exp\left(-\frac{M_{X'/Y'}^2}{T^2}\right) &= \int_{16m_c^2}^{s'_0} ds \int_{z_i}^{z_f} dz \int_{t_i}^{t_f} dt \int_{r_i}^{r_f} dr \rho(s, z, t, r) \\
&\quad \exp\left(-\frac{s}{T^2}\right), \quad (217)
\end{aligned}$$

	$T^2(\text{GeV}^2)$	$s_0(\text{GeV}^2)$	$\mu(\text{GeV})$	pole	$M_X(\text{GeV})$	$\lambda_X(\text{GeV}^5)$
$cc\bar{c}\bar{c}(0^{++})$	4.2 – 4.6	42 ± 1	2.0	(46 – 62)%	5.99 ± 0.08	$(3.72 \pm 0.54) \times 10^{-1}$
$cc\bar{c}\bar{c}(1^{+-})$	4.5 – 4.9	43 ± 1	2.0	(46 – 61)%	6.05 ± 0.08	$(2.97 \pm 0.44) \times 10^{-1}$
$cc\bar{c}\bar{c}(2^{++})$	4.6 – 5.2	44 ± 1	2.0	(46 – 63)%	6.09 ± 0.08	$(3.36 \pm 0.45) \times 10^{-1}$
$cc\bar{c}\bar{c}(1^{--})$	4.2 – 4.6	44 ± 1	2.0	(46 – 62)%	6.11 ± 0.08	$(1.82 \pm 0.33) \times 10^{-1}$
$bb\bar{b}\bar{b}(0^{++})$	13.0 – 13.6	374 ± 3	3.1	(49 – 61)%	18.84 ± 0.09	6.79 ± 1.27
$bb\bar{b}\bar{b}(1^{+-})$	13.3 – 13.9	374 ± 3	3.1	(48 – 60)%	18.84 ± 0.09	5.45 ± 1.01
$bb\bar{b}\bar{b}(2^{++})$	13.0 – 13.6	375 ± 3	3.1	(51 – 63)%	18.85 ± 0.09	5.55 ± 1.00
$bb\bar{b}\bar{b}(1^{--})$	11.7 – 12.3	376 ± 3	3.1	(47 – 60)%	18.89 ± 0.09	1.64 ± 0.36

Table 36: The Borel parameters, continuum threshold parameters, energy scales, pole contributions, masses and pole residues for the 1S and 1P fully heavy tetraquark states [610, 611].

J^{PC}	$T^2(\text{GeV}^2)$	$\sqrt{s_0'}(\text{GeV})$	$\mu(\text{GeV})$	pole	$M_{X/Y}(\text{GeV})$	$\lambda_{X/Y}(10^{-1}\text{GeV}^5)$
$0^{++}(2S)$	4.4 – 4.8	6.80 ± 0.10	2.5	(65 – 79)%	6.48 ± 0.08	7.41 ± 1.12
$1^{+-}(2S)$	4.4 – 4.8	6.85 ± 0.10	2.5	(69 – 82)%	6.52 ± 0.08	5.56 ± 0.80
$2^{++}(2S)$	4.9 – 5.3	6.90 ± 0.10	2.5	(63 – 76)%	6.56 ± 0.08	5.92 ± 0.83
$1^{--}(2P)$	4.5 – 4.9	6.90 ± 0.10	2.2	(57 – 73)%	6.58 ± 0.09	3.46 ± 0.58

Table 37: The Borel parameters, continuum threshold parameters, energy scales, pole contributions, masses and pole residues for the 2S and 2P $cc\bar{c}\bar{c}$ tetraquark states [614].

where the QCD spectral densities $\rho(s, z, t, r) = \rho_S(s, z, t, r)$, $\rho_A(s, z, t, r)$, $\rho_V(s, z, t, r)$ and $\rho_T(s, z, t, r)$ [610, 611, 614].

In Fig.21, we plot the masses of the $cc\bar{c}\bar{c}$ tetraquark states with variations of the energy scales and Borel parameters for the threshold parameters $s_S^0 = 42 \text{ GeV}^2$ and $s_T^0 = 44 \text{ GeV}^2$. The predicted masses decrease monotonously and slowly with increase of the energy scales, the QCD sum rules are stable with variations of the Borel parameters at the energy scales $1.2 \text{ GeV} < \mu < 2.2 \text{ GeV}$. We take the largest energy scale $\mu = 2.0 \text{ GeV}$ in Ref.[610]. In Refs.[610, 611], we obtain the predictions for the masses of the ground states, see Table 36, where $M_{cc\bar{c}\bar{c}(0^{++})} < 2M_{J/\psi}$.

In 2020, the LHCb collaboration observed a broad structure above the $J/\psi J/\psi$ threshold ranging from 6.2 to 6.8 GeV and a narrow structure at about 6.9 GeV in the $J/\psi J/\psi$ mass spectrum, and they also observed some vague structures around 7.2 GeV [142]. Accordingly, we obtain the masses of the 2S and 2P states from the QCDSR II in Eq.(217), and obtain the 3/4S and 3/4P masses by fitting the Regge trajectories,

$$M_n^2 = \alpha(n-1) + \alpha_0, \quad (218)$$

where the α and α_0 are constants, see Tables 37-38, which support assigning the broad structure from 6.2 to 6.8 GeV in the di- J/ψ mass spectrum as the 2S or 2P tetraquark state, and assigning the narrow structure at about 6.9 GeV in the di- J/ψ mass spectrum as the 3S tetraquark state [614].

In 2023, the ATLAS collaboration observed a narrow resonance at about 6.9 GeV and a broader structure at much lower mass in the $J/\psi J/\psi$ channel, moreover, they observed a statistically significant excess at about 7.0 GeV in the $J/\psi \psi'$ channel [143]. In 2024, the CMS collaboration

J^{PC}	$M_1(\text{GeV})$	$M_2(\text{GeV})$	$M_3(\text{GeV})$	$M_4(\text{GeV})$
0^{++}	5.99 ± 0.08	6.48 ± 0.08	6.94 ± 0.08	7.36 ± 0.08
1^{+-}	6.05 ± 0.08	6.52 ± 0.08	6.96 ± 0.08	6.37 ± 0.08
2^{++}	6.09 ± 0.08	6.56 ± 0.08	7.00 ± 0.08	7.41 ± 0.08
1^{--}	6.11 ± 0.08	6.58 ± 0.09	7.02 ± 0.09	7.43 ± 0.09

Table 38: The masses of the $cc\bar{c}\bar{c}$ tetraquark states with the radial quantum numbers $n = 1, 2, 3$ and 4 [614].

J^{PC}	$T^2(\text{GeV}^2)$	$\sqrt{s_0}(\text{GeV})$	$\mu(\text{GeV})$	pole	$M_{X/Y}(\text{GeV})$	$\lambda_{X/Y}(10^{-1}\text{GeV}^5)$
$0^{++}(1S)$	$3.6 - 4.0$	6.55 ± 0.10	1.4	$(39 - 61)\%$	6.20 ± 0.10	2.68 ± 0.57
$1^{+-}(1S)$	$3.8 - 4.2$	6.60 ± 0.10	1.4	$(40 - 61)\%$	6.24 ± 0.10	2.18 ± 0.44
$2^{++}(1S)$	$4.0 - 4.4$	6.65 ± 0.10	1.4	$(39 - 60)\%$	6.27 ± 0.09	2.35 ± 0.46
$1^{--}(1P)$	$3.2 - 3.6$	6.70 ± 0.10	1.2	$(39 - 63)\%$	6.33 ± 0.10	0.86 ± 0.24

Table 39: The Borel parameters, continuum threshold parameters, energy scales, pole contributions, masses and pole residues for the 1S and 1P $cc\bar{c}\bar{c}$ tetraquark states [615].

observed three resonant structures in the $J/\psi J/\psi$ mass spectrum,

$$\begin{aligned}
X(6600) : M &= 6552 \pm 10 \pm 12 \text{ MeV}, \Gamma = 124_{-26}^{+32} \pm 33 \text{ MeV}, \\
X(6900) : M &= 6927 \pm 9 \pm 4 \text{ MeV}, \Gamma = 122_{-21}^{+24} \pm 18 \text{ MeV}, \\
X(7300) : M &= 7287_{-18}^{+20} \pm 5 \text{ MeV}, \Gamma = 95_{-40}^{+59} \pm 19 \text{ MeV},
\end{aligned} \tag{219}$$

in the no-interference model [144].

In Ref.[615], we update the calculations by taking the energy scale $\mu = 1.4 \text{ GeV}$, the lower bound in Fig.21, and adopt the relation,

$$M_1 < \sqrt{s_0} < M_2 < \sqrt{s'_0} < M_3, \tag{220}$$

and obtain the predictions, see Tables 39-40, and make the possible assignments, see Table 41. From Table 41, we can see explicitly that **the lowest state lies at about 6.2 GeV**, which is consistent with the recent coupled-channel analysis [616].

The thresholds of the $J/\psi J/\psi$, $J/\psi \psi \psi'$ and $J/\psi \psi \psi(3770)$ are 6194 MeV, 6783 MeV and 6875 MeV, respectively [97], we cannot obtain a simple molecule scenario to interpret those X states without introducing complex coupled-channel effects [617, 618, 619, 620], or just assign them as the **$\bar{3}3$** and **$6\bar{6}$** type tetraquark states [334, 337, 344, 352, 460, 595, 621, 622, 623, 624, 625, 626, 627, 628, 629, 630, 631], or with gluonic constituent [632].

J^{PC}	$T^2(\text{GeV}^2)$	$\sqrt{s'_0}(\text{GeV})$	$\mu(\text{GeV})$	pole	$M_{X/Y}(\text{GeV})$	$\lambda_{X/Y}(10^{-1}\text{GeV}^5)$
$0^{++}(2S)$	$4.8 - 5.2$	6.90 ± 0.10	2.4	$(61 - 75)\%$	6.57 ± 0.09	8.12 ± 1.21
$1^{+-}(2S)$	$5.2 - 5.6$	7.00 ± 0.10	2.4	$(61 - 75)\%$	6.64 ± 0.09	6.43 ± 0.88
$2^{++}(2S)$	$5.3 - 5.7$	7.05 ± 0.10	2.4	$(62 - 75)\%$	6.69 ± 0.09	6.84 ± 0.92
$1^{--}(2P)$	$5.0 - 5.4$	7.10 ± 0.10	2.4	$(60 - 74)\%$	6.74 ± 0.09	4.74 ± 0.71

Table 40: The Borel parameters, continuum threshold parameters, energy scales, pole contributions, masses and pole residues for the 2S and 2P $cc\bar{c}\bar{c}$ tetraquark states [615].

J^{PC}	$M_1(\text{GeV})$	$M_2(\text{GeV})$	$M_3(\text{GeV})$	$M_4(\text{GeV})$
0^{++}	6.20 ± 0.10 ? $X(6220)$	6.57 ± 0.09 ? $X(6600/6620)$	6.92 ± 0.09 ? $X(6900)$	7.25 ± 0.09 ? $X(7220/7300)$
1^{+-}	6.24 ± 0.10 ? $X(6220)$	6.64 ± 0.09 ? $X(6600/6620)$	7.03 ± 0.09	7.40 ± 0.09
2^{++}	6.27 ± 0.09	6.69 ± 0.09	7.09 ± 0.09	7.46 ± 0.09
1^{--}	6.33 ± 0.10	6.74 ± 0.09	7.13 ± 0.09	7.50 ± 0.09

Table 41: The masses of the fully-charm tetraquark states with the radial quantum numbers $n = 1, 2, 3$ and 4. In the lower lines, we present the possible assignments [615].

We perform Fierz transformation for the currents $J(x)$ and $J_{\mu\nu}(x)$, and obtain particular superpositions of a series of color **11** type currents,

$$\begin{aligned}
J &= 2\bar{Q}Q\bar{Q}Q + 2\bar{Q}i\gamma_5 Q\bar{Q}i\gamma_5 Q + \bar{Q}\gamma_\alpha Q\bar{Q}\gamma^\alpha Q - \bar{Q}\gamma_\alpha\gamma_5 Q\bar{Q}\gamma^\alpha\gamma_5 Q, \\
J_{\mu\nu}^1 &= 2i\bar{Q}\sigma_{\mu\nu}Q\bar{Q}Q + 2i\varepsilon_{\mu\nu\alpha\beta}\bar{Q}\gamma_\alpha\gamma_5 Q\bar{Q}\gamma_\beta Q - 2\bar{Q}\sigma_{\mu\nu}\gamma_5 Q\bar{Q}i\gamma_5 Q, \\
\tilde{J}_{\mu\nu}^2 &= 2\bar{Q}\gamma_\mu\gamma_5 Q\bar{Q}\gamma_\nu\gamma_5 Q - 2\bar{Q}\gamma_\mu Q\bar{Q}\gamma_\nu Q + g^{\alpha\beta}(\bar{Q}\sigma_{\mu\alpha}Q\bar{Q}\sigma_{\nu\beta}Q + \bar{Q}\sigma_{\nu\alpha}Q\bar{Q}\sigma_{\mu\beta}Q) + \\
&\quad g_{\mu\nu}\left(\bar{Q}Q\bar{Q}Q + \bar{Q}i\gamma_5 Q\bar{Q}i\gamma_5 Q + \bar{Q}\gamma_\alpha Q\bar{Q}\gamma^\alpha Q - \bar{Q}\gamma_\alpha\gamma_5 Q\bar{Q}\gamma^\alpha\gamma_5 Q - \frac{1}{2}\bar{Q}\sigma_{\alpha\beta}Q\bar{Q}\sigma^{\alpha\beta}Q\right),
\end{aligned} \tag{221}$$

with $\tilde{J}_{\mu\nu}^2 = \sqrt{2}J_{\mu\nu}^2$, the components $\bar{Q}\Gamma Q\bar{Q}\Gamma'Q$ couple potentially to the molecular states, where the Γ and Γ' stand for some Dirac γ -matrixes. Therefore the **33** type tetraquark states have some important **11** type Fock components, which would decay to their constituents via the Okubo-Zweig-Iizuka super-allowed fall apart mechanism if they are kinematically permitted. There exists a term $\bar{Q}\gamma_\mu Q\bar{Q}\gamma_\nu Q$, the decay to the di- J/ψ is super-allowed, which is consistent with the observations of the ATLAS, CMS and LHCb experiments.

If we insist on that the di- J/ψ system should have positive charge conjugation, we would like to construct a cousin of currents, $J_{-, \mu}^{\tilde{A}A}(x)$ and $J_{+, \mu}^{\tilde{A}A}(x)$,

$$\begin{aligned}
J_{-, \mu}^{\tilde{A}A}(x) &= \frac{\varepsilon^{ijk}\varepsilon^{imn}}{\sqrt{2}}\left[c_j^T(x)C\sigma_{\mu\nu}\gamma_5 c_k(x)\bar{c}_m(x)\gamma^\nu C\bar{c}_n^T(x) - c_j^T(x)C\gamma^\nu c_k(x)\bar{c}_m(x)\gamma_5\sigma_{\mu\nu}C\bar{c}_n^T(x)\right], \\
J_{+, \mu}^{\tilde{A}A}(x) &= \frac{\varepsilon^{ijk}\varepsilon^{imn}}{\sqrt{2}}\left[c_j^T(x)C\sigma_{\mu\nu}\gamma_5 c_k(x)\bar{c}_m(x)\gamma^\nu C\bar{c}_n^T(x) + c_j^T(x)C\gamma^\nu c_k(x)\bar{c}_m(x)\gamma_5\sigma_{\mu\nu}C\bar{c}_n^T(x)\right],
\end{aligned} \tag{222}$$

which couple potentially to the fully-charm tetraquark states with the $J^{PC} = 1^{+-}$ and 1^{++} , respectively.

In Ref.[633], we introduce a relative P-wave to construct the doubly-charmed vector diquark operator \tilde{V} , then construct the scalar and tensor four-quark currents,

$$\begin{aligned}
J(x) &= \varepsilon^{ijk}\varepsilon^{imn}c_j^T(x)C\gamma_5\overleftrightarrow{\partial}_\mu c_k(x)\bar{c}_m(x)\overleftrightarrow{\partial}_\nu\gamma_5 C\bar{c}_n^T(x)g^{\mu\nu}, \\
J_{\mu\nu}^1(x) &= \varepsilon^{ijk}\varepsilon^{imn}\left\{c_j^T(x)C\gamma_5\overleftrightarrow{\partial}_\mu c_k(x)\bar{c}_m(x)\overleftrightarrow{\partial}_\nu\gamma_5 C\bar{c}_n^T(x) \right. \\
&\quad \left. - c_j^T(x)C\gamma_5\overleftrightarrow{\partial}_\nu c_k(x)\bar{c}_m(x)\overleftrightarrow{\partial}_\mu\gamma_5 C\bar{c}_n^T(x)\right\}, \\
J_{\mu\nu}^2(x) &= \varepsilon^{ijk}\varepsilon^{imn}\left\{c_j^T(x)C\gamma_5\overleftrightarrow{\partial}_\mu c_k(x)\bar{c}_m(x)\overleftrightarrow{\partial}_\nu\gamma_5 C\bar{c}_n^T(x) \right. \\
&\quad \left. + c_j^T(x)C\gamma_5\overleftrightarrow{\partial}_\nu c_k(x)\bar{c}_m(x)\overleftrightarrow{\partial}_\mu\gamma_5 C\bar{c}_n^T(x)\right\},
\end{aligned} \tag{223}$$

to study the scalar, axialvector and tensor fully-charm tetraquark states with the QCD sum rules. And we observe that the ground state $\hat{V}\hat{V}$ type tetraquark states and the first radial excited states of the AA type tetraquark states have almost degenerated masses.

We can extend this subsection directly to study the $\bar{\mathbf{3}}\mathbf{3}\bar{\mathbf{3}}$ type fully heavy pentaquark states and $\mathbf{3}\mathbf{3}\mathbf{3}$ type fully heavy hexaquark states [634, 635].

4 11 type tetraquark states

The X , Y , Z , T and P states always lie near the two-particle thresholds, such as

$$\begin{aligned}
D\bar{D}^*/\bar{D}D^* &: X(3872), Z_c(3885/3900), \\
DD^* &: T_{cc}(3875), \\
D^*\bar{D}^* &: Z_c(4020/4025), \\
D\bar{D}_s^*/D^*\bar{D}_s &: Z_{cs}(3985/4000), \\
D_s^*\bar{D}_s^* &: X(4140), \\
D\bar{D}_1/\bar{D}D_1 &: Y(4260/4220), Z_c(4250), \\
D^*\bar{D}_0/\bar{D}^*D_0 &: Y(4360/4320), \\
\bar{D}\Sigma_c &: P_c(4312), \\
\bar{D}\Xi_c &: P_{cs}(4338), \\
\bar{D}\Xi'_c/\bar{D}^*\Xi_c &: P_{cs}(4459), \\
\bar{D}\Sigma_c^* &: P_c(4380), \\
\bar{D}^*\Sigma_c &: P_c(4440/4457), \\
\Lambda_c^+\Lambda_c^-/f_0(980)\psi' &: Y(4660), \\
B\bar{B}^*/\bar{B}B^* &: Z_b(10610), \\
B^*\bar{B}^* &: Z_b(10650),
\end{aligned} \tag{224}$$

naively, we expect that they consist of two color-neutral clusters, and they are molecular states, more precisely, they are the **11** type hidden-charm or doubly-charmed tetraquark or pentaquark states [636]. The establishment of the $J^{PC} = 1^{++}$ of the $Y(4140)$ by the LHCb collaboration [113, 114] excludes its assignment as the $D_s^*\bar{D}_s^*$ molecular state with the $J^{PC} = 0^{++}$ [432, 435, 477, 478, 637, 638], however, which does not mean non-existence of the $D_s^*\bar{D}_s^*$ molecular state with the $J^{PC} = 0^{++}$.

The $\bar{\mathbf{3}}\mathbf{3}$ type four-quark currents could be reformed in a series of **11** type four-quark currents through Fierz transformation [424, 639], some useful examples are given explicitly in the appendix, see Eqs.(482)-(489).

According to the quark-hadron duality, the $\bar{\mathbf{3}}\mathbf{3}$ and **11** type local currents couple potentially to the $\bar{\mathbf{3}}\mathbf{3}$ and **11** type tetraquark states, respectively. The $\bar{\mathbf{3}}\mathbf{3}$ type tetraquark states could be taken as a particular superposition of a series of the **11** type tetraquark states, while the **11** type tetraquark states could decay through the Okubo-Zweig-Iizuka super-allowed fall-apart mechanism. We usually use the identities in Eqs.(482)-(489) to analyze the strong decays [424, 639]. For example, the current in Eq.(482) couples potentially to the $Z_c(3900)$, in the nonrelativistic and heavy quark limit, the component $\bar{c}\sigma^{\mu\nu}\gamma_5 u \bar{d}\gamma_\nu c$ can be reduced to the form,

$$\begin{aligned}
\bar{c}\sigma^{0j}\gamma_5 u \bar{d}\gamma_j c &\propto \xi_c^\dagger \sigma^j \zeta_u \chi_d^\dagger \vec{\sigma} \cdot \vec{k}_d \sigma^j \xi_c \propto \xi_c^\dagger \frac{\sigma^j}{2} \zeta_u \chi_d^\dagger \frac{\sigma^j}{2} \xi_c = \vec{S}_{D^*} \cdot \vec{S}_{D^*}, \\
\bar{c}\sigma^{ij}\gamma_5 u \bar{d}\gamma_j c &\propto \epsilon^{ijk} \xi_c^\dagger \sigma^k \vec{\sigma} \cdot \vec{k}_u \zeta_u \chi_d^\dagger \vec{\sigma} \cdot \vec{k}_d \sigma^j \xi_c \propto \epsilon^{ijk} \xi_c^\dagger \frac{\sigma^k}{2} \zeta_u \chi_d^\dagger \frac{\sigma^j}{2} \xi_c = \vec{S}_{D^*} \times \vec{S}_{D^*},
\end{aligned} \tag{225}$$

where the ξ , ζ and χ are two-component spinors of the quark fields, the \vec{k} are the three-vectors of the quark fields, the σ^i are the pauli matrixes, and the \vec{S} are the spin operators. It is obvious that

the currents $\bar{c}\sigma^{\mu\nu}\gamma_5 u \bar{d}\gamma_\nu c$ and $\bar{c}\gamma_\nu u \bar{d}\sigma^{\mu\nu}\gamma_5 c$ couple potentially to the $J^P = 0^+$ and 1^+ ($D^*\bar{D}^*$) $^+$ states. However, the strong decays $Z_c^\pm(3900) \rightarrow (D^*\bar{D}^*)^\pm$ are kinematically forbidden.

4.1 Hidden heavy tetraquark states

Again, let us adopt the correlation functions $\Pi(p)$, $\Pi_{\mu\nu}(p)$ and $\Pi_{\mu\nu\alpha\beta}(p)$ defined in Eq.(125) and write down the currents

$$\begin{aligned} J(x) &= J_{D\bar{D}}(x), J_{D\bar{D}_s}(x), J_{D_s\bar{D}_s}(x), J_{D^*\bar{D}^*}(x), J_{D^*\bar{D}_s^*}(x), J_{D_s^*\bar{D}_s^*}(x), \\ J_\mu(x) &= J_{D\bar{D}^*,\pm,\mu}(x), J_{D\bar{D}_s^*,\pm,\mu}(x), J_{D_s\bar{D}_s^*,\pm,\mu}(x), \\ J_{\mu\nu}(x) &= J_{\pm,\mu\nu}(x), \\ J_{\pm,\mu\nu}(x) &= J_{D^*\bar{D}^*,\pm,\mu\nu}(x), J_{D^*\bar{D}_s^*,\pm,\mu\nu}(x), J_{D_s^*\bar{D}_s^*,\pm,\mu\nu}(x), \end{aligned} \quad (226)$$

and

$$\begin{aligned} J_{D\bar{D}}(x) &= \bar{q}(x)i\gamma_5 c(x) \bar{c}(x)i\gamma_5 q(x), \\ J_{D\bar{D}_s}(x) &= \bar{q}(x)i\gamma_5 c(x) \bar{c}(x)i\gamma_5 s(x), \\ J_{D_s\bar{D}_s}(x) &= \bar{s}(x)i\gamma_5 c(x) \bar{c}(x)i\gamma_5 s(x), \\ J_{D^*\bar{D}^*}(x) &= \bar{q}(x)\gamma_\mu c(x) \bar{c}(x)\gamma^\mu q(x), \\ J_{D^*\bar{D}_s^*}(x) &= \bar{q}(x)\gamma_\mu c(x) \bar{c}(x)\gamma^\mu s(x), \\ J_{D_s^*\bar{D}_s^*}(x) &= \bar{s}(x)\gamma_\mu c(x) \bar{c}(x)\gamma^\mu s(x), \end{aligned} \quad (227)$$

$$\begin{aligned} J_{D\bar{D}^*,\pm,\mu}(x) &= \frac{1}{\sqrt{2}} \left[\bar{u}(x)i\gamma_5 c(x) \bar{c}(x)\gamma_\mu d(x) \mp \bar{u}(x)\gamma_\mu c(x) \bar{c}(x)i\gamma_5 d(x) \right], \\ J_{D\bar{D}_s^*,\pm,\mu}(x) &= \frac{1}{\sqrt{2}} \left[\bar{q}(x)i\gamma_5 c(x) \bar{c}(x)\gamma_\mu s(x) \mp \bar{q}(x)\gamma_\mu c(x) \bar{c}(x)i\gamma_5 s(x) \right], \\ J_{D_s\bar{D}_s^*,\pm,\mu}(x) &= \frac{1}{\sqrt{2}} \left[\bar{s}(x)i\gamma_5 c(x) \bar{c}(x)\gamma_\mu s(x) \mp \bar{s}(x)\gamma_\mu c(x) \bar{c}(x)i\gamma_5 s(x) \right], \end{aligned} \quad (228)$$

$$\begin{aligned} J_{D^*\bar{D}^*,\pm,\mu\nu}(x) &= \frac{1}{\sqrt{2}} \left[\bar{u}(x)\gamma_\mu c(x) \bar{c}(x)\gamma_\nu d(x) \pm \bar{u}(x)\gamma_\nu c(x) \bar{c}(x)\gamma_\mu d(x) \right], \\ J_{D^*\bar{D}_s^*,\pm,\mu\nu}(x) &= \frac{1}{\sqrt{2}} \left[\bar{q}(x)\gamma_\mu c(x) \bar{c}(x)\gamma_\nu s(x) \pm \bar{q}(x)\gamma_\nu c(x) \bar{c}(x)\gamma_\mu s(x) \right], \\ J_{D_s^*\bar{D}_s^*,\pm,\mu\nu}(x) &= \frac{1}{\sqrt{2}} \left[\bar{s}(x)\gamma_\mu c(x) \bar{c}(x)\gamma_\nu s(x) \pm \bar{s}(x)\gamma_\nu c(x) \bar{c}(x)\gamma_\mu s(x) \right], \end{aligned} \quad (229)$$

and $q = u, d$. The subscripts $D\bar{D}$, $D\bar{D}_s$, \dots and $D_s^*\bar{D}_s^*$ stand for the two color-neutral clusters; especially, the subscripts $D\bar{D}^*, \pm$, $D\bar{D}_s^*, \pm$ and $D_s\bar{D}_s^*, \pm$ correspond to the two color-neutral clusters $D\bar{D}^* \mp D^*\bar{D}$, $D\bar{D}_s^* \mp D^*\bar{D}_s$ and $D_s\bar{D}_s^* \mp D_s^*\bar{D}_s$, respectively, etc.

Again, we take the isospin limit, the currents with the symbolic quark structures $\bar{c}c\bar{d}u$, $\bar{c}c\bar{u}d$, $\bar{c}c\frac{\bar{u}u-\bar{d}d}{\sqrt{2}}$, $\bar{c}c\frac{\bar{u}u+\bar{d}d}{\sqrt{2}}$ couple potentially to the hidden-charm molecular states with degenerated masses, the currents with the isospin $I = 1$ and 0 lead to the same QCD sum rules [81, 82, 83, 422].

Under parity transformation \hat{P} , the currents $J(x)$, $J_\mu(x)$ and $J_{\mu\nu}(x)$ have the properties,

$$\begin{aligned} \hat{P}J(x)\hat{P}^{-1} &= +J(\tilde{x}), \\ \hat{P}J_\mu(x)\hat{P}^{-1} &= -J^\mu(\tilde{x}), \\ \hat{P}J_{\pm,\mu\nu}(x)\hat{P}^{-1} &= +J_{\pm,\mu\nu}^{\mu\nu}(\tilde{x}), \end{aligned} \quad (230)$$

where $x^\mu = (t, \vec{x})$ and $\tilde{x}^\mu = (t, -\vec{x})$. Under charge conjugation transformation \hat{C} , the currents $J(x)$, $J_\mu(x)$ and $J_{\mu\nu}(x)$ have the properties,

$$\begin{aligned}\hat{C}J(x)\hat{C}^{-1} &= +J(x), \\ \hat{C}J_{\pm,\mu}(x)\hat{C}^{-1} &= \pm J_{\pm,\mu}(x), \\ \hat{C}J_{\pm,\mu\nu}(x)\hat{C}^{-1} &= \pm J_{\pm,\mu\nu}(x).\end{aligned}\tag{231}$$

At the hadron side, we obtain the hadronic representation and isolate the ground state hidden-charm molecule contributions [82, 83],

$$\begin{aligned}\Pi(p) &= \frac{\lambda_{Z_+}^2}{M_{Z_+}^2 - p^2} + \dots = \Pi_+(p^2), \\ \Pi_{\mu\nu}(p) &= \frac{\lambda_{Z_+}^2}{M_{Z_+}^2 - p^2} \left(-g_{\mu\nu} + \frac{p_\mu p_\nu}{p^2} \right) + \dots \\ &= \Pi_+(p^2) \left(-g_{\mu\nu} + \frac{p_\mu p_\nu}{p^2} \right) + \dots, \\ \Pi_{-,\mu\nu\alpha\beta}(p) &= \frac{\tilde{\lambda}_{Z_+}^2}{M_{Z_+}^2 - p^2} (p^2 g_{\mu\alpha} g_{\nu\beta} - p^2 g_{\mu\beta} g_{\nu\alpha} - g_{\mu\alpha} p_\nu p_\beta - g_{\nu\beta} p_\mu p_\alpha + g_{\mu\beta} p_\nu p_\alpha + g_{\nu\alpha} p_\mu p_\beta) \\ &\quad + \frac{\tilde{\lambda}_{Z_-}^2}{M_{Z_-}^2 - p^2} (-g_{\mu\alpha} p_\nu p_\beta - g_{\nu\beta} p_\mu p_\alpha + g_{\mu\beta} p_\nu p_\alpha + g_{\nu\alpha} p_\mu p_\beta) + \dots \\ &= \tilde{\Pi}_+(p^2) (p^2 g_{\mu\alpha} g_{\nu\beta} - p^2 g_{\mu\beta} g_{\nu\alpha} - g_{\mu\alpha} p_\nu p_\beta - g_{\nu\beta} p_\mu p_\alpha + g_{\mu\beta} p_\nu p_\alpha + g_{\nu\alpha} p_\mu p_\beta) \\ &\quad + \tilde{\Pi}_-(p^2) (-g_{\mu\alpha} p_\nu p_\beta - g_{\nu\beta} p_\mu p_\alpha + g_{\mu\beta} p_\nu p_\alpha + g_{\nu\alpha} p_\mu p_\beta), \\ \Pi_{+,\mu\nu\alpha\beta}(p) &= \frac{\lambda_{Z_+}^2}{M_{Z_+}^2 - p^2} \left(\frac{\tilde{g}_{\mu\alpha} \tilde{g}_{\nu\beta} + \tilde{g}_{\mu\beta} \tilde{g}_{\nu\alpha}}{2} - \frac{\tilde{g}_{\mu\nu} \tilde{g}_{\alpha\beta}}{3} \right) + \dots, \\ &= \Pi_+(p^2) \left(\frac{\tilde{g}_{\mu\alpha} \tilde{g}_{\nu\beta} + \tilde{g}_{\mu\beta} \tilde{g}_{\nu\alpha}}{2} - \frac{\tilde{g}_{\mu\nu} \tilde{g}_{\alpha\beta}}{3} \right) + \dots,\end{aligned}\tag{232}$$

where the Z represents the molecular states Z_c , X_c , Z_{cs} , etc. We add the subscripts \pm in the hidden-charm molecular states Z_\pm and the components $\Pi_\pm(p^2)$ and $\tilde{\Pi}_\pm(p^2)$ to represent the positive and negative parity contributions, respectively, and define the pole residues λ_{Z_\pm} analogous to Eq.(127) with $\lambda_{Z_\pm} = M_{Z_\pm} \tilde{\lambda}_{Z_\pm}$. We choose the components $\Pi_+(p^2)$ and $p^2 \tilde{\Pi}_+(p^2)$ to study the scalar, axialvector and tensor hidden-charm molecular states. According to the discussions in Sect.2.3, we have no reason to worry about the contaminations from the two-meson scattering states.

At the QCD side, we carry out the operator product expansion up to the vacuum condensates of dimension 10, and take account of the vacuum condensates $\langle \bar{q}q \rangle$, $\langle \frac{\alpha_s GG}{\pi} \rangle$, $\langle \bar{q}g_s \sigma Gq \rangle$, $\langle \bar{q}q \rangle^2$, $g_s^2 \langle \bar{q}q \rangle^2$, $\langle \bar{q}q \rangle \langle \frac{\alpha_s GG}{\pi} \rangle$, $\langle \bar{q}q \rangle \langle \bar{q}g_s \sigma Gq \rangle$, $\langle \bar{q}g_s \sigma Gq \rangle^2$ and $\langle \bar{q}q \rangle^2 \langle \frac{\alpha_s GG}{\pi} \rangle$, where $q = u, d$ or s quark, just like in Sect.3.1.1.

According to analogous routine of Sect.3.1.1, we obtain the QCD sum rules:

$$\lambda_{Z_+}^2 \exp\left(-\frac{M_{Z_+}^2}{T^2}\right) = \int_{4m_c^2}^{s_0} ds \rho_{QCD}(s) \exp\left(-\frac{s}{T^2}\right),\tag{233}$$

and

$$M_{Z_+}^2 = -\frac{\int_{4m_c^2}^{s_0} ds \frac{d}{d\tau} \rho_{QCD}(s) \exp(-\tau s)}{\int_{4m_c^2}^{s_0} ds \rho_{QCD}(s) \exp(-\tau s)} \Big|_{\tau=\frac{1}{T^2}}.\tag{234}$$

$Z_c(X_c)$	J^{PC}	$T^2(\text{GeV}^2)$	$\sqrt{s_0}(\text{GeV})$	$\mu(\text{GeV})$	pole	$ D(10) $
DD	0^{++}	$2.7 - 3.1$	4.30 ± 0.10	1.3	$(40 - 63)\%$	$\ll 1\%$
$D\bar{D}_s$	0^{++}	$2.8 - 3.2$	4.40 ± 0.10	1.3	$(40 - 63)\%$	$\ll 1\%$
$D_s\bar{D}_s$	0^{++}	$2.9 - 3.3$	4.50 ± 0.10	1.3	$(41 - 62)\%$	$\ll 1\%$
D^*D^*	0^{++}	$2.8 - 3.2$	4.55 ± 0.10	1.6	$(40 - 62)\%$	$\leq 1\%$
$D^*\bar{D}_s^*$	0^{++}	$2.9 - 3.3$	4.65 ± 0.10	1.6	$(41 - 63)\%$	$< 1\%$
$D_s^*\bar{D}_s^*$	0^{++}	$3.1 - 3.5$	4.75 ± 0.10	1.6	$(40 - 61)\%$	$\ll 1\%$
$D\bar{D}^* - D^*\bar{D}$	1^{+-}	$2.7 - 3.1$	4.40 ± 0.10	1.3	$(40 - 63)\%$	$\ll 1\%$
$D\bar{D}_s^* - D^*\bar{D}_s$	1^{+-}	$2.9 - 3.3$	4.55 ± 0.10	1.3	$(41 - 63)\%$	$\ll 1\%$
$D_s\bar{D}_s^* - D_s^*\bar{D}_s$	1^{+-}	$3.0 - 3.4$	4.65 ± 0.10	1.3	$(42 - 63)\%$	$\ll 1\%$
$D\bar{D}^* + D^*\bar{D}$	1^{+-}	$2.7 - 3.1$	4.40 ± 0.10	1.3	$(40 - 63)\%$	$\ll 1\%$
$D\bar{D}_s^* + D^*\bar{D}_s$	1^{+-}	$2.9 - 3.3$	4.55 ± 0.10	1.3	$(41 - 63)\%$	$\ll 1\%$
$D_s\bar{D}_s^* + D_s^*\bar{D}_s$	1^{+-}	$3.0 - 3.4$	4.65 ± 0.10	1.3	$(42 - 63)\%$	$\ll 1\%$
D^*D^*	1^{+-}	$3.0 - 3.4$	4.55 ± 0.10	1.6	$(42 - 63)\%$	$< 1\%$
$D^*\bar{D}_s^*$	1^{+-}	$3.2 - 3.6$	4.65 ± 0.10	1.6	$(41 - 61)\%$	$\ll 1\%$
$D_s^*\bar{D}_s^*$	1^{+-}	$3.3 - 3.7$	4.75 ± 0.10	1.6	$(42 - 61)\%$	$\ll 1\%$
D^*D^*	2^{++}	$3.0 - 3.4$	4.55 ± 0.10	1.6	$(41 - 62)\%$	$< 1\%$
$D^*\bar{D}_s^*$	2^{++}	$3.2 - 3.6$	4.65 ± 0.10	1.6	$(40 - 60)\%$	$\ll 1\%$
$D_s^*\bar{D}_s^*$	2^{++}	$3.3 - 3.7$	4.75 ± 0.10	1.6	$(41 - 61)\%$	$\ll 1\%$

Table 42: The Borel parameters, continuum threshold parameters, energy scales of the QCD spectral densities, pole contributions and contributions of the vacuum condensates of dimension 10 for the ground states [82, 83].

In the heavy quark limit, we describe the $Q\bar{Q}q\bar{q}$ systems by a double-well potential model, the heavy quark Q (\bar{Q}) serves as a static well potential and attracts the light antiquark \bar{q} (q) to form a color-neutral cluster. We introduce the effective heavy quark mass \mathbb{M}_Q and divide the molecular states into both the heavy and light degrees of freedom, i.e. $2\mathbb{M}_Q$ and $\mu = \sqrt{M_{X/Y/Z}^2 - (2\mathbb{M}_Q)^2}$, respectively.

Analysis of the J/ψ and Υ mass spectrum with the famous Cornell potential or Coulomb-potential-plus-linear-potential leads to the constituent quark masses $m_c = 1.84 \text{ GeV}$ and $m_b = 5.17 \text{ GeV}$ [640], we can set the effective c -quark mass as the constituent quark mass $\mathbb{M}_c = m_c = 1.84 \text{ GeV}$. The old value $\mathbb{M}_c = 1.84 \text{ GeV}$ and updated value $\mathbb{M}_c = 1.85 \text{ GeV}$, which are fitted for the hidden-charm molecular states, are all consistent with the constituent quark mass $m_c = 1.84 \text{ GeV}$ [81, 422, 641]. We choose the value $\mathbb{M}_c = 1.84 \text{ GeV}$ to determine the ideal energy scales of the QCD spectral densities, and add an uncertainty $\delta\mu = \pm 0.1 \text{ GeV}$ to account for the difference between the values $\mathbb{M}_c = 1.84 \text{ GeV}$ and 1.85 GeV . Furthermore, we take the modified energy scale formula

$$\mu = \sqrt{M_{X/Y/Z}^2 - (2\mathbb{M}_c)^2} - k\mathbb{M}_s, \quad (235)$$

with $k = 0, 1, 2$ and $\mathbb{M}_s = 0.2 \text{ GeV}$ to account for the light flavor $SU(3)$ breaking effects.

After trial and error, we obtain the Borel windows, continuum threshold parameters, energy scales of the QCD spectral densities, pole contributions, and contributions of the vacuum condensates of dimension 10, which are shown explicitly in Table 42. At the hadron side, the pole contributions are about $(40 - 60)\%$, while the central values are larger than 50%, the pole dominance condition is well satisfied. At the QCD side, the contributions of the vacuum condensates of dimension 10 are $|D(10)| \leq 1\%$ or $\ll 1\%$, the convergent behaviors of the operator product expansion are very good.

We take account of all the uncertainties of the relevant parameters, and obtain the masses and pole residues of the molecular states without strange, with strange and with hidden-strange, which

$Z_c(X_c)$	J^{PC}	$M_Z(\text{GeV})$	$\lambda_Z(\text{GeV}^5)$
DD	0^{++}	3.74 ± 0.09	$(1.61 \pm 0.23) \times 10^{-2}$
$D\bar{D}_s$	0^{++}	3.88 ± 0.10	$(1.98 \pm 0.30) \times 10^{-2}$
$D_s\bar{D}_s$	0^{++}	3.98 ± 0.10	$(2.36 \pm 0.45) \times 10^{-2}$
D^*D^*	0^{++}	4.02 ± 0.09	$(4.30 \pm 0.72) \times 10^{-2}$
$D^*\bar{D}_s^*$	0^{++}	4.10 ± 0.09	$(5.00 \pm 0.83) \times 10^{-2}$
$D_s^*\bar{D}_s^*$	0^{++}	4.20 ± 0.09	$(5.86 \pm 0.98) \times 10^{-2}$
$D\bar{D}^* - D^*\bar{D}$	1^{++}	3.89 ± 0.09	$(1.72 \pm 0.30) \times 10^{-2}$
$D\bar{D}_s^* - D^*\bar{D}_s$	1^{++}	3.99 ± 0.09	$(1.96 \pm 0.35) \times 10^{-2}$
$D_s\bar{D}_s^* - D_s^*\bar{D}_s$	1^{++}	4.07 ± 0.09	$(2.07 \pm 0.37) \times 10^{-2}$
$D\bar{D}^* + D^*\bar{D}$	1^{+-}	3.89 ± 0.09	$(1.72 \pm 0.30) \times 10^{-2}$
$D\bar{D}_s^* + D^*\bar{D}_s$	1^{+-}	3.99 ± 0.09	$(1.96 \pm 0.35) \times 10^{-2}$
$D_s\bar{D}_s^* + D_s^*\bar{D}_s$	1^{+-}	4.07 ± 0.09	$(2.07 \pm 0.37) \times 10^{-2}$
D^*D^*	1^{+-}	4.02 ± 0.09	$(2.33 \pm 0.35) \times 10^{-2}$
$D^*\bar{D}_s^*$	1^{+-}	4.11 ± 0.09	$(2.71 \pm 0.41) \times 10^{-2}$
$D_s^*\bar{D}_s^*$	1^{+-}	4.19 ± 0.09	$(3.12 \pm 0.47) \times 10^{-2}$
D^*D^*	2^{++}	4.02 ± 0.09	$(3.29 \pm 0.51) \times 10^{-2}$
$D^*\bar{D}_s^*$	2^{++}	4.11 ± 0.09	$(3.84 \pm 0.59) \times 10^{-2}$
$D_s^*\bar{D}_s^*$	2^{++}	4.19 ± 0.09	$(4.42 \pm 0.67) \times 10^{-2}$

Table 43: The masses and pole residues of the ground state hidden-charm molecular states [82, 83].

are shown explicitly in Table 43. From Tables 42–43, it is obvious that the modified energy scale formula in Eq.(235) is well satisfied [82, 83].

In Fig.22, we plot the masses of the axialvector molecular states $D\bar{D}^* + D^*\bar{D}$, $D\bar{D}^* - D^*\bar{D}$, $D\bar{D}_s^* + D^*\bar{D}_s$ and $D^*\bar{D}^*$ with variations of the Borel parameters at much larger ranges than the Borel widows as an example. From the figure, we can see plainly that there appear very flat platforms in the Borel windows indeed, where the regions between the two short vertical lines are the Borel windows.

In Fig.22, we also present the experimental values of the masses of the $Z_c(3900)$, $X_c(3872)$, $Z_{cs}(3985)$ and $Z_c(4020)$ [169, 642], the predicted masses are in excellent agreement with the experimental data. The calculations support assigning the $Z_c(3900)$, $X_c(3872)$, $Z_{cs}(3985)$ and $Z_c(4020)$ to be the $D\bar{D}^* + D^*\bar{D}$, $D\bar{D}^* - D^*\bar{D}$, $D\bar{D}_s^* + D^*\bar{D}_s$ and $D^*\bar{D}^*$ tetraquark molecular states with the quantum numbers $J^{PC} = 1^{+-}$, 1^{++} , 1^{+-} and 1^{+-} , respectively. In Table 44, we present the possible assignments of the ground state hidden-charm molecular states. However, the lattice QCD calculations do not favor the existence of the $Z_c(3900)$ [357, 370, 643, 644].

We could reproduce the experimental masses of the $X_c(3872)$, $Z_c(3900)$, $Z_{cs}(3985)$, $Z_{cs}(4123)$ and $Z_c(4020)$ both in the scenarios of tetraquark states and molecular states, see Tables 9-11 and 44, the tetraquark scenario can accommodate much more exotic X and Z states than the molecule scenario. Even in the tetraquark scenario, there are no rooms to accommodate the $X(3940)$, $X(4160)$, $Z_c(4100)$ and $Z_c(4200)$ without resorting to fine tuning. The $X(3940)$ and $X(4160)$ might be the conventional $\eta_c(3S)$ and $\eta_c(4S)$ states with the $J^{PC} = 0^{-+}$, respectively. The $Z_c(4100)$ might be a mixing scalar tetraquark state with the $J^{PC} = 0^{++}$, and the $Z_c(4200)$ might be an axialvector color **88** type tetraquark state with the $J^{PC} = 1^{+-}$. For detailed discussions about this subject, one can consult Ref.[61].

The $Z_c(3900)$ and $Z_c(3885)$ have almost degenerated masses but quite different decay widths [162, 163, 167], they are taken as the same particle by the Particle Data Group [97] (also Ref.[60]), however, it is difficult to explain the large ratio,

$$R_{exp} = \frac{\Gamma(Z_c(3885) \rightarrow D\bar{D}^*)}{\Gamma(Z_c(3900) \rightarrow J/\psi\pi)} = 6.2 \pm 1.1 \pm 2.7, \quad (236)$$

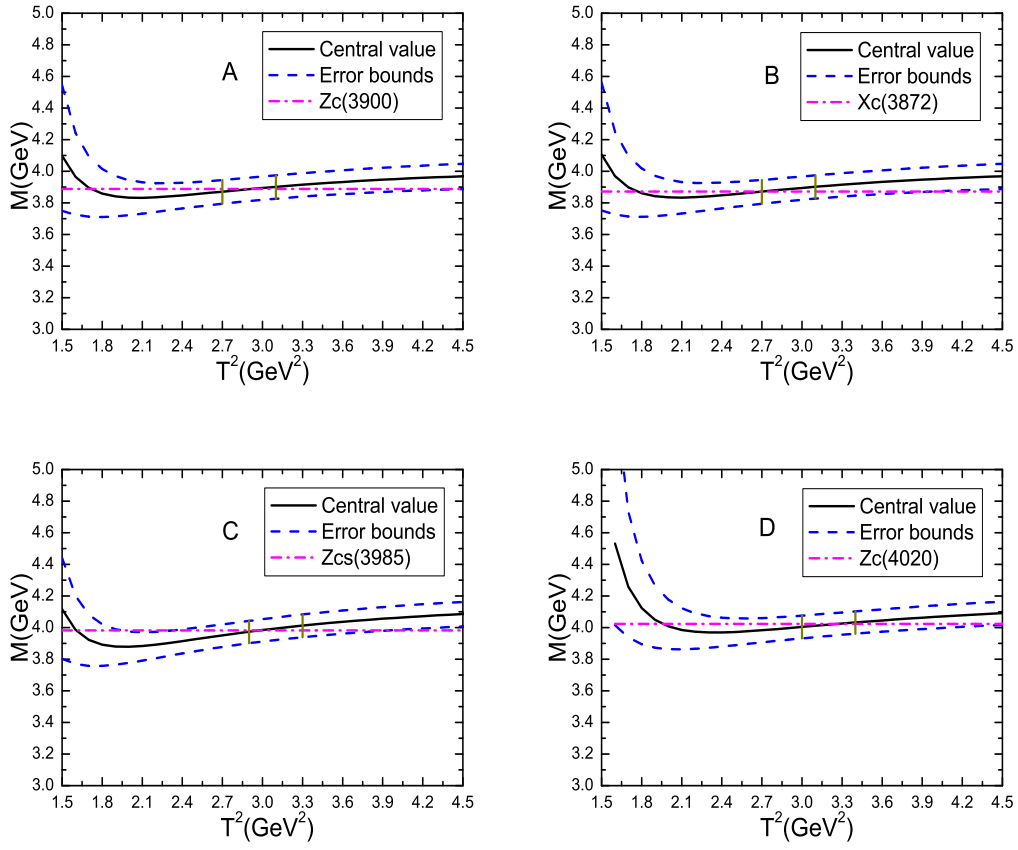


Figure 22: The masses of the molecular states with variations of the Borel parameters T^2 , where the A, B, C and D correspond to the axialvector $D\bar{D}^* + D^*\bar{D}$, $D\bar{D}^* - D^*\bar{D}$, $D\bar{D}_s^* + D^*\bar{D}_s$ and $D^*\bar{D}^*$ molecular states, respectively.

$Z_c(X_c)$	J^{PC}	$M_Z(\text{GeV})$	Assignments
DD	0^{++}	3.74 ± 0.09	? $X(3960)$
$D\bar{D}_s$	0^{++}	3.88 ± 0.10	
$D_s\bar{D}_s$	0^{++}	3.98 ± 0.10	
$D^*\bar{D}^*$	0^{++}	4.02 ± 0.09	
$D^*\bar{D}_s^*$	0^{++}	4.10 ± 0.09	
$D_s^*\bar{D}_s^*$	0^{++}	4.20 ± 0.09	
$DD^* - D^*D$	1^{++}	3.89 ± 0.09	? $X_c(3872)$
$D\bar{D}_s^* - D^*\bar{D}_s$	1^{++}	3.99 ± 0.09	
$D_s\bar{D}_s^* - D_s^*\bar{D}_s$	1^{++}	4.07 ± 0.09	
$DD^* + D^*D$	1^{+-}	3.89 ± 0.09	? $Z_c(3900)$
$D\bar{D}_s^* + D^*\bar{D}_s$	1^{+-}	3.99 ± 0.09	? $Z_{cs}(3985/4000)$
$D_s\bar{D}_s^* + D_s^*\bar{D}_s$	1^{+-}	4.07 ± 0.09	
$D^*\bar{D}^*$	1^{+-}	4.02 ± 0.09	? $Z_c(4020)$
$D^*\bar{D}_s^*$	1^{+-}	4.11 ± 0.09	? $Z_{cs}(4100/4123)$
$D_s^*\bar{D}_s^*$	1^{+-}	4.19 ± 0.09	
$D^*\bar{D}^*$	2^{++}	4.02 ± 0.09	? X₂(4014)
$D^*\bar{D}_s^*$	2^{++}	4.11 ± 0.09	
$D_s^*\bar{D}_s^*$	2^{++}	4.19 ± 0.09	

Table 44: The possible assignments of the ground state hidden-charm molecular states, the isospin limit is implied [82, 83].

from the BESIII collaboration [167]. If we assign the $Z_c(3900)$ as the $\bar{\mathbf{3}}\mathbf{3}$ type tetraquark state, and assign the $Z_c(3885)$ as the $D\bar{D} + D^*\bar{D}$ molecular state, it is easy to explain the large ratio R_{exp} .

The $Z_{cs}(3985)$ observed by the BESIII collaboration near the $D_s^- D^{*0}$ and $D_s^{*-} D^0$ thresholds in the K^+ recoil-mass spectrum in the processes $e^+e^- \rightarrow K^+(D_s^- D^{*0} + D_s^{*-} D^0)$, its Breit-Wigner mass and width are $3985.2_{-2.0}^{+2.1} \pm 1.7 \text{ MeV}$ and $13.8_{-5.2}^{+8.1} \pm 4.9 \text{ MeV}$ respectively with an assignment of the spin-parity $J^P = 1^+$ [169]. The $Z_{cs}(4000)$ observed in the $J/\psi K^+$ mass spectrum by the LHCb collaboration has a mass of $4003 \pm 6_{-14}^{+4} \text{ MeV}$, a width of $131 \pm 15 \pm 26 \text{ MeV}$, and the spin-parity $J^P = 1^+$ [115]. The $Z_{cs}(3885)$ and $Z_{cs}(4000)$ are two quite different particles, although they have almost degenerated masses.

In the $J/\psi K^+$ mass spectrum from the LHCb collaboration, there is a hint of a dip at the energy about 4.1 GeV [115], which maybe due to the $Z_{cs}^-(4123)$ observed by the BESIII collaboration with a mass about $(4123.5 \pm 0.7 \pm 4.7) \text{ MeV}$ [170]. More experimental data are still needed to obtain a precise resolution.

After Ref.[82] was published, the Belle collaboration observed weak evidences for two structures in the $\gamma\psi(2S)$ invariant mass spectrum in the two-photon process $\gamma\gamma \rightarrow \gamma\psi(2S)$, one at $3922.4 \pm 6.5 \pm 2.0 \text{ MeV}$ with a width $22 \pm 17 \pm 4 \text{ MeV}$, and another at $4014.3 \pm 4.0 \pm 1.5 \text{ MeV}$ with a width $4 \pm 11 \pm 6 \text{ MeV}$ [645]. The first structure is consistent with the $X(3915)$ or $\chi_{c2}(3930)$, the second one might be an exotic charmonium-like state. We present its possible assignment in Table 44, see **X₂(4014)**, which cannot be accommodated in the scenario of tetraquark state.

In Table 43, the central values of the predicted molecule masses lie at the thresholds of the corresponding two-meson scattering states, where we have taken the currents having two color-neutral clusters, in each cluster, the constituents q and \bar{Q} (or Q and \bar{q}) are in relative S-wave, see Eq.(226).

Now let us see the possible outcomes, if one of the color-neutral clusters has a relative P-wave between the constituents q and \bar{Q} (or Q and \bar{q}), as one of the possible assignments of the $Y(4260)$ is the $D\bar{D}_1$ molecular state with the $J^{PC} = 1^{--}$ [227, 229, 280, 555, 556].

For example, in the isospin limit, we write the valence quarks of the $D\bar{D}_1(2420)$ and $D^*\bar{D}_0^*(2400)$ molecular states symbolically as

$$\bar{u}d\bar{c}c, \quad \frac{\bar{u}u - \bar{d}d}{\sqrt{2}}\bar{c}c, \quad \bar{d}u\bar{c}c, \quad \frac{\bar{u}u + \bar{d}d}{\sqrt{2}}\bar{c}c, \quad (237)$$

the isospin triplet and singlet have degenerate masses. We take the isospin limit to study those molecular states [641].

Again we resort to the correlation functions $\Pi_{\mu\nu}(p)$ in Eq.(125) with the currents $J_\mu(x) = J_\mu^1(x)$, $J_\mu^2(x)$, $J_\mu^3(x)$ and $J_\mu^4(x)$ to study the $D\bar{D}_1(2420)$ and $D^*\bar{D}_0^*(2400)$ molecular states, where

$$\begin{aligned} J_\mu^{1/2}(x) &= \frac{1}{\sqrt{2}} \{ \bar{u}(x)i\gamma_5 c(x)\bar{c}(x)\gamma_\mu\gamma_5 d(x) \mp \bar{u}(x)\gamma_\mu\gamma_5 c(x)\bar{c}(x)i\gamma_5 d(x) \}, \\ J_\mu^{3/4}(x) &= \frac{1}{\sqrt{2}} \{ \bar{u}(x)c(x)\bar{c}(x)\gamma_\mu d(x) \pm \bar{u}(x)\gamma_\mu c(x)\bar{c}(x)d(x) \}. \end{aligned} \quad (238)$$

Under charge conjugation transformation \hat{C} , the currents $J_\mu(x)$ have the properties,

$$\begin{aligned} \hat{C}J_\mu^{1/3}(x)\hat{C}^{-1} &= -J_\mu^{1/3}(x)|_{u\leftrightarrow d}, \\ \hat{C}J_\mu^{2/4}(x)\hat{C}^{-1} &= +J_\mu^{2/4}(x)|_{u\leftrightarrow d}. \end{aligned} \quad (239)$$

According to the quark-hadron duality, we isolate the ground state contributions of the vector molecular states,

$$\Pi_{\mu\nu}(p) = \frac{\lambda_Y^2}{M_Y^2 - p^2} \left(-g_{\mu\nu} + \frac{p_\mu p_\nu}{p^2} \right) + \dots, \quad (240)$$

where the λ_Y are the pole residues.

We carry out the operator product expansion up to the vacuum condensates of dimension 10 in a consistent way routinely [82, 83, 641], and obtain the QCD sum rules for the masses and pole residues.

We adopt the energy scale formula in Eq.(235) to choose the best energy scales of the QCD spectral densities, and take the updated value $M_c = 1.85$ GeV [641].

After trial and error, we obtain the Borel parameters, continuum threshold parameters, pole contributions and energy scales, see Table 45, where the central values of the pole contributions are larger than 50%, the pole dominance is well satisfied. In the Borel windows, the contributions $D_{10} \ll 1\%$, the operator product expansion is well convergent.

We take account of all the uncertainties of the relevant parameters, and obtain the values of the masses and pole residues, which are also shown Table 45 [641].

The prediction $M_{D\bar{D}_1(1^{--})} = 4.36 \pm 0.08$ GeV is consistent with the experimental data $M_{Y(4390)} = 4391.6 \pm 6.3 \pm 1.0$ MeV from the BESIII collaboration within uncertainties [153], while the predictions $M_{D\bar{D}_1(1^{--})} = 4.60 \pm 0.08$ GeV, $M_{D^*\bar{D}_0^*(1^{--})} = 4.78 \pm 0.07$ GeV and $M_{D^*\bar{D}_0^*(1^{--})} = 4.73 \pm 0.07$ GeV are much larger than upper bound of the experimental data $M_{Y(4220)} = 4218.4 \pm 4.0 \pm 0.9$ MeV and $M_{Y(4390)} = 4391.6 \pm 6.3 \pm 1.0$ MeV [153], moreover, they are much larger than the near thresholds $M_{D^+D_1(2420)^-} = 4293$ MeV, $M_{D^0D_1(2420)^0} = 4285$ MeV, $M_{D^{*+}D_0^*(2400)^-} = 4361$ MeV, $M_{D^{*0}D_0^*(2400)^0} = 4325$ MeV [646]. The present predictions only support assigning the $Y(4390)$ to be the $D\bar{D}_1(1^{--})$ molecular state. Or the $Y(4260)$ has sizable non $D\bar{D}_1$ component [647].

In Ref.[434], Zhang and Huang study the $Q\bar{q}Q'q$ type scalar, vector and axialvector molecular states with the QCD sum rules systematically by calculating the operator product expansion up to the vacuum condensates of dimension 6. The predicted molecule masses $M_{D^*\bar{D}_0^*} = 4.26 \pm 0.07$ GeV and $M_{D\bar{D}_1} = 4.34 \pm 0.07$ GeV are consistent with the $Y(4220)$ and $Y(4390)$, respectively. However, they do not distinguish the charge conjugation of the molecular states and neglect the higher dimensional vacuum condensates.

	$T^2(\text{GeV}^2)$	$\sqrt{s_0}(\text{GeV})$	pole	$\mu(\text{GeV})$	$M_Y(\text{GeV})$	$\lambda_Y(10^{-2}\text{GeV}^5)$
$DD_1(1^{--})$	3.2 – 3.6	4.9 ± 0.1	(45 – 65)%	2.3	4.36 ± 0.08	3.97 ± 0.54
$DD_1(1^{-+})$	3.5 – 3.9	5.1 ± 0.1	(44 – 63)%	2.7	4.60 ± 0.08	5.26 ± 0.65
$D^*D_0^*(1^{--})$	4.0 – 4.4	5.3 ± 0.1	(44 – 61)%	3.0	4.78 ± 0.07	7.56 ± 0.84
$D^*D_0^*(1^{-+})$	3.8 – 4.2	5.2 ± 0.1	(44 – 61)%	2.9	4.73 ± 0.07	6.83 ± 0.84

Table 45: The Borel parameters, continuum threshold parameters, pole contributions, energy scales, masses and pole residues of the vector molecular states [641].

In Ref.[430], Lee, Morita and Nielsen distinguish the charge conjugation, calculate the operator product expansion up to the vacuum condensates of dimension 6 including dimension 8 partly. They obtain the mass of the $D\bar{D}_1(2420)$ molecular state with the $J^{PC} = 1^{-+}$, $M_{D\bar{D}_1} = 4.19 \pm 0.22 \text{ GeV}$, which differs from the prediction $M_{D\bar{D}_1} = 4.34 \pm 0.07 \text{ GeV}$ significantly [434].

In Refs.[430, 434], **Scheme II** is chosen, some higher dimensional vacuum condensates are neglected, which are associated with $\frac{1}{T^2}$, $\frac{1}{T^4}$, $\frac{1}{T^6}$ in the QCD spectral densities and manifest themselves at small values of the T^2 , thus we have to choose large values of T^2 to warrant convergence of the operator product expansion. The higher dimensional vacuum condensates, see Fig.23, play an important role in determining the Borel windows therefore the ground state masses and pole residues, we should take them into account consistently. All in all, we observe that the QCD sum rules favor much larger masses than the two-meson thresholds if there exists a P-wave in one constituent, and we should bear in mind that the continuum threshold parameters should not be large enough to include contaminations from the higher resonances [648], i.e. if a bound state really exists, the continuum threshold $\sqrt{s_0}$ should be less than $M_{\text{ground}} + 0.7 \text{ GeV}$ in the case of the hidden-charm four-quark systems.

Besides the $Y(4260)$, it is also difficult to reproduce the mass of the $Y(4660)$ with a $c\bar{q} - q\bar{c}$ type current, however, we can reproduce its mass with a $c\bar{c} - q\bar{q}$ type current [482, 485], i.e. it might be a $\psi' f_0(980)$ bound state [482, 485, 649, 650].

With the simple replacement $c \rightarrow b$, we obtain the corresponding QCD sum rules for the hidden-bottom tetraquark molecular states from Eq.(234). We can reproduce the experimental masses of the $Z_b(10610)$ and $Z_b(10650)$ as the $B\bar{B}^* - B^*\bar{B}$ and $B^*\bar{B}^*$ molecular states respectively with the $J^{PC} = 1^{+-}$ via the QCD sum rules [81, 422, 443, 445, 451], although those QCD sum rules suffer from shortcomings in one way or the other. It is more easy to reproduce a weak bound state if there exist weak attractive interactions between the two constituents [76, 211, 271, 274, 282, 651, 652, 653, 654, 655].

In Ref.[557], Qiao assigns the $Y(4260)$ as the $\bar{\Lambda}_c \Lambda_c$ baryonium state with the $J^{PC} = 1^{--}$. In Ref.[558], Qiao includes the Σ_c^0 constituent, and suggests a triplet and a singlet baryonium states,

$$\begin{aligned}
B_1^+ &\equiv |\Lambda_c^+ \bar{\Sigma}_c^0 \rangle, \\
\text{Triplet : } B_1^0 &\equiv \frac{1}{\sqrt{2}}(|\Lambda_c^+ \bar{\Lambda}_c^- \rangle - |\Sigma_c^0 \bar{\Sigma}_c^0 \rangle), \\
B_1^- &\equiv |\Lambda_c^- \Sigma_c^0 \rangle,
\end{aligned} \tag{241}$$

and

$$\text{Singlet : } B_0^0 \equiv \frac{1}{\sqrt{2}}(|\Lambda_c^+ \bar{\Lambda}_c^- \rangle + |\Sigma_c^0 \bar{\Sigma}_c^0 \rangle), \tag{242}$$

then he assigns the $Z_c^\pm(4430)$ as the 2S B_1^\pm state with the $J^{PC} = 1^{+-}$, and the $Y(4360)$ ($Y(4660)$) as the 2S $\bar{\Lambda}_c \Lambda_c$ ($\bar{\Sigma}_c \Sigma_c$) baryonium state with the $J^{PC} = 1^{--}$.

We study the $\bar{\Lambda}_c \Lambda_c$ and $\bar{\Sigma}_c \Sigma_c$ type hidden-charm baryonium states via the QCD sum rules consistently by carrying out the operator product expansion up to the vacuum condensates of

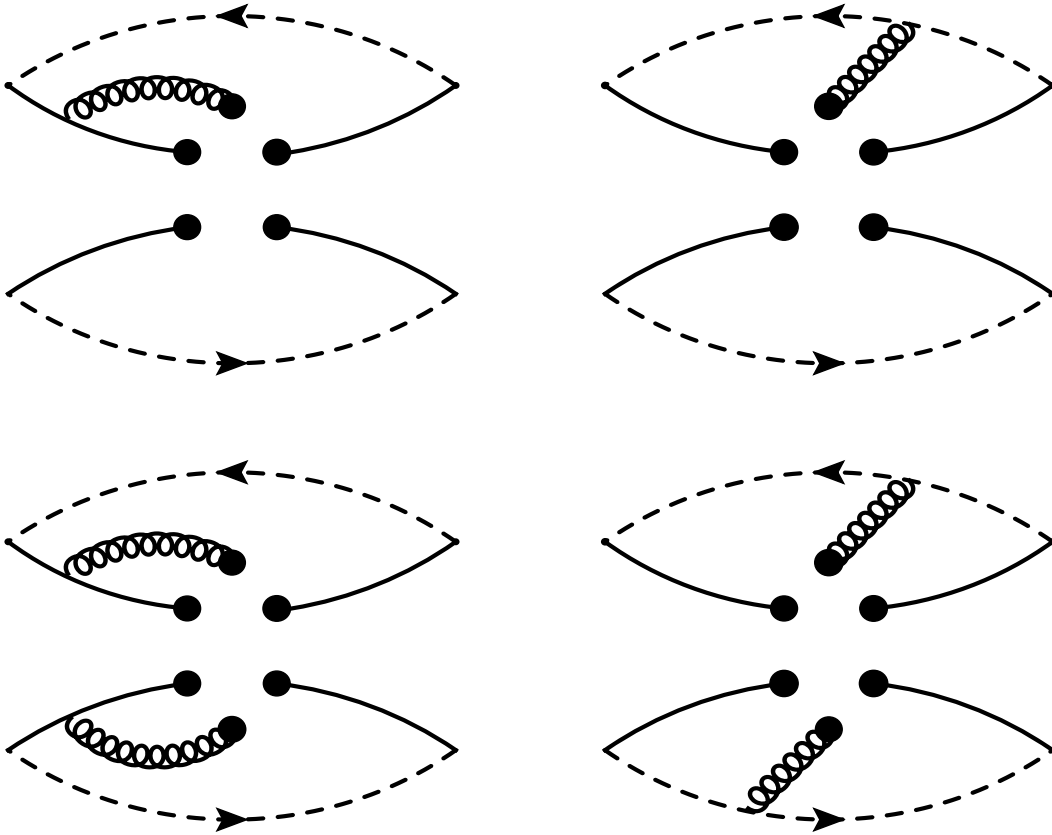


Figure 23: The Feynman diagrams contribute to the $\langle \bar{q}q \rangle \langle \bar{q}g_s \sigma G q \rangle$ and $\langle \bar{q}g_s \sigma G q \rangle^2$. Other diagrams obtained by interchanging of the light and heavy quark lines are implied.

dimension 16 according to the counting rules in Sects. 2.2 and 3.1.1, and observe that the $\bar{\Lambda}_c \Lambda_c$ state with the $J^P = 1^-$ and $\bar{\Sigma}_c \Sigma_c$ states with the $J^P = 0^-, 1^-$ lie at the corresponding baryon-antibaryon thresholds, respectively, while the $\bar{\Lambda}_c \Lambda_c$ states with the $J^P = 0^-, 1^+$ and $\bar{\Sigma}_c \Sigma_c$ states with the $J^P = 0^+, 1^+$ lie above the corresponding baryon-antibaryon thresholds, respectively, whose masses are all much larger than the $Y(4260)$ [656]. In Ref.[657], Wan, Tang and Qiao study the $\bar{\Lambda}_Q \Lambda_Q$ states with the $J^{PC} = 0^{++}, 0^{-+}, 1^{++}$ and 1^{--} via the QCD sum rules by taking account of the vacuum condensates up to dimension 12, and observe that only the baryonium states with the $J^{PC} = 0^{++}$ and 1^{--} could exist, they also obtain masses much larger than the corresponding $\bar{\Lambda}_Q \Lambda_Q$ thresholds, respectively.

In Ref.[658], we construct the color singlet-singlet type six-quark current,

$$\begin{aligned} J(x) &= \bar{J}_{cc}(x) i\gamma_5 J_{cc}(x), \\ J_{cc}(x) &= \varepsilon^{ijk} c_i^T(x) C \gamma_\alpha c_j(x) \gamma^\alpha \gamma^5 q_k(x), \end{aligned} \quad (243)$$

with $q = u$ or d , to study the $\Xi_{cc} \Xi_{cc}$ hexaquark molecular state by calculating the vacuum condensates up to dimension 14, the predicted mass $M_X \sim 7.2 \text{ GeV}$ supports assigning the $X(7200)$ to be the $\Xi_{cc} \Xi_{cc}$ hexaquark molecular state with the $J^{PC} = 0^{-+}$. However, the pole contribution is not larger than 40%, which would weaken the predictive ability.

In Ref.[659], we construct the color singlet-singlet-singlet type six-quark current with the $I(J^P) = \frac{3}{2}(1^-)$ to study the $D\bar{D}^*K$ system via the QCD sum rules by considering the contributions of the vacuum condensates up to dimension-16, and observe that there indeed exists a resonance state which lies above the $D\bar{D}^*K$ threshold, and suggest to search for it in the $J/\psi\pi K$ mass spectrum.

Such subjects need further studies to obtain definite conclusion, at the present time, they are open problems.

4.2 Doubly heavy tetraquark states

Before and after the observation of the doubly-charmed tetraquark candidate $T_{cc}^+(3875)$, especially after the observation, there have been many works on the doubly-charmed tetraquark (molecular) states with different theoretical approaches [371, 372, 373, 375, 471, 472, 513, 660, 661, 662, 663, 664, 665, 666, 667, 668, 669].

If we perform Fierz rearrangements for the four-quark axialvector current $J_\mu(x)$ [576], see Eq.(194), we obtain a special superposition of the color singlet-singlet type currents,

$$\begin{aligned} J_\mu(x) &= \varepsilon^{ijk} \varepsilon^{imn} Q_j^T(x) C \gamma_\mu Q_k(x) \bar{u}_m(x) \gamma_5 C \bar{d}_n^T(x), \\ &= \frac{i}{2} [\bar{u} i \gamma_5 Q \bar{d} \gamma_\mu Q - \bar{d} i \gamma_5 Q \bar{u} \gamma_\mu Q] + \frac{1}{2} [\bar{u} Q \bar{d} \gamma_\mu \gamma_5 Q - \bar{d} Q \bar{u} \gamma_\mu \gamma_5 Q] \\ &\quad - \frac{i}{2} [\bar{u} \sigma_{\mu\nu} \gamma_5 Q \bar{d} \gamma^\nu Q - \bar{d} \sigma_{\mu\nu} \gamma_5 Q \bar{u} \gamma^\nu Q] + \frac{i}{2} [\bar{u} \sigma_{\mu\nu} Q \bar{d} \gamma^\nu \gamma_5 Q - \bar{d} \sigma_{\mu\nu} Q \bar{u} \gamma^\nu \gamma_5 Q], \\ &= \frac{i}{2} J_\mu^1(x) + \frac{1}{2} J_\mu^2(x) - \frac{i}{2} J_\mu^3(x) + \frac{i}{2} J_\mu^4(x). \end{aligned} \quad (244)$$

The currents $J_\mu^1(x)$, $J_\mu^2(x)$, $J_\mu^3(x)$ and $J_\mu^4(x)$ couple potentially to the color singlet-singlet type tetraquark states or two-meson scattering states. In fact, there exist spatial separations between the diquark and antidiquark pair, the currents $J_\mu(x)$ should be modified to $J_\mu(x, \epsilon)$,

$$J_\mu(x, \epsilon) = \varepsilon^{ijk} \varepsilon^{imn} Q_j^T(x) C \gamma_\mu Q_k(x) \bar{u}_m(x + \epsilon) \gamma_5 C \bar{d}_n^T(x + \epsilon), \quad (245)$$

where the four-vector $\epsilon^\alpha = (0, \vec{\epsilon})$. The spatial distance between the diquark and antidiquark pair maybe frustrate the Fierz rearrangements or recombination, although we usually take the local limit $\epsilon \rightarrow 0$, we should not take it for granted that the Fierz rearrangements are feasible [401], we cannot obtain the conclusion that the T_{cc}^+ has the $D^*D - DD^*$ Fock component according to the

component $\bar{q}i\gamma_5 c \otimes \bar{q}\gamma_\mu c$ in Eq.(244). According to the predictions in Table 34, we can only obtain the conclusion tentatively that the T_{cc}^+ has a diquark-antidiquark type tetraquark Fock component with the spin-parity $J^P = 1^+$ and isospin $I = 0$ [576]. It is interesting to explore whether or not there exists a color **11** type Fock component indeed.

Again, we resort to the correlation functions $\Pi(p)$, $\Pi_{\mu\nu}(p)$ and $\Pi_{\mu\nu\alpha\beta}(p)$ defined in Eq.(125), and construct the currents $J(x)$, $J_\mu(x)$ and $J_{\mu\nu}(x)$,

$$J(x) = J_{DD}(x), J_{DD_s}(x), J_{D_s D_s}(x), J_{D^* D^*}(x), J_{D^* D_s^*}(x), J_{D_s^* D_s^*}(x), \quad (246)$$

$$J_\mu(x) = J_{DD^*, L, \mu}(x), J_{DD^*, H, \mu}(x), J_{DD_s^*, L, \mu}(x), J_{DD_s^*, H, \mu}(x), J_{D_s D_s^*, \mu}(x), \\ J_{D_1 D_0^*, L, \mu}(x), J_{D_1 D_0^*, H, \mu}(x), J_{D_{s1} D_0^*, L, \mu}(x), J_{D_{s1} D_0^*, H, \mu}(x), J_{D_{s1} D_{s0}^*, \mu}(x), \quad (247)$$

$$J_{\mu\nu}(x) = J_{D^* D^*, L, \mu\nu}(x), J_{D^* D^*, H, \mu\nu}(x), J_{D^* D_s^*, L, \mu\nu}(x), J_{D^* D_s^*, H, \mu\nu}(x), J_{D_s^* D_s^*, L, \mu\nu}(x), \\ J_{D_s^* D_s^*, H, \mu\nu}(x), \quad (248)$$

$$\begin{aligned} J_{DD}(x) &= \bar{u}(x)i\gamma_5 c(x) \bar{d}(x)i\gamma_5 c(x), \\ J_{DD_s}(x) &= \bar{q}(x)i\gamma_5 c(x) \bar{s}(x)i\gamma_5 c(x), \\ J_{D_s D_s}(x) &= \bar{s}(x)i\gamma_5 c(x) \bar{s}(x)i\gamma_5 c(x), \\ J_{D^* D^*}(x) &= \bar{u}(x)\gamma_\mu c(x) \bar{d}(x)\gamma^\mu c(x), \\ J_{D^* D_s^*}(x) &= \bar{q}(x)\gamma_\mu c(x) \bar{s}(x)\gamma^\mu c(x), \\ J_{D_s^* D_s^*}(x) &= \bar{s}(x)\gamma_\mu c(x) \bar{s}(x)\gamma^\mu c(x), \end{aligned} \quad (249)$$

$$\begin{aligned} J_{DD^*, L/H, \mu}(x) &= \frac{1}{\sqrt{2}} \left[\bar{u}(x)i\gamma_5 c(x) \bar{d}(x)\gamma_\mu c(x) \mp \bar{u}(x)\gamma_\mu c(x) \bar{d}(x)i\gamma_5 c(x) \right], \\ J_{DD_s^*, L/H, \mu}(x) &= \frac{1}{\sqrt{2}} \left[\bar{q}(x)i\gamma_5 c(x) \bar{s}(x)\gamma_\mu c(x) \mp \bar{q}(x)\gamma_\mu c(x) \bar{s}(x)i\gamma_5 c(x) \right], \\ J_{D_s D_s^*, \mu}(x) &= \bar{s}(x)i\gamma_5 c(x) \bar{s}(x)\gamma_\mu c(x), \end{aligned} \quad (250)$$

$$\begin{aligned} J_{D_1 D_0^*, L/H, \mu}(x) &= \frac{1}{\sqrt{2}} \left[\bar{u}(x)c(x) \bar{d}(x)\gamma_\mu \gamma_5 c(x) \pm \bar{u}(x)\gamma_\mu \gamma_5 c(x) \bar{d}(x)c(x) \right], \\ J_{D_{s1} D_0^*, L/H, \mu}(x) &= \frac{1}{\sqrt{2}} \left[\bar{q}(x)c(x) \bar{s}(x)\gamma_\mu \gamma_5 c(x) \pm \bar{q}(x)\gamma_\mu \gamma_5 c(x) \bar{s}(x)c(x) \right], \\ J_{D_{s1} D_{s0}^*, \mu}(x) &= \bar{s}(x)c(x) \bar{s}(x)\gamma_\mu \gamma_5 c(x), \end{aligned} \quad (251)$$

$$\begin{aligned} J_{D^* D^*, L/H, \mu\nu}(x) &= \frac{1}{\sqrt{2}} \left[\bar{u}(x)\gamma_\mu c(x) \bar{d}(x)\gamma_\nu c(x) \mp \bar{u}(x)\gamma_\nu c(x) \bar{d}(x)\gamma_\mu c(x) \right], \\ J_{D^* D_s^*, L/H, \mu\nu}(x) &= \frac{1}{\sqrt{2}} \left[\bar{q}(x)\gamma_\mu c(x) \bar{s}(x)\gamma_\nu c(x) \mp \bar{q}(x)\gamma_\nu c(x) \bar{s}(x)\gamma_\mu c(x) \right], \\ J_{D_s^* D_s^*, L/H, \mu\nu}(x) &= \frac{1}{\sqrt{2}} \left[\bar{s}(x)\gamma_\mu c(x) \bar{s}(x)\gamma_\nu c(x) \mp \bar{s}(x)\gamma_\nu c(x) \bar{s}(x)\gamma_\mu c(x) \right], \end{aligned} \quad (252)$$

and $q = u, d$, the subscripts DD , DD^* , \dots and $D_s^* D_s^*$ stand for the two color-neutral clusters, we add the subscripts L and H to distinguish the lighter and heavier states in the same doublet due to the mixing effects, as direct calculations indicate that there exists such a tendency.

Under parity transformation \hat{P} , the currents have the properties,

$$\begin{aligned} \hat{P}J(x)\hat{P}^{-1} &= +J(\tilde{x}), \\ \hat{P}J_\mu(x)\hat{P}^{-1} &= -J^\mu(\tilde{x}), \\ \hat{P}J_{\mu\nu}(x)\hat{P}^{-1} &= +J^{\mu\nu}(\tilde{x}), \end{aligned} \quad (253)$$

where $x^\mu = (t, \vec{x})$ and $\tilde{x}^\mu = (t, -\vec{x})$. We rewrite Eq.(253) in more explicit form,

$$\begin{aligned}\hat{P}J_i(x)\hat{P}^{-1} &= +J_i(\tilde{x}), \\ \hat{P}J_{ij}(x)\hat{P}^{-1} &= +J_{ij}(\tilde{x}),\end{aligned}\tag{254}$$

$$\begin{aligned}\hat{P}J_0(x)\hat{P}^{-1} &= -J_0(\tilde{x}), \\ \hat{P}J_{0i}(x)\hat{P}^{-1} &= -J_{0i}(\tilde{x}),\end{aligned}\tag{255}$$

where the space indexes $i, j = 1, 2, 3$. There are both positive and negative components, and they couple potentially to the axialvector/tensor and pseudoscalar/vector molecular states, respectively. We will introduce an superscript $-$ to denote the negative parity.

According to the quark-hadron duality, we obtain the hadronic representation and isolate the ground state contributions of the scalar, axialvector and tensor molecular states [83, 513],

$$\begin{aligned}\Pi(p) &= \frac{\lambda_T^2}{M_T^2 - p^2} + \cdots = \Pi_T^0(p^2) + \cdots, \\ \Pi_{\mu\nu}(p) &= \frac{\lambda_T^2}{M_T^2 - p^2} \left(-g_{\mu\nu} + \frac{p_\mu p_\nu}{p^2} \right) + \cdots \\ &= \Pi_T^1(p^2) \left(-g_{\mu\nu} + \frac{p_\mu p_\nu}{p^2} \right) + \cdots, \\ \Pi_{L,\mu\nu\alpha\beta}(p) &= \frac{\tilde{\lambda}_T^2}{M_T^2 - p^2} (p^2 g_{\mu\alpha} g_{\nu\beta} - p^2 g_{\mu\beta} g_{\nu\alpha} - g_{\mu\alpha} p_\nu p_\beta - g_{\nu\beta} p_\mu p_\alpha + g_{\mu\beta} p_\nu p_\alpha + g_{\nu\alpha} p_\mu p_\beta) \\ &\quad + \frac{\tilde{\lambda}_{T-}^2}{M_{T-}^2 - p^2} (-g_{\mu\alpha} p_\nu p_\beta - g_{\nu\beta} p_\mu p_\alpha + g_{\mu\beta} p_\nu p_\alpha + g_{\nu\alpha} p_\mu p_\beta) + \cdots \\ &= \tilde{\Pi}_T^1(p^2) (p^2 g_{\mu\alpha} g_{\nu\beta} - p^2 g_{\mu\beta} g_{\nu\alpha} - g_{\mu\alpha} p_\nu p_\beta - g_{\nu\beta} p_\mu p_\alpha + g_{\mu\beta} p_\nu p_\alpha + g_{\nu\alpha} p_\mu p_\beta) \\ &\quad + \tilde{\Pi}_T^{1,-}(p^2) (-g_{\mu\alpha} p_\nu p_\beta - g_{\nu\beta} p_\mu p_\alpha + g_{\mu\beta} p_\nu p_\alpha + g_{\nu\alpha} p_\mu p_\beta), \\ \Pi_{H,\mu\nu\alpha\beta}(p) &= \frac{\lambda_T^2}{M_T^2 - p^2} \left(\frac{\tilde{g}_{\mu\alpha} \tilde{g}_{\nu\beta} + \tilde{g}_{\mu\beta} \tilde{g}_{\nu\alpha}}{2} - \frac{\tilde{g}_{\mu\nu} \tilde{g}_{\alpha\beta}}{3} \right) + \cdots, \\ &= \Pi_T^2(p^2) \left(\frac{\tilde{g}_{\mu\alpha} \tilde{g}_{\nu\beta} + \tilde{g}_{\mu\beta} \tilde{g}_{\nu\alpha}}{2} - \frac{\tilde{g}_{\mu\nu} \tilde{g}_{\alpha\beta}}{3} \right) + \cdots,\end{aligned}\tag{256}$$

where the pole residues λ_T and λ_{T-} are defined analogous to Eq.(127) with the simple replacements $Z^+ \rightarrow T$ and $Z^- \rightarrow T^-$, and $\lambda_T = \tilde{\lambda}_T M_T$ and $\lambda_{T-} = \tilde{\lambda}_{T-} M_{T-}$, we introduce the superscripts 0, 1 and 2 denote the spins of the molecular states. Thereafter, we choose the components $\Pi_T^{0/2}(p^2)$ and $p^2 \tilde{\Pi}_T^1(p^2)$.

We accomplish the operator product expansion up to the vacuum condensates of dimension 10 and take account of the vacuum condensates $\langle \bar{q}q \rangle$, $\langle \frac{\alpha_s GG}{\pi} \rangle$, $\langle \bar{q}g_s \sigma G q \rangle$, $\langle \bar{q}q \rangle^2$, $\langle \bar{q}q \rangle \langle \frac{\alpha_s GG}{\pi} \rangle$, $\langle \bar{q}q \rangle \langle \bar{q}g_s \sigma G q \rangle$, $\langle \bar{q}g_s \sigma G q \rangle^2$ and $\langle \bar{q}q \rangle^2 \langle \frac{\alpha_s GG}{\pi} \rangle$ with the vacuum saturation in a consistent way [670], where $q = u, d$ or s [60, 61, 82, 83, 171, 172, 418, 425, 513, 514, 515]. Again, we neglect the u and d quark masses, and take account of the terms $\propto m_s$ according to the light-flavor $SU(3)$ breaking effects.

Then we match the hadron side with the QCD side below the continuum thresholds s_0 , perform the Borel transformation, and obtain the QCD sum rules for the masses and pole residues. With

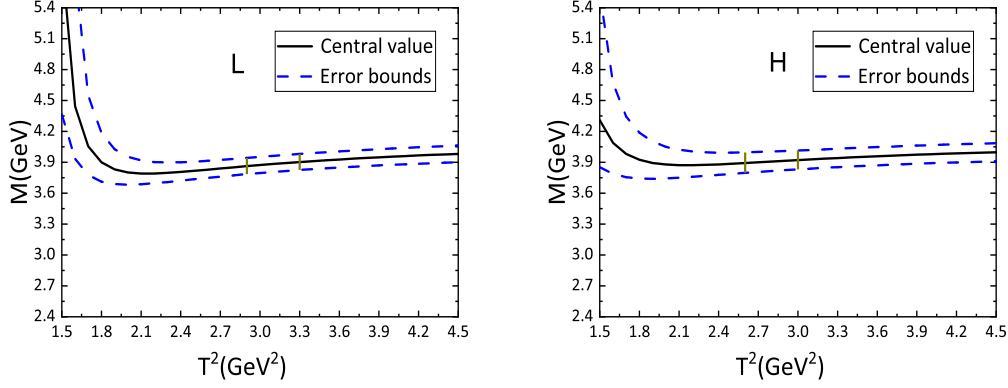


Figure 24: The masses with variations of the Borel parameters for the axialvector tetraquark molecular states, where the L and H denote the lighter and heavier DD^* states, respectively.

a simple replacement $c \rightarrow b$, we obtain the corresponding QCD sum rules for the doubly-bottom tetraquark states, the calculations are straightforward.

We take the modified energy scale formula shown in Eq.(235) and the effective c/s -quark masses $\mathbb{M}_c = 1.82 \text{ GeV}$ and $\mathbb{M}_s = 0.2 \text{ GeV}$ to determine the optimal energy scales of the QCD spectral densities. After trial and error, we obtain the Borel parameters, continuum threshold parameters, energy scales of the QCD spectral densities, pole contributions and contributions of the vacuum condensates of dimension 10, which are shown in Table 46 [83, 513]. The pole contributions are about $(40 - 60)\%$ at the hadron side, the central values are larger than 50% , the pole dominance is satisfied very good. Moreover, the contributions of the vacuum condensates of dimension 10 are $|D(10)| < 1\%$ or $\ll 1\%$ at the QCD side, the operator product expansion converges very good [83, 513].

We take account of all the uncertainties of the relevant parameters, and obtain the masses and pole residues of the doubly-charmed molecular states without strange, with strange and with doubly-strange, which are presented explicitly in Table 47 [83, 513].

In Fig.24, as an example, we plot the masses of the axialvector $(D^*D - DD^*)_L$ and $(D^*D + DD^*)_H$ molecular states with variations of the Borel parameters at much larger ranges than the Borel widows. There appear very flat platforms in the Borel windows, the regions between the two short perpendicular lines.

There exist both a lighter and a heavier state for the $cc\bar{u}\bar{d}$ and $cc\bar{q}\bar{s}$ molecular states, the lighter state $(D^*D - DD^*)_L$ with the isospin $(I, I_3) = (0, 0)$ has a mass $3.88 \pm 0.11 \text{ GeV}$, which is in excellent agreement with the mass of the doubly-charmed tetraquark candidate T_{cc}^+ from the LHCb collaboration [194, 195], and supports assigning the T_{cc}^+ to be the $(D^*D - DD^*)_L$ molecular state, as the T_{cc}^+ has the isospin $I = 0$. In other words, the exotic state T_{cc}^+ maybe have a $(D^*D - DD^*)_L$ Fock component. The heavier state $(D^*D + DD^*)_H$ with the isospin $(I, I_3) = (1, 0)$ has a mass $3.90 \pm 0.11 \text{ GeV}$, the central value lies slightly above the DD^* threshold, the strong decays to the final states $DD\pi$ are kinematically allowed but with small phase-space. If we choose the same input parameters, the DD^* molecular state with the isospin $I = 1$ has slightly larger mass than the corresponding molecule with the isospin $I = 0$, it is indeed that the isoscalar DD^* molecular state is lighter.

For the $(D_0^*D_1 + D_1D_0^*)_L$, $(D_0^*D_1 - D_1D_0^*)_H$, $(D_0^*D_{s1} + D_{s0}^*D_1)_L$ and $(D_0^*D_{s1} - D_{s0}^*D_1)_H$ molecular states, there exists a P-wave in the color-singlet constituents, the P-wave is embodied implicitly in the underlined $\underline{\gamma_5}$ in the scalar currents $\bar{q}i\underline{\gamma_5}\underline{\gamma_5}c$, $\bar{s}i\underline{\gamma_5}\underline{\gamma_5}c$ and axialvector currents $\bar{q}\gamma_\mu\underline{\gamma_5}c$, $\bar{s}\gamma_\mu\underline{\gamma_5}c$, as multiplying γ_5 to the pseudoscalar currents $\bar{q}i\gamma_5c$, $\bar{s}i\gamma_5c$ and vector currents $\bar{q}\gamma_\mu c$,

T_{cc}	Isospin	$T^2(\text{GeV}^2)$	$\sqrt{s_0}(\text{GeV})$	$\mu(\text{GeV})$	pole	$ D(10) $
DD	1	$2.6 - 3.0$	4.30 ± 0.10	1.4	(40 – 64)%	$\ll 1\%$
DD_s	$\frac{1}{2}$	$2.7 - 3.1$	4.40 ± 0.10	1.4	(41 – 64)%	$\ll 1\%$
$D_s D_s$	0	$2.8 - 3.2$	4.50 ± 0.10	1.4	(41 – 63)%	$\ll 1\%$
$D^* D^*$	1	$2.8 - 3.2$	4.55 ± 0.10	1.7	(41 – 61)%	$< 1\%$
$D_s^* D^*$	$\frac{1}{2}$	$2.9 - 3.3$	4.65 ± 0.10	1.7	(42 – 62)%	$\ll 1\%$
$D_s^* D_s^*$	0	$3.2 - 3.5$	4.80 ± 0.10	1.8	(42 – 61)%	$\ll 1\%$
$D^* D - DD^*$	0	$2.9 - 3.3$	4.45 ± 0.10	1.4	(42 – 62)%	$\ll 1\%$
$D^* D + DD^*$	1	$2.6 - 3.0$	4.40 ± 0.10	1.4	(42 – 63)%	$\ll 1\%$
$D_s^* D - D_s D^*$	$\frac{1}{2}$	$3.0 - 3.4$	4.50 ± 0.10	1.5	(40 – 62)%	$< 1\%$
$D_s^* D + D_s D^*$	$\frac{1}{2}$	$2.9 - 3.3$	4.50 ± 0.10	1.5	(40 – 60)%	$\ll 1\%$
$D_s^* D_s$	0	$3.0 - 3.4$	4.60 ± 0.10	1.5	(41 – 63)%	$\ll 1\%$
$D_0^* D_1 - D_1 D_0^*$	0	$5.6 - 7.0$	6.35 ± 0.10	4.6	(41 – 60)%	$\ll 1\%$
$D_0^* D_1 + D_1 D_0^*$	1	$4.7 - 6.1$	5.90 ± 0.10	4.0	(42 – 61)%	$\ll 1\%$
$D_0^* D_{s1} - D_{s0}^* D_1$	$\frac{1}{2}$	$5.8 - 7.2$	6.50 ± 0.10	4.6	(43 – 60)%	$< 1\%$
$D_0^* D_{s1} + D_{s0}^* D_1$	$\frac{1}{2}$	$4.7 - 6.1$	6.05 ± 0.10	4.0	(42 – 62)%	$< 1\%$
$D_{s1} D_{s0}^*$	0	$4.9 - 6.3$	6.20 ± 0.10	4.0	(43 – 61)%	$< 1\%$
$D^* D^* - D^* D^*$	0	$3.2 - 3.6$	4.55 ± 0.10	1.7	(42 – 61)%	$< 1\%$
$D^* D^* + D^* D^*$	1	$3.0 - 3.4$	4.55 ± 0.10	1.7	(41 – 60)%	$< 1\%$
$D_s^* D^* - D_s^* D^*$	$\frac{1}{2}$	$3.3 - 3.7$	4.65 ± 0.10	1.7	(40 – 59)%	$\ll 1\%$
$D_s^* D^* + D_s^* D^*$	$\frac{1}{2}$	$3.1 - 3.5$	4.65 ± 0.10	1.7	(42 – 61)%	$< 1\%$
$D_s^* D_s^* - D_s^* D_s^*$	0	$3.6 - 4.0$	4.80 ± 0.10	1.8	(40 – 60)%	$\ll 1\%$
$D_s^* D_s^* + D_s^* D_s^*$	0	$3.4 - 3.9$	4.80 ± 0.10	1.8	(41 – 61)%	$< 1\%$

Table 46: The Borel parameters, continuum threshold parameters, energy scales of the QCD spectral densities, pole contributions and contributions of the vacuum condensates of dimension 10 for the doubly-charmed molecular states [83, 513].

$\bar{s}\gamma_\mu c$ changes their parity. We should introduce the spin-orbit interactions to account for the large mass gaps between the lighter and heavier states (L, H), i.e. $((D_0^* D_1 + D_1 D_0^*)_L, (D_0^* D_1 - D_1 D_0^*)_H)$, $((D_0^* D_{s1} + D_{s0}^* D_1)_L, (D_0^* D_{s1} - D_{s0}^* D_1)_H)$ [83, 513].

From Table 47, we can see explicitly that the $D_0^* D_1 - D_1 D_0^*$, $D_0^* D_1 + D_1 D_0^*$, $D_0^* D_{s1} - D_{s0}^* D_1$, $D_0^* D_{s1} + D_{s0}^* D_1$ and $D_{s1} D_{s0}^*$ molecular states have much larger masses than the corresponding two-meson thresholds, just like in the case of the hidden-charm molecular states studied in the previous sub-section, where there exist a relative P-wave in one of the color-neutral clusters.

Beyond those color **11** tetraquark states, there maybe also exist some corresponding hexaquark states. The QCD sum rules indicate that there exist the $\Lambda_c \Lambda_c$, $\Sigma_c \Sigma_c$ and $\Xi_{cc} \Sigma_c$ dibaryon states [413, 656, 657], the **333** type triply-charmed hexaquark states [671], and the color **111** type triply-charmed hexaquark molecular states [426]. However, for the light dibaryon/baryonium states, we can only obtain very small pole contributions at the hadron side or bad convergent behaviors of the operator product expansion at the QCD side [205, 672, 673], which weakens the predictive ability. If we adopt the truncation rule in Sects. 2.2 and 3.1.1, i.e. each heavy quark line emits a gluon and each light quark contributes a quark-antiquark pair, which leads to a quark-gluon operator to reach the highest dimensional vacuum condensates, the two basic criteria of the QCD sum rules are difficult to satisfy. Such subjects need further studies.

On the other hand, Lattice calculations indicate that there maybe exist the $N\Omega$, $\Omega\Omega$, $\Omega(ccc)\Omega(ccc)$, $\Omega(bbb)\Omega(bbb)$, \dots dibaryon states [674, 675, 676, 677, 678, 679]. While the heavy-antiquark-diquark symmetry implies that there exists a model-independent relation between the spin-splitting in the masses of the hidden-charm pentaquark states and corresponding splitting for the triply-charmed dibaryon states [680].

T_{cc}	Isospin	$M_T(\text{GeV})$	$\lambda_T(\text{GeV}^5)$
DD	1	3.75 ± 0.09	$(1.48 \pm 0.23) \times 10^{-2}$
DD_s	$\frac{1}{2}$	3.85 ± 0.09	$(1.69 \pm 0.26) \times 10^{-2}$
$D_s D_s$	0	3.95 ± 0.09	$(2.00 \pm 0.32) \times 10^{-2}$
$D^* D^*$	1	4.04 ± 0.11	$(4.99 \pm 0.66) \times 10^{-2}$
$D_s^* D^*$	$\frac{1}{2}$	4.12 ± 0.10	$(5.74 \pm 0.78) \times 10^{-2}$
$D_s^* D_s^*$	0	4.22 ± 0.10	$(7.46 \pm 0.89) \times 10^{-2}$
$D^* D - DD^*$	0	3.88 ± 0.11	$(1.92 \pm 0.29) \times 10^{-2}$
$D^* D + DD^*$	1	3.90 ± 0.11	$(1.50 \pm 0.22) \times 10^{-2}$
$D_s^* D - D_s D^*$	$\frac{1}{2}$	3.97 ± 0.10	$(2.40 \pm 0.41) \times 10^{-2}$
$D_s^* D + D_s D^*$	$\frac{1}{2}$	3.98 ± 0.11	$(2.06 \pm 0.30) \times 10^{-2}$
$D_s^* D_s$	0	4.10 ± 0.12	$(2.31 \pm 0.45) \times 10^{-2}$
$D_0^* D_1 - D_1 D_0^*$	0	5.79 ± 0.15	$(2.13 \pm 0.19) \times 10^{-1}$
$D_0^* D_1 + D_1 D_0^*$	1	5.37 ± 0.13	$(1.30 \pm 0.11) \times 10^{-1}$
$D_0^* D_{s1} - D_{s0}^* D_1$	$\frac{1}{2}$	5.93 ± 0.27	$(2.80 \pm 0.33) \times 10^{-1}$
$D_0^* D_{s1} + D_{s0}^* D_1$	$\frac{1}{2}$	5.54 ± 0.20	$(1.51 \pm 0.16) \times 10^{-1}$
$D_{s1} D_{s0}^*$	0	5.67 ± 0.27	$(1.77 \pm 0.27) \times 10^{-1}$
$D^* D^* - D^* D^*$	0	4.00 ± 0.11	$(2.47 \pm 0.32) \times 10^{-2}$
$D^* D^* + D^* D^*$	1	4.02 ± 0.11	$(2.83 \pm 0.30) \times 10^{-2}$
$D_s^* D^* - D_s^* D^*$	$\frac{1}{2}$	4.08 ± 0.10	$(2.81 \pm 0.40) \times 10^{-2}$
$D_s^* D^* + D_s^* D^*$	$\frac{1}{2}$	4.10 ± 0.11	$(3.19 \pm 0.44) \times 10^{-2}$
$D_s^* D_s^* - D_s^* D_s^*$	0	4.19 ± 0.09	$(3.49 \pm 0.49) \times 10^{-2}$
$D_s^* D_s^* + D_s^* D_s^*$	0	4.20 ± 0.10	$(4.00 \pm 0.53) \times 10^{-2}$

Table 47: The masses and pole residues of the ground state doubly-charmed molecular states [83, 513].

5 Hidden heavy pentaquark states

If a baryon current $J(x)$ has the spin-parity $J^P = \frac{1}{2}^+$, then the current $i\gamma_5 J(x)$ would have the spin-parity $J^P = \frac{1}{2}^-$, as multiplying $i\gamma_5$ changes the parity of the current $J(x)$ [681]. In 1993, Bagan et al took the infinite heavy quark limit to separate the contributions of the positive and negative parity heavy baryon states unambiguously [682]. In 1996, Jido et al introduced a novel approach to separate the contributions of the negative-parity light-flavor baryons from the positive-parity ones [683].

At first, we write down the correlation functions $\Pi_{\pm}(p)$,

$$\Pi_{\pm}(p) = i \int d^4x e^{ip \cdot x} \langle 0 | T \{ J_{\pm}(x) \bar{J}_{\pm}(0) \} | 0 \rangle, \quad (257)$$

where we add the subscripts \pm to denote the positive and negative parity, respectively, $J_- = i\gamma_5 J_+$. We decompose the correlation functions $\Pi_{\pm}(p)$,

$$\Pi_{\pm}(p) = \not{p} \Pi_1(p^2) \pm \Pi_0(p^2), \quad (258)$$

according to Lorentz covariance, because

$$\Pi_-(p) = -\gamma_5 \Pi_+(p) \gamma_5. \quad (259)$$

The currents J_+ couple potentially to both the positive- and negative-parity baryons [681],

$$\langle 0 | J_+ | B^{\pm} \rangle \langle B^{\pm} | \bar{J}_+ | 0 \rangle = -\gamma_5 \langle 0 | J_- | B^{\pm} \rangle \langle B^{\pm} | \bar{J}_- | 0 \rangle \gamma_5, \quad (260)$$

where the B^{\pm} denote the positive and negative parity baryons, respectively.

According to the relation in Eq.(260), we obtain the hadronic representation [683],

$$\Pi_+(p) = \lambda_+^2 \frac{\not{p} + M_+}{M_+^2 - p^2} + \lambda_-^2 \frac{\not{p} - M_-}{M_-^2 - p^2} + \dots, \quad (261)$$

where the M_{\pm} are the baryon masses, the pole residues are defined by $\langle 0 | J_{\pm}(0) | B^{\pm}(p) \rangle = \lambda_{\pm} U_{\pm}$, the U_{\pm} are the Dirac spinors.

If we take $\vec{p} = 0$, then

$$\begin{aligned} \lim_{\epsilon \rightarrow 0} \frac{\text{Im} \Pi_+(p_0 + i\epsilon)}{\pi} &= \lambda_+^2 \frac{\gamma_0 + 1}{2} \delta(p_0 - M_+) + \lambda_-^2 \frac{\gamma_0 - 1}{2} \delta(p_0 - M_-) + \dots \\ &= \gamma_0 A(p_0) + B(p_0) + \dots, \end{aligned} \quad (262)$$

where

$$\begin{aligned} A(p_0) &= \frac{1}{2} [\lambda_+^2 \delta(p_0 - M_+) + \lambda_-^2 \delta(p_0 - M_-)], \\ B(p_0) &= \frac{1}{2} [\lambda_+^2 \delta(p_0 - M_+) - \lambda_-^2 \delta(p_0 - M_-)], \end{aligned} \quad (263)$$

the contribution $A(p_0) + B(p_0)$ ($A(p_0) - B(p_0)$) contains contributions from the positive parity (negative parity) states only.

We carry out the operator product expansion at large $P^2 = -p_0^2$ region, then use the dispersion relation to obtain the spectral densities $\rho^A(p_0)$ and $\rho^B(p_0)$ at the quark-gluon level. At last, we introduce the weight functions $\exp\left[-\frac{p_0^2}{T^2}\right]$, $p_0^2 \exp\left[-\frac{p_0^2}{T^2}\right]$, and obtain the QCD sum rules,

$$\int_{\Delta}^{\sqrt{s_0}} dp_0 [A(p_0) + B(p_0)] \exp\left[-\frac{p_0^2}{T^2}\right] = \int_{\Delta}^{\sqrt{s_0}} dp_0 [\rho^A(p_0) + \rho^B(p_0)] \exp\left[-\frac{p_0^2}{T^2}\right], \quad (264)$$

$$\int_{\Delta}^{\sqrt{s_0}} dp_0 [A(p_0) + B(p_0)] p_0^2 \exp \left[-\frac{p_0^2}{T^2} \right] = \int_{\Delta}^{\sqrt{s_0}} dp_0 [\rho^A(p_0) + \rho^B(p_0)] p_0^2 \exp \left[-\frac{p_0^2}{T^2} \right], \quad (265)$$

where the Δ and $\sqrt{s_0}$ are the threshold and continuum threshold respectively, the T^2 is the Borel parameter [683]. Thereafter, such semi-analytical method was applied to study the heavy, doubly-heavy and triply-heavy baryons with the $J^P = \frac{1}{2}^{\pm}$ and $\frac{3}{2}^{\pm}$ [684, 685, 686, 687, 688, 689].

As the procedure introduced in Ref.[683] is semi-analytical, in 2016, we suggested an analytical procedure to study the pentaquark states [423]. For a correlation function $\Pi(p^2) = \Pi_{-}(p)$, at the hadron side, we obtain the spectral densities through the dispersion relation,

$$\begin{aligned} \frac{\text{Im}\Pi(s)}{\pi} &= \not{p} [\lambda_-^2 \delta(s - M_-^2) + \lambda_+^2 \delta(s - M_+^2)] + [M_- \lambda_-^2 \delta(s - M_-^2) - M_+ \lambda_+^2 \delta(s - M_+^2)], \\ &= \not{p} \rho_H^1(s) + \rho_H^0(s), \end{aligned} \quad (266)$$

where the subscript H denotes the hadron side, then we introduce the weight function $\exp(-\frac{s}{T^2})$ to obtain the QCD sum rules at the hadron side,

$$\int_{\Delta^2}^{s_0} ds [\sqrt{s} \rho_H^1(s) \pm \rho_H^0(s)] \exp\left(-\frac{s}{T^2}\right) = 2M_{\mp} \lambda_{\mp}^2 \exp\left(-\frac{M_{\mp}^2}{T^2}\right), \quad (267)$$

where the s_0 are the continuum threshold parameters. We separate the contributions of the negative parity pentaquark states from that of the positive parity ones unambiguously [423]. The calculations at the QCD side are analytical as we do not set $\vec{p} = 0$.

For the early works on the pentaquark states, one can consult the QCD sum rules on the $\Theta(1540)$, where the currents $J_Z(x)$ [690], $J_O(x)$ [691] and $J_N(x)$ [692],

$$\begin{aligned} J_Z(x) &= \frac{1}{\sqrt{2}} \varepsilon^{ijk} u_i^T(x) C \gamma_5 d_j(x) \{u_m(x) \bar{s}_m(x) i \gamma_5 d_k(x) - (u \leftrightarrow d)\}, \\ J_O(x) &= \varepsilon^{ijk} \varepsilon^{lmn} \varepsilon^{knb} u_i^T(x) C d_j(x) u_l^T(x) C \gamma_5 d_m(x) C \bar{s}_b^T(x), \\ J_N(x) &= \frac{\cos \theta}{\sqrt{2}} \varepsilon^{ijk} u_i^T(x) C \gamma_5 d_j(x) u_k^T(x) C \gamma_5 d_m(x) C \bar{s}_m^T(x) - (u \leftrightarrow d) \\ &\quad + \frac{\sin \theta}{\sqrt{2}} \varepsilon^{ijk} u_i^T(x) C d_j(x) u_k^T(x) C d_m(x) C \bar{s}_m^T(x) - (u \leftrightarrow d), \end{aligned} \quad (268)$$

were constructed to interpolate it. The current $J_O(x)$ was studied in the semi-analytical method [691].

5.1 $\bar{3}\bar{3}\bar{3}$ type pentaquark states

Now, let us turn to the pentaquark states completely and write down the correlation functions $\Pi(p)$, $\Pi_{\mu\nu}(p)$ and $\Pi_{\mu\nu\alpha\beta}(p)$,

$$\begin{aligned} \Pi(p) &= i \int d^4x e^{ip \cdot x} \langle 0 | T \{ J(x) \bar{J}(0) \} | 0 \rangle, \\ \Pi_{\mu\nu}(p) &= i \int d^4x e^{ip \cdot x} \langle 0 | T \{ J_{\mu}(x) \bar{J}_{\nu}(0) \} | 0 \rangle, \\ \Pi_{\mu\nu\alpha\beta}(p) &= i \int d^4x e^{ip \cdot x} \langle 0 | T \{ J_{\mu\nu}(x) \bar{J}_{\alpha\beta}(0) \} | 0 \rangle, \end{aligned} \quad (269)$$

where

$$\begin{aligned} J(x) &= J^1(x), J^2(x), J^3(x), J^4(x), \\ J_{\mu}(x) &= J_{\mu}^1(x), J_{\mu}^2(x), J_{\mu}^3(x), J_{\mu}^4(x), \\ J_{\mu\nu}(x) &= J_{\mu\nu}^1(x), J_{\mu\nu}^2(x), \end{aligned} \quad (270)$$

$$\begin{aligned}
J^1(x) &= \varepsilon^{ila} \varepsilon^{ijk} \varepsilon^{lmn} u_j^T(x) C \gamma_5 d_k(x) u_m^T(x) C \gamma_5 c_n(x) C \bar{c}_a^T(x), \\
J^2(x) &= \varepsilon^{ila} \varepsilon^{ijk} \varepsilon^{lmn} u_j^T(x) C \gamma_5 d_k(x) u_m^T(x) C \gamma_\mu c_n(x) \gamma_5 \gamma^\mu C \bar{c}_a^T(x), \\
J^3(x) &= \frac{\varepsilon^{ila} \varepsilon^{ijk} \varepsilon^{lmn}}{\sqrt{3}} [u_j^T(x) C \gamma_\mu u_k(x) d_m^T(x) C \gamma_5 c_n(x) + 2u_j^T(x) C \gamma_\mu d_k(x) u_m^T(x) C \gamma_5 c_n(x)] \gamma_5 \gamma^\mu C \bar{c}_a^T(x), \\
J^4(x) &= \frac{\varepsilon^{ila} \varepsilon^{ijk} \varepsilon^{lmn}}{\sqrt{3}} [u_j^T(x) C \gamma_\mu u_k(x) d_m^T(x) C \gamma^\mu c_n(x) + 2u_j^T(x) C \gamma_\mu d_k(x) u_m^T(x) C \gamma^\mu c_n(x)] C \bar{c}_a^T(x), \\
J_\mu^1(x) &= \varepsilon^{ila} \varepsilon^{ijk} \varepsilon^{lmn} u_j^T(x) C \gamma_5 d_k(x) u_m^T(x) C \gamma_\mu c_n(x) C \bar{c}_a^T(x), \\
J_\mu^2(x) &= \frac{\varepsilon^{ila} \varepsilon^{ijk} \varepsilon^{lmn}}{\sqrt{3}} [u_j^T(x) C \gamma_\mu u_k(x) d_m^T(x) C \gamma_5 c_n(x) + 2u_j^T(x) C \gamma_\mu d_k(x) u_m^T(x) C \gamma_5 c_n(x)] C \bar{c}_a^T(x), \\
J_\mu^3(x) &= \frac{\varepsilon^{ila} \varepsilon^{ijk} \varepsilon^{lmn}}{\sqrt{3}} [u_j^T(x) C \gamma_\mu u_k(x) d_m^T(x) C \gamma_\alpha c_n(x) + 2u_j^T(x) C \gamma_\mu d_k(x) u_m^T(x) C \gamma_\alpha c_n(x)] \gamma_5 \gamma^\alpha C \bar{c}_a^T(x), \\
J_\mu^4(x) &= \frac{\varepsilon^{ila} \varepsilon^{ijk} \varepsilon^{lmn}}{\sqrt{3}} [u_j^T(x) C \gamma_\alpha u_k(x) d_m^T(x) C \gamma_\mu c_n(x) + 2u_j^T(x) C \gamma_\alpha d_k(x) u_m^T(x) C \gamma_\mu c_n(x)] \gamma_5 \gamma^\alpha C \bar{c}_a^T(x), \\
J_{\mu\nu}^1(x) &= \frac{\varepsilon^{ila} \varepsilon^{ijk} \varepsilon^{lmn}}{\sqrt{6}} [u_j^T(x) C \gamma_\mu u_k(x) d_m^T(x) C \gamma_\nu c_n(x) + 2u_j^T(x) C \gamma_\mu d_k(x) u_m^T(x) C \gamma_\nu c_n(x)] \\
&\quad C \bar{c}_a^T(x) + (\mu \leftrightarrow \nu), \\
J_{\mu\nu}^2(x) &= \frac{1}{\sqrt{2}} \varepsilon^{ila} \varepsilon^{ijk} \varepsilon^{lmn} u_j^T(x) C \gamma_5 d_k(x) [u_m^T(x) C \gamma_\mu c_n(x) \gamma_5 \gamma_\nu C \bar{c}_a^T(x) \\
&\quad + u_m^T(x) C \gamma_\nu c_n(x) \gamma_5 \gamma_\mu C \bar{c}_a^T(x)], \tag{271}
\end{aligned}$$

we choose the $C\gamma_5$ and $C\gamma_\mu$ diquarks in the color $\bar{\mathbf{3}}$, the most stable diquark configurations, as the basic constituents to construct the diquark-diquark-antiquark type currents $J(x)$, $J_\mu(x)$ and $J_{\mu\nu}(x)$ with the spin-parity $J^P = \frac{1}{2}^-$, $\frac{3}{2}^-$ and $\frac{5}{2}^-$, respectively, which are expected to couple potentially to the lowest pentaquark states [402, 423, 514].

In the currents $J(x)$, $J_\mu(x)$ and $J_{\mu\nu}(x)$, there are diquark constituents $\varepsilon^{ijk} u_j^T C \gamma_5 d_k$, $\varepsilon^{ijk} u_j^T C \gamma_\mu d_k$, $\varepsilon^{ijk} u_j^T C \gamma_\mu u_k$, $\varepsilon^{ijk} q_j^T C \gamma_5 c_k$, $\varepsilon^{ijk} q_j^T C \gamma_\mu c_k$ with $q = u, d$. If we use the S_L and S_H to represent the spins of the light and heavy diquarks, respectively, the light diquarks $\varepsilon^{ijk} u_j^T C \gamma_5 d_k$, $\varepsilon^{ijk} u_j^T C \gamma_\mu d_k$ and $\varepsilon^{ijk} u_j^T C \gamma_\mu u_k$ have the spins $S_L = 0, 1$ and 1 , respectively, the heavy diquarks $\varepsilon^{ijk} q_j^T C \gamma_5 c_k$ and $\varepsilon^{ijk} q_j^T C \gamma_\mu c_k$ have the spins $S_H = 0$ and 1 , respectively. A light diquark and a heavy diquark form a charmed tetraquark in the color $\mathbf{3}$ with the angular momentum $\vec{J}_{LH} = \vec{S}_L + \vec{S}_H$, which has the values $J_{LH} = 0, 1$ or 2 . The \bar{c} -quark operator $C \bar{c}_a^T$ has the spin-parity $J^P = \frac{1}{2}^-$, the \bar{c} -quark operator $\gamma_5 \gamma_\mu C \bar{c}_a^T$ has the spin-parity $J^P = \frac{3}{2}^-$ due to the factor $\gamma_5 \gamma_\mu$. The total angular momenta are $\vec{J} = \vec{J}_{LH} + \vec{J}_{\bar{c}}$ with the values $J = \frac{1}{2}, \frac{3}{2}$ or $\frac{5}{2}$, which are shown explicitly in Table 48. In Table 48, we present the quark structures of the currents explicitly [402]. For example, in the current $J_{\mu\nu}^2(x)$, there are a scalar diquark $\varepsilon^{ijk} u_j^T(x) C \gamma_5 d_k(x)$ with the spin-parity $J^P = 0^+$, an axialvector diquark $\varepsilon^{lmn} u_m^T(x) C \gamma_\mu c_n(x)$ with the spin-parity $J^P = 1^+$, and an antiquark $\gamma_5 \gamma_\nu C \bar{c}_a^T(x)$ with the spin-parity $J^P = \frac{3}{2}^-$, the total angular momentum is $J = \frac{5}{2}$. For more intuitive and simple diquark models for the pentaquark states, one can consult Refs.[693, 694, 695, 696, 697, 698].

Although the currents $J(x)$, $J_\mu(x)$ and $J_{\mu\nu}(x)$ have negative parity, but they couple potentially to the pentaquark states with positive parity, as multiplying $i\gamma_5$ to the currents $J(x)$, $J_\mu(x)$ and $J_{\mu\nu}(x)$ changes their parity [681, 682, 683, 684, 685, 686, 687, 688, 689, 699, 700, 701].

Now we write down the current-pentaquark couplings explicitly,

$$\begin{aligned}
\langle 0 | J(0) | P_{\frac{1}{2}}^-(p) \rangle &= \lambda_{\frac{1}{2}}^- U^-(p, s), \\
\langle 0 | J(0) | P_{\frac{1}{2}}^+(p) \rangle &= \lambda_{\frac{1}{2}}^+ i \gamma_5 U^+(p, s), \tag{272}
\end{aligned}$$

$[qq'] [q''\bar{c}]\bar{c} (S_L, S_H, J_{LH}, J)$	J^P	Currents
$[ud][uc]\bar{c} (0, 0, 0, \frac{1}{2})$	$\frac{1}{2}^-$	$J^1(x)$
$[ud][uc]\bar{c} (0, 1, 1, \frac{1}{2})$	$\frac{1}{2}^-$	$J^2(x)$
$[uu][dc]\bar{c} + 2[ud][uc]\bar{c} (1, 0, 1, \frac{1}{2})$	$\frac{1}{2}^-$	$J^3(x)$
$[uu][dc]\bar{c} + 2[ud][uc]\bar{c} (1, 1, 0, \frac{1}{2})$	$\frac{1}{2}^-$	$J^4(x)$
$[ud][uc]\bar{c} (0, 1, 1, \frac{3}{2})$	$\frac{3}{2}^-$	$J_\mu^1(x)$
$[uu][dc]\bar{c} + 2[ud][uc]\bar{c} (1, 0, 1, \frac{3}{2})$	$\frac{3}{2}^-$	$J_\mu^2(x)$
$[uu][dc]\bar{c} + 2[ud][uc]\bar{c} (1, 1, 2, \frac{3}{2})$	$\frac{3}{2}^-$	$J_\mu^3(x)$
$[uu][dc]\bar{c} + 2[ud][uc]\bar{c} (1, 1, 2, \frac{3}{2})$	$\frac{3}{2}^-$	$J_\mu^4(x)$
$[uu][dc]\bar{c} + 2[ud][uc]\bar{c} (1, 1, 2, \frac{5}{2})$	$\frac{5}{2}^-$	$J_{\mu\nu}^1(x)$
$[ud][uc]\bar{c} (0, 1, 1, \frac{5}{2})$	$\frac{5}{2}^-$	$J_{\mu\nu}^2(x)$

Table 48: The quark structures of the currents, where the S_L and S_H denote the spins of the light and heavy diquarks respectively, $\vec{J}_{LH} = \vec{S}_L + \vec{S}_H$, $\vec{J} = \vec{J}_{LH} + \vec{J}_{\bar{c}}$, the $\vec{J}_{\bar{c}}$ is the angular momentum of the \bar{c} -quark [402].

$$\begin{aligned}
\langle 0 | J_\mu(0) | P_{\frac{3}{2}}^-(p) \rangle &= \lambda_{\frac{3}{2}}^- U_\mu^-(p, s), \\
\langle 0 | J_\mu(0) | P_{\frac{3}{2}}^+(p) \rangle &= \lambda_{\frac{3}{2}}^+ i\gamma_5 U_\mu^+(p, s), \\
\langle 0 | J_\mu(0) | P_{\frac{1}{2}}^+(p) \rangle &= f_{\frac{1}{2}}^+ p_\mu U^+(p, s), \\
\langle 0 | J_\mu(0) | P_{\frac{1}{2}}^-(p) \rangle &= f_{\frac{1}{2}}^- p_\mu i\gamma_5 U^-(p, s),
\end{aligned} \tag{273}$$

$$\begin{aligned}
\langle 0 | J_{\mu\nu}(0) | P_{\frac{5}{2}}^-(p) \rangle &= \sqrt{2} \lambda_{\frac{5}{2}}^- U_{\mu\nu}^-(p, s), \\
\langle 0 | J_{\mu\nu}(0) | P_{\frac{5}{2}}^+(p) \rangle &= \sqrt{2} \lambda_{\frac{5}{2}}^+ i\gamma_5 U_{\mu\nu}^+(p, s), \\
\langle 0 | J_{\mu\nu}(0) | P_{\frac{3}{2}}^+(p) \rangle &= f_{\frac{3}{2}}^+ [p_\mu U_\nu^+(p, s) + p_\nu U_\mu^+(p, s)], \\
\langle 0 | J_{\mu\nu}(0) | P_{\frac{3}{2}}^-(p) \rangle &= f_{\frac{3}{2}}^- i\gamma_5 [p_\mu U_\nu^-(p, s) + p_\nu U_\mu^-(p, s)], \\
\langle 0 | J_{\mu\nu}(0) | P_{\frac{1}{2}}^-(p) \rangle &= g_{\frac{1}{2}}^- p_\mu p_\nu U^-(p, s), \\
\langle 0 | J_{\mu\nu}(0) | P_{\frac{1}{2}}^+(p) \rangle &= g_{\frac{1}{2}}^+ p_\mu p_\nu i\gamma_5 U^+(p, s),
\end{aligned} \tag{274}$$

where the superscripts \pm denote the positive parity and negative parity, respectively, the subscripts $\frac{1}{2}$, $\frac{3}{2}$ and $\frac{5}{2}$ denote the spins of the pentaquark states, the λ , f and g are the pole residues.

The spinors $U^\pm(p, s)$ satisfy the Dirac equations $(\not{p} - M_\pm)U^\pm(p) = 0$, while the spinors $U_\mu^\pm(p, s)$ and $U_{\mu\nu}^\pm(p, s)$ satisfy the Rarita-Schwinger equations $(\not{p} - M_\pm)U_\mu^\pm(p) = 0$ and $(\not{p} - M_\pm)U_{\mu\nu}^\pm(p) = 0$, and relations $\gamma^\mu U_\mu^\pm(p, s) = 0$, $p^\mu U_\mu^\pm(p, s) = 0$, $\gamma^\mu U_{\mu\nu}^\pm(p, s) = 0$, $p^\mu U_{\mu\nu}^\pm(p, s) = 0$, $U_{\nu\mu}^\pm(p, s) = U_{\mu\nu}^\pm(p, s)$, respectively [423, 565].

At the hadron side, we insert a complete set of intermediate pentaquark states with the same quantum numbers as the currents $J(x)$, $i\gamma_5 J(x)$, $J_\mu(x)$, $i\gamma_5 J_\mu(x)$, $J_{\mu\nu}(x)$ and $i\gamma_5 J_{\mu\nu}(x)$ into the correlation functions $\Pi(p)$, $\Pi_{\mu\nu}(p)$ and $\Pi_{\mu\nu\alpha\beta}(p)$ to obtain the hadronic representation, and isolate the lowest states of the hidden-charm pentaquark states with negative and positive parity [402, 423, 514]:

$$\begin{aligned}
\Pi(p) &= \lambda_{\frac{1}{2}}^{-2} \frac{\not{p} + M_-}{M_-^2 - p^2} + \lambda_{\frac{1}{2}}^{+2} \frac{\not{p} - M_+}{M_+^2 - p^2} + \cdots, \\
&= \Pi_{\frac{1}{2}}^1(p^2) \not{p} + \Pi_{\frac{1}{2}}^0(p^2),
\end{aligned} \tag{275}$$

$$\begin{aligned}
\Pi_{\mu\nu}(p) &= \lambda_{\frac{3}{2}}^{-2} \frac{\not{p} + M_-}{M_-^2 - p^2} \left(-g_{\mu\nu} + \frac{\gamma_\mu \gamma_\nu}{3} + \frac{2p_\mu p_\nu}{3p^2} - \frac{p_\mu \gamma_\nu - p_\nu \gamma_\mu}{3\sqrt{p^2}} \right) \\
&\quad + \lambda_{\frac{3}{2}}^{+2} \frac{\not{p} - M_+}{M_+^2 - p^2} \left(-g_{\mu\nu} + \frac{\gamma_\mu \gamma_\nu}{3} + \frac{2p_\mu p_\nu}{3p^2} - \frac{p_\mu \gamma_\nu - p_\nu \gamma_\mu}{3\sqrt{p^2}} \right) \\
&\quad + f_{\frac{1}{2}}^{+2} \frac{\not{p} + M_+}{M_+^2 - p^2} p_\mu p_\nu + f_{\frac{1}{2}}^{-2} \frac{\not{p} - M_-}{M_-^2 - p^2} p_\mu p_\nu + \dots, \\
&= \left[\Pi_{\frac{3}{2}}^1(p^2) \not{p} + \Pi_{\frac{3}{2}}^0(p^2) \right] (-g_{\mu\nu}) + \dots,
\end{aligned} \tag{276}$$

$$\begin{aligned}
\Pi_{\mu\nu\alpha\beta}(p) &= 2\lambda_{\frac{5}{2}}^{-2} \frac{\not{p} + M_-}{M_-^2 - p^2} \left[\frac{\tilde{g}_{\mu\alpha}\tilde{g}_{\nu\beta} + \tilde{g}_{\mu\beta}\tilde{g}_{\nu\alpha}}{2} - \frac{\tilde{g}_{\mu\nu}\tilde{g}_{\alpha\beta}}{5} - \frac{1}{10} \left(\gamma_\mu \gamma_\alpha + \frac{\gamma_\mu p_\alpha - \gamma_\alpha p_\mu}{\sqrt{p^2}} - \frac{p_\mu p_\alpha}{p^2} \right) \tilde{g}_{\nu\beta} \right. \\
&\quad \left. - \frac{1}{10} \left(\gamma_\nu \gamma_\alpha + \frac{\gamma_\nu p_\alpha - \gamma_\alpha p_\nu}{\sqrt{p^2}} - \frac{p_\nu p_\alpha}{p^2} \right) \tilde{g}_{\mu\beta} + \dots \right] \\
&\quad + 2\lambda_{\frac{5}{2}}^{+2} \frac{\not{p} - M_+}{M_+^2 - p^2} \left[\frac{\tilde{g}_{\mu\alpha}\tilde{g}_{\nu\beta} + \tilde{g}_{\mu\beta}\tilde{g}_{\nu\alpha}}{2} - \frac{\tilde{g}_{\mu\nu}\tilde{g}_{\alpha\beta}}{5} - \frac{1}{10} \left(\gamma_\mu \gamma_\alpha + \frac{\gamma_\mu p_\alpha - \gamma_\alpha p_\mu}{\sqrt{p^2}} - \frac{p_\mu p_\alpha}{p^2} \right) \tilde{g}_{\nu\beta} \right. \\
&\quad \left. - \frac{1}{10} \left(\gamma_\nu \gamma_\alpha + \frac{\gamma_\nu p_\alpha - \gamma_\alpha p_\nu}{\sqrt{p^2}} - \frac{p_\nu p_\alpha}{p^2} \right) \tilde{g}_{\mu\beta} + \dots \right] \\
&\quad + f_{\frac{3}{2}}^{+2} \frac{\not{p} + M_+}{M_+^2 - p^2} \left[p_\mu p_\alpha \left(-g_{\nu\beta} + \frac{\gamma_\nu \gamma_\beta}{3} + \frac{2p_\nu p_\beta}{3p^2} - \frac{p_\nu \gamma_\beta - p_\beta \gamma_\nu}{3\sqrt{p^2}} \right) + \dots \right] \\
&\quad + f_{\frac{3}{2}}^{-2} \frac{\not{p} - M_-}{M_-^2 - p^2} \left[p_\mu p_\alpha \left(-g_{\nu\beta} + \frac{\gamma_\nu \gamma_\beta}{3} + \frac{2p_\nu p_\beta}{3p^2} - \frac{p_\nu \gamma_\beta - p_\beta \gamma_\nu}{3\sqrt{p^2}} \right) + \dots \right] \\
&\quad + g_{\frac{1}{2}}^{-2} \frac{\not{p} + M_-}{M_-^2 - p^2} p_\mu p_\nu p_\alpha p_\beta + g_{\frac{1}{2}}^{+2} \frac{\not{p} - M_+}{M_+^2 - p^2} p_\mu p_\nu p_\alpha p_\beta + \dots, \\
&= \left[\Pi_{\frac{5}{2}}^1(p^2) \not{p} + \Pi_{\frac{5}{2}}^0(p^2) \right] (g_{\mu\alpha}g_{\nu\beta} + g_{\mu\beta}g_{\nu\alpha}) + \dots,
\end{aligned} \tag{277}$$

where we have used the summations of the spinors [702],

$$\begin{aligned}
\sum_s U \bar{U} &= (\not{p} + M_\pm), \\
\sum_s U_\mu \bar{U}_\nu &= (\not{p} + M_\pm) \left(-g_{\mu\nu} + \frac{\gamma_\mu \gamma_\nu}{3} + \frac{2p_\mu p_\nu}{3p^2} - \frac{p_\mu \gamma_\nu - p_\nu \gamma_\mu}{3\sqrt{p^2}} \right), \\
\sum_s U_{\mu\nu} \bar{U}_{\alpha\beta} &= (\not{p} + M_\pm) \left\{ \frac{\tilde{g}_{\mu\alpha}\tilde{g}_{\nu\beta} + \tilde{g}_{\mu\beta}\tilde{g}_{\nu\alpha}}{2} - \frac{\tilde{g}_{\mu\nu}\tilde{g}_{\alpha\beta}}{5} - \frac{1}{10} \left(\gamma_\mu \gamma_\alpha + \frac{\gamma_\mu p_\alpha - \gamma_\alpha p_\mu}{\sqrt{p^2}} - \frac{p_\mu p_\alpha}{p^2} \right) \tilde{g}_{\nu\beta} \right. \\
&\quad - \frac{1}{10} \left(\gamma_\nu \gamma_\alpha + \frac{\gamma_\nu p_\alpha - \gamma_\alpha p_\nu}{\sqrt{p^2}} - \frac{p_\nu p_\alpha}{p^2} \right) \tilde{g}_{\mu\beta} - \frac{1}{10} \left(\gamma_\mu \gamma_\beta + \frac{\gamma_\mu p_\beta - \gamma_\beta p_\mu}{\sqrt{p^2}} - \frac{p_\mu p_\beta}{p^2} \right) \tilde{g}_{\nu\alpha} \\
&\quad \left. - \frac{1}{10} \left(\gamma_\nu \gamma_\beta + \frac{\gamma_\nu p_\beta - \gamma_\beta p_\nu}{\sqrt{p^2}} - \frac{p_\nu p_\beta}{p^2} \right) \tilde{g}_{\mu\alpha} \right\},
\end{aligned} \tag{278}$$

and $p^2 = M_\pm^2$ on mass-shell. We study the components $\Pi_{\frac{1}{2}}^1(p^2)$, $\Pi_{\frac{1}{2}}^0(p^2)$, $\Pi_{\frac{3}{2}}^1(p^2)$, $\Pi_{\frac{3}{2}}^0(p^2)$, $\Pi_{\frac{5}{2}}^1(p^2)$ and $\Pi_{\frac{5}{2}}^0(p^2)$ to avoid possible contaminations from other pentaquark states with different spins.

We obtain the spectral densities at the hadron side through dispersion relation,

$$\frac{\text{Im}\Pi_j^1(s)}{\pi} = \lambda_j^{-2}\delta(s - M_-^2) + \lambda_j^{+2}\delta(s - M_+^2) = \rho_{j,H}^1(s), \quad (279)$$

$$\frac{\text{Im}\Pi_j^0(s)}{\pi} = M_- \lambda_j^{-2}\delta(s - M_-^2) - M_+ \lambda_j^{+2}\delta(s - M_+^2) = \rho_{j,H}^0(s), \quad (280)$$

where $j = \frac{1}{2}, \frac{3}{2}, \frac{5}{2}$, the subscript H denotes the hadron side, then we introduce the weight functions $\sqrt{s} \exp(-\frac{s}{T^2})$ and $\exp(-\frac{s}{T^2})$ to obtain the QCD sum rules at the hadron side,

$$\int_{4m_c^2}^{s_0} ds [\sqrt{s} \rho_{j,H}^1(s) \pm \rho_{j,H}^0(s)] \exp\left(-\frac{s}{T^2}\right) = 2M_{\mp} \lambda_j^{\mp 2} \exp\left(-\frac{M_{\mp}^2}{T^2}\right), \quad (281)$$

where the s_0 are the continuum threshold parameters, and the T^2 are the Borel parameters. We distinguish the contributions of the negative and positive parity pentaquark states unambiguously, and there is no contamination.

Now we briefly outline the operator product expansion. Firstly, we contract the u , d and c quark fields in the correlation functions $\Pi(p)$, $\Pi_{\mu\nu}(p)$ and $\Pi_{\mu\nu\alpha\beta}(p)$ with Wick theorem, for example,

$$\begin{aligned} \Pi(p) = & i \varepsilon^{ila} \varepsilon^{ijk} \varepsilon^{lmn} \varepsilon^{i'l'a'} \varepsilon^{i'j'k'} \varepsilon^{l'm'n'} \int d^4x e^{ip \cdot x} \\ & \left\{ -Tr \left[\gamma_5 D_{kk'}(x) \gamma_5 C U_{jj'}^T(x) C \right] Tr \left[\gamma_5 C_{nn'}(x) \gamma_5 C U_{mm'}^T(x) C \right] C C_{a'a}^T(-x) C \right. \\ & \left. + Tr \left[\gamma_5 D_{kk'}(x) \gamma_5 C U_{mj'}^T(x) C \gamma_5 C_{nn'}(x) \gamma_5 C U_{jm'}^T(x) C \right] C C_{a'a}^T(-x) C \right\}, \end{aligned} \quad (282)$$

for the current $J(x) = J^1(x)$, where the $U_{ij}(x)$, $D_{ij}(x)$ and $C_{ij}(x)$ are the full u , d and c quark propagators, respectively, see Eqs.(129)-(130). Then we compute all the integrals in the coordinate and momentum spaces sequentially to obtain the $\Pi(p)$, $\Pi_{\mu\nu}(p)$ and $\Pi_{\mu\nu\alpha\beta}(p)$ at the quark-gluon level, and finally we obtain the QCD spectral densities through dispersion relation,

$$\begin{aligned} \rho_{j,QCD}^1(s) &= \frac{\text{Im}\Pi_j^1(s)}{\pi}, \\ \rho_{j,QCD}^0(s) &= \frac{\text{Im}\Pi_j^0(s)}{\pi}, \end{aligned} \quad (283)$$

where $j = \frac{1}{2}, \frac{3}{2}, \frac{5}{2}$. In computing the integrals, we draw up all the Feynman diagrams from Eq.(282) and calculate them one by one. In Eq.(282), there are two c -quark propagators and three light quark propagators, if each c -quark line emits a gluon and each light quark line contributes a quark-antiquark pair, we obtain an operator $G_{\mu\nu} G_{\alpha\beta} \bar{u}u \bar{u}d \bar{d}d$ according to the counting rule in Eq.(38), which is of dimension 13, see Fig.25. We should take account of the vacuum condensates at least up to dimension 13 in stead of dimension 10, which is adopted in most literatures. The vacuum condensates $\langle \bar{q}q \rangle^2 \langle \bar{q}g_s \sigma G q \rangle$, $\langle \bar{q}q \rangle \langle \bar{q}g_s \sigma G q \rangle^2$, $\langle \bar{q}q \rangle^3 \langle \frac{\alpha_s}{\pi} GG \rangle$ are of dimension 11 and 13 respectively, and come from the Feynman diagrams shown in Fig.25 [402]. Those vacuum condensates are associated with the $\frac{1}{T^2}$, $\frac{1}{T^4}$ and $\frac{1}{T^6}$, which manifest themselves at the small T^2 and play an important role in choosing the Borel windows. We take the truncations $n \leq 13$ and $k \leq 1$ in a consistent way, the quark-gluon operators of the orders $\mathcal{O}(\alpha_s^k)$ with $k > 1$ and dimension $n > 13$ are discarded.

In Refs.[423, 703, 704, 705, 706], we take the truncations $n \leq 10$ and $k \leq 1$ and discard the quark-gluon operators of the orders $\mathcal{O}(\alpha_s^k)$ with $k > 1$ and dimension $n > 10$. Sometimes we also neglected the vacuum condensates $\langle \frac{\alpha_s}{\pi} GG \rangle$, $\langle \bar{q}q \rangle \langle \frac{\alpha_s}{\pi} GG \rangle$, $\langle \bar{s}s \rangle \langle \frac{\alpha_s}{\pi} GG \rangle$, $\langle \bar{q}q \rangle^2 \langle \frac{\alpha_s}{\pi} GG \rangle$, $\langle \bar{q}q \rangle \langle \bar{s}s \rangle \langle \frac{\alpha_s}{\pi} GG \rangle$, $\langle \bar{s}s \rangle^2 \langle \frac{\alpha_s}{\pi} GG \rangle$, which are not associated with the $\frac{1}{T^2}$, $\frac{1}{T^4}$ and $\frac{1}{T^6}$ to manifest themselves at the small T^2 . Such an approximation would impair the predictive ability.

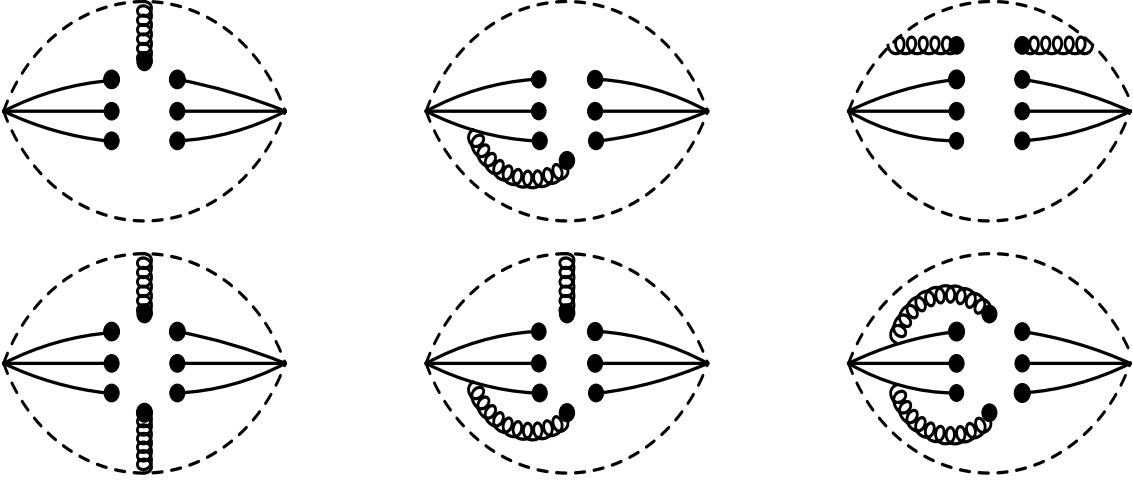


Figure 25: The diagrams contribute to the condensates $\langle \bar{q}q \rangle^2 \langle \bar{q}g_s \sigma G q \rangle$, $\langle \bar{q}q \rangle \langle \bar{q}g_s \sigma G q \rangle^2$, $\langle \bar{q}q \rangle^3 \langle \frac{\alpha_s}{\pi} GG \rangle$. Other diagrams obtained by interchanging of the c quark lines (dashed lines) or light quark lines (solid lines) are implied [402].

Then let us match the hadron side with the QCD side of the correlation functions, take the quark-hadron duality below the continuum thresholds s_0 , and obtain the QCD sum rules:

$$2M_{\mp} \lambda_j^{\mp 2} \exp\left(-\frac{M_{\mp}^2}{T^2}\right) = \int_{4m_c^2}^{s_0} ds \rho_{QCD,j}(s) \exp\left(-\frac{s}{T^2}\right), \quad (284)$$

where $\rho_{QCD,j}(s) = \sqrt{s} \rho_{QCD,j}^1(s) \pm \rho_{QCD,j}^0(s)$.

We derive Eq.(284) with respect to $\frac{1}{T^2}$, then eliminate the pole residues λ_j^{\mp} and obtain the QCD sum rules for the masses of the hidden-charm pentaquark states,

$$M_{\mp}^2 = \frac{-\int_{4m_c^2}^{s_0} ds \frac{d}{d(1/T^2)} \rho_{QCD,j}(s) \exp\left(-\frac{s}{T^2}\right)}{\int_{4m_c^2}^{s_0} ds \rho_{QCD,j}(s) \exp\left(-\frac{s}{T^2}\right)}. \quad (285)$$

With a simple replacement $c \rightarrow b$, we obtain the corresponding QCD sum rules for the hidden-bottom pentaquark states.

According to the discussions in Sect.2.4, we take the energy scale formula,

$$\mu = \sqrt{M_{X/Y/Z/P}^2 - (2\mathbb{M}_Q)^2}, \quad (286)$$

to determine the best energy scales of the QCD spectral densities [402, 423, 703, 704, 705, 706], and choose the updated value of the effective c -quark mass $\mathbb{M}_c = 1.82 \text{ GeV}$ [512].

After trial and error, we obtain the Borel windows T^2 , continuum threshold parameters s_0 , ideal energy scales of the QCD spectral densities, pole contributions of the ground states and contributions of the vacuum condensates of dimension 13, which are shown explicitly in Table 49 [402].

In Fig.26, we plot the contributions of the vacuum condensates of dimension 11 and 13 with variation of the Borel parameter T^2 for the hidden-charm pentaquark state $[ud][uc]\bar{c}$ (0, 0, 0, $\frac{1}{2}$) with the central values of the parameters shown in Table 49 as an example. The vacuum condensates of dimension 13 manifest themselves at the region $T^2 < 2 \text{ GeV}^2$, we should choose the value $T^2 > 2 \text{ GeV}^2$. While the vacuum condensates of dimension 11 manifest themselves at the region $T^2 < 2.6 \text{ GeV}^2$, which requires a larger Borel parameter $T^2 > 2.6 \text{ GeV}^2$ to warrant the

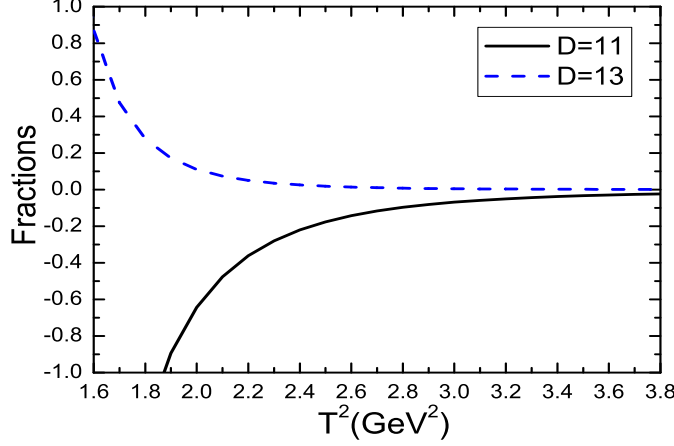


Figure 26: The contributions of the vacuum condensates of dimension 11 and 13 with variation of the Borel parameter T^2 for the hidden-charm pentaquark state $[ud][uc]\bar{c}$ $(0, 0, 0, \frac{1}{2})$ [402].

convergence of the operator product expansion. The higher dimensional vacuum condensates play an important role in choosing the Borel windows, where they play an minor important role as the operator product expansion should be convergent, we should take them into account in a consistent way, for example, the $|D(13)|$ is less than 1% [402].

In Fig.27, we plot the mass of the hidden-charm pentaquark state $[ud][uc]\bar{c}$ $(0, 0, 0, \frac{1}{2})$ with variation of the Borel parameter T^2 for truncations of the operator product expansion up to the vacuum condensates of dimension 10 and 13, respectively [402]. The vacuum condensates of dimension 11 and 13 play an important role to obtain stable QCD sum rules, we should take them into account.

In Table 49, the pole contributions are about $(40 - 60)\%$ and the contributions of the vacuum condensates of dimension 13 are $\leq 1\%$ or $\ll 1\%$, the pole dominance and convergence of the operator product expansion are all satisfied, **the two basic criteria of the QCD sum rules are satisfied in the case of the hidden-charm pentaquark states for the first time.**

We take account of all uncertainties of the relevant parameters, and obtain the masses and pole residues of the hidden-charm pentaquark states with negative parity, which are shown explicitly in Table 50.

The predicted masses $M_P = 4.31 \pm 0.11$ GeV for the ground state $[ud][uc]\bar{c}$ $(0, 0, 0, \frac{1}{2})$ pentaquark state and $M_P = 4.34 \pm 0.14$ GeV for the ground state $[uu][dc]\bar{c} + 2[ud][uc]\bar{c}$ $(1, 1, 0, \frac{1}{2})$ pentaquark state are both in excellent agreement with the experimental data $M_{P(4312)} = 4311.9 \pm 0.7^{+6.8}_{-0.6}$ MeV from the LHCb collaboration [197], and support assigning the $P_c(4312)$ to be the hidden-charm pentaquark state with the $J^P = \frac{1}{2}^-$.

After the work was published [402], the LHCb collaboration observed an evidence for a structure $P_c(4337)$ in the $J/\psi p$ and $J/\psi \bar{p}$ systems with a significance about $3.1 - 3.7\sigma$ depending on the J^P hypothesis [199], the Breit-Wigner mass and width are 4337^{+7+2}_{-4-2} MeV and 29^{+26+14}_{-12-14} MeV respectively. The $P_c(4337)$ can be assigned as the ground state $[uu][dc]\bar{c} + 2[ud][uc]\bar{c}$ $(1, 1, 0, \frac{1}{2})$ pentaquark state with the mass 4.34 ± 0.14 GeV.

The predicted masses $M_P = 4.45 \pm 0.11$ GeV for the ground state $[ud][uc]\bar{c}$ $(0, 1, 1, \frac{1}{2})$ pentaquark state, $M_P = 4.46 \pm 0.11$ GeV for the ground state $[uu][dc]\bar{c} + 2[ud][uc]\bar{c}$ $(1, 0, 1, \frac{1}{2})$ pentaquark state and $M_P = 4.39 \pm 0.11$ for the ground state $[ud][uc]\bar{c}$ $(0, 1, 1, \frac{3}{2})$, $[uu][dc]\bar{c} + 2[ud][uc]\bar{c}$ $(1, 1, 2, \frac{5}{2})$, $[ud][uc]\bar{c}$ $(0, 1, 1, \frac{5}{2})$ pentaquark states are in excellent agreement (or compatible with)

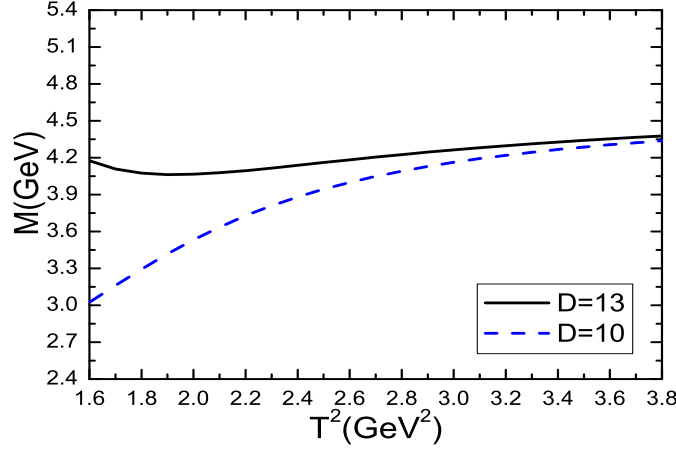


Figure 27: The mass with variation of the Borel parameter T^2 for the hidden-charm pentaquark state $[ud][uc]\bar{c}$ $(0, 0, 0, \frac{1}{2})$, the $D = 10, 13$ denote truncations of the operator product expansion [402].

the experimental data $M_{P(4440)} = 4440.3 \pm 1.3^{+4.1}_{-4.7}$ MeV from the LHCb collaboration [197], and support assigning the $P_c(4440)$ to be the hidden-charm pentaquark state with $J^P = \frac{1}{2}^-$, $\frac{3}{2}^-$ or $\frac{5}{2}^-$.

The predicted masses $M_P = 4.45 \pm 0.11$ GeV for the ground state $[ud][uc]\bar{c}$ $(0, 1, 1, \frac{1}{2})$ pentaquark state, $M_P = 4.46 \pm 0.11$ GeV for the ground state $[uu][dc]\bar{c} + 2[ud][uc]\bar{c}$ $(1, 0, 1, \frac{1}{2})$ pentaquark state and $M_P = 4.47 \pm 0.11$ GeV for the ground state $[uu][dc]\bar{c} + 2[ud][uc]\bar{c}$ $(1, 0, 1, \frac{3}{2})$ pentaquark states are in excellent agreement the experimental data $M_{P(4457)} = 4457.3 \pm 0.6^{+4.1}_{-1.7}$ MeV from the LHCb collaboration [197], and support assigning the $P_c(4457)$ to be the hidden-charm pentaquark state with $J^P = \frac{1}{2}^-$ or $\frac{3}{2}^-$.

In Table 50, we present the possible assignments of the $P_c(4312)$, $P_c(4440)$ and $P_c(4457)$ explicitly as a summary. In Table 51, we compare the present predictions with our previous calculations [423, 703, 704, 705], where the vacuum condensates of dimension 11 and 13 were neglected, sometimes the vacuum condensates $\langle \frac{\alpha_s GG}{\pi} \rangle$, $\langle \bar{q}q \rangle \langle \frac{\alpha_s GG}{\pi} \rangle$ and $\langle \bar{q}q \rangle^2 \langle \frac{\alpha_s GG}{\pi} \rangle$ were also neglected. From the Table 51, we can see that in some cases the predicted masses change remarkably, while in other cases the predicted masses change slightly. In Ref.[423], we construct the current $\gamma_5 J_{\mu\nu}^2(x)$ to interpolate the hidden-charm tetraquark state with the $J^P = \frac{5}{2}^+$, which should be updated.

In Ref.[704], we construct the $J_{q_1 q_2 q_3}^{j_L j_H}(x)$ with the spin-parity $J^P = \frac{1}{2}^-$ to study the hidden-charm pentaquark states with the $J^P = \frac{1}{2}^\pm$ according to the rules,

$$\begin{aligned}
 1_{q_1 q_2}^+ \otimes 0_{q_3 c}^+ \otimes \frac{1}{2}_{\bar{c}}^- &= \frac{1}{2}_{q_1 q_2 q_3 c \bar{c}}^- \oplus \frac{3}{2}_{q_1 q_2 q_3 c \bar{c}}^-, \\
 1_{q_1 q_2}^+ \otimes 1_{q_3 c}^+ \otimes \frac{1}{2}_{\bar{c}}^- &= [0_{q_1 q_2 q_3 c}^+ \oplus 1_{q_1 q_2 q_3 c}^+ \oplus 2_{q_1 q_2 q_3 c}^+] \otimes \frac{1}{2}_{\bar{c}}^- \\
 &= \frac{1}{2}_{q_1 q_2 q_3 c \bar{c}}^- \oplus \left[\frac{1}{2}_{q_1 q_2 q_3 c \bar{c}}^- \oplus \frac{3}{2}_{q_1 q_2 q_3 c \bar{c}}^- \right] \oplus \left[\frac{3}{2}_{q_1 q_2 q_3 c \bar{c}}^- \oplus \frac{5}{2}_{q_1 q_2 q_3 c \bar{c}}^- \right],
 \end{aligned}$$

	$T^2(\text{GeV}^2)$	$\sqrt{s_0}(\text{GeV})$	$\mu(\text{GeV})$	pole	D_{13}
$J^1(x)$	3.1 – 3.5	4.96 ± 0.10	2.3	(41 – 62)%	$< 1\%$
$J^2(x)$	3.2 – 3.6	5.10 ± 0.10	2.6	(42 – 63)%	$< 1\%$
$J^3(x)$	3.2 – 3.6	5.11 ± 0.10	2.6	(42 – 63)%	$\ll 1\%$
$J^4(x)$	2.9 – 3.3	5.00 ± 0.10	2.4	(40 – 64)%	$\leq 1\%$
$J_\mu^1(x)$	3.1 – 3.5	5.03 ± 0.10	2.4	(42 – 63)%	$\leq 1\%$
$J_\mu^2(x)$	3.3 – 3.7	5.11 ± 0.10	2.6	(40 – 61)%	$\ll 1\%$
$J_\mu^3(x)$	3.4 – 3.8	5.26 ± 0.10	2.8	(42 – 62)%	$\ll 1\%$
$J_\mu^4(x)$	3.3 – 3.7	5.17 ± 0.10	2.7	(41 – 61)%	$< 1\%$
$J_{\mu\nu}^1(x)$	3.2 – 3.6	5.03 ± 0.10	2.4	(40 – 61)%	$\leq 1\%$
$J_{\mu\nu}^2(x)$	3.1 – 3.5	5.03 ± 0.10	2.4	(42 – 63)%	$\leq 1\%$

Table 49: The Borel windows, continuum threshold parameters, ideal energy scales, pole contributions and contributions of the vacuum condensates of dimension 13 for the hidden-charm pentaquark states [402].

$[qq'][q''c]\bar{c} (S_L, S_H, J_{LH}, J)$	$M(\text{GeV})$	$\lambda(10^{-3}\text{GeV}^6)$	Assignments	Currents
$[ud][uc]\bar{c} (0, 0, 0, \frac{1}{2})$	4.31 ± 0.11	1.40 ± 0.23	? $P_c(4312)$	$J^1(x)$
$[ud][uc]\bar{c} (0, 1, 1, \frac{1}{2})$	4.45 ± 0.11	3.02 ± 0.48	? $P_c(4440/4457)$	$J^2(x)$
$[uu][dc]\bar{c} + 2[ud][uc]\bar{c} (1, 0, 1, \frac{1}{2})$	4.46 ± 0.11	4.32 ± 0.71	? $P_c(4440/4457)$	$J^3(x)$
$[uu][dc]\bar{c} + 2[ud][uc]\bar{c} (1, 1, 0, \frac{1}{2})$	4.34 ± 0.14	3.23 ± 0.61	? $P_c(4312/\mathbf{4337})$	$J^4(x)$
$[ud][uc]\bar{c} (0, 1, 1, \frac{3}{2})$	4.39 ± 0.11	1.44 ± 0.23	? $P_c(4440)$	$J_\mu^1(x)$
$[uu][dc]\bar{c} + 2[ud][uc]\bar{c} (1, 0, 1, \frac{3}{2})$	4.47 ± 0.11	2.41 ± 0.38	? $P_c(4440/4457)$	$J_\mu^2(x)$
$[uu][dc]\bar{c} + 2[ud][uc]\bar{c} (1, 1, 2, \frac{3}{2})$	4.61 ± 0.11	5.13 ± 0.79		$J_\mu^3(x)$
$[uu][dc]\bar{c} + 2[ud][uc]\bar{c} (1, 1, 2, \frac{3}{2})$	4.52 ± 0.11	4.49 ± 0.72		$J_\mu^4(x)$
$[uu][dc]\bar{c} + 2[ud][uc]\bar{c} (1, 1, 2, \frac{5}{2})$	4.39 ± 0.11	1.94 ± 0.31	? $P_c(4440)$	$J_{\mu\nu}^1(x)$
$[ud][uc]\bar{c} (0, 1, 1, \frac{5}{2})$	4.39 ± 0.11	1.44 ± 0.23	? $P_c(4440)$	$J_{\mu\nu}^2(x)$

Table 50: The masses and pole residues of the hidden-charm pentaquark states [402].

$[qq'][q''c]\bar{c} (S_L, S_H, J_{LH}, J)$	Ref.[402]	Old calculations	Currents
$[ud][uc]\bar{c} (0, 0, 0, \frac{1}{2})$	4.31 ± 0.11	4.29 ± 0.13	$J^1(x)$
$[ud][uc]\bar{c} (0, 1, 1, \frac{1}{2})$	4.45 ± 0.11	4.30 ± 0.13	$J^2(x)$
$[uu][dc]\bar{c} + 2[ud][uc]\bar{c} (1, 0, 1, \frac{1}{2})$	4.46 ± 0.11	4.42 ± 0.12	$J^3(x)$
$[uu][dc]\bar{c} + 2[ud][uc]\bar{c} (1, 1, 0, \frac{1}{2})$	4.34 ± 0.14	4.35 ± 0.15	$J^4(x)$
$[ud][uc]\bar{c} (0, 1, 1, \frac{3}{2})$	4.39 ± 0.11	4.38 ± 0.13	$J_\mu^1(x)$
$[uu][dc]\bar{c} + 2[ud][uc]\bar{c} (1, 0, 1, \frac{3}{2})$	4.47 ± 0.11	4.39 ± 0.13	$J_\mu^2(x)$
$[uu][dc]\bar{c} + 2[ud][uc]\bar{c} (1, 1, 2, \frac{3}{2})$	4.61 ± 0.11	4.39 ± 0.14	$J_\mu^3(x)$
$[uu][dc]\bar{c} + 2[ud][uc]\bar{c} (1, 1, 2, \frac{3}{2})$	4.52 ± 0.11	4.39 ± 0.14	$J_\mu^4(x)$
$[uu][dc]\bar{c} + 2[ud][uc]\bar{c} (1, 1, 2, \frac{5}{2})$	4.39 ± 0.11		$J_{\mu\nu}^1(x)$
$[ud][uc]\bar{c} (0, 1, 1, \frac{5}{2})$	4.39 ± 0.11		$J_{\mu\nu}^2(x)$

Table 51: The masses (in unit of GeV) are compared with the old calculations [423, 703, 704, 705].

$$\begin{aligned}
1_{q_1 q_2}^+ \otimes 0_{q_3 c}^+ \otimes \left[1^- \otimes \frac{1^-}{2_{\bar{c}}} \right] &= 1_{q_1 q_2}^+ \otimes 0_{q_3 c}^+ \otimes \left[\frac{1^+}{2_{\bar{c}}} \oplus \frac{3^+}{2_{\bar{c}}} \right] \\
&= \left[\frac{1^+}{2_{q_1 q_2 q_3 c \bar{c}}} \oplus \frac{3^+}{2_{q_1 q_2 q_3 c \bar{c}}} \right] \oplus \left[\frac{1^+}{2_{q_1 q_2 q_3 c \bar{c}}} \oplus \frac{3^+}{2_{q_1 q_2 q_3 c \bar{c}}} \oplus \frac{5^+}{2_{q_1 q_2 q_3 c \bar{c}}} \right], \\
\\
1_{q_1 q_2}^+ \otimes 1_{q_3 c}^+ \otimes \left[1^- \otimes \frac{1^-}{2_{\bar{c}}} \right] &= [0_{q_1 q_2 q_3 c}^+ \oplus 1_{q_1 q_2 q_3 c}^+ \oplus 2_{q_1 q_2 q_3 c}^+] \otimes \left[\frac{1^+}{2_{\bar{c}}} \oplus \frac{3^+}{2_{\bar{c}}} \right] \\
&= \frac{1^+}{2_{q_1 q_2 q_3 c \bar{c}}} \oplus \left[\frac{1^+}{2_{q_1 q_2 q_3 c \bar{c}}} \oplus \frac{3^+}{2_{q_1 q_2 q_3 c \bar{c}}} \right] \oplus \left[\frac{3^+}{2_{q_1 q_2 q_3 c \bar{c}}} \oplus \frac{5^+}{2_{q_1 q_2 q_3 c \bar{c}}} \right] \\
&\quad \oplus \frac{3^+}{2_{q_1 q_2 q_3 c \bar{c}}} \oplus \left[\frac{1^+}{2_{q_1 q_2 q_3 c \bar{c}}} \oplus \frac{3^+}{2_{q_1 q_2 q_3 c \bar{c}}} \oplus \frac{5^+}{2_{q_1 q_2 q_3 c \bar{c}}} \right] \\
&\quad \oplus \left[\frac{1^+}{2_{q_1 q_2 q_3 c \bar{c}}} \oplus \frac{3^+}{2_{q_1 q_2 q_3 c \bar{c}}} \oplus \frac{5^+}{2_{q_1 q_2 q_3 c \bar{c}}} \oplus \frac{7^+}{2_{q_1 q_2 q_3 c \bar{c}}} \right], \tag{287}
\end{aligned}$$

where the 1^- denotes the additional P-wave and is embodied by a γ_5 in constructing the currents, the subscripts $q_1 q_2, q_3 c, \dots$ denote the quark constituents. The quark and antiquark have opposite parity, we usually take it for granted that the quarks (antiquarks) have positive (negative) parity, and the \bar{c} -quark has the $J^P = \frac{1}{2}^-$.

We write down the currents $J_{q_1 q_2 q_3}^{j_L j_H}(x)$ explicitly,

$$\begin{aligned}
J_{uuu}^{11}(x) &= \varepsilon^{ila} \varepsilon^{ijk} \varepsilon^{lmn} u_j^T(x) C \gamma_\mu u_k(x) u_m^T(x) C \gamma^\mu c_n(x) C \bar{c}_a^T(x), \\
J_{uud}^{11}(x) &= \frac{\varepsilon^{ila} \varepsilon^{ijk} \varepsilon^{lmn}}{\sqrt{3}} [u_j^T(x) C \gamma_\mu u_k(x) d_m^T(x) C \gamma^\mu c_n(x) + 2u_j^T(x) C \gamma_\mu d_k(x) u_m^T(x) C \gamma^\mu c_n(x)] C \bar{c}_a^T(x), \\
J_{udd}^{11}(x) &= \frac{\varepsilon^{ila} \varepsilon^{ijk} \varepsilon^{lmn}}{\sqrt{3}} [d_j^T(x) C \gamma_\mu d_k(x) u_m^T(x) C \gamma^\mu c_n(x) + 2d_j^T(x) C \gamma_\mu u_k(x) d_m^T(x) C \gamma^\mu c_n(x)] C \bar{c}_a^T(x), \\
J_{ddd}^{11}(x) &= \varepsilon^{ila} \varepsilon^{ijk} \varepsilon^{lmn} d_j^T(x) C \gamma_\mu d_k(x) d_m^T(x) C \gamma^\mu c_n(x) C \bar{c}_a^T(x), \tag{288}
\end{aligned}$$

$$\begin{aligned}
J_{uus}^{11}(x) &= \frac{\varepsilon^{ila} \varepsilon^{ijk} \varepsilon^{lmn}}{\sqrt{3}} [u_j^T(x) C \gamma_\mu u_k(x) s_m^T(x) C \gamma^\mu c_n(x) + 2u_j^T(x) C \gamma_\mu s_k(x) u_m^T(x) C \gamma^\mu c_n(x)] C \bar{c}_a^T(x), \\
J_{uds}^{11}(x) &= \frac{\varepsilon^{ila} \varepsilon^{ijk} \varepsilon^{lmn}}{\sqrt{3}} [u_j^T(x) C \gamma_\mu d_k(x) s_m^T(x) C \gamma^\mu c_n(x) + u_j^T(x) C \gamma_\mu s_k(x) d_m^T(x) C \gamma^\mu c_n(x) \\
&\quad + d_j^T(x) C \gamma_\mu s_k(x) u_m^T(x) C \gamma^\mu c_n(x)] C \bar{c}_a^T(x), \\
J_{dds}^{11}(x) &= \frac{\varepsilon^{ila} \varepsilon^{ijk} \varepsilon^{lmn}}{\sqrt{3}} [d_j^T(x) C \gamma_\mu d_k(x) s_m^T(x) C \gamma^\mu c_n(x) + 2d_j^T(x) C \gamma_\mu s_k(x) d_m^T(x) C \gamma^\mu c_n(x)] C \bar{c}_a^T(x), \tag{289}
\end{aligned}$$

$$\begin{aligned}
J_{uss}^{11}(x) &= \frac{\varepsilon^{ila} \varepsilon^{ijk} \varepsilon^{lmn}}{\sqrt{3}} [s_j^T(x) C \gamma_\mu s_k(x) u_m^T(x) C \gamma^\mu c_n(x) + 2s_j^T(x) C \gamma_\mu u_k(x) s_m^T(x) C \gamma^\mu c_n(x)] C \bar{c}_a^T(x), \\
J_{dss}^{11}(x) &= \frac{\varepsilon^{ila} \varepsilon^{ijk} \varepsilon^{lmn}}{\sqrt{3}} [s_j^T(x) C \gamma_\mu s_k(x) d_m^T(x) C \gamma^\mu c_n(x) + 2s_j^T(x) C \gamma_\mu d_k(x) s_m^T(x) C \gamma^\mu c_n(x)] C \bar{c}_a^T(x), \tag{290}
\end{aligned}$$

$$J_{sss}^{11}(x) = \varepsilon^{ila} \varepsilon^{ijk} \varepsilon^{lmn} s_j^T(x) C \gamma_\mu s_k(x) s_m^T(x) C \gamma^\mu c_n(x) C \bar{c}_a^T(x), \tag{291}$$

$$\begin{aligned}
J_{uuu}^{10}(x) &= \varepsilon^{ila} \varepsilon^{ijk} \varepsilon^{lmn} u_j^T(x) C \gamma_\mu u_k(x) u_m^T(x) C \gamma_5 c_n(x) \gamma_5 \gamma^\mu C \bar{c}_a^T(x), \\
J_{uud}^{10}(x) &= \frac{\varepsilon^{ila} \varepsilon^{ijk} \varepsilon^{lmn}}{\sqrt{3}} [u_j^T(x) C \gamma_\mu u_k(x) d_m^T(x) C \gamma_5 c_n(x) + 2u_j^T(x) C \gamma_\mu d_k(x) u_m^T(x) C \gamma_5 c_n(x)] \gamma_5 \gamma^\mu C \bar{c}_a^T(x), \\
J_{udd}^{10}(x) &= \frac{\varepsilon^{ila} \varepsilon^{ijk} \varepsilon^{lmn}}{\sqrt{3}} [d_j^T(x) C \gamma_\mu d_k(x) u_m^T(x) C \gamma_5 c_n(x) + 2d_j^T(x) C \gamma_\mu u_k(x) d_m^T(x) C \gamma_5 c_n(x)] \gamma_5 \gamma^\mu C \bar{c}_a^T(x), \\
J_{ddd}^{10}(x) &= \varepsilon^{ila} \varepsilon^{ijk} \varepsilon^{lmn} d_j^T(x) C \gamma_\mu d_k(x) d_m^T(x) C \gamma_5 c_n(x) \gamma_5 \gamma^\mu C \bar{c}_a^T(x), \tag{292}
\end{aligned}$$

$$\begin{aligned}
J_{uus}^{10}(x) &= \frac{\varepsilon^{ila} \varepsilon^{ijk} \varepsilon^{lmn}}{\sqrt{3}} [u_j^T(x) C \gamma_\mu u_k(x) s_m^T(x) C \gamma_5 c_n(x) + 2u_j^T(x) C \gamma_\mu s_k(x) u_m^T(x) C \gamma_5 c_n(x)] \gamma_5 \gamma^\mu C \bar{c}_a^T(x), \\
J_{uds}^{10}(x) &= \frac{\varepsilon^{ila} \varepsilon^{ijk} \varepsilon^{lmn}}{\sqrt{3}} [u_j^T(x) C \gamma_\mu d_k(x) s_m^T(x) C \gamma_5 c_n(x) + u_j^T(x) C \gamma_\mu s_k(x) d_m^T(x) C \gamma_5 c_n(x) \\
&\quad + d_j^T(x) C \gamma_\mu s_k(x) u_m^T(x) C \gamma_5 c_n(x)] \gamma_5 \gamma^\mu C \bar{c}_a^T(x), \\
J_{dds}^{10}(x) &= \frac{\varepsilon^{ila} \varepsilon^{ijk} \varepsilon^{lmn}}{\sqrt{3}} [d_j^T(x) C \gamma_\mu d_k(x) s_m^T(x) C \gamma_5 c_n(x) + 2d_j^T(x) C \gamma_\mu s_k(x) d_m^T(x) C \gamma_5 c_n(x)] \gamma_5 \gamma^\mu C \bar{c}_a^T(x), \tag{293}
\end{aligned}$$

$$\begin{aligned}
J_{uss}^{10}(x) &= \frac{\varepsilon^{ila} \varepsilon^{ijk} \varepsilon^{lmn}}{\sqrt{3}} [s_j^T(x) C \gamma_\mu s_k(x) u_m^T(x) C \gamma_5 c_n(x) + 2s_j^T(x) C \gamma_\mu u_k(x) s_m^T(x) C \gamma_5 c_n(x)] \gamma_5 \gamma^\mu C \bar{c}_a^T(x), \\
J_{dss}^{10}(x) &= \frac{\varepsilon^{ila} \varepsilon^{ijk} \varepsilon^{lmn}}{\sqrt{3}} [s_j^T(x) C \gamma_\mu s_k(x) d_m^T(x) C \gamma_5 c_n(x) + 2s_j^T(x) C \gamma_\mu d_k(x) s_m^T(x) C \gamma_5 c_n(x)] \gamma_5 \gamma^\mu C \bar{c}_a^T(x), \tag{294}
\end{aligned}$$

$$J_{sss}^{10}(x) = \varepsilon^{ila} \varepsilon^{ijk} \varepsilon^{lmn} s_j^T(x) C \gamma_\mu s_k(x) s_m^T(x) C \gamma_5 c_n(x) \gamma_5 \gamma^\mu C \bar{c}_a^T(x), \tag{295}$$

where the superscripts j_L and j_H are the spins of the light and heavy diquarks, respectively.

We take the isospin limit and classify the currents which couple potentially to the pentaquark states with degenerate masses into the following 8 types,

$$\begin{aligned}
&J_{uuu}^{11}(x), J_{uud}^{11}(x), J_{udd}^{11}(x), J_{ddd}^{11}(x); \\
&J_{uus}^{11}(x), J_{uds}^{11}(x), J_{dds}^{11}(x); \\
&J_{uss}^{11}(x), J_{dss}^{11}(x); \\
&J_{sss}^{11}(x); \\
&J_{uuu}^{10}(x), J_{uud}^{10}(x), J_{udd}^{10}(x), J_{ddd}^{10}(x); \\
&J_{uus}^{10}(x), J_{uds}^{10}(x), J_{dds}^{10}(x); \\
&J_{uss}^{10}(x), J_{dss}^{10}(x); \\
&J_{sss}^{10}(x), \tag{296}
\end{aligned}$$

and perform the operator product expansion up to the vacuum condensates of dimension 10 to obtain the QCD sum rules, the predictions for the hidden-charm pentaquark states $P_{q_1 q_2 q_3}^{j_L j_H \frac{1}{2}}$ with the spin-parity $J^P = \frac{1}{2}^\pm$ are presented in Table 61 in the Appendix.

From Table 61, we can see that the two-body strong decays to the $J/\psi B_{10}$,

$$P_{q_1 q_2 q_3}^{11 \frac{1}{2}} \left(\frac{1}{2}^- \right), P_{q_1 q_2 q_3}^{10 \frac{1}{2}} \left(\frac{1}{2}^- \right) \rightarrow J/\psi B_{10}, \tag{297}$$

for example,

$$\begin{aligned}
P_{uu\bar{u}}^{11\frac{1}{2}}\left(\frac{1}{2}^{-}\right), P_{uu\bar{u}}^{10\frac{1}{2}}\left(\frac{1}{2}^{-}\right) &\rightarrow J/\psi\Delta^{++}, \\
P_{uus}^{11\frac{1}{2}}\left(\frac{1}{2}^{-}\right), P_{uus}^{10\frac{1}{2}}\left(\frac{1}{2}^{-}\right) &\rightarrow J/\psi\Sigma^{*+}, \\
P_{uss}^{11\frac{1}{2}}\left(\frac{1}{2}^{-}\right), P_{uss}^{10\frac{1}{2}}\left(\frac{1}{2}^{-}\right) &\rightarrow J/\psi\Xi^{*0}, \\
P_{sss}^{11\frac{1}{2}}\left(\frac{1}{2}^{-}\right), P_{sss}^{10\frac{1}{2}}\left(\frac{1}{2}^{-}\right) &\rightarrow J/\psi\Omega^{-},
\end{aligned} \tag{298}$$

could take place, but the decay widths are rather small due to the small available phase-spaces; on the other hand, the two-body strong decays,

$$P_{q_1q_2q_3}^{11\frac{1}{2}}\left(\frac{1}{2}^{-}\right), P_{q_1q_2q_3}^{10\frac{1}{2}}\left(\frac{1}{2}^{-}\right) \rightarrow J/\psi B_8, \tag{299}$$

$$P_{q_1q_2q_3}^{11\frac{1}{2}}\left(\frac{1}{2}^{+}\right) \rightarrow J/\psi B_{10}, J/\psi B_8, \tag{300}$$

for example,

$$\begin{aligned}
P_{uud}^{11\frac{1}{2}}\left(\frac{1}{2}^{\pm}\right), P_{uud}^{10\frac{1}{2}}\left(\frac{1}{2}^{-}\right) &\rightarrow J/\psi p, \\
P_{uus}^{11\frac{1}{2}}\left(\frac{1}{2}^{\pm}\right), P_{uus}^{10\frac{1}{2}}\left(\frac{1}{2}^{-}\right) &\rightarrow J/\psi\Sigma^{+}, \\
P_{uss}^{11\frac{1}{2}}\left(\frac{1}{2}^{\pm}\right), P_{uss}^{10\frac{1}{2}}\left(\frac{1}{2}^{-}\right) &\rightarrow J/\psi\Xi^0, \\
P_{uuu}^{11\frac{1}{2}}\left(\frac{1}{2}^{+}\right) &\rightarrow J/\psi\Delta^{++}, \\
P_{uus}^{11\frac{1}{2}}\left(\frac{1}{2}^{+}\right) &\rightarrow J/\psi\Sigma^{*+}, \\
P_{uss}^{11\frac{1}{2}}\left(\frac{1}{2}^{+}\right) &\rightarrow J/\psi\Xi^{*0}, \\
P_{sss}^{11\frac{1}{2}}\left(\frac{1}{2}^{+}\right) &\rightarrow J/\psi\Omega^{-},
\end{aligned} \tag{301}$$

can take place more easily, the decay widths are larger due to the larger available phase-spaces; furthermore, the two-body strong decays

$$P_{q_1q_2q_3}^{10\frac{1}{2}}\left(\frac{1}{2}^{+}\right) \rightarrow J/\psi B_8, J/\psi B_{10}, \tag{302}$$

for example,

$$\begin{aligned}
P_{uud}^{10\frac{1}{2}}\left(\frac{1}{2}^{+}\right) &\rightarrow J/\psi p, \\
P_{uus}^{10\frac{1}{2}}\left(\frac{1}{2}^{+}\right) &\rightarrow J/\psi \Sigma^{+}, \\
P_{uss}^{10\frac{1}{2}}\left(\frac{1}{2}^{+}\right) &\rightarrow J/\psi \Xi^{0}, \\
P_{uuu}^{10\frac{1}{2}}\left(\frac{1}{2}^{+}\right) &\rightarrow J/\psi \Delta^{++}, \\
P_{uus}^{10\frac{1}{2}}\left(\frac{1}{2}^{+}\right) &\rightarrow J/\psi \Sigma^{*+}, \\
P_{uss}^{10\frac{1}{2}}\left(\frac{1}{2}^{+}\right) &\rightarrow J/\psi \Xi^{*0}, \\
P_{sss}^{10\frac{1}{2}}\left(\frac{1}{2}^{+}\right) &\rightarrow J/\psi \Omega^{-},
\end{aligned} \tag{303}$$

can take place fluently, the decay widths are rather large due to the large available phase-spaces. We can search for those pentaquark states in the $J/\psi B_8$ and $J/\psi B_{10}$ mass spectra in the decays of the bottom baryons to the final states $J/\psi B_8$ and $J/\psi B_{10}$ associated with the light vector mesons or pseudoscalar mesons [693, 707, 708], for example,

$$\begin{aligned}
\Omega_b^{-} &\rightarrow P_{uss}^{11\frac{1}{2}}\left(\frac{1}{2}^{\pm}\right) K^{-} \rightarrow J/\psi \Xi^{*0} K^{-}, \\
\Omega_b^{-} &\rightarrow P_{sss}^{11\frac{1}{2}}\left(\frac{1}{2}^{\pm}\right) \phi \rightarrow J/\psi \Omega^{-} \phi.
\end{aligned} \tag{304}$$

In Ref.[705], we construct the currents $J_{q_1 q_2 q_3, \mu}^{j_L j_H j}(x)$ to interpolate the $J^P = \frac{3}{2}^{\pm}$ hidden-charm tetraquark states, where the superscripts j_L and j_H are the spins of the light and heavy diquarks, respectively, $\vec{j} = \vec{j}_H + \vec{j}_{\bar{c}}$, the $j_{\bar{c}}$ is the spin of the heavy antiquark, the subscripts q_1, q_2, q_3 are the light quark constituents u, d or s . We write down the currents $J_{q_1 q_2 q_3, \mu}^{j_L j_H j}(x)$ explicitly,

$$\begin{aligned}
J_{uuu, \mu}^{10\frac{1}{2}}(x) &= \varepsilon^{ila} \varepsilon^{ijk} \varepsilon^{lmn} u_j^T(x) C \gamma_{\mu} u_k(x) u_m^T(x) C \gamma_5 c_n(x) C \bar{c}_a^T(x), \\
J_{uud, \mu}^{10\frac{1}{2}}(x) &= \frac{\varepsilon^{ila} \varepsilon^{ijk} \varepsilon^{lmn}}{\sqrt{3}} [u_j^T(x) C \gamma_{\mu} u_k(x) d_m^T(x) C \gamma_5 c_n(x) + 2u_j^T(x) C \gamma_{\mu} d_k(x) u_m^T(x) C \gamma_5 c_n(x)] C \bar{c}_a^T(x), \\
J_{udd, \mu}^{10\frac{1}{2}}(x) &= \frac{\varepsilon^{ila} \varepsilon^{ijk} \varepsilon^{lmn}}{\sqrt{3}} [d_j^T(x) C \gamma_{\mu} d_k(x) u_m^T(x) C \gamma_5 c_n(x) + 2d_j^T(x) C \gamma_{\mu} u_k(x) d_m^T(x) C \gamma_5 c_n(x)] C \bar{c}_a^T(x), \\
J_{ddd, \mu}^{10\frac{1}{2}}(x) &= \varepsilon^{ila} \varepsilon^{ijk} \varepsilon^{lmn} d_j^T(x) C \gamma_{\mu} d_k(x) d_m^T(x) C \gamma_5 c_n(x) C \bar{c}_a^T(x),
\end{aligned} \tag{305}$$

$$\begin{aligned}
J_{uus, \mu}^{10\frac{1}{2}}(x) &= \frac{\varepsilon^{ila} \varepsilon^{ijk} \varepsilon^{lmn}}{\sqrt{3}} [u_j^T(x) C \gamma_{\mu} u_k(x) s_m^T(x) C \gamma_5 c_n(x) + 2u_j^T(x) C \gamma_{\mu} s_k(x) u_m^T(x) C \gamma_5 c_n(x)] C \bar{c}_a^T(x), \\
J_{uds, \mu}^{10\frac{1}{2}}(x) &= \frac{\varepsilon^{ila} \varepsilon^{ijk} \varepsilon^{lmn}}{\sqrt{3}} [u_j^T(x) C \gamma_{\mu} d_k(x) s_m^T(x) C \gamma_5 c_n(x) + u_j^T(x) C \gamma_{\mu} s_k(x) d_m^T(x) C \gamma_5 c_n(x) \\
&\quad + d_j^T(x) C \gamma_{\mu} s_k(x) u_m^T(x) C \gamma_5 c_n(x)] C \bar{c}_a^T(x), \\
J_{dds, \mu}^{10\frac{1}{2}}(x) &= \frac{\varepsilon^{ila} \varepsilon^{ijk} \varepsilon^{lmn}}{\sqrt{3}} [d_j^T(x) C \gamma_{\mu} d_k(x) s_m^T(x) C \gamma_5 c_n(x) + 2d_j^T(x) C \gamma_{\mu} s_k(x) d_m^T(x) C \gamma_5 c_n(x)] C \bar{c}_a^T(x),
\end{aligned} \tag{306}$$

$$\begin{aligned}
J_{uss,\mu}^{10\frac{1}{2}}(x) &= \frac{\varepsilon^{ila}\varepsilon^{ijk}\varepsilon^{lmn}}{\sqrt{3}} \left[s_j^T(x)C\gamma_\mu s_k(x)u_m^T(x)C\gamma_5 c_n(x) + 2s_j^T(x)C\gamma_\mu u_k(x)s_m^T(x)C\gamma_5 c_n(x) \right] C\bar{c}_a^T(x), \\
J_{dss,\mu}^{10\frac{1}{2}}(x) &= \frac{\varepsilon^{ila}\varepsilon^{ijk}\varepsilon^{lmn}}{\sqrt{3}} \left[s_j^T(x)C\gamma_\mu s_k(x)d_m^T(x)C\gamma_5 c_n(x) + 2s_j^T(x)C\gamma_\mu d_k(x)s_m^T(x)C\gamma_5 c_n(x) \right] C\bar{c}_a^T(x),
\end{aligned} \tag{307}$$

$$J_{sss,\mu}^{10\frac{1}{2}}(x) = \varepsilon^{ila}\varepsilon^{ijk}\varepsilon^{lmn}s_j^T(x)C\gamma_\mu s_k(x)s_m^T(x)C\gamma_5 c_n(x)C\bar{c}_a^T(x), \tag{308}$$

$$\begin{aligned}
J_{uuu,\mu}^{11\frac{1}{2}}(x) &= \varepsilon^{ila}\varepsilon^{ijk}\varepsilon^{lmn}u_j^T(x)C\gamma_\mu u_k(x)u_m^T(x)C\gamma_\alpha c_n(x)\gamma_5\gamma^\alpha C\bar{c}_a^T(x), \\
J_{uud,\mu}^{11\frac{1}{2}}(x) &= \frac{\varepsilon^{ila}\varepsilon^{ijk}\varepsilon^{lmn}}{\sqrt{3}} \left[u_j^T(x)C\gamma_\mu u_k(x)d_m^T(x)C\gamma_\alpha c_n(x) + 2u_j^T(x)C\gamma_\mu d_k(x)u_m^T(x)C\gamma_\alpha c_n(x) \right] \gamma_5\gamma^\alpha C\bar{c}_a^T(x), \\
J_{udd,\mu}^{11\frac{1}{2}}(x) &= \frac{\varepsilon^{ila}\varepsilon^{ijk}\varepsilon^{lmn}}{\sqrt{3}} \left[d_j^T(x)C\gamma_\mu d_k(x)u_m^T(x)C\gamma_\alpha c_n(x) + 2d_j^T(x)C\gamma_\mu u_k(x)d_m^T(x)C\gamma_\alpha c_n(x) \right] \gamma_5\gamma^\alpha C\bar{c}_a^T(x), \\
J_{ddd,\mu}^{11\frac{1}{2}}(x) &= \varepsilon^{ila}\varepsilon^{ijk}\varepsilon^{lmn}d_j^T(x)C\gamma_\mu d_k(x)d_m^T(x)C\gamma_\alpha c_n(x)\gamma_5\gamma^\alpha C\bar{c}_a^T(x),
\end{aligned} \tag{309}$$

$$\begin{aligned}
J_{uus,\mu}^{11\frac{1}{2}}(x) &= \frac{\varepsilon^{ila}\varepsilon^{ijk}\varepsilon^{lmn}}{\sqrt{3}} \left[u_j^T(x)C\gamma_\mu u_k(x)s_m^T(x)C\gamma_\alpha c_n(x) + 2u_j^T(x)C\gamma_\mu s_k(x)u_m^T(x)C\gamma_\alpha c_n(x) \right] \gamma_5\gamma^\alpha C\bar{c}_a^T(x), \\
J_{uds,\mu}^{11\frac{1}{2}}(x) &= \frac{\varepsilon^{ila}\varepsilon^{ijk}\varepsilon^{lmn}}{\sqrt{3}} \left[u_j^T(x)C\gamma_\mu d_k(x)s_m^T(x)C\gamma_\alpha c_n(x) + u_j^T(x)C\gamma_\mu s_k(x)d_m^T(x)C\gamma_\alpha c_n(x) \right. \\
&\quad \left. + d_j^T(x)C\gamma_\mu s_k(x)u_m^T(x)C\gamma_\alpha c_n(x) \right] \gamma_5\gamma^\alpha C\bar{c}_a^T(x), \\
J_{dds,\mu}^{11\frac{1}{2}}(x) &= \frac{\varepsilon^{ila}\varepsilon^{ijk}\varepsilon^{lmn}}{\sqrt{3}} \left[d_j^T(x)C\gamma_\mu d_k(x)s_m^T(x)C\gamma_\alpha c_n(x) + 2d_j^T(x)C\gamma_\mu s_k(x)d_m^T(x)C\gamma_\alpha c_n(x) \right] \gamma_5\gamma^\alpha C\bar{c}_a^T(x),
\end{aligned} \tag{310}$$

$$\begin{aligned}
J_{uss,\mu}^{11\frac{1}{2}}(x) &= \frac{\varepsilon^{ila}\varepsilon^{ijk}\varepsilon^{lmn}}{\sqrt{3}} \left[s_j^T(x)C\gamma_\mu s_k(x)u_m^T(x)C\gamma_\alpha c_n(x) + 2s_j^T(x)C\gamma_\mu u_k(x)s_m^T(x)C\gamma_\alpha c_n(x) \right] \gamma_5\gamma^\alpha C\bar{c}_a^T(x), \\
J_{dss,\mu}^{11\frac{1}{2}}(x) &= \frac{\varepsilon^{ila}\varepsilon^{ijk}\varepsilon^{lmn}}{\sqrt{3}} \left[s_j^T(x)C\gamma_\mu s_k(x)d_m^T(x)C\gamma_\alpha c_n(x) + 2s_j^T(x)C\gamma_\mu d_k(x)s_m^T(x)C\gamma_\alpha c_n(x) \right] \gamma_5\gamma^\alpha C\bar{c}_a^T(x),
\end{aligned} \tag{311}$$

$$J_{sss,\mu}^{11\frac{1}{2}}(x) = \varepsilon^{ila}\varepsilon^{ijk}\varepsilon^{lmn}s_j^T(x)C\gamma_\mu s_k(x)s_m^T(x)C\gamma_\alpha c_n(x)\gamma_5\gamma^\alpha C\bar{c}_a^T(x), \tag{312}$$

$$\begin{aligned}
J_{uuu,\mu}^{11\frac{3}{2}}(x) &= \varepsilon^{ila}\varepsilon^{ijk}\varepsilon^{lmn}u_j^T(x)C\gamma_\alpha u_k(x)u_m^T(x)C\gamma_\mu c_n(x)\gamma_5\gamma^\alpha C\bar{c}_a^T(x), \\
J_{uud,\mu}^{11\frac{3}{2}}(x) &= \frac{\varepsilon^{ila}\varepsilon^{ijk}\varepsilon^{lmn}}{\sqrt{3}} \left[u_j^T(x)C\gamma_\alpha u_k(x)d_m^T(x)C\gamma_\mu c_n(x) + 2u_j^T(x)C\gamma_\alpha d_k(x)u_m^T(x)C\gamma_\mu c_n(x) \right] \gamma_5\gamma^\alpha C\bar{c}_a^T(x), \\
J_{udd,\mu}^{11\frac{3}{2}}(x) &= \frac{\varepsilon^{ila}\varepsilon^{ijk}\varepsilon^{lmn}}{\sqrt{3}} \left[d_j^T(x)C\gamma_\alpha d_k(x)u_m^T(x)C\gamma_\mu c_n(x) + 2d_j^T(x)C\gamma_\alpha u_k(x)d_m^T(x)C\gamma_\mu c_n(x) \right] \gamma_5\gamma^\alpha C\bar{c}_a^T(x), \\
J_{ddd,\mu}^{11\frac{3}{2}}(x) &= \varepsilon^{ila}\varepsilon^{ijk}\varepsilon^{lmn}d_j^T(x)C\gamma_\alpha d_k(x)d_m^T(x)C\gamma_\mu c_n(x)\gamma_5\gamma^\alpha C\bar{c}_a^T(x),
\end{aligned} \tag{313}$$

$$\begin{aligned}
J_{uus,\mu}^{11\frac{3}{2}}(x) &= \frac{\varepsilon^{ila}\varepsilon^{ijk}\varepsilon^{lmn}}{\sqrt{3}} [u_j^T(x)C\gamma_\alpha u_k(x)s_m^T(x)C\gamma_\mu c_n(x) + 2u_j^T(x)C\gamma_\alpha s_k(x)u_m^T(x)C\gamma_\mu c_n(x)] \gamma_5\gamma^\alpha C\bar{c}_a^T(x), \\
J_{uds,\mu}^{11\frac{3}{2}}(x) &= \frac{\varepsilon^{ila}\varepsilon^{ijk}\varepsilon^{lmn}}{\sqrt{3}} [u_j^T(x)C\gamma_\alpha d_k(x)s_m^T(x)C\gamma_\mu c_n(x) + u_j^T(x)C\gamma_\alpha s_k(x)d_m^T(x)C\gamma_\mu c_n(x) \\
&\quad + d_j^T(x)C\gamma_\alpha s_k(x)u_m^T(x)C\gamma_\mu c_n(x)] \gamma_5\gamma^\alpha C\bar{c}_a^T(x), \\
J_{dds,\mu}^{11\frac{3}{2}}(x) &= \frac{\varepsilon^{ila}\varepsilon^{ijk}\varepsilon^{lmn}}{\sqrt{3}} [d_j^T(x)C\gamma_\alpha d_k(x)s_m^T(x)C\gamma_\mu c_n(x) + 2d_j^T(x)C\gamma_\alpha s_k(x)d_m^T(x)C\gamma_\mu c_n(x)] \gamma_5\gamma^\alpha C\bar{c}_a^T(x),
\end{aligned} \tag{314}$$

$$\begin{aligned}
J_{uss,\mu}^{11\frac{3}{2}}(x) &= \frac{\varepsilon^{ila}\varepsilon^{ijk}\varepsilon^{lmn}}{\sqrt{3}} [s_j^T(x)C\gamma_\alpha s_k(x)u_m^T(x)C\gamma_\mu c_n(x) + 2s_j^T(x)C\gamma_\alpha u_k(x)s_m^T(x)C\gamma_\mu c_n(x)] \gamma_5\gamma^\alpha C\bar{c}_a^T(x), \\
J_{dss,\mu}^{11\frac{3}{2}}(x) &= \frac{\varepsilon^{ila}\varepsilon^{ijk}\varepsilon^{lmn}}{\sqrt{3}} [s_j^T(x)C\gamma_\alpha s_k(x)d_m^T(x)C\gamma_\mu c_n(x) + 2s_j^T(x)C\gamma_\alpha d_k(x)s_m^T(x)C\gamma_\mu c_n(x)] \gamma_5\gamma^\alpha C\bar{c}_a^T(x),
\end{aligned} \tag{315}$$

$$J_{sss,\mu}^{11\frac{3}{2}}(x) = \varepsilon^{ila}\varepsilon^{ijk}\varepsilon^{lmn}s_j^T(x)C\gamma_\alpha s_k(x)s_m^T(x)C\gamma_\mu c_n(x)\gamma_5\gamma^\alpha C\bar{c}_a^T(x). \tag{316}$$

We take the isospin limit and classify the thirty currents couple potentially to the hidden-charm pentaquark states with degenerate masses into the following twelve types,

$$\begin{aligned}
&J_{uuu,\mu}^{10\frac{1}{2}}(x), J_{uud,\mu}^{10\frac{1}{2}}(x), J_{udd,\mu}^{10\frac{1}{2}}(x), J_{ddd,\mu}^{10\frac{1}{2}}(x); \\
&J_{uus,\mu}^{10\frac{1}{2}}(x), J_{uds,\mu}^{10\frac{1}{2}}(x), J_{dds,\mu}^{10\frac{1}{2}}(x); \\
&J_{uss,\mu}^{10\frac{1}{2}}(x), J_{dss,\mu}^{10\frac{1}{2}}(x); \\
&J_{sss,\mu}^{10\frac{1}{2}}(x); \\
&J_{uuu,\mu}^{11\frac{1}{2}}(x), J_{uud,\mu}^{11\frac{1}{2}}(x), J_{udd,\mu}^{11\frac{1}{2}}(x), J_{ddd,\mu}^{11\frac{1}{2}}(x); \\
&J_{uus,\mu}^{11\frac{1}{2}}(x), J_{uds,\mu}^{11\frac{1}{2}}(x), J_{dds,\mu}^{11\frac{1}{2}}(x); \\
&J_{uss,\mu}^{11\frac{1}{2}}(x), J_{dss,\mu}^{11\frac{1}{2}}(x); \\
&J_{sss,\mu}^{11\frac{1}{2}}(x); \\
&J_{uuu,\mu}^{11\frac{3}{2}}(x), J_{uud,\mu}^{11\frac{3}{2}}(x), J_{udd,\mu}^{11\frac{3}{2}}(x), J_{ddd,\mu}^{11\frac{3}{2}}(x); \\
&J_{uus,\mu}^{11\frac{3}{2}}(x), J_{uds,\mu}^{11\frac{3}{2}}(x), J_{dds,\mu}^{11\frac{3}{2}}(x); \\
&J_{uss,\mu}^{11\frac{3}{2}}(x), J_{dss,\mu}^{11\frac{3}{2}}(x); \\
&J_{sss,\mu}^{11\frac{3}{2}}(x),
\end{aligned} \tag{317}$$

and perform the operator product expansion up to the vacuum condensates of dimension 10 to obtain the QCD sum rules, the predictions are presented in Table 62 in the Appendix.

According to Figs.26-27, the vacuum condensates of the dimensions 11 and 13 play an important role, we should update the old calculations, just like in Ref.[402].

In Ref.[514], we extend our previous works [402, 703] to explore the possible assignment of the $P_{cs}(4459)$ as the $[ud][sc]\bar{c}$ (0, 0, 0, $\frac{1}{2}$) pentaquark state with the spin-parity $J^P = \frac{1}{2}^-$. We choose

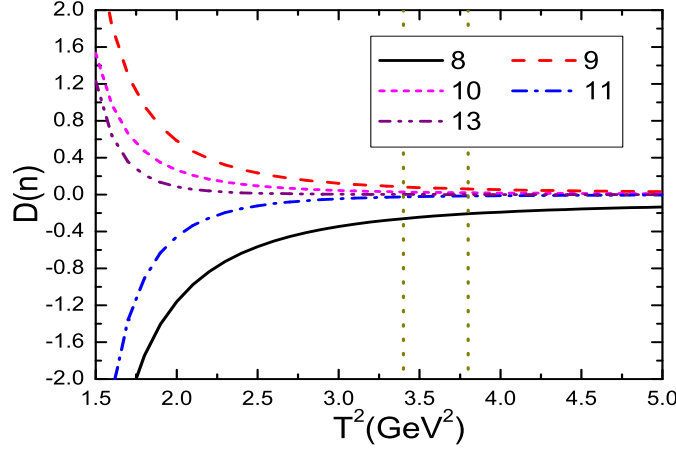


Figure 28: The contributions of the higher dimensional vacuum condensates $D(n)$ with variation of the Borel parameter T^2 , where the $n = 8, 9, 10, 11$ and 13 , the region between the two vertical lines is the Borel window.

the current $J(x)$ and carry out the operator product expansion up to the vacuum condensates of dimension 13, where

$$J(x) = \varepsilon^{ila} \varepsilon^{ijk} \varepsilon^{lmn} u_j^T(x) C \gamma_5 d_k(x) s_m^T(x) C \gamma_5 c_n(x) C \bar{c}_a^T(x). \quad (318)$$

In calculations, we take the modified energy scale formula $\mu = \sqrt{M_P - (2\mathbb{M}_c)^2} - m_s(\mu) = 2.4 \text{ GeV}$ to constraint the QCD spectral densities.

We obtain the Borel window $T^2 = 3.4 - 3.8 \text{ GeV}^2$ via trial and error, the pole contribution is about $(40 - 61)\%$, which is large enough to extract the pentaquark mass reliably. In Fig.28, we plot the contributions of the higher dimensional vacuum condensates with variation of the Borel parameter T^2 . The higher dimensional vacuum condensates manifest themselves at the region $T^2 < 2.5 \text{ GeV}^2$, we should choose the value $T^2 > 2.5 \text{ GeV}^2$. Their values decrease monotonously and quickly with the increase of the Borel parameter, in the Borel window $T^2 = 3.4 - 3.8 \text{ GeV}^2$, the contributions of the higher dimensional vacuum condensates are $D(8) = -(21 - 26)\%$, $D(9) = (6 - 8)\%$, $D(10) = (2 - 3)\%$, $D(11) = -(1 - 2)\%$, $D(13) \ll 1\%$, the convergent behavior is very good [514].

In Fig.29, we plot the predicted pentaquark mass with variation of the Borel parameter T^2 with the truncations of the operator product expansion up to the vacuum condensates of dimensions $n = 10$ and 13 , respectively. From the figure, we can see explicitly that the vacuum condensates of dimensions 11 and 13 play an important role to obtain the flat platform, we should take them into account in a consistent way, just like in the case of Ref.[402], where no s -quark is present. All in all, the higher dimensional vacuum condensates play an important role in obtaining the flat platform, especially those associated with the inverse Borel parameters $\frac{1}{T^2}$, $\frac{1}{T^4}$, $\frac{1}{T^6}$ and $\frac{1}{T^8}$.

At last, we obtain the mass and pole residue [514],

$$\begin{aligned} M_P &= 4.47 \pm 0.11 \text{ GeV}, \\ \lambda_P &= (1.86 \pm 0.31) \times 10^{-3} \text{ GeV}^6. \end{aligned} \quad (319)$$

The predicted mass $M_P = 4.47 \pm 0.11 \text{ GeV}$ is in excellent agreement with the experimental data $4458.8 \pm 2.9_{-1.1}^{+4.7} \text{ MeV}$ from the LHCb collaboration [198], and supports assigning the $P_{cs}(4459)$ as the $[ud][sc]\bar{c}$ $(0, 0, 0, \frac{1}{2})$ pentaquark state with the spin-parity $J^P = \frac{1}{2}^-$. In Ref.[402], we

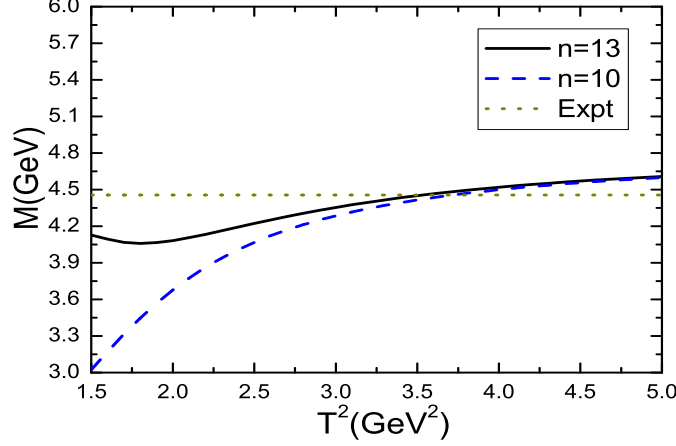


Figure 29: The predicted mass with variation of the Borel parameter T^2 , where the $n = 10$ and 13 denote truncations of the operator product expansion, the expt denotes the experimental value of the mass of the $P_{cs}(4459)$.

observe that the $P_c(4312)$ can be assigned to be the $[ud][uc]\bar{c}$ $(0, 0, 0, \frac{1}{2})$ pentaquark state with the spin-parity $J^P = \frac{1}{2}^-$. The light-flavor $SU(3)$ mass-breaking effect is about $\Delta = m_s = 147$ MeV, the estimations presented in Table 52 are reasonable and reliable, where we take the experimental value of the mass of the $P_{cs}(4459)$. In Refs.[704, 705], we study the $J^P = \frac{1}{2}^\pm$ and $\frac{3}{2}^\pm$ hidden-charm pentaquark states with the strangeness $S = 0, -1, -2$ and -3 in a systematic way by carrying out the operator product expansion up to the vacuum condensates of dimension 10 and choosing the old value $\mathbb{M}_c = 1.80$ GeV, and observe that the light-flavor $SU(3)$ mass-breaking effects are $\Delta = (90 - 130)$ MeV for the negative-parity pentaquark states. The new analysis supports a larger light-flavor $SU(3)$ mass-breaking effect.

We can extend this section directly to study the $\bar{3}\bar{3}\bar{3}$ type triply-heavy pentaquark states [709].

5.2 11 type pentaquark states

In Ref.[710], Chen et al construct the color singlet-singlet type currents,

$$\begin{aligned} J_\mu^{\bar{D}^*\Sigma_c}(x) &= \bar{c}(x)\gamma_\mu d(x)\varepsilon^{ijk}u_i^T(x)C\gamma_\nu u_j(x)\gamma^\nu\gamma_5 c_k(x), \\ J_\mu^{\bar{D}\Sigma_c^*}(x) &= \bar{c}(x)\gamma_5 d(x)\varepsilon^{ijk}u_i^T(x)C\gamma_\mu u_j(x)c_k(x), \end{aligned} \quad (320)$$

$$\begin{aligned} J_\mu^{\bar{D}^*\Sigma_c^*}(x) &= \bar{c}(x)\gamma_\mu d(x)\varepsilon^{ijk}u_i^T(x)C\gamma_\nu u_j(x)\gamma_5 c_k(x) + (\mu \leftrightarrow \nu), \\ J_\mu^{\bar{D}\Sigma_c^*}(x) &= \bar{c}(x)\gamma_\mu\gamma_5 d(x)\varepsilon^{ijk}u_i^T(x)C\gamma_\nu u_j(x)c_k(x) + (\mu \leftrightarrow \nu), \\ J_\mu^{\bar{D}^*\Lambda_c}(x) &= \bar{c}(x)\gamma_\mu u(x)\varepsilon^{ijk}u_i^T(x)C\gamma_\nu\gamma_5 d_j(x)c(x) + (\mu \leftrightarrow \nu), \end{aligned} \quad (321)$$

for the first time, and take the currents $J_\mu^{\bar{D}^*\Sigma_c}(x)$ and $J_\mu^{\bar{D}\Sigma_c^*}(x)$ to study the $P_c(4380)$ and $P_c(4450)$ by carrying out the operator product expansion up to the vacuum condensates of dimension 8. Thereafter, the **11** type currents were used to interpolate the pentaquark molecular states [418, 487, 711, 712, 713, 714, 715, 716, 717, 718, 719]. However, in those works, the isospins of the currents are not specified and should be improved, as the two-body strong decays to the final states $J/\psi p$ and $J/\psi \Lambda$ conserve isospins.

$[qq'] [q''\bar{c}] \bar{c} (S_L, S_H, J_{LH}, J)$	New analysis [402]	u or $d \rightarrow s$	Assignments
$[ud][uc]\bar{c} (0, 0, 0, \frac{1}{2})$	4.31 ± 0.11	4.46 ± 0.11	? $P_{cs}(4459)$
$[ud][uc]\bar{c} (0, 1, 1, \frac{1}{2})$	4.45 ± 0.11	4.60 ± 0.11	
$[uu][dc]\bar{c} + 2[ud][uc]\bar{c} (1, 0, 1, \frac{1}{2})$	4.46 ± 0.11	4.61 ± 0.11	
$[uu][dc]\bar{c} + 2[ud][uc]\bar{c} (1, 1, 0, \frac{1}{2})$	4.34 ± 0.14	4.49 ± 0.14	
$[ud][uc]\bar{c} (0, 1, 1, \frac{3}{2})$	4.39 ± 0.11	4.54 ± 0.11	
$[uu][dc]\bar{c} + 2[ud][uc]\bar{c} (1, 0, 1, \frac{3}{2})$	4.47 ± 0.11	4.62 ± 0.11	
$[uu][dc]\bar{c} + 2[ud][uc]\bar{c} (1, 1, 2, \frac{3}{2})$	4.61 ± 0.11	4.76 ± 0.11	
$[uu][dc]\bar{c} + 2[ud][uc]\bar{c} (1, 1, 2, \frac{5}{2})$	4.52 ± 0.11	4.67 ± 0.11	
$[uu][dc]\bar{c} + 2[ud][uc]\bar{c} (1, 1, 2, \frac{5}{2})$	4.39 ± 0.11	4.54 ± 0.11	
$[ud][uc]\bar{c} (0, 1, 1, \frac{5}{2})$	4.39 ± 0.11	4.54 ± 0.11	

Table 52: The masses (in unit of GeV) of the pentaquark states with the strangeness $S = -1$, where the S_L and S_H denote the spins of the light and heavy diquarks respectively, $\vec{J}_{LH} = \vec{S}_L + \vec{S}_H$, $\vec{J} = \vec{J}_{LH} + \vec{J}_{\bar{c}}$, the $\vec{J}_{\bar{c}}$ is the angular momentum of the \bar{c} -quark [514].

The u and d quarks have the isospin $I = \frac{1}{2}$, i.e. $\hat{I}u = \frac{1}{2}u$ and $\hat{I}d = -\frac{1}{2}d$, where the \hat{I} is the isospin operator. Then the \bar{D}^0 , \bar{D}^{*0} , \bar{D}^- , \bar{D}^{*-} , \bar{D}_s^- , \bar{D}_s^{*-} , Σ_c^+ , Σ_c^{*+} , Σ_c^{++} , Σ_c^{*++} , $\Xi_c'^0$, $\Xi_c'^*$, $\Xi_c'^+$, $\Xi_c'^{*+}$, Ξ_c^0 , Ξ_c^{*0} , Ξ_c^+ and Λ_c^+ correspond to the eigenstates $|\frac{1}{2}, \frac{1}{2}\rangle$, $|\frac{1}{2}, \frac{1}{2}\rangle$, $|\frac{1}{2}, -\frac{1}{2}\rangle$, $|\frac{1}{2}, -\frac{1}{2}\rangle$, $|\frac{1}{2}, -\frac{1}{2}\rangle$, $|\frac{1}{2}, -\frac{1}{2}\rangle$, $|0, 0\rangle$, $|0, 0\rangle$, $|1, 0\rangle$, $|1, 0\rangle$, $|1, 1\rangle$, $|1, 1\rangle$, $|\frac{1}{2}, -\frac{1}{2}\rangle$, $|\frac{1}{2}, -\frac{1}{2}\rangle$, $|\frac{1}{2}, \frac{1}{2}\rangle$, $|\frac{1}{2}, \frac{1}{2}\rangle$, $|\frac{1}{2}, -\frac{1}{2}\rangle$, $|\frac{1}{2}, \frac{1}{2}\rangle$ and $|0, 0\rangle$ in the isospin space $|I, I_3\rangle$, respectively. We construct the color-singlet currents to interpolate them,

$$\begin{aligned}
J^{\bar{D}^{0/-}}(x) &= \bar{c}(x)i\gamma_5 u/d(x), \\
J^{\bar{D}_s^-}(x) &= \bar{c}(x)i\gamma_5 s(x), \\
J_\mu^{\bar{D}^{*0/-}}(x) &= \bar{c}(x)\gamma_\mu u/d(x), \\
J_\mu^{\bar{D}_s^{*-}}(x) &= \bar{c}(x)\gamma_\mu s(x),
\end{aligned} \tag{322}$$

$$\begin{aligned}
J^{\Sigma_c^+}(x) &= \varepsilon^{ijk} u_i^T(x) C \gamma_\mu d_j(x) \gamma^\mu \gamma_5 c_k(x), \\
J^{\Sigma_c^{*+}}(x) &= \varepsilon^{ijk} u_i^T(x) C \gamma_\mu u_j(x) \gamma^\mu \gamma_5 c_k(x), \\
J_\mu^{\Sigma_c^{*+}}(x) &= \varepsilon^{ijk} u_i^T(x) C \gamma_\mu d_j(x) c_k(x), \\
J_\mu^{\Sigma_c^{*++}}(x) &= \varepsilon^{ijk} u_i^T(x) C \gamma_\mu u_j(x) c_k(x),
\end{aligned} \tag{323}$$

$$\begin{aligned}
J^{\Xi_c'^0}(x) &= \varepsilon^{ijk} d_i^T(x) C \gamma_\mu s_j(x) \gamma^\mu \gamma_5 c_k(x), \\
J_\mu^{\Xi_c'^0}(x) &= \varepsilon^{ijk} d_i^T(x) C \gamma_\mu s_j(x) c_k(x), \\
J^{\Xi_c'^+}(x) &= \varepsilon^{ijk} u_i^T(x) C \gamma_\mu s_j(x) \gamma^\mu \gamma_5 c_k(x), \\
J_\mu^{\Xi_c'^+}(x) &= \varepsilon^{ijk} u_i^T(x) C \gamma_\mu s_j(x) c_k(x),
\end{aligned} \tag{324}$$

$$\begin{aligned}
J^{\Xi_c^0}(x) &= \varepsilon^{ijk} d_i^T(x) C \gamma_5 s_j(x) c_k(x), \\
J^{\Xi_c^+}(x) &= \varepsilon^{ijk} u_i^T(x) C \gamma_5 s_j(x) c_k(x), \\
J^{\Lambda_c^+}(x) &= \varepsilon^{ijk} u_i^T(x) C \gamma_5 d_j(x) c_k(x).
\end{aligned} \tag{325}$$

Accordingly, we construct the **11** type five-quark currents to interpolate the $\bar{D}^{(*)}\Sigma_c^{(*)}$, $\bar{D}^{(*)}\Xi_c^{(*)}$, $\bar{D}^{(*)}\Xi'_c$ and $\bar{D}^{(*)}\Lambda_c$ type pentaquark states, where the $\bar{D}^{(*)}$, $\Sigma_c^{(*)}$, $\Xi_c^{(*)}$, Ξ'_c and Λ_c represent the color-singlet clusters having the same quantum numbers as the physical states $\bar{D}^{(*)}$, $\Sigma_c^{(*)}$, $\Xi_c^{(*)}$, Ξ'_c and Λ_c respectively except for the masses,

$$\begin{aligned}
J(x) &= J_{\frac{1}{2}}^{\bar{D}\Sigma_c}(x), J_{\frac{3}{2}}^{\bar{D}\Sigma_c}(x), J_0^{\bar{D}\Xi'_c}(x), J_1^{\bar{D}\Xi'_c}(x), \\
&\quad J_0^{\bar{D}\Xi_c}(x), J_1^{\bar{D}\Xi_c}(x), J_{\frac{1}{2}}^{\bar{D}\Lambda_c}(x), J_{\frac{1}{2}}^{\bar{D}_s\Xi_c}(x), J_0^{\bar{D}_s\Lambda_c}(x), \\
J_\mu(x) &= J_{\frac{1}{2};\mu}^{\bar{D}\Sigma_c^*}(x), J_{\frac{3}{2};\mu}^{\bar{D}\Sigma_c^*}(x), J_{\frac{1}{2};\mu}^{\bar{D}^*\Sigma_c}(x), J_{\frac{3}{2};\mu}^{\bar{D}^*\Sigma_c}(x), \\
&\quad J_{0;\mu}^{\bar{D}\Xi_c^*}(x), J_{1;\mu}^{\bar{D}\Xi_c^*}(x), J_{0;\mu}^{\bar{D}^*\Xi'_c}(x), J_{1;\mu}^{\bar{D}^*\Xi'_c}(x), \\
&\quad J_{0;\mu}^{\bar{D}^*\Xi_c}(x), J_{1;\mu}^{\bar{D}^*\Xi_c}(x), J_{\frac{1}{2};\mu}^{\bar{D}^*\Lambda_c}(x), J_{\frac{1}{2};\mu}^{\bar{D}_s^*\Xi_c}(x), J_{0;\mu}^{\bar{D}_s^*\Lambda_c}(x), \\
J_{\mu\nu}(x) &= J_{\frac{1}{2};\mu\nu}^{\bar{D}^*\Sigma_c^*}(x), J_{\frac{3}{2};\mu\nu}^{\bar{D}^*\Sigma_c^*}(x), J_{0;\mu\nu}^{\bar{D}^*\Xi'_c}(x), J_{1;\mu\nu}^{\bar{D}^*\Xi'_c}(x),
\end{aligned} \tag{326}$$

$$\begin{aligned}
J_{\frac{1}{2}}^{\bar{D}\Sigma_c}(x) &= \frac{1}{\sqrt{3}}J^{\bar{D}^0}(x)J^{\Sigma_c^+}(x) - \sqrt{\frac{2}{3}}J^{\bar{D}^-}(x)J^{\Sigma_c^{++}}(x), \\
J_{\frac{3}{2}}^{\bar{D}\Sigma_c}(x) &= \sqrt{\frac{2}{3}}J^{\bar{D}^0}(x)J^{\Sigma_c^+}(x) + \frac{1}{\sqrt{3}}J^{\bar{D}^-}(x)J^{\Sigma_c^{++}}(x), \\
J_{\frac{1}{2};\mu}^{\bar{D}\Sigma_c^*}(x) &= \frac{1}{\sqrt{3}}J^{\bar{D}^0}(x)J_\mu^{\Sigma_c^{*+}}(x) - \sqrt{\frac{2}{3}}J^{\bar{D}^-}(x)J_\mu^{\Sigma_c^{*++}}(x), \\
J_{\frac{3}{2};\mu}^{\bar{D}\Sigma_c^*}(x) &= \sqrt{\frac{2}{3}}J^{\bar{D}^0}(x)J_\mu^{\Sigma_c^{*+}}(x) + \frac{1}{\sqrt{3}}J^{\bar{D}^-}(x)J_\mu^{\Sigma_c^{*++}}(x),
\end{aligned} \tag{327}$$

$$\begin{aligned}
J_{\frac{1}{2};\mu}^{\bar{D}^*\Sigma_c}(x) &= \frac{1}{\sqrt{3}}J_\mu^{\bar{D}^{*0}}(x)J^{\Sigma_c^+}(x) - \sqrt{\frac{2}{3}}J_\mu^{\bar{D}^{*-}}(x)J^{\Sigma_c^{++}}(x), \\
J_{\frac{3}{2};\mu}^{\bar{D}^*\Sigma_c}(x) &= \sqrt{\frac{2}{3}}J_\mu^{\bar{D}^{*0}}(x)J^{\Sigma_c^+}(x) + \frac{1}{\sqrt{3}}J_\mu^{\bar{D}^{*-}}(x)J^{\Sigma_c^{++}}(x), \\
J_{\frac{1}{2};\mu\nu}^{\bar{D}^*\Sigma_c^*}(x) &= \frac{1}{\sqrt{3}}J_\mu^{\bar{D}^{*0}}(x)J_\nu^{\Sigma_c^{*+}}(x) - \sqrt{\frac{2}{3}}J_\mu^{\bar{D}^{*-}}(x)J_\nu^{\Sigma_c^{*++}}(x) + (\mu \leftrightarrow \nu), \\
J_{\frac{3}{2};\mu\nu}^{\bar{D}^*\Sigma_c^*}(x) &= \sqrt{\frac{2}{3}}J_\mu^{\bar{D}^{*0}}(x)J_\nu^{\Sigma_c^{*+}}(x) + \frac{1}{\sqrt{3}}J_\mu^{\bar{D}^{*-}}(x)J_\nu^{\Sigma_c^{*++}}(x) + (\mu \leftrightarrow \nu),
\end{aligned} \tag{328}$$

$$\begin{aligned}
J_0^{\bar{D}\Xi'_c}(x) &= \frac{1}{\sqrt{2}}J^{\bar{D}^0}(x)J^{\Xi_c'^0}(x) - \frac{1}{\sqrt{2}}J^{\bar{D}^-}(x)J^{\Xi_c'^+}(x), \\
J_1^{\bar{D}\Xi'_c}(x) &= \frac{1}{\sqrt{2}}J^{\bar{D}^0}(x)J^{\Xi_c'^0}(x) + \frac{1}{\sqrt{2}}J^{\bar{D}^-}(x)J^{\Xi_c'^+}(x), \\
J_{0;\mu}^{\bar{D}\Xi_c^*}(x) &= \frac{1}{\sqrt{2}}J^{\bar{D}^0}(x)J_\mu^{\Xi_c^{*0}}(x) - \frac{1}{\sqrt{2}}J^{\bar{D}^-}(x)J_\mu^{\Xi_c^{*+}}(x), \\
J_{1;\mu}^{\bar{D}\Xi_c^*}(x) &= \frac{1}{\sqrt{2}}J^{\bar{D}^0}(x)J_\mu^{\Xi_c^{*0}}(x) + \frac{1}{\sqrt{2}}J^{\bar{D}^-}(x)J_\mu^{\Xi_c^{*+}}(x),
\end{aligned} \tag{329}$$

$$\begin{aligned}
J_{0;\mu}^{\bar{D}^*\Xi'_c}(x) &= \frac{1}{\sqrt{2}}J_{\mu}^{\bar{D}^*0}(x)J^{\Xi'^0}_c(x) - \frac{1}{\sqrt{2}}J_{\mu}^{\bar{D}^{*-}}(x)J^{\Xi'^+}_c(x), \\
J_{1;\mu}^{\bar{D}^*\Xi'_c}(x) &= \frac{1}{\sqrt{2}}J_{\mu}^{\bar{D}^*0}(x)J^{\Xi'^0}_c(x) + \frac{1}{\sqrt{2}}J_{\mu}^{\bar{D}^{*-}}(x)J^{\Xi'^+}_c(x), \\
J_{0;\mu\nu}^{\bar{D}^*\Xi_c^*}(x) &= \frac{1}{\sqrt{2}}J_{\mu}^{\bar{D}^*0}(x)J_{\nu}^{\Xi_c^{*0}}(x) - \frac{1}{\sqrt{2}}J_{\mu}^{\bar{D}^{*-}}(x)J_{\nu}^{\Xi_c^{*+}}(x) + (\mu \leftrightarrow \nu), \\
J_{1;\mu\nu}^{\bar{D}^*\Xi_c^*}(x) &= \frac{1}{\sqrt{2}}J_{\mu}^{\bar{D}^*0}(x)J_{\nu}^{\Xi_c^{*0}}(x) + \frac{1}{\sqrt{2}}J_{\mu}^{\bar{D}^{*-}}(x)J_{\nu}^{\Xi_c^{*+}}(x) + (\mu \leftrightarrow \nu), \tag{330}
\end{aligned}$$

$$\begin{aligned}
J_0^{\bar{D}\Xi_c}(x) &= \frac{1}{\sqrt{2}}J^{\bar{D}^0}(x)J^{\Xi_c^0}(x) - \frac{1}{\sqrt{2}}J^{\bar{D}^-}(x)J^{\Xi_c^+}(x), \\
J_1^{\bar{D}\Xi_c}(x) &= \frac{1}{\sqrt{2}}J^{\bar{D}^0}(x)J^{\Xi_c^0}(x) + \frac{1}{\sqrt{2}}J^{\bar{D}^-}(x)J^{\Xi_c^+}(x), \\
J_{\frac{1}{2}}^{\bar{D}\Lambda_c}(x) &= J^{\bar{D}^0}(x)J^{\Lambda_c^+}(x), \\
J_{\frac{1}{2}}^{\bar{D}_s\Xi_c}(x) &= J^{\bar{D}_s^-}(x)J^{\Xi_c^+}(x), \\
J_0^{\bar{D}_s\Lambda_c}(x) &= J^{\bar{D}_s^-}(x)J^{\Lambda_c^+}(x), \tag{331}
\end{aligned}$$

$$\begin{aligned}
J_{0;\mu}^{\bar{D}^*\Xi_c}(x) &= \frac{1}{\sqrt{2}}J_{\mu}^{\bar{D}^*0}(x)J^{\Xi_c^0}(x) - \frac{1}{\sqrt{2}}J_{\mu}^{\bar{D}^{*-}}(x)J^{\Xi_c^+}(x), \\
J_{1;\mu}^{\bar{D}^*\Xi_c}(x) &= \frac{1}{\sqrt{2}}J_{\mu}^{\bar{D}^*0}(x)J^{\Xi_c^0}(x) + \frac{1}{\sqrt{2}}J_{\mu}^{\bar{D}^{*-}}(x)J^{\Xi_c^+}(x), \\
J_{\frac{1}{2};\mu}^{\bar{D}^*\Lambda_c}(x) &= J_{\mu}^{\bar{D}^*0}(x)J^{\Lambda_c^+}(x), \\
J_{\frac{1}{2};\mu}^{\bar{D}_s^*\Xi_c}(x) &= J_{\mu}^{\bar{D}_s^{*-}}(x)J^{\Xi_c^+}(x), \\
J_{0;\mu}^{\bar{D}_s^*\Lambda_c}(x) &= J_{\mu}^{\bar{D}_s^{*-}}(x)J^{\Lambda_c^+}(x), \tag{332}
\end{aligned}$$

the subscripts $\frac{1}{2}$, $\frac{3}{2}$, 0 and 1 represent the isospins I [418, 720, 721, 722]. They are the isospin eigenstates $|I, I_3\rangle = |\frac{1}{2}, \frac{1}{2}\rangle$, $|\frac{3}{2}, \frac{1}{2}\rangle$, $|1, 0\rangle$ or $|0, 0\rangle$.

For example, from Eq.(327), we obtain the relations,

$$\begin{aligned}
J^{\bar{D}^0}(x)J^{\Sigma_c^+}(x) &= \frac{1}{\sqrt{3}}J_{\frac{1}{2}}^{\bar{D}\Sigma_c}(x) + \sqrt{\frac{2}{3}}J_{\frac{3}{2}}^{\bar{D}\Sigma_c}(x), \\
J^{\bar{D}^-}(x)J^{\Sigma_c^{++}}(x) &= \frac{1}{\sqrt{3}}J_{\frac{3}{2}}^{\bar{D}\Sigma_c}(x) - \sqrt{\frac{2}{3}}J_{\frac{1}{2}}^{\bar{D}\Sigma_c}(x), \tag{333}
\end{aligned}$$

the currents $J^{\bar{D}^0}(x)J^{\Sigma_c^+}(x)$ and $J^{\bar{D}^-}(x)J^{\Sigma_c^{++}}(x)$ have both the isospin $(I, I_3) = (\frac{1}{2}, \frac{1}{2})$ and $(\frac{3}{2}, \frac{1}{2})$ components, and couple potentially to the pentaquark molecular states with the isospins $(\frac{1}{2}, \frac{1}{2})$ and $(\frac{3}{2}, \frac{1}{2})$, which decay to the final states $J/\psi p$ and $J/\psi \Delta^+$, respectively. As the $P_c(4312)$, $\bar{P}_c(4380)$, $P_c(4440)$, $P_c(4457)$ and $P_c(4337)$ are observed in the $J/\psi p$ mass spectrum, it is better to choose the current $J_{\frac{1}{2}}^{\bar{D}\Sigma_c}(x)$ with the definite isospin, we prefer the color singlet-singlet type currents with the definite isospins [418, 720, 721, 722], and thereafter those currents are adopted in Refs.[723, 724, 725]. Although the mass splitting between the isospin cousins is of several 10-MeV in most cases, in some cases, the mass splitting can be as large as 150 MeV, see Table 54. Phenomenologically, the molecule-type P states have been studied extensively with the help of heavy quark symmetry

[214, 257, 268, 269, 277, 287, 288, 289, 726, 727, 728, 729, 730, 731, 732, 733, 734, 735, 736, 737, 738], it is more easy to apply isospin eigenstates in the effective field theory than in QCD.

We resort to the correlation functions $\Pi(p)$, $\Pi_{\mu\nu}(p)$ and $\Pi_{\mu\alpha\beta}(p)$ in Eq.(269), and perform analogous analysis to obtain the QCD sum rules for the masses and pole residues like Eqs.(284)-(285),

$$2M_- \lambda_j^{-2} \exp\left(-\frac{M_-^2}{T^2}\right) = \int_{4m_c^2}^{s_0} ds \rho_{QCD,j}(s) \exp\left(-\frac{s}{T^2}\right), \quad (334)$$

$$M_-^2 = \frac{-\int_{4m_c^2}^{s_0} ds \frac{d}{d(1/T^2)} \rho_{QCD,j}(s) \exp\left(-\frac{s}{T^2}\right)}{\int_{4m_c^2}^{s_0} ds \rho_{QCD,j}(s) \exp\left(-\frac{s}{T^2}\right)}, \quad (335)$$

where $j = \frac{1}{2}, \frac{3}{2}$ and $\frac{5}{2}$, the pole residues are defined analogous to Eqs.(272)-(274).

As we study the **11** type pentaquark states, it is better to choose the updated values $\mathbb{M}_c = 1.85 \pm 0.01$ GeV and $\mathbb{M}_s = 0.2$ GeV to determine the optimal energy scales of the QCD spectral densities with the formula [641],

$$\mu = \sqrt{M_{X/Y/Z/P}^2 - (2\mathbb{M}_c)^2 - k\mathbb{M}_s}. \quad (336)$$

After trial and error, we obtain the Borel windows, continuum threshold parameters, energy scales and pole contributions, see Table 53 [720, 721, 722], the pole contributions are about or slightly larger than (40–60)%, we obtain the **largest pole contributions** up to now. In the Borel windows, the highest dimensional condensate contributions $|D(12)|$ and $|D(13)|$ are approximately zero, the most important contributions are mainly from the lowest order contributions $\langle \bar{q}q \rangle$, $\langle \bar{q}q \rangle^2$ and $\langle \bar{q}q_s \sigma G q \rangle \langle \bar{q}q \rangle$. The operator product expansion converges very well.

Then we calculate the uncertainties of the masses and pole residues, which are shown in Table 54 [720, 721, 722]. The central value of the mass of the $\bar{D}\Sigma_c$ molecular state with the $IJ^P = \frac{1}{2}\frac{1}{2}^-$ is 4.31 GeV, it is only about 10 MeV below the $\bar{D}^0\Sigma_c^+$ threshold, we assign it as the $P_c(4312)$ tentatively. For the $\bar{D}\Sigma_c$ molecular state with the $IJ^P = \frac{3}{2}\frac{1}{2}^-$, the central value of the mass is 4.33 GeV, which is about 10 MeV above the $\bar{D}^-\Sigma_c^{++}$ threshold, we tentatively assign it as the $\bar{D}\Sigma_c$ resonance, the isospin cousin of the $P_c(4312)$.

In a similar way, we assign the $P_c(4380)$, $P_c(4440)$ and $P_c(4457)$ as the $\bar{D}\Sigma_c^*$, $\bar{D}^*\Sigma_c$ and $\bar{D}^*\Sigma_c^*$ molecular states with the $IJ^P = \frac{1}{2}\frac{3}{2}^-$, $\frac{1}{2}\frac{3}{2}^-$ and $\frac{1}{2}\frac{5}{2}^-$, respectively. For the molecular states (resonances) $\bar{D}\Sigma_c^*$ with the $IJ^P = \frac{3}{2}\frac{3}{2}^-$, $\bar{D}^*\Sigma_c$ with the $IJ^P = \frac{3}{2}\frac{3}{2}^-$ and $\bar{D}^*\Sigma_c^*$ with the $IJ^P = \frac{3}{2}\frac{5}{2}^-$, the central values of the masses are about 20 MeV, 10 MeV and 90 MeV above the corresponding meson-baryon thresholds, respectively.

If we choose the same input parameters, the **11** type pentaquark states with the isospin $I = \frac{3}{2}$ (1) have slightly larger masses than the corresponding ones with the isospin $I = \frac{1}{2}$ (0).

The $P_c(4312)$, $P_c(4380)$, $P_c(4440)$ and $P_c(4457)$ can be assigned as the $\bar{D}\Sigma_c$, $\bar{D}\Sigma_c^*$, $\bar{D}^*\Sigma_c$ and $\bar{D}^*\Sigma_c^*$ molecular states with the isospin $I = \frac{1}{2}$ respectively, since the two-body strong decays $P_c \rightarrow J/\psi p$ conserve isospin. If the assignments are robust, there exist four slightly higher molecular states $\bar{D}\Sigma_c$, $\bar{D}\Sigma_c^*$, $\bar{D}^*\Sigma_c$ and $\bar{D}^*\Sigma_c^*$ with the isospin $I = \frac{3}{2}$, we can search for the four resonances in the $J/\psi\Delta^+$ mass spectrum, as the two-body strong decays $P_c \rightarrow J/\psi\Delta^+$ also conserve isospin, the J/ψ , p and Δ have the isospins $I = 0$, $\frac{1}{2}$ and $\frac{3}{2}$, respectively.

The $\bar{D}^*\Xi_c'$ and $\bar{D}^*\Xi_c^*$ molecular states lie about 0.1 GeV and 0.2 GeV above the $P_{cs}(4459)$ respectively, the $P_{cs}(4459)$ is unlikely to be the $\bar{D}^*\Xi_c'$ or $\bar{D}^*\Xi_c^*$ molecular state. The mass of the $\bar{D}\Xi'$ molecular state with the isospin $I = 1$ is $4.45_{-0.08}^{+0.07}$ GeV, which is near the value 4459 MeV, but lies slightly above the corresponding meson-baryon threshold, it is a resonance, from the decay channel $P_{cs}(4459) \rightarrow J/\psi\Lambda$ [198], the isospin of the $P_{cs}(4459)$ is zero, which excludes assigning the $P_{cs}(4459)$ as the $\bar{D}\Xi_c^*$ molecular state with the isospin $I = 1$. The mass of the $\bar{D}\Xi_c^*$ molecular

	IJ^P	$T^2(\text{GeV}^2)$	$\sqrt{s_0}(\text{GeV})$	$\mu(\text{GeV})$	PC
$\bar{D}\Sigma_c$	$\frac{1}{2}\frac{1}{2}^-$	3.2 – 3.8	5.00 ± 0.10	2.2	(42 – 60)%
$\bar{D}\Sigma_c$	$\frac{3}{2}\frac{1}{2}^-$	2.8 – 3.4	4.98 ± 0.10	2.2	(44 – 65)%
$\bar{D}\Sigma_c^*$	$\frac{1}{2}\frac{3}{2}^-$	3.3 – 3.9	5.06 ± 0.10	2.3	(42 – 60)%
$\bar{D}\Sigma_c^*$	$\frac{3}{2}\frac{3}{2}^-$	2.9 – 3.5	5.03 ± 0.10	2.4	(44 – 64)%
$\bar{D}^*\Sigma_c$	$\frac{1}{2}\frac{3}{2}^-$	3.3 – 3.9	5.12 ± 0.10	2.5	(42 – 60)%
$\bar{D}^*\Sigma_c$	$\frac{3}{2}\frac{3}{2}^-$	3.0 – 3.6	5.10 ± 0.10	2.5	(41 – 61)%
$\bar{D}^*\Sigma_c^*$	$\frac{1}{2}\frac{5}{2}^-$	3.2 – 3.8	5.08 ± 0.10	2.5	(43 – 60)%
$\bar{D}^*\Sigma_c^*$	$\frac{3}{2}\frac{5}{2}^-$	3.0 – 3.6	5.24 ± 0.10	2.8	(42 – 61)%
$\bar{D}\Xi'_c$	$0\frac{1}{2}^-$	3.4 – 4.0	5.12 ± 0.10	2.2	(41 – 58)%
$\bar{D}\Xi'_c$	$1\frac{1}{2}^-$	3.2 – 3.8	5.14 ± 0.10	2.3	(43 – 61)%
$\bar{D}\Xi_c^*$	$0\frac{3}{2}^-$	3.4 – 4.0	5.15 ± 0.10	2.3	(43 – 60)%
$\bar{D}\Xi_c^*$	$1\frac{3}{2}^-$	3.3 – 3.9	5.22 ± 0.10	2.4	(44 – 62)%
$\bar{D}^*\Xi'_c$	$0\frac{3}{2}^-$	3.5 – 4.1	5.26 ± 0.10	2.5	(42 – 59)%
$\bar{D}^*\Xi'_c$	$1\frac{3}{2}^-$	3.4 – 4.0	5.31 ± 0.10	2.6	(43 – 60)%
$\bar{D}^*\Xi_c^*$	$0\frac{5}{2}^-$	3.6 – 4.2	5.31 ± 0.10	2.6	(42 – 58)%
$\bar{D}^*\Xi_c^*$	$1\frac{5}{2}^-$	3.4 – 4.0	5.35 ± 0.10	2.6	(44 – 61)%
$\bar{D}\Xi_c$	$0\frac{1}{2}^-$	3.2 – 3.8	5.00 ± 0.10	2.1	(41 – 60)%
$\bar{D}\Xi_c$	$1\frac{1}{2}^-$	3.1 – 3.7	5.09 ± 0.10	2.3	(42 – 61)%
$\bar{D}\Lambda_c$	$\frac{1}{2}\frac{1}{2}^-$	3.2 – 3.8	5.11 ± 0.10	2.5	(42 – 60)%
$\bar{D}_s\Xi_c$	$\frac{1}{2}\frac{1}{2}^-$	3.2 – 3.8	5.15 ± 0.10	2.2	(41 – 59)%
$\bar{D}_s\Lambda_c$	$0\frac{1}{2}^-$	3.2 – 3.8	5.13 ± 0.10	2.3	(43 – 61)%
$\bar{D}^*\Xi_c$	$0\frac{3}{2}^-$	3.2 – 3.8	5.10 ± 0.10	2.3	(43 – 61)%
$\bar{D}^*\Xi_c$	$1\frac{3}{2}^-$	3.3 – 3.9	5.27 ± 0.10	2.6	(43 – 61)%
$\bar{D}^*\Lambda_c$	$\frac{1}{2}\frac{3}{2}^-$	3.3 – 3.9	5.23 ± 0.10	2.7	(41 – 61)%
$\bar{D}_s^*\Xi_c$	$\frac{1}{2}\frac{3}{2}^-$	3.3 – 3.9	5.28 ± 0.10	2.4	(42 – 59)%
$\bar{D}_s^*\Lambda_c$	$0\frac{3}{2}^-$	3.2 – 3.8	5.14 ± 0.10	2.4	(42 – 60)%

Table 53: The Borel parameters, continuum threshold parameters, energy scales and pole contributions for the **11** type pentaquark states [720, 721, 722].

state with the isospin $I = 0$ is $4.46_{-0.07}^{+0.07}$ GeV, which is in very good agreement with the $P_{cs}(4459)$, it is very good to assign the $P_{cs}(4459)$ as the $\bar{D}\Xi_c^*$ molecular state with the isospin $I = 0$ and the spin-parity $J^P = \frac{3}{2}^-$. The predications also favor assigning the $P_{cs}(4459)$ as the $\bar{D}^*\Xi_c$ molecular state with the spin-parity $J^P = \frac{3}{2}^-$ and isospin $I = 0$.

The predictions support assigning the $P_{cs}(4338)$ as the $\bar{D}\Xi_c$ molecular state with the spin-parity $J^P = \frac{1}{2}^-$ and isospin $I = 0$, the observation of its cousin with the isospin $I = 1$ in the $J/\psi\Sigma^0/\eta_c\Sigma^0$ mass spectrum would decipher the inner structure of the $P_{cs}(4338)$. However, there exists no candidate for the $P_c(4337)$ [199].

Beyond the **333** type currents, in Ref.[739], Pimikov, Lee and Zhang construct the color **88** type currents $J^A(\Gamma_2, \Gamma_3)$ and $J_\mu^S(\Gamma_2, \Gamma_3)$ to interpolate the hidden-charm pentaquark states,

$$\begin{aligned}
J^A(\Gamma_2, \Gamma_3) &= \varepsilon_{f_1 f_2 f_3} \varepsilon_{c_1 c_3 c} t_{cc_2}^m [q_1^T C q_2 \Gamma_2 q_3 - q_1^T C \gamma_5 q_2 \gamma_5 \Gamma_2 q_3] [\bar{q}_5 t^m \Gamma_3 q_4], \\
J_\mu^S(\Gamma_2, \Gamma_3) &= \varepsilon_{f_1 f_2 f_3} \varepsilon_{c_1 c_3 c} t_{cc_2}^m q_1^T C \gamma_\mu q_2 \Gamma_2 q_3 [\bar{q}_5 t^m \Gamma_3 q_4],
\end{aligned} \tag{337}$$

	IJ^P	$M(\text{GeV})$	$\lambda(10^{-3}\text{GeV}^6)$	Assignments	Thresholds (MeV)
$\bar{D}\Sigma_c$	$\frac{1}{2}\frac{1}{2}^-$	$4.31^{+0.07}_{-0.07}$	$3.25^{+0.43}_{-0.41}$	$P_c(4312)$	4321
$\bar{D}\Sigma_c$	$\frac{3}{2}\frac{1}{2}^-$	$4.33^{+0.09}_{-0.08}$	$1.97^{+0.28}_{-0.26}$		4321
$\bar{D}\Sigma_c^*$	$\frac{1}{2}\frac{3}{2}^-$	$4.38^{+0.07}_{-0.07}$	$1.97^{+0.26}_{-0.24}$	$P_c(4380)$	4385
$\bar{D}\Sigma_c^*$	$\frac{3}{2}\frac{3}{2}^-$	$4.41^{+0.08}_{-0.08}$	$1.24^{+0.17}_{-0.16}$		4385
$\bar{D}^*\Sigma_c$	$\frac{1}{2}\frac{3}{2}^-$	$4.44^{+0.07}_{-0.08}$	$3.60^{+0.47}_{-0.44}$	$P_c(4440)$	4462
$\bar{D}^*\Sigma_c$	$\frac{3}{2}\frac{3}{2}^-$	$4.47^{+0.09}_{-0.09}$	$2.31^{+0.33}_{-0.31}$		4462
$\bar{D}^*\Sigma_c^*$	$\frac{1}{2}\frac{5}{2}^-$	$4.46^{+0.08}_{-0.08}$	$4.05^{+0.54}_{-0.50}$	$P_c(4457)$	4527
$\bar{D}^*\Sigma_c^*$	$\frac{3}{2}\frac{5}{2}^-$	$4.62^{+0.09}_{-0.09}$	$2.40^{+0.37}_{-0.35}$		4527
$\bar{D}\Xi'_c$	$0\frac{1}{2}^-$	$4.43^{+0.07}_{-0.07}$	$3.02^{+0.39}_{-0.37}$		4446
$\bar{D}\Xi'_c$	$1\frac{1}{2}^-$	$4.45^{+0.07}_{-0.08}$	$2.50^{+0.33}_{-0.31}$		4446
$\bar{D}\Xi_c^*$	$0\frac{3}{2}^-$	$4.46^{+0.07}_{-0.07}$	$1.71^{+0.22}_{-0.21}$	$P_{cs}(4459)$	4513
$\bar{D}\Xi_c^*$	$1\frac{3}{2}^-$	$4.53^{+0.07}_{-0.07}$	$1.56^{+0.20}_{-0.19}$		4513
$\bar{D}^*\Xi'_c$	$0\frac{3}{2}^-$	$4.57^{+0.07}_{-0.07}$	$3.41^{+0.43}_{-0.41}$		4588
$\bar{D}^*\Xi'_c$	$1\frac{3}{2}^-$	$4.62^{+0.08}_{-0.08}$	$3.05^{+0.39}_{-0.37}$		4588
$\bar{D}^*\Xi_c^*$	$0\frac{5}{2}^-$	$4.64^{+0.07}_{-0.07}$	$4.36^{+0.54}_{-0.51}$		4655
$\bar{D}^*\Xi_c^*$	$1\frac{5}{2}^-$	$4.67^{+0.08}_{-0.08}$	$3.25^{+0.41}_{-0.39}$		4655
$\bar{D}\Xi_c$	$0\frac{1}{2}^-$	$4.34^{+0.07}_{-0.07}$	$1.43^{+0.19}_{-0.18}$? $P_{cs}(4338)$	4337
$\bar{D}\Xi_c$	$1\frac{1}{2}^-$	$4.46^{+0.07}_{-0.07}$	$1.37^{+0.19}_{-0.18}$		4337
$\bar{D}\Lambda_c$	$\frac{1}{2}\frac{1}{2}^-$	$4.46^{+0.07}_{-0.08}$	$1.47^{+0.20}_{-0.18}$		4151
$\bar{D}_s\Xi_c$	$\frac{1}{2}\frac{1}{2}^-$	$4.54^{+0.07}_{-0.07}$	$1.58^{+0.21}_{-0.20}$		4437
$\bar{D}_s\Lambda_c$	$0\frac{1}{2}^-$	$4.48^{+0.07}_{-0.07}$	$1.57^{+0.21}_{-0.20}$		4255
$\bar{D}^*\Xi_c$	$0\frac{3}{2}^-$	$4.46^{+0.07}_{-0.07}$	$1.55^{+0.20}_{-0.19}$? $P_{cs}(4459)$	4479
$\bar{D}^*\Xi_c$	$1\frac{3}{2}^-$	$4.63^{+0.08}_{-0.08}$	$1.69^{+0.22}_{-0.21}$		4479
$\bar{D}^*\Lambda_c$	$\frac{1}{2}\frac{3}{2}^-$	$4.59^{+0.08}_{-0.08}$	$1.67^{+0.22}_{-0.21}$		4293
$\bar{D}_s^*\Xi_c$	$\frac{1}{2}\frac{3}{2}^-$	$4.65^{+0.08}_{-0.08}$	$1.66^{+0.22}_{-0.21}$		4580
$\bar{D}_s^*\Lambda_c$	$0\frac{3}{2}^-$	$4.50^{+0.07}_{-0.07}$	$1.52^{+0.21}_{-0.19}$		4398

Table 54: The masses, pole residues and possible assignments for the **11** type pentaquark states, where the thresholds denote the corresponding thresholds of the meson-baryon scattering states [720, 721, 722].

where the quark fields have the flavors f_i and color c_i , the Γ_2 and Γ_3 are some Dirac matrixes. Then, they calculate the mass spectrum by taking account of the vacuum condensates $\langle \bar{q}q \rangle$, $\langle \frac{\alpha_s GG}{\pi} \rangle$, $\langle \bar{q}g_s \sigma Gq \rangle$, $\langle \bar{q}q \rangle^2$, $\langle \bar{q}q \rangle \langle \bar{q}g_s \sigma Gq \rangle$, $\langle \bar{q}q \rangle^3$ and $\langle \bar{q}g_s \sigma Gq \rangle^2$.

6 Singly-heavy exotic states

6.1 Singly-heavy tetraquark states

The $X_0(2900)$ and $X_1(2900)$ observed in the $D^- K^+$ mass spectrum are the first exotic structures with fully open flavor [101, 102], they have the valence quarks $ud\bar{c}\bar{s}$. The $T_{c\bar{s}}^0(2900)$ and $T_{c\bar{s}}^{++}(2900)$ are observed in the $D_s^+ \pi^-$ and $D_s^+ \pi^+$ mass spectra, respectively [130, 131], they have the valence quarks $c\bar{s}u\bar{d}$ and $c\bar{s}\bar{u}d$, respectively.

Based on the predicted masses of the AA -type scalar tetraquark states from the QCD sum rules [61, 740],

$$\begin{aligned} M_{qq\bar{q}\bar{q}} &= 1.86 \pm 0.11 \text{ GeV}, \\ M_{ss\bar{s}\bar{s}} &= 2.08 \pm 0.13 \text{ GeV}, \\ M_{cq\bar{c}\bar{q}} &= 3.95 \pm 0.09 \text{ GeV}, \end{aligned} \quad (338)$$

we estimate the mass of the AA -type $c\bar{s}u\bar{d}$ tetraquark state crudely,

$$M_{c\bar{s}u\bar{d}} = \frac{M_{qq\bar{q}\bar{q}} + M_{ss\bar{s}\bar{s}} + 2M_{cq\bar{c}\bar{q}}}{4} = 2.96 \pm 0.11 \text{ GeV}, \quad (339)$$

which is consistent with the mass of the $X_0(2900)$ within uncertainties [119].

In Ref.[119], we construct the AA and SS -type scalar four-quark currents,

$$\begin{aligned} J_{AA}(x) &= \varepsilon^{ijk} \varepsilon^{imn} s_j^T(x) C \gamma_\alpha c_k(x) \bar{u}_m(x) \gamma^\alpha C \bar{d}_n^T(x), \\ J_{SS}(x) &= \varepsilon^{ijk} \varepsilon^{imn} s_j^T(x) C \gamma_5 c_k(x) \bar{u}_m(x) \gamma_5 C \bar{d}_n^T(x), \end{aligned} \quad (340)$$

to study the $c\bar{s}u\bar{d}$ tetraquark states with the correlation function $\Pi(p)$, see Eq.(125). We carry out the operator product expansion up to the vacuum condensates of dimension-11 and assume vacuum saturation for the higher dimensional vacuum condensates according to the routine in Sect.2.2 and Sect.3.1.1. As there are three q -quark lines and one Q -quark line, if each Q -quark line emits a gluon and each q -quark line contributes a quark-antiquark pair, we obtain a quark-gluon operator $g_s G_{\mu\nu} \bar{q}q \bar{q}q \bar{s}s$, which is of dimension 11, and leads to the vacuum condensates $\langle \bar{q}q \rangle^2 \langle \bar{s}g_s \sigma Gs \rangle$ and $\langle \bar{q}q \rangle \langle \bar{s}s \rangle \langle \bar{q}g_s \sigma Gq \rangle$.

We obtain the QCD sum rules routinely, at the QCD side, we choose the flavor numbers $n_f = 4$ and the typical energy scale $\mu = 1 \text{ GeV}$. After trial and error, we obtain the Borel windows and continuum threshold parameters, therefore the pole contributions of the ground states and convergent behaviors of the operator product expansion, see Table 55. In the Borel windows, the pole contributions are about (38 – 67)%, the central values exceed 52%. The contributions of the vacuum condensates $|D(11)|$ are about (2 – 4)% and (0 – 1)% for the AA and SS -type tetraquark states, respectively.

At last, we obtain the values of the masses and pole residues, which are also shown in Table 55. In Fig.30, we plot the masses of the AA and SS -type scalar $c\bar{s}u\bar{d}$ tetraquark states with variations of the Borel parameters T^2 in much larger ranges than the Borel windows, there appear platforms in the Borel windows indeed.

The predicted mass $M_{AA} = 2.91 \pm 0.12 \text{ GeV}$ is consistent with the experimental value $2866 \pm 7 \text{ MeV}$ from the LHCb collaboration [101, 102], and supports assigning the $X_0(2900)$ to be the AA -type $c\bar{s}u\bar{d}$ tetraquark state with the spin-parity $J^P = 0^+$. While the predicted mass $M_{SS} = 3.05 \pm 0.10 \text{ GeV}$ lies above the experimental value $2866 \pm 7 \text{ MeV}$ [101, 102].

	$T^2(\text{GeV}^2)$	$\sqrt{s_0}(\text{GeV})$	pole	$ D(11) $	$M(\text{GeV})$	$\lambda(\text{GeV}^5)$
$[cs]_A[\bar{u}\bar{d}]_A$	$1.9 - 2.3$	3.5 ± 0.1	$(38 - 67)\%$	$(2 - 4)\%$	2.91 ± 0.12	$(1.60 \pm 0.33) \times 10^{-2}$
$[cs]_S[\bar{u}\bar{d}]_S$	$2.1 - 2.5$	3.6 ± 0.1	$(39 - 66)\%$	$(0 - 1)\%$	3.05 ± 0.10	$(1.20 \pm 0.21) \times 10^{-2}$

Table 55: The Borel windows, continuum threshold parameters, pole contributions, contributions of the vacuum condensates of dimension 11, masses and pole residues for the scalar tetraquark states [119].

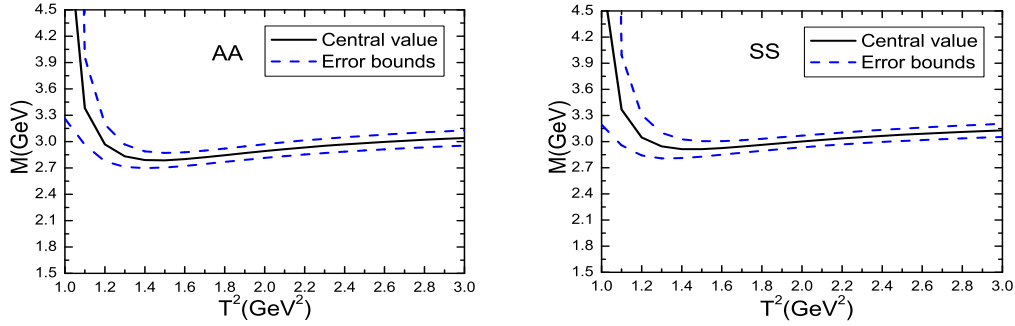


Figure 30: The masses of the AA and SS -type tetraquark states with variations of the Borel parameters T^2 .

In Ref.[741], we construct the $A\bar{A}$ -type currents to study the ground state mass spectrum of the tetraquark states with strange and doubly-strange via the QCD sum rules to verify the inner structures of the $T_{c\bar{s}}(2900)$, where

$$\begin{aligned} J(x) &= J_s^0(x), J_{ss}^0(x), \\ J_{\mu\nu}(x) &= J_{s,\mu\nu}^1(x), J_{ss,\mu\nu}^1(x), J_{s,\mu\nu}^2(x), J_{ss,\mu\nu}^2(x), \end{aligned} \quad (341)$$

$$\begin{aligned} J_s^0(x) &= \varepsilon^{ijk} \varepsilon^{imn} u_j^T(x) C \gamma_\mu c_k(x) \bar{d}_m(x) \gamma^\mu C \bar{s}_n^T(x), \\ J_{ss}^0(x) &= \varepsilon^{ijk} \varepsilon^{imn} u_j^T(x) C \gamma_\mu c_k(x) \bar{s}_m(x) \gamma^\mu C \bar{s}_n^T(x), \\ J_{s,\mu\nu}^1(x) &= \varepsilon^{ijk} \varepsilon^{imn} [u_j^T(x) C \gamma_\mu c_k(x) \bar{d}_m(x) \gamma_\nu C \bar{s}_n^T(x) - u_j^T(x) C \gamma_\nu c_k(x) \bar{d}_m(x) \gamma_\mu C \bar{s}_n^T(x)], \\ J_{ss,\mu\nu}^1(x) &= \varepsilon^{ijk} \varepsilon^{imn} [u_j^T(x) C \gamma_\mu c_k(x) \bar{s}_m(x) \gamma_\nu C \bar{s}_n^T(x) - u_j^T(x) C \gamma_\nu c_k(x) \bar{s}_m(x) \gamma_\mu C \bar{s}_n^T(x)], \\ J_{s,\mu\nu}^2(x) &= \varepsilon^{ijk} \varepsilon^{imn} [u_j^T(x) C \gamma_\mu c_k(x) \bar{d}_m(x) \gamma_\nu C \bar{s}_n^T(x) + u_j^T(x) C \gamma_\nu c_k(x) \bar{d}_m(x) \gamma_\mu C \bar{s}_n^T(x)], \\ J_{ss,\mu\nu}^2(x) &= \varepsilon^{ijk} \varepsilon^{imn} [u_j^T(x) C \gamma_\mu c_k(x) \bar{s}_m(x) \gamma_\nu C \bar{s}_n^T(x) + u_j^T(x) C \gamma_\nu c_k(x) \bar{s}_m(x) \gamma_\mu C \bar{s}_n^T(x)], \end{aligned} \quad (342)$$

the superscripts 0, 1 and 2 denote the spins. With a simple replacement $u \leftrightarrow d$, we obtain the corresponding currents in the same isospin multiplets. In the isospin limit, the tetraquark states in the same multiplets have the same masses.

Again, we resort to the correlation functions $\Pi(p)$ and $\Pi_{\mu\nu\alpha\beta}(p)$, see Eq.(125), and obtain the ground state contributions according to the hadron representations in Eqs.(202)-(204), and obtain the QCD sum rules routinely, again we take the flavor numbers $n_f = 4$ and the typical energy scale $\mu = 1.0 \text{ GeV}$.

After trial and error, we obtain the Borel windows, continuum threshold parameters and pole contributions, see Table 56, where the pole contributions are $38\% - 66\%$ and the central values

	J^P	$T^2(\text{GeV}^2)$	$\sqrt{s_0}(\text{GeV})$	pole	$M_T(\text{GeV})$	$\lambda_T(10^{-2}\text{GeV}^5)$
$cud\bar{s}$	0^+	$1.9 - 2.3$	3.50 ± 0.10	$(40 - 65)\%$	2.92 ± 0.12	1.62 ± 0.33
$cud\bar{s}$	1^+	$2.2 - 2.6$	3.65 ± 0.10	$(40 - 62)\%$	3.10 ± 0.10	1.59 ± 0.27
$cud\bar{s}$	2^+	$2.5 - 2.9$	3.95 ± 0.10	$(42 - 61)\%$	3.40 ± 0.10	3.51 ± 0.55
$cu\bar{s}\bar{s}$	0^+	$2.0 - 2.4$	3.60 ± 0.10	$(38 - 66)\%$	3.02 ± 0.12	2.72 ± 0.43
$cu\bar{s}\bar{s}$	1^+	$2.3 - 2.7$	3.75 ± 0.10	$(40 - 65)\%$	3.20 ± 0.10	2.64 ± 0.33
$cu\bar{s}\bar{s}$	2^+	$2.6 - 3.0$	4.05 ± 0.10	$(41 - 64)\%$	3.49 ± 0.10	5.70 ± 0.65

Table 56: The spin-parity, Borel parameters, continuum threshold parameters, pole contributions, masses and pole residues for the singly-charmed tetraquark states [741].

for the six states are larger than 50%, furthermore, the contributions of the vacuum condensates show a descending trend $|D(6)| > |D(8)| > |D(9)| > |D(10)| \sim |D(11)| \sim 0$. At last, we obtain the masses and pole residues, which are also shown in Table 56 [741].

In Table 56, the predicted mass of the $J^P = 0^+$ state $cud\bar{s}$, $M = 2.92 \pm 0.12 \text{ GeV}$, is in very good agreement with the experimental values $M = 2.892 \pm 0.014 \pm 0.015 \text{ GeV}$ and $2.921 \pm 0.017 \pm 0.020 \text{ GeV}$ from the LHCb collaboration [130, 131], and supports assigning the $T_{c\bar{s}}(2900)$ to be the $A\bar{A}$ -type $c\bar{s}q\bar{q}$ tetraquark states with the spin-parity $J^P = 0^+$.

Those typical singly-charmed tetraquark candidates, which lie at 2.9 GeV, have attracted many theoretical works, and are assigned as the $\bar{\mathbf{3}}\mathbf{3}$ type tetraquark states [118, 119, 120, 121, 742], or their radial/orbital excitations [122], or non-tetraquark states [123], $D^*\bar{K}^*$ molecular states [121, 124, 125, 126, 127, 128, 743, 744, 745], triangle singularities [129, 746, 747], etc. We could only obtain a mass about 2.3 GeV for the singly-charmed tetraquark states at the cost of sacrificing the pole dominance [748, 749, 750].

At the bottom sector, the singly-bottom tetraquark candidate $X(5568)$ is not confirmed [751, 752]. The lowest mass of the ground state $b\bar{s}u\bar{d}$ might have a mass $M_{T/X} + m_b(m_b) - m_c(m_c) \approx 5.81 \text{ GeV}$, which lies above the $X(5568)$.

6.2 Singly-heavy pentaquark states

The experimental candidates for the singly-charmed pentaquark states are not as robust as that of the singly-charmed tetraquark states, the assignments in the scenario of pentaquark states are only conjectures.

In 2017, the LHCb collaboration observed five narrow structures $\Omega_c(3000)$, $\Omega_c(3050)$, $\Omega_c(3066)$, $\Omega_c(3090)$ and $\Omega_c(3119)$ [753]. Also in 2017, the Belle collaboration confirmed the $\Omega_c(3000)$, $\Omega_c(3050)$, $\Omega_c(3066)$ and $\Omega_c(3090)$ in the $\Xi_c^+ K^-$ decay mode [754]. In 2023, the LHCb collaboration observed the $\Omega_c(3185)$ and $\Omega_c(3327)$ in the $\Xi_c^+ K^-$ mass spectrum [755], which lie near the $D\Xi$ and $D^*\Xi$ thresholds, respectively, the measured Breit-Wigner masses and decay widths are

$$\begin{aligned}
\Omega_c(3185) : M &= 3185.1 \pm 1.7_{-0.9}^{+7.4} \pm 0.2 \text{ MeV}, \Gamma = 50 \pm 7_{-20}^{+10} \text{ MeV}, \\
\Omega_c(3327) : M &= 3327.1 \pm 1.2_{-1.3}^{+0.1} \pm 0.2 \text{ MeV}, \Gamma = 20 \pm 5_{-1}^{+13} \text{ MeV}.
\end{aligned} \tag{343}$$

As early as 2005, the Belle collaboration tentatively assigned the $\Sigma_c^0(2800)$, $\Sigma_c^+(2800)$ and $\Sigma_c^{++}(2800)$ in the $\Lambda_c^+ \pi^- / 0^+ / +$ mass spectra as the isospin triplet states with the spin-parity $J^P = \frac{3}{2}^-$ [756], the measured masses and decay widths are

$$\begin{aligned}
\Sigma_c^0(2800) : M &= M_{\Lambda^+} + 515.4_{-3.1-6.0}^{+3.2+2.1} \text{ MeV}, \Gamma = 61_{-13-13}^{+18+22} \text{ MeV}, \\
\Sigma_c^+(2800) : M &= M_{\Lambda^+} + 505.4_{-4.6-2.0}^{+5.8+12.4} \text{ MeV}, \Gamma = 62_{-23-38}^{+37+52} \text{ MeV}, \\
\Sigma_c^{++}(2800) : M &= M_{\Lambda^+} + 514.5_{-3.1-4.9}^{+3.4+2.8} \text{ MeV}, \Gamma = 75_{-13-11}^{+18+12} \text{ MeV}.
\end{aligned} \tag{344}$$

In 2008, the BaBar collaboration observed the $\Sigma_c^0(2800)$ in the $\Lambda_c^+ \pi^-$ mass spectrum with the possible spin-parity $J^P = \frac{1}{2}^-$ [757], the mass and decay width are,

$$\Sigma_c^0(2800) : M = 2846 \pm 8 \pm 10 \text{ MeV}, \Gamma = 86_{-22}^{+33} \pm 7 \text{ MeV}. \quad (345)$$

In 2007, the BaBar collaboration observed the $\Lambda_c(2940)$ in the $D^0 p$ invariant mass spectrum [758]. Subsequently, the Belle collaboration verified the $\Lambda_c(2940)$ in the decay mode $\Lambda_c(2940) \rightarrow \Sigma_c(2455) \pi$ [759]. In 2017, the LHCb collaboration determined the spin-parity of the $\Lambda(2940)^+$ to be $J^P = \frac{3}{2}^-$ by analyzing the process $\Lambda_b^0 \rightarrow D^0 p \pi^-$ [760]. The measured masses and decay widths are,

$$\begin{aligned} \Lambda_c(2940) : M &= 2939.8 \pm 1.3 \pm 1.0 \text{ MeV}, \Gamma = 17.5 \pm 5.0 \pm 5.9 \text{ MeV} \quad (\text{BaBar}), \\ \Lambda_c(2940) : M &= 2938.0 \pm 1.3_{-4.0}^{+2.0} \text{ MeV}, \Gamma = 13_{-5-7}^{+8+27} \text{ MeV} \quad (\text{Belle}), \\ \Lambda_c(2940) : M &= 2944.8_{-2.5}^{+3.5} \pm 0.4_{-4.6}^{+0.1} \text{ MeV}, \Gamma = 27.7_{-6.0}^{+8.2} \pm 0.9_{-10.4}^{+5.2} \text{ MeV} \quad (\text{LHCb}). \end{aligned} \quad (346)$$

In 2023, the Belle collaboration studied the decays $\bar{B}^0 \rightarrow \Sigma_c(2455)^{0,++} \pi^\pm \bar{p}$ and found a new structure $\Lambda_c^+(2910)$ in the $\Sigma_c(2455)^{0,++} \pi^\pm$ mass spectrum [761], the mass and decay width are,

$$\Lambda_c(2910) : M = 2913.8 \pm 5.6 \pm 3.8 \text{ MeV}, \Gamma = 51.8 \pm 20.0 \pm 18.8 \text{ MeV}. \quad (347)$$

The $\Sigma_c(2800)$, $\Lambda_c(2940)$ and $\Lambda_c(2910)$ lie near the $D^{(*)}N$ thresholds, and they might be the $D^{(*)}N$ molecular states. For example, we can assign the $\Sigma_c(2800)$ as the DN molecular (bound) state [762, 763, 764, 765], and assign the $\Lambda_c(2940)$ as the D^*N molecular state [763, 765, 766, 767, 768, 769, 770]. We would like to study the **11** type charmed pentaquark states and explore the possible assignments in the scenario of molecular states.

Again, we resort to the correlation functions $\Pi(p)$, $\Pi_{\mu\nu}(p)$ and $\Pi_{\mu\nu\alpha\beta}(p)$ defined in Eq.(269), and write down the currents,

$$\begin{aligned} J(x) &= J_{|1,0\rangle}^{DN}(x), J_{|0,0\rangle}^{DN}(x), J_{|1,0\rangle}^{D\Xi}(x), J_{|0,0\rangle}^{D\Xi}(x), J_{|\frac{1}{2},\pm\frac{1}{2}\rangle}^{D_s\Xi}(x), \\ J_\mu(x) &= J_{|1,0\rangle}^{D^*N}(x), J_{|0,0\rangle}^{D^*N}(x), J_{|1,0\rangle}^{D^*\Xi}(x), J_{|0,0\rangle}^{D^*\Xi}(x), J_{|\frac{1}{2},\pm\frac{1}{2}\rangle}^{D_s^*\Xi}(x), J_{|1,0\rangle}^{D\Xi^*}(x), J_{|0,0\rangle}^{D\Xi^*}(x), J_{|\frac{1}{2},\pm\frac{1}{2}\rangle}^{D_s\Xi^*}(x), \\ J_{\mu\nu}(x) &= J_{|1,0\rangle}^{D^*\Xi^*}(x), J_{|0,0\rangle}^{D^*\Xi^*}(x), J_{|\frac{1}{2},\pm\frac{1}{2}\rangle}^{D_s^*\Xi^*}(x), \end{aligned} \quad (348)$$

$$\begin{aligned} J_{|1,0\rangle}^{DN}(x) &= \frac{1}{\sqrt{2}} J_{|\frac{1}{2},-\frac{1}{2}\rangle}^{D^0}(x) J_{|\frac{1}{2},\frac{1}{2}\rangle}^{N^+}(x) + \frac{1}{\sqrt{2}} J_{|\frac{1}{2},\frac{1}{2}\rangle}^{D^+}(x) J_{|\frac{1}{2},-\frac{1}{2}\rangle}^{N^0}(x), \\ J_{|0,0\rangle}^{DN}(x) &= \frac{1}{\sqrt{2}} J_{|\frac{1}{2},-\frac{1}{2}\rangle}^{D^0}(x) J_{|\frac{1}{2},\frac{1}{2}\rangle}^{N^+}(x) - \frac{1}{\sqrt{2}} J_{|\frac{1}{2},\frac{1}{2}\rangle}^{D^+}(x) J_{|\frac{1}{2},-\frac{1}{2}\rangle}^{N^0}(x), \\ J_{|1,0\rangle}^{D\Xi}(x) &= \frac{1}{\sqrt{2}} J_{|\frac{1}{2},-\frac{1}{2}\rangle}^{D^0}(x) J_{|\frac{1}{2},\frac{1}{2}\rangle}^{\Xi^0}(x) + \frac{1}{\sqrt{2}} J_{|\frac{1}{2},\frac{1}{2}\rangle}^{D^+}(x) J_{|\frac{1}{2},-\frac{1}{2}\rangle}^{\Xi^-}(x), \\ J_{|0,0\rangle}^{D\Xi}(x) &= \frac{1}{\sqrt{2}} J_{|\frac{1}{2},-\frac{1}{2}\rangle}^{D^0}(x) J_{|\frac{1}{2},\frac{1}{2}\rangle}^{\Xi^0}(x) - \frac{1}{\sqrt{2}} J_{|\frac{1}{2},\frac{1}{2}\rangle}^{D^+}(x) J_{|\frac{1}{2},-\frac{1}{2}\rangle}^{\Xi^-}(x), \\ J_{|\frac{1}{2},\pm\frac{1}{2}\rangle}^{D_s\Xi}(x) &= J_{|0,0\rangle}^{D_s^+}(x) J_{|\frac{1}{2},\pm\frac{1}{2}\rangle}^{\Xi^{0/-}}(x), \end{aligned} \quad (349)$$

$$\begin{aligned}
J_{|1,0\rangle}^{D^*N}(x) &= \frac{1}{\sqrt{2}}J_{|\frac{1}{2},-\frac{1}{2}\rangle}^{D^{*0}}(x)J_{|\frac{1}{2},\frac{1}{2}\rangle}^{N^+}(x) + \frac{1}{\sqrt{2}}J_{|\frac{1}{2},\frac{1}{2}\rangle}^{D^{*+}}(x)J_{|\frac{1}{2},-\frac{1}{2}\rangle}^{N^0}(x), \\
J_{|0,0\rangle}^{D^*N}(x) &= \frac{1}{\sqrt{2}}J_{|\frac{1}{2},-\frac{1}{2}\rangle}^{D^{*0}}(x)J_{|\frac{1}{2},\frac{1}{2}\rangle}^{N^+}(x) - \frac{1}{\sqrt{2}}J_{|\frac{1}{2},\frac{1}{2}\rangle}^{D^{*+}}(x)J_{|\frac{1}{2},-\frac{1}{2}\rangle}^{N^0}(x), \\
J_{|1,0\rangle}^{D^*\Xi}(x) &= \frac{1}{\sqrt{2}}J_{|\frac{1}{2},-\frac{1}{2}\rangle}^{D^{*0}}(x)J_{|\frac{1}{2},\frac{1}{2}\rangle}^{\Xi^0}(x) + \frac{1}{\sqrt{2}}J_{|\frac{1}{2},\frac{1}{2}\rangle}^{D^{*+}}(x)J_{|\frac{1}{2},-\frac{1}{2}\rangle}^{\Xi^-}(x), \\
J_{|0,0\rangle}^{D^*\Xi}(x) &= \frac{1}{\sqrt{2}}J_{|\frac{1}{2},-\frac{1}{2}\rangle}^{D^{*0}}(x)J_{|\frac{1}{2},\frac{1}{2}\rangle}^{\Xi^0}(x) - \frac{1}{\sqrt{2}}J_{|\frac{1}{2},\frac{1}{2}\rangle}^{D^{*+}}(x)J_{|\frac{1}{2},-\frac{1}{2}\rangle}^{\Xi^-}(x), \\
J_{|\frac{1}{2},\pm\frac{1}{2}\rangle}^{D_s^*\Xi}(x) &= J_{|0,0\rangle}^{D_s^{*+}}(x)J_{|\frac{1}{2},\pm\frac{1}{2}\rangle}^{\Xi^{0/-}}(x), \\
J_{|1,0\rangle}^{D\Xi^*}(x) &= \frac{1}{\sqrt{2}}J_{|\frac{1}{2},-\frac{1}{2}\rangle}^{D^0}(x)J_{|\frac{1}{2},\frac{1}{2}\rangle}^{\Xi^{*0}}(x) + \frac{1}{\sqrt{2}}J_{|\frac{1}{2},\frac{1}{2}\rangle}^{D^+}(x)J_{|\frac{1}{2},-\frac{1}{2}\rangle}^{\Xi^{*-}}(x), \\
J_{|0,0\rangle}^{D\Xi^*}(x) &= \frac{1}{\sqrt{2}}J_{|\frac{1}{2},-\frac{1}{2}\rangle}^{D^0}(x)J_{|\frac{1}{2},\frac{1}{2}\rangle}^{\Xi^{*0}}(x) - \frac{1}{\sqrt{2}}J_{|\frac{1}{2},\frac{1}{2}\rangle}^{D^+}(x)J_{|\frac{1}{2},-\frac{1}{2}\rangle}^{\Xi^{*-}}(x), \\
J_{|\frac{1}{2},\pm\frac{1}{2}\rangle}^{D_s^*\Xi^*}(x) &= J_{|0,0\rangle}^{D_s^+}(x)J_{|\frac{1}{2},\pm\frac{1}{2}\rangle}^{\Xi^{*0/-}}(x), \tag{350}
\end{aligned}$$

$$\begin{aligned}
J_{|1,0\rangle}^{D^*\Xi^*}(x) &= \frac{1}{\sqrt{2}}J_{|\frac{1}{2},-\frac{1}{2}\rangle}^{D^{*0}}(x)J_{|\frac{1}{2},\frac{1}{2}\rangle}^{\Xi^{*0}}(x) + \frac{1}{\sqrt{2}}J_{|\frac{1}{2},\frac{1}{2}\rangle}^{D^{*+}}(x)J_{|\frac{1}{2},-\frac{1}{2}\rangle}^{\Xi^{*-}}(x), \\
J_{|0,0\rangle}^{D^*\Xi^*}(x) &= \frac{1}{\sqrt{2}}J_{|\frac{1}{2},-\frac{1}{2}\rangle}^{D^{*0}}(x)J_{|\frac{1}{2},\frac{1}{2}\rangle}^{\Xi^{*0}}(x) - \frac{1}{\sqrt{2}}J_{|\frac{1}{2},\frac{1}{2}\rangle}^{D^{*+}}(x)J_{|\frac{1}{2},-\frac{1}{2}\rangle}^{\Xi^{*-}}(x), \\
J_{|\frac{1}{2},\pm\frac{1}{2}\rangle}^{D_s^*\Xi^*}(x) &= J_{|0,0\rangle}^{D_s^{*+}}(x)J_{|\frac{1}{2},\pm\frac{1}{2}\rangle}^{\Xi^{*0/-}}(x), \tag{351}
\end{aligned}$$

and

$$\begin{aligned}
J_{|\frac{1}{2},-\frac{1}{2}\rangle}^{D^0}(x) &= \bar{u}(x)i\gamma_5 c(x), \\
J_{|\frac{1}{2},\frac{1}{2}\rangle}^{D^+}(x) &= -\bar{d}(x)i\gamma_5 c(x), \\
J_{|0,0\rangle}^{D_s^+}(x) &= \bar{s}(x)i\gamma_5 c(x), \\
J_{|\frac{1}{2},-\frac{1}{2}\rangle}^{D^{*0}}(x) &= \bar{u}(x)\gamma_\mu c(x), \\
J_{|\frac{1}{2},\frac{1}{2}\rangle}^{D^{*+}}(x) &= -\bar{d}(x)\gamma_\mu c(x), \\
J_{|0,0\rangle}^{D_s^{*+}}(x) &= \bar{s}(x)\gamma_\mu c(x), \tag{352}
\end{aligned}$$

$$\begin{aligned}
J_{|\frac{1}{2},\frac{1}{2}\rangle}^{N^+}(x) &= \varepsilon^{ijk}u_i^T(x)C\gamma_\mu u_j(x)\gamma^\mu\gamma_5 d_k(x), \\
J_{|\frac{1}{2},-\frac{1}{2}\rangle}^{N^0}(x) &= \varepsilon^{ijk}d_i^T(x)C\gamma_\mu d_j(x)\gamma^\mu\gamma_5 u_k(x), \\
J_{|\frac{1}{2},\frac{1}{2}\rangle}^{\Xi^0}(x) &= \varepsilon^{ijk}s_i^T(x)C\gamma_\mu s_j(x)\gamma^\mu\gamma_5 u_k(x), \\
J_{|\frac{1}{2},-\frac{1}{2}\rangle}^{\Xi^-}(x) &= \varepsilon^{ijk}s_i^T(x)C\gamma_\mu s_j(x)\gamma^\mu\gamma_5 d_k(x), \\
J_{|\frac{1}{2},\frac{1}{2}\rangle}^{\Xi^{*0}}(x) &= \varepsilon^{ijk}s_i^T(x)C\gamma_\mu s_j(x)u_k(x), \\
J_{|\frac{1}{2},-\frac{1}{2}\rangle}^{\Xi^{*-}}(x) &= \varepsilon^{ijk}s_i^T(x)C\gamma_\mu s_j(x)d_k(x), \tag{353}
\end{aligned}$$

the subscripts $|1,0\rangle$, $|0,0\rangle$, $|\frac{1}{2},\frac{1}{2}\rangle$ and $|\frac{1}{2},-\frac{1}{2}\rangle$ are isospin indexes $|I, I_3\rangle$, we choose the convention $|\frac{1}{2},\frac{1}{2}\rangle = -\bar{d}$ [771].

The currents $J(0)$, $J_\mu(0)$ and $J_{\mu\nu}(0)$ couple potentially to the $J^P = \frac{1}{2}^\mp$, $\frac{3}{2}^\mp$ and $\frac{5}{2}^\mp$ singly-charmed molecular states $P_{\frac{1}{2}}^\mp$, $P_{\frac{3}{2}}^\mp$, and $P_{\frac{5}{2}}^\mp$, respectively, for more details, see Sect.5.1. At the hadron side, we isolate the ground state contributions,

$$\begin{aligned}\Pi(p) &= \lambda_{\frac{1}{2}}^{-2} \frac{\not{p} + M_-}{M_-^2 - p^2} + \lambda_{\frac{1}{2}}^{+2} \frac{\not{p} - M_+}{M_+^2 - p^2} + \dots, \\ &= \Pi_{\frac{1}{2}}^1(p^2) \not{p} + \Pi_{\frac{1}{2}}^0(p^2),\end{aligned}\quad (354)$$

$$\begin{aligned}\Pi_{\mu\nu}(p) &= \lambda_{\frac{3}{2}}^{-2} \frac{\not{p} + M_-}{M_-^2 - p^2} \left(-g_{\mu\nu} + \frac{\gamma_\mu \gamma_\nu}{3} + \frac{2p_\mu p_\nu}{3p^2} - \frac{p_\mu \gamma_\nu - p_\nu \gamma_\mu}{3\sqrt{p^2}} \right) \\ &\quad + \lambda_{\frac{3}{2}}^{+2} \frac{\not{p} - M_+}{M_+^2 - p^2} \left(-g_{\mu\nu} + \frac{\gamma_\mu \gamma_\nu}{3} + \frac{2p_\mu p_\nu}{3p^2} - \frac{p_\mu \gamma_\nu - p_\nu \gamma_\mu}{3\sqrt{p^2}} \right) + \dots, \\ &= -\Pi_{\frac{3}{2}}^1(p^2) \not{p} g_{\mu\nu} - \Pi_{\frac{3}{2}}^0(p^2) g_{\mu\nu} + \dots,\end{aligned}\quad (355)$$

$$\begin{aligned}\Pi_{\mu\nu\alpha\beta}(p) &= \lambda_{\frac{5}{2}}^{-2} \frac{\not{p} + M_-}{M_-^2 - p^2} \left[\frac{\tilde{g}_{\mu\alpha} \tilde{g}_{\nu\beta} + \tilde{g}_{\mu\beta} \tilde{g}_{\nu\alpha}}{2} - \frac{\tilde{g}_{\mu\nu} \tilde{g}_{\alpha\beta}}{5} - \frac{1}{10} (\gamma_\alpha \gamma_\mu + \dots) \tilde{g}_{\nu\beta} + \dots \right] \\ &\quad + \lambda_{\frac{5}{2}}^{+2} \frac{\not{p} - M_+}{M_+^2 - p^2} \left[\frac{\tilde{g}_{\mu\alpha} \tilde{g}_{\nu\beta} + \tilde{g}_{\mu\beta} \tilde{g}_{\nu\alpha}}{2} - \frac{\tilde{g}_{\mu\nu} \tilde{g}_{\alpha\beta}}{5} + \dots \right] + \dots, \\ &= \Pi_{\frac{5}{2}}^1(p^2) \not{p} \frac{g_{\mu\alpha} g_{\nu\beta} + g_{\mu\beta} g_{\nu\alpha}}{2} + \Pi_{\frac{5}{2}}^0(p^2) \frac{g_{\mu\alpha} g_{\nu\beta} + g_{\mu\beta} g_{\nu\alpha}}{2} + \dots.\end{aligned}\quad (356)$$

We choose the components $\Pi_{\frac{1}{2}}^1(p^2)$, $\Pi_{\frac{1}{2}}^0(p^2)$, $\Pi_{\frac{3}{2}}^1(p^2)$, $\Pi_{\frac{3}{2}}^0(p^2)$, $\Pi_{\frac{5}{2}}^1(p^2)$ and $\Pi_{\frac{5}{2}}^0(p^2)$ to explore the spin-parity $J^P = \frac{1}{2}^-$, $\frac{3}{2}^-$ and $\frac{5}{2}^-$ molecular states, respectively. Again see Sect.5.1 for technical details in tensor analysis.

Again we obtain the spectral densities through dispersion relation,

$$\begin{aligned}\frac{\text{Im}\Pi_j^1(s)}{\pi} &= \lambda_j^{-2} \delta(s - M_-^2) + \lambda_j^{+2} \delta(s - M_+^2) = \rho_{j,H}^1(s), \\ \frac{\text{Im}\Pi_j^0(s)}{\pi} &= M_- \lambda_j^{-2} \delta(s - M_-^2) - M_+ \lambda_j^{+2} \delta(s - M_+^2) = \rho_{j,H}^0(s),\end{aligned}\quad (357)$$

where $j = \frac{1}{2}, \frac{3}{2}, \frac{5}{2}$, the subscript H denotes the hadron side, then we introduce the weight functions $\sqrt{s} \exp(-\frac{s}{T^2})$ and $\exp(-\frac{s}{T^2})$ to obtain the QCD sum rules at the hadron side,

$$\int_{m_c^2}^{s_0} ds [\sqrt{s} \rho_{j,H}^1(s) + \rho_{j,H}^0(s)] \exp\left(-\frac{s}{T^2}\right) = 2M_- \lambda_j^{-2} \exp\left(-\frac{M_-^2}{T^2}\right), \quad (358)$$

which are free from contaminations of the positive-parity molecular states.

At the QCD side, we accomplish the operator product expansion with the full light/heavy-quark propagators up to the vacuum condensates of dimension 13 in a consistent way, and obtain the QCD spectral densities through dispersion relation,

$$\frac{\text{Im}\Pi_j^{1/0}(s)}{\pi} = \rho_{j,QCD}^{1/0}(s), \quad (359)$$

where $j = \frac{1}{2}, \frac{3}{2}, \frac{5}{2}$. See Sect.3.1.1 for technical details.

	J^P	Isospin	μ	$T^2(\text{GeV}^2)$	$\sqrt{s_0}(\text{GeV})$	pole	$ D(13) $
DN	$\frac{1}{2}^-$	0	2.1	1.9 – 2.3	3.45 ± 0.10	(41 – 70)%	4.9%
DN	$\frac{1}{2}^-$	1	2.1	1.9 – 2.3	3.45 ± 0.10	(41 – 70)%	4.9%
$D\Xi$	$\frac{1}{2}^-$	0	2.2	2.3 – 2.7	3.85 ± 0.10	(41 – 67)%	1.2%
$D\Xi$	$\frac{1}{2}^-$	1	2.2	2.3 – 2.7	3.85 ± 0.10	(41 – 67)%	1.2%
$D_s\Xi$	$\frac{1}{2}^-$	$\frac{1}{2}$	2.2	2.4 – 2.8	3.95 ± 0.10	(41 – 65)%	0.9%
D^*N	$\frac{3}{2}^-$	0	2.3	2.1 – 2.5	3.60 ± 0.10	(37 – 64)%	1.2%
D^*N	$\frac{3}{2}^-$	1	2.3	2.1 – 2.5	3.60 ± 0.10	(37 – 64)%	1.2%
$D^*\Xi$	$\frac{3}{2}^-$	0	2.4	2.5 – 2.9	4.00 ± 0.10	(38 – 62)%	0.3%
$D^*\Xi$	$\frac{3}{2}^-$	1	2.4	2.5 – 2.9	4.00 ± 0.10	(38 – 62)%	0.3%
$D_s^*\Xi$	$\frac{3}{2}^-$	$\frac{1}{2}$	2.4	2.5 – 2.9	4.05 ± 0.10	(38 – 62)%	0.3%
$D\Xi^*$	$\frac{3}{2}^-$	0	2.5	2.5 – 2.9	4.10 ± 0.10	(41 – 66)%	0.5%
$D\Xi^*$	$\frac{3}{2}^-$	1	2.5	2.5 – 2.9	4.10 ± 0.10	(41 – 66)%	0.5%
$D_s\Xi^*$	$\frac{3}{2}^-$	$\frac{1}{2}$	2.5	2.6 – 3.0	4.20 ± 0.10	(40 – 64)%	0.5%
$D^*\Xi^*$	$\frac{5}{2}^-$	0	2.6	2.6 – 3.0	4.20 ± 0.10	(41 – 64)%	0.4%
$D^*\Xi^*$	$\frac{5}{2}^-$	1	2.6	2.6 – 3.0	4.20 ± 0.10	(41 – 64)%	0.4%
$D_s^*\Xi^*$	$\frac{5}{2}^-$	$\frac{1}{2}$	2.6	2.8 – 3.2	4.30 ± 0.10	(40 – 63)%	0.2%

Table 57: The spin-parity, isospin, energy scales μ , Borel parameters T^2 , continuum threshold parameters s_0 , pole contributions and vacuum condensate contributions $|D(13)|$ for the singly-charmed pentaquark molecular states [771].

At last, we obtain the QCD sum rules,

$$2M_- \lambda_j^{-2} \exp\left(-\frac{M_-^2}{T^2}\right) = \int_{m_c^2}^{s_0} ds [\sqrt{s} \rho_{j,QCD}^1(s) + \rho_{j,QCD}^0(s)] \exp\left(-\frac{s}{T^2}\right). \quad (360)$$

We differentiate Eq.(360) with respect to $\tau = \frac{1}{T^2}$, then eliminate the pole residues to obtain the QCD sum rules for the masses,

$$M_-^2 = \frac{-\frac{d}{d\tau} \int_{m_c^2}^{s_0} ds [\sqrt{s} \rho_{QCD}^1(s) + \rho_{QCD}^0(s)] \exp(-\tau s)}{\int_{m_c^2}^{s_0} ds [\sqrt{s} \rho_{QCD}^1(s) + \rho_{QCD}^0(s)] \exp(-\tau s)}, \quad (361)$$

where the spectral densities $\rho_{QCD}^1(s) = \rho_{j,QCD}^1(s)$ and $\rho_{QCD}^0(s) = \rho_{j,QCD}^0(s)$.

We take the quark flavor number $n_f = 4$ and resort to the modified energy scale formula

$$\mu = \sqrt{M_P^2 - \mathbb{M}_c^2 - k \mathbb{M}_s}, \quad (362)$$

to choose the ideal energy scales of the QCD spectral densities, where $M_P = M_-$, the effective c -quark mass $\mathbb{M}_c = 1.82 \text{ GeV}$ and effective s -quark mass $\mathbb{M}_s = 0.2 \text{ GeV}$, the k is the number of the s -quark in the currents/states, see Sect.4.1 for details.

Routinely, we obtain the Borel windows, continuum threshold parameters, energy scales of the QCD spectral densities and contributions of the $D(13)$, see Table 57, where the pole dominance is well satisfied. On the other hand, the highest dimensional vacuum condensate contributions have the relation $|D(11)| \gg |D(12)| > |D(13)|$, the operator product expansion is convergent very well.

At last, we obtain the masses and pole residues of the pentaquark molecular states, see Table 58 [771]. From Tables 57-58, it is obvious that the modified energy scale formula $\mu = \sqrt{M_P^2 - \mathbb{M}_c^2 -$

	J^P	Isospin	$M(\text{GeV})$	$\lambda(10^{-4}\text{GeV}^6)$	Thresholds (MeV)	Assignments
DN	$\frac{1}{2}^-$	0	$2.81^{+0.13}_{-0.16}$	$7.98^{+1.98}_{-1.56}$	2806	
DN	$\frac{1}{2}^-$	1	$2.81^{+0.13}_{-0.16}$	$7.98^{+1.98}_{-1.56}$	2806	? $\Sigma_c(2800)$
$D\Xi$	$\frac{1}{2}^-$	0	$3.19^{+0.11}_{-0.13}$	$14.22^{+2.74}_{-2.40}$	3186	? $\Omega_c(3185)$
$D\Xi$	$\frac{1}{2}^-$	1	$3.19^{+0.11}_{-0.13}$	$14.22^{+2.74}_{-2.40}$	3186	
$D_s\Xi$	$\frac{1}{2}^-$	$\frac{1}{2}$	$3.28^{+0.12}_{-0.12}$	$16.04^{+3.04}_{-2.66}$	3287	
D^*N	$\frac{3}{2}^-$	0	$2.96^{+0.13}_{-0.14}$	$8.87^{+1.84}_{-1.59}$	2947	?? $\Lambda_c(2940)/\Lambda_c(2910)$
D^*N	$\frac{3}{2}^-$	1	$2.96^{+0.13}_{-0.14}$	$8.87^{+1.84}_{-1.59}$	2947	
$D^*\Xi$	$\frac{3}{2}^-$	0	$3.35^{+0.11}_{-0.13}$	$15.89^{+2.93}_{-2.56}$	3327	? $\Omega_c(3327)$
$D^*\Xi$	$\frac{3}{2}^-$	1	$3.35^{+0.11}_{-0.13}$	$15.89^{+2.93}_{-2.56}$	3327	
$D_s^*\Xi$	$\frac{3}{2}^-$	$\frac{1}{2}$	$3.44^{+0.11}_{-0.11}$	$17.24^{+3.06}_{-2.66}$	3430	
$D\Xi^*$	$\frac{3}{2}^-$	0	$3.41^{+0.11}_{-0.12}$	$10.67^{+1.92}_{-1.68}$	3399	
$D\Xi^*$	$\frac{3}{2}^-$	1	$3.41^{+0.11}_{-0.12}$	$10.67^{+1.92}_{-1.68}$	3399	
$D_s\Xi^*$	$\frac{3}{2}^-$	$\frac{1}{2}$	$3.51^{+0.11}_{-0.13}$	$11.93^{+2.11}_{-1.85}$	3500	
$D^*\Xi^*$	$\frac{5}{2}^-$	0	$3.54^{+0.11}_{-0.12}$	$10.93^{+1.94}_{-1.71}$	3540	
$D^*\Xi^*$	$\frac{5}{2}^-$	1	$3.54^{+0.11}_{-0.12}$	$10.93^{+1.94}_{-1.71}$	3540	
$D_s^*\Xi^*$	$\frac{5}{2}^-$	$\frac{1}{2}$	$3.65^{+0.11}_{-0.11}$	$12.91^{+2.19}_{-1.93}$	3644	

Table 58: The masses, pole residues, (corresponding meson-baryon) thresholds and possible assignments for the singly-charmed pentaquark molecular states [771].

$k\mathbb{M}_s$ is satisfied in most cases. The energy scales $\sqrt{M_P^2 - \mathbb{M}_c^2} - 3\mathbb{M}_s$ for the $D_s\Xi$, $D_s^*\Xi$ and $D_s\Xi^*$ states are smaller than the energy scales $\sqrt{M_P^2 - \mathbb{M}_c^2} - 2\mathbb{M}_s$ for the corresponding $D\Xi$, $D^*\Xi$ and $D\Xi^*$ states, respectively, we choose the same energy scales $\sqrt{M_P^2 - \mathbb{M}_c^2} - 2\mathbb{M}_s$ for those cousins, as larger masses correspond to larger energy scales naively.

The predicted masses $2.81^{+0.13}_{-0.16}$ GeV and $3.19^{+0.11}_{-0.13}$ GeV for the DN and $D\Xi$ molecular states (respectively) with the $J^P = \frac{1}{2}^-$ support assigning the $\Sigma_c(2800)$ and $\Omega_c(3185)$ as the DN and $D\Xi$ molecular states, respectively. The predicted mass $3.35^{+0.11}_{-0.13}$ GeV for the $D^*\Xi$ molecular state with the $J^P = \frac{3}{2}^-$ supports assigning the $\Omega_c(3327)$ as the $D^*\Xi$ molecular state. The predicted mass $2.96^{+0.14}_{-0.13}$ GeV for the D^*N molecular state is consistent with the $\Lambda_c(2940)/\Lambda_c(2910)$ within uncertainties, which does not exclude the possibility that they are molecular states.

In Ref.[767], J. R. Zhang studies the $\Sigma_c(2800)$ and $\Lambda_c(2940)$ as the S -wave DN and D^*N molecule candidates respectively with the QCD sum rules, obtains the masses 3.64 ± 0.33 GeV and 3.73 ± 0.35 GeV for the S -wave DN state with the $J^P = \frac{1}{2}^-$ and S -wave D^*N state with the $J^P = \frac{3}{2}^-$, respectively, which are somewhat bigger than the experimental data for the $\Sigma_c(2800)$ and $\Lambda_c(2940)$, respectively, and differ from the present calculations significantly. We should bear in mind that J. R. Zhang chooses **Scheme II** while we choose **Scheme I**.

Taking the $D\Xi$ ($D^*\Xi$) pentaquark molecular states with the $J^P = \frac{1}{2}^-$ ($\frac{3}{2}^-$) as an example, we obtain a symmetric isotriplet $|1, 1\rangle$, $|1, 0\rangle$, $|1, -1\rangle$ and an antisymmetric isosinglet $|0, 0\rangle$. The $\Omega_c(3185)$ ($\Omega_c(3327)$) is a good candidate for the $D\Xi$ ($D^*\Xi$) molecular state with the isospin $|0, 0\rangle$. We expect to search for the molecular states with the isospin $|1, 1\rangle$ and $|1, -1\rangle$ in the $\Xi_c^+ \bar{K}^0$ and $\Xi_c^0 \bar{K}^-$ mass spectra respectively to shed light on the nature of the $\Omega_c(3185)$ ($\Omega_c(3327)$).

Other interpretations also exist, the $\Sigma_c(2800)$ could be assigned as overlap of the $\Sigma_c(2813)$ and $\Sigma_c(2840)$ [772] or P-wave charmed baryon state with the $J^P = \frac{1}{2}^-/\frac{3}{2}^-/\frac{5}{2}^-$ [773, 774, 775, 776]. Cheng et al suggest that the $\Sigma_c(2800)$ is not possible to be a $J^P = \frac{1}{2}^-$ charmed baryon state [777].

The $\Lambda_c^+(2940)$ is most likely to be the $J^P = \frac{1}{2}^-$ or $\frac{3}{2}^-$ (2P) state [776, 777, 778, 779]. And the $\Lambda_c^+(2910)$ is probably the $J^P = \frac{1}{2}^-$ (2P) [780] or $\frac{5}{2}^-$ (1P) state [781]. The $\Omega_c(3185)$ lies in the region of the 2S state [782, 783], while the $\Omega_c(3327)$ is a good candidate for the 2S Ω_c state [783] or D-wave Ω_c baryon state with the $J^P = \frac{1}{2}^+/\frac{3}{2}^+/\frac{5}{2}^+$ [782, 784, 785].

With a simple replacement $c \rightarrow b$, we obtain the corresponding QCD sum rules for the singly-bottom pentaquark molecular states, see Eqs.(360)-(361). In Ref.[786], we choose the current,

$$J(x) = \bar{u}(x)i\gamma_5 s(x)\varepsilon^{ijk}u_i^T(x)C\gamma_\alpha d_j(x)\gamma^\alpha\gamma_5 b_k(x), \quad (363)$$

to interpolate the molecular states with the $J^P = \frac{1}{2}^\pm$, the prediction supports assigning the $\Xi_b(6227)$ as the pentaquark molecular state with the $J^P = \frac{1}{2}^-$.

In Ref.[787], we construct the **333** type five-quark currents,

$$\begin{aligned} J_{SS}(x) &= \varepsilon^{ila}\varepsilon^{ijk}\varepsilon^{lmn}s_j^T(x)C\gamma_5 u_k(x)s_m^T(x)C\gamma_5 c_n(x)C\bar{u}_a^T(x), \\ J_{AA}(x) &= \varepsilon^{ila}\varepsilon^{ijk}\varepsilon^{lmn}s_j^T(x)C\gamma_\mu u_k(x)s_m^T(x)C\gamma^\mu c_n(x)C\bar{u}_a^T(x), \end{aligned} \quad (364)$$

to interpolate the singly-charmed pentaquark states $susc\bar{u}$ with the $J^P = \frac{1}{2}^\pm$. With a simple replacement,

$$susc\bar{u} \rightarrow \frac{1}{\sqrt{2}}(susc\bar{u} + sdsc\bar{d}), \quad (365)$$

we obtain the isospin singlet current, the expressions of the QCD sum rules survive. The predictions support assigning the excited Ω_c states from the LHCb collaboration as the SS or AA -type pentaquark states with the $J^P = \frac{1}{2}^-$ and the mass about 3.08 GeV. We group the quark flavors as $[su][sc]\bar{u}$ to construct the currents, if we group the quark flavors as $[ss][cu]\bar{u}$, the SS -type current will vanish due to Fermi-Dirac statistics, but the AA -type current survives and leads to almost degenerated mass according to the light-flavor $SU(3)$ symmetry.

In Ref.[788], we study the **333** type singly-charmed pentaquark states with the $J^P = \frac{3}{2}^\pm$ via the QCD sum rules. We distinguish the isospins in constructing the interpolating currents via two clusters, a diquark $q_j^T C\gamma_\mu q_k''$ (D_i) plus a triquark $q_m''' C\gamma_5 c_n C\bar{q}_a^T$ (T_{mna}), which have the properties,

$$\begin{aligned} \hat{I}^2 \varepsilon_{ijk} q_j^T C\gamma_\mu q_k' &= 1(1+1) \varepsilon_{ijk} q_j^T C\gamma_\mu q_k', \\ \hat{I}^2 \varepsilon_{ijk} q_j^T C\gamma_\mu s_j &= \frac{1}{2} \left(\frac{1}{2} + 1 \right) \varepsilon_{ijk} q_j^T C\gamma_\mu s_j, \\ \hat{I}^2 \varepsilon_{ijk} s_j^T C\gamma_\mu s_j &= 0(0+1) \varepsilon_{ijk} s_j^T C\gamma_\mu s_j, \\ \hat{I}^2 u_m^T C\gamma_5 c_n C\bar{d}_a^T &= 1(1+1) u_m^T C\gamma_5 c_n C\bar{d}_a^T, \\ \hat{I}^2 d_m^T C\gamma_5 c_n C\bar{u}_a^T &= 1(1+1) d_m^T C\gamma_5 c_n C\bar{u}_a^T, \\ \hat{I}^2 [u_m^T C\gamma_5 c_n C\bar{u}_a^T - d_m^T C\gamma_5 c_n C\bar{d}_a^T] &= 1(1+1) [u_m^T C\gamma_5 c_n C\bar{u}_a^T - d_m^T C\gamma_5 c_n C\bar{d}_a^T], \\ \hat{I}^2 [u_m^T C\gamma_5 c_n C\bar{u}_a^T + d_m^T C\gamma_5 c_n C\bar{d}_a^T] &= 0(0+1) [u_m^T C\gamma_5 c_n C\bar{u}_a^T + d_m^T C\gamma_5 c_n C\bar{d}_a^T], \\ \hat{I}^2 q_m^T C\gamma_5 c_n C\bar{s}_a^T &= \frac{1}{2} \left(\frac{1}{2} + 1 \right) q_m^T C\gamma_5 c_n C\bar{s}_a^T, \\ \hat{I}^2 s_m^T C\gamma_5 c_n C\bar{q}_a^T &= \frac{1}{2} \left(\frac{1}{2} + 1 \right) s_m^T C\gamma_5 c_n C\bar{q}_a^T, \\ \hat{I}^2 s_m^T C\gamma_5 c_n C\bar{s}_a^T &= 0(0+1) s_m^T C\gamma_5 c_n C\bar{s}_a^T, \end{aligned} \quad (366)$$

with $q, q' = u, d$, the \hat{I}^2 is the isospin operator. The diquark clusters D_i and triquark clusters T_{mna} have the isospins $I = 1, \frac{1}{2}$ or 0. We could obtain some mass relations based on the $SU(3)$ breaking

effects of the u , d , s quarks, the mass relation among the diquark clusters D_i is $m_{I=0} - m_{I=\frac{1}{2}} = m_{I=\frac{1}{2}} - m_{I=1}$, while the mass relation among the triquark clusters T_{mna} is $m_{I=0} - m_{I=\frac{1}{2}} = m_{I=\frac{1}{2}} - m_{I=1}$, if the hidden-flavor (for u and d) isospin singlet $u_m^T C \gamma_5 c_n C \bar{u}_a^T + d_m^T C \gamma_5 c_n C \bar{d}_a^T$ is excluded. Moreover, the isospin triplet $u_m^T C \gamma_5 c_n C \bar{u}_a^T - d_m^T C \gamma_5 c_n C \bar{d}_a^T$ and isospin singlet $u_m^T C \gamma_5 c_n C \bar{u}_a^T + d_m^T C \gamma_5 c_n C \bar{d}_a^T$ are expected to have degenerate masses, which can be inferred from the tiny mass difference between the vector mesons $\rho^0(770)$ and $\omega(780)$. In fact, if we choose the currents $J_\mu(x) = \bar{u}(x)\gamma_\mu u(x) - \bar{d}(x)\gamma_\mu d(x)$ and $\bar{u}(x)\gamma_\mu u(x) + \bar{d}(x)\gamma_\mu d(x)$ to interpolate the $\rho^0(770)$ and $\omega(780)$, respectively, we obtain the same QCD sum rules.

We write down the currents explicitly,

$$J_{q'q''q'''\bar{q},\mu}(x) = \varepsilon^{ila}\varepsilon^{ijk}\varepsilon^{lmn}q_j'^T(x)C\gamma_\mu q_k''(x)q_m'''^T(x)C\gamma_5 c_n(x)C\bar{q}_a^T(x), \quad (368)$$

and study the singly-charmed pentaquark states $uuuc\bar{u}$ and $sssc\bar{s}$ with the QCD sum rules in details. Then we estimate the masses of the singly-charmed pentaquark states $ssuc\bar{u}$, $susc\bar{u}$, $ssdc\bar{d}$ and $sdsd\bar{d}$ with $J^P = \frac{3}{2}^-$ to be 3.15 ± 0.13 GeV according to the light-flavor $SU(3)$ breaking effects, which is compatible with the experimental values of the masses of the $\Omega_c(3050)$, $\Omega_c(3066)$, $\Omega_c(3090)$, $\Omega_c(3119)$.

7 Strong decays of exotic states

In Refs.[520, 789], we suggest rigorous quark-hadron duality to calculate the hadronic coupling constants in the two-body strong decays of the tetraquark states with the QCD sum rules. At first, we write down the three-point correlation functions $\Pi(p, q)$,

$$\Pi(p, q) = i^2 \int d^4x d^4y e^{ip \cdot x} e^{iq \cdot y} \langle 0 | T \{ J_B(x) J_C(y) J_A^\dagger(0) \} | 0 \rangle, \quad (369)$$

where the currents $J_A(0)$ interpolate the tetraquark states A , the currents $J_B(x)$ and $J_C(y)$ interpolate the conventional mesons B and C , respectively,

$$\begin{aligned} \langle 0 | J_A(0) | A(p') \rangle &= \lambda_A, \\ \langle 0 | J_B(0) | B(p) \rangle &= \lambda_B, \\ \langle 0 | J_C(0) | C(q) \rangle &= \lambda_C, \end{aligned} \quad (370)$$

the λ_A , λ_B and λ_C are the pole residues or decay constants.

At the hadron side, we insert a complete set of intermediate hadronic states with the same quantum numbers as the currents $J_A(0)$, $J_B(x)$, $J_C(y)$ into the three-point correlation functions $\Pi(p, q)$ and isolate the ground state contributions to obtain the result [789],

$$\begin{aligned} \Pi(p, q) &= \frac{\lambda_A \lambda_B \lambda_C G_{ABC}}{(m_A^2 - p'^2)(m_B^2 - p^2)(m_C^2 - q^2)} + \frac{1}{(m_A^2 - p'^2)(m_B^2 - p^2)} \int_{s_C^0}^\infty dt \frac{\rho_{AC'}(p'^2, p^2, t)}{t - q^2} \\ &\quad + \frac{1}{(m_A^2 - p'^2)(m_C^2 - q^2)} \int_{s_B^0}^\infty dt \frac{\rho_{AB'}(p'^2, t, q^2)}{t - p^2} \\ &\quad + \frac{1}{(m_B^2 - p^2)(m_C^2 - q^2)} \int_{s_A^0}^\infty dt \frac{\rho_{A'B}(t, p^2, q^2) + \rho_{A'C}(t, p^2, q^2)}{t - p'^2} + \dots \\ &= \Pi(p'^2, p^2, q^2), \end{aligned} \quad (371)$$

where $p' = p + q$, the G_{ABC} are the hadronic coupling constants defined by

$$\langle B(p) C(q) | A(p') \rangle = i G_{ABC}, \quad (372)$$

the four functions $\rho_{AC'}(p'^2, p^2, t)$, $\rho_{AB'}(p'^2, t, q^2)$, $\rho_{A'B}(t', p^2, q^2)$ and $\rho_{A'C}(t', p^2, q^2)$ have complex dependence on the transitions between the ground states and the higher resonances or continuum states.

We rewrite the correlation functions $\Pi_H(p'^2, p^2, q^2)$ at the hadron side as

$$\begin{aligned} \Pi_H(p'^2, p^2, q^2) &= \int_{\Delta^2}^{s_A^0} ds' \int_{\Delta_s^2}^{s_B^0} ds \int_{\Delta_u^2}^{u_C^0} du \frac{\rho_H(s', s, u)}{(s' - p'^2)(s - p^2)(u - q^2)} \\ &+ \int_{s_A^0}^{\infty} ds' \int_{\Delta_s^2}^{s_B^0} ds \int_{\Delta_u^2}^{u_C^0} du \frac{\rho_H(s', s, u)}{(s' - p'^2)(s - p^2)(u - q^2)} + \cdots, \end{aligned} \quad (373)$$

through triple-dispersion relation, where the $\rho_H(s', s, u)$ are the hadronic spectral densities,

$$\rho_H(s', s, u) = \lim_{\epsilon_3 \rightarrow 0} \lim_{\epsilon_2 \rightarrow 0} \lim_{\epsilon_1 \rightarrow 0} \frac{\text{Im}_{s'} \text{Im}_s \text{Im}_u \Pi_H(s' + i\epsilon_3, s + i\epsilon_2, u + i\epsilon_1)}{\pi^3}, \quad (374)$$

where the Δ^2 , Δ_s^2 and Δ_u^2 are the thresholds, the s_A^0 , s_B^0 , u_C^0 are the continuum thresholds.

Now we carry out the operator product expansion at the QCD side, and write the correlation functions $\Pi_{QCD}(p'^2, p^2, q^2)$ as

$$\Pi_{QCD}(p'^2, p^2, q^2) = \int_{\Delta_s^2}^{s_B^0} ds \int_{\Delta_u^2}^{u_C^0} du \frac{\rho_{QCD}(p'^2, s, u)}{(s - p^2)(u - q^2)} + \cdots, \quad (375)$$

through double-dispersion relation, where the $\rho_{QCD}(p'^2, s, u)$ are the QCD spectral densities,

$$\rho_{QCD}(p'^2, s, u) = \lim_{\epsilon_2 \rightarrow 0} \lim_{\epsilon_1 \rightarrow 0} \frac{\text{Im}_s \text{Im}_u \Pi_{QCD}(p'^2, s + i\epsilon_2, u + i\epsilon_1)}{\pi^2}. \quad (376)$$

As the QCD spectral densities $\rho_{QCD}(s', s, u)$ do not exist,

$$\begin{aligned} \rho_{QCD}(s', s, u) &= \lim_{\epsilon_3 \rightarrow 0} \lim_{\epsilon_2 \rightarrow 0} \lim_{\epsilon_1 \rightarrow 0} \frac{\text{Im}_{s'} \text{Im}_s \text{Im}_u \Pi_{QCD}(s' + i\epsilon_3, s + i\epsilon_2, u + i\epsilon_1)}{\pi^3} \\ &= 0, \end{aligned} \quad (377)$$

because

$$\lim_{\epsilon_3 \rightarrow 0} \frac{\text{Im}_{s'} \Pi_{QCD}(s' + i\epsilon_3, p^2, q^2)}{\pi} = 0. \quad (378)$$

Thereafter we will write the QCD spectral densities $\rho_{QCD}(p'^2, s, u)$ as $\rho_{QCD}(s, u)$ for simplicity.

We match the hadron side with the QCD side of the correlation functions, and accomplish the integral over ds' firstly to obtain the rigorous quark-hadron duality [520],

$$\int_{\Delta_s^2}^{s_B^0} ds \int_{\Delta_u^2}^{u_C^0} du \frac{\rho_{QCD}(s, u)}{(s - p^2)(u - q^2)} = \int_{\Delta_s^2}^{s_B^0} ds \int_{\Delta_u^2}^{u_C^0} du \frac{1}{(s - p^2)(u - q^2)} \left[\int_{\Delta^2}^{\infty} ds' \frac{\rho_H(s', s, u)}{s' - p'^2} \right], \quad (379)$$

the Δ^2 denotes the thresholds $(\Delta_s + \Delta_u)^2$. Now we write down the quark-hadron duality explicitly,

$$\begin{aligned} \int_{\Delta_s^2}^{s_B^0} ds \int_{\Delta_u^2}^{u_C^0} du \frac{\rho_{QCD}(s, u)}{(s - p^2)(u - q^2)} &= \int_{\Delta_s^2}^{s_B^0} ds \int_{\Delta_u^2}^{u_C^0} du \int_{\Delta^2}^{\infty} ds' \frac{\rho_H(s', s, u)}{(s' - p'^2)(s - p^2)(u - q^2)} \\ &= \frac{\lambda_A \lambda_B \lambda_C G_{ABC}}{(m_A^2 - p'^2)(m_B^2 - p^2)(m_C^2 - q^2)} + \frac{C_{A'B} + C_{A'C}}{(m_B^2 - p^2)(m_C^2 - q^2)}. \end{aligned} \quad (380)$$

No approximation is needed, we do not need the continuum threshold parameter s_A^0 in the s' channel, as we match the hadron side with the QCD side below the continuum thresholds s_0 and u_0 to obtain rigorous quark-hadron duality, and we take account of the continuum contributions in the s' channel.

In Eq.(480), we introduce the parameters $C_{AC'}$, $C_{AB'}$, $C_{A'B}$ and $C_{A'C}$ to parameterize the net effects,

$$\begin{aligned} C_{AC'} &= \int_{s_C^0}^{\infty} dt \frac{\rho_{AC'}(p'^2, p^2, t)}{t - q^2}, \\ C_{AB'} &= \int_{s_B^0}^{\infty} dt \frac{\rho_{AB'}(p'^2, t, q^2)}{t - p^2}, \\ C_{A'B} &= \int_{s_A^0}^{\infty} dt \frac{\rho_{A'B}(t, p^2, q^2)}{t - p'^2}, \\ C_{A'C} &= \int_{s_A^0}^{\infty} dt \frac{\rho_{A'C}(t, p^2, q^2)}{t - p'^2}. \end{aligned} \quad (381)$$

In numerical calculations, we take the relevant functions $C_{A'B}$ and $C_{A'C}$ as free parameters, and choose suitable values to eliminate the contaminations from the higher resonances and continuum states to obtain the stable QCD sum rules with the variations of the Borel parameters T^2 .

According to the discussions in Sect.2.3, the quantum field theory does not forbid the couplings between the four-quark currents $J_A(0)$ and two-meson scattering states BC , if they have the same quantum numbers. The local currents $J_A(0)$ have direct non-vanishing couplings to the two-meson scattering states BC , although the overlaps of the wave-functions are very small [417], which leads to a finite width to modify the dispersion relation, see Eqs.(78)-(79).

There exists another term $\Pi_H^D(p'^2, p^2, q^2)$ at the hadron side beyond that shown in Eq.(480),

$$\Pi_H^D(p'^2, p^2, q^2) = \frac{\lambda_B \lambda_C \lambda_{BC}}{(m_B^2 - p^2)(m_C^2 - q^2)} + \dots, \quad (382)$$

where

$$\langle 0 | J_A(0) | B(p) C(q) \rangle = \lambda_{BC}. \quad (383)$$

Such terms $\Pi_H^D(p'^2, p^2, q^2)$ shown in Eq.(382) could be absorbed into the parameters $C_{A'B} + C_{A'C}$ with the simple replacement,

$$C_{A'B} + C_{A'C} \rightarrow C_{A'B} + C_{A'C} + \lambda_B \lambda_C \lambda_{BC}. \quad (384)$$

In Ref.[446, 790], Nielsen et al approximate the hadron side of the correlation functions as

$$\Pi_H(p'^2, p^2, q^2) = \frac{\lambda_A \lambda_B \lambda_C G_{ABC}}{(m_A^2 - p'^2)(m_B^2 - p^2)(m_C^2 - q^2)} + \frac{B_H}{(s'_0 - p'^2)(m_C^2 - q^2)}, \quad (385)$$

then match them with the QCD side below the continuum threshold s_0 by taking the chiral limit $m_C^2 \rightarrow 0$ and $q^2 \rightarrow 0$ sequentially, where the B_H stands for the pole-continuum transitions, and we have rewritten their notations into the present form for convenience. Although Nielsen et al take account of the continuum contributions by introducing a parameter s'_0 in the s' channel phenomenologically, they neglect the continuum contributions in the u channel at the hadron side by hand. Such an approximation is also adopted in Refs.[47, 532, 791, 792].

There is another scheme to study the strong hadronic coupling constants with the correlation functions $\Pi(p, p')$,

$$\Pi(p, p') = i^2 \int d^4x d^4y e^{-ip \cdot x} e^{ip' \cdot y} \langle 0 | T \left\{ J_B(y) J_C(0) J_A^\dagger(x) \right\} | 0 \rangle. \quad (386)$$

At the QCD side, a double-dispersion relation,

$$\Pi(p^2, p'^2, q^2) = \int_{\Delta_s^2}^{s_0} ds \int_{\Delta_{s'}^2}^{s'_0} ds' \frac{\rho(s, s', q^2)}{(s - p^2)(s' - p'^2)} + \dots, \quad (387)$$

with $q = p' - p$ is adopted [465, 472]. However, we cannot obtain the QCD spectral densities $\rho(s, s', q^2)$. Such an scheme is also adopted in the case of pentaquark states [793, 794, 795, 796].

Let us turn to Eq.(480) again. If the B are charmonium or bottomonium states, we set $p'^2 = p^2$ and perform the double Borel transformation with respect to the variables $P^2 = -p^2$ and $Q^2 = -q^2$, respectively to obtain the QCD sum rules,

$$\frac{\lambda_A \lambda_B \lambda_C G_{ABC}}{m_A^2 - m_B^2} \left[\exp\left(-\frac{m_B^2}{T_1^2}\right) - \exp\left(-\frac{m_A^2}{T_1^2}\right) \right] \exp\left(-\frac{m_C^2}{T_2^2}\right) + (C_{A'B} + C_{A'C}) \exp\left(-\frac{m_B^2}{T_1^2} - \frac{m_C^2}{T_2^2}\right) = \int_{\Delta_s^2}^{s_B^0} ds \int_{\Delta_u^2}^{u_C^0} du \rho_{QCD}(s, u) \exp\left(-\frac{s}{T_1^2} - \frac{u}{T_2^2}\right) \quad (388)$$

where the T_1^2 and T_2^2 are the Borel parameters. If the B are open-charm or open-bottom mesons, we set $p'^2 = 4p^2$ and perform the double Borel transformation with respect to the variables $P^2 = -p^2$ and $Q^2 = -q^2$, respectively to obtain the QCD sum rules,

$$\frac{\lambda_A \lambda_B \lambda_C G_{ABC}}{4(\tilde{m}_A^2 - m_B^2)} \left[\exp\left(-\frac{m_B^2}{T_1^2}\right) - \exp\left(-\frac{\tilde{m}_A^2}{T_1^2}\right) \right] \exp\left(-\frac{m_C^2}{T_2^2}\right) + (C_{A'B} + C_{A'C}) \exp\left(-\frac{m_B^2}{T_1^2} - \frac{m_C^2}{T_2^2}\right) = \int_{\Delta_s^2}^{s_B^0} ds \int_{\Delta_u^2}^{u_C^0} du \rho_{QCD}(s, u) \exp\left(-\frac{s}{T_1^2} - \frac{u}{T_2^2}\right) \quad (389)$$

where $\tilde{m}_A^2 = \frac{m_A^2}{4}$. Or set $p'^2 = p^2$, just like in the first case. The scheme based on the rigorous quark-hadron duality is adopted in Refs.[62, 171, 507, 523, 797, 798, 799, 800, 801, 802, 803, 804, 805, 806].

7.1 Strong decays of the $Y(4500)$ as an example

In this sub-section, we would like to use a typical example to illustrate the procedure in details.

After Ref.[543] was published, the $Y(4500)$ was observed by the BESIII collaboration [155, 156, 159]. At the energy about 4.5 GeV, we obtain three hidden-charm tetraquark states with the $J^{PC} = 1^{--}$, the $[uc]_{\tilde{V}}[\bar{u}\bar{c}]_A + [dc]_{\tilde{V}}[\bar{d}\bar{c}]_A - [uc]_A[\bar{u}\bar{c}]_{\tilde{V}} - [dc]_A[\bar{d}\bar{c}]_{\tilde{V}}, [uc]_{\tilde{A}}[\bar{u}\bar{c}]_V + [dc]_{\tilde{A}}[\bar{d}\bar{c}]_V + [uc]_V[\bar{u}\bar{c}]_{\tilde{A}} + [dc]_V[\bar{d}\bar{c}]_{\tilde{A}}$ and $[uc]_S[\bar{u}\bar{c}]_{\tilde{V}} + [dc]_S[\bar{d}\bar{c}]_{\tilde{V}} - [uc]_{\tilde{V}}[\bar{u}\bar{c}]_S - [dc]_{\tilde{V}}[\bar{d}\bar{c}]_S$ tetraquark states have the masses 4.53 ± 0.07 GeV, 4.48 ± 0.08 GeV and 4.50 ± 0.09 GeV, respectively [543], see Table 22. In Ref.[546], we study their two-body strong decays systematically with the three-point correlation functions,

$$\Pi_{\mu}^{\bar{D}D\tilde{A}V}(p, q) = i^2 \int d^4x d^4y e^{ip \cdot x} e^{iq \cdot y} \langle 0 | T \left\{ J^{\bar{D}}(x) J^D(y) J_{-, \mu}^{\tilde{A}V \dagger}(0) \right\} | 0 \rangle, \quad (390)$$

$$\Pi_{\alpha\mu}^{\bar{D}^*D\tilde{A}V}(p, q) = i^2 \int d^4x d^4y e^{ip \cdot x} e^{iq \cdot y} \langle 0 | T \left\{ J_{\alpha}^{\bar{D}^*}(x) J^D(y) J_{-, \mu}^{\tilde{A}V \dagger}(0) \right\} | 0 \rangle, \quad (391)$$

$$\Pi_{\alpha\beta\mu}^{\bar{D}^*D^*\tilde{A}V}(p, q) = i^2 \int d^4x d^4y e^{ip \cdot x} e^{iq \cdot y} \langle 0 | T \left\{ J_{\alpha}^{\bar{D}^*}(x) J_{\beta}^{D^*}(y) J_{-, \mu}^{\tilde{A}V \dagger}(0) \right\} | 0 \rangle, \quad (392)$$

$$\Pi_{\alpha\mu}^{\bar{D}_0D^*\tilde{A}V}(p, q) = i^2 \int d^4x d^4y e^{ip \cdot x} e^{iq \cdot y} \langle 0 | T \left\{ J^{\bar{D}_0}(x) J_{\alpha}^{D^*}(y) J_{-, \mu}^{\tilde{A}V \dagger}(0) \right\} | 0 \rangle, \quad (393)$$

$$\Pi_{\alpha\mu}^{\bar{D}_1 D \tilde{A}V}(p, q) = i^2 \int d^4x d^4y e^{ip \cdot x} e^{iq \cdot y} \langle 0 | T \left\{ J_{\alpha}^{\bar{D}_1}(x) J^D(y) J_{-\mu}^{\tilde{A}V \dagger}(0) \right\} | 0 \rangle, \quad (394)$$

$$\Pi_{\alpha\mu}^{\eta_c \tilde{A}V}(p, q) = i^2 \int d^4x d^4y e^{ip \cdot x} e^{iq \cdot y} \langle 0 | T \left\{ J^{\eta_c}(x) J_{\alpha}^{\omega}(y) J_{-\mu}^{\tilde{A}V \dagger}(0) \right\} | 0 \rangle, \quad (395)$$

$$\Pi_{\alpha\beta\mu}^{J/\psi \omega \tilde{A}V}(p, q) = i^2 \int d^4x d^4y e^{ip \cdot x} e^{iq \cdot y} \langle 0 | T \left\{ J_{\alpha}^{J/\psi}(x) J_{\beta}^{\omega}(y) J_{-\mu}^{\tilde{A}V \dagger}(0) \right\} | 0 \rangle, \quad (396)$$

$$\Pi_{\alpha\mu}^{\chi_{c0} \omega \tilde{A}V}(p, q) = i^2 \int d^4x d^4y e^{ip \cdot x} e^{iq \cdot y} \langle 0 | T \left\{ J^{\chi_{c0}}(x) J_{\alpha}^{\omega}(y) J_{-\mu}^{\tilde{A}V \dagger}(0) \right\} | 0 \rangle, \quad (397)$$

$$\Pi_{\alpha\beta\mu}^{\chi_{c1} \omega \tilde{A}V}(p, q) = i^2 \int d^4x d^4y e^{ip \cdot x} e^{iq \cdot y} \langle 0 | T \left\{ J_{\alpha}^{\chi_{c1}}(x) J_{\beta}^{\omega}(y) J_{-\mu}^{\tilde{A}V \dagger}(0) \right\} | 0 \rangle, \quad (398)$$

$$\Pi_{\alpha\mu}^{J/\psi f_0 \tilde{A}V}(p, q) = i^2 \int d^4x d^4y e^{ip \cdot x} e^{iq \cdot y} \langle 0 | T \left\{ J_{\alpha}^{J/\psi}(x) J^{f_0}(y) J_{-\mu}^{\tilde{A}V \dagger}(0) \right\} | 0 \rangle. \quad (399)$$

With the simple replacement $\tilde{A}V \rightarrow \tilde{V}A$, we obtain the corresponding correlation functions for the current $J_{-\mu}^{\tilde{V}A}$. And with the simple replacements $\tilde{A}V \rightarrow S\tilde{V}$ and $\mu \rightarrow \mu\nu$, we obtain the corresponding correlation functions for the current $J_{-\mu\nu}^{S\tilde{V}}$, where the currents

$$\begin{aligned} J^{\bar{D}}(x) &= \bar{c}(x) i \gamma_5 u(x), \\ J^D(y) &= \bar{u}(y) i \gamma_5 c(y), \\ J_{\alpha}^{\bar{D}^*}(x) &= \bar{c}(x) \gamma_{\alpha} u(x), \\ J_{\beta}^{D^*}(y) &= \bar{u}(y) \gamma_{\beta} c(y), \\ J^{\bar{D}_0}(x) &= \bar{c}(x) u(x), \\ J_{\alpha}^{\bar{D}_1}(x) &= \bar{c}(x) \gamma_{\alpha} \gamma_5 u(x), \end{aligned} \quad (400)$$

$$\begin{aligned} J^{\eta_c}(x) &= \bar{c}(x) i \gamma_5 c(x), \\ J_{\alpha}^{J/\psi}(x) &= \bar{c}(x) \gamma_{\alpha} c(x), \\ J^{\chi_{c0}}(x) &= \bar{c}(x) c(x), \\ J_{\alpha}^{\chi_{c1}}(x) &= \bar{c}(x) \gamma_{\alpha} \gamma_5 c(x), \end{aligned} \quad (401)$$

$$\begin{aligned} J_{\alpha}^{\omega}(y) &= \frac{\bar{u}(y) \gamma_{\alpha} u(y) + \bar{d}(y) \gamma_{\alpha} d(y)}{\sqrt{2}}, \\ J^{f_0}(y) &= \frac{\bar{u}(y) u(y) + \bar{d}(y) d(y)}{\sqrt{2}}, \end{aligned} \quad (402)$$

$$\begin{aligned} J_{-\mu}^{\tilde{A}V}(x) &= \frac{\varepsilon^{ijk} \varepsilon^{imn}}{2} \left[u_j^T(x) C \sigma_{\mu\nu} \gamma_5 c_k(x) \bar{u}_m(x) \gamma_5 \gamma^{\nu} C \bar{c}_n^T(x) + d_j^T(x) C \sigma_{\mu\nu} \gamma_5 c_k(x) \bar{d}_m(x) \gamma_5 \gamma^{\nu} C \bar{c}_n^T(x) \right. \\ &\quad \left. + u_j^T(x) C \gamma^{\nu} \gamma_5 c_k(x) \bar{u}_m(x) \gamma_5 \sigma_{\mu\nu} C \bar{c}_n^T(x) + d_j^T(x) C \gamma^{\nu} \gamma_5 c_k(x) \bar{d}_m(x) \gamma_5 \sigma_{\mu\nu} C \bar{c}_n^T(x) \right], \end{aligned} \quad (403)$$

$$J_{-, \mu}^{\tilde{V}A}(x) = \frac{\varepsilon^{ijk} \varepsilon^{imn}}{2} \left[u_j^T(x) C \sigma_{\mu\nu} c_k(x) \bar{u}_m(x) \gamma^\nu C \bar{c}_n^T(x) + d_j^T(x) C \sigma_{\mu\nu} c_k(x) \bar{d}_m(x) \gamma^\nu C \bar{c}_n^T(x) \right. \\ \left. - u_j^T(x) C \gamma^\nu c_k(x) \bar{u}_m(x) \sigma_{\mu\nu} C \bar{c}_n^T(x) - d_j^T(x) C \gamma^\nu c_k(x) \bar{d}_m(x) \sigma_{\mu\nu} C \bar{c}_n^T(x) \right], \quad (404)$$

$$J_{-, \mu\nu}^{S\tilde{V}}(x) = \frac{\varepsilon^{ijk} \varepsilon^{imn}}{2} \left[u_j^T(x) C \gamma_5 c_k(x) \bar{u}_m(x) \sigma_{\mu\nu} C \bar{c}_n^T(x) + d_j^T(x) C \gamma_5 c_k(x) \bar{d}_m(x) \sigma_{\mu\nu} C \bar{c}_n^T(x) \right. \\ \left. - u_j^T(x) C \sigma_{\mu\nu} c_k(x) \bar{u}_m(x) \gamma_5 C \bar{c}_n^T(x) - d_j^T(x) C \sigma_{\mu\nu} c_k(x) \bar{d}_m(x) \gamma_5 C \bar{c}_n^T(x) \right]. \quad (405)$$

According to quark-hadron duality, we obtain the hadron representation and isolate the ground state contributions explicitly,

$$\Pi_\mu^{\bar{D}D\tilde{A}V}(p, q) = \Pi_{\bar{D}D\tilde{A}V}(p'^2, p^2, q^2) i(p - q)_\mu + \cdots, \quad (406)$$

$$\Pi_{\alpha\mu}^{\bar{D}^*D\tilde{A}V}(p, q) = \Pi_{\bar{D}^*D\tilde{A}V}(p'^2, p^2, q^2) (-i\varepsilon_{\alpha\mu\lambda\tau} p^\lambda q^\tau) + \cdots, \quad (407)$$

$$\Pi_{\alpha\beta\mu}^{\bar{D}^*D^*\tilde{A}V}(p, q) = \Pi_{\bar{D}^*D^*\tilde{A}V}(p'^2, p^2, q^2) (-ig_{\alpha\beta} p_\mu) + \cdots, \quad (408)$$

$$\Pi_{\alpha\mu}^{\bar{D}_0D^*\tilde{A}V}(p, q) = \Pi_{\bar{D}_0D^*\tilde{A}V}(p'^2, p^2, q^2) (-ig_{\alpha\mu} p \cdot q) + \cdots, \quad (409)$$

$$\Pi_{\alpha\mu}^{\bar{D}_1D\tilde{A}V}(p, q) = \Pi_{\bar{D}_1D\tilde{A}V}(p'^2, p^2, q^2) g_{\alpha\mu} + \cdots, \quad (410)$$

$$\Pi_{\alpha\mu}^{\eta_c\omega\tilde{A}V}(p, q) = \Pi_{\eta_c\omega\tilde{A}V}(p'^2, p^2, q^2) (i\varepsilon_{\alpha\mu\lambda\tau} p^\lambda q^\tau) + \cdots, \quad (411)$$

$$\Pi_{\alpha\beta\mu}^{J/\psi\omega\tilde{A}V}(p, q) = \Pi_{J/\psi\omega\tilde{A}V}(p'^2, p^2, q^2) (ig_{\alpha\beta} p_\mu) + \cdots, \quad (412)$$

$$\Pi_{\alpha\mu}^{\chi_{c0}\omega\tilde{A}V}(p, q) = \Pi_{\chi_{c0}\omega\tilde{A}V}(p'^2, p^2, q^2) ig_{\alpha\mu} + \cdots, \quad (413)$$

$$\Pi_{\alpha\beta\mu}^{\chi_{c1}\omega\tilde{A}V}(p, q) = \Pi_{\chi_{c1}\omega\tilde{A}V}(p'^2, p^2, q^2) (\varepsilon_{\alpha\beta\mu\lambda} p^\lambda p \cdot q) + \cdots, \quad (414)$$

$$\Pi_{\alpha\mu}^{J/\psi f_0\tilde{A}V}(p, q) = \Pi_{J/\psi f_0\tilde{A}V}(p'^2, p^2, q^2) (-ig_{\alpha\mu}) + \cdots, \quad (415)$$

other ground state contributions are given in Ref.[546], where

$$\Pi_{\bar{D}D\tilde{A}V}(p'^2, p^2, q^2) = \frac{\lambda_{\bar{D}D\tilde{A}V}}{(m_Y^2 - p'^2)(m_D^2 - p^2)(m_D^2 - q^2)} + \frac{C_{\bar{D}D\tilde{A}V}}{(m_D^2 - p^2)(m_D^2 - q^2)} \\ + \cdots, \quad (416)$$

$$\begin{aligned} \Pi_{\bar{D}^* D \tilde{A} V}(p'^2, p^2, q^2) &= \frac{\lambda_{\bar{D}^* D \tilde{A} V}}{(m_Y^2 - p'^2)(m_{D^*}^2 - p^2)(m_D^2 - q^2)} + \frac{C_{\bar{D}^* D \tilde{A} V}}{(m_{D^*}^2 - p^2)(m_D^2 - q^2)} \\ &+ \dots, \end{aligned} \quad (417)$$

$$\begin{aligned} \Pi_{\bar{D}^* D^* \tilde{A} V}(p'^2, p^2, q^2) &= \frac{\lambda_{\bar{D}^* D^* \tilde{A} V}}{(m_Y^2 - p'^2)(m_{D^*}^2 - p^2)(m_{D^*}^2 - q^2)} + \frac{C_{\bar{D}^* D^* \tilde{A} V}}{(m_{D^*}^2 - p^2)(m_{D^*}^2 - q^2)} \\ &+ \dots, \end{aligned} \quad (418)$$

$$\begin{aligned} \Pi_{\bar{D}_0 D^* \tilde{A} V}(p'^2, p^2, q^2) &= \frac{\lambda_{\bar{D}_0 D^* \tilde{A} V}}{(m_Y^2 - p'^2)(m_{D_0}^2 - p^2)(m_{D^*}^2 - q^2)} + \frac{C_{\bar{D}_0 D^* \tilde{A} V}}{(m_{D_0}^2 - p^2)(m_{D^*}^2 - q^2)} \\ &+ \dots, \end{aligned} \quad (419)$$

$$\begin{aligned} \Pi_{\bar{D}_1 D \tilde{A} V}(p'^2, p^2, q^2) &= \frac{\lambda_{\bar{D}_1 D \tilde{A} V}}{(m_Y^2 - p'^2)(m_{D_1}^2 - p^2)(m_D^2 - q^2)} + \frac{C_{\bar{D}_1 D \tilde{A} V}}{(m_{D_1}^2 - p^2)(m_D^2 - q^2)} \\ &+ \dots, \end{aligned} \quad (420)$$

$$\begin{aligned} \Pi_{\eta_c \omega \tilde{A} V}(p'^2, p^2, q^2) &= \frac{\lambda_{\eta_c \omega \tilde{A} V}}{(m_Y^2 - p'^2)(m_{\eta_c}^2 - p^2)(m_\omega^2 - q^2)} + \frac{C_{\eta_c \omega \tilde{A} V}}{(m_{\eta_c}^2 - p^2)(m_\omega^2 - q^2)} \\ &+ \dots, \end{aligned} \quad (421)$$

with the simple replacements $\eta_c \rightarrow J/\psi$, χ_{c0} and χ_{c1} , we obtain the hadronic representation for the $J/\psi \omega \tilde{A} V$, $\chi_{c0} \omega \tilde{A} V$ and $\chi_{c1} \omega \tilde{A} V$ channels, respectively,

$$\begin{aligned} \Pi_{J/\psi f_0 \tilde{A} V}(p'^2, p^2, q^2) &= \frac{\lambda_{J/\psi f_0 \tilde{A} V}}{(m_Y^2 - p'^2)(m_{J/\psi}^2 - p^2)(m_{f_0}^2 - q^2)} + \frac{C_{J/\psi f_0 \tilde{A} V}}{(m_{J/\psi}^2 - p^2)(m_{f_0}^2 - q^2)} \\ &+ \dots. \end{aligned} \quad (422)$$

With the simple replacements $\tilde{A} V \rightarrow \tilde{V} A$ and $S \tilde{V}$, we obtain the corresponding components $\Pi(p'^2, p^2, q^2)$ for the currents $J_{-, \mu}^{\tilde{V} A}(0)$ and $J_{-, \mu \nu}^{S \tilde{V}}(0)$, except for the component $\Pi_{\eta_c \omega S \tilde{V}}(p'^2, p^2, q^2)$,

$$\begin{aligned} \Pi_{\eta_c \omega S \tilde{V}}(p'^2, p^2, q^2) &= \frac{\lambda_{\eta_c \omega S \tilde{V}}}{(m_Y^2 - p'^2)(m_{\eta_c}^2 - p^2)(m_\omega^2 - q^2)} + \frac{C_{\eta_c \omega S \tilde{V}}}{(m_{\eta_c}^2 - p^2)(m_\omega^2 - q^2)} \\ &+ \frac{\bar{\lambda}_{\eta_c \omega S \tilde{A}}}{(m_X^2 - p'^2)(m_{\eta_c}^2 - p^2)(m_\omega^2 - q^2)} + \dots. \end{aligned} \quad (423)$$

We introduce the collective notations to simplify the expressions,

$$\begin{aligned} \lambda_{\bar{D} D \tilde{A} V} &= \frac{f_D^2 m_D^4}{m_c^2} \lambda_{\tilde{A} V} G_{\bar{D} D \tilde{A} V}, \\ \lambda_{\bar{D}^* D \tilde{A} V} &= \frac{f_{D^*} m_{D^*} f_D m_D^2}{m_c} \lambda_{\tilde{A} V} G_{\bar{D}^* D \tilde{A} V}, \\ \lambda_{\bar{D}^* D^* \tilde{A} V} &= f_{D^*}^2 m_{D^*}^2 \lambda_{\tilde{A} V} G_{\bar{D}^* D^* \tilde{A} V}, \\ \lambda_{\bar{D}_0 D^* \tilde{A} V} &= f_{D_0} m_{D_0} f_{D^*} m_{D^*} \lambda_{\tilde{A} V} G_{\bar{D}_0 D^* \tilde{A} V}, \\ \lambda_{\bar{D}_1 D \tilde{A} V} &= \frac{f_{D_1} m_{D_1} f_D m_D^2}{m_c} \lambda_{\tilde{A} V} G_{\bar{D}_1 D \tilde{A} V}, \end{aligned} \quad (424)$$

$$\begin{aligned}
\lambda_{\eta_c \omega \tilde{A}V} &= \frac{f_{\eta_c} m_{\eta_c}^2 f_{\omega} m_{\omega}}{2m_c} \lambda_{\tilde{A}V} G_{\eta_c \omega \tilde{A}V}, \\
\lambda_{J/\psi \omega \tilde{A}V} &= f_{J/\psi} m_{J/\psi} f_{\omega} m_{\omega} \lambda_{\tilde{A}V} G_{J/\psi \omega \tilde{A}V} \left(1 + \frac{m_{\omega}^2}{m_Y^2} - \frac{m_{J/\psi}^2}{m_Y^2} \right), \\
\lambda_{\chi_{c0} \omega \tilde{A}V} &= f_{\chi_{c0}} m_{\chi_{c0}} f_{\omega} m_{\omega} \lambda_{\tilde{A}V} G_{\chi_{c0} \omega \tilde{A}V}, \\
\lambda_{\chi_{c1} \omega \tilde{A}V} &= f_{\chi_{c1}} m_{\chi_{c1}} f_{\omega} m_{\omega} \lambda_{\tilde{A}V} G_{\chi_{c1} \omega \tilde{A}V}, \\
\lambda_{J/\psi f_0 \tilde{A}V} &= f_{J/\psi} m_{J/\psi} f_{f_0} m_{f_0} \lambda_{\tilde{A}V} G_{J/\psi f_0 \tilde{A}V}.
\end{aligned} \tag{425}$$

With the simple replacements $\tilde{A}V \rightarrow \tilde{V}A$ and $S\tilde{V}$, we obtain the collective notations λ for the currents $J_{-, \mu}^{\tilde{V}A}(0)$ and $J_{-, \mu\nu}^{S\tilde{V}}(0)$, except for the $\lambda_{\eta_c \omega S\tilde{V}}$, $\lambda_{J/\psi \omega S\tilde{V}}$, $\lambda_{\chi_{c1} \omega S\tilde{V}}$, where

$$\begin{aligned}
\lambda_{\eta_c \omega S\tilde{V}} &= \frac{f_{\eta_c} m_{\eta_c}^2 f_{\omega} m_{\omega}^3}{2m_c} \lambda_{S\tilde{V}} G_{\eta_c \omega S\tilde{V}}, \\
\lambda_{J/\psi \omega S\tilde{V}} &= f_{J/\psi} m_{J/\psi} f_{\omega} m_{\omega} \lambda_{S\tilde{V}} G_{J/\psi \omega S\tilde{V}}, \\
\lambda_{\chi_{c1} \omega S\tilde{V}} &= f_{\chi_{c1}} m_{\chi_{c1}}^3 f_{\omega} m_{\omega} \lambda_{S\tilde{V}} G_{\chi_{c1} \omega S\tilde{V}},
\end{aligned} \tag{426}$$

and

$$\bar{\lambda}_{\eta_c \omega S\tilde{A}} = \frac{f_{\eta_c} m_{\eta_c}^2 f_{\omega} m_{\omega}}{2m_c} \bar{\lambda}_{S\tilde{A}} \bar{G}_{\eta_c \omega S\tilde{A}}. \tag{427}$$

We adopt the standard definitions for the decay constants and pole residues [546], and we define the hadronic coupling constants,

$$\begin{aligned}
\langle \bar{D}(p) D(q) | Y_{\tilde{A}V}(p') \rangle &= (p - q) \cdot \varepsilon G_{\bar{D}D\tilde{A}V}, \\
\langle \bar{D}(p) D(q) | Y_{\tilde{V}A}(p') \rangle &= (p - q) \cdot \varepsilon G_{\bar{D}D\tilde{V}A}, \\
\langle \bar{D}(p) D(q) | Y_{S\tilde{V}}(p') \rangle &= -i(p - q) \cdot \varepsilon G_{\bar{D}DS\tilde{V}},
\end{aligned} \tag{428}$$

$$\begin{aligned}
\langle \bar{D}^*(p) D(q) | Y_{\tilde{A}V}(p') \rangle &= -\varepsilon^{\lambda\tau\rho\sigma} p_{\lambda} \xi_{\tau}^* p'_{\rho} \varepsilon_{\sigma} G_{\bar{D}^*D\tilde{A}V}, \\
\langle \bar{D}^*(p) D(q) | Y_{\tilde{V}A}(p') \rangle &= \varepsilon^{\lambda\tau\rho\sigma} p_{\lambda} \xi_{\tau}^* p'_{\rho} \varepsilon_{\sigma} G_{\bar{D}^*D\tilde{V}A}, \\
\langle \bar{D}^*(p) D(q) | Y_{S\tilde{V}}(p') \rangle &= -i\varepsilon^{\lambda\tau\rho\sigma} p_{\lambda} \xi_{\tau}^* p'_{\rho} \varepsilon_{\sigma} G_{\bar{D}^*DS\tilde{V}},
\end{aligned} \tag{429}$$

etc [546].

In Eq.(423), there are contributions come from the $J^{PC} = 1^{+-}$ and 1^{--} tetraquark states, and we cannot choose the pertinent structures to exclude the contaminations from the $J^{PC} = 1^{+-}$ tetraquark state X , so we include it at the hadron side. The unknown parameters $C_{\bar{D}D\tilde{A}V}$, $C_{\bar{D}^*D\tilde{A}V}$, $C_{\bar{D}^*D\tilde{V}A}$, etc, parameterize the complex interactions among the excitations in the p'^2 channels and the ground state charmed meson pairs or charmonium plus ω/f_0 . It is difficult to choose the pertinent tensor structures in Eqs.(406)-(423) to obtain good QCD sum rules without contaminations, we have to reach the satisfactory results via trial and error.

At the QCD side, we accomplish the operator product expansion up to the vacuum condensates of dimension 5 and take account of both the connected and disconnected Feynman diagrams in the color space, see Fig.31 (in Refs.[47, 446, 532, 790, 791], only the connected Feynman diagrams are taken into account, i.e. the D , E and I in Fig.31), and choose the components $\Pi_H(p'^2, p^2, q^2)$ to study the hadronic coupling constants G_H based on the rigorous quark-hadron duality [520, 789].

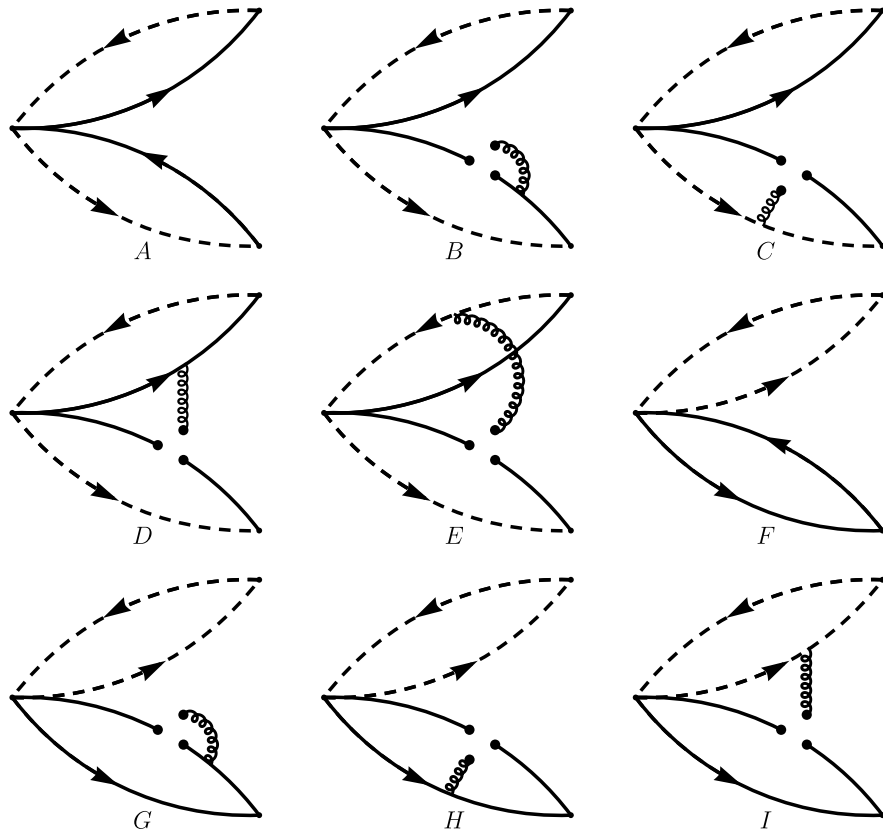


Figure 31: The connected and disconnected Feynman diagrams, where the dashed (solid) lines denote the heavy (light) quark lines, the interchanges of the heavy (light) quark lines are implied.

Then we set $p'^2 = p^2$ in the components $\Pi(p'^2, p^2, q^2)$, and carry out the double Borel transformation with respect to the variables $P^2 = -p^2$ and $Q^2 = -q^2$ respectively, and set $T_1^2 = T_2^2 = T^2$ to obtain thirty QCD sum rules,

$$\begin{aligned} & \frac{\lambda_{\bar{D}D\tilde{A}V}}{m_Y^2 - m_D^2} \left[\exp\left(-\frac{m_D^2}{T^2}\right) - \exp\left(-\frac{m_Y^2}{T^2}\right) \right] \exp\left(-\frac{m_D^2}{T^2}\right) + C_{\bar{D}D\tilde{A}V} \exp\left(-\frac{m_D^2}{T^2} - \frac{m_D^2}{T^2}\right) \\ &= \Pi_{\bar{D}D\tilde{A}V}^{QCD}(T^2), \end{aligned} \quad (430)$$

$$\begin{aligned} & \frac{\lambda_{\bar{D}^*D\tilde{A}V}}{m_Y^2 - m_{D^*}^2} \left[\exp\left(-\frac{m_{D^*}^2}{T^2}\right) - \exp\left(-\frac{m_Y^2}{T^2}\right) \right] \exp\left(-\frac{m_D^2}{T^2}\right) + C_{\bar{D}^*D\tilde{A}V} \exp\left(-\frac{m_{D^*}^2}{T^2} - \frac{m_D^2}{T^2}\right) \\ &= \Pi_{\bar{D}^*D\tilde{A}V}^{QCD}(T^2), \end{aligned} \quad (431)$$

$$\begin{aligned} & \frac{\lambda_{\bar{D}^*D^*\tilde{A}V}}{m_Y^2 - m_{D^*}^2} \left[\exp\left(-\frac{m_{D^*}^2}{T^2}\right) - \exp\left(-\frac{m_Y^2}{T^2}\right) \right] \exp\left(-\frac{m_{D^*}^2}{T^2}\right) + C_{\bar{D}^*D^*\tilde{A}V} \exp\left(-\frac{m_{D^*}^2}{T^2} - \frac{m_{D^*}^2}{T^2}\right) \\ &= \Pi_{\bar{D}^*D^*\tilde{A}V}^{QCD}(T^2), \end{aligned} \quad (432)$$

$$\begin{aligned} & \frac{\lambda_{\bar{D}_0D^*\tilde{A}V}}{m_Y^2 - m_{D_0}^2} \left[\exp\left(-\frac{m_{D_0}^2}{T^2}\right) - \exp\left(-\frac{m_Y^2}{T^2}\right) \right] \exp\left(-\frac{m_{D^*}^2}{T^2}\right) + C_{\bar{D}_0D^*\tilde{A}V} \exp\left(-\frac{m_{D_0}^2}{T^2} - \frac{m_{D^*}^2}{T^2}\right) \\ &= \Pi_{\bar{D}_0D^*\tilde{A}V}^{QCD}(T^2), \end{aligned} \quad (433)$$

$$\begin{aligned} & \frac{\lambda_{\bar{D}_1D\tilde{A}V}}{m_Y^2 - m_{D_1}^2} \left[\exp\left(-\frac{m_{D_1}^2}{T^2}\right) - \exp\left(-\frac{m_Y^2}{T^2}\right) \right] \exp\left(-\frac{m_D^2}{T^2}\right) + C_{\bar{D}_1D\tilde{A}V} \exp\left(-\frac{m_{D_1}^2}{T^2} - \frac{m_D^2}{T^2}\right) \\ &= \Pi_{\bar{D}_1D\tilde{A}V}^{QCD}(T^2), \end{aligned} \quad (434)$$

$$\begin{aligned} & \frac{\lambda_{\eta_c\omega\tilde{A}V}}{m_Y^2 - m_{\eta_c}^2} \left[\exp\left(-\frac{m_{\eta_c}^2}{T^2}\right) - \exp\left(-\frac{m_Y^2}{T^2}\right) \right] \exp\left(-\frac{m_\omega^2}{T^2}\right) + C_{\eta_c\omega\tilde{A}V} \exp\left(-\frac{m_{\eta_c}^2}{T^2} - \frac{m_\omega^2}{T^2}\right) \\ &= \Pi_{\eta_c\omega\tilde{A}V}^{QCD}(T^2), \end{aligned} \quad (435)$$

with the simple replacements $\eta_c \rightarrow J/\psi$, χ_{c0} and χ_{c1} , we obtain the QCD sum rules for the $J/\psi\omega\tilde{A}V$, $\chi_{c0}\omega\tilde{A}V$ and $\chi_{c1}\omega\tilde{A}V$ channels, respectively,

$$\begin{aligned} & \frac{\lambda_{J/\psi f_0\tilde{A}V}}{m_Y^2 - m_{J/\psi}^2} \left[\exp\left(-\frac{m_{J/\psi}^2}{T^2}\right) - \exp\left(-\frac{m_Y^2}{T^2}\right) \right] \exp\left(-\frac{m_{f_0}^2}{T^2}\right) + C_{J/\psi f_0\tilde{A}V} \exp\left(-\frac{m_{J/\psi}^2}{T^2} - \frac{m_{f_0}^2}{T^2}\right) \\ &= \Pi_{J/\psi f_0\tilde{A}V}^{QCD}(T^2). \end{aligned} \quad (436)$$

With the simple replacements $\tilde{A}V \rightarrow \tilde{V}A$ and $S\tilde{V}$, we obtain the QCD sum rules for the $J_{-, \mu}^{\tilde{V}A}(0)$ and $J_{-, \mu\nu}^{S\tilde{V}}(0)$, except for the $\eta_c\omega$ channel,

$$\begin{aligned} & \frac{\lambda_{\eta_c\omega S\tilde{V}}}{m_Y^2 - m_{\eta_c}^2} \left[\exp\left(-\frac{m_{\eta_c}^2}{T^2}\right) - \exp\left(-\frac{m_Y^2}{T^2}\right) \right] \exp\left(-\frac{m_\omega^2}{T^2}\right) + C_{\eta_c\omega S\tilde{V}} \exp\left(-\frac{m_{\eta_c}^2}{T^2} - \frac{m_\omega^2}{T^2}\right) \\ &+ \frac{\bar{\lambda}_{\eta_c\omega S\tilde{A}}}{m_X^2 - m_{\eta_c}^2} \left[\exp\left(-\frac{m_{\eta_c}^2}{T^2}\right) - \exp\left(-\frac{m_X^2}{T^2}\right) \right] \exp\left(-\frac{m_\omega^2}{T^2}\right) = \Pi_{\eta_c\omega S\tilde{V}}^{QCD}(T^2), \end{aligned} \quad (437)$$

the explicit expressions of the QCD side are given in Ref.[546].

We take the unknown parameters $C_{\bar{D}D\tilde{A}V}$, $C_{\bar{D}^*D\tilde{A}V}$, $C_{\bar{D}^*D^*\tilde{A}V}$, \dots as free parameters, and adjust the suitable values to obtain flat Borel platforms for the hadronic coupling constants [546],

$$\begin{aligned}
C_{\bar{D}D\tilde{A}V} &= 0.00045 \text{ GeV}^5 \times T^2, \\
C_{\bar{D}^*D\tilde{A}V} &= -0.000003 \text{ GeV}^4 \times T^2, \\
C_{\bar{D}^*D^*\tilde{A}V} &= 0.0001 \text{ GeV}^5 \times T^2, \\
C_{\bar{D}_0D^*\tilde{A}V} &= 0.000055 \text{ GeV}^4 \times T^2, \\
C_{\bar{D}_1D\tilde{A}V} &= 0.0031 \text{ GeV}^6 \times T^2, \\
C_{\eta_c\omega\tilde{A}V} &= -0.000082 \text{ GeV}^4 \times T^2, \\
C_{J/\psi\omega\tilde{A}V} &= 0.0, \\
C_{\chi_{c0}\omega\tilde{A}V} &= 0.00085 \text{ GeV}^6 \times T^2, \\
C_{\chi_{c1}\omega\tilde{A}V} &= -0.000019 \text{ GeV}^3 \times T^2, \\
C_{J/\psi f_0\tilde{A}V} &= 0.00085 \text{ GeV}^6 \times T^2,
\end{aligned} \tag{438}$$

$$\begin{aligned}
C_{\bar{D}D\tilde{V}A} &= 0.0000015 \text{ GeV}^5 \times T^2, \\
C_{\bar{D}^*D\tilde{V}A} &= 0.000038 \text{ GeV}^4 \times T^2, \\
C_{\bar{D}^*D^*\tilde{V}A} &= 0.0000054 \text{ GeV}^5 \times T^2, \\
C_{\bar{D}_0D^*\tilde{V}A} &= 0.00264 \text{ GeV}^6 \times T^2, \\
C_{\bar{D}_1D\tilde{V}A} &= 0.000055 \text{ GeV}^4 \times T^2, \\
C_{\eta_c\omega\tilde{V}A} &= -0.00006 \text{ GeV}^4 \times T^2, \\
C_{J/\psi\omega\tilde{V}A} &= 0.0, \\
C_{\chi_{c0}\omega\tilde{V}A} &= 0.00087 \text{ GeV}^6 \times T^2, \\
C_{\chi_{c1}\omega\tilde{V}A} &= -0.000018 \text{ GeV}^3 \times T^2, \\
C_{J/\psi f_0\tilde{V}A} &= 0.00075 \text{ GeV}^6 \times T^2,
\end{aligned} \tag{439}$$

$$\begin{aligned}
C_{\bar{D}DS\tilde{V}} &= 0.00014 \text{ GeV}^6 + 0.00002 \text{ GeV}^4 \times T^2, \\
C_{\bar{D}^*DS\tilde{V}} &= 0.0000006 \text{ GeV}^3 \times T^2, \\
C_{\bar{D}^*D^*S\tilde{V}} &= -0.000002 \text{ GeV}^4 \times T^2, \\
C_{\bar{D}_0D^*S\tilde{V}} &= 0.0012 \text{ GeV}^7 + 0.000164 \text{ GeV}^5 \times T^2, \\
C_{\bar{D}_1DS\tilde{V}} &= 0.0017 \text{ GeV}^7 + 0.000205 \text{ GeV}^5 \times T^2, \\
C_{\eta_c\omega S\tilde{V}} &= 0.00014 \text{ GeV}^7, \\
\bar{\lambda}_{\eta_c\omega S\tilde{A}} &= 0.0012 \text{ GeV}^7 \times T^2, \\
C_{J/\psi\omega S\tilde{V}} &= -0.0005 \text{ GeV}^6 - 0.0000216 \text{ GeV}^4 \times T^2, \\
C_{\chi_{c0}\omega S\tilde{V}} &= -0.0018 \text{ GeV}^7 - 0.000156 \text{ GeV}^5 \times T^2, \\
C_{\chi_{c1}\omega S\tilde{V}} &= 0.0012 \text{ GeV}^8 + 0.00015 \text{ GeV}^6 \times T^2, \\
C_{J/\psi f_0S\tilde{V}} &= 0.0005 \text{ GeV}^7 + 0.00006 \text{ GeV}^5 \times T^2,
\end{aligned} \tag{440}$$

the Borel windows are shown explicitly in Table 59. We obtain uniform flat platforms $T_{max}^2 - T_{min}^2 = 1 \text{ GeV}^2$, where the max and min denote the maximum and minimum, respectively. In calculations,

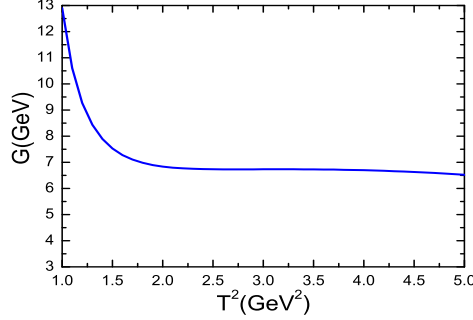


Figure 32: The hadron-coupling constant $G_{\bar{D}_1 D \tilde{A} V}$ with the Borel parameter.

we choose quark flavor numbers $n_f = 4$, and evolve all the input parameters to the energy scale $\mu = 1$ GeV. For detailed information about the parameters, one can consult Ref.[546].

In Fig.32, we plot the $G_{\bar{D}_1 D \tilde{A} V}$ with variation of the Borel parameter at a large interval as an example, in the Borel window, there appears very flat platform indeed.

We estimate the uncertainties of the hadronic coupling constants routinely. For an input parameter ξ , $\xi = \bar{\xi} + \delta\xi$, the left side can be written as $\lambda_{\tilde{A}V} f_{\bar{D}} f_D G_{\bar{D} D \tilde{A} V} = \bar{\lambda}_{\tilde{A}V} \bar{f}_{\bar{D}} \bar{f}_D \bar{G}_{\bar{D} D \tilde{A} V} + \delta\lambda_{\tilde{A}V} \bar{f}_{\bar{D}} \bar{f}_D \bar{G}_{\bar{D} D \tilde{A} V} + \bar{\lambda}_{\tilde{A}V} \delta f_{\bar{D}} \bar{f}_D \bar{G}_{\bar{D} D \tilde{A} V} + \bar{\lambda}_{\tilde{A}V} \bar{f}_{\bar{D}} \delta f_D \bar{G}_{\bar{D} D \tilde{A} V} + \bar{\lambda}_{\tilde{A}V} \bar{f}_{\bar{D}} \bar{f}_D \delta G_{\bar{D} D \tilde{A} V}$, where

$$\delta\lambda_{\tilde{A}V} \bar{f}_{\bar{D}} \bar{f}_D \bar{G}_{\bar{D} D \tilde{A} V} = \bar{\lambda}_{\tilde{A}V} \bar{f}_{\bar{D}} \bar{f}_D \bar{G}_{\bar{D} D \tilde{A} V} \left(\frac{\delta f_{\bar{D}}}{\bar{f}_{\bar{D}}} + \frac{\delta f_D}{\bar{f}_D} + \frac{\delta\lambda_{\tilde{A}V}}{\bar{\lambda}_{\tilde{A}V}} + \frac{\delta G_{\bar{D} D \tilde{A} V}}{\bar{G}_{\bar{D} D \tilde{A} V}} \right), \quad (441)$$

... We set $\delta C_{\bar{D} D \tilde{A} V} = 0$, $\frac{\delta f_{\bar{D}}}{\bar{f}_{\bar{D}}} = \frac{\delta f_D}{\bar{f}_D} = \frac{\delta\lambda_{\tilde{A}V}}{\bar{\lambda}_{\tilde{A}V}} = \frac{\delta G_{\bar{D} D \tilde{A} V}}{\bar{G}_{\bar{D} D \tilde{A} V}}$, ... approximately.

After taking into account the uncertainties, we obtain the values of the hadronic coupling constants, which are shown explicitly in Table 59, then we obtain the partial decay widths directly, and show them explicitly in Table 60.

At last, we saturate the total widths with the summary of partial decay widths,

$$\begin{aligned} \Gamma(Y_{\tilde{A}V}) &= 241.6 \pm 9.0 \text{ MeV}, \\ \Gamma(Y_{\tilde{V}A}) &= 210.6 \pm 9.4 \text{ MeV}, \\ \Gamma(Y_{S\tilde{V}}) &= 229.4 \pm 39.9 \text{ MeV}. \end{aligned} \quad (442)$$

The widths of the $Y(4484)$, $Y(4469)$ and $Y(4544)$ are $111.1 \pm 30.1 \pm 15.2$ MeV, $246.3 \pm 36.7 \pm 9.4$ MeV and $116.1 \pm 33.5 \pm 1.7$ MeV, respectively, from the BESIII collaboration [155, 156, 159], which are compatible with the theoretical predictions in magnitude.

From Table 60, we obtain the typical decay modes. For the $Y_{\tilde{A}V}$ state, the decays,

$$Y_{\tilde{A}V} \rightarrow \frac{\bar{D}_1^0 D^0 - \bar{D}^0 D_1^0}{\sqrt{2}}, \frac{\bar{D}_1^- D^+ - \bar{D}^- D_1^+}{\sqrt{2}}, \quad (443)$$

have the largest partial decay width 59.7 ± 5.5 MeV; while the decay,

$$Y_{\tilde{A}V} \rightarrow J/\psi \omega, \quad (444)$$

has zero partial decay width. For the $Y_{\tilde{V}A}$ state, the decays,

$$Y_{\tilde{V}A} \rightarrow \frac{\bar{D}_0^0 D^{*0} - \bar{D}^{*0} D_0^0}{\sqrt{2}}, \frac{\bar{D}_0^- D^{*+} - \bar{D}^{*-} D_0^+}{\sqrt{2}}, \quad (445)$$

Channels	$T^2(\text{GeV}^2)$	G
$\bar{D}\bar{D}\tilde{A}V$	3.8 – 4.8	2.11 ± 0.10
$\bar{D}^*\bar{D}\tilde{A}V$	4.7 – 5.7	$(4.49 \pm 0.15) \times 10^{-2} \text{ GeV}^{-1}$
$\bar{D}^*D^*\tilde{A}V$	4.1 – 5.1	0.95 ± 0.04
$\bar{D}_0D^*\tilde{A}V$	4.4 – 5.4	$0.30 \pm 0.01 \text{ GeV}^{-1}$
$\bar{D}_1D\tilde{A}V$	2.5 – 3.5	$6.73 \pm 0.31 \text{ GeV}$
$\eta_c\omega\tilde{A}V$	3.7 – 4.7	$-(0.35 \pm 0.03) \text{ GeV}^{-1}$
$J/\psi\omega\tilde{A}V$	— — —	0.0
$\chi_{c0}\omega\tilde{A}V$	3.8 – 4.8	$2.72 \pm 0.20 \text{ GeV}$
$\chi_{c1}\omega\tilde{A}V$	5.2 – 6.2	$-(0.25 \pm 0.01) \text{ GeV}^{-2}$
$J/\psi f_0\tilde{A}V$	3.8 – 4.8	$2.51 \pm 0.15 \text{ GeV}$
$\bar{D}D\tilde{V}A$	4.4 – 5.4	$-(4.02 \pm 0.16) \times 10^{-2}$
$\bar{D}^*D\tilde{V}A$	4.0 – 5.0	$0.30 \pm 0.01 \text{ GeV}^{-1}$
$\bar{D}^*D^*\tilde{V}A$	4.6 – 5.6	$-(6.00 \pm 0.20) \times 10^{-2}$
$\bar{D}_0D^*\tilde{V}A$	2.6 – 3.6	$8.00 \pm 0.37 \text{ GeV}$
$\bar{D}_1D\tilde{V}A$	2.8 – 3.8	$0.30 \pm 0.01 \text{ GeV}^{-1}$
$\eta_c\omega\tilde{V}A$	5.3 – 6.3	$-(0.40 \pm 0.03) \text{ GeV}^{-1}$
$J/\psi\omega\tilde{V}A$	— — —	0.0
$\chi_{c0}\omega\tilde{V}A$	3.0 – 4.0	$2.56 \pm 0.19 \text{ GeV}$
$\chi_{c1}\omega\tilde{V}A$	5.4 – 6.4	$-(0.24 \pm 0.01) \text{ GeV}^{-2}$
$J/\psi f_0\tilde{V}A$	4.6 – 5.6	$2.60 \pm 0.15 \text{ GeV}$
$\bar{D}DS\tilde{V}$	2.5 – 3.5	0.60 ± 0.06
$\bar{D}^*DS\tilde{V}$	4.7 – 5.7	$-(7.00 \pm 0.24) \times 10^{-2} \text{ GeV}^{-1}$
$\bar{D}^*D^*S\tilde{V}$	4.0 – 5.0	0.18 ± 0.01
$\bar{D}_0D^*S\tilde{V}$	3.3 – 4.3	$2.23 \pm 0.24 \text{ GeV}$
$\bar{D}_1DS\tilde{V}$	3.5 – 4.5	$4.21 \pm 0.37 \text{ GeV}$
$\eta_c\omega S\tilde{V}$	2.8 – 3.8	$1.71 \pm 0.31 \text{ GeV}^{-1}$
$J/\psi\omega S\tilde{V}$	3.7 – 4.7	$-(1.08 \pm 0.19)$
$\chi_{c0}\omega S\tilde{V}$	4.4 – 5.4	$-(5.56 \pm 0.97) \text{ GeV}$
$\chi_{c1}\omega S\tilde{V}$	3.1 – 4.1	0.29 ± 0.04
$J/\psi f_0S\tilde{V}$	3.5 – 4.5	$0.47 \pm 0.14 \text{ GeV}$

Table 59: The Borel parameters and hadronic coupling constants [546].

Channels	$\Gamma(\text{MeV})$
$Y_{\tilde{A}V} \rightarrow D^0 \bar{D}^0, D^- D^+$	22.5 ± 2.1
$Y_{\tilde{A}V} \rightarrow \frac{Y_{\tilde{A}V} \rightarrow D^{0*} \bar{D}^0 - \bar{D}^0 D^{*0}}{\sqrt{2}}, \frac{\bar{D}^{-*} D^+ - \bar{D}^- D^{*+}}{\sqrt{2}}$	0.08 ± 0.01
$Y_{\tilde{A}V} \rightarrow \frac{Y_{\tilde{A}V} \rightarrow \bar{D}^{*0} D^{*0}}{\sqrt{2}}, \frac{\bar{D}^{*-} D^{*+}}{\sqrt{2}}$	9.93 ± 0.84
$Y_{\tilde{A}V} \rightarrow \frac{\bar{D}_0^0 D^{*0} - \bar{D}^{*0} D_0^0}{\sqrt{2}}, \frac{\bar{D}_0^- D^{*+} - \bar{D}^{*-} D_0^+}{\sqrt{2}}$	1.92 ± 0.13
$Y_{\tilde{A}V} \rightarrow \frac{\bar{D}_1^0 D^0 - \bar{D}^0 D_1^0}{\sqrt{2}}, \frac{\bar{D}_1^- D^+ - \bar{D}^- D_1^+}{\sqrt{2}}$	59.7 ± 5.5
$Y_{\tilde{A}V} \rightarrow \eta_c \omega$	3.83 ± 0.66
$Y_{\tilde{A}V} \rightarrow J/\psi \omega$	0.0
$Y_{\tilde{A}V} \rightarrow \chi_{c0} \omega$	11.3 ± 1.7
$Y_{\tilde{A}V} \rightarrow \chi_{c1} \omega$	24.4 ± 1.9
$Y_{\tilde{A}V} \rightarrow J/\psi f_0(500)$	13.9 ± 1.7
$Y_{\tilde{V}A} \rightarrow D^0 \bar{D}^0, D^- D^+$	0.009 ± 0.001
$Y_{\tilde{V}A} \rightarrow \frac{Y_{\tilde{V}A} \rightarrow D^{0*} \bar{D}^0 - \bar{D}^0 D^{*0}}{\sqrt{2}}, \frac{\bar{D}^{-*} D^+ - \bar{D}^- D^{*+}}{\sqrt{2}}$	3.88 ± 0.26
$Y_{\tilde{V}A} \rightarrow \frac{Y_{\tilde{V}A} \rightarrow \bar{D}^{*0} D^{*0}}{\sqrt{2}}, \frac{\bar{D}^{*-} D^{*+}}{\sqrt{2}}$	0.047 ± 0.003
$Y_{\tilde{V}A} \rightarrow \frac{\bar{D}_0^0 D^{*0} - \bar{D}^{*0} D_0^0}{\sqrt{2}}, \frac{\bar{D}_0^- D^{*+} - \bar{D}^{*-} D_0^+}{\sqrt{2}}$	66.3 ± 6.1
$Y_{\tilde{V}A} \rightarrow \frac{\bar{D}_1^0 D^0 - \bar{D}^0 D_1^0}{\sqrt{2}}, \frac{\bar{D}_1^- D^+ - \bar{D}^- D_1^+}{\sqrt{2}}$	4.10 ± 0.27
$Y_{\tilde{V}A} \rightarrow \eta_c \omega$	5.65 ± 0.85
$Y_{\tilde{V}A} \rightarrow J/\psi \omega$	0.0
$Y_{\tilde{V}A} \rightarrow \chi_{c0} \omega$	11.1 ± 1.6
$Y_{\tilde{V}A} \rightarrow \chi_{c1} \omega$	29.9 ± 2.5
$Y_{\tilde{V}A} \rightarrow J/\psi f_0(500)$	15.2 ± 1.8
$Y_{S\tilde{V}} \rightarrow D^0 \bar{D}^0, D^- D^+$	1.88 ± 0.38
$Y_{S\tilde{V}} \rightarrow \frac{Y_{S\tilde{V}} \rightarrow D^{0*} \bar{D}^0 - \bar{D}^0 D^{*0}}{\sqrt{2}}, \frac{\bar{D}^{-*} D^+ - \bar{D}^- D^{*+}}{\sqrt{2}}$	0.20 ± 0.01
$Y_{S\tilde{V}} \rightarrow \frac{Y_{S\tilde{V}} \rightarrow \bar{D}^{*0} D^{*0}}{\sqrt{2}}, \frac{\bar{D}^{*-} D^{*+}}{\sqrt{2}}$	0.38 ± 0.04
$Y_{S\tilde{V}} \rightarrow \frac{\bar{D}_0^0 D^{*0} - \bar{D}^{*0} D_0^0}{\sqrt{2}}, \frac{\bar{D}_0^- D^{*+} - \bar{D}^{*-} D_0^+}{\sqrt{2}}$	4.51 ± 0.97
$Y_{S\tilde{V}} \rightarrow \frac{\bar{D}_1^0 D^0 - \bar{D}^0 D_1^0}{\sqrt{2}}, \frac{\bar{D}_1^- D^+ - \bar{D}^- D_1^+}{\sqrt{2}}$	24.4 ± 4.3
$Y_{S\tilde{V}} \rightarrow \eta_c \omega$	96.0 ± 34.8
$Y_{S\tilde{V}} \rightarrow J/\psi \omega$	18.0 ± 6.3
$Y_{S\tilde{V}} \rightarrow \chi_{c0} \omega$	49.4 ± 17.2
$Y_{S\tilde{V}} \rightarrow \chi_{c1} \omega$	2.76 ± 0.76
$Y_{S\tilde{V}} \rightarrow J/\psi f_0(500)$	0.49 ± 0.29

Table 60: The partial decay widths [546].

have the largest partial decay width 66.3 ± 6.1 MeV; while the decay,

$$Y_{\tilde{V}A} \rightarrow J/\psi\omega, \quad (446)$$

has zero partial decay width. For the $Y_{S\tilde{V}}$ state, the decay,

$$Y_{S\tilde{V}} \rightarrow \eta_c\omega, \quad (447)$$

has the largest partial decay width 96.0 ± 34.8 MeV; while the decay,

$$Y_{S\tilde{V}} \rightarrow J/\psi\omega, \quad (448)$$

has the partial decay width 18.0 ± 6.3 MeV. We can search for the $Y(4500)$ in those typical decays to diagnose its nature.

7.2 Light-cone QCD sum rules for the $Y(4500)$ as an example

The light-cone QCD sum rules have been applied extensively to study the two-body strong decays of the tetraquark (molecular) states [127, 462, 467, 807, 808, 809, 810, 811], where only the ground state contributions are isolated, and an unknown parameter is (or not) introduced by hand to parameterize the higher resonance contributions, then the Ioffe-Smilga-type trick,

$$1 - T^2 \frac{d}{dT^2}, \quad (449)$$

is (or not) adopted to subtract this parameter [812, 813]. The Ioffe-Smilga-type trick was suggested to deal with the traditional hadrons, where there exists a triangle Feynman diagram. In the case of tetraquark (molecular) states, we deal with two disconnected loop diagrams approximately, see Fig.31, we would like not to resort to the Ioffe-Smilga trick, and write down the higher resonance contributions explicitly.

We would like to use an example to illustrate how to study the strong decays of the tetraquark states via the light-cone QCD sum rules, and write down the three-point correlation function $\Pi_{\mu\alpha\beta}(p)$,

$$\Pi_{\mu\alpha\beta}(p, q) = i^2 \int d^4x d^4y e^{-ip \cdot x} e^{-iq \cdot y} \langle 0 | T \left\{ J_\mu^Y(0) J_\alpha^{D^{*+}}(x) J_\beta^{\bar{D}^{*0}}(y) \right\} | \pi(r) \rangle \rangle, \quad (450)$$

where

$$\begin{aligned} J_\mu^Y(0) &= \frac{\varepsilon^{ijk} \varepsilon^{imn}}{2} \left[u_j^T(0) C \sigma_{\mu\nu} \gamma_5 c_k(0) \bar{u}_m(0) \gamma_5 \gamma^\nu C \bar{c}_n^T(0) + u_j^T(0) C \gamma^\nu \gamma_5 c_k(0) \bar{u}_m(0) \gamma_5 \sigma_{\mu\nu} C \bar{c}_n^T(0) \right. \\ &\quad \left. + d_j^T(x) C \sigma_{\mu\nu} \gamma_5 c_k(0) \bar{d}_m(0) \gamma_5 \gamma^\nu C \bar{c}_n^T(0) + d_j^T(0) C \gamma^\nu \gamma_5 c_k(0) \bar{d}_m(0) \gamma_5 \sigma_{\mu\nu} C \bar{c}_n^T(0) \right], \\ J_\alpha^{D^{*+}}(y) &= \bar{d}(x) \gamma_\alpha c(x), \\ J_\beta^{\bar{D}^{*0}}(x) &= \bar{c}(y) \gamma_\beta u(y), \end{aligned} \quad (451)$$

interpolate the $Y(4500)$, \bar{D}^* and D^* , respectively [547], the $|\pi(r)\rangle$ is the external π state.

At the hadron side, we insert a complete set of intermediate hadronic states with the same quantum numbers as the interpolating currents into the three-point correlation function, and isolate the ground state contributions,

$$\begin{aligned} \Pi_{\mu\alpha\beta}(p, q) &= \lambda_Y f_{D^*}^2 M_{D^*}^2 \frac{-iG_\pi r_\tau + iG_Y p'_\tau}{(M_Y^2 - p^2)(M_{D^*}^2 - p^2)(M_{D^*}^2 - q^2)} \varepsilon^{\rho\sigma\lambda\tau} \left(-g_{\mu\rho} + \frac{p'_\mu p'_\rho}{p'^2} \right) \\ &\quad \left(-g_{\alpha\sigma} + \frac{p_\alpha p_\sigma}{p^2} \right) \left(-g_{\lambda\beta} + \frac{q_\lambda q_\beta}{q^2} \right) + \dots, \end{aligned} \quad (452)$$

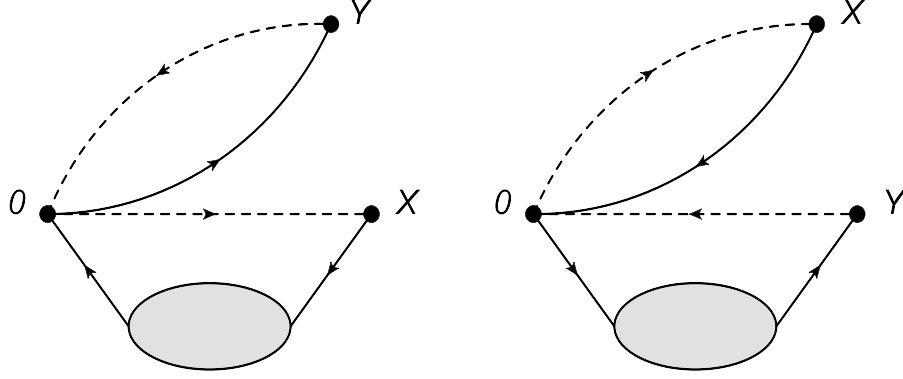


Figure 33: The lowest order Feynman diagrams, where the dashed (solid) lines denote the heavy (light) quark lines, the ovals denote the external π^+ meson.

where $p' = p + q + r$, we adopt the standard definitions for the decay constants λ_Y , f_{D^*} , $f_{\bar{D}^*}$, and define the hadronic coupling constants G_π and G_Y ,

$$\langle Y_c(p') | \bar{D}^*(p) D^*(q) \pi(r) \rangle = G_\pi \varepsilon^{\rho\sigma\lambda\tau} \varepsilon_\rho^* \xi_\sigma \zeta_\lambda r_\tau - G_Y \varepsilon^{\rho\sigma\lambda\tau} \varepsilon_\rho^* \xi_\sigma \zeta_\lambda p'_\tau, \quad (453)$$

the ε_μ , ξ_α and ζ_β are polarization vectors of the $Y(4500)$, \bar{D}^* and D^* , respectively. In the isospin limit, $m_u = m_d$, $f_{D^*} = f_{\bar{D}^*}$ and $M_{D^*} = M_{\bar{D}^*}$.

We multiply Eq.(452) with the tensor $\varepsilon_{\theta\omega}^{\alpha\beta}$ and obtain

$$\begin{aligned} \tilde{\Pi}_{\mu\theta\omega}(p, q) &= \varepsilon_{\theta\omega}^{\alpha\beta} \Pi_{\mu\alpha\beta}(p, q) \\ &= \lambda_Y f_{D^*}^2 M_{D^*}^2 \frac{iG_\pi (g_{\mu\omega} r_\theta - g_{\mu\theta} r_\omega) - iG_Y (g_{\mu\omega} p'_\theta - g_{\mu\theta} p'_\omega)}{(M_Y^2 - p'^2)(M_{\bar{D}^*}^2 - p^2)(M_{D^*}^2 - q^2)} + \dots \end{aligned} \quad (454)$$

Again, we take the isospin limit, then $\tilde{\Pi}_{\mu\theta\omega}(p, q) = \tilde{\Pi}_{\mu\theta\omega}(q, p)$, and we write down the relevant components explicitly,

$$\begin{aligned} \tilde{\Pi}_{\mu\theta\omega}(p, q) &= [i\Pi_\pi(p'^2, p^2, q^2) - i\Pi_Y(p'^2, p^2, q^2)] (g_{\mu\omega} r_\theta - g_{\mu\theta} r_\omega) \\ &\quad + i\Pi_Y(p'^2, p^2, q^2) (g_{\mu\omega} q_\theta - g_{\mu\theta} q_\omega) + \dots, \end{aligned} \quad (455)$$

where

$$\begin{aligned} \Pi_\pi(p'^2, p^2, q^2) &= \frac{\lambda_Y f_{D^*}^2 M_{D^*}^2 G_\pi}{(M_Y^2 - p'^2)(M_{\bar{D}^*}^2 - p^2)(M_{D^*}^2 - q^2)} + \dots, \\ \Pi_Y(p'^2, p^2, q^2) &= \frac{\lambda_Y f_{D^*}^2 M_{D^*}^2 G_Y}{(M_Y^2 - p'^2)(M_{\bar{D}^*}^2 - p^2)(M_{D^*}^2 - q^2)} + \dots. \end{aligned} \quad (456)$$

Then we choose the tensor structures $g_{\mu\omega} r_\theta - g_{\mu\theta} r_\omega$ and $g_{\mu\omega} q_\theta - g_{\mu\theta} q_\omega$ to study the hadronic coupling constants G_π and G_Y , respectively. We obtain the hadronic spectral densities $\rho_H(s', s, u)$ through triple dispersion relation,

$$\Pi_H(p'^2, p^2, q^2) = \int_{\Delta_s'^2}^\infty ds' \int_{\Delta_s^2}^\infty ds \int_{\Delta_u^2}^\infty du \frac{\rho_H(s', s, u)}{(s' - p'^2)(s - p^2)(u - q^2)}, \quad (457)$$

where the $\Delta_s'^2$, Δ_s^2 and Δ_u^2 are the thresholds, and we add the subscript H to represent the hadron side.

We carry out the operator product expansion up to the vacuum condensates of dimension 5 and neglect the tiny gluon condensate contributions [520, 789],

$$\begin{aligned}
\Pi_\pi(p^2, q'^2, q^2) = & f_\pi m_c \int_0^1 du \varphi_\pi(u) \left[\int_0^1 dx x \bar{x} \frac{\Gamma(\epsilon-1)}{2\pi^2(p^2 - \tilde{m}_c^2)^{\epsilon-1}} - \frac{2m_c \langle \bar{q}q \rangle}{3(p^2 - m_c^2)} \right. \\
& + \left. \frac{m_c^3 \langle \bar{q}g_s \sigma Gq \rangle}{3(p^2 - m_c^2)^3} \right] \frac{1}{(q+ur)^2 - m_c^2} \\
& + \frac{f_\pi m_\pi^2}{m_u + m_d} \int_0^1 du \varphi_5(u) \bar{u} \left[\int_0^1 dx x \bar{x} \frac{\Gamma(\epsilon-1)}{2\pi^2(p^2 - \tilde{m}_c^2)^{\epsilon-1}} - \frac{2m_c \langle \bar{q}q \rangle}{3(p^2 - m_c^2)} \right. \\
& + \left. \frac{m_c^3 \langle \bar{q}g_s \sigma Gq \rangle}{3(p^2 - m_c^2)^3} \right] \frac{1}{(q+ur)^2 - m_c^2} \\
& - \frac{f_\pi m_c^2 \langle \bar{q}g_s \sigma Gq \rangle}{36} \int_0^1 du \varphi_\pi(u) \frac{1}{(p^2 - m_c^2)((q+ur)^2 - m_c^2)^2} \\
& + \frac{f_\pi m_\pi^2 m_c \langle \bar{q}g_s \sigma Gq \rangle}{36(m_u + m_d)} \int_0^1 du \varphi_5(u) \bar{u} \frac{1}{(p^2 - m_c^2)((q+ur)^2 - m_c^2)^2}, \quad (458)
\end{aligned}$$

$$\begin{aligned}
\Pi_Y(p^2, q'^2, q^2) = & \frac{f_\pi m_\pi^2}{m_u + m_d} \int_0^1 du \varphi_5(u) \left[\int_0^1 dx x \bar{x} \frac{\Gamma(\epsilon-1)}{2\pi^2(p^2 - \tilde{m}_c^2)^{\epsilon-1}} - \frac{2m_c \langle \bar{q}q \rangle}{3(p^2 - m_c^2)} \right. \\
& + \left. \frac{m_c^3 \langle \bar{q}g_s \sigma Gq \rangle}{3(p^2 - m_c^2)^3} \right] \frac{1}{(q+ur)^2 - m_c^2} \\
& + \frac{f_\pi m_\pi^2 m_c \langle \bar{q}g_s \sigma Gq \rangle}{36(m_u + m_d)} \int_0^1 du \varphi_5(u) \frac{1}{(p^2 - m_c^2)((q+ur)^2 - m_c^2)^2} \\
& + f_{3\pi} m_\pi^2 \int_0^1 dx \bar{x} \left[\frac{3\Gamma(\epsilon)}{8\pi^2(p^2 - \tilde{m}_c^2)^\epsilon} - \frac{p^2}{2\pi^2(p^2 - \tilde{m}_c^2)} \right] \frac{1}{q^2 - m_c^2} \\
& - f_{3\pi} m_\pi^2 \int_0^1 dx x \bar{x} \left[\frac{\Gamma(\epsilon-1)}{2\pi^2(p^2 - \tilde{m}_c^2)^{\epsilon-1}} + \frac{p^2 \Gamma(\epsilon)}{2\pi^2(p^2 - \tilde{m}_c^2)^\epsilon} \right] \frac{1}{(q^2 - m_c^2)^2} \\
& - f_{3\pi} m_\pi^2 \int_0^1 dx x \left[\frac{3\Gamma(\epsilon)}{8\pi^2(p^2 - \tilde{m}_c^2)^\epsilon} + \frac{p^2}{4\pi^2(p^2 - \tilde{m}_c^2)} \right] \frac{1}{q^2 - m_c^2}, \quad (459)
\end{aligned}$$

where $q' = q+r$, $\bar{u} = 1-u$, $\bar{x} = 1-x$, $\tilde{m}_c^2 = \frac{m_c^2}{x}$, $(q-ur)^2 - m_c^2 = (1-u)q^2 + u(q+r)^2 - u\bar{u}m_\pi^2 - m_c^2$. And we have used the π light-cone distribution functions [814],

$$\begin{aligned}
\langle 0 | \bar{d}(0) \gamma_\mu \gamma_5 u(x) | \pi(r) \rangle &= i f_\pi r_\mu \int_0^1 du e^{-iur \cdot x} \varphi_\pi(u) + \dots, \\
\langle 0 | \bar{d}(0) \sigma_{\mu\nu} \gamma_5 u(x) | \pi(r) \rangle &= \frac{i}{6} \frac{f_\pi m_\pi^2}{m_u + m_d} (r_\mu x_\nu - r_\nu x_\mu) \int_0^1 du e^{-iur \cdot x} \varphi_\sigma(u), \\
\langle 0 | \bar{d}(0) i \gamma_5 u(x) | \pi(r) \rangle &= \frac{f_\pi m_\pi^2}{m_u + m_d} \int_0^1 du e^{-iur \cdot x} \varphi_5(u), \quad (460)
\end{aligned}$$

and the approximation,

$$\langle 0 | \bar{d}(x_1) \sigma_{\mu\nu} \gamma_5 g_s G_{\alpha\beta}(x_2) u(x_3) | \pi(r) \rangle = i f_{3\pi} (r_\mu r_\alpha g_{\nu\beta} + r_\nu r_\beta g_{\mu\alpha} - r_\nu r_\alpha g_{\mu\beta} - r_\mu r_\beta g_{\nu\alpha}), \quad (461)$$

for the twist-3 quark-gluon light-cone distribution functions with the value $f_{3\pi} = 0.0035 \text{ GeV}^2$ at the energy scale $\mu = 1 \text{ GeV}$ [814, 815]. Such terms proportional to m_π^2 and their contributions are greatly suppressed, and we also neglect the twist-4 light-cone distribution functions due to their

small contributions. According to the Gell-Mann-Oakes-Renner relation $\frac{f_\pi m_\pi^2}{m_u+m_d} = -\frac{2\langle\bar{q}q\rangle}{f_\pi}$, we take account of the Chiral enhanced contributions fully in Eqs.(458)-(459).

In Fig.33, we draw the lowest order Feynman diagrams as an example to illustrate the operator product expansion.

In the soft limit $r_\mu \rightarrow 0$, $(q+r)^2 = q^2$, we can set $\Pi_{\pi/Y}(p^2, q'^2, q^2) = \Pi_{\pi/Y}(p^2, q^2)$, then we obtain the QCD spectral densities $\rho_{QCD}(s, u)$ through double dispersion relation,

$$\Pi_{\pi/Y}^{QCD}(p^2, q^2) = \int_{\Delta_s^2}^\infty ds \int_{\Delta_u^2}^\infty du \frac{\rho_{QCD}(s, u)}{(s-p^2)(u-q^2)}, \quad (462)$$

we add the superscript (subscript) QCD to stand for the QCD side.

We match the hadron side with the QCD side below the continuum thresholds s_0 and u_0 to acquire rigorous quark-hadron duality [520, 789],

$$\int_{\Delta_s^2}^{s_0} ds \int_{\Delta_u^2}^{u_0} du \frac{\rho_{QCD}(s, u)}{(s-p^2)(u-q^2)} = \int_{\Delta_s^2}^{s_0} ds \int_{\Delta_u^2}^{u_0} du \left[\int_{\Delta_{s'}^2}^\infty ds' \frac{\rho_H(s', s, u)}{(s'-p'^2)(s-p^2)(u-q^2)} \right], \quad (463)$$

and we carry out the integral over ds' firstly, then

$$\begin{aligned} \Pi_H(p'^2, p^2, q^2) &= \frac{\lambda_Y f_{D^*}^2 M_{D^*}^2 G_{\pi/Y}}{(M_Y^2 - p'^2)(M_{D^*}^2 - p^2)(M_{D^*}^2 - q^2)} + \int_{s'_0}^\infty ds' \frac{\tilde{\rho}_H(s', M_{D^*}^2, M_{D^*}^2)}{(s' - p'^2)(M_{D^*}^2 - p^2)(M_{D^*}^2 - q^2)} \\ &\quad + \dots, \\ &= \frac{\lambda_Y f_{D^*}^2 M_{D^*}^2 G_{\pi/Y}}{(M_Y^2 - p'^2)(M_{D^*}^2 - p^2)(M_{D^*}^2 - q^2)} + \frac{C_{\pi/Y}}{(M_{D^*}^2 - p^2)(M_{D^*}^2 - q^2)} + \dots, \end{aligned} \quad (464)$$

where $\rho_H(s', s, u) = \tilde{\rho}_H(s', s, u)\delta(s - M_{D^*}^2)\delta(u - M_{D^*}^2)$, and we introduce the parameters $C_{\pi/Y}$ to parameterize the contributions concerning the higher resonances and continuum states in the s' channel,

$$C_{\pi/Y} = \int_{s'_0}^\infty ds' \frac{\tilde{\rho}_H(s', M_{D^*}^2, M_{D^*}^2)}{s' - p'^2}. \quad (465)$$

As the strong interactions among the ground states π , D^* , \bar{D}^* and excited Y' states are complex, and we have no knowledge about the corresponding four-hadron contact vertex. In practical calculations, we can take the unknown functions $C_{\pi/Y}$ as free parameters and adjust the values to acquire flat platforms for the hadronic coupling constants $G_{\pi/Y}$ with variations of the Borel parameters. Such a method works well in the case of three-hadron contact vertexes [520, 789], and we expect it also works here.

In Eq.(452) and Eq.(454), there exist three poles in the limit $p'^2 \rightarrow M_Y^2$, $p^2 \rightarrow M_{D^*}^2$ and $q^2 \rightarrow M_{D^*}^2$. According to the relation $M_Y \approx M_{\bar{D}^*} + M_{D^*}$, we set $p'^2 = 4q^2$ and perform double Borel transformation with respect to the variables $P^2 = -p^2$ and $Q^2 = -q^2$ respectively, then we

set $T_1^2 = T_2^2 = T^2$ to obtain two QCD sum rules,

$$\begin{aligned}
& \frac{\lambda_{YD^*D^*}G_\pi}{4(\widetilde{M}_Y^2 - M_{D^*}^2)} \left[\exp\left(-\frac{M_{D^*}^2}{T^2}\right) - \exp\left(-\frac{\widetilde{M}_Y^2}{T^2}\right) \right] \exp\left(-\frac{M_{D^*}^2}{T^2}\right) + C_\pi \exp\left(-\frac{M_{D^*}^2 + M_{D^*}^2}{T^2}\right) \\
&= f_\pi m_c \int_{m_c^2}^{s_0} ds \int_0^1 du \varphi_\pi(u) \left[\frac{1}{2\pi^2} \int_{x_i}^1 dx x \bar{x} (s - \tilde{m}_c^2) - \left(\frac{2m_c \langle \bar{q}q \rangle}{3} - \frac{m_c^3 \langle \bar{q}g_s \sigma Gq \rangle}{6T^4} \right) \delta(s - m_c^2) \right] \\
&\exp\left(-\frac{s + m_c^2 + u\bar{u}m_\pi^2}{T^2}\right) \\
&+ \frac{f_\pi m_\pi^2}{m_u + m_d} \int_{m_c^2}^{s_0} ds \int_0^1 du \varphi_5(u) \bar{u} \left[\frac{1}{2\pi^2} \int_{x_i}^1 dx x \bar{x} (s - \tilde{m}_c^2) - \left(\frac{2m_c \langle \bar{q}q \rangle}{3} - \frac{m_c^3 \langle \bar{q}g_s \sigma Gq \rangle}{6T^4} \right) \delta(s - m_c^2) \right] \\
&\exp\left(-\frac{s + m_c^2 + u\bar{u}m_\pi^2}{T^2}\right) + \frac{f_\pi m_c^2 \langle \bar{q}g_s \sigma Gq \rangle}{36T^2} \int_0^1 du \varphi_\pi(u) \exp\left(-\frac{2m_c^2 + u\bar{u}m_\pi^2}{T^2}\right) \\
&- \frac{f_\pi m_\pi^2 m_c \langle \bar{q}g_s \sigma Gq \rangle}{36(m_u + m_d)T^2} \int_0^1 du \varphi_5(u) \bar{u} \exp\left(-\frac{2m_c^2 + u\bar{u}m_\pi^2}{T^2}\right), \tag{466}
\end{aligned}$$

$$\begin{aligned}
& \frac{\lambda_{YD^*D^*}G_Y}{4(\widetilde{M}_Y^2 - M_{D^*}^2)} \left[\exp\left(-\frac{M_{D^*}^2}{T^2}\right) - \exp\left(-\frac{\widetilde{M}_Y^2}{T^2}\right) \right] \exp\left(-\frac{M_{D^*}^2}{T^2}\right) + C_Y \exp\left(-\frac{M_{D^*}^2 + M_{D^*}^2}{T^2}\right) \\
&= \frac{f_\pi m_\pi^2}{m_u + m_d} \int_{m_c^2}^{s_0} ds \int_0^1 du \varphi_5(u) \left[\frac{1}{2\pi^2} \int_{x_i}^1 dx x \bar{x} (s - \tilde{m}_c^2) - \left(\frac{2m_c \langle \bar{q}q \rangle}{3} - \frac{m_c^3 \langle \bar{q}g_s \sigma Gq \rangle}{6T^4} \right) \delta(s - m_c^2) \right] \\
&\exp\left(-\frac{s + m_c^2 + u\bar{u}m_\pi^2}{T^2}\right) - \frac{f_\pi m_\pi^2 m_c \langle \bar{q}g_s \sigma Gq \rangle}{36(m_u + m_d)T^2} \int_0^1 du \varphi_5(u) \exp\left(-\frac{2m_c^2 + u\bar{u}m_\pi^2}{T^2}\right) \\
&- \frac{f_{3\pi} m_\pi^2}{2\pi^2} \int_{m_c^2}^{s_0} ds \int_{x_i}^1 dx \bar{x} \left[\frac{3}{4} + s \delta(s - \tilde{m}_c^2) \right] \exp\left(-\frac{s + m_c^2}{T^2}\right) \\
&- \frac{f_{3\pi} m_\pi^2}{2\pi^2 T^2} \int_{m_c^2}^{s_0} ds \int_{x_i}^1 dx x \bar{x} \tilde{m}_c^2 \exp\left(-\frac{s + m_c^2}{T^2}\right) \\
&+ \frac{f_{3\pi} m_\pi^2}{4\pi^2} \int_{m_c^2}^{s_0} ds \int_{x_i}^1 dx x \left[\frac{3}{2} - s \delta(s - \tilde{m}_c^2) \right] \exp\left(-\frac{s + m_c^2}{T^2}\right), \tag{467}
\end{aligned}$$

where $\lambda_{YD^*D^*} = \lambda_Y f_{D^*}^2 M_{D^*}^2$, $\widetilde{M}_Y^2 = \frac{M_Y^2}{4}$ and $x_i = \frac{m_c^2}{s}$.

In calculations, we fit the free parameters as $C_\pi = 0.00101(T^2 - 3.6 \text{ GeV}^2) \text{ GeV}^4$ and $C_Y = 0.00089(T^2 - 3.2 \text{ GeV}^2) \text{ GeV}^4$ to acquire uniform flat Borel platforms $T_{max}^2 - T_{min}^2 = 1 \text{ GeV}^2$. The Borel windows are $T_\pi^2 = (4.6 - 5.6) \text{ GeV}^2$ and $T_Y^2 = (4.4 - 5.4) \text{ GeV}^2$, where the subscripts π and Y represent the corresponding channels. In Fig.34, we plot the hadronic coupling constants G_π and G_Y with variations of the Borel parameters. In the Borel windows, there appear very flat platforms indeed.

We obtain the hadronic coupling constants routinely,

$$\begin{aligned}
G_\pi &= 15.9 \pm 0.5 \text{ GeV}^{-1}, \\
G_Y &= 10.4 \pm 0.6 \text{ GeV}^{-1}, \tag{468}
\end{aligned}$$

by setting

$$\delta \bar{\lambda}_Y \bar{f}_{D^*} \bar{f}_{D^*} \bar{G}_{\pi/Y} = \bar{\lambda}_Y \bar{f}_{D^*} \bar{f}_{D^*} \bar{G}_{\pi/Y} \frac{4\delta G_{\pi/Y}}{\bar{G}_{\pi/Y}}. \tag{469}$$

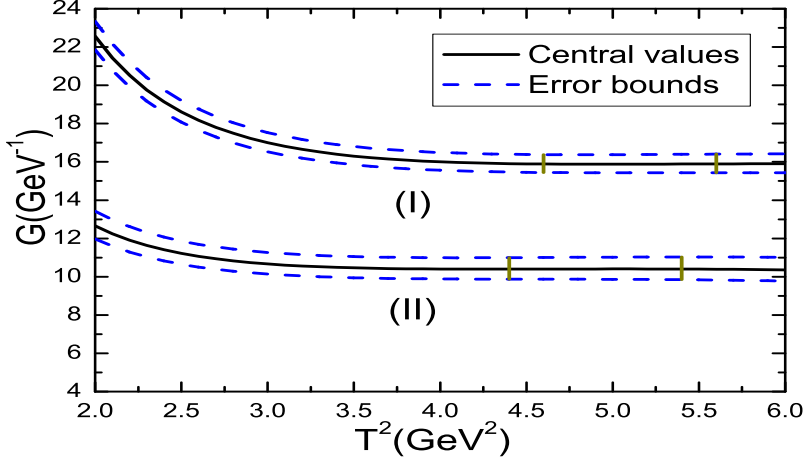


Figure 34: The hadronic coupling constants with variations of the Borel parameters T^2 , where the (I) and (II) denote the G_π and G_Y , respectively, the regions between the two vertical lines are the Borel windows.

It is direct to obtain the partial decay width,

$$\begin{aligned}
 \Gamma(Y(4500) \rightarrow D^* \bar{D}^* \pi^+) &= \frac{1}{24\pi M_Y} \int dk^2 (2\pi)^4 \delta^4(p' - k - p) \frac{d^3 \vec{k}}{(2\pi)^3 2k_0} \frac{d^3 \vec{p}}{(2\pi)^3 2p_0} \\
 &\quad (2\pi)^4 \delta^4(k - q - r) \frac{d^3 \vec{q}}{(2\pi)^3 2q_0} \frac{d^3 \vec{r}}{(2\pi)^3 2r_0} \Sigma |T|^2 \\
 &= 6.43_{-0.76}^{+0.80} \text{ MeV},
 \end{aligned} \tag{470}$$

where $T = \langle Y_c(p') | \bar{D}^*(p) D^*(q) \pi(r) \rangle$.

The partial decay width $\Gamma(Y(4500) \rightarrow D^* \bar{D}^* \pi^+) = 6.43_{-0.76}^{+0.80} \text{ MeV}$ is much smaller than the total width $\Gamma = 246.3 \pm 36.7 \pm 9.4 \text{ MeV}$ from the BESIII collaboration [156].

The three-body strong decays of the $Y(4230)$ are also studied in this scheme [816], this scheme could be applied to the two-body strong decays of the tetraquark (molecular) states straightforwardly.

We write down the two-point correlation functions $\Pi(p, r)$,

$$\Pi(p, r) = i \int d^4x e^{-ip \cdot x} \langle 0 | T \{ J_A(0) J_B(x) \} | P(r) \rangle, \tag{471}$$

where the currents $J_A(0)$ and $J_B(x)$ interpolate the tetraquark (molecular) states and traditional mesons, respectively, the $P(r)$ are external states.

At the hadron side, we obtain

$$\begin{aligned}
 \Pi(p, r) &= \frac{\lambda_A \lambda_B G_{ABP}}{(M_A^2 - (p+r)^2)(M_B^2 - p^2)} + \dots, \\
 &= \Pi_H(p'^2, p^2),
 \end{aligned} \tag{472}$$

where $p' = p + r$, and we rewrite the correlation functions $\Pi_H(p'^2, p^2)$ as

$$\Pi_H(p'^2, p^2) = \int_{\Delta^2}^{s_A^0} ds' \int_{\Delta_s^2}^{s_B^0} ds \frac{\rho_H(s', s)}{(s' - p'^2)(s - p^2)} + \int_{s_A^0}^{\infty} ds' \int_{\Delta_s^2}^{s_B^0} ds \frac{\rho_H(s', s)}{(s' - p'^2)(s - p^2)} + \dots, \quad (473)$$

through double-dispersion relation, where the $\rho_H(s', s)$ are the hadronic spectral densities,

$$\rho_H(s', s) = \lim_{\epsilon_2 \rightarrow 0} \lim_{\epsilon_1 \rightarrow 0} \frac{\text{Im}_{s'} \text{Im}_s \Pi_H(s' + i\epsilon_2, s + i\epsilon_1)}{\pi^2}, \quad (474)$$

where the Δ^2 and Δ_s^2 are the thresholds, the s_A^0 and s_B^0 are the continuum thresholds.

Then we carry out the operator product expansion (not necessary on the light-cone) at the QCD side, and write the correlation functions $\Pi_{QCD}(p'^2, p^2)$ as

$$\Pi_{QCD}(p'^2, p^2) = \int_{\Delta_s^2}^{s_B^0} ds \frac{\rho_{QCD}(p'^2, s)}{s - p^2} + \dots, \quad (475)$$

through single-dispersion relation, where the $\rho_{QCD}(p'^2, s)$ are the QCD spectral densities,

$$\rho_{QCD}(p'^2, s) = \lim_{\epsilon_1 \rightarrow 0} \frac{\text{Im}_s \Pi_{QCD}(p'^2, s + i\epsilon_1)}{\pi}. \quad (476)$$

As the QCD spectral densities $\rho_{QCD}(s', s)$ do not exist,

$$\begin{aligned} \rho_{QCD}(s', s) &= \lim_{\epsilon_2 \rightarrow 0} \lim_{\epsilon_1 \rightarrow 0} \frac{\text{Im}_{s'} \text{Im}_s \Pi_{QCD}(s' + i\epsilon_2, s + i\epsilon_1)}{\pi^2} \\ &= 0, \end{aligned} \quad (477)$$

because

$$\lim_{\epsilon_2 \rightarrow 0} \frac{\text{Im}_{s'} \Pi_{QCD}(s' + i\epsilon_2, p^2)}{\pi} = 0. \quad (478)$$

And we will write the QCD spectral densities $\rho_{QCD}(p'^2, s)$ as $\rho_{QCD}(s)$ for simplicity.

We match the hadron side with the QCD side of the correlation functions, and accomplish the integral over ds' firstly to obtain the rigorous quark-hadron duality [520],

$$\int_{\Delta_s^2}^{s_B^0} ds \frac{\rho_{QCD}(s)}{s - p^2} = \int_{\Delta_s^2}^{s_B^0} ds \frac{1}{s - p^2} \left[\int_{\Delta^2}^{\infty} ds' \frac{\rho_H(s', s)}{s' - p'^2} \right]. \quad (479)$$

And we write down the quark-hadron duality explicitly,

$$\int_{\Delta_s^2}^{s_B^0} ds \frac{\rho_{QCD}(s)}{s - p^2} = \frac{\lambda_A \lambda_B G_{ABP}}{(m_A^2 - p'^2)(m_B^2 - p^2)} + \frac{C_{A'B}}{m_B^2 - p^2}. \quad (480)$$

Again, we introduce the parameters $C_{A'B}$ to parameterize the net effects. In numerical calculations, we take the $C_{A'B}$ as free parameters, and choose suitable values to obtain the stable QCD sum rules with the variations of the Borel parameters T^2 .

8 Conclusion and Perspective

At the present time, we can only say confidently that the tetraquark and pentaquark states are established in sense of that there are four and five valence quarks, respectively. The under-structures are still under hot debates, more experimental and theoretical works are still needed before reaching definite conclusion. The QCD sum rules method is a reliable and powerful theoretical tool in studying the multiquark states and has given many successful descriptions, however, the predictions have arbitrariness depending on the treating schemes, only comprehensive and systematic works would work.

Appendix

Some typical and useful examples of the Borel transformations,

$$\begin{aligned}
\mathcal{B}[(P^2)^k] &= 0, \\
\mathcal{B}\left[\frac{\Gamma(k)}{(P^2)^k}\right] &= \frac{1}{(T^2)^{k-1}}, \\
\mathcal{B}\left[\frac{\Gamma(k)}{(s+P^2)^k}\right] &= \frac{1}{(T^2)^{k-1}} \exp\left(-\frac{s}{T^2}\right).
\end{aligned} \tag{481}$$

Some useful examples of the Fierz transformations.

$$\begin{aligned}
2\sqrt{2}J_{1+-}^\mu &= 2\varepsilon^{ijk}\varepsilon^{imn}\{u_j^T C\gamma_5 c_k \bar{d}_m \gamma^\mu C \bar{c}_n^T - u_j^T C\gamma^\mu c_k \bar{d}_m \gamma_5 C \bar{c}_n^T\}, \\
&= i\bar{c}i\gamma_5 c \bar{d}\gamma^\mu u - i\bar{c}\gamma^\mu c \bar{d}i\gamma_5 u + \bar{c}u \bar{d}\gamma^\mu \gamma_5 c - \bar{c}\gamma^\mu \gamma_5 u \bar{d}c - i\bar{c}\gamma_\nu \gamma_5 c \bar{d}\sigma^{\mu\nu} u \\
&\quad + i\bar{c}\sigma^{\mu\nu} c \bar{d}\gamma_\nu \gamma_5 u - i\bar{c}\sigma^{\mu\nu} \gamma_5 u \bar{d}\gamma_\nu c + i\bar{c}\gamma_\nu u \bar{d}\sigma^{\mu\nu} \gamma_5 c,
\end{aligned} \tag{482}$$

$$\begin{aligned}
2\sqrt{2}J_{1+-}^{\mu\nu} &= 2\varepsilon^{ijk}\varepsilon^{imn}\{u_j^T C\gamma^\mu c_k \bar{d}_m \gamma^\nu C \bar{c}_n^T - u_j^T C\gamma^\nu c_k \bar{d}_m \gamma^\mu C \bar{c}_n^T\}, \\
&= i\bar{d}u \bar{c}\sigma^{\mu\nu} c + i\bar{d}\sigma^{\mu\nu} u \bar{c}c + i\bar{d}c \bar{c}\sigma^{\mu\nu} u + i\bar{d}\sigma^{\mu\nu} c \bar{c}u \\
&\quad - \bar{c}\sigma^{\mu\nu} \gamma_5 c \bar{d}i\gamma_5 u - \bar{c}i\gamma_5 c \bar{d}\sigma^{\mu\nu} \gamma_5 u - \bar{d}\sigma^{\mu\nu} \gamma_5 c \bar{c}i\gamma_5 u - \bar{d}i\gamma_5 c \bar{c}\sigma^{\mu\nu} \gamma_5 u \\
&\quad + i\varepsilon^{\mu\nu\alpha\beta} \bar{c}\gamma^\alpha \gamma_5 c \bar{d}\gamma^\beta u - i\varepsilon^{\mu\nu\alpha\beta} \bar{c}\gamma^\alpha c \bar{d}\gamma^\beta \gamma_5 u \\
&\quad + i\varepsilon^{\mu\nu\alpha\beta} \bar{c}\gamma^\alpha \gamma_5 u \bar{d}\gamma^\beta c - i\varepsilon^{\mu\nu\alpha\beta} \bar{c}\gamma^\alpha u \bar{d}\gamma^\beta \gamma_5 c,
\end{aligned} \tag{483}$$

$$\begin{aligned}
2\sqrt{2}J_{1--}^\mu &= 2\varepsilon^{ijk}\varepsilon^{imn}\{u_j^T C c_k \bar{d}_m \gamma^\mu C \bar{c}_n^T - u_j^T C\gamma^\mu c_k \bar{d}_m C \bar{c}_n^T\}, \\
&= \bar{c}\gamma^\mu c \bar{d}u - \bar{c}c \bar{d}\gamma^\mu u + i\bar{c}\gamma^\mu \gamma_5 u \bar{d}i\gamma_5 c - i\bar{c}i\gamma_5 u \bar{d}\gamma^\mu \gamma_5 c \\
&\quad - i\bar{c}\gamma_\nu \gamma_5 c \bar{d}\sigma^{\mu\nu} \gamma_5 u + i\bar{c}\sigma^{\mu\nu} \gamma_5 c \bar{d}\gamma_\nu \gamma_5 u - i\bar{d}\gamma_\nu c \bar{c}\sigma^{\mu\nu} u + i\bar{d}\sigma^{\mu\nu} c \bar{c}\gamma_\nu u,
\end{aligned} \tag{484}$$

$$\begin{aligned}
2\sqrt{2}J_{1-+}^\mu &= 2\varepsilon^{ijk}\varepsilon^{imn}\{u_j^T C c_k \bar{d}_m \gamma^\mu C \bar{c}_n^T + u_j^T C\gamma^\mu c_k \bar{d}_m C \bar{c}_n^T\}, \\
&= i\bar{c}i\gamma_5 c \bar{d}\gamma^\mu \gamma_5 u - i\bar{c}\gamma^\mu \gamma_5 c \bar{d}i\gamma_5 u - \bar{c}\gamma^\mu u \bar{d}c + \bar{c}u \bar{d}\gamma^\mu c \\
&\quad + i\bar{c}\sigma^{\mu\nu} c \bar{d}\gamma_\nu u - i\bar{c}\gamma_\nu c \bar{d}\sigma^{\mu\nu} u - i\bar{d}\gamma_\nu \gamma_5 c \bar{c}\sigma^{\mu\nu} \gamma_5 u + i\bar{d}\sigma^{\mu\nu} \gamma_5 c \bar{c}\gamma_\nu \gamma_5 u,
\end{aligned} \tag{485}$$

$$\begin{aligned}
2\sqrt{2}J_{1--}^\mu &= 2\varepsilon^{ijk}\varepsilon^{imn}\{s_j^T C c_k \bar{s}_m \gamma^\mu C \bar{c}_n^T - s_j^T C\gamma^\mu c_k \bar{s}_m C \bar{c}_n^T\}, \\
&= \bar{c}\gamma^\mu c \bar{s}s - \bar{c}c \bar{s}\gamma^\mu s + i\bar{c}\gamma^\mu \gamma_5 s \bar{s}i\gamma_5 c - i\bar{c}i\gamma_5 s \bar{s}\gamma^\mu \gamma_5 c \\
&\quad - i\bar{c}\gamma_\nu \gamma_5 c \bar{s}\sigma^{\mu\nu} \gamma_5 s + i\bar{c}\sigma^{\mu\nu} \gamma_5 c \bar{s}\gamma_\nu \gamma_5 s - i\bar{s}\gamma_\nu c \bar{c}\sigma^{\mu\nu} s + i\bar{s}\sigma^{\mu\nu} c \bar{c}\gamma_\nu s,
\end{aligned} \tag{486}$$

$$\begin{aligned}
2\sqrt{2}J_{1-+}^\mu &= 2\varepsilon^{ijk}\varepsilon^{imn}\{s_j^T C c_k \bar{s}_m \gamma^\mu C \bar{c}_n^T + s_j^T C\gamma^\mu c_k \bar{s}_m C \bar{c}_n^T\}, \\
&= i\bar{c}i\gamma_5 c \bar{s}\gamma^\mu \gamma_5 s - i\bar{c}\gamma^\mu \gamma_5 c \bar{s}i\gamma_5 s - \bar{c}\gamma^\mu s \bar{s}c + \bar{c}s \bar{s}\gamma^\mu c \\
&\quad + i\bar{c}\sigma^{\mu\nu} c \bar{s}\gamma_\nu s - i\bar{c}\gamma_\nu c \bar{s}\sigma^{\mu\nu} s - i\bar{s}\gamma_\nu \gamma_5 c \bar{c}\sigma^{\mu\nu} \gamma_5 s + i\bar{s}\sigma^{\mu\nu} \gamma_5 c \bar{c}\gamma_\nu \gamma_5 s,
\end{aligned} \tag{487}$$

	$M_P(\text{GeV})$	$\lambda_P(\text{GeV}^6)$	$M_{B_{10}J/\psi(B_8J/\psi)}(\text{GeV})$
$P_{uuu}^{11\frac{1}{2}}\left(\frac{1}{2}^-\right)$	4.35 ± 0.15	$(3.72 \pm 0.76) \times 10^{-3}$	4.33 (4.04)
$P_{uus}^{11\frac{1}{2}}\left(\frac{1}{2}^-\right)$	4.47 ± 0.15	$(4.50 \pm 0.85) \times 10^{-3}$	4.48 (4.29)
$P_{uss}^{11\frac{1}{2}}\left(\frac{1}{2}^-\right)$	4.58 ± 0.14	$(5.43 \pm 0.96) \times 10^{-3}$	4.63 (4.41)
$P_{sss}^{11\frac{1}{2}}\left(\frac{1}{2}^-\right)$	4.68 ± 0.13	$(6.47 \pm 1.10) \times 10^{-3}$	4.77
$P_{uuu}^{10\frac{1}{2}}\left(\frac{1}{2}^-\right)$	4.42 ± 0.12	$(4.14 \pm 0.70) \times 10^{-3}$	4.33 (4.04)
$P_{uus}^{10\frac{1}{2}}\left(\frac{1}{2}^-\right)$	4.51 ± 0.11	$(4.97 \pm 0.79) \times 10^{-3}$	4.48 (4.29)
$P_{uss}^{10\frac{1}{2}}\left(\frac{1}{2}^-\right)$	4.60 ± 0.11	$(5.87 \pm 0.89) \times 10^{-3}$	4.63 (4.41)
$P_{sss}^{10\frac{1}{2}}\left(\frac{1}{2}^-\right)$	4.71 ± 0.11	$(6.84 \pm 1.00) \times 10^{-3}$	4.77
$P_{uuu}^{11\frac{1}{2}}\left(\frac{1}{2}^+\right)$	4.56 ± 0.15	$(1.97 \pm 0.40) \times 10^{-3}$	4.33 (4.04)
$P_{uus}^{11\frac{1}{2}}\left(\frac{1}{2}^+\right)$	4.67 ± 0.14	$(2.42 \pm 0.47) \times 10^{-3}$	4.48 (4.29)
$P_{uss}^{11\frac{1}{2}}\left(\frac{1}{2}^+\right)$	4.78 ± 0.13	$(2.88 \pm 0.53) \times 10^{-3}$	4.63 (4.41)
$P_{sss}^{11\frac{1}{2}}\left(\frac{1}{2}^+\right)$	4.89 ± 0.13	$(3.44 \pm 0.61) \times 10^{-3}$	4.77
$P_{uuu}^{10\frac{1}{2}}\left(\frac{1}{2}^+\right)$	5.12 ± 0.08	$(8.01 \pm 0.92) \times 10^{-3}$	4.33 (4.04)
$P_{uus}^{10\frac{1}{2}}\left(\frac{1}{2}^+\right)$	5.19 ± 0.08	$(8.92 \pm 1.05) \times 10^{-3}$	4.48 (4.29)
$P_{uss}^{10\frac{1}{2}}\left(\frac{1}{2}^+\right)$	5.26 ± 0.08	$(9.93 \pm 1.21) \times 10^{-3}$	4.63 (4.41)
$P_{sss}^{10\frac{1}{2}}\left(\frac{1}{2}^+\right)$	5.40 ± 0.08	$(12.17 \pm 1.28) \times 10^{-3}$	4.77

Table 61: The masses and pole residues of the hidden-charm pentaquark states with the $J^P = \frac{1}{2}^\pm$, where the B_{10} and B_8 denote the decuplet and octet baryons with the quark constituents $q_1q_2q_3$ respectively [704].

$$\begin{aligned}
2\sqrt{2}J_{2^{++}}^{\mu\nu} &= 2\varepsilon^{ijk}\varepsilon^{imn}\{u_j^T C\gamma^\mu c_k \bar{d}_m \gamma^\nu C\bar{c}_n^T + u_j^T C\gamma^\nu c_k \bar{d}_m \gamma^\mu C\bar{c}_n^T\}, \\
&= \bar{c}\gamma^\mu \gamma_5 c \bar{d}\gamma^\nu \gamma_5 u + \bar{c}\gamma^\nu \gamma_5 c \bar{d}\gamma^\mu \gamma_5 u - \bar{c}\gamma^\mu c \bar{d}\gamma^\nu u - \bar{c}\gamma^\nu c \bar{d}\gamma^\mu u + \bar{c}\gamma^\mu \gamma_5 u \bar{d}\gamma^\nu \gamma_5 c \\
&\quad + \bar{c}\gamma^\nu \gamma_5 u \bar{d}\gamma^\mu \gamma_5 c - \bar{c}\gamma^\mu u \bar{d}\gamma^\nu c - \bar{c}\gamma^\nu u \bar{d}\gamma^\mu c + g_{\alpha\beta} \bar{c}\sigma^{\mu\alpha} c \bar{d}\sigma^{\nu\beta} u + g_{\alpha\beta} \bar{c}\sigma^{\nu\alpha} c \bar{d}\sigma^{\mu\beta} u \\
&\quad + g_{\alpha\beta} \bar{c}\sigma^{\mu\alpha} u \bar{d}\sigma^{\nu\beta} c + g_{\alpha\beta} \bar{c}\sigma^{\nu\alpha} u \bar{d}\sigma^{\mu\beta} c + g^{\mu\nu} \bar{c}c \bar{d}u + g^{\mu\nu} \bar{c}i\gamma_5 c \bar{d}i\gamma_5 u + g^{\mu\nu} \bar{c}\gamma_\alpha c \bar{d}\gamma^\alpha u \\
&\quad - g^{\mu\nu} \bar{c}\gamma_\alpha \gamma_5 c \bar{d}\gamma^\alpha \gamma_5 u - \frac{1}{2}g^{\mu\nu} \bar{c}\sigma_{\alpha\beta} c \bar{d}\sigma^{\alpha\beta} u + g^{\mu\nu} \bar{c}u \bar{d}c + g^{\mu\nu} \bar{c}i\gamma_5 u \bar{d}i\gamma_5 c \\
&\quad + g^{\mu\nu} \bar{c}\gamma_\alpha u \bar{d}\gamma^\alpha c - g^{\mu\nu} \bar{c}\gamma_\alpha \gamma_5 u \bar{d}\gamma^\alpha \gamma_5 c - \frac{1}{2}g^{\mu\nu} \bar{c}\sigma_{\alpha\beta} u \bar{d}\sigma^{\alpha\beta} c, \tag{488}
\end{aligned}$$

$$\begin{aligned}
J_{0^{++}} &= \varepsilon^{ijk}\varepsilon^{imn}u_j^T C\gamma_\mu c_k \bar{d}_m \gamma^\mu C\bar{c}_n^T, \\
&= \bar{c}c \bar{d}u + \bar{c}i\gamma_5 c \bar{d}i\gamma_5 u + \frac{1}{2}\bar{c}\gamma_\alpha c \bar{d}\gamma^\alpha u - \frac{1}{2}\bar{c}\gamma_\alpha \gamma_5 c \bar{d}\gamma^\alpha \gamma_5 u \\
&\quad + \bar{c}u \bar{d}c + \bar{c}i\gamma_5 u \bar{d}i\gamma_5 c + \frac{1}{2}\bar{c}\gamma_\alpha u \bar{d}\gamma^\alpha c - \frac{1}{2}\bar{c}\gamma_\alpha \gamma_5 u \bar{d}\gamma^\alpha \gamma_5 c. \tag{489}
\end{aligned}$$

	$M_P(\text{GeV})$	$\lambda_P(10^{-3}\text{GeV}^6)$
$P_{uuu}^{10\frac{1}{2}}\left(\frac{3}{2}^{-}\right)$	4.39 ± 0.13	2.25 ± 0.40
$P_{uus}^{10\frac{1}{2}}\left(\frac{3}{2}^{-}\right)$	4.51 ± 0.12	2.75 ± 0.45
$P_{uss}^{10\frac{1}{2}}\left(\frac{3}{2}^{-}\right)$	4.60 ± 0.11	3.19 ± 0.50
$P_{sss}^{10\frac{1}{2}}\left(\frac{3}{2}^{-}\right)$	4.70 ± 0.11	3.78 ± 0.57
$P_{uuu}^{11\frac{1}{2}}\left(\frac{3}{2}^{-}\right)$	4.39 ± 0.14	3.75 ± 0.68
$P_{uus}^{11\frac{1}{2}}\left(\frac{3}{2}^{-}\right)$	4.51 ± 0.12	4.64 ± 0.77
$P_{uss}^{11\frac{1}{2}}\left(\frac{3}{2}^{-}\right)$	4.62 ± 0.11	5.60 ± 0.88
$P_{sss}^{11\frac{1}{2}}\left(\frac{3}{2}^{-}\right)$	4.71 ± 0.11	6.47 ± 1.00
$P_{uuu}^{11\frac{3}{2}}\left(\frac{3}{2}^{-}\right)$	4.39 ± 0.14	3.74 ± 0.70
$P_{uus}^{11\frac{3}{2}}\left(\frac{3}{2}^{-}\right)$	4.52 ± 0.12	4.64 ± 0.79
$P_{uss}^{11\frac{3}{2}}\left(\frac{3}{2}^{-}\right)$	4.61 ± 0.12	5.52 ± 0.90
$P_{sss}^{11\frac{3}{2}}\left(\frac{3}{2}^{-}\right)$	4.72 ± 0.11	6.52 ± 1.02
$P_{uuu}^{10\frac{1}{2}}\left(\frac{3}{2}^{+}\right)$	4.51 ± 0.13	0.99 ± 0.19
$P_{uus}^{10\frac{1}{2}}\left(\frac{3}{2}^{+}\right)$	4.60 ± 0.12	1.21 ± 0.22
$P_{uss}^{10\frac{1}{2}}\left(\frac{3}{2}^{+}\right)$	4.72 ± 0.11	1.45 ± 0.25
$P_{sss}^{10\frac{1}{2}}\left(\frac{3}{2}^{+}\right)$	4.81 ± 0.12	1.71 ± 0.29
$P_{uuu}^{11\frac{1}{2}}\left(\frac{3}{2}^{+}\right)$	4.91 ± 0.09	5.04 ± 0.68
$P_{uus}^{11\frac{1}{2}}\left(\frac{3}{2}^{+}\right)$	4.99 ± 0.09	5.83 ± 0.82
$P_{uss}^{11\frac{1}{2}}\left(\frac{3}{2}^{+}\right)$	5.08 ± 0.09	6.72 ± 0.98
$P_{sss}^{11\frac{1}{2}}\left(\frac{3}{2}^{+}\right)$	5.18 ± 0.09	7.73 ± 1.10
$P_{uuu}^{11\frac{3}{2}}\left(\frac{3}{2}^{+}\right)$	5.14 ± 0.08	7.86 ± 0.91
$P_{uus}^{11\frac{3}{2}}\left(\frac{3}{2}^{+}\right)$	5.21 ± 0.08	8.79 ± 1.07
$P_{uss}^{11\frac{3}{2}}\left(\frac{3}{2}^{+}\right)$	5.28 ± 0.08	9.91 ± 1.25
$P_{sss}^{11\frac{3}{2}}\left(\frac{3}{2}^{+}\right)$	5.36 ± 0.08	11.20 ± 1.42

Table 62: The masses and pole residues of the hidden-charm pentaquark states with the $J^P = \frac{3}{2}^{\pm}$ [705].

Acknowledgements

This work is supported by National Natural Science Foundation, Grant Number 11775079.

References

- [1] M. Gell-Mann, *A Schematic Model of Baryons and Mesons*, Phys. Lett. **8** (1964) 214.
- [2] R. L. Jaffe, *Multi-Quark Hadrons. 1. The Phenomenology of $Q^2\bar{Q}^2$ Mesons*, Phys. Rev. **D15** (1977) 267.
- [3] R. L. Jaffe, *Multi-Quark Hadrons. 2. Methods*, Phys. Rev. **D15** (1977) 281.
- [4] D. Strottman, *Multi-Quark Baryons and the MIT Bag Model*, Phys. Rev. **D20** (1979) 748.
- [5] H. J. Lipkin, *New Possibilities for Exotic Hadrons: Anticharmed Strange Baryons*, Phys. Lett. **B195** (1987) 484.
- [6] F. Dyson and N. H. Xuong, *$Y=2$ States in $Su(6)$ Theory*, Phys. Rev. Lett. **13** (1964) 815.
- [7] H. Clement, *On the History of Dibaryons and their Final Observation*, Prog. Part. Nucl. Phys. **93** (2017) 195.
- [8] T. Sakai, K. Shimizu and K. Yazaki, *H dibaryon*, Prog. Theor. Phys. Suppl. **137** (2000) 121.
- [9] R. L. Jaffe and K. Johnson, *Unconventional States of Confined Quarks and Gluons*, Phys. Lett. **B60** (1976) 201.
- [10] K. L. Au, D. Morgan and M. R. Pennington, *Meson Dynamics Beyond the Quark Model: A Study of Final State Interactions*, Phys. Rev. **D35** (1987) 1633.
- [11] T. Barnes, F. E. Close and F. de Viron, *$Q\bar{Q}G$ Hermaphrodite Mesons in the MIT Bag Model*, Nucl. Phys. **B224** (1983) 241.
- [12] S. K. Choi et al, *Observation of a narrow charmonium-like state in exclusive $B^+ \rightarrow K^+\pi^+\pi^- J/\psi$ decays*, Phys. Rev. Lett. **91** (2003) 262001.
- [13] J. D. Weinstein and N. Isgur, *Do Multi-Quark Hadrons Exist?*, Phys. Rev. Lett. **48** (1982) 659.
- [14] J. D. Weinstein and N. Isgur, *$K\bar{K}$ Molecules*, Phys. Rev. **D41** (1990) 2236.
- [15] N. N. Achasov, V. V. Gubin and V. I. Shevchenko, *Production of scalar $K\bar{K}$ molecules in ϕ radiative decays*, Phys. Rev. **D56** (1997) 203.
- [16] M. Boglione and M. R. Pennington, *Dynamical generation of scalar mesons*, Phys. Rev. **D65** (2002) 114010.
- [17] L. Maiani, F. Piccinini, A. D. Polosa and V. Riquer, *A New look at scalar mesons*, Phys. Rev. Lett. **93** (2004) 212002.
- [18] R. L. Jaffe and F. Wilczek, *Diquarks and exotic spectroscopy*, Phys. Rev. Lett. **91** (2003) 232003.
- [19] T. V. Brito, F. S. Navarra, M. Nielsen and M. E. Bracco, *QCD sum rule approach for the light scalar mesons as four-quark states*, Phys. Lett. **B608** (2005) 69.
- [20] Z. G. Wang and W. M. Yang, *Analysis the $f_0(980)$ and $a_0(980)$ mesons as four-quark states with the QCD sum rules*, Eur. Phys. J. **C42** (2005) 89.

- [21] Z. G. Wang, W. M. Yang and S. L. Wan, *Analysis the 0^{++} nonet mesons as four-quark states with the QCD sum rules*, J. Phys. **G31** (2005) 971.
- [22] H. J. Lee, *A QCD sum rule study of the light scalar meson*, Eur. Phys. J. **A30** (2006) 423.
- [23] H. J. Lee and N. I. Kochelev, *Instanton interpolating current for sigma-tetraquark*, Phys. Lett. **B642** (2006) 358.
- [24] S. Groote, J. G. Korner and D. Niinepuu, *Perturbative $\mathcal{O}(\alpha_s)$ corrections to the correlation functions of light tetraquark currents*, Phys. Rev. **D90** (2014) 054028.
- [25] Z. G. Wang, *Analysis of the scalar nonet mesons with QCD sum rules*, Eur. Phys. J. **C76** (2016) 427.
- [26] S. S. Agaev, K. Azizi and H. Sundu, *The strong decays of the light scalar mesons $f_0(500)$ and $f_0(980)$* , Phys. Lett. **B784** (2018) 266.
- [27] S. S. Agaev, K. Azizi and H. Sundu, *The nonet of the light scalar tetraquarks: The mesons $a_0(980)$ and $K_0^*(800)$* , Phys. Lett. **B789** (2019) 405.
- [28] H. J. Lee, K. S. Kim and H. Kim, *Testing the tetraquark mixing framework from QCD sum rules for $a_0(980)$* , Phys. Rev. **D100** (2019) 034021.
- [29] S. Weinberg, *Tetraquark Mesons in Large- N Quantum Chromodynamics*, Phys. Rev. Lett. **110** (2013) 261601.
- [30] C. Amsler and N. A. Tornqvist, *Mesons beyond the naive quark model*, Phys. Rept. **389** (2004) 61.
- [31] F. E. Close and N. A. Tornqvist, *Scalar mesons above and below 1-GeV*, J. Phys. **G28** (2002) R249.
- [32] E. Klempt and A. Zaitsev, *Glueballs, Hybrids, Multiquarks. Experimental facts versus QCD inspired concepts*, Phys. Rept. **454** (2007) 1.
- [33] A. Hosaka, T. Iijima, K. Miyabayashi, Y. Sakai and S. Yasui, *Exotic hadrons with heavy flavors: X , Y , Z , and related states*, Prog. Theor. Exp. Phys. **2016** (2016) 062C01.
- [34] H. X. Chen, W. Chen, X. Liu and S. L. Zhu, *The hidden-charm pentaquark and tetraquark states*, Phys. Rept. **639** (2016) 1.
- [35] R. F. Lebed, R. E. Mitchell and E. S. Swanson, *Heavy-Quark QCD Exotica*, Prog. Part. Nucl. Phys. **93** (2017) 143.
- [36] A. Ali, J. S. Lange and S. Stone, *Exotics: Heavy Pentaquarks and Tetraquarks*, Prog. Part. Nucl. Phys. **97** (2017) 123.
- [37] A. Esposito, A. Pilloni and A. D. Polosa, *Multiquark Resonances*, Phys. Rept. **668** (2017) 1.
- [38] F. K. Guo, C. Hanhart, U. G. Meissner, Q. Wang, Q. Zhao and B. S. Zou, *Hadronic molecules*, Rev. Mod. Phys. **90** (2018) 015004.
- [39] S. L. Olsen and T. Skwarnicki, *Non-standard heavy mesons and baryons: Experimental evidence*, Rev. Mod. Phys. **90** (2018) 015003.
- [40] M. Karliner, J. L. Rosner and T. Skwarnicki, *Multiquark States*, Ann. Rev. Nucl. Part. Sci. **68** (2018) 17.

- [41] N. Brambilla, S. Eidelman, C. Hanhart, A. Nefediev, C. P. Shen, C. E. Thomas, A. Vairo and C. Z. Yuan, *The XYZ states: experimental and theoretical status and perspectives*, Phys. Rept. **873** (2020) 1.
- [42] Y. R. Liu, H. X. Chen, W. Chen, X. Liu and S. L. Zhu, *Pentaquark and Tetraquark states*, Prog. Part. Nucl. Phys. **107** (2019) 237.
- [43] H. X. Chen, W. Chen, X. Liu, Y. R. Liu and S. L. Zhu, *An updated review of the new hadron states*, Rept. Prog. Phys. **86** (2023) 026201.
- [44] L. Meng, B. Wang, G. J. Wang and S. L. Zhu, *Chiral perturbation theory for heavy hadrons and chiral effective field theory for heavy hadronic molecules*, Phys. Rept. **1019** (2023) 1.
- [45] M. Z. Liu, Y. W. Pan, Z. W. Liu, T. W. Wu, J. X. Lu and L. S. Geng, *Three ways to decipher the nature of exotic hadrons: Multiplets, three-body hadronic molecules, and correlation functions*, Phys. Rept. **1108** (2025) 1.
- [46] M. Nielsen, F. S. Navarra and S. H. Lee, *New Charmonium States in QCD Sum Rules: A Concise Review*, Phys. Rept. **497** (2010) 41.
- [47] R. M. Albuquerque, J. M. Dias, K. P. Khemchandani, A. M. Torres, F. S. Navarra, M. Nielsen and C. M. Zanetti, *QCD sum rules approach to the X, Y and Z states*, J. Phys. **G46** (2019) 093002.
- [48] K. Abe et al, *Evidence for $X(3872) \rightarrow \gamma J/\psi$ and the sub-threshold decay $X(3872) \rightarrow \omega J/\psi$* , hep-ex/0505037.
- [49] B. Aubert et al, *Search for $B^+ \rightarrow X(3872)K^+$, $X(3872) \rightarrow J/\psi\gamma$* , Phys. Rev. **D74** (2006) 071101.
- [50] B. Aubert et al, *Evidence for $X(3872) \rightarrow \psi(2S)\gamma$ in $B^\pm \rightarrow X(3872)K^\pm$ decays, and a study of $B \rightarrow c\bar{c}\gamma K$* , Phys. Rev. Lett. **102** (2009) 132001.
- [51] A. Abulencia et al, *Analysis of the Quantum Numbers J^{PC} of the $X(3872)$ Particle*, Phys. Rev. Lett. **98** (2007) 132002.
- [52] S. K. Choi et al, *Bounds on the width, mass difference and other properties of $X(3872) \rightarrow \pi^+\pi^-J/\psi$ decays*, Phys. Rev. **D84** (2011) 052004.
- [53] R. Aaij et al, *Determination of the $X(3872)$ meson quantum numbers*, Phys. Rev. Lett. **110** (2013) 222001.
- [54] R. Aaij et al, *Quantum numbers of the $X(3872)$ state and orbital angular momentum in its $\rho^0 J/\psi$ decay*, Phys. Rev. **D92** (2015) 011102.
- [55] L. Maiani, F. Piccinini, A. D. Polosa and V. Riquer, *Diquark-antidiquarks with hidden or open charm and the nature of $X(3872)$* , Phys. Rev. **D71** (2005) 014028.
- [56] L. Maiani, F. Piccinini, A. D. Polosa and V. Riquer, *The $Z(4430)$ and a New Paradigm for Spin Interactions in Tetraquarks*, Phys. Rev. **D89** (2014) 114010.
- [57] S. J. Brodsky, D. S. Hwang and R. F. Lebed, *Dynamical Picture for the Formation and Decay of the Exotic XYZ Mesons*, Phys. Rev. Lett. **113** (2014) 112001.
- [58] R. D. Matheus, S. Narison, M. Nielsen and J. M. Richard, *Can the $X(3872)$ be a 1^{++} four-quark state?*, Phys. Rev. **D75** (2007) 014005.
- [59] D. Ebert, R. N. Faustov and V. O. Galkin, *Masses of heavy tetraquarks in the relativistic quark model*, Phys. Lett. **B634** (2006) 214.

- [60] Z. G. Wang and T. Huang, *Analysis of the $X(3872)$, $Z_c(3900)$ and $Z_c(3885)$ as axial-vector tetraquark states with QCD sum rules*, Phys. Rev. **D89** (2014) 054019.
- [61] Z. G. Wang, *Analysis of the hidden-charm tetraquark mass spectrum with the QCD sum rules*, Phys. Rev. **D102** (2020) 014018.
- [62] Z. G. Wang, *Decipher the width of the $X(3872)$ via the QCD sum rules*, Phys. Rev. **D109** (2024) 014017.
- [63] Y. R. Liu, X. Liu, W. Z. Deng and S. L. Zhu, *Is $X(3872)$ Really a Molecular State?*, Eur. Phys. J. **C56** (2008) 63.
- [64] N. A. Tornqvist, *Isospin breaking of the narrow charmonium state of Belle at 3872 MeV as a deuson*, Phys. Lett. **B590** (2004) 209.
- [65] E. S. Swanson, *Short range structure in the $X(3872)$* , Phys. Lett. **B588** (2004) 189.
- [66] E. S. Swanson, *Diagnostic decays of the $X(3872)$* , Phys. Lett. **B598** (2004) 197.
- [67] S. Fleming, M. Kusunoki, T. Mehen and U. v. Kolck, *Pion interactions in the $X(3872)$* , Phys. Rev. **D76** (2007) 034006.
- [68] C. Bignamini, B. Grinstein, F. Piccinini, A. D. Polosa and C. Sabelli, *Is the $X(3872)$ Production Cross Section at Tevatron Compatible with a Hadron Molecule Interpretation?*, Phys. Rev. Lett. **103** (2009) 162001.
- [69] F. E. Close and P. R. Page, *The $D^{*0}\bar{D}^0$ threshold resonance*, Phys. Lett. **B578** (2004) 119.
- [70] D. Gamermann, J. Nieves, E. Oset and E. R. Arriola, *Couplings in coupled channels versus wave functions: application to the $X(3872)$ resonance*, Phys. Rev. **D81** (2010) 014029.
- [71] M. B. Voloshin, *Interference and binding effects in decays of possible molecular component of $X(3872)$* , Phys. Lett. **B579** (2004) 316.
- [72] F. K. Guo, C. Hidalgo-Duque, J. Nieves and M. P. Valderrama, *Consequences of Heavy Quark Symmetries for Hadronic Molecules*, Phys. Rev. **D88** (2013) 054007.
- [73] F. K. Guo, C. Hanhart, U. G. Meissner, Q. Wang and Q. Zhao, *Production of the $X(3872)$ in charmonia radiative decays*, Phys. Lett. **B725** (2013) 127.
- [74] C. Y. Wong, *Molecular states of heavy quark mesons*, Phys. Rev. **C69** (2004) 055202.
- [75] M. T. AlFiky, F. Gabbiani and A. A. Petrov, *$X(3872)$: Hadronic molecules in effective field theory*, Phys. Lett. **B640** (2006) 238.
- [76] J. Nieves and M. P. Valderrama, *The Heavy Quark Spin Symmetry Partners of the $X(3872)$* , Phys. Rev. **D86** (2012) 056004.
- [77] C. Hanhart, Y. S. Kalashnikova, A. E. Kudryavtsev and A. V. Nefediev, *Reconciling the $X(3872)$ with the near-threshold enhancement in the $D^0\bar{D}^{*0}$ final state*, Phys. Rev. **D76** (2007) 034007.
- [78] Y. S. Kalashnikova, *Coupled-channel model for charmonium levels and an option for $X(3872)$* , Phys. Rev. **D72** (2005) 034010.
- [79] P. Artoisenet and E. Braaten, *Production of the $X(3872)$ at the Tevatron and the LHC*, Phys. Rev. **D81** (2010) 114018.

- [80] Y. B. Dong, A. Faessler, T. Gutsche and V. E. Lyubovitskij, *Estimate for the $X(3872) \rightarrow \gamma J/\psi$ decay width*, Phys. Rev. **D77** (2008) 094013.
- [81] Z. G. Wang and T. Huang, *Possible assignments of the $X(3872)$, $Z_c(3900)$ and $Z_b(10610)$ as axial-vector molecular states*, Eur. Phys. J. **C74** (2014) 2891.
- [82] Z. G. Wang, *Analysis of the Hidden-charm Tetraquark molecule mass spectrum with the QCD sum rules*, Int. J. Mod. Phys. **A36** (2021) 2150107.
- [83] Q. Xin and Z. G. Wang, *Analysis of the $X(3960)$ and related tetraquark molecular states via the QCD sum rules*, AAPPS Bull. **32** (2022) 37.
- [84] H. Mutuk, Y. Sarac, H. Gumus and A. Ozpineci, *$X(3872)$ and Its Heavy Quark Spin Symmetry Partners in QCD Sum Rules*, Eur. Phys. J. **C78** (2018) 904.
- [85] E. J. Eichten, K. Lane and C. Quigg, *New states above charm threshold*, Phys. Rev. **D73** (2006) 014014.
- [86] T. Barnes and S. Godfrey, *Charmonium options for the $X(3872)$* , Phys. Rev. **D69** (2004) 054008.
- [87] M. Suzuki, *The $X(3872)$ boson: Molecule or charmonium*, Phys. Rev. **D72** (2005) 114013.
- [88] B. Q. Li and K. T. Chao, *Higher Charmonia and X , Y , Z states with Screened Potential*, Phys. Rev. **D79** (2009) 094004.
- [89] D. V. Bugg, *Reinterpreting several narrow resonances as threshold cusps*, Phys. Lett. **B598** (2004) 8.
- [90] S. K. Choi et al, *Observation of a near-threshold $\omega J/\psi$ mass enhancement in exclusive $B \rightarrow K \omega J/\psi$ decays*, Phys. Rev. Lett. **94** (2005) 182002.
- [91] B. Aubert et al, *Observation of $Y(3940) \rightarrow J/\psi \omega$ in $B \rightarrow J/\psi \omega K$ at BABAR*, Phys. Rev. Lett. **101** (2008) 082001.
- [92] P. del Amo Sanchez et al, *Evidence for the decay $X(3872) \rightarrow J/\psi \omega$* , Phys. Rev. **D82** (2010) 011101.
- [93] K. Abe et al, *Observation of a new charmonium state in double charmonium production in e^+e^- annihilation at $\sqrt{s} \approx 10.6$ GeV*, Phys. Rev. Lett. **98** (2007) 082001.
- [94] K. Abe et al, *Search for new charmonium states in the processes $e^+e^- \rightarrow J/\psi D^{(*)} \bar{D}^{(*)}$ at $\sqrt{s} \approx 10.6$ GeV*, Phys. Rev. Lett. **100** (2008) 202001.
- [95] S. Uehara et al, *Observation of a charmonium-like enhancement in the $\gamma\gamma \rightarrow \omega J/\psi$ process*, Phys. Rev. Lett. **104** (2010) 092001.
- [96] J. P. Lees et al, *Study of $X(3915) \rightarrow J/\psi \omega$ in two-photon collisions*, Phys. Rev. **D86** (2012) 072002.
- [97] S. Navas et al, *The Review of Particle Physics*, Phys. Rev. **D110** (2024) 030001.
- [98] S. Uehara et al, *Observation of a χ'_{c2} candidate in $\gamma\gamma \rightarrow D\bar{D}$ production at Belle*, Phys. Rev. Lett. **96** (2006) 082003.
- [99] B. Aubert et al, *Observation of the $\chi_{c2}(2P)$ meson in the reaction $\gamma\gamma \rightarrow D\bar{D}$ at BABAR*, Phys. Rev. **D81** (2010) 092003.

- [100] K. Chilikin et al, *Observation of an alternative $\chi_{c0}(2P)$ candidate in $e^+e^- \rightarrow J/\psi D\bar{D}$* , Phys. Rev. **D95** (2017) 112003.
- [101] R. Aaij et al, *Model-independent study of structure in $B^+ \rightarrow D^+ D^- K^+$ decays*, Phys. Rev. Lett. **125** (2020) 242001.
- [102] R. Aaij et al, *Amplitude analysis of the $B^+ \rightarrow D^+ D^- K^+$ decay*, Phys. Rev. **D102** (2020) 112003.
- [103] R. Aaij et al, *Observation of a resonant structure near the $D_s^+ D_s^-$ threshold in the $B^+ \rightarrow D_s^+ D_s^- K^+$ decay*, Phys. Rev. Lett. **131** (2023) 071901.
- [104] F. K. Guo and U. G. Meissner, *Where is the $\chi_{c0}(2P)$?*, Phys. Rev. **D86** (2012) 091501.
- [105] T. Ji, X. K. Dong, M. Albaladejo, M. L. Du, F. K. Guo, J. Nieves and B. S. Zou, *Understanding the 0^{++} and 2^{++} charmonium(-like) states near 3.9 GeV*, Sci. Bull. **68** (2023) 688.
- [106] Z. G. Wang, *Analysis of the mass and width of the $X^*(3860)$ with QCD sum rules*, Eur. Phys. J. **A53** (2017) 192.
- [107] Z. Y. Zhou, Z. Xiao and H. Q. Zhou, *Could the $X(3915)$ and the $X(3930)$ Be the Same Tensor State?*, Phys. Rev. Lett. **115** (2015) 022001.
- [108] T. Barnes, S. Godfrey and E. S. Swanson, *Higher charmonia*, Phys. Rev. **D72** (2005) 054026.
- [109] R. Aaij et al, *Observation of new charmonium(-like) states in $B^+ \rightarrow D^{*\pm} D^\mp K^+$* , Phys. Rev. Lett. **133** (2024) 131902.
- [110] T. Aaltonen et al, *Evidence for a Narrow Near-Threshold Structure in the $J/\psi\phi$ Mass Spectrum in $B^+ \rightarrow J/\psi\phi K^+$ Decays*, Phys. Rev. Lett. **102** (2009) 242002.
- [111] T. Aaltonen et al, *Observation of the $Y(4140)$ structure in the $J/\psi\phi$ Mass Spectrum in $B^\pm \rightarrow J/\psi\phi K^\pm$ Decays*, Mod. Phys. Lett. **A32** (2017) 1750139.
- [112] S. Chatrchyan et al, *Observation of a peaking structure in the $J/\psi\phi$ mass spectrum from $B^\pm \rightarrow J/\psi\phi K^\pm$ decays*, Phys. Lett. **B734** (2014) 261.
- [113] R. Aaij et al, *Observation of $J/\psi\phi$ structures consistent with exotic states from amplitude analysis of $B^+ \rightarrow J/\psi\phi K^+$ decays*, Phys. Rev. Lett. **118** (2017) 022003.
- [114] R. Aaij et al, *Amplitude analysis of $B^+ \rightarrow J/\psi\phi K^+$ decays*, Phys. Rev. **D95** (2017) 012002.
- [115] R. Aaij et al, *Observation of new resonances decaying to $J/\psi K^+$ and $J/\psi\phi$* , Phys. Rev. Lett. **127** (2021) 082001.
- [116] R. Aaij et al, *Amplitude analysis of $B^+ \rightarrow \psi(2S) K^+ \pi^+ \pi^-$ decays*, JHEP **01** (2025) 054.
- [117] C. P. Shen et al, *Evidence for a new resonance and search for the $Y(4140)$ in $\gamma\gamma \rightarrow \phi J/\psi$* , Phys. Rev. Lett. **104** (2010) 112004.
- [118] M. Karliner and J. L. Rosner, *First exotic hadron with open heavy flavor: $c\bar{s}\bar{u}\bar{d}$ tetraquark*, Phys. Rev. **D102** (2020) 094016.
- [119] Z. G. Wang, *Analysis of the $X_0(2900)$ as the scalar tetraquark state via the QCD sum rules*, Int. J. Mod. Phys. **A35** (2020) 2050187.
- [120] J. R. Zhang, *Open-charm tetraquark candidate: Note on $X_0(2900)$* , Phys. Rev. **D103** (2021) 054019.

- [121] H. X. Chen, W. Chen, R. R. Dong and N. Su, $X_0(2900)$ and $X_1(2900)$: *Hadronic Molecules or Compact Tetraquarks*, Chin. Phys. Lett. **37** (2020) 101201.
- [122] X. G. He, W. Wang and R. L. Zhu, *Open-charm tetraquark X_c and open-bottom tetraquark X_b* , Eur. Phys. J. **C80** (2020) 1026.
- [123] Q. F. Lu, D. Y. Chen and Y. B. Dong, *Open charm and bottom tetraquarks in an extended relativized quark model*, Phys. Rev. **D102** (2020) 074021.
- [124] M. Z. Liu, J. J. Xie and L. S. Geng, $X_0(2866)$ as a $D^* \bar{K}^*$ molecular state, Phys. Rev. **D102** (2020) 091502.
- [125] M. W. Hu, X. Y. Lao, P. Ling and Q. Wang, $X_0(2900)$ and its heavy quark spin partners in molecular picture, Chin. Phys. **C45** (2021) 021003.
- [126] R. Molina and E. Oset, *Molecular picture for the $X_0(2866)$ as a $D^* \bar{K}^*$ $J^P = 0^+$ state and related 1^+ , 2^+ states*, Phys. Lett. **B811** (2020) 135870.
- [127] S. S. Agaev, K. Azizi and H. Sundu, *New scalar resonance $X_0(2900)$ as a molecule: mass and width*, J. Phys. **G48** (2021) 085012.
- [128] R. M. Albuquerque, S. Narison, D. Rabetiarivony and G. Randriamanatrika, $X_{0,1}(2900)$ and $(D^- K^+)$ invariant mass from *QCD Laplace sum rules at NLO*, Nucl. Phys. **A1007** (2021) 122113.
- [129] X. H. Liu, M. J. Yan, H. W. Ke, G. Li and J. J. Xie, *Triangle singularity as the origin of $X_0(2900)$ and $X_1(2900)$ observed in $B^+ \rightarrow D^+ D^- K^+$* , Eur. Phys. J. **C80** (2020) 1178.
- [130] R. Aaij et al, *First Observation of a Doubly Charged Tetraquark and Its Neutral Partner*, Phys. Rev. Lett. **131** (2023) 041902.
- [131] R. Aaij et al, *Amplitude analysis of $B^0 \rightarrow \bar{D}^0 D_s^+ \pi^-$ and $B^+ \rightarrow D^- D_s^+ \pi^+$ decays*, Phys. Rev. **D108** (2023) 012017.
- [132] V. M. Abazov et al, *Evidence for a $B_s^0 \pi^\pm$ State*, Phys. Rev. Lett. **117** (2016) 022003.
- [133] Z. G. Wang, *Analysis of the $X(5568)$ as scalar tetraquark state in the diquark-antidiquark model with *QCD* sum rules*, Commun. Theor. Phys. **66** (2016) 335.
- [134] W. Chen, H. X. Chen, X. Liu, T. G. Steele and S. L. Zhu, *Decoding the $X(5568)$ as a fully open-flavor $\text{sub}\bar{d}$ tetraquark state*, Phys. Rev. Lett. **117** (2016) 022002.
- [135] S. S. Agaev, K. Azizi and H. Sundu, *Mass and decay constant of the newly observed exotic $X(5568)$ state*, Phys. Rev. **D93** (2016) 074024.
- [136] W. Wang and R. L. Zhu, *Can $X(5568)$ be a tetraquark state?*, Chin. Phys. **C40** (2016) 093101.
- [137] C. M. Zanetti, M. Nielsen and K. P. Khemchandani, *QCD sum rule study of a charged bottom-strange scalar meson*, Phys. Rev. **D93** (2016) 096011.
- [138] R. Aaij et al, *Search for structure in the $B_s^0 \pi^\pm$ invariant mass spectrum*, Phys. Rev. Lett. **117** (2016) 152003.
- [139] A. M. Sirunyan et al, *Search for the $X(5568)$ state decaying into $B_s^0 \pi^\pm$ in proton-proton collisions at $\sqrt{s} = 8$ TeV*, Phys. Rev. Lett. **120** (2018) 202005.
- [140] M. Aaboud et al, *Search for a Structure in the $B_s^0 \pi^\pm$ Invariant Mass Spectrum with the ATLAS Experiment*, Phys. Rev. Lett. **120** (2018) 202007.

- [141] T. Aaltonen et al, *A search for the exotic meson $X(5568)$ with the Collider Detector at Fermilab*, Phys. Rev. Lett. **120** (2018) 202006.
- [142] R. Aaij et al, *Observation of structure in the J/ψ -pair mass spectrum*, Sci. Bull. **65** (2020) 1983.
- [143] G. Aad et al, *Observation of an Excess of Dicharmonium Events in the Four-Muon Final State with the ATLAS Detector*, Phys. Rev. Lett. **131** (2023) 151902.
- [144] A. Hayrapetyan et al, *New Structures in the $J/\psi J/\psi$ Mass Spectrum in Proton-Proton Collisions at $\sqrt{s} = 13$ TeV*, Phys. Rev. Lett. **132** (2024) 111901.
- [145] B. Aubert et al, *Observation of a Broad Structure in the $\pi^+\pi^- J/\psi$ Mass Spectrum around 4.26 GeV/c²*, Phys. Rev. Lett. **95** (2005) 142001.
- [146] C. Z. Yuan et al, *Measurement of $e^+e^- \rightarrow \pi^+\pi^- J/\psi$ Cross Section via Initial State Radiation at Belle*, Phys. Rev. Lett. **99** (2007) 182004.
- [147] Q. He et al, *Confirmation of the $Y(4260)$ Resonance Production in ISR*, Phys. Rev. **D74** (2006) 091104.
- [148] X. L. Wang et al, *Observation of Two Resonant Structures in $e^+e^- \rightarrow \pi^+\pi^-\psi(2S)$ via Initial State Radiation at Belle*, Phys. Rev. Lett. **99** (2007) 142002.
- [149] X. L. Wang et al, *Measurement of $e^+e^- \rightarrow \pi^+\pi^-\psi(2S)$ via Initial State Radiation at Belle*, Phys. Rev. **D91** (2015) 112007.
- [150] J. P. Lees et al, *Study of the reaction $e^+e^- \rightarrow \psi(2S)\pi^-\pi^-$ via initial state radiation at BaBar*, Phys. Rev. **D89** (2014) 111103.
- [151] G. Pakhlova et al, *Observation of a near-threshold enhancement in the $e^+e^- \rightarrow \Lambda_c^+\Lambda_c^-$ cross section using initial-state radiation*, Phys. Rev. Lett. **101** (2008) 172001.
- [152] M. Ablikim et al, *Study of $e^+e^- \rightarrow \omega\chi_{cJ}$ at center-of-mass energies from 4.21 to 4.42 GeV*, Phys. Rev. Lett. **114** (2015) 092003.
- [153] M. Ablikim et al, *Evidence of Two Resonant Structures in $e^+e^- \rightarrow \pi^+\pi^-h_c$* , Phys. Rev. Lett. **118** (2017) 092002.
- [154] M. Ablikim et al, *Precise measurement of the $e^+e^- \rightarrow \pi^+\pi^- J/\psi$ cross section at center-of-mass energies from 3.77 to 4.60 GeV*, Phys. Rev. Lett. **118** (2017) 092001.
- [155] M. Ablikim et al, *Observation of the $Y(4230)$ and a new structure in $e^+e^- \rightarrow K^+K^- J/\psi$* , Chin. Phys. **C46** (2022) 111002.
- [156] M. Ablikim et al, *Observation of Three Charmoniumlike States with $J^{PC} = 1^{--}$ in $e^+e^- \rightarrow D^{*0}D^{*-}\pi^+$* , Phys. Rev. Lett. **130** (2023) 121901.
- [157] M. Ablikim et al, *Precise measurement of the $e^+e^- \rightarrow D_s^{*+}D_s^{*-}$ cross sections at center-of-mass energies from threshold to 4.95 GeV*, Phys. Rev. Lett. **131** (2023) 151903.
- [158] M. Ablikim et al, *Observation of a vector charmoniumlike state at 4.7 GeV/c² and search for Z_{cs} in $e^+e^- \rightarrow K^+K^- J/\psi$* , Phys. Rev. Lett. **131** (2023) 211902.
- [159] M. Ablikim et al, *Observation of structures in the processes $e^+e^- \rightarrow \omega\chi_{c1}$ and $\omega\chi_{c2}$* , Phys. Rev. Lett. **132** (2024) 161901.
- [160] M. Ablikim et al, *Study of $e^+e^- \rightarrow \omega X(3872)$ and $\gamma X(3872)$ from 4.66 to 4.95 GeV*, Phys. Rev. **D110** (2024) 012006.

- [161] M. Ablikim et al, *Measurement of Energy-Dependent Pair-Production Cross Section and Electromagnetic Form Factors of a Charmed Baryon*, Phys. Rev. Lett. **131** (2023) 191901.
- [162] M. Ablikim et al, *Observation of a charged charmoniumlike structure in $e^+e^- \rightarrow \pi^+\pi^- J/\psi$ at $\sqrt{s} = 4.26$ GeV*, Phys. Rev. Lett. **110** (2013) 252001.
- [163] Z. Q. Liu et al, *Study of $e^+e^- \rightarrow \pi^+\pi^- J/\psi$ and Observation of a Charged Charmonium-like State at Belle*, Phys. Rev. Lett. **110** (2013) 252002.
- [164] T. Xiao, S. Dobbs, A. Tomaradze and K. K. Seth, *Observation of the Charged Hadron $Z_c^\pm(3900)$ and Evidence for the Neutral $Z_c^0(3900)$ in $e^+e^- \rightarrow \pi^+\pi^- J/\psi$ at $\sqrt{s} = 4170$ MeV*, Phys. Lett. **B727** (2013) 366.
- [165] M. Ablikim et al, *Observation of a charged charmoniumlike structure in $e^+e^- \rightarrow (D^*\bar{D}^*)^\pm \pi^\mp$ at $\sqrt{s} = 4.26$ GeV*, Phys. Rev. Lett. **112** (2014) 132001.
- [166] M. Ablikim et al, *Observation of a charged charmoniumlike structure $Z_c(4020)$ and search for the $Z_c(3900)$ in $e^+e^- \rightarrow \pi^+\pi^- h_c$* , Phys. Rev. Lett. **111** (2013) 242001.
- [167] M. Ablikim et al, *Observation of a charged $(D\bar{D}^*)^\pm$ mass peak in $e^+e^- \rightarrow \pi D\bar{D}^*$ at $\sqrt{s} = 4.26$ GeV*, Phys. Rev. Lett. **112** (2014) 022001.
- [168] M. Ablikim et al, *Determination of spin and parity of the $Z_c(3900)$* , Phys. Rev. Lett. **119** (2017) 072001.
- [169] M. Ablikim et al, *Observation of a near-threshold structure in the K^+ recoil-mass spectra in $e^+e^- \rightarrow K^+(D_s^- D^{*0} + D_s^{*-} D^0)$* , Phys. Rev. Lett. **126** (2021) 102001.
- [170] M. Ablikim et al, *Search for hidden-charm tetraquark with strangeness in $e^+e^- \rightarrow K^+ D_s^{*-} D^{*0} + c.c.$* , Chin. Phys. **C47** (2023) 033001.
- [171] Z. G. Wang, *Strange cousin of $Z_c(4020/4025)$ as a tetraquark state*, Chin. Phys. **C46** (2022) 123106.
- [172] Z. G. Wang, *Analysis of $Z_{cs}(3985)$ as the axialvector tetraquark state*, Chin. Phys. **C45** (2021) 073107.
- [173] R. Mizuk et al, *Observation of two resonance-like structures in the $\pi^+ \chi_{c1}$ mass distribution in exclusive $\bar{B}^0 \rightarrow K^- \pi^+ \chi_{c1}$ decays*, Phys. Rev. **D78** (2008) 072004.
- [174] J. P. Lees et al, *Search for the $Z_1(4050)^+$ and $Z_2(4250)^+$ states in $\bar{B}^0 \rightarrow \chi_{c1} K^- \pi^+$ and $B^+ \rightarrow \chi_{c1} K_S^0 \pi^+$* , Phys. Rev. **D85** (2012) 052003.
- [175] R. Aaij et al, *Evidence for an $\eta_c(1S)\pi^-$ resonance in $B^0 \rightarrow \eta_c(1S)K^+\pi^-$ decays*, Eur. Phys. J. **C78** (2018) 1019.
- [176] S. K. Choi et al, *Observation of a resonance-like structure in the $\pi^\pm \psi'$ mass distribution in exclusive $B \rightarrow K \pi^\pm \psi'$ decays*, Phys. Rev. Lett. **100** (2008) 142001.
- [177] R. Mizuk et al, *Dalitz analysis of $B \rightarrow K \pi^+ \psi'$ decays and the $Z(4430)^+$* , Phys. Rev. **D80** (2009) 031104.
- [178] K. Chilikin et al, *Experimental constraints on the spin and parity of the $Z(4430)^+$* , Phys. Rev. **D88** (2013) 074026.
- [179] R. Aaij et al, *Observation of the resonant character of the $Z(4430)^-$ state*, Phys. Rev. Lett. **112** (2014) 222002.

- [180] S. H. Lee, A. Mihara, F. S. Navarra and M. Nielsen, *QCD sum rules study of the meson $Z^+(4430)$* , Phys. Lett. **B661** (2008) 28.
- [181] M. Nielsen and F. S. Navarra, *Charged Exotic Charmonium States*, Mod. Phys. Lett. **A29** (2014) 1430005.
- [182] Z. G. Wang, *Analysis of the $Z(4430)$ as the first radial excitation of the $Z_c(3900)$* , Commun. Theor. Phys. **63** (2015) 325.
- [183] R. Aaij et al, *Model-independent observation of exotic contributions to $B^0 \rightarrow J/\psi K^+ \pi^-$ decays*, Phys. Rev. Lett. **122** (2019) 152002.
- [184] Z. G. Wang, *Axialvector tetraquark candidates for the $Z_c(3900)$, $Z_c(4020)$, $Z_c(4430)$, $Z_c(4600)$* , Chin. Phys. **C44** (2020) 063105.
- [185] H. X. Chen and W. Chen, *Settling the $Z_c(4600)$ in the charged charmonium-like family*, Phys. Rev. **D99** (2019) 074022.
- [186] K. Chilikin et al, *Observation of a new charged charmoniumlike state in $\bar{B}^0 \rightarrow J/\psi K^- \pi^+$ decays*, Phys. Rev. **D90** (2014) 112009.
- [187] I. Adachi et al, *Observation of two charged bottomonium-like resonances*, arXiv:1105.4583 [hep-ex].
- [188] A. Bondar et al, *Observation of two charged bottomonium-like resonances in $\Upsilon(5S)$ decays*, Phys. Rev. Lett. **108** (2012) 122001.
- [189] P. Krokovny et al, *First Observation of the $Z_b^0(10610)$ in a Dalitz Analysis of $\Upsilon(5S) \rightarrow \Upsilon(nS)\pi^0\pi^0$* , Phys. Rev. **D88** (2013) 052016.
- [190] A. Abdesselam et al, *Observation of a new structure near 10.75 GeV in the energy dependence of the $e^+e^- \rightarrow \Upsilon(nS)\pi^+\pi^-$ ($n = 1, 2, 3$) cross sections*, JHEP **10** (2019) 220.
- [191] I. Adachi et al, *Observation of $e^+e^- \rightarrow \omega\chi_{bJ}(1P)$ and search for $X_b \rightarrow \omega\Upsilon(1S)$ at \sqrt{s} near 10.75 GeV*, Phys. Rev. Lett. **130** (2023) 091902.
- [192] I. Adachi et al, *Study of $Y(10753)$ decays to $\pi^+\pi^-\Upsilon(nS)$ final states at Belle II*, JHEP **07** (2024) 116.
- [193] I. Adachi et al, *Search for the $e^+e^- \rightarrow \eta_b(1S)\omega$ and $e^+e^- \rightarrow \chi_{b0}(1P)\omega$ processes at $\sqrt{s} = 10.745$ GeV*, Phys. Rev. **D109** (2024) 072013.
- [194] R. Aaij et al, *Observation of an exotic narrow doubly charmed tetraquark*, Nature Phys. **18** (2022) 751.
- [195] R. Aaij et al, *Study of the doubly charmed tetraquark T_{cc}^+* , Nature Commun. **13** (2022) 3351.
- [196] R. Aaij et al, *Observation of $J/\psi p$ Resonances Consistent with Pentaquark States in $\Lambda_b^0 \rightarrow J/\psi K^- p$ Decays*, Phys. Rev. Lett. **115** (2015) 072001.
- [197] R. Aaij et al, *Observation of a narrow pentaquark state, $P_c(4312)^+$, and of two-peak structure of the $P_c(4450)^+$* , Phys. Rev. Lett. **122** (2019) 222001.
- [198] R. Aaij et al, *Evidence of a $J/\psi\Lambda$ structure and observation of excited Ξ^- states in the $\Xi_b^- \rightarrow J/\psi\Lambda K^-$ decay*, Sci. Bull. **66** (2021) 1278.
- [199] R. Aaij et al, *Evidence for a new structure in the $J/\psi p$ and $J/\psi\bar{p}$ systems in $\bar{B}_s^0 \rightarrow J/\psi p\bar{p}$ decays*, Phys. Rev. Lett. **128** (2022) 062001.

- [200] R. Aaij et al, *Observation of a $J/\psi\Lambda$ resonance consistent with a strange pentaquark candidate in $B^- \rightarrow J/\psi\Lambda\bar{p}$ decays*, Phys. Rev. Lett. **131** (2023) 031901.
- [201] P. Adlarson et al, *Evidence for a New Resonance from Polarized Neutron-Proton Scattering*, Phys. Rev. Lett. **112** (2014) 202301.
- [202] P. Adlarson et al, *Neutron-proton scattering in the context of the $d^*(2380)$ resonance*, Phys. Rev. **C90** (2014) 035204.
- [203] F. Huang, Z. Y. Zhang, P. N. Shen and W. L. Wang, *Is d^* a candidate for a hexaquark-dominated exotic state?*, Chin. Phys. **C39** (2015) 071001.
- [204] W. Park, A. Park and S. H. Lee, *Dibaryons in a constituent quark model*, Phys. Rev. **D92** (2015) 014037.
- [205] H. X. Chen, E. L. Cui, W. Chen, T. G. Steele and S. L. Zhu, *QCD sum rule study of the $d^*(2380)$* , Phys. Rev. **C91** (2015) 025204.
- [206] A. Gal, *The $d^*(2380)$ dibaryon resonance width and decay branching ratios*, Phys. Lett. **B769** (2017) 436.
- [207] F. Huang, *Progress on $d^*(2380)$ in a chiral $SU(3)$ quark model*, Rev. Mex. Fis. Suppl. **3** (2022) 0308031.
- [208] N. A. Tornqvist, *From the deuteron to deusons, an analysis of deuteron-like meson meson bound states*, Z. Phys. **C61** (1994) 525.
- [209] M. Karliner and J. L. Rosner, *New Exotic Meson and Baryon Resonances from Doubly-Heavy Hadronic Molecules*, Phys. Rev. Lett. **115** (2015) 122001.
- [210] C. E. Thomas and F. E. Close, *Is $X(3872)$ a molecule?*, Phys. Rev. **D78** (2008) 034007.
- [211] C. Hidalgo-Duque, J. Nieves and M. P. Valderrama, *Light flavor and heavy quark spin symmetry in heavy meson molecules*, Phys. Rev. **D87** (2013) 076006.
- [212] Y. R. Liu and M. Oka, *$\Lambda_c N$ bound states revisited*, Phys. Rev. **D85** (2012) 014015.
- [213] M. Cleven, F. K. Guo, C. Hanhart, Q. Wang and Q. Zhao, *Employing spin symmetry to disentangle different models for the XYZ states*, Phys. Rev. **D92** (2015) 014005.
- [214] Y. Yamaguchi, A. Giachino, A. Hosaka, E. Santopinto, S. Takeuchi and M. Takizawa, *Hidden-charm and bottom meson-baryon molecules coupled with five-quark states*, Phys. Rev. **D96** (2017) 114031.
- [215] F. Close, C. Downum and C. E. Thomas, *Novel Charmonium and Bottomonium Spectroscopies due to Deeply Bound Hadronic Molecules from Single Pion Exchange*, Phys. Rev. **D81** (2010) 074033.
- [216] F. K. Guo, X. H. Liu and S. Sakai, *Threshold cusps and triangle singularities in hadronic reactions*, Prog. Part. Nucl. Phys. **112** (2020) 103757.
- [217] D. V. Bugg, *How Resonances can synchronise with Thresholds*, J. Phys. **G35** (2008) 075005.
- [218] E. S. Swanson, *Z_b and Z_c Exotic States as Coupled Channel Cusps*, Phys. Rev. **D91** (2015) 034009.
- [219] E. S. Swanson, *Cusps and Exotic Charmonia*, Int. J. Mod. Phys. **E25** (2016) 1642010.

- [220] D. Y. Chen and X. Liu, *$Z_b(10610)$ and $Z_b(10650)$ structures produced by the initial single pion emission in the $\Upsilon(5S)$ decays*, Phys. Rev. **D84** (2011) 094003.
- [221] D. Y. Chen, X. Liu and T. Matsuki, *Reproducing the $Z_c(3900)$ structure through the initial-single-pion-emission mechanism*, Phys. Rev. **D88** (2013) 036008.
- [222] D. Y. Chen, X. Liu and T. Matsuki, *Predictions of Charged Charmoniumlike Structures with Hidden-Charm and Open-Strange Channels*, Phys. Rev. Lett. **110** (2013) 232001.
- [223] X. K. Dong, F. K. Guo and B. S. Zou, *Explaining the Many Threshold Structures in the Heavy-Quark Hadron Spectrum*, Phys. Rev. Lett. **126** (2021) 152001.
- [224] X. H. Liu and G. Li, *Exploring the threshold behavior and implications on the nature of $Y(4260)$ and $Z_c(3900)$* , Phys. Rev. **D88** (2013) 014013.
- [225] X. H. Liu, Q. Wang and Q. Zhao, *Understanding the newly observed heavy pentaquark candidates*, Phys. Lett. **B757** (2016) 231.
- [226] F. K. Guo, U. G. Meissner, J. Nieves and Z. Yang, *Remarks on the P_c structures and triangle singularities*, Eur. Phys. J. **A52** (2016) 318.
- [227] Q. Wang, C. Hanhart and Q. Zhao, *Decoding the riddle of $Y(4260)$ and $Z_c(3900)$* , Phys. Rev. Lett. **111** (2013) 132003.
- [228] Q. Wang, C. Hanhart and Q. Zhao, *Systematic study of the singularity mechanism in heavy quarkonium decays*, Phys. Lett. **B725** (2013) 106.
- [229] M. Cleven, Q. Wang, F. K. Guo, C. Hanhart, U. G. Meissner and Q. Zhao, *$Y(4260)$ as the first S -wave open charm vector molecular state?*, Phys. Rev. **D90** (2014) 074039.
- [230] M. L. Du, M. Albaladejo, F. K. Guo and J. Nieves, *A combined analysis of the $Z_c(3900)$ and the $Z_{cs}(3985)$ exotic states*, Phys. Rev. **D105** (2022) 074018.
- [231] L. W. Yan, Z. H. Guo, F. K. Guo, D. L. Yao and Z. Y. Zhou, *Reconciling experimental and lattice data of $Z_c(3900)$ in a $J/\psi\pi - D\bar{D}^*$ coupled-channel analysis*, Phys. Rev. **D109** (2024) 014026.
- [232] Q. Wu, D. Y. Chen and F. K. Guo, *Production of the $Z_b^{(\prime)}$ states from the $\Upsilon(5S, 6S)$ decays*, Phys. Rev. **D99** (2019) 034022.
- [233] Y. H. Chen, M. Cleven, J. T. Daub, F. K. Guo, C. Hanhart, B. Kubis, U. G. Meissner and B. S. Zou, *Effects of Z_b states and bottom meson loops on $\Upsilon(4S) \rightarrow \Upsilon(1S, 2S)\pi^+\pi^-$ transitions*, Phys. Rev. **D95** (2017) 034022.
- [234] M. Albaladejo, F. K. Guo, C. Hidalgo-Duque and J. Nieves, *$Z_c(3900)$: What has been really seen?*, Phys. Lett. **B755** (2016) 337.
- [235] F. K. Guo, C. Hanhart, Q. Wang and Q. Zhao, *Could the near-threshold XYZ states be simply kinematic effects?*, Phys. Rev. **D91** (2015) 051504.
- [236] A. P. Szczepaniak, *Triangle Singularities and XYZ Quarkonium Peaks*, Phys. Lett. **B747** (2015) 410.
- [237] Y. H. Chen, M. L. Du and F. K. Guo, *Precise determination of the pole position of the exotic $Z_c(3900)$* , Sci. China Phys. Mech. Astron. **67** (2024) 291011.
- [238] B. A. Li, *Is $X(3872)$ a possible candidate of hybrid meson?*, Phys. Lett. **B605** (2005) 306.

- [239] X. H. Liu, Q. Zhao and F. E. Close, *Search for tetraquark candidate $Z(4430)$ in meson photoproduction*, Phys. Rev. **D77** (2008) 094005.
- [240] X. Y. Wang, J. He, X. R. Chen, Q. J. Wang and X. M. Zhu, *Pion-induced production of hidden-charm pentaquarks $P_c(4312)$, $P_c(4440)$ and $P_c(4457)$* , Phys. Lett. **B797** (2019) 134862.
- [241] J. Chen, F. K. Guo, Y. G. Ma, C. P. Shen, Q. Shou, Q. Wang, J. J. Wu and B. S. Zou, *Production of exotic hadrons in pp and nuclear collisions*, Nucl. Sci. Tech. **36** (2025) 55.
- [242] R. Casalbuoni, A. Deandrea, N. Di Bartolomeo, F. Feruglio, R. Gatto and G. Nardulli, *Phenomenology of Heavy Meson Chiral Lagrangians*, Phys. Rept. **281** (1997) 145.
- [243] Z. G. Wang, *Strong decays of the bottom mesons $B_1(5721)$, $B_2(5747)$, $B_{s1}(5830)$, $B_{s2}(5840)$ and $B(5970)$* , Eur. Phys. J. Plus **129** (2014) 186.
- [244] S. Campanella, P. Colangelo and F. De Fazio, *Excited heavy meson decays to light vector mesons: implications for spectroscopy*, Phys. Rev. **D98** (2018) 114028.
- [245] J. A. Oller, E. Oset and A. Ramos, *Chiral unitary approach to meson-meson and meson-baryon interactions and nuclear applications*, Prog. Part. Nucl. Phys. **45** (2000) 157.
- [246] T. Hyodo, D. Jido and A. Hosaka, *Compositeness of dynamically generated states in a chiral unitary approach*, Phys. Rev. **C85** (2012) 015201.
- [247] D. Gamermann and E. Oset, *Axial resonances in the open and hidden charm sectors*, Eur. Phys. J. **A33** (2007) 119.
- [248] R. Molina and E. Oset, *The $Y(3940)$, $Z(3930)$ and the $X(4160)$ as dynamically generated resonances from the vector-vector interaction*, Phys. Rev. **D80** (2009) 114013.
- [249] F. Aceti, M. Bayar, E. Oset, A. Martinez Torres, K. P. Khemchandani, J. M. Dias, F. S. Navarra and M. Nielsen, *Prediction of an $I = 1$ $D\bar{D}^*$ state and relationship to the claimed $Z_c(3900)$, $Z_c(3885)$* , Phys. Rev. **D90** (2014) 016003.
- [250] T. Ji, X. K. Dong, M. Albaladejo, M. L. Du, F. K. Guo and J. Nieves, *Establishing the heavy quark spin and light flavor molecular multiplets of the $X(3872)$, $Z_c(3900)$ and $X(3960)$* , Phys. Rev. **D106** (2022) 094002.
- [251] J. M. Dias, F. Aceti and E. Oset, *Study of $B\bar{B}^*$ and $B^*\bar{B}^*$ interactions in $I = 1$ and relationship to the $Z_b(10610)$, $Z_b(10650)$ states*, Phys. Rev. **D91** (2015) 076001.
- [252] M. Cleven, Q. Wang, F. K. Guo, C. Hanhart, U. G. Meissner and Q. Zhao, *Confirming the molecular nature of the $Z_b(10610)$ and the $Z_b(10650)$* , Phys. Rev. **D87** (2013) 074006.
- [253] M. Cleven, F. K. Guo, C. Hanhart and U. G. Meissner, *Bound state nature of the exotic Z_b states*, Eur. Phys. J. **A47** (2011) 120.
- [254] F. K. Guo, P. N. Shen, H. C. Chiang and R. G. Ping, *Heavy Quarkonium $\pi^+\pi^-$ Transitions and a Possible $b\bar{b}q\bar{q}$ State*, Nucl. Phys. **A761** (2005) 269.
- [255] J. J. Wu, R. Molina, E. Oset and B. S. Zou, *Dynamically generated N^* and Λ^* resonances in the hidden charm sector around 4.3 GeV*, Phys. Rev. **C84** (2011) 015202.
- [256] C. W. Xiao, J. Nieves and E. Oset, *Combining heavy quark spin and local hidden gauge symmetries in the dynamical generation of hidden charm baryons*, Phys. Rev. **D88** (2013) 056012.
- [257] L. Roca, J. Nieves and E. Oset, *The LHCb pentaquark as a $\bar{D}^*\Sigma_c - \bar{D}^*\Sigma_c^*$ molecular state*, Phys. Rev. **D92** (2015) 094003.

- [258] T. Uchino, W. H. Liang and E. Oset, *Baryon states with hidden charm in the extended local hidden gauge approach*, Eur. Phys. J. **A52** (2016) 43.
- [259] C. W. Xiao, J. Nieves and E. Oset, *Heavy quark spin symmetric molecular states from $\bar{D}^{(*)}\Sigma_c^{(*)}$ and other coupled channels in the light of the recent LHCb pentaquarks*, Phys. Rev. **D100** (2019) 014021.
- [260] T. Hyodo, *Structure of Near-Threshold s-Wave Resonances*, Phys. Rev. Lett. **111** (2013) 132002.
- [261] Z. H. Guo and J. A. Oller, *Probabilistic interpretation of compositeness relation for resonances*, Phys. Rev. **D93** (2016) 096001.
- [262] Y. Kamiya and T. Hyodo, *Structure of near-threshold quasibound states*, Phys. Rev. **C93** (2016) 035203.
- [263] X. W. Kang, Z. H. Guo and J. A. Oller, *General considerations on the nature of $Z_b(10610)$ and $Z_b(10650)$ from their pole positions*, Phys. Rev. **D94** (2016) 014012.
- [264] Y. Li, F. K. Guo, J. Y. Pang and J. J. Wu, *Generalization of Weinberg's compositeness relations*, Phys. Rev. **D105** (2022) L071502.
- [265] Z. H. Zhang, T. Ji, X. K. Dong, F. K. Guo, C. Hanhart, U. G. Meissner and A. Rusetsky, *Predicting isovector charmonium-like states from $X(3872)$ properties*, JHEP **08** (2024) 130.
- [266] T. Ji, X. K. Dong, F. K. Guo, C. Hanhart, and U. G. Meissner, *Precise determination of the properties of $X(3872)$ and of its isovector partner W_{c1}* , arXiv:2502.04458 [hep-ph].
- [267] J. He, *The $Z_c(3900)$ as a resonance from the $D\bar{D}^*$ interaction*, Phys. Rev. **D92** (2015) 034004.
- [268] J. He, *$\bar{D}\Sigma_c^*$ and $\bar{D}^*\Sigma_c$ interactions and the LHCb hidden-charmed pentaquarks*, Phys. Lett. **B753** (2016) 547.
- [269] J. He, *Study of $P_c(4457)$, $P_c(4440)$, and $P_c(4312)$ in a quasipotential Bethe-Salpeter equation approach*, Eur. Phys. J. **C79** (2019) 393.
- [270] P. G. Ortega, J. Segovia, D. R. Entem and F. Fernandez, *The Z_c structures in a coupled-channels model*, Eur. Phys. J. **C79** (2019) 78.
- [271] H. W. Ke, X. Q. Li, Y. L. Shi, G. L. Wang and X. H. Yuan, *Is $Z_b(10610)$ a Molecular State?*, JHEP **04** (2012) 056.
- [272] H. W. Ke, M. Li, X. H. Liu and X. Q. Li, *Study on possible molecular states composed of $\Lambda_c\bar{D}(\Lambda_b B)$ and $\Sigma_c\bar{D}(\Sigma_b B)$ within the Bethe-Salpeter framework*, Phys. Rev. **D101** (2020) 014024.
- [273] M. J. Zhao, Z. Y. Wang, C. Wang and X. H. Guo, *Investigation of the possible $D\bar{D}^*/B\bar{B}^*$ and $DD^*/\bar{B}\bar{B}^*$ molecule states*, Phys. Rev. **D105** (2022) 096016.
- [274] J. Nieves and M. P. Valderrama, *Deriving the existence of $B\bar{B}^*$ bound states from the $X(3872)$ and Heavy Quark Symmetry*, Phys. Rev. **D84** (2011) 056015.
- [275] M. Z. Liu, T. W. Wu, J. J. Xie, M. P. Valderrama and L. S. Geng, *$D\Xi$ and $D^*\Xi$ molecular states from one boson exchange*, Phys. Rev. **D98** (2018) 014014.
- [276] M. Z. Liu, T. W. Wu, M. P. Valderrama, J. J. Xie and L. S. Geng, *Heavy-quark spin and flavor symmetry partners of the $X(3872)$* , Phys. Rev. **D99** (2019) 094018.

- [277] M. Z. Liu, Y. W. Pan, F. Z. Peng, M. S. Sanchez, L. S. Geng, A. Hosaka and M. Pa. Valderrama, *Emergence of a complete heavy-quark spin symmetry multiplet: seven molecular pentaquarks in light of the latest LHCb analysis*, Phys. Rev. Lett. **122** (2019) 242001.
- [278] M. Z. Liu, Y. W. Pan and L. S. Geng, *Can discovery of hidden charm strange pentaquark states help determine the spins of $P_c(4440)$ and $P_c(4457)$?*, Phys. Rev. **D103** (2021) 034003.
- [279] X. Liu, Z. G. Luo, Y. R. Liu and S. L. Zhu, *$X(3872)$ and Other Possible Heavy Molecular States*, Eur. Phys. J. **C61** (2009) 411.
- [280] G. J. Ding, *Are $Y(4260)$ and $Z_2^+(4250)$ D_1D or D^0D Hadronic Molecules?*, Phys. Rev. **D79** (2009) 014001.
- [281] I. W. Lee, A. Faessler, T. Gutsche and V. E. Lyubovitskij, *$X(3872)$ as a molecular DD^* state in a potential model*, Phys. Rev. **D80** (2009) 094005.
- [282] Z. F. Sun, J. He, X. Liu, Z. G. Luo and S. L. Zhu, *$Z_b(10610)^\pm$ and $Z_b(10650)^\pm$ as the $B^*\bar{B}$ and $B^*\bar{B}^*$ molecular states*, Phys. Rev. **D84** (2011) 054002.
- [283] Z. C. Yang, Z. F. Sun, J. He, X. Liu and S. L. Zhu, *The possible hidden-charm molecular baryons composed of anti-charmed meson and charmed baryon*, Chin. Phys. **C36** (2012) 6.
- [284] S. Ohkoda, Y. Yamaguchi, S. Yasui, K. Sudoh and A. Hosaka, *Exotic mesons with double charm and bottom flavor*, Phys. Rev. **D86** (2012) 034019.
- [285] N. Li, Z. F. Sun, X. Liu and S. L. Zhu, *Coupled-channel analysis of the possible $D^{(*)}D^{(*)}$, $\bar{B}^{(*)}\bar{B}^{(*)}$ and $D^{(*)}\bar{B}^{(*)}$ molecular states*, Phys. Rev. **D88** (2013) 114008.
- [286] H. Xu, B. Wang, Z. W. Liu and X. Liu, *DD^* potentials in chiral perturbation theory and possible molecular states*, Phys. Rev. **D99** (2019) 014027.
- [287] L. Meng, B. Wang, G. J. Wang and S. L. Zhu, *The hidden charm pentaquark states and $\Sigma_c\bar{D}^{(*)}$ interaction in chiral perturbation theory*, Phys. Rev. **D100** (2019) 014031.
- [288] B. Wang, L. Meng and S. L. Zhu, *Hidden-charm and hidden-bottom molecular pentaquarks in chiral effective field theory*, JHEP **11** (2019) 108.
- [289] M. Z. Liu, T. W. Wu, M. S. Sanchez, M. P. Valderrama, L. S. Geng and J. J. Xie, *Spin-parities of the $P_c(4440)$ and $P_c(4457)$ in the one-boson-exchange model*, Phys. Rev. **D103** (2021) 054004.
- [290] S. Y. Yu and X. W. Kang, *Nature of $X(3872)$ from its radiative decay*, Phys. Lett. **B848** (2024) 138404.
- [291] E. Braaten and M. Kusunoki, *Low-energy universality and the new charmonium resonance at 3870-MeV*, Phys. Rev. **D69** (2004) 074005.
- [292] P. G. Ortega, J. Segovia, D. R. Entem and F. Fernandez, *Coupled channel approach to the structure of the $X(3872)$* , Phys. Rev. **D81** (2010) 054023.
- [293] S. Coito, G. Rupp and E. van Beveren, *$X(3872)$ is not a true molecule*, Eur. Phys. J. **C73** (2013) 2351.
- [294] P. G. Ortega, J. Segovia, D. R. Entem and F. Fernandez, *Charmonium resonances in the 3.9 GeV/ c^2 energy region and the $X(3915)/X(3930)$ puzzle*, Phys. Lett. **B778** (2018) 5.
- [295] Z. Y. Zhou and Z. Xiao, *Understanding $X(3862)$, $X(3872)$, and $X(3930)$ in a Friedrichs-model-like scheme*, Phys. Rev. **D96** (2017) 054031.

- [296] Z. Y. Zhou and Z. Xiao, *Comprehending Isospin breaking effects of $X(3872)$ in a Friedrichs-model-like scheme*, Phys. Rev. **D97** (2018) 034011.
- [297] J. Ferretti and E. Santopinto, *Threshold corrections of $\chi_c(2P)$ and $\chi_b(3P)$ states and $J/\psi\rho$ and $J/\psi\omega$ transitions of the $X(3872)$ in a coupled-channel model*, Phys. Lett. **B789** (2019) 550.
- [298] Y. S. Kalashnikova and A. V. Nefediev, *$X(3872)$ in the molecular model*, Phys. Usp. **62** (2019) 568.
- [299] Y. Yamaguchi, A. Hosaka, S. Takeuchi and M. Takizawa, *Heavy hadronic molecules with pion exchange and quark core couplings: a guide for practitioners*, J. Phys. **G47** (2020) 053001.
- [300] Q. Deng, R. H. Ni, Q. Li and X. H. Zhong, *Charmonia in an unquenched quark model*, Phys. Rev. **D110** (2024) 056034.
- [301] E. Braaten, *How the $Z_c(3900)$ Reveals the Spectra of Quarkonium Hybrid and Tetraquark Mesons*, Phys. Rev. Lett. **111** (2013) 162003.
- [302] E. Braaten, C. Langmack, D. H. Smith, *Selection Rules for Hadronic Transitions of XYZ Mesons*, Phys. Rev. Lett. **112** (2014) 222001.
- [303] E. Braaten, C. Langmack and D. H. Smith, *Born-Oppenheimer Approximation for the XYZ Mesons*, Phys. Rev. **D90** (2014) 014044.
- [304] M. Berwein, N. Brambilla, J. T. Castella and A. Vairo, *Quarkonium Hybrids with Nonrelativistic Effective Field Theories*, Phys. Rev. **D92** (2015) 114019.
- [305] R. Oncala and J. Soto, *Heavy Quarkonium Hybrids: Spectrum, Decay and Mixing*, Phys. Rev. **D96** (2017) 014004.
- [306] N. Brambilla, W. K. Lai, J. Segovia, J. T. Castella and A. Vairo, *Spin structure of heavy-quark hybrids*, Phys. Rev. **D99** (2019) 014017.
- [307] K. J. Juge, J. Kuti and C. J. Morningstar, *Ab initio study of hybrid $\bar{b}gb$ mesons*, Phys. Rev. Lett. **82** (1999) 4400.
- [308] G. S. Bali, B. Bolder, N. Eicker, T. Lippert, B. Orth, P. Ueberholz, K. Schilling and T. Struckmann, *Static potentials and glueball masses from QCD simulations with Wilson sea quarks*, Phys. Rev. **D62** (2000) 054503.
- [309] G. S. Bali, H. Neff, T. Duessell, T. Lippert and K. Schilling, *Observation of String Breaking in QCD*, Phys. Rev. **D71** (2005) 114513.
- [310] M. Foster and C. Michael, *Hadrons with a heavy colour-adjoint particle*, Phys. Rev. **D59** (2009) 094509.
- [311] R. L. Jaffe, *Exotica*, Phys. Rept. **409** (2005) 1.
- [312] R. Faccini, L. Maiani, F. Piccinini, A. Pilloni, A. D. Polosa and V. Riquer, *A $J^{PG} = 1^{++}$ Charged Resonance in the $Y(4260)$ to $\pi^+\pi^-J/\psi$ Decay?*, Phys. Rev. **D87** (2013) 111102.
- [313] L. Maiani, V. Riquer, F. Piccinini and A. D. Polosa, *Four Quark Interpretation of $Y(4260)$* , Phys. Rev. **D72** (2005) 031502.
- [314] N. V. Drenska, R. Faccini and A. D. Polosa, *Exotic Hadrons with Hidden Charm and Strangeness*, Phys. Rev. **D79** (2009) 077502.

- [315] R. F. Lebed and A. D. Polosa, $\chi_{c0}(3915)$ *As the Lightest $c\bar{c}s\bar{s}$ State*, Phys. Rev. **D93** (2016) 094024.
- [316] L. Maiani, A. D. Polosa and V. Riquer, *Interpretation of Axial Resonances in $J/\psi\phi$ at LHCb*, Phys. Rev. **D94** (2016) 054026.
- [317] L. Maiani, A. D. Polosa and V. Riquer, *A Theory of X and Z Multiquark Resonances*, Phys. Lett. **B778** (2018) 247.
- [318] A. Ali, L. Maiani, A. V. Borisov, I. Ahmed, M. Jamil Aslam, A. Y. Parkhomenko, A. D. Polosa and A. Rehman, *A New Look at the Y Tetraquarks and Ω_c Baryons in the Diquark Model*, Eur. Phys. J. **C78** (2018) 29.
- [319] L. Maiani, A. D. Polosa and V. Riquer, *The new resonances $Z_{cs}(3985)$ and $Z_{cs}(4003)$ (almost) fill two tetraquark nonets of broken $SU(3)_f$* , Sci. Bull. **66** (2021) 1616.
- [320] H. Hogaasen, J. M. Richard and P. Sorba, *A Chromomagnetic mechanism for the X(3872) resonance*, Phys. Rev. **D73** (2006) 054013.
- [321] F. Buccella, H. Hogaasen, J. M. Richard and P. Sorba, *Chromomagnetism, flavour symmetry breaking and S-wave tetraquarks*, Eur. Phys. J. **C49** (2007) 743.
- [322] L. Zhao, W. Z. Deng and S. L. Zhu, *Hidden-Charm Tetraquarks and Charged Z_c States*, Phys. Rev. **D90** (2014) 094031.
- [323] J. Wu, Y. R. Liu, K. Chen, X. Liu and S. L. Zhu, *Heavy-flavored tetraquark states with the $QQ\bar{Q}\bar{Q}$ configuration*, Phys. Rev. **D97** (2018) 094015.
- [324] T. Guo, J. Li, J. Zhao and L. He, *Mass spectra of doubly heavy tetraquarks in an improved chromomagnetic interaction model*, Phys. Rev. **D105** (2022) 014021.
- [325] R. F. Lebed, *Spectroscopy of Exotic Hadrons Formed from Dynamical Diquarks*, Phys. Rev. **D96** (2017) 116003.
- [326] J. F. Giron and R. F. Lebed, *The Dynamical Diquark Model: First Numerical Results*, JHEP **05** (2019) 061.
- [327] J. F. Giron, R. F. Lebed and C. T. Peterson, *The Dynamical Diquark Model: Fine Structure and Isospin*, JHEP **01** (2020) 124.
- [328] J. F. Giron and R. F. Lebed, *Spectrum of p-wave hidden-charm exotic mesons in the diquark model*, Phys. Rev. **D101** (2020) 074032.
- [329] J. F. Giron and R. F. Lebed, *Spectrum of the hidden-bottom and the hidden-charm-strange exotics in the dynamical diquark model*, Phys. Rev. **D102** (2020) 014036.
- [330] J. F. Giron, R. F. Lebed and S. R. Martinez, *Spectrum of hidden-charm, open-strange exotics in the dynamical diquark model*, Phys. Rev. **D104** (2021) 054001.
- [331] R. F. Lebed and S. R. Martinez, *T_{cc} in the diabatic diquark model: Effects of D^*D isospin*, Phys. Rev. **D110** (2024) 034033.
- [332] Q. F. Lu and Y. B. Dong, *X(4140), X(4274), X(4500), and X(4700) in the relativized quark model*, Phys. Rev. **D94** (2016) 074007.
- [333] M. N. Anwar, J. Ferretti and E. Santopinto, *Spectroscopy of the hidden-charm $[qc][\bar{q}\bar{c}]$ and $[sc][\bar{s}\bar{c}]$ tetraquarks*, Phys. Rev. **D98** (2018) 094015.

- [334] M. A. Bedolla, J. Ferretti, C. D. Roberts and E. Santopinto, *Spectrum of fully-heavy tetraquarks from a diquark+antidiquark perspective*, Eur. Phys. J. **C80** (2020) 1004.
- [335] J. Ferretti and E. Santopinto, *Hidden-charm and bottom tetra- and pentaquarks with strangeness in the hadro-quarkonium and compact tetraquark models*, JHEP **04** (2020) 119.
- [336] Q. F. Lu, D. Y. Chen and Y. B. Dong, *Masses of doubly heavy tetraquarks $T_{QQ'}$ in a relativized quark model*, Phys. Rev. **D102** (2020) 034012.
- [337] Q. F. Lu, D. Y. Chen and Y. B. Dong, *Masses of fully heavy tetraquarks $QQ\bar{Q}\bar{Q}$ in an extended relativized quark model*, Eur. Phys. J. **C80** (2020) 871.
- [338] G. L. Yu, Z. Y. Li, Z. G. Wang, J. Lu and M. Yan, *The S- and P-wave fully charmed tetraquark states and their radial excitations*, Eur. Phys. J. **C83** (2023) 416.
- [339] W. C. Dong and Z. G. Wang, *Going in quest of potential tetraquark interpretations for the newly observed states in light of the diquark-antidiquark scenarios*, Phys. Rev. **D107** (2023) 074010.
- [340] G. L. Yu, Z. Y. Li, Z. G. Wang, B. Wu and Z. Zhou, *The ground states of hidden-charm tetraquarks and their radial excitations*, Eur. Phys. J. **C84** (2024) 1130.
- [341] W. C. Dong and Z. G. Wang, *Hunting for the prospective T_{cc} family based on the diquark-antidiquark configuration*, Nucl. Phys. **B1012** (2025) 116828.
- [342] D. Ebert, R. N. Faustov, V. O. Galkin and W. Lucha, *Masses of tetraquarks with two heavy quarks in the relativistic quark model*, Phys. Rev. **D76** (2007) 114015.
- [343] D. Ebert, R. N. Faustov and V. O. Galkin, *Excited heavy tetraquarks with hidden charm*, Eur. Phys. J. **C58** (2008) 399.
- [344] R. N. Faustov, V. O. Galkin, E. M. Savchenko, *Masses of the $QQ\bar{Q}\bar{Q}$ tetraquarks in the relativistic diquark-antidiquark picture*, Phys. Rev. **D102** (2020) 114030.
- [345] J. Vijande, F. Fernandez, A. Valcarce and B. Silvestre-Brac, *Tetraquarks in a chiral constituent quark model*, Eur. Phys. J. **A19** (2004) 383.
- [346] N. Barnea, J. Vijande and A. Valcarce, *Four-quark spectroscopy within the hyperspherical formalism*, Phys. Rev. **D73** (2006) 054004.
- [347] J. Vijande, E. Weissma, N. Barnea and A. Valcarce, *Do $c\bar{c}n\bar{n}$ bound states exist?*, Phys. Rev. **D76** (2007) 094022.
- [348] Y. R. Liu and Z. Y. Zhang, *$X(3872)$ and the bound state problem of $D^0\bar{D}^{*0}$ (\bar{D}^0D^{*0}) in a chiral quark model*, Phys. Rev. **C79** (2009) 035206.
- [349] G. J. Wang, L. Meng and S. L. Zhu, *Spectrum of the fully-heavy tetraquark state $QQ\bar{Q}'\bar{Q}'$* , Phys. Rev. **D100** (2019) 096013.
- [350] G. Yang, J. L. Ping and J. Segovia, *Tetra- and penta-quark structures in the constituent quark model*, Symmetry **12** (2020) 1869.
- [351] S. Noh, W. Park and S. H. Lee, *The Doubly-heavy Tetraquarks ($qq'\bar{Q}\bar{Q}'$) in a Constituent Quark Model with a Complete Set of Harmonic Oscillator Bases*, Phys. Rev. **D103** (2021) 114009.
- [352] Z. Zhao, K. Xu, A. Kaewsnod, X. Liu, A. Limphirat and Y. Yan, *Study of charmoniumlike and fully-charm tetraquark spectroscopy*, Phys. Rev. **D103** (2021) 116027.

- [353] C. R. Deng, J. L. Ping, H. X. Huang and F. Wang, *Hidden charmed states and multibody color flux-tube dynamics*, Phys. Rev. **D98** (2018) 014026.
- [354] C. R. Deng, H. Chen and J. L. Ping, *Systematical investigation on the stability of doubly heavy tetraquark states*, Eur. Phys. J. **A56** (2020) 9.
- [355] C. Michael, *Adjoint Sources in Lattice Gauge Theory*, Nucl. Phys. **B259** (1985) 58.
- [356] B. Blossier, M. D. Morte, G. v. Hippel, T. Mendes and R. Sommer, *On the generalized eigenvalue method for energies and matrix elements in lattice field theory*, JHEP **04** (2009) 094.
- [357] S. Prelovsek, C. B. Lang, L. Leskovec and D. Mohler, *Study of the Z_c^+ channel using lattice QCD*, Phys. Rev. **D91** (2015) 014504.
- [358] M. Padmanath, C. B. Lang and S. Prelovsek, *$X(3872)$ and $Y(4140)$ using diquark-antidiquark operators with lattice QCD*, Phys. Rev. **D92** (2015) 034501.
- [359] A. Francis, R. J. Hudspith, R. Lewis and K. Maltman, *Lattice Prediction for Deeply Bound Doubly Heavy Tetraquarks*, Phys. Rev. Lett. **118** (2017) 142001.
- [360] G. K. C. Cheung, C. E. Thomas, J. J. Dudek and R. G. Edwards, *Tetraquark operators in lattice QCD and exotic flavour states in the charm sector*, JHEP **11** (2017) 033.
- [361] P. Junnarkar, N. Mathur and M. Padmanath, *Study of doubly heavy tetraquarks in Lattice QCD*, Phys. Rev. **D99** (2019) 034507.
- [362] L. Leskovec, S. Meinel, M. Pflaumer and M. Wagner, *Lattice QCD investigation of a doubly-bottom $\bar{b}b u d$ tetraquark with quantum numbers $I(J^P) = 0(1^+)$* , Phys. Rev. **D100** (2019) 014503.
- [363] A. Francis, R. J. Hudspith, R. Lewis and K. Maltman, *Evidence for charm-bottom tetraquarks and the mass dependence of heavy-light tetraquark states from lattice QCD*, Phys. Rev. **D99** (2019) 054505.
- [364] A. Francis, *Lattice perspectives on doubly heavy tetraquarks*, Prog. Part. Nucl. Phys. **140** (2025) 104143.
- [365] P. Bicudo, *Tetraquarks and pentaquarks in lattice QCD with light and heavy quarks*, Phys. Rept. **1039** (2023) 1.
- [366] M. Luscher, *Two particle states on a torus and their relation to the scattering matrix*, Nucl. Phys. **B354** (1991) 531.
- [367] M. Luscher, *Signatures of unstable particles in finite volume*, Nucl. Phys. **B364** (1991) 237.
- [368] R. A. Briceno, J. J. Dudek and R. D. Young, *Scattering processes and resonances from lattice QCD*, Rev. Mod. Phys. **90** (2018) 025001.
- [369] S. Prelovsek and L. Leskovec, *Evidence for $X(3872)$ from DD^* scattering on the lattice*, Phys. Rev. Lett. **111** (2013) 192001.
- [370] Y. Chen et al, *Low-energy Scattering of $(D\bar{D}^*)^\pm$ System And the Resonance-like Structure $Z_c(3900)$* , Phys. Rev. **D89** (2014) 094506.
- [371] M. Padmanath and S. Prelovsek, *Signature of a Doubly Charm Tetraquark Pole in DD^* Scattering on the Lattice*, Phys. Rev. Lett. **129** (2022) 032002.

- [372] S. Chen, C. Shi, Y. Chen, M. Gong, Z. Liu, W. Sun and R. Zhang, $T_{cc}^+(3875)$ relevant DD^* scattering from $N_f = 2$ lattice QCD, Phys. Lett. **B833** (2022) 137391.
- [373] M. L. Du, A. Filin, V. Baru, X. K. Dong, E. Epelbaum, F. K. Guo, C. Hanhart, A. Nefediev, J. Nieves and Q. Wang, Role of left-hand cut contributions on pole extractions from lattice data: Case study for $T_{cc}(3875)^+$, Phys. Rev. Lett. **131** (2023) 131903.
- [374] S. Aoki, T. Doi, T. Hatsuda, Y. Ikeda, T. Inoue, N. Ishii, K. Murano, H. Nemura and K. Sasaki, Lattice QCD approach to Nuclear Physics, PTEP **2012** (2012) 01A105.
- [375] Y. Lyu, S. Aoki, T. Doi, T. Hatsuda, Y. Ikeda and J. Meng, Doubly Charmed Tetraquark T_{cc}^+ from Lattice QCD near Physical Point, Phys. Rev. Lett. **131** (2023) 161901.
- [376] M. A. Shifman, A. I. Vainshtein and V. I. Zakharov, QCD and Resonance Physics. Theoretical Foundations, Nucl. Phys. **B147** (1979) 385.
- [377] M. A. Shifman, A. I. Vainshtein and V. I. Zakharov, QCD and Resonance Physics: Applications, Nucl. Phys. **B147** (1979) 448.
- [378] B. L. Ioffe, Calculation of Baryon Masses in Quantum Chromodynamics, Nucl. Phys. **B188** (1981) 317.
- [379] V. L. Chernyak and I. R. Zhitnitsky, Nucleon Wave Function and Nucleon Form-Factors in QCD, Nucl. Phys. **B246** (1984) 52.
- [380] V. L. Chernyak and A. R. Zhitnitsky, Asymptotic Behavior of Exclusive Processes in QCD, Phys. Rept. **112** (1984) 173.
- [381] L. J. Reinders, H. Rubinstein and S. Yazaki, Hadron Properties from QCD Sum Rules, Phys. Rept. **127** (1985) 1.
- [382] I. I. Balitsky, V. M. Braun and A. V. Kolesnichenko, Radiative Decay $\Sigma^+ \rightarrow p\gamma$ in Quantum Chromodynamics, Nucl. Phys. **B312** (1989) 509.
- [383] V. M. Braun and I. E. Filyanov, QCD Sum Rules in Exclusive Kinematics and Pion Wave Function, Z. Phys. **C44** (1989) 157.
- [384] M. A. Shifman, Vacuum structure and QCD sum rules, North-Holland, 1992.
- [385] P. Colangelo and A. Khodjamirian, QCD sum rules, a modern perspective, arXiv: hep-ph/0010175.
- [386] S. Narison, QCD as a Theory of Hadrons: From Partons to Confinement, Camb. Monogr. Part. Phys. Nucl. Phys. Cosmol. **17** (2007) 1.
- [387] P. Gubler and D. Satow, Recent Progress in QCD Condensate Evaluations and Sum Rules, Prog. Part. Nucl. Phys. **106** (2019) 1.
- [388] D. B. Leinweber, QCD sum rules for skeptics, Annals Phys. **254** (1997) 328.
- [389] I. I. Balitsky, D. Diakonov and A. V. Yung, Exotic mesons with $J^{PC} = 1^{-+}$ from QCD sum rules, Phys. Lett. **B112** (1982) 71.
- [390] J. Govaerts, F. de Viron, D. Gusbin and J. Weyers, Exotic mesons from QCD sum rules, Phys. Lett. **B128** (1983) 262.
- [391] J. Govaerts, F. de Viron, D. Gusbin and J. Weyers, QCD Sum Rules and Hybrid Mesons, Nucl. Phys. **B248** (1984) 1.

- [392] J. I. Latorre, S. Narison, P. Pascual and R. Tarrach, *Hermaphrodite Mesons and QCD Sum Rules*, Phys. Lett. **B147** (1984) 169.
- [393] J. Govaerts, L. J. Reinders and J. Weyers, *Radial Excitations and Exotic Mesons via QCD Sum Rules*, Nucl. Phys. **B262** (1985) 575.
- [394] S. A. Larin, V. A. Matveev, A. A. Ovchinnikov and A. A. Pivovarov, *Determination of the mass of the $\Lambda\Lambda$ dibaryon by the method of QCD sum rules*, Sov. J. Nucl. Phys. **44** (1986) 690.
- [395] I. I. Balitsky, D. Diakonov and A. V. Yung, *Exotic mesons with $J^{PC} = 1^{-+}$ strange and non-strange*, Z. Phys. **C33** (1986) 265.
- [396] V. M. Braun and A. V. Kolesnichenko, *Exotic Scalar $J^{PC} = 0^{+-}$ Meson From QCD Sum Rules*, Phys. Lett. **B175** (1986) 485.
- [397] J. I. Latorre, P. Pascual and S. Narison, *Spectra and Hadronic Couplings of Light Hermaphrodite Mesons*, Z. Phys. **C34** (1987) 347.
- [398] J. Govaerts, L. J. Reinders, P. Francken, X. Gonze and J. Weyers, *Coupled QCD Sum Rules for Hybrid Mesons*, Nucl. Phys. **B284** (1987) 674.
- [399] V. M. Braun and Y. M. Shabelski, *Four quark exotic mesons $\bar{u}usd$ from QCD sum rules*, Sov. J. Nucl. Phys. **50** (1989) 306.
- [400] L. S. Kisslinger and Z. P. Li, *Hybrid baryons via QCD sum rules*, Phys. Rev. **D51** (1995) R5986.
- [401] Z. G. Wang, *Two-particle contributions and nonlocal effects in the QCD sum rules for the axial vector tetraquark candidate $Z_c(3900)$* , Int. J. Mod. Phys. **A35** (2020) 2050138.
- [402] Z. G. Wang, *Analysis of the $P_c(4312)$, $P_c(4440)$, $P_c(4457)$ and related hidden-charm pentaquark states with QCD sum rules*, Int. J. Mod. Phys. **A35** (2020) 2050003.
- [403] Y. Kondo, O. Morimatsu and T. Nishikawa, *Two-hadron-irreducible QCD sum rule for pentaquark baryon*, Phys. Lett. **B611** (2005) 93.
- [404] S. H. Lee, H. Kim and Y. Kwon, *Parity of $\Theta^+(1540)$ from QCD sum rules*, Phys. Lett. **B609** (2005) 252.
- [405] H. J. Lee and N. I. Kochelev, *On the $\pi\pi$ contribution to the QCD sum rules for the light tetraquark*, Phys. Rev. **D78** (2008) 076005.
- [406] H. X. Chen, A. Hosaka, H. Toki and S. L. Zhu, *Light Scalar Meson $\sigma(600)$ in QCD Sum Rule with Continuum*, Phys. Rev. **D81** (2010) 114034.
- [407] W. Lucha, D. Melikhov and H. Sazdjian, *Tetraquark-adequate formulation of QCD sum rules*, Phys. Rev. **D100** (2019) 014010.
- [408] W. Lucha, D. Melikhov and H. Sazdjian, *Tetraquark-adequate QCD sum rules for quark-exchange processes*, Phys. Rev. **D100** (2019) 074029.
- [409] Z. G. Wang, *Landau equation and QCD sum rules for the tetraquark molecular states*, Phys. Rev. **D101** (2020) 074011.
- [410] L. D. Landau, *On analytic properties of vertex parts in quantum field theory*, Nucl. Phys. **13** (1959) 181.
- [411] M. Tanabashi et al, *The Review of Particle Physics*, Phys. Rev. **D98** (2018) 030001.

- [412] N. Gray, D. J. Broadhurst, W. Grafe and K. Schilcher, *Three Loop Relation of Quark (Modified) \overline{MS} and Pole Masses*, Z. Phys. **C48** (1990) 673.
- [413] Z. G. Wang, *Triply-charmed dibaryon states or two-baryon scattering states from the QCD sum rules?*, Phys. Rev. **D102** (2020) 034008.
- [414] K. U. Can, G. Erkol, B. Isildak, M. Oka and T. Takahashi, *Electromagnetic structure of charmed baryons in Lattice QCD*, PoS LATTICE2014 (2015) 157.
- [415] J. Y. Kim and H. C. Kim, *Electromagnetic form factors of singly heavy baryons in the self-consistent $SU(3)$ chiral quark-soliton model*, Phys. Rev. **D97** (2018) 114009.
- [416] C. W. Hwang, *Charge radii of light and heavy mesons*, Eur. Phys. J. **C23** (2002) 585.
- [417] Z. G. Wang, *Comment on "OPE and quark-hadron duality for two-point functions of tetraquark currents in $1/N_c$ expansion"*, arXiv:2102.07520 [hep-ph].
- [418] Z. G. Wang and Q. Xin, *Analysis of the hidden-charm pentaquark molecular states with and without strangeness via the QCD sum rules*, Chin. Phys. **C45** (2021) 123105.
- [419] Z. G. Wang, *Analysis of the masses and decay constants of the heavy-light mesons with QCD sum rules*, Eur. Phys. J. **C75** (2015) 427.
- [420] K. G. Chetyrkin and M. Steinhauser, *Three loop nondiagonal current correlators in QCD and NLO corrections to single top quark production*, Phys. Lett. **B502** (2001) 104.
- [421] K. G. Chetyrkin and M. Steinhauser, *Heavy-light current correlators at order α_s^2 in QCD and HQET*, Eur. Phys. J. **C21** (2001) 319.
- [422] Z. G. Wang, *Reanalysis of the $Y(3940)$, $Y(4140)$, $Z_c(4020)$, $Z_c(4025)$ and $Z_b(10650)$ as molecular states with QCD sum rules*, Eur. Phys. J. **C74** (2014) 2963.
- [423] Z. G. Wang, *Analysis of $P_c(4380)$ and $P_c(4450)$ as pentaquark states in the diquark model with QCD sum rules*, Eur. Phys. J. **C76** (2016) 70.
- [424] Z. G. Wang, *Analysis of the $Z_c(4020)$, $Z_c(4025)$, $Y(4360)$ and $Y(4660)$ as vector tetraquark states with QCD sum rules*, Eur. Phys. J. **C74** (2014) 2874.
- [425] Z. G. Wang, *Analysis of the hidden-charm-hidden-strange tetraquark mass spectrum via the QCD sum rules*, Nucl. Phys. **1007** (2024) 116661.
- [426] Z. G. Wang, *Analysis of the tetraquark and hexaquark molecular states with the QCD sum rules*, Commun. Theor. Phys. **73** (2021) 065201.
- [427] S. H. Lee, K. Morita and M. Nielsen, *Width of exotics from QCD sum rules: Tetraquarks or molecules?*, Phys. Rev. **D78** (2008) 076001.
- [428] S. H. Lee, M. Nielsen and U. Wiedner, *$D_s D^*$ molecule as an axial meson*, J. Korean Phys. Soc. **55** (2009) 424.
- [429] M. E. Bracco, S. H. Lee, M. Nielsen, R. Rodrigues da Silva, *The Meson $Z^+(4430)$ as a tetraquark state*, Phys. Lett. **B671** (2009) 240.
- [430] S. H. Lee, K. Morita and M. Nielsen, *Can the $\pi^+ \chi_{c1}$ resonance structures be $D^* \bar{D}^*$ and $D_1 \bar{D}$ molecules?*, Nucl. Phys. **A815** (2009) 29.
- [431] R. M. Albuquerque and M. Nielsen, *QCD sum rules study of the $J^{PC} = 1^{--}$ charmonium Y mesons*, Nucl. Phys. **A815** (2009) 53; Erratum-ibid. **A857** (2011) 48.

- [432] R. M. Albuquerque, M. E. Bracco and M. Nielsen, *A QCD sum rule calculation for the $Y(4140)$ narrow structure*, Phys. Lett. **B678** (2009) 186.
- [433] R. D. Matheus, F. S. Navarra, M. Nielsen and C. M. Zanetti, *QCD Sum Rules for the $X(3872)$ as a mixed molecule-charmonium state*, Phys. Rev. **D80** (2009) 056002.
- [434] J. R. Zhang and M. Q. Huang, $\{Q\bar{q}\}\{\bar{Q}^{(\prime)}q\}$ *molecular states*, Phys. Rev. **D80** (2009) 056004.
- [435] J. R. Zhang and M. Q. Huang, $(Q\bar{s})^{(*)}(\bar{Q}s)^{(*)}$ *molecular states from QCD sum rules: a view on $Y(4140)$* , J. Phys. **G37** (2010) 025005.
- [436] J. R. Zhang and M. Q. Huang, $\{Q\bar{s}\}\{\bar{Q}^{(\prime)}s\}$ *molecular states in QCD sum rules*, Commun. Theor. Phys. **54** (2010) 1075.
- [437] W. Chen and S. L. Zhu, *Possible $J^{PC} = 0^{-+}$ Charmonium-like State*, Phys. Rev. **D81** (2010) 105018.
- [438] M. Nielsen and C. M. Zanetti, *Radiative decay of the $X(3872)$ as a mixed molecule-charmonium state in QCD Sum Rules*, Phys. Rev. **D82** (2010) 116002.
- [439] S. Narison, F. S. Navarra and M. Nielsen, *On the nature of the $X(3872)$ from QCD*, Phys. Rev. **D83** (2011) 016004.
- [440] R. M. Albuquerque, M. Nielsen, R. Rodrigues da Silva, *Exotic 1^{--} States in QCD Sum Rules*, Phys. Rev. **D84** (2011) 116004.
- [441] J. M. Dias, S. Narison, F. S. Navarra, M. Nielsen and J. M. Richard, *Relation between $T_{cc,bb}$ and $X_{c,b}$ from QCD*, Phys. Lett. **B703** (2011) 274.
- [442] S. I. Finazzo, X. Liu and M. Nielsen, *QCD sum rule calculation for the charmonium-like structures in the $J/\psi\phi$ and $J/\psi\omega$ invariant mass spectra*, Phys. Lett. **B701** (2011) 101.
- [443] J. R. Zhang, M. Zhong and M. Q. Huang, *Could $Z_b(10610)$ be a $B^*\bar{B}$ molecular state?*, Phys. Lett. **B704** (2011) 312.
- [444] W. Chen and S. L. Zhu, *The Vector and Axial-Vector Charmonium-like States*, Phys. Rev. **D83** (2011) 034010.
- [445] C. Y. Cui, Y. L. Liu and M. Q. Huang, *Investigating different structures of the $Z_b(10610)$ and $Z_b(10650)$* , Phys. Rev. **D85** (2012) 074014.
- [446] J. M. Dias, F. S. Navarra, M. Nielsen and C. M. Zanetti, *$Z_c^+(3900)$ decay width in QCD sum rules*, Phys. Rev. **D88** (2013) 016004.
- [447] W. Chen, H. Y. Jin, R. T. Kleiv, T. G. Steele, M. Wang and Q. Xu, *QCD Sum-Rule Interpretation of $X(3872)$ with $J^{PC} = 1^{++}$ Mixtures of Hybrid Charmonium and $\bar{D}D^*$ Molecular Currents*, Phys. Rev. **D88** (2013) 045027.
- [448] J. R. Zhang, *Improved QCD sum rule study of $Z_c(3900)$ as a $\bar{D}D^*$ molecular state*, Phys. Rev. **D87** (2013) 116004.
- [449] C. F. Qiao and L. Tang, *Estimating the mass of the hidden charm $1^+(1^+)$ tetraquark state via QCD sum rules*, Eur. Phys. J. **C74** (2014) 3122.
- [450] C. F. Qiao and L. Tang, *Interpretation of $Z_c(4025)$ as the hidden charm tetraquark states via QCD Sum Rules*, Eur. Phys. J. **C74** (2014) 2810.
- [451] W. Chen, T. G. Steele, H. X. Chen and S. L. Zhu, *Mass spectra of Z_c and Z_b exotic states as hadron molecules*, Phys. Rev. **D92** (2015) 054002.

- [452] R. Albuquerque, S. Narison, F. Fanomezana, A. Rabemananjara, D. Rabetiarivony and G. Randriamanatrika, *XYZ-like Spectra from Laplace Sum Rule at N²LO in the Chiral Limit*, Int. J. Mod. Phys. **A31** (2016) 1650196.
- [453] L. Tang and C. F. Qiao, *Tetraquark States with Open Flavors*, Eur. Phys. J. **C76** (2016) 558.
- [454] R. Albuquerque, S. Narison, D. Rabetiarivony and G. Randriamanatrika, *XYZ-SU3 Breakings from Laplace Sum Rules at Higher Orders*, Int. J. Mod. Phys. **A33** (2018) 1850082.
- [455] L. Tang, B. D. Wan, K. Maltman and C. F. Qiao, *Doubly Heavy Tetraquarks in QCD Sum Rules*, Phys. Rev. **D101** (2020) 094032.
- [456] R. M. Albuquerque, S. Narison, A. Rabemananjara, D. Rabetiarivony and G. Randriamanatrika, *Doubly-hidden scalar heavy molecules and tetraquarks states from QCD at NLO*, Phys. Rev. **D102** (2020) 094001.
- [457] B. D. Wan and C. F. Qiao, *About the exotic structure of Z_{cs}* , Nucl. Phys. **B968** (2021) 115450.
- [458] W. Chen, T. G. Steele and S. L. Zhu, *Exotic open-flavor $bc\bar{q}\bar{q}$, $bc\bar{s}\bar{s}$ and $qc\bar{q}\bar{b}$, $sc\bar{s}\bar{b}$ tetraquark states*, Phys. Rev. **D89** (2014) 054037.
- [459] B. C. Yang, L. Tang and C. F. Qiao, *Scalar Fully-heavy Tetraquark States $QQ'\bar{Q}\bar{Q}'$ in QCD Sum Rules*, Eur. Phys. J. **C81** (2021) 324.
- [460] J. R. Zhang, 0^+ *fully-charmed tetraquark states*, Phys. Rev. **D103** (2021) 014018.
- [461] R. M. Albuquerque, S. Narison and D. Rabetiarivony, *Z_c -like spectra from QCD Laplace sum rules at NLO*, Phys. Rev. **D103** (2021) 074015.
- [462] S. S. Agaev, K. Azizi and H. Sundu, *Strong $Z_c^+(3900) \rightarrow J/\psi\pi^+$; $\eta_c\rho^+$ decays in QCD*, Phys. Rev. **D93** (2016) 074002.
- [463] U. Ozdem and K. Azizi, *Magnetic and quadrupole moments of the $Z_c(3900)$* , Phys. Rev. **D96** (2017) 074030.
- [464] S. S. Agaev, K. Azizi and H. Sundu, *Treating $Z_c(3900)$ and $Z(4430)$ as the ground-state and first radially excited tetraquarks*, Phys. Rev. **D96** (2017) 034026.
- [465] H. Sundu, S. S. Agaev and K. Azizi, *New charged resonance $Z_c(4100)$: the spectroscopic parameters and width*, Eur. Phys. J. **C79** (2019) 215.
- [466] S. S. Agaev, K. Azizi, B. Barsbay and H. Sundu, *The doubly charmed pseudoscalar tetraquarks $T_{cc;\bar{s}\bar{s}}^{+++}$ and $T_{cc;\bar{d}\bar{s}}^{+++}$* , Nucl. Phys. **B939** (2019) 130.
- [467] S. Agaev, K. Azizi and H. Sundu, *Four-quark exotic mesons*, Turk. J. Phys. **44** (2020) 95.
- [468] U. Ozdem and K. Azizi, *Magnetic dipole moment of the $Z_{cs}(3985)$ state: diquark-antidiquark and molecular pictures*, Eur. Phys. J. Plus **136** (2021) 968.
- [469] U. Ozdem and A. K. Yildirim, *Magnetic dipole moments of the $Z_c(4020)^+$, $Z_c(4200)^+$, $Z_{cs}(4000)^+$ and $Z_{cs}(4220)^+$ states in light-cone QCD*, Phys. Rev. **D104** (2021) 054017.
- [470] K. Azizi and N. Er, *The newly observed $Z_{cs}(3985)^-$ state: in vacuum and a dense medium*, Eur. Phys. J. **C81** (2021) 61.
- [471] S. S. Agaev, K. Azizi and H. Sundu, *Hadronic molecule model for the doubly charmed state T_{cc}^+* , JHEP **06** (2022) 057.

- [472] S. S. Agaev, K. Azizi and H. Sundu, *Newly observed exotic doubly charmed meson T_{cc}^+* , Nucl. Phys. **B975** (2022) 115650.
- [473] H. Mutuk, *Molecular Interpretation of $X(3960)$ as $D_s^+ D_s^-$ State*, Eur. Phys. J. **C82** (2022) 1142.
- [474] H. Mutuk, *Monte-Carlo based QCD sum rules analysis of $X_0(2900)$ and $X_1(2900)$* , J. Phys. **G48** (2021) 055007.
- [475] Z. G. Wang, *Mass spectrum of the vector hidden charmed and bottomed tetraquark states*, J. Phys. **G36** (2009) 085002.
- [476] Z. G. Wang, *Mass spectrum of the scalar hidden charmed and bottomed tetraquark states*, Phys. Rev. **D79** (2009) 094027.
- [477] Z. G. Wang, *Analysis of the $Y(4140)$ with QCD sum rules*, Eur. Phys. J. **C63** (2009) 115.
- [478] Z. G. Wang, Z. C. Liu and X. H. Zhang, *Analysis of the $Y(4140)$ and related molecular states with QCD sum rules*, Eur. Phys. J. **C64** (2009) 373.
- [479] Z. G. Wang, *Possible tetraquark state in the $\pi^+ \chi_{c1}$ invariant mass distribution*, Eur. Phys. J. **C59** (2009) 675.
- [480] Z. G. Wang, *Another tetraquark structure in the $\pi^+ \chi_{c1}$ invariant mass distribution*, Eur. Phys. J. **C62** (2009) 375.
- [481] Z. G. Wang, *Reanalysis of the mass spectrum of the scalar hidden charm and hidden bottom tetraquark states*, Eur. Phys. J. **C67** (2010) 411.
- [482] Z. G. Wang and X. H. Zhang, *Analysis of the pseudoscalar partner of the $Y(4660)$ and related bound states*, Eur. Phys. J. **C66** (2010) 419.
- [483] Z. G. Wang, *Mass spectrum of the axial-vector hidden charmed and hidden bottom tetraquark states*, Eur. Phys. J. **C70** (2010) 139.
- [484] Z. G. Wang, *Analysis of the $X(4350)$ as a scalar $\bar{c}c$ and $D_s^* \bar{D}_s^*$ mixing state with QCD sum rules*, Phys. Lett. **B690** (2010) 403.
- [485] Z. G. Wang and X. H. Zhang, *Analysis of $Y(4660)$ and related bound states with QCD sum rules*, Commun. Theor. Phys. **54** (2010) 323.
- [486] Z. G. Wang, *Analysis of the $Y(4274)$ with QCD sum rules*, Int. J. Mod. Phys. **A26** (2011) 4929.
- [487] Z. G. Wang, *Analysis of the $\bar{D}\Sigma_c$, $\bar{D}\Sigma_c^*$, $\bar{D}^*\Sigma_c$ and $\bar{D}^*\Sigma_c^*$ pentaquark molecular states with QCD sum rules*, Int. J. Mod. Phys. **A34** (2019) 1950097.
- [488] H. X. Chen, A. Hosaka and S. L. Zhu, *Light Scalar Tetraquark Mesons in the QCD Sum Rule*, Phys. Rev. **D76** (2007) 094025.
- [489] H. X. Chen, A. Hosaka and S. L. Zhu, *The $I^G J^{PC} = 1^- 1^{++}$ Tetraquark States*, Phys. Rev. **D78** (2008) 054017.
- [490] C. K. Jiao, W. Chen, H. X. Chen and S. L. Zhu, *The Possible $J^{PC} = 0^{--}$ Exotic State*, Phys. Rev. **D79** (2009) 114034.
- [491] Z. R. Huang, W. Chen, T. G. Steele, Z. F. Zhang and H. Y. Jin, *Investigation of the light four-quark states with exotic $J^{PC} = 0^{--}$* , Phys. Rev. **D95** (2017) 076017.

- [492] W. Chen, H. X. Chen, X. Liu, T. G. Steele and S. L. Zhu, *Mass spectra for $qc\bar{q}\bar{c}$, $sc\bar{s}\bar{c}$, $qb\bar{q}\bar{b}$, $sb\bar{s}\bar{b}$ tetraquark states with $J^{PC} = 0^{++}$ and 2^{++}* , Phys. Rev. **D96** (2017) 114017.
- [493] W. Chen, H. X. Chen, X. Liu, T. G. Steele and S. L. Zhu, *Hunting for exotic doubly hidden-charm/bottom tetraquark states*, Phys. Lett. **B773** (2017) 247.
- [494] Z. G. Wang, *Analysis of the $Y(2175)$ as a tetraquark state with QCD sum rules*, Nucl. Phys. **A791** (2007) 106.
- [495] Z. G. Wang, *Analysis of the mass and width of the $Y(4274)$ as axialvector molecule-like state*, Eur. Phys. J. **C77** (2017) 174.
- [496] Z. G. Wang, *Analysis of the $Z_c(4200)$ as axial-vector molecule-like state*, Int. J. Mod. Phys. **A30** (2015) 1550168.
- [497] C. M. Tang, C. G. Duan and L. Tang, *Fully Charmed Tetraquark States in $8_{[c\bar{c}]} \otimes 8_{[c\bar{c}]}$ Color Structure via QCD Sum Rules*, Eur. Phys. J. **C84** (2024) 743.
- [498] Z. G. Wang, *Analysis of the scalar and axial-vector heavy diquark states with QCD sum rules*, Eur. Phys. J. **C71** (2011) 1524.
- [499] L. Tang and X. Q. Li, *Discussions on Stability of Diquarks*, Chin. Phys. **C36** (2012) 578.
- [500] R. T. Kleiv, T. G. Steele, A. L. Zhang and I. Blokland, *Heavy-light diquark masses from QCD sum rules and constituent diquark models of tetraquarks*, Phys. Rev. **D87** (2013) 125018.
- [501] Z. G. Wang, *Analysis of the light-flavor scalar and axial-vector diquark states with QCD sum rules*, Commun. Theor. Phys. **59** (2013) 451.
- [502] H. G. Dosch, M. Jamin and B. Stech, *Diquarks, QCD Sum Rules and Weak Decays*, Z. Phys. **C42** (1989) 167.
- [503] M. Jamin and M. Neubert, *Diquark Decay Constants From QCD Sum Rules*, Phys. Lett. **B238** (1990) 387.
- [504] A. L. Zhang, T. Huang and T. G. Steele, *Diquark and light four-quark states*, Phys. Rev. **D76** (2007) 036004.
- [505] Z. G. Wang, *Scalar or vector tetraquark state candidate: $Z_c(4100)$* , Commun. Theor. Phys. **71** (2019) 1319.
- [506] Z. G. Wang and Y. F. Tian, *Tetraquark state candidates: $Y(4140)$, $Y(4274)$ and $X(4350)$* , Int. J. Mod. Phys. **A30** (2015) 1550004.
- [507] Z. G. Wang and Z. Y. Di, *Analysis of the mass and width of the $X(4140)$ as axialvector tetraquark state*, Eur. Phys. J. **C79** (2019) 72.
- [508] P. Pascual and R. Tarrach, *QCD : renormalization for the practitioner*, Lect. Notes Phys. **194** (1984) 1.
- [509] X. W. Wang, Z. G. Wang and G. L. Yu, *Study of $\Lambda_c\Lambda_c$ dibaryon and $\Lambda_c\bar{\Lambda}_c$ baryonium states via QCD sum rules*, Eur. Phys. J. **A57** (2021) 275.
- [510] J. Beringer et al, *Review of Particle Physics*, Phys. Rev. **D86** (2012) 010001.
- [511] S. Narison and R. Tarrach, *Higher Dimensional Renormalization Group Invariant Vacuum Condensates in Quantum Chromodynamics*, Phys. Lett. **B125** (1983) 217.

- [512] Z. G. Wang, *Tetraquark state candidates: $Y(4260)$, $Y(4360)$, $Y(4660)$ and $Z_c(4020/4025)$* , Eur. Phys. J. **C76** (2016) 387.
- [513] Q. Xin and Z. G. Wang, *Analysis of the doubly-charmed tetraquark molecular states with the QCD sum rules*, Eur. Phys. J. **A58** (2022) 110.
- [514] Z. G. Wang, *Analysis of the $P_{cs}(4459)$ as the hidden-charm pentaquark state with QCD sum rules*, Int. J. Mod. Phys. **A36** (2021) 2150071.
- [515] Z. G. Wang and Q. Xin, *Analysis of the pseudoscalar hidden-charm tetraquark states with the QCD sum rules*, Nucl. Phys. **B978** (2022) 115761.
- [516] R. Albuquerque, S. Narison, A. Rabemananjara and D. Rabetiarivony, *Nature of the $X(5568)$: a critical Laplace sum rule analysis at N^2LO* , Int. J. Mod. Phys. **A31** (2016) 1650093.
- [517] R. M. Albuquerque, S. Narison and D. Rabetiarivony, *Tests of the Z_c -like Laplace sum rule results using finite energy sum rule at NLO* , Phys. Rev. **D105** (2022) 114035.
- [518] R. H. Wu, C. Y. Wang, C. Meng, Y. Q. Ma and K. T. Chao, *Z_c and Z_{cs} systems with operator mixing at NLO in QCD sum rules*, JHEP **06** (2024) 216.
- [519] R. H. Wu, Y. S. Zuo, C. Y. Wang, C. Meng, Y. Q. Ma and K. T. Chao, *NLO results with operator mixing for fully heavy tetraquarks in QCD sum rules*, JHEP **11** (2022) 023.
- [520] Z. G. Wang and J. X. Zhang, *The decay width of the $Z_c(3900)$ as an axialvector tetraquark state in solid quark-hadron duality*, Eur. Phys. J. **C78** (2018) 14.
- [521] A. Esposito, A. L. Guerrieri and A. Pilloni, *Probing the nature of $Z_c^{(\prime)}$ states via the $\eta_c\rho$ decay*, Phys. Lett. **B746** (2015) 194.
- [522] Z. G. Wang, *Assignments of the $X(4140)$, $X(4500)$, $X(4630)$ and $X(4685)$ Based on the QCD Sum Rules*, Adv. High Energy Phys. **2021** (2021) 4426163.
- [523] Z. G. Wang, *Revisit the $X(4274)$ as the Axialvector Tetraquark State*, Acta Phys. Polon. **B51** (2020) 435.
- [524] F. Stancu, *Can $Y(4140)$ be a $c\bar{c}s\bar{s}$ tetraquark?*, J. Phys. **G37** (2010) 075017.
- [525] R. L. Zhu, *Hidden charm octet tetraquarks from a diquark-antidiquark model*, Phys. Rev. **D94** (2016) 054009.
- [526] J. Wu, Y. R. Liu, K. Chen, X. Liu and S. L. Zhu, *$X(4140)$, $X(4270)$, $X(4500)$ and $X(4700)$ and their $c\bar{c}s\bar{s}$ tetraquark partners*, Phys. Rev. **D94** (2016) 094031.
- [527] H. X. Chen, E. L. Cui, W. Chen, X. Liu and S. L. Zhu, *Understanding the internal structures of the $X(4140)$, $X(4274)$, $X(4500)$ and $X(4700)$* , Eur. Phys. J. **C77** (2017) 160.
- [528] N. Mahajan, *$Y(4140)$: Possible options*, Phys. Lett. **B679** (2009) 228.
- [529] X. H. Liu, *How to understand the underlying structures of $X(4140)$, $X(4274)$, $X(4500)$ and $X(4700)$* , Phys. Lett. **B766** (2017) 117.
- [530] Z. G. Wang, *Analysis of the $X(4475)$, $X(4500)$, $Z_{\bar{c}s}$ (4600) and related tetraquark states with the QCD sum rules*, arXiv: 2409.19348 [hep-ph].
- [531] Z. G. Wang, *Analysis of the hidden-bottom tetraquark mass spectrum with the QCD sum rules*, Eur. Phys. J. **C79** (2019) 489.

- [532] Z. G. Wang and T. Huang, *The $Z_b(10610)$ and $Z_b(10650)$ as axial-vector tetraquark states in the QCD sum rules*, Nucl. Phys. **A930** (2014) 63.
- [533] A. Ali, C. Hambrock and W. Wang, *Tetraquark Interpretation of the Charged Bottomonium-like states $Z_b^\pm(10610)$ and $Z_b^\pm(10650)$ and Implications*, Phys. Rev. **D85** (2012) 054011.
- [534] A. Ali, L. Maiani, A. D. Polosa and V. Riquer, *Hidden-Beauty Charged Tetraquarks and Heavy Quark Spin Conservation*, Phys. Rev. **D91** (2015) 017502.
- [535] Z. G. Wang, *Analysis of the axialvector B_c -like tetraquark states with the QCD sum rules*, EPL **128** (2019) 11001.
- [536] S. S. Agaev, K. Azizi and H. Sundu, *Open charm-bottom scalar tetraquarks and their strong decays*, Phys. Rev. **D95** (2017) 034008.
- [537] U. Ozdem, *Electromagnetic form factors of the B_c -like tetraquarks: Molecular and diquark-antidiquark pictures*, Phys. Lett. **B838** (2023) 137750.
- [538] M. S. Maior de Sousa and R. Rodrigues da Silva, *The $\rho(1S, 2S)$, $\psi(1S, 2S)$, $\Upsilon(1S, 2S)$ and $\psi_t(1S, 2S)$ mesons in a double pole QCD Sum Rule*, Braz. J. Phys. **46** (2016) 730.
- [539] K. Azizi and N. Er, *Modifications on parameters of $Z(4430)$ in a dense medium*, Phys. Lett. **B811** (2020) 135979.
- [540] Z. G. Wang, *Scalar tetraquark state candidates: $X(3915)$, $X(4500)$ and $X(4700)$* , Eur. Phys. J. **C77** (2017) 78.
- [541] Z. G. Wang, *Reanalysis of the $X(3915)$, $X(4500)$ and $X(4700)$ with QCD sum rules*, Eur. Phys. J. **A53** (2017) 19.
- [542] Z. G. Wang and H. J. Wang, *Analysis of the $1S$ and $2S$ states of Λ_Q and Ξ_Q with QCD sum rules*, Chin. Phys. **C45** (2021) 013109.
- [543] Z. G. Wang, *Analysis of the vector hidden-charm tetraquark states without explicit P -waves via the QCD sum rules*, Nucl. Phys. **B973** (2021) 115592.
- [544] Z. G. Wang, *Vector tetraquark state candidates: $Y(4260/4220)$, $Y(4360/4320)$, $Y(4390)$ and $Y(4660/4630)$* , Eur. Phys. J. **C78** (2018) 518.
- [545] Z. G. Wang, *Analysis of the vector hidden-charm-hidden-strange tetraquark states with implicit P -waves via the QCD sum rules*, Nucl. Phys. **B1002** (2024) 116514.
- [546] Z. G. Wang, *Strong decays of the vector tetraquark states with the masses about 4.5 GeV via the QCD sum rules*, Nucl. Phys. **B1005** (2024) 116580.
- [547] Z. G. Wang, *Analysis of the decay $Y(4500) \rightarrow D^* \bar{D}^* \pi$ with the light-cone QCD sum rules*, Nucl. Phys. **B993** (2023) 116265.
- [548] J. R. Zhang and M. Q. Huang, *The P -wave $[cs][\bar{c}\bar{s}]$ tetraquark state: $Y(4260)$ or $Y(4660)?$* , Phys. Rev. **D83** (2011) 036005.
- [549] Z. G. Wang, *Lowest vector tetraquark states: $Y(4260/4220)$ or $Z_c(4100)$* , Eur. Phys. J. **C78** (2018) 933.
- [550] Z. G. Wang, *Analysis of the vector tetraquark states with P -waves between the diquarks and antidiquarks via the QCD sum rules*, Eur. Phys. J. **C79** (2019) 29.
- [551] S. L. Zhu, *The Possible interpretations of $Y(4260)$* , Phys. Lett. **B625** (2005) 212.

- [552] F. E. Close and P. R. Page, *Gluonic charmonium resonances at BaBar and BELLE?*, Phys. Lett. **B628** (2005) 215.
- [553] E. Kou and O. Pene, *Suppressed decay into open charm for the $Y(4260)$ being an hybrid*, Phys. Lett. **B631** (2005) 164.
- [554] L. Liu et al, *Excited and exotic charmonium spectroscopy from lattice QCD*, JHEP **07** (2012) 126.
- [555] X. K. Dong, F. K. Guo and B. S. Zou, *A survey of heavy-antiheavy hadronic molecules*, Progr. Phys. **41** (2021) 65.
- [556] T. W. Chiu and T. H. Hsieh, *$Y(4260)$ on the lattice*, Phys. Rev. **D73** (2006) 094510.
- [557] C. F. Qiao, *One explanation for the exotic state $Y(4260)$* , Phys. Lett. **B639** (2006) 263.
- [558] C. F. Qiao, *A Uniform description of the states recently observed at B-factories*, J. Phys. **G35** (2008) 075008.
- [559] X. Li and M. B. Voloshin, *$Y(4260)$ and $Y(4360)$ as mixed hadrocharmonium*, Mod. Phys. Lett. **A29** (2014) 1450060.
- [560] D. Y. Chen, J. He and X. Liu, *Nonresonant explanation for the $Y(4260)$ structure observed in the $e^+e^- \rightarrow J/\psi\pi^+\pi^-$ process*, Phys. Rev. **D83** (2011) 054021.
- [561] D. Y. Chen, X. Liu, X. Q. Li and H. W. Ke, *Unified Fano-like interference picture for charmoniumlike states $Y(4008)$, $Y(4260)$ and $Y(4360)$* , Phys. Rev. **D93** (2016) 014011.
- [562] Z. G. Wang, *Ground states and first radial excitations of vector tetraquark states with explicit P -waves via QCD sum rules*, Chin. Phys. **C48** (2024) 103103.
- [563] Z. G. Wang, *Vector hidden-bottom tetraquark candidate: $Y(10750)$* , Chin. Phys. **C43** (2019) 123102.
- [564] R. Aaij et al, *Observation of the doubly charmed baryon Ξ_{cc}^{++}* , Phys. Rev. Lett. **119** (2017) 112001.
- [565] Z. G. Wang, *Analysis of the doubly heavy baryon states and pentaquark states with QCD sum rules*, Eur. Phys. J. **C78** (2018) 826.
- [566] M. Karliner and J. L. Rosner, *Discovery of doubly-charmed Ξ_{cc} baryon implies a stable $b\bar{b}u\bar{d}$ tetraquark*, Phys. Rev. Lett. **119** (2017) 202001.
- [567] E. J. Eichten and C. Quigg, *Heavy-quark symmetry implies stable heavy tetraquark mesons $Q_i Q_j \bar{q}_k \bar{q}_l$* , Phys. Rev. Lett. **119** (2017) 202002.
- [568] Q. Qin, Y. F. Shen and F. S. Yu, *Discovery potentials of double-charm tetraquarks*, Chin. Phys. **C45** (2021) 103106.
- [569] J. P. Ader, J. M. Richard and P. Taxil, *Do narrow heavy multiquark states exist?*, Phys. Rev. **D25** (1982) 2370.
- [570] L. Heller and J. A. Tjon, *On the Existence of Stable Dimesons*, Phys. Rev. **D35** (1987) 969.
- [571] J. Carlson, L. Heller and J. A. Tjon, *Stability of Dimesons*, Phys. Rev. **D37** (1988) 744.
- [572] S. Zouzou, B. Silvestre-Brac, C. Gignoux and J. M. Richard, *Four-quark bound states*, Z. Phys. **C30** (1986) 457.

- [573] D. M. Brink and F. Stancu, *Tetraquarks with heavy flavors*, Phys. Rev. **D57** (1998) 6778.
- [574] A. Czarnecki, B. Leng and M. B. Voloshin, *Stability of tetrons*, Phys. Lett. **B778** (2018) 233.
- [575] A. V. Manohar and M. B. Wise, *Exotic $QQ\bar{q}\bar{q}$ states in QCD*, Nucl. Phys. **B399** (1993) 17.
- [576] Z. G. Wang, *Analysis of the axialvector doubly heavy tetraquark states with QCD sum rules*, Acta Phys. Polon. **B49** (2018) 1781.
- [577] M. L. Du, W. Chen, X. L. Chen and S. L. Zhu, *Exotic $QQ\bar{q}\bar{q}$, $QQ\bar{q}\bar{s}$ and $QQ\bar{s}\bar{s}$ states*, Phys. Rev. **D87** (2013) 014003.
- [578] Z. G. Wang and Z. H. Yan, *Analysis of the scalar, axialvector, vector, tensor doubly charmed tetraquark states with QCD sum rules*, Eur. Phys. J. **C78** (2018) 19.
- [579] M. A. Moinester, *How to search for doubly charmed baryons and tetraquarks*, Z. Phys. **A355** (1996) 349.
- [580] S. Pepin, F. Stancu, M. Genovese and J. M. Richard, *Tetraquarks with color blind forces in chiral quark models*, Phys. Lett. **B393** (1997) 119.
- [581] B. A. Gelman and S. Nussinov, *Does a narrow tetraquark $cc\bar{u}\bar{d}$ state exist?*, Phys. Lett. **B551** (2003) 296.
- [582] D. Janc and M. Rosina, *The $T_{cc} = DD^*$ molecular state*, Few Body Syst. **35** (2004) 175.
- [583] F. S. Navarra, M. Nielsen and S. H. Lee, *QCD sum rules study of $QQ\bar{u}\bar{d}$ mesons*, Phys. Lett. **B649** (2007) 166.
- [584] Z. G. Wang, Y. M. Xu and H. J. Wang, *Analysis of the scalar doubly heavy tetraquark states with QCD sum rules*, Commun. Theor. Phys. **55** (2011) 1049.
- [585] J. Vijande, E. Weissman, A. Valcarce and N. Barnea, *Are there compact heavy four-quark bound states?*, Phys. Rev. **D76** (2007) 094027.
- [586] S. H. Lee and S. Yasui, *Stable multiquark states with heavy quarks in a diquark model*, Eur. Phys. J. **C64** (2009) 283.
- [587] Y. Yang, C. Deng, J. Ping and T. Goldman, *S-wave $QQ\bar{q}\bar{q}$ state in the constituent quark model*, Phys. Rev. **D80** (2009) 114023.
- [588] S. Q. Luo, K. Chen, X. Liu, Y. R. Liu and S. L. Zhu, *Exotic tetraquark states with the $qq\bar{Q}\bar{Q}$ configuration*, Eur. Phys. J. **C77** (2017) 709.
- [589] W. Park, S. Noh and S. H. Lee, *Masses of the doubly heavy tetraquarks in a constituent quark model*, Nucl. Phys. **A 983** (2019) 1.
- [590] L. Maiani, A. D. Polosa and V. Riquer, *Hydrogen bond of QCD in doubly heavy baryons and tetraquarks*, Phys. Rev. **D100** (2019) 074002.
- [591] G. Yang, J. Ping and J. Segovia, *Doubly-heavy tetraquarks*, Phys. Rev. **D101** (2020) 014001.
- [592] E. Braaten, L. P. He and A. Mohapatra, *Masses of doubly heavy tetraquarks with error bars*, Phys. Rev. **D103** (2021) 016001.
- [593] D. Gao, D. Jia and Y. J. Sun, *Masses of doubly heavy tetraquarks $QQ\bar{n}\bar{q}$ with $J^P = 1^+$* , Mod. Phys. Lett. **A37** (2022) 2250223.
- [594] J. B. Cheng, S. Y. Li, Y. R. Liu, Z. G. Si and T. Yao, *Double-heavy tetraquark states with heavy diquark-antiquark symmetry*, Chin. Phys. **C45** (2021) 043102.

- [595] R. N. Faustov, V. O. Galkin and E. M. Savchenko, *Heavy tetraquarks in the relativistic quark model*, Universe **7** (2021) 94.
- [596] Y. Ikeda et al, *Charmed Tetraquarks T_{cc} and T_{cs} from Dynamical Lattice QCD Simulations*, Phys. Lett. **B729** (2014) 85.
- [597] X. Z. Weng, W. Z. Deng and S. L. Zhu, *Doubly heavy tetraquarks in an extended chromo-magnetic model*, Chin. Phys. **C46** (2022) 013102.
- [598] K. Azizi and U. Ozdem, *Magnetic dipole moments of the T_{cc}^+ and Z_V^{++} tetraquark states*, Phys. Rev. **D104** (2021) 114002.
- [599] Y. Kim, M. Oka and K. Suzuki, *Doubly heavy tetraquarks in a chiral-diquark picture*, Phys. Rev. **D105** (2022) 074021.
- [600] T. W. Wu and Y. L. Ma, *Doubly heavy tetraquark multiplets as heavy antiquark-diquark symmetry partners of heavy baryons*, Phys. Rev. **D107** (2023) L071501.
- [601] M. Karliner and J. L. Rosner, *Doubly charmed strange tetraquark*, Phys. Rev. **D105** (2022) 034020.
- [602] Y. Iwasaki, *Is a State $c\bar{c}c\bar{c}$ Found at 6.0 GeV?*, Phys. Rev. Lett. **36** (1976) 1266.
- [603] K. T. Chao, *The $cc\text{-}\bar{c}\bar{c}$ (Diquark-Anti-Diquark) States in e^+e^- Annihilation*, Z. Phys. **C7** (1981) 317.
- [604] A. M. Badalyan, B. L. Ioffe and A. V. Smilga, *Four-quark states in heavy quark systems*, Nucl. Phys. **B281** (1987) 85.
- [605] A. V. Berezhnoy, A. V. Luchinsky and A. A. Novoselov, *Tetraquarks Composed of 4 Heavy Quarks*, Phys. Rev. **D86** (2012) 034004.
- [606] M. Karliner, J. L. Rosner and S. Nussinov, *$QQ\bar{Q}\bar{Q}$ states: masses, production, and decays*, Phys. Rev. **D95** (2017) 034011.
- [607] V. R. Debastiani and F. S. Navarra, *A non-relativistic model for the $cc\bar{c}\bar{c}$ tetraquark*, Chin. Phys. **C43** (2019) 013105.
- [608] M. S. Liu, Q. F. Lu, X. H. Zhong and Q. Zhao, *All-heavy tetraquarks*, Phys. Rev. **D100** (2019) 016006.
- [609] R. J. Lloyd and J. P. Vary, *All charm tetraquarks*, Phys. Rev. **D70** (2004) 014009.
- [610] Z. G. Wang, *Analysis of the $QQ\bar{Q}\bar{Q}$ tetraquark states with QCD sum rules*, Eur. Phys. J. **C77** (2017) 432.
- [611] Z. G. Wang and Z. Y. Di, *Analysis of the vector and axialvector $QQ\bar{Q}\bar{Q}$ tetraquark states with QCD sum rules*, Acta Phys. Polon. **B50** (2019) 1335.
- [612] M. N. Anwar, J. Ferretti, F. K. Guo, E. Santopinto and B. S. Zou, *Spectroscopy and decays of the fully-heavy tetraquarks*, Eur. Phys. J. **C78** (2018) 647.
- [613] C. Hughes, E. Eichten and C. T. H. Davies, *Searching for beauty-fully bound tetraquarks using lattice nonrelativistic QCD*, Phys. Rev. **D97** (2018) 054505.
- [614] Z. G. Wang, *Tetraquark candidates in the LHCb's $di\text{-}J/\psi$ mass spectrum*, Chin. Phys. **C44** (2020) 113106.

- [615] Z. G. Wang, *Analysis of the $X(6600)$, $X(6900)$, $X(7300)$ and related tetraquark states with the QCD sum rules*, Nucl. Phys. **B985** (2022) 115983.
- [616] Y. L. Song, Y. Zhang, V. Baru, F. K. Guo, C. Hanhart and A. Nefediev, *Towards a precision determination of the $X(6200)$ parameters from data*, Phys. Rev. **D111** (2025) 034038.
- [617] X. K. Dong, V. Baru, F. K. Guo, C. Hanhart and A. Nefediev, *Coupled-channel interpretation of the LHCb double- J/ψ spectrum and hints of a new state near the $J/\psi J/\psi$ threshold*, Phys. Rev. Lett. **126** (2021) 132001.
- [618] Z. H. Guo and J. A. Oller, *Insights into the inner structures of the fully charmed tetraquark state $X(6900)$* , Phys. Rev. **D103** (2021) 034024.
- [619] Z. R. Liang, X. Y. Wu and D. L. Yao, *Hunting for states in the recent LHCb di- J/ψ invariant mass spectrum*, Phys. Rev. **D104** (2021) 034034.
- [620] Q. F. Cao, H. Chen, H. R. Qi and H. Q. Zheng, *Some remarks on $X(6900)$* , Chin. Phys. **C45** (2021) 103102.
- [621] J. F. Giron and R. F. Lebed, *The Simple Spectrum of $c\bar{c}c\bar{c}$ States in the Dynamical Diquark Model*, Phys. Rev. **D102** (2020) 074003.
- [622] M. Karliner and J. L. Rosner, *Interpretation of structure in the di- J/ψ spectrum*, Phys. Rev. **D102** (2020) 114039.
- [623] C. R. Deng, H. Chen and J. L. Ping, *Towards the understanding of fully-heavy tetraquark states from various models*, Phys. Rev. **D103** (2021) 014001.
- [624] X. Z. Weng, X. L. Chen, W. Z. Deng and S. L. Zhu, *Systematics of fully heavy tetraquarks*, Phys. Rev. **D103** (2021) 034001.
- [625] R. L. Zhu, *Fully-heavy tetraquark spectra and production at hadron colliders*, Nucl. Phys. **B966** (2021) 115393.
- [626] M. C. Gordillo, F. De Soto and J. Segovia, *Diffusion Monte Carlo calculations of fully-heavy multi-quark bound states*, Phys. Rev. **D102** (2020) 114007.
- [627] H. W. Ke, X. Han, X. H. Liu and Y. L. Shi, *Tetraquark state $X(6900)$ and the interaction between diquark and antidiquark*, Eur. Phys. J. **C81** (2021) 427.
- [628] H. Mutuk, *Nonrelativistic treatment of fully-heavy tetraquarks as diquark-antidiquark states*, Eur. Phys. J. **C81** (2021) 367.
- [629] K. T. Chao and S. L. Zhu, *The possible tetraquark states $cc\bar{c}\bar{c}$ observed by the LHCb experiment*, Sci. Bull. **65** (2020) 1952.
- [630] Q. Li, C. H. Chang, G. L. Wang and T. Wang, *Mass spectra and wave functions of $T_{QQ\bar{Q}\bar{Q}}$ tetraquarks*, Phys. Rev. **D104** (2021) 014018.
- [631] F. X. Liu, M. S. Liu, X. H. Zhong and Q. Zhao, *Higher mass spectra of the fully-charmed and fully-bottom tetraquarks*, Phys. Rev. **D104** (2021) 116029.
- [632] B. D. Wan and C. F. Qiao, *Gluonic tetracharm configuration of $X(6900)$* , Phys. Lett. **B817** (2021) 136339.
- [633] Z. G. Wang, *Revisit the tetraquark candidates in the $J/\psi J/\psi$ mass spectrum*, Int. J. Mod. Phys. **A36** (2021) 2150014.

- [634] Z. G. Wang, *Analysis of the fully-heavy pentaquark states via the QCD sum rules*, Nucl. Phys. **B973** (2021) 115579.
- [635] Z. G. Wang, *Fully heavy hexaquark states via the QCD sum rules*, Int. J. Mod. Phys. **A37** (2022) 2250166.
- [636] X. K. Dong, F. K. Guo and B. S. Zou, *A survey of heavy-heavy hadronic molecules*, Commun. Theor. Phys. **73** (2021) 125201.
- [637] X. Liu and S. L. Zhu, *$Y(4143)$ is probably a molecular partner of $Y(3930)$* , Phys. Rev. **D80** (2009) 017502.
- [638] G. J. Ding, *Possible Molecular States of $D_s^* \bar{D}_s^*$ System and $Y(4140)$* , Eur. Phys. J. **C64** (2009) 297.
- [639] Z. G. Wang, *Reanalysis of the $Z_c(4020)$, $Z_c(4025)$, $Z(4050)$ and $Z(4250)$ as tetraquark states with QCD sum rules*, Commun. Theor. Phys. **63** (2015) 466.
- [640] E. J. Eichten and C. Quigg, *Mesons with Beauty and Charm: New Horizons in Spectroscopy*, Phys. Rev. **D99** (2019) 054025.
- [641] Z. G. Wang, *Analysis of the $Y(4220)$ and $Y(4390)$ as molecular states with QCD sum rules*, Chin. Phys. **C41** (2017) 083103.
- [642] P. A. Zyla et al, *Review of Particle Physics*, PTEP **2020** (2020) 083C01.
- [643] S. Prelovsek and L. Leskovec, *Search for $Z_c^+(3900)$ in the 1^{+-} channel on the lattice*, Phys. Lett. **B727** (2013) 172.
- [644] Y. Ikeda et al, *Fate of the Tetraquark Candidate $Z_c(3900)$ from Lattice QCD*, Phys. Rev. Lett. **117** (2016) 242001.
- [645] X. L. Wang et al, *The study of $\gamma\gamma \rightarrow \gamma\psi(2S)$ at Belle*, Phys. Rev. **D105** (2022) 112011.
- [646] C. Patrignani et al, *Review of Particle Physics*, Chin. Phys. **C40** (2016) 100001.
- [647] Y. H. Chen, L. Y. Dai, F. K. Guo and B. Kubis, *Nature of the $Y(4260)$: A light-quark perspective*, Phys. Rev. **D99** (2019) 074016.
- [648] Z. G. Wang, *Comment on "Z_c-like spectra from QCD Laplace sum rules at NLO"*, arXiv:2202.06058 [hep-ph].
- [649] F. K. Guo, C. Hanhart, U. G. Meissner, *Evidence that the $Y(4660)$ is a $f_0(980)\psi'$ bound state*, Phys. Lett. **B665** (2008) 26.
- [650] F. K. Guo, J. Haidenbauer, C. Hanhart and U. G. Meissner, *Reconciling the $X(4630)$ with the $Y(4660)$* , Phys. Rev. **D82** (2010) 094008.
- [651] T. Mehen and J. W. Powell, *Heavy Quark Symmetry Predictions for Weakly Bound B-Meson Molecules*, Phys. Rev. **D84** (2011) 114013.
- [652] Q. Wang, V. Baru, A. A. Filin, C. Hanhart, A. V. Nefediev and J. L. Winyen, *The line shapes of the $Z_b(10610)$ and $Z_b(10650)$ in the elastic and inelastic channels revisited*, Phys. Rev. **D98** (2018) 074023.
- [653] S. Ohkoda, Y. Yamaguchi, S. Yasui, K. Sudoh and A. Hosaka, *Exotic Mesons with Hidden Bottom near Thresholds*, Phys. Rev. **D86** (2012) 014004.

- [654] V. Baru, E. Epelbaum, A. A. Filin, C. Hanhart, A. V. Nefediev and Q. Wang, *Spin partners W_{bJ} from the line shapes of the $Z_b(10610)$ and $Z_b(10650)$* , Phys. Rev. **D99** (2019) 094013.
- [655] M. Karliner and S. Nussinov, *The doubly heavies: $\bar{Q}Q\bar{q}q$ and $QQ\bar{q}\bar{q}$ tetraquarks and QQq baryons*, JHEP **07** (2013) 153.
- [656] X. W. Wang and Z. G. Wang, *Search for the Charmed Baryonium and Dibaryon Structures via the QCD Sum Rules*, Adv. High Energy Phys. **2022** (2022) 6224597.
- [657] B. D. Wan, L. Tang and C. F. Qiao, *Hidden-bottom and -charm hexaquark states in QCD sum rules*, Eur. Phys. J. **C80** (2020) 121.
- [658] Z. G. Wang, *Analysis of the $\bar{\Xi}_{cc}\Xi_{cc}$ hexaquark molecular state with the QCD sum rules*, Phys. Lett. **B819** (2021) 136464.
- [659] Z. Y. Di and Z. G. Wang, *Analysis of the $D\bar{D}^*K$ system with QCD sum rules*, Adv. High Energy Phys. **2019** (2019) 8958079.
- [660] M. L. Du, V. Baru, X. K. Dong, A. Filin, F. K. Guo, C. Hanhart, A. Nefediev, J. Nieves and Q. Wang, *Coupled-channel approach to T_{cc}^+ including three-body effects*, Phys. Rev. **D105** (2022) 014024.
- [661] A. Feijoo, W. H. Liang and E. Oset, *$D^0D^0\pi^+$ mass distribution in the production of the T_{cc} exotic state*, Phys. Rev. **D104** (2021) 114015.
- [662] M. Albaladejo, *T_{cc}^+ coupled channel analysis and predictions*, Phys. Lett. **B829** (2022) 137052.
- [663] X. Z. Ling, M. Z. Liu, L. S. Geng, E. Wang and J. J. Xie, *Can we understand the decay width of the T_{cc}^+ state?*, Phys. Lett. **B826** (2022) 136897.
- [664] L. Meng, G. J. Wang, B. Wang and S. L. Zhu, *Probing the long-range structure of the T_{cc}^+ with the strong and electromagnetic decays*, Phys. Rev. **D104** (2021) 051502.
- [665] C. R. Deng and S. L. Zhu, *T_{cc}^+ and its partners*, Phys. Rev. **D105** (2022) 054015.
- [666] S. Fleming, R. Hodges and T. Mehen, *T_{cc}^+ decays: Differential spectra and two-body final states*, Phys. Rev. **D104** (2021) 116010.
- [667] M. J. Yan and M. P. Valderrama, *Subleading contributions to the decay width of the T_{cc}^+ tetraquark*, Phys. Rev. **D105** (2022) 014007.
- [668] R. Chen, Q. Huang, X. Liu and S. L. Zhu, *Predicting another doubly charmed molecular resonance $T_{cc}'^+(3876)$* , Phys. Rev. **D104** (2021) 114042.
- [669] H. Ren, F. Wu and R. L. Zhu, *Hadronic Molecule Interpretation of T_{cc}^+ and Its Beauty Partners*, Adv. High Energy Phys. **2022** (2022) 9103031.
- [670] Z. G. Wang, *Does vacuum saturation work for the higher-dimensional vacuum condensates in the QCD sum rules?*, Int. J. Mod. Phys. **A36** (2021) 2150246.
- [671] Z. G. Wang, *Triply-charmed hexaquark states with the QCD sum rules*, Int. J. Mod. Phys. **A35** (2020) 2050073.
- [672] N. Kodama, M. Oka and T. Hatsuda, *H dibaryon in the QCD sum rule*, Nucl. Phys. **A580** (1994) 445.
- [673] Z. G. Wang, *$X(1835)$ as a baryonium state with QCD sum rules*, J. Phys. **G34** (2007) 505.

- [674] T. Iritani et al, *$N\Omega$ dibaryon from lattice QCD near the physical point*, Phys. Lett. **B792** (2019) 284.
- [675] S. Gongyo et al, *Most Strange Dibaryon from Lattice QCD*, Phys. Rev. Lett. **120** (2018) 212001.
- [676] P. Junnarkar and N. Mathur, *Deuteronlike Heavy Dibaryons from Lattice Quantum Chromodynamics*, Phys. Rev. Lett. **123** (2019) 162003.
- [677] Y. Lyu et al, *Dibaryon with highest charm number near unitarity from lattice QCD*, Phys. Rev. Lett. **127** (2021) 072003.
- [678] N. Mathur, M. Padmanath and D. Chakraborty, *Strongly Bound Dibaryon with Maximal Beauty Flavor from Lattice QCD*, Phys. Rev. Lett. **130** (2023) 111901.
- [679] P. M. Junnarkar and N. Mathur, *Spectrum of two-flavored spin-zero heavy dibaryons in lattice QCD*, Phys. Rev. **D111** (2025) 014512.
- [680] Y. W. Pan, M. Z. Liu, F. Z. Peng, M. S. Sanchez, L. S. Geng and M. P. Valderrama, *Model independent determination of the spins of the $P_c(4440)$ and $P_c(4457)$ from the spectroscopy of the triply charmed dibaryons*, Phys. Rev. **D102** (2020) 011504.
- [681] Y. Chung, H. G. Dosch, M. Kremer and D. Schall, *Baryon Sum Rules and Chiral Symmetry Breaking*, Nucl. Phys. **B197** (1982) 55.
- [682] E. Bagan, M. Chabab, H. G. Dosch and S. Narison, *Baryon sum rules in the heavy quark effective theory*, Phys. Lett. **B301**, 243 (1993).
- [683] D. Jido, N. Kodama and M. Oka, *Negative parity nucleon resonance in the QCD sum rule*, Phys. Rev. **D54** (1996) 4532.
- [684] Z. G. Wang, *Reanalysis of the heavy baryon states Ω_b , Ω_c , Ξ'_b , Ξ'_c , Σ_b and Σ_c with QCD sum rules*, Phys. Lett. **B685** (2010) 59.
- [685] Z. G. Wang, *Analysis of the $\frac{1}{2}^+$ doubly heavy baryon states with QCD sum rules*, Eur. Phys. J. **A45** (2010) 267.
- [686] Z. G. Wang, *Analysis of the $\frac{3}{2}^+$ heavy and doubly heavy baryon states with QCD sum rules*, Eur. Phys. J. **C68** (2010) 459.
- [687] Z. G. Wang, *Analysis of the $\frac{1}{2}^\pm$ antitriplet heavy baryon states with QCD sum rules*, Eur. Phys. J. **C68** (2010) 479.
- [688] Z. G. Wang, *Analysis of the $\frac{1}{2}^-$ and $\frac{3}{2}^-$ heavy and doubly heavy baryon states with QCD sum rules*, Eur. Phys. J. **A47** (2011) 81.
- [689] Z. G. Wang, *Analysis of the Triply Heavy Baryon States with QCD Sum Rules*, Commun. Theor. Phys. **58** (2012) 723.
- [690] S. L. Zhu, *Understanding pentaquark states in QCD*, Phys. Rev. Lett. **91** (2003) 232002.
- [691] J. Sugiyama, T. Doi and M. Oka, *Pentaquark baryon from the QCD sum rule*, Phys. Lett. **B581** (2004) 167.
- [692] R. D. Matheus, F. S. Navarra, M. Nielsen, R. Rodrigues da Silva and S. H. Lee, *Are Θ^+ and the Roper resonance diquark-diquark-antiquark states?*, Phys. Lett. **B578** (2004) 323.

- [693] L. Maiani, A. D. Polosa and V. Riquer, *The New Pentaquarks in the Diquark Model*, Phys. Lett. **B749** (2015) 289.
- [694] A. Ali and A. Y. Parkhomenko, *Interpretation of the Narrow $J/\psi p$ Peaks in $\Lambda_b \rightarrow J/\psi p K^-$ Decay*, Phys. Lett. **B793** (2019) 365.
- [695] R. F. Lebed, *The Pentaquark Candidates in the Dynamical Diquark Picture*, Phys. Lett. **B749** (2015) 454.
- [696] R. L. Zhu and C. F. Qiao, *Pentaquark states in a diquark-triquark model*, Phys. Lett. **B756** (2016) 259.
- [697] A. Ali, I. Ahmed, M. J. Aslam and A. Rehman, *Heavy quark symmetry and weak decays of the b -baryons in pentaquarks with a $c\bar{c}$ component*, Phys. Rev. **D94** (2016) 054001.
- [698] L. Maiani, A. D. Polosa and V. Riquer, *From Pentaquarks to Dibaryons in $\Lambda_b(5620)$ decays*, Phys. Lett. **B750** (2015) 37.
- [699] Z. G. Wang, *Analysis of the $\Lambda_c(2860)$, $\Lambda_c(2880)$, $\Xi_c(3055)$ and $\Xi_c(3080)$ as D -wave baryon states with QCD sum rules*, Nucl. Phys. **B926** (2018) 467.
- [700] Q. Xin, Z. G. Wang and F. Lu, *The Λ -type P -wave bottom baryon states via the QCD sum rules*, Chin. Phys. **C47** (2023) 093106.
- [701] G. L. Yu, Z. G. Wang and X. W. Wang, *The $1D$, $2D$ Ξ_b and Λ_b baryons*, Chin. Phys. **C46** (2022) 093102.
- [702] Shi-Zhong Huang, *Free particles and fields of high spins (in chinese)*, Anhui peoples Publishing House, 2006.
- [703] Z. G. Wang and T. Huang *Analysis of the $\frac{1}{2}^\pm$ pentaquark states in the diquark model with QCD sum rules*, Eur. Phys. J. **C76** (2016) 43.
- [704] Z. G. Wang, *Analysis of the $\frac{1}{2}^\pm$ pentaquark states in the diquark-diquark-antiquark model with QCD sum rules*, Eur. Phys. J. **C76** (2016) 142.
- [705] Z. G. Wang, *Analysis of the $\frac{3}{2}^\pm$ pentaquark states in the diquark-diquark-antiquark model with QCD sum rules*, Nucl. Phys. **B913** (2016) 163.
- [706] J. X. Zhang, Z. G. Wang and Z. Y. Di, *Analysis of the $\frac{3}{2}^\pm$ pentaquark states in the diquark model with QCD sum rules*, Acta Phys. Polon. **B48** (2017) 2013.
- [707] G. N. Li, X. G. He and M. He, *Some Predictions of Diquark Model for Hidden Charm Pentaquark Discovered at the LHCb*, JHEP **12** (2015) 128.
- [708] H. Y. Cheng and C. K. Chua, *Bottom Baryon Decays to Pseudoscalar Meson and Pentaquark*, Phys. Rev. **D92** (2015) 096009.
- [709] Z. G. Wang, *Analysis of the triply-charmed pentaquark states with QCD sum rules*, Eur. Phys. J. **C78** (2018) 300.
- [710] H. X. Chen, W. Chen, X. Liu, T. G. Steele and S. L. Zhu, *Towards exotic hidden-charm pentaquarks in QCD*, Phys. Rev. Lett. **115** (2015) 172001.
- [711] H. X. Chen, E. L. Cui, W. Chen, T. G. Steele, X. Liu and S. L. Zhu, *QCD sum rule study of hidden-charm pentaquarks*, Eur. Phys. J. **C76** (2016) 572.
- [712] K. Azizi, Y. Sarac and H. Sundu, *Analysis of $P_c^+(4380)$ and $P_c^+(4450)$ as pentaquark states in the molecular picture with QCD sum rules*, Phys. Rev. **D95** (2017) 094016.

- [713] K. Azizi, Y. Sarac and H. Sundu, *Strong Decay of $P_c(4380)$ Pentaquark in a Molecular Picture*, Phys. Lett. **B782** (2018) 694.
- [714] H. X. Chen, W. Chen and S. L. Zhu, *Possible interpretations of the $P_c(4312)$, $P_c(4440)$, and $P_c(4457)$* , Phys. Rev. **D100** (2019) 051501.
- [715] J. R. Zhang, *Exploring a $\Sigma_c \bar{D}$ state: with focus on $P_c(4312)^+$* , Eur. Phys. J. **C79** (2019) 1001.
- [716] H. X. Chen, W. Chen, X. Liu and X. H. Liu, *Establishing the first hidden-charm pentaquark with strangeness*, Eur. Phys. J. **C81** (2021) 409.
- [717] K. Azizi, Y. Sarac and H. Sundu, *Properties of the $P_c(4312)$ pentaquark and its bottom partner*, Chin. Phys. **C45** (2021) 053103.
- [718] K. Azizi, Y. Sarac and H. Sundu, *Hidden Bottom Pentaquark States with Spin $\frac{3}{2}$ and $\frac{5}{2}$* , Phys. Rev. **D96** (2017) 094030.
- [719] J. B. Xiang, H. X. Chen, W. Chen, X. B. Li, X. Q. Yao and S. L. Zhu, *Revisiting hidden-charm pentaquarks from QCD sum rules*, Chin. Phys. **C43** (2019) 034104.
- [720] X. W. Wang, Z. G. Wang, G. L. Yu and Q. Xin, *Isospin eigenstates of the color singlet-singlet-type pentaquark states*, Sci. China Phys. Mech. Astron. **65** (2022) 291011.
- [721] X. W. Wang and Z. G. Wang, *Study of isospin eigenstates of the pentaquark molecular states with strangeness*, Int. J. Mod. Phys. **A37** (2022) 2250189.
- [722] X. W. Wang and Z. G. Wang, *Analysis of $P_{cs}(4338)$ and related pentaquark molecular states via QCD sum rules*, Chin. Phys. **C47** (2023) 013109.
- [723] U. Ozdem, *Investigation of magnetic moment of $P_{cs}(4338)$ and $P_{cs}(4459)$ pentaquark states*, Phys. Lett. **B836** (2023) 137635.
- [724] U. Ozdem, *Electromagnetic properties of $\bar{D}^{(*)}\Xi'_c$, $\bar{D}^{(*)}\Lambda_c$, $\bar{D}_s^{(*)}\Lambda_c$ and $\bar{D}_s^{(*)}\Xi_c$ pentaquarks*, Phys. Lett. **B846** (2023) 138267.
- [725] U. Ozdem, *Analysis of the isospin eigenstate $\bar{D}\Sigma_c$, $\bar{D}^*\Sigma_c$, and $\bar{D}\Sigma_c^*$ pentaquarks by their electromagnetic properties*, Eur. Phys. J. **C84** (2024) 769.
- [726] R. Chen, X. Liu, X. Q. Li and S. L. Zhu, *Identifying exotic hidden-charm pentaquarks*, Phys. Rev. Lett. **115** (2015) 132002.
- [727] F. K. Guo, U. G. Meissner, W. Wang and Z. Yang, *How to reveal the exotic nature of the $P_c(4450)$* , Phys. Rev. **D92** (2015) 071502.
- [728] R. Chen, Z. F. Sun, X. Liu and S. L. Zhu, *Strong LHCb evidence supporting the existence of the hidden-charm molecular pentaquarks*, Phys. Rev. **D100** (2019) 011502.
- [729] C. J. Xiao, Y. Huang, Y. B. Dong, L. S. Geng and D. Y. Chen, *Exploring the molecular scenario of $P_c(4312)$, $P_c(4440)$, and $P_c(4457)$* , Phys. Rev. **D100** (2019) 014022.
- [730] T. J. Burns, *Phenomenology of $P_c(4380)^+$, $P_c(4450)^+$ and related states*, Eur. Phys. J. **A51** (2015) 152.
- [731] F. K. Guo, H. J. Jing, U. G. Meissner and S. Sakai, *Isospin breaking decays as a diagnosis of the hadronic molecular structure of the $P_c(4457)$* , Phys. Rev. **D99** (2019) 091501.

- [732] H. X. Chen, L. S. Geng, We. H. Liang, E. Oset, E. Wang and J. J. Xie, *Looking for a hidden-charm pentaquark state with strangeness $S = -1$ from Ξ_b^- decay into $J/\psi K^- \Lambda$* , Phys. Rev. **C93** (2016) 065203.
- [733] T. J. Burns and E. S. Swanson, *Molecular Interpretation of the $P_c(4440)$ and $P_c(4457)$ States*, Phys. Rev. **D100** (2019) 114033.
- [734] Y. Yamaguchi, H. Garcia-Tecocoatzi, A. Giachino, A. Hosaka, E. Santopinto, S. Takeuchi and M. Takizawa, *P_c pentaquarks with chiral tensor and quark dynamics*, Phys. Rev. **D101** (2020) 091502.
- [735] Y. Shimizu, D. Suenaga and M. Harada, *Coupled channel analysis of molecule picture of $P_c(4380)$* , Phys. Rev. **D93** (2016) 114003.
- [736] Y. Yamaguchi and E. Santopinto, *Hidden-charm pentaquarks as a meson-baryon molecule with coupled channels for $\bar{D}^{(*)}\Lambda_c$ and $\bar{D}^{(*)}\Sigma_c^{(*)}$* , Phys. Rev. **D96** (2017) 014018.
- [737] M. L. Du, V. Baru, F. K. Guo, C. Hanhart, U. G. Meissner, J. A. Oller and Q. Wang, *Interpretation of the LHCb P_c States as Hadronic Molecules and Hints of a Narrow $P_c(4380)$* , Phys. Rev. Lett. **124** (2020) 072001.
- [738] M. L. Du, V. Baru, F. K. Guo, C. Hanhart, U. G. Meissner, J. A. Oller and Q. Wang, *Revisiting the nature of the P_c pentaquarks*, JHEP **08** (2021) 157.
- [739] A. Pimikov, H. J. Lee and P. M. Zhang, *Hidden charm pentaquarks with color-octet substructure in QCD Sum Rules*, Phys. Rev. **D101** (2020) 014002.
- [740] Z. G. Wang, *Light tetraquark state candidates*, Adv. High Energy Phys. **2020** (2020) 6438730.
- [741] X. S. Yang, Q. Xin and Z. G. Wang, *Analysis of the $T_{c\bar{s}}(2900)$ and related tetraquark states with the QCD sum rules*, Int. J. Mod. Phys. **A38** (2023) 2350056.
- [742] G. J. Wang, L. Meng, L. Y. Xiao, M. Oka and S. L. Zhu, *Mass spectrum and strong decays of tetraquark $\bar{c}sqq$ states*, Eur. Phys. J. **C81** (2021) 188.
- [743] Y. Huang, J. X. Lu, J. J. Xie and L. S. Geng, *Strong decays of \bar{D}^*K^* molecules and the newly observed $X_{0,1}$ states*, Eur. Phys. J. **C80** (2020) 973.
- [744] C. J. Xiao, D. Y. Chen, Y. B. Dong and G. W. Meng, *A study of the decays of S -wave \bar{D}^*K^* hadronic molecules: the scalar $X_0(2900)$ and its spin partners $X_{J(J=1,2)}$* , Phys. Rev. **D103** (2021) 034004.
- [745] B. Wang and S. L. Zhu, *How to understand the $X(2900)?$* , Eur. Phys. J. **C82** (2022) 419.
- [746] T. J. Burns and E. S. Swanson, *Kinematical cusp and resonance interpretations of the $X(2900)$* , Phys. Lett. **B813** (2021) 136057.
- [747] T. J. Burns and E. S. Swanson, *Discriminating among interpretations for the $X(2900)$ states*, Phys. Rev. **D103** (2021) 014004.
- [748] M. E. Bracco, A. Lozea, R. D. Matheus, F. S. Navarra and M. Nielsen, *Disentangling two- and four-quark state pictures of the charmed scalar mesons*, Phys. Lett. **B624** (2005) 217.
- [749] H. Kim and Y. Oh, *$D_s(2317)$ as a four-quark state in QCD sum rules*, Phys. Rev. **D72** (2005) 074012.
- [750] Z. G. Wang and S. L. Wan, *$D_{s0}(2317)$ as a tetraquark state with QCD sum rules in heavy quark limit*, Nucl. Phys. **A778** (2006) 22.

- [751] T. J. Burns and E. S. Swanson, *Interpreting the $X(5568)$* , Phys. Lett. **B760** (2016) 627.
- [752] F. K. Guo, U. G. Meissner and B. S. Zou, *How the $X(5568)$ challenges our understanding of QCD*, Commun. Theor. Phys. **65** (2016) 593.
- [753] R. Aaij et al, *Observation of five new narrow Ω_c^0 states decaying to $\Xi_c^+ K^-$* , Phys. Rev. Lett. **118** (2017) 182001.
- [754] J. Yelton et al, *Observation of Excited Ω_c Charmed Baryons in e^+e^- Collisions*, Phys. Rev. **D97** (2018) 051102.
- [755] R. Aaij et al, *Observation of new Ω_c^0 states decaying to the $\Xi_c^+ K^-$ final state*, Phys. Rev. Lett. **131** (2023) 131902.
- [756] R. Mizuk et al, *Observation of an Isotriplet of Excited Charmed Baryons Decaying to $\Lambda_c^+ \pi$* , Phys. Rev. Lett. **94** (2005) 122002.
- [757] B. Aubert et al, *Measurements of $\mathcal{B}(\bar{B}^0 \rightarrow \Lambda_c^+ \bar{p})$ and $\mathcal{B}(B^- \rightarrow \Lambda_c^+ \bar{p} \pi^-)$ and Studies of $\Lambda_c^+ \pi^-$ Resonances*, Phys. Rev. **D78** (2008) 112003.
- [758] B. Aubert et al, *Observation of a Charmed Baryon Decaying to $D^0 p$ at a Mass Near 2.94 GeV/c²*, Phys. Rev. Lett. **98** (2007) 012001.
- [759] K. Abe et al, *Experimental Constraints on the Spin and Parity of the $\Lambda_c(2880)$* , Phys. Rev. Lett. **98** (2007) 262001.
- [760] R. Aaij et al, *Study of the $D^0 p$ amplitude in $\Lambda_b^0 \rightarrow D^0 p \pi^-$ decays*, JHEP **05** (2017) 030.
- [761] Y. B. Li et al, *Evidence of a new excited charmed baryon decaying to $\Sigma_c(2455)^{0,++} \pi^\pm$* , Phys. Rev. Lett. **130** (2023) 031901.
- [762] S. Sakai, F. K. Guo and B. Kubis, *Extraction of ND scattering lengths from the $\Lambda_b \rightarrow \pi^- p D^0$ decay and properties of the $\Sigma_c(2800)^+$* , Phys. Lett. **B808** (2020) 135623.
- [763] L. F. Zhao, H. X. Huang and J. L. Ping, *ND and NB systems in quark delocalization color screening model*, Eur. Phys. J. **A53** (2017) 28.
- [764] Z. Y. Wang, J. J. Qi, X. H. Guo and K. W. Wei, *Study of molecular ND bound states in the Bethe-Salpeter equation approach*, Phys. Rev. **D97** (2018) 094025.
- [765] M. J. Yan, F. Z. Peng and M. P. Valderrama, *Molecular charmed baryons and pentaquarks from light-meson exchange saturation*, Phys. Rev. **D109** (2024) 014023.
- [766] Y. Yan, X. H. Hu, Y. H. Wu, H. X. Huang and J. L. Ping, *Molecular state interpretation of charmed baryons in the quark model*, Eur. Phys. J. **C83** (2023) 524.
- [767] J. R. Zhang, *S -wave $D^{(*)}N$ molecular states: $\Sigma_c(2800)$ and $\Lambda_c(2940)^+?$* , Phys. Rev. **D89** (2014) 096006.
- [768] Z. L. Zhang, Z. W. Liu, S. Q. Luo, F. L. Wang, B. Wang and H. Xu, *$\Lambda_c(2910)$ and $\Lambda_c(2940)$ as the conventional baryons dressed with the D^*N channel*, Phys. Rev. **D107** (2023) 034036.
- [769] B. Wang, L. Meng and S. L. Zhu, *$D^{(*)}N$ interaction and the structure of $\Sigma_c(2800)$ and $\Lambda_c(2940)$ in chiral effective field theory*, Phys. Rev. **D101** (2020) 094035.
- [770] Y. Huang, J. He, J. J. Xie and L. S. Geng, *Production of the $\Lambda_c(2940)$ by kaon-induced reactions on a proton target*, Phys. Rev. **D99** (2019) 014045.

- [771] Q. Xin, X. S. Yang and Z. G. Wang, *The singly charmed pentaquark molecular states via the QCD sum rules*, Int. J. Mod. Phys. **A38** (2023) 2350123.
- [772] K. L. Wang and X. H. Zhong, *Toward establishing the low-lying P-wave excited Σ_c baryon states*, Chin. Phys. **C46** (2022) 023103.
- [773] K. L. Wang, Y. X. Yao, X. H. Zhong and Q. Zhao, *Strong and radiative decays of the low-lying S- and P-wave singly heavy baryons*, Phys. Rev. **D96** (2017) 116016.
- [774] H. M. Yang and H. X. Chen, *P-wave charmed baryons of the SU(3) flavor 6_F* , Phys. Rev. **D104** (2021) 034037.
- [775] D. J. Jia, W. N. Liu and A. Hosaka, *Regge behaviors in orbitally excited spectroscopy of charmed and bottom baryons*, Phys. Rev. **D101** (2020) 034016.
- [776] G. L. Yu, Z. Y. Li, Z. G. Wang, J. Lu and M. Yan, *Systematic analysis of single heavy baryons Λ_Q , Σ_Q and Ω_Q* , Nucl. Phys. **B990** (2023) 116183.
- [777] H. Y. Cheng and C. W. Chiang, *Quantum numbers of Ω_c states and other charmed baryons*, Phys. Rev. **D95** (2017) 094018.
- [778] S. Q. Luo, B. Chen, Z. W. Liu and X. Liu, *Resolving the low mass puzzle of $\Lambda_c(2940)^+$* , Eur. Phys. J. **C80** (2020) 301.
- [779] Q. F. Lu, Z. Y. Wang and X. H. Zhong, *Strong decay of $\Lambda_c(2940)$ as a $2P$ state in the Λ_c family*, Eur. Phys. J. **C78** (2018) 599.
- [780] K. Azizi, Y. Sarac and H. Sundu, *Interpretation of the $\Lambda_c(2910)^+$ baryon newly seen by Belle Collaboration and its possible bottom partner*, Eur. Phys. J. **C82** (2022) 920.
- [781] W. J. Wang, L. Y. Xiao and X. H. Zhong, *The strong decays of the low-lying ρ -mode $1P$ -wave singly heavy baryons*, Phys. Rev. **D106** (2022) 074020.
- [782] G. L. Yu, M. Yan, Z. Y. Li, Z. G. Wang and J. Lu, *Strong decay properties of single heavy baryons Λ_Q , Σ_Q and Ω_Q* , Int. J. Mod. Phys. **A38** (2023) 2350082.
- [783] M. Karliner and J. L. Rosner, *Excited Ω_c baryons as $2S$ states*, Phys. Rev. **D108** (2023) 014006.
- [784] S. Q. Luo and X. Liu, *The newly observed $\Omega_c(3327)$: A good candidate for a D-wave charmed baryon*, Phys. Rev. **D107** (2023) 074041.
- [785] Z. G. Wang, F. Lu and Y. Liu, *Analysis of the D-wave Σ -type charmed baryon states with the QCD sum rules*, Eur. Phys. J. **C83** (2023) 689.
- [786] H. J. Wang, Z. Y. Di and Z. G. Wang, *Analysis of the $\Xi_b(6227)$ as the $\frac{1}{2}^\pm$ Pentaquark Molecular States with QCD Sum Rules*, Int. J. Theor. Phys. **59** (2020) 3124.
- [787] H. J. Wang, Z. Y. Di and Z. G. Wang, *Analysis of the excited Ω_c states as the $\frac{1}{2}^\pm$ pentaquark states with QCD sum rules*, Commun. Theor. Phys. **73** (2021) 035201.
- [788] Z. G. Wang and J. X. Zhang, *Possible pentaquark candidates: new excited Ω_c states*, Eur. Phys. J. **C78** (2018) 503.
- [789] Z. G. Wang, *Strong decays of the $Y(4660)$ as a vector tetraquark state in solid quark-hadron duality*, Eur. Phys. J. **C79** (2019) 184.
- [790] F. S. Navarra and M. Nielsen, *$X(3872) \rightarrow J/\psi \pi^+ \pi^-$ and $X(3872) \rightarrow J/\psi \pi^+ \pi^- \pi^0$ decay widths from QCD sum rules*, Phys. Lett. **B639** (2006) 272.

- [791] J. M. Dias, K. P. Khemchandani, A. M. Torres, M. Nielsen and C. M. Zanetti, *A QCD sum rule calculation of the $X^\pm(5568) \rightarrow B_s^0 \pi^\pm$ decay width*, Phys. Lett. **B758** (2016) 235.
- [792] W. Chen, T. G. Steele, H. X. Chen and S. L. Zhu, *$Z_c(4200)^+$ decay width as a charmonium-like tetraquark state*, Eur. Phys. J. **C75** (2015) 358.
- [793] K. Azizi, Y. Sarac and H. Sundu, *Investigation of $P_{cs}(4459)^0$ pentaquark via its strong decay to $\Lambda J/\psi$* , Phys. Rev. **D103** (2021) 094033.
- [794] K. Azizi, Y. Sarac and H. Sundu, *Investigation of a candidate spin- $\frac{1}{2}$ hidden-charm triple strange pentaquark state P_{csss}* , Phys. Rev. **D107** (2023) 014023.
- [795] K. Azizi, Y. Sarac and H. Sundu, *Investigation of hidden-charm double strange pentaquark candidate P_{css} via its mass and strong decays*, Eur. Phys. J. **C82** (2022) 543.
- [796] K. Azizi, Y. Sarac and H. Sundu, *Investigation of the strange pentaquark candidate $P_{\psi s}^\Lambda(4338)^0$ recently observed by LHCb*, Phys. Rev. **D108** (2023) 074010.
- [797] Z. G. Wang, *Analysis of strong decays of the $Z_c(4600)$ with the QCD sum rules*, Int. J. Mod. Phys. **A34** (2019) 1950110.
- [798] Z. G. Wang and X. Wang, *Analysis of the strong decays of the $P_c(4312)$ as a pentaquark molecular state with QCD sum rules*, Chin. Phys. **C44** (2020) 103102.
- [799] Z. G. Wang, H. J. Wang and Q. Xin, *The hadronic coupling constants of the lowest hidden-charm pentaquark state with the QCD sum rules in rigorous quark-hadron duality*, Chin. Phys. **C45** (2021) 063104.
- [800] Y. J. Xu, Y. L. Liu and M. Q. Huang, *The magnetic moment of $P_c(4312)$ as a $\bar{D}\Sigma_c$ molecular state*, Eur. Phys. J. **C81** (2021) 421.
- [801] Z. G. Wang, *Decay widths of $Z_{cs}(3985/4000)$ based on rigorous quark-hadron duality*, Chin. Phys. **C46** (2022) 103106.
- [802] Z. G. Wang and X. S. Yang, *The two-body strong decays of the fully-charm tetraquark states*, AAPPs Bull. **34** (2024) 5.
- [803] X. W. Wang and Z. G. Wang, *Strong decays of the $P_c(4312)$ and its isospin cousin via the QCD sum rules*, Chin. Phys. **C48** (2024) 053102.
- [804] X. W. Wang and Z. G. Wang, *Strong decays of $P_{cs}(4338)$ and its high isospin cousin via QCD sum rules*, Phys. Rev. **D110** (2024) 014008.
- [805] Y. J. Xu, C. Y. Cui, Y. L. Liu and M. Q. Huang, *Partial decay widths of $P_c(4312)$ as a $\bar{D}\Sigma_c$ molecular state*, Phys. Rev. **D102** (2020) 034028.
- [806] Z. G. Wang, *The magnetic moment of the $Z_c(3900)$ as an axialvector tetraquark state with QCD sum rules*, Eur. Phys. J. **C78** (2018) 297.
- [807] S. S. Agaev, K. Azizi and H. Sundu, *Exploring the resonances $X(4140)$ and $X(4274)$ through their decay channels*, Phys. Rev. **D95** (2017) 114003.
- [808] S. S. Agaev, K. Azizi and H. Sundu, *Spectroscopic parameters and decays of the resonance $Z_b(10610)$* , Eur. Phys. J. **C77** (2017) 836.
- [809] H. Sundu, S. S. Agaev and K. Azizi, *Resonance $Y(4660)$ as a vector tetraquark and its strong decay channels*, Phys. Rev. **D98** (2018) 054021.

- [810] Y. Xie and H. Sun, *Investigate the strong coupling of $g_{XJ/\psi\phi}$ in $X(4500) \rightarrow J/\psi\phi$ by using the three-point sum rules and the light-cone sum rules*, Nucl. Phys. **B1000** (2024) 116471.
- [811] U. Ozdem and K. Azizi, *Electromagnetic multipole moments of the $P_c^+(4380)$ pentaquark in light-cone QCD*, Eur. Phys. J. **C78** (2018) 379.
- [812] B. L. Ioffe and A. V. Smilga, *Nucleon Magnetic Moments and Magnetic Properties of Vacuum in QCD*, Nucl. Phys. **B232** (1984) 109.
- [813] V. M. Belyaev, V. M. Braun, A. Khodjamirian and R. Ruckl, *$D^*D\pi$ and $B^*B\pi$ couplings in QCD*, Phys. Rev. **D51** (1995) 6177.
- [814] P. Ball, *Theoretical update of pseudoscalar meson distribution amplitudes of higher twist: The Nonsinglet case*, JHEP **01** (1999) 010.
- [815] V. M. Braun and I. E. Filyanov, *Conformal Invariance and Pion Wave Functions of Non-leading Twist*, Z. Phys. **C48** (1990) 239.
- [816] Z. G. Wang, *Three-body strong decays of the $Y(4230)$ via the light-cone QCD sum rules*, Int. J. Mod. Phys. **A38** (2023) 2350175.